METHODS IN MOLECULAR MEDICINE™

Drug Targeting

Strategies, Principles, and Applications

Edited by

G. E. Francis
Cristina Delgado

Humana Press

1

Chemical Construction of Immunotoxins

Victor Ghetie and Ellen S. Vitetta

1. Introduction

Immunotoxins (ITs) are chimeric proteins consisting of an antibody linked to a toxin. The antibody confers specificity (ability to recognize and react with the target), whereas the toxin confers cytotoxicity (ability to kill the target) ***(1–3)***. ITs have been used in both mice and humans to eliminate tumor cells, autoimmune cells, and virus-infected cells ***(4–6)***.

The linkage of the antibody to the toxin can be accomplished by one of two general methods, chemical or genetic. Chemical construction of ITs utilizes reagents that crosslink antibody and toxin (**Fig. 1A**) ***(7,8)***. Genetic construction uses hybrid genes to produce antibody-toxin fusion proteins in *Escherichia coli* (**Fig. 1B**) ***(9,10)***. Two major types of chemical bonds can be used to form ITs: disulfide bonds ***(11)*** and thioether bonds ***(12)*** (**Fig. 2**). Disulfide bonds are susceptible to reduction in the cytoplasm of the target cells, thereby releasing the toxin so that it can exert its inhibitory activity only in the cells binding the antibody moiety ***(13)***. This type of covalent bond has been used to construct ITs containing single-chain plant toxins (ricin A chain [RTA], pokeweed antiviral protein [PAP], saporin, gelonin, and so forth). Since mammalian enzymes cannot hydrolyze thioether bonds, thioether-linked conjugates of toxins and antibodies are not cytotoxic to target cells ***(1,14)***. However there are two exceptions. The first is an IT with the intact ricin toxin (RT). RT is composed of two polypeptide chains (the cell-binding B chain [RTB] and the RTA) linked by a disulfide bond. If the antibody is bound to the toxin through the RTB, the toxic chain can be released in the target cell cytosol by reduction of the interchain disulfide bond ***(15)*** (**Fig. 2**). The second exception is an IT prepared with *Pseudomonas* exotoxin (PE). PE can be coupled to antibody by

From: *Methods in Molecular Medicine, Vol. 25: Drug Targeting: Strategies, Principles, and Applications*
Edited by: G. E. Francis and C. Delgado

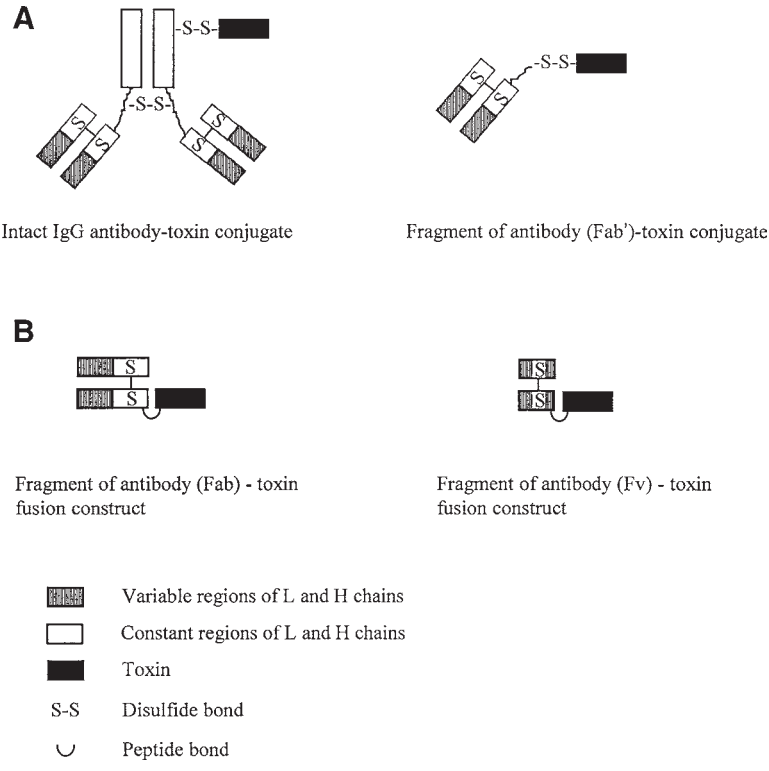

Fig. 1. The structure of antibody–toxin constructs obtained by **(A)** chemical and **(B)** genetic engineering procedures.

a thioether bond, since this toxin contains a protease-sensitive peptide bond that is cleaved intracellularly to generate a toxic moiety bound to the rest of the molecule by a disulfide bond (**Fig. 2**).

This chapter presents methods for preparing ITs with disulfide-linked toxins as exemplified by RTA, PAP, and a truncated recombinant *Pseudomonas* exotoxin (PE35) and with thioether-linked toxins exemplified by blocked ricin (bRT) and truncated recombinant *Pseudomonas* exotoxin (PE38).

2. Materials

The following reagents have been used for the preparation of ITs:

1. From Pharmacia (Piscataway, NJ): Protein A-Sepharose Fast Flow, Protein G-Sepharose Fast Flow, Sephacryl S-200HR, DEAE-Sepharose CL-4B, Sephadex G-25M, Blue-Sepharose CL-4B, Sephadex G-25 MicroSpin, CM-Sepharose CL-4B, SP-Sepharose Fast Flow.

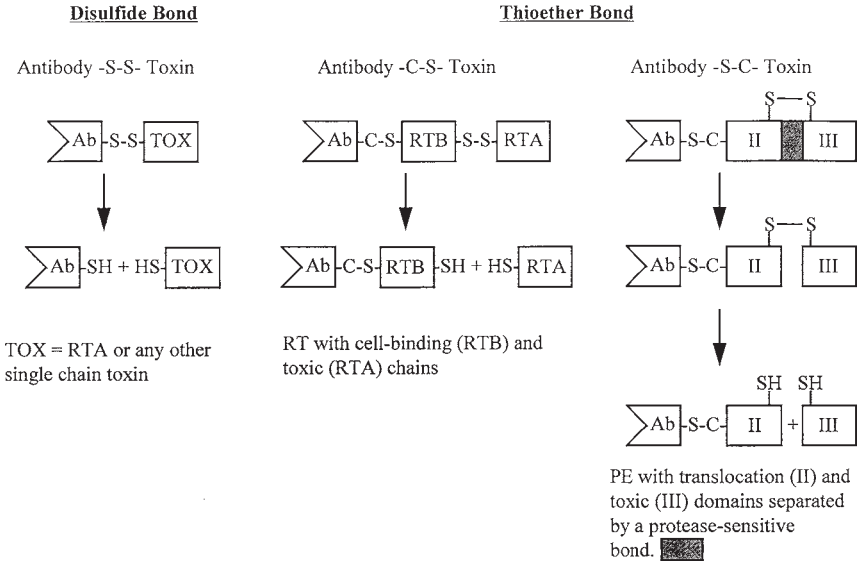

Fig. 2. Covalent bonds crosslinking antibody to toxin.

2. From Pierce (Rockford, IL): 4-succinimidyloxycarbonyl-α-methyl-α-(2-pyridyldithio)-toluene (SMPT), *N*-succinimidyl 3-(2-pyridyldithio)propionate (SPDP), *N*-succinimidyl 5-acetylthioacetate (SATA), succinimidyl 4-(*N*-maleimidomethyl) cyclohexane-1-carboxylate (SMCC), 2-iminothiolane (2-IT), dithiothreitol (DTT), dimethylformamide (DMF), 5,5'-dithio-bis-(2-nitrobenzoic)acid (DTNB), (Ellman's reagent), 2-mercaptoethanol.
3. From Sigma (St. Louis, MO): sodium hydroxyde, sodium chloride, potassium chloride, potassium and sodium phosphate (monobasic and dibasic), ethylenediaminetetra-acetic acid (EDTA; disodium salt), acetic acid (glacial), penicillin G (sodium salt), pepsin (crystallized and insoluble enzyme attached to 4% crosslinked agarose), boric acid, glycine, ricin toxin (Toxin RCA60), ricin A chain, saporin, pockweed mitogen (PAP), pseudomonas exotin A (PE), lactose, galactose, cyanuric chloride, sodium metaperiodate, sodium cyanoborohydride, Trizma hydrochloride (Tris), fetuin, triethanolamine hydrochloride, orcinol, streptomicin sulfate, L-glutamine, RPMI-1640 medium, fetal calf serum.
4. From Amersham (Arlington Heights, IL): ^{35}S-methionine, ^{3}H-thymidine, ^{3}H-Leucine.
5. The following equipment has been used for the preparation of ITs: spectrophotometer (DU640 Beckman, Beckman Instruments, Houston, TX), electrophoresis system (Phastsystem, Pharmacia, Piscataway, NJ), chromatographic system (BioLogic system, Bio-Rad, Hercules, CA), HPLC system (LKB-Pharmacia), HPLC columns (TSK, TosoHaas, Montgomeryville, PA), centrifuge (RC3C, Sorvall, Newton, CT), ultracentrifuge (Optima, Beckman).

6. For the in vivo testing of ITs, SCID mice were obtained from Charles River Labs (Wilmington, MA) and Taconic (Germantown, NY).

3. Methods

3.1. Preparation of the IgG Antibody and Its Fab' Fragments

The antibody most frequently used for the preparation of ITs belongs to the IgG isotype of murine monoclonal antibodies (MAbs). However, Fab' fragments as well as chimeric mouse–human IgG antibodies have also been used ***(16)***.

3.1.1. IgG

Many procedures for the preparation of monoclonal mouse IgG are available ***(17)***.

The method used in our laboratory is as follows:

1. The MAb preparation (from cell culture supernatants or ascites) is chromatographed over a protein G Sepharose column equilibrated with 50 m*M* phosphate buffer containing 3 m*M* Na_2EDTA at pH 7.5 (PBE).
2. The bound MAb is eluted with 25 m*M* acetic acid and after neutralization is subjected to gel filtration on a column of Sephacryl S-200 HR (length 60–90 cm) equilibrated with PBE containing 0.15 *M* NaCl (PBS) at pH 7.5.
3. The fraction containing purified IgG is concentrated to 5 mg/mL by ultrafiltration (e.g., using the Millipore ultrafiltration centrifugal device) and then used for chemical derivatization.
4. If the MAb is used for the preparation of a clinical IT, an additional chromatographic purification is performed on a DEAE-Sepharose column equilibrated with PBS to remove the murine DNA and bacterial endotoxin contaminating the MAb.

3.1.2. Fab' Fragments

Fab' fragments can be obtained by pepsin digestion of purified IgG molecules. As a result of the hydrolysis, $F(ab')_2$ fragments are obtained. Following reduction with DTT, the $F(ab')_2$ yields two Fab' fragments with one or more free sulfhydryl (SH) groups in the hinge region which are available for crosslinking to the toxin moiety (**Fig. 1A**). Therefore, Fab' fragments do not require chemical derivation with thiol-containing crosslinkers. The pH and duration of pepsinolyis depend on the IgG isotype ***(18,19)***. Therefore, preliminary experiments should be carried out to select the optimal conditions for obtaining Fab' fragments with the highest purity and the yields. The method used in our laboratory is as follows ***(20)***:

1. IgG is brought to 2.5 mg/mL in 0.1 *M* citrate buffer, pH 3.7, pepsin (Sigma) is added (1 mg pepsin/50 mg), and digestion is performed at 37°C for 2–8 h (depending on the IgG isotype).

2. The pH of the digest is then brought to pH 8.0 with 0.1 *M* NaOH and the mixture is applied to a Sephacryl S-200 HR column equilibrated with PBE.
3. The $F(ab')_2$ is collected and concentrated to 5 mg/mL.
4. DTT is then added to a final concentration of 5 m*M* and the mixture is incubated at room temperature for 1 h in the dark.
5. The reduced Fab' fragments are chromatographed on a Sephadex G-25M column (length 30–60 cm) equilibrated with PBE and flushed with N_2 by loading a volume not greater than 2% of the volume of the gel. Thus, for a column of 1.8×30 cm containing 75 mL gel, <1.5 mL of mixture should be added.
6. The Fab' fraction is eluted in the void volume, concentrated to 5 mg/mL, and treated with a 1/100 volume of DTNB (Ellman reagent) dissolved in DMF (80 mg/mL).
7. After a 1 h incubation at 25°C, the mixture is rechromatographed on a Sephadex G-25M column as described in **Subheading 3.1.2.**, **step 5**.
8. The Ellmanized Fab' eluted in the void volume is collected, concentrated to 5 mg/mL, and stored at 4°C until it can be used for reaction with the toxin.

3.2. Chemical Derivatization of the IgG Antibody

MAbs cannot be linked to toxins unless they are derivatized with crosslinking agents since the IgG molecule, in contrast to Fab', does not contain a free cysteine residue. Disulfide or sulfhydryl groups are therefore introduced into the antibody molecule to form a disulfide bond between the antibody and the toxin. For crosslinking the toxin to the antibody through a thioether bond, a maleimide group should be introduced into the IgG, thus allowing a reaction with the sulfhydryl groups of the toxin.

3.2.1. Introduction of Disulfide Groups

Disulfide groups are introduced using one of two heterobifunctional crosslinkers, which can be obtained commercially in water soluble (sulfo) or insoluble form (Pierce) (**Fig. 3**). We prefer SMPT to SPDP as the pyridyldisulfide crosslinker since it generates a molecule with increased stability in vivo because of the protective effect exerted upon the disulfide bond by the methyl group and the benzene ring on the carbon atoms adjacent to the -ss- bond (**Fig. 3**) *(21,22)*. The procedure used in our laboratory is as follows *(23)*:

1. IgG is dissolved in PBE or PBS, pH 7.5, at a concentration of 5 mg/mL.
2. 10 µL of SMPT (or SPDP) dissolved in DMF (5 mg/mL) or sulfo-SMPT (or Sulfo-SPDP) dissolved in buffer (10 mg/mL) is added to each milliliter of the MAb and the mixture is incubated at 25°C for 1 h.
3. The mixture is chromatographed on Sephadex G-25M as described in **Subheading 1.2.** and the material eluted in the void volume is collected and concentrated to 3–5 mg/mL. This material should be stored at 4°C before mixing it with the toxin.

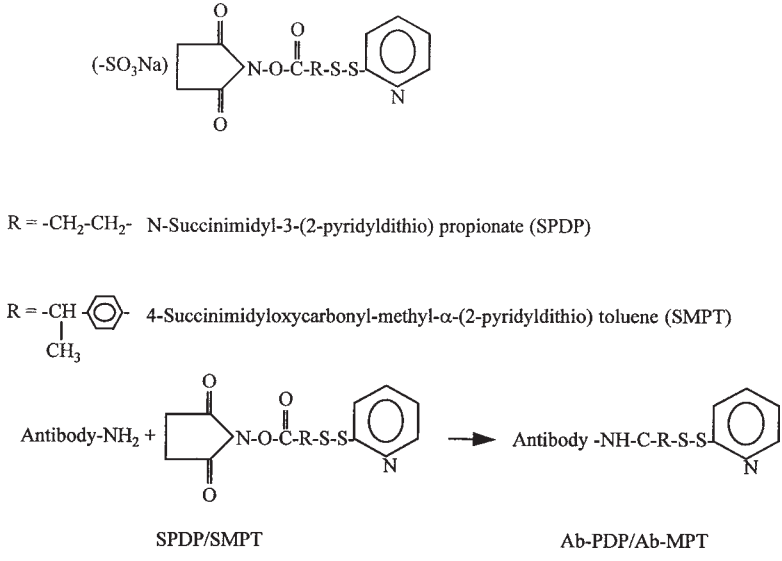

Fig. 3. The structure of the pyridyldisulfide crosslinkers and their reaction with the antibody molecule.

4. The average number of disulfide groups introduced into the antibody molecule can be measured on an aliquot as follows:
   a. To 1 mL of modified IgG with a known absorbance at 280 nm (1–2 absorbance units is optimal), 20 µL of 0.3 *M* DTT is added and the absorbance at 343 nm is measured after an incubation of 5 min.
   b. The MPT/IgG molar ratio (MR) is calculated using the formula: $MR = 26 \times A_{343} / [A_{280} - 0.63 \times A_{343}]$.

The MR of a correctly prepared antibody–MPT derivative should range between 2.0 and 2.5. For example, if A_{280} nm = 1.35 and A_{343} nm = 0.11, MR = 2.86/1.28 = 2.2.

3.2.2. Introduction of Sulfhydryl Groups

Sulfhydryl groups are introduced using one of two reagents that can be obtained commercially: 2-iminothiolane (2-IT) and SATA (**Fig. 4**). SATA contains a protected sulfhydryl group to confer stability on the molecule. When a free sulfhydryl group is needed, it can be generated by treatment with hydroxylamine. (**Fig. 4**).

3.2.2.1. 2-Iminothiolane ***(22,24)***

1. The IgG is dissolved at 10 mg/mL in 50 m*M* borate buffer containing 0.3 *M* NaCl, pH 9.0.
2. 25 µL of 2-IT (4.4 mg/mL in the same buffer) is added and the mixture is stirred at room temperature for 1 h.

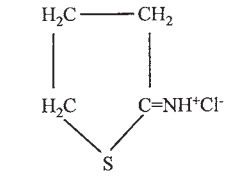

2-Iminothiolane (2-IT)
(Traut reagent)

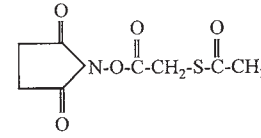

N-Succinimidyl-S-Acetylthioacetate
(SATA)

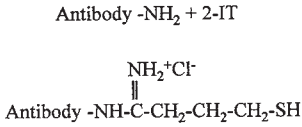

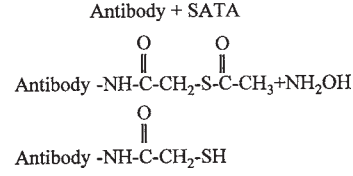

Fig. 4. The structure of thiolation reagents and their reaction with IgG.

3. The reaction is stopped by adding glycine to 0.22 *M* final concentration.
4. Excess reagents are removed by gel filtration on Sephadex G-25M equilibrated with 0.1 *M* phosphate buffer containing 0.1 *M* NaCl and 1 m*M* Na_2EDTA, pH 7.5.
5. The fraction eluted in the void volume containing the thiolated IgG is concentrated to 3–5 mg/mL and then mixed with the toxin.

The number of sulfhydryl groups introduced ranges from 1.5 to 1.8 per molecule of antibody. This can be determined as follows:

1. 1 mL of buffer is placed in a spectrophotometer cuvet.
2. 10 µL DTNB (80 mg/mL DMF) is added and the spectrophotometer is zeroed at 412 nm.
3. The buffer is discarded and 1 mL of the derivatized IgG solution (with a known protein concentration, A_{280} nm ≈ 1.0) is placed in the same cuvet.
4. 10 µL DTNB (80 mg/mL DMF) is added and the A_{412} is determined.
5. The number of SH groups per molecule of IgG is calculated using the formula $21 \times A_{412}/1.36 \times A_{280}$. For example, if A_{280} nm = 1.4 and A_{412} nm = 0.2; SH/IgG = 4.2/1.9 = 2.2.

The sulfhydryl yields a disulfide group following treatment of the thiolated IgG with Ellman's reagent:

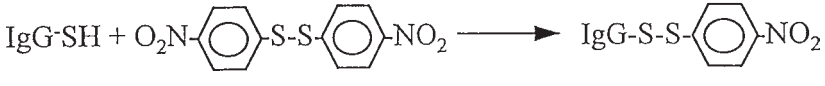

In this case, the mixture is treated with 10 µL Ellman's reagent (80 mg/mL DMF)/1 mL of mixture after stopping the reaction of 2-IT with IgG by the

addition of glycine. After 1 h the solution is chromatographed on Sephadex G25M. The protein eluted in the void volume is concentrated to 5 mg/mL. This can be stored at 4°C before reaction with the chosen toxin.

The number of disulfide groups can be determined as follows:

1. 1 mL of IgG-S-S-R solution with a known A_{280} nm is placed in a cuvet and 10 µL of 0.25 *M* DTT is added, mixed, and the A_{412} determined.
2. The number of disulfide groups per molecule of IgG is calculated using the formula: $15 \times A_{412} / [(1.36 \times A_{280}) - (0.24 \times A_{412})]$. For example, if A_{280} nm = 1.2 and A_{412} nm = 0.2; MR= 3/1.58 = 1.9.

3.2.2.2. SATA *(25)*

1. IgG is dissolved in PBE or PBS, pH 7.5, at a concentration of 5 mg/mL and 10 µL of SATA (5 mg/mL DMF) per mL of antibody solution is added.
2. After incubation at 25°C for 30 min, the mixture is chromatographed on a column of Sephadex G-25M equilibrated with PBE or PBS.
3. The thioacetylated IgG is collected in the void volume and concentrated to 3–5 mg/mL.
4. Before it is reacted with the toxin, the thioacetylated IgG is deacetylated by treatment with hydroxylamine at pH 7.5 to 100 m*M* final concentration.
5. The number of SH groups introduced into the molecule of IgG is determined as described in **Subheading 3.2.1.**

3.2.3. Introduction of Maleimide Groups (26)

The most frequently used crosslinker for the preparation of ITs is SMCC, commercially available in a water soluble (sulfo) or insoluble form (**Fig. 5**).

1. IgG (1 mL) dissolved in PBE or PBS, pH 7.5, is mixed with 10 µL of SMCC dissolved in DM2F at 10 mg/mL or in PBE (PBS) at 20 mg/mL if sulfo-SMCC is used.
2. The mixture is incubated at 25°C for 1 h and the derivatized IgG is separated from the excess SMCC by gel filtration on Sephadex G-25M equilibrated with PBE or PBS but at lower pH (6.5–7.0).
3. The modified IgG is concentrated to 3–5 mg/mL and stored at 4°C for only a limited period of time because of the slow hydrolysis of the maleimide groups at pHs above 7.0.

3.3. Preparation and Modification of Toxins

The toxins used for the chemical construction of ITs are bRT, RTA in deglycosylated form (dgRTA), two ribosome-inactivatiing proteins (RlPs) (PAP and saporin), and PE. The preparation of some of these toxins is described in **Subheading 3.3.1.** It should be noted that presently almost all plant and bacterial toxins used for the preparation of ITs can also be expressed in recombinant form in *E. coli*.

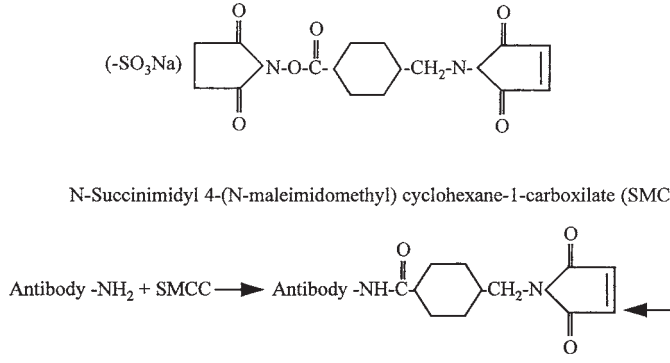

Fig. 5. The structure of SMCC and its reaction with an IgG. The arrow indicates the carbon atom involved in the reaction with the sulfhydryl group of toxins.

3.3.1. RTA and RT

RT is the major protein of the *Ricinus communis* seed. It is composed of two polypeptide chains, RTA and RTB, of approx the same molecular mass (30–32 kDa) linked to each other with a disulfide bond (**Fig. 2**). RTA is an *N* glycosidase, which removes a specific adenine residue from the 28S ribosomal RNA, thereby inhibiting protein synthesis. The RTB chain is a galactose-specific lectin that allows the RT to bind to the cell-surface glycoproteins and glycolipids on virtually all mammalian cells. Both chains also contain carbohydrate moieties, which are responsible, at least in part, for their interaction with the carbobydrate-binding lectins of liver cells. The procedure used in our laboratory for isolation and purification of RT and its RTA chain is as follows (**Fig. 6**).

1. *R. communis* seeds are ground up and extracted repeatedly with acetone.
2. The dry acetone powder is further extracted with PBS, pH 7.5, and the extract is clarified by filtration and centrifugation.
3. The extract is then chromatographed on an acid-treated Sepharose 4B (2 wk at 37°C with 1 *M* propionic acid) column equilibrated with 50 m*M* borate buffer with 50 m*M* NaCl (borate-saline), pH 8.0. This binds to both RT and ricin agglutinin (RCA1) and removes all other seed proteins.
4. RT and RCA1 are eluted with 0.2 *M* galactose in borate-saline buffer and further chromatographed on a 90-cm column of Sephacryl S-200HR equilibrated with 0.2 *M* acetate buffer pH3.5.
5. Two main peaks are obtained, the second of which corresponds to a protein with a molecular mass of 60–62 kDa containing purified RT.

Since ITs with RT can bind to cells through RTB, a method has been developed ***(15,27)*** to block the galactose-binding sites on RTB and to use the blocking molecule as a linker for the binding of RT to the IgG (**Fig. 7**). The blocking

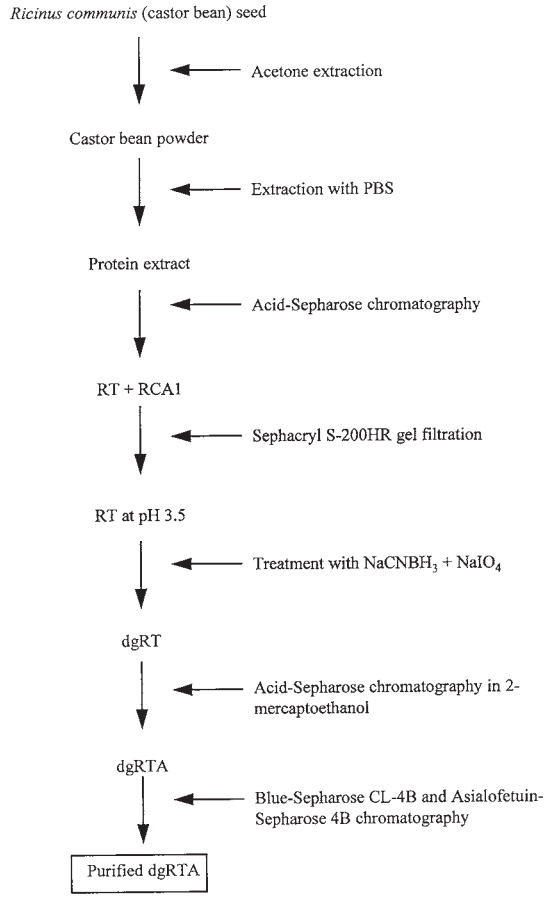

Fig. 6. Flow diagram for the preparation of RT and dgRTA.

molecule contains galactose-rich oligosaccharides derived from chemically modified fetuin. To this end, fetuin is treated with cyanuric chloride to generate an active group able to bind covalently to the RTB chain in the neighborhood of the galactose-binding site (**Fig. 7**) and a disulfide bond susceptible to reduction prior to it reacting with the SMCC-derivatized MAb (*see* **Subheading 3.3.**). Therefore, bRT is bound to the antibody through a stable thioether bond involving only RTB. The RTA is linked to the RTB by the natural disulfide bond that binds these two chains together (**Fig. 2**). The preparation of bRT is as follows ***(27)***:

1. RT (2 mg/mL in 50 m*M* triethanolamine buffer, pH 8.0) is mixed with a fivefold molar excess of the blocking reagent (**Fig. 7**) (for the preparation of blocking reagent; *see* **ref. *27***) and incubated for 24–48 h at 25°C.

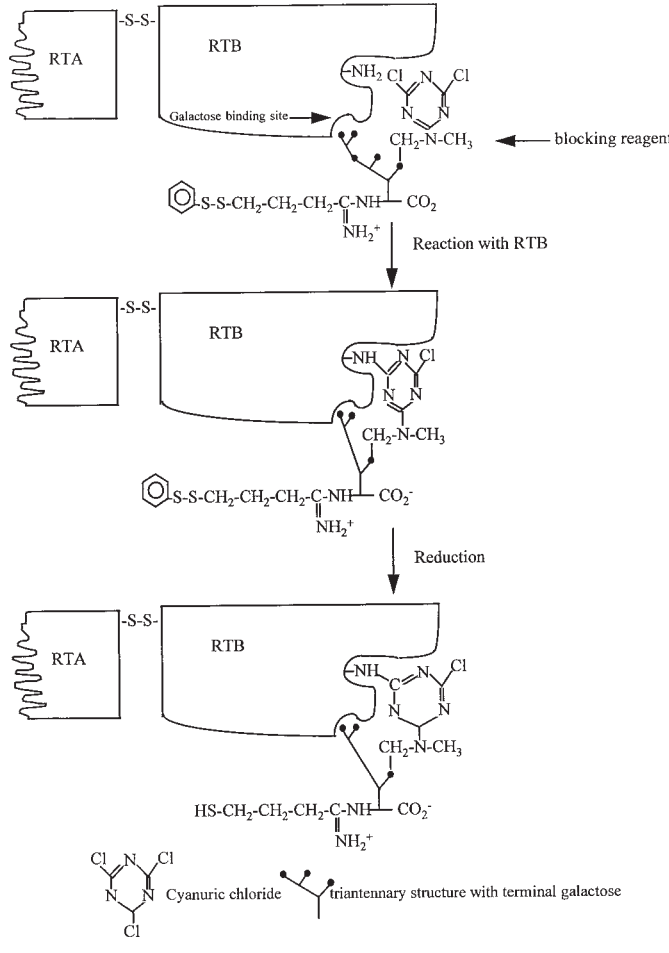

Fig. 7. Reaction of an activated glycopeptide with RT to form bRT (adapted from **ref. *27***).

2. The mixture is then acidified with acetic acid and chromatographed on a Bio-Gel P-60 column (column volume ≥10× sample volume) equilibrated with 0.1 *M* acetic acid containing 0.145 *M* NaCl and 0.25 *M* lactose.
3. The fraction eluted in the void volume is dialyzed against 10 m*M* phosphate buffer, pH 6.8, with 0.145 *M* NaCl and passed successively over two columns, of immobilized lactose and asialofetuin (1 mg bRT/1 mL gel) equilibrated with the abovementioned phosphate buffer.
4. The unbound fractions contain bRT with a molar ratio blocking reagent/bRT of approx 1.

The RTA chain can be obtained from RT using the procedure depicted in **Fig. 5**. RTA contains a complex oligosaccharide unit rich in mannose that is

recognized by the lectin receptor of the reticuloendothelial cells of the liver and spleen and is responsible for the liver toxicity of both RT and RTA ***(28)***. Therefore, deglycosylation of RTA is a procedure that is currently used for the preparation of ITs with RT ***(29,30)***. Deglycosylation is carried out using the whole RT, and the dgRTA is subsequently obtained by reducing the dgRT molecule and separating the dgRTB from the dgRTA. The following procedure is used in our laboratory.

1. A solution of RT at 2.5 mg/mL in 0.2 *M* acetate buffer, pH 3.5 (*see* **Subheading 3.3.1.**) is treated with an equal volume of the deglycosylation agent consisting of a mixture of 80 m*M* sodium cyanoborohydride ($NaCNBH_3$) and 40 m*M* sodium metaperiodate ($NaIO_4$) in the same buffer.
2. The mixture is incubated at 4°C for 4 h and the reaction is stopped by adding glycerol to a final concentration of 1%.
3. The mixture is brought to pH 8.0 with 2 *M* Tris-HCl, and chromatographed on an acid-sepharose 4B column equilibrated with borate-saline buffer (*see* preparation of RT) at 4°C.
4. The column is washed with this buffer until all unbound protein is removed.
5. The column is then eluted with 4% 2-mercaptoethanol (2-ME) in borate-saline buffer until the protein/absorbance at 280 nm increases.
6. The column is then closed and incubated for 4 h. During this time the disulfide bond between the dgRTA and the dgRTB is reduced ***(31)***.
7. The elution is resumed until all the dgRTA is collected.
8. The thiolated dgRTA is loaded onto a Blue-Sepharose CL-4B column equilibrated with borate-saline buffer.
9. The column is washed with borate-saline until all the 2-ME is removed, with 0.2 *M* galactose in borate-saline buffer until dgRTB/dgRT impurities are removed, and with borate-saline buffer until all galactose is removed (determined using the orcinol reaction).
10. The dgRTA bound to the column is eluted with 1 *M* NaCl in borate-saline, then diluted 1:2 with distilled water and affinity-chromatographed on an asialofetuin-Sepharose CL-4B column equilibrated with borate-saline buffer.
11. The unbound protein fraction containing highly purified dgRTA is collected, concentrated to 5 mg/mL, diluted 1:1 with glycerol, and stored at –10°C.

3.3.2. PAP

PAP belongs to a family of enzymes known as ribosome inactivating proteins (RIPs), which exert their inhibitory effects on protein synthesis by specifically removing a single adenine from the 28S ribosomal RNA in the same manner as dgRTA does. PAP is found in the leaves of the pokeweed plant (*Phytolacca americana*) in the form of a single-chain RIP that lacks a cell-binding domain, such as RTB, has a molecular mass of 30 kDa, and is not glycosylated. Therefore, for the production of PAP no dissociation and deglycosylation steps (as for RTA) are necessary. However, PAP as well as the

other single-chain RIPs (saporin, gelonin, and others) lack a free cysteine residue and therefore must have a thiol group introduced by chemical derivatization. The preparation of PAP is as follows ***(32–34)***:

1. Frozen pokeweed leaves are squeezed in a kitchen juicer and the juice is clarified by centrifugation.
2. The supernatant is fractioned using 40 and 100% saturated with ammonium sulfate, and the precipitate is dissolved in 10 m*M* Tris-HCl with 0.1 m*M* 2-ME and 0.2 m*M* Na_2EDTA, pH 7.5, and dialyzed against this buffer.
3. The dialyzed fraction is chromatographed on a DEAE-cellulose column equilibrated with the above buffer and the unbound fraction is collected.
4. This fraction is adjusted to 20 m*M* potassium phosphate, pH 6.0, by the addition of the appropriate volume of 1 *M* potassium phosphate, pH 6.0, and chromatographed on a SP-Sepharose column equilibrated with 20 m*M* phosphate buffer, pH 6.0.
5. The unbound fraction is discarded and a linear gradient of 0–0.5 *M* KCl in the phosphate buffer is used.
6. PAP is eluted as a sharp peak at the start of the gradient (0.12–0.2 *M*).
7. The protein is dialyzed against distilled water and lyophilized.
8. Purified PAP at 10 mg/mL in PBS pH 8.0 is mixed with a threefold molar excess of freshly prepared 2-IT.
9. The mixture is incubated at room temperature for 2 h with gentle rocking and then chromatographed on Sephadex G-25M equilibrated with PBS, pH 7.5.
10. The thiolated PAP eluted in the void volume is collected and concentrated to 3–5 mg/mL. It contains an average of 0.4 reactive thiol groups per molecule of PAP and should be used immediately.

3.3.3. PE ***(10,35,36)***

PE is a single-chain protein with a molecular mass of 66 kDa composed of three distinct domains (**Fig. 2**). In the PE protein, domain I (1–252) binds to the PE receptor on normal animal cells, which has been identified as the α2-macroglobulin receptor. Domain II (253–364) mediates translocation of domain III (400–613) into the cytosol. The translocation domain contains a proteolytic cleavage site within a disulfide loop, which, after proteolytic cleavage, leaves the cell-binding site (I) and translocation domain (II) bound to the catalytic/toxic site (III) by a disulfide bond (**Fig. 2**). Following reduction of this bond in the cytosol, the ADP-ribosylation activity of domain III inactivates elongation factor (EF2) and causes inhibition of protein synthesis and cell death.

PE cannot be used for construction of ITs since its cell-binding domain (I) confers nonspecific toxicity ***(37)***. Deletion of the cell-binding domain has been achieved by cloning truncated DNAs encoding this protein and expressing them in *E. coli*. Many truncated forms of PE have been obtained, free or fused to the

antigen-binding moiety, but only two have been used for the chemical construction of ITs: PE35 (280–613), which does not require intracellular proteolysis for activity, and PE38 (253–613), which does, since it contains the proteolytic cleavage site. In PE35, serine-287 is replaced with cysteine to provide a free sulfhydryl for conjugation. The preparation of these two truncated recombinant PEs is fully described elsewhere ***(38)***. Today, many ITs containing recombinant PEs are obtained as fusion proteins (**Fig. 1B**). The derivatization of PE38 requires SMCC in a 10-fold molar excess ***(39)*** at 25°C, pH 7.4. The mixture is chromatographed on a PD-10 column equilibrated with PBS at pH 7.4. The fraction eluted in the void volume is concentrated to 1 mg/mL and is used for reaction with the thiolated IgG. PE35 containing a free cysteine is reduced with 0.1 m*M* DTT at 25°C and desalted over PD-10 as described in this section.

3.4. Preparation and Purification of ITs

The antibody and toxin components of the IT molecule can be linked together only after chemical activation as described above. There are two possibilities for preparing chemically conjugated ITs:

1. Derivatized IgGs containing disulfide or maleimide group(s) reacted with derivatized toxins containing sulfhydryl groups.
2. Derivatized IgGs containing sulfhydryl groups reacted with derivatized toxins containing disulfide groups or maleimide groups.

The chemical construction of some ITs are presented in **Table 1**. The introduction of SH groups into the IgG is restricted to agents that do not require reduction (e.g., 2-IT or SATA). Reduction of the disulfide groups introduced into the molecule of IgG (e.g., by SPDP or SMPT) also splits the inter- and intrachain disulfide bonds of the IgG, thus decreasing its antigen-binding capacity.

The reaction between an activated IgG and a toxin should proceed at pH 7.5 to generate a disulfide bond and at pH 7.0 to generate a thioether bond. The stringency of the pH is determined by the ratio between the IgG–toxin reaction rate and the rate of their active site decomposition. Another consideration necessary for obtaining good yields of IT is the protein concentration of the IgG and toxin. Concentrations between 3 and 5 mg/mL allow a reaction of relatively short duration (2–4 h) with a good yield.

ITs prepared by chemical methods are not homogeneous products. Because of the stochastic nature of the derivatization, products with various degrees of active group substitutions are produced. Even a highly purified IT preparation devoid of any free IgG or toxin will contain several species of molecules with variable toxin/IgG ratios. Further purification of IgG–toxin conjugates to obtain

Table 1
Chemical Construction of Some Immunotoxins

Mouse monoclonal antibody				Toxin		
Name	Specificity	Activation agent	Active group	Name	Activation agent	Active group
RFB4	CD22	SMPT	-S-S-R	dgRTA	DTT	-SH
HD37	CD19	SMPT	-S-S-R	dgRTA	DTT	-SH
B43	CD19	SPDP	-S-S-R	PAP	2-IT	-SH
RFB4	CD22	2-IT/DTNB	-S-S-R	PE35	DTT	-SH
B4	CD19	SMCC	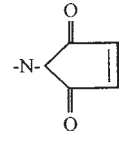	bRT	DTT	-SH
RFB4(Fab')	CD22	DTT	-SH	dgRTA	DTT/DTNB	-S-S-R
RFB4	CD22	2-IT	-SH	PE35	SMCC	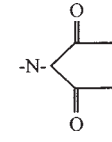

homogeneous products containing only one toxin molecule bound to each molecule of IgG is sometimes possible ***(40,41)*** but, because of the decrease in the yield, has been used infrequently.

3.4.1. ITs Containing RTA

1. IgGs modified by treatment with crosslinkers (SPDP, SMPT) (*see* **Subheading 2.1.**) are reacted with RTdgA (*see* **Subheading 3.1.**) previously treated with 5 m*M* DTT (final concentration) and chromatographed on Sephadex G-25M equilibrated with PBE, pH 7.5. The dgRTA/IgG molar ratio is 2:1.
2. The concentrations of both IgG-MPT and dgRTA-SH are brought to 3–5 mg/mL (after filtration through a 0.22 µm filter) and the mixture is incubated for 24–48 h at 25°C. The purification involves removing the unreacted IgG by affinity chromatography on Blue-Sepharose CL-4B equilibrated with PBE.
3. Both bound IT and the unreacted dgRTA are eluted with 0.5 *M* NaCl in PBE and chromatographed on Sephacryl S-200HR equilibrated with PBS to separate the IT from the dgRTA (**Fig. 8**).

When Fab' fragments are used (*see* **Subheading 1.2.**) the reaction with dgRTA (*see* **Subheading 3.1.**) takes place at 25°C for 2 h at a dgrRTA/Fab' molar ratio of 1:1. The solution becomes yellow as the Fab'-TNB conjugates to

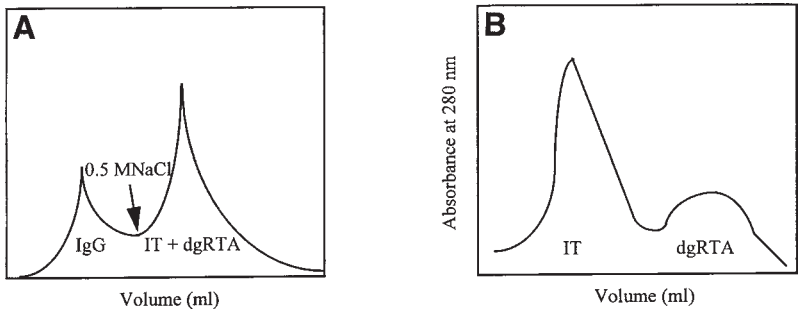

Fig. 8. Purification of RFB4-dgRTA by chromatography on Blue-Sepharose CL-4B **(A)** and Sephacryl S-200HR **(B)**.

the dgRTA-SH (elimination of TNB). The reaction can be monitored by reading the absorbance at 412 nm. When a reading close to 0.5 is reached the reaction is complete. The purification of Fab'-S-S-dgRTA follows the steps indicated above for the IgG-S-S-dgRTA conjugate (Blue-Sepharose Cl-4B and Sephacryl-S-200 HR chromatography).

3.4.2. ITs Containing PAP

Antibodies modified with SPDP (2.5 PDP groups/IgG) are reacted with 2-IT-treated PAP (*see* **Subheading 3.2.**) after excess SPDP and 2-IT are removed by gel filtration on Sephadex G-25M. The PAP /IgG molar ratio is 3:1. After incubation at 25°C for 2 h the mixture is chromatographed on a TSK-3000-SW column (HPLC) or a Sephacryl S-200 HR (gel filtration) column, both equilibrated with 100 m*M* phosphate buffer, pH 6.8. The fractions containing IT and the unreacted IgG are further chromatographed in columns of CM-Sepharose equilibrated in 10 m*M* phosphate buffer, pH 6.2. At this pH all the free IgG is washed out, whereas the bound IT is eluted by increasing the pH to 7.8 and adding 20 m*M* NaCl to the phosphate buffer. The purification scheme is presented in **Fig. 9**.

3.4.3. ITs Containing bRT

The IgG modified with SMCC (*see* **Subheading 2.3.**) and bRT (*see* **Subheading 3.1.**), both dissolved in 50 m*M* phosphate buffer with 50 m*M* NaCl, pH 7.0, are mixed at a bRT/IgG molar ratio of 1:2 and stored at 4°C for 16 h. The B4-bRT conjugate is purified by ion-exchange chromatography on a column of SP-Sepharose equilibrated with 50 m*M* sodium acetate buffer, pH 5.0. The IT and free IgG are eluted with 0.4 *M* sodium chloride and chromatographed on a column of immobilized anti-bRT to remove the free IgG. The conjugate is eluted with 0.1 *M* glycine buffer, pH 2.7, and after

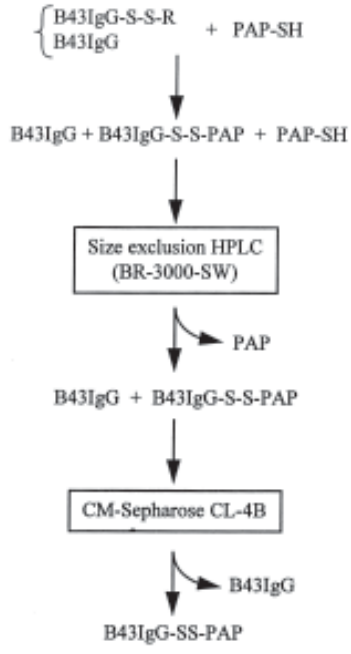

Fig. 9. Purification of a B43-SPDP-PAP IT (adapted from **ref. *34***).

neutralization is further purified by gel-filtration on a Sephacryl S-300 column equilibrated with 10 m*M* potassium phosphate buffer with 0.15 *M* NaCl, pH 7.4.

3.4.4. ITs Containing PE

The IgG modified with 2-IT (*see* **Subheading 2.2.1.**) is mixed with SMCC-treated PE38 (*see* **Subheading 3.3.**), concentrated to 1 mg/mL final concentration and incubated at 25°C for several hours and for 12–16 h at 4°C. Conjugated IgG-S-C-PE38 is passed over a Mono-Q anion exchange column to remove the free IgG and free PE38 from the IT. The conjugate (plus free PE38) is eluted with a NaCl gradient up to 0.5 *M* and the unreacted PE38 is further removed by size-exclusion chromatography on a TSK-3000-SW preparative column (HPLC) equilibrated with PBS at pH 7.4. The preparation is filtered through a 0.22-µm filter and stored frozen at –80°C.

If PE35 is used as the toxin moiety, the IgG modified with 2-IT is further treated with DTNB at a final concentration of 1 m*M* and the excess DTNB is removed by gel filtration on Sephadex G-25M. The Ellmanized IgG is mixed with reduced PE35 (*see* **Subheading 3.3.**) and the mixture is processed as indicated above.

3.5. Analysis of ITs

The components of the IT should be tested for their ability to exert their specific effects at levels comparable to those measured before conjugation. Thus, the IgG moiety of the IT should have the same specificity and antigen-binding capacity as the non-conjugated IgG. Similarly, the toxin moiety of the ITs should exhibit protein synthesis inhibition at the same concentration as the native toxin.

3.5.1. Analysis of Antibody Activity

The antibody activity of the IT is compared to that of the free antibody and the activity of the IT is therefore expressed as a percentage of the activity of the free antibody. The most widely used procedure is to radiolabel both the IT and the antibody and to measure the percentage of binding of both ligands to increasing concentrations of target cells. A procedure used in our laboratory is as follows:

1. Radiolabeling of IT/antibody is accomplished by using the Iodo-Gen method ***(42)***, i.e., adding 0.1 mCi ^{125}INa to 50–100 µg protein and removing the free iodine by gel filtration on Sephadex G-25 Microspin column (Pharmacia).
2. At different cell concentrations of the target cells suspended in medium (e.g., RPMI-1640 with 10% fetal calf serum) ranging from 10^6 to 10^8 cells /mL, a fixed amount of radioligand is added (e.g., 100,000 cpm), and after incubation at 4°C for 1 h and three washings by centrifugation with ice-cold medium, the radioactivity bound to the cells is measured in a gamma-counter.
3. By representing the percentage of bound radioacitvity vs 1/cell concentration, as shown in **Fig. 10**, the maximum percentage of binding for the antibody and the IT, respectively, can be calculated using routine methods that can be found in standard manuals.

3.5.2. Analysis of the Toxin Activity

The toxic activity of the IT in comparison with the toxin used for its construction is measured by evaluating the protein-synthesis inhibiting activity of each in a cell-free rabbit reticulocite assay ***(31)***. The method used in our laboratory is as follows:

1. The IT is reduced with 5 m*M* DTT (1 h at 25°C) to dissociate the dgRTA from the MAb.
2. The sample is diluted to concentrations ranging from 10^{-8} to 10^{-12} *M*.
3. 5 µL of dissociated IT in triplicate (using a 96-well plate) is added to 50 µL of rabbit reticulocyte lysate system, nuclease treated (Promega, Madison, WI) and incubated at 25°C for 20 min.
4. The plate is pulsed with ^{35}S-methionine (3 µCi/well) and incubated for another 40 min.
5. The plate is harvested and the radioactivity is measured in a beta-counter.

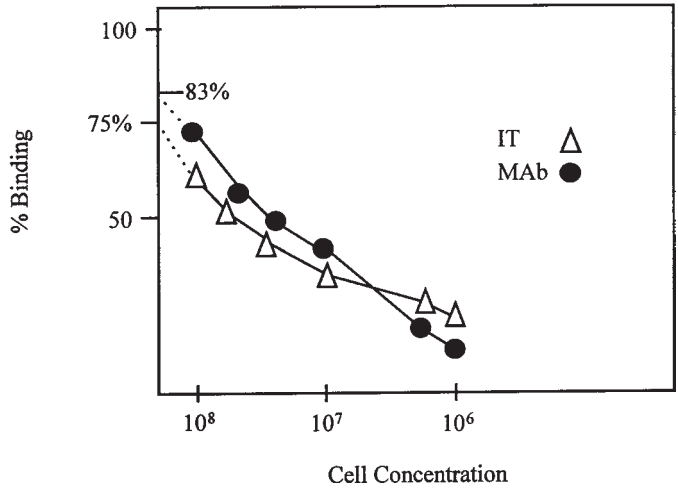

Fig. 10. IT/MAb binding to target cells. IT activity = 75/83 × 100 = 90.3%.

6. The IC_{50} of the IT sample is then compared with that of a dgRTA standard as shown in **Fig. 11**.

3.5.3. Analysis of IT Activity

3.5.3.1. In Vitro

The most important test for evaluating the potency of an IT preparation is its ability to kill an antigen-positive target cell. This is currently measured by the ability of the IT to inhibit the incorporation of ^{3}H-thymidine or ^{3}H-leucine into the target cells ***(29)***. The potency of the IT is defined as the concentration of IT that inhibits 50% of the thymidine/leucine incorporation of untreated cells in a determined interval of time (IC_{50}). The IC_{50} of an acceptable IT should be at least 10^{-10} *M* and at least 1000 times lower than the IC_{50} of the unconjugated toxin on the same target cells (**Fig. 12**) or of the IT on antigen-negative target cells. Moreover, the killing curve should reach values under 5% incorporation at a concentration not more than 100 times higher than the IC_{50} as shown in **Fig. 12**. The method used in our laboratory is as follows:

1. 10^5 cells/20 µL in RPMI-1640 containing 10% fetal calf serum, L-glutamine (100 m*M*), and antibiotics (100 µg/mL streptomicin + 100 U/mL penicillin) are distributed in triplicate in 96-well microtiter plates containing 100 µL medium and concentrations of IT ranging from 10^{-13} to 10^{-7} *M*, and incubated for 24–48 h at 37°C in a 5% CO_2 incubator.
2. The cells are centrifuged and washed twice with leucine-free medium and are resuspended in 200 µL of the same medium.
3. Cells are pulsed for 4 h at 37°C with 5 µCi ^{3}H-leucine.

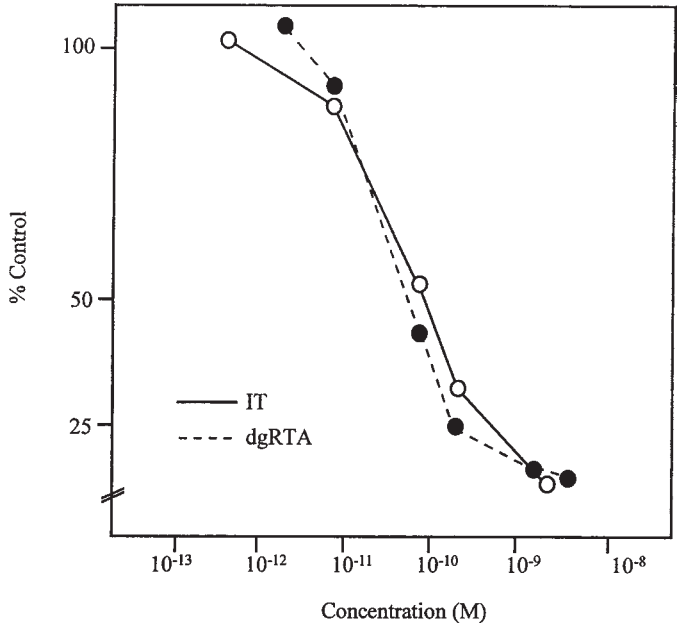

Fig. 11. The inhibition of protein synthesis by RFB4-SMPT-dgRTA and the corresponding dgRTA.

4. Cells are harvested on a Titertek cell harvester and the radioactivity on the filters is counted in a liquid scintillation beta-spectrometer.
5. The percentage reduction in ^{3}H-leucine incorporation as compared with untreated controls is presented as a function of the concentration of the IT and the IC_{50} calculated as indicated in **Fig. 12**.

3.5.3.2. In Vivo

SCID or nude mice with human tumor xenographs are used. SCID mice have been used to study the therapy of disseminated human tumors, whereas nude mice have been used for the study of solid tumors grown subcutaneously.

In our laboratory the curative effect of different ITs in SCID mice with disseminated human lymphomas has been studied and the methods are presented as follows ***(43–45)***:

Cultured lines of human lymphoma cells (e.g., Daudi cells) are injected in the tail vein of SCID mice (5×10^6 cells) (SCID/Daudi mice). After 30–40 d all mice show paralysis of the hind legs just prior to death. The paralysis is associated with the presence of neoplastic nodules within the spinal cord but tumor infiltrates can be observed in lungs, liver, kidney, ovaries, bone marrow, and other organs ***(43)***. The mean paralysis time (MPT) represents an accurate measure-

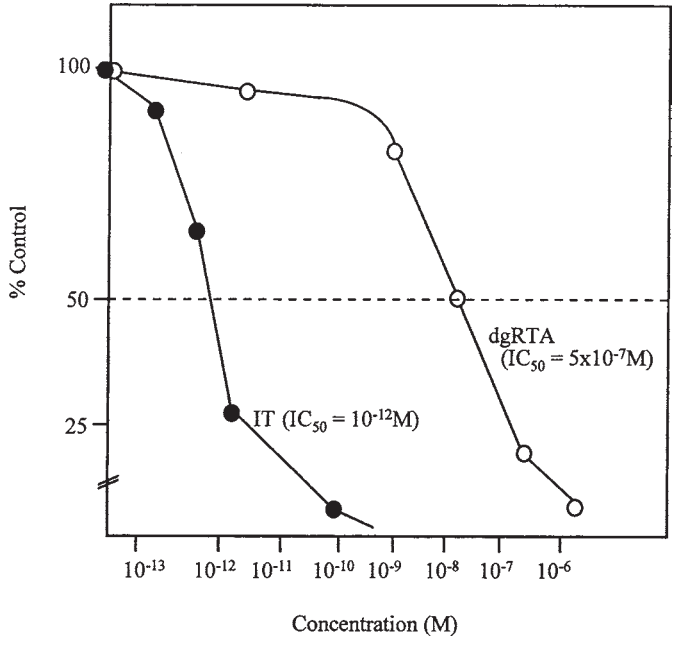

Fig. 12. Evaluation of the in vitro cytotoxicity of ITs.

ment of the antitumor effect following treatment with ITs. Mice injected with tumor cells are treated with ITs immediately after inoculation of the tumor cells or at different intervals of time (<20 d). The regimen might consist of a single dose of IT or several doses administered either daily or at various intervals of time. The effect of two IT constructs in SCID/Daudi mice given 25 µg IT/animal/d by injections on d 1, 2, 3, and 4 after tumor cell inoculation (5×10^6 cells) is presented in **Fig. 13**. The data demonstrate that RFB4-SMPT-dgRTA is more effective in extending the MPT than is HD37-SMPT-dgRTA, but that both ITs significantly prolong the MPT compared with controls treated with saline.

3.5.4. Quality Controls

Each batch of IT prepared for clinical use should pass quality-control tests described in **Table 2** as well as evaluations of purity and sterility. An example of the quality control tests performed on two ITs is presented in **Table 2**.

4. Notes

1. Preparation of the Fab' fragment: Sometimes the Sephacryl S-200HR gel filtration does not completely eliminate the undigested IgG. In these cases an additional affinity chromatography on protein A-Sepharose is performed at neutral pH, collecting the nonbound fraction.

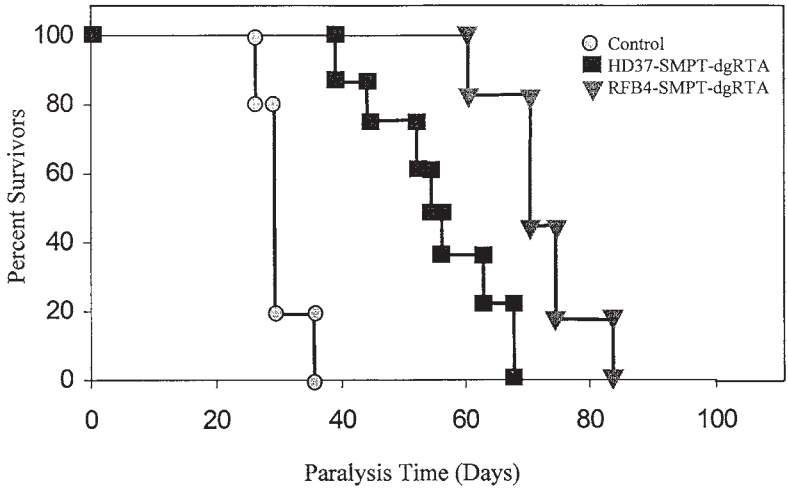

Fig. 13. Effect of two ITs in SCID/Daudi mice.

Table 2
Quality Control Analysis of Purified Anti-CD19 Immunotoxins Containing dgRTA *(23)* and PAP *(34)* Toxins

Parameter	HD37-SMPT-dgRTA	B-43-SPDP-PAP
Antibody activity (% of initial activity)	82.0	76.9
Reticulocyte assay (IC_{50}) (*M*)	6.4×10^{-11}[a]	4.1×10^{-11} *M*[b]
Cell-killing assay (IC_{50})(*M*)	1.0×10^{-11}	$5.5 \times 10–9$ *M*[c]
LD_{50} in mice[d] (μg/mouse)	280	60
Endotoxin (unit/mg)	2.0	0.5
Purity (%)		
180 kDa (ab/toxin = 1:1)	85	56
210 kDa (ab/toxin = 1:2)	15	41

[a]IC_{50} for free RTdgA = 8×10^{-11} *M*.
[b]IC_{50} for free PAP = 1.2×10^{-11} *M*.
[c]Data from **ref. *46***.
[d]Lethal dose for 50% of injected animals.

2. Introduction of disulfide groups: If the antibody solution becomes turbid when treated with the crosslinker dissolved in DMF, the sulfo-derivative should be used dissolved in the conjugation buffer.
3. Introduction of sulfhydryl groups: When 2-IT is used the number of SH groups may be variable depending upon the source of IgG or the "age" of the reagent.

Therefore, a preliminary study on aliquots of IgG using 2-IT in molar excesses of 10–100 should be performed. When SATA is used the deacetylation of the substituted IgG should be performed with a freshly prepared solution of 1 *M* hydroxylamine. Sometimes this solution becomes turbid when the pH is brought to 7.5. This is a sign that the reagent is old and should be changed.

4. Preparation of ITs: The ITs prepared by chemical methods are heterogeneous, comprising conjugates with one, two, or more toxin molecules per molecule of IgG. These conjugates can be evaluated by SDS-PAGE and can be further purified to homogeneity by affinity chromatography on Blue-Sepharose using a NaCl gradient from 0.2 *M* to 1.0 *M* ***(40)***.

Acknowledgments

We thank Ms. C. Self for expert secretarial and graphic work.

References

1. Ghetie, V. and Vitetta, E. S. (1994) Immunotoxins in the therapy of cancer: from bench to clinic. *Pharmacol. Ther.* **63(3),** 209–234.
2. Thrush, G. R., Lark, L. R., and Vitetta, E. S. (1996) Immunotoxins (review), in *Therapeutic Immunology* (Austen, K. F., Burakoff, S. J., Rosen, F. S., and Strom, T. B., eds.), Blackwell Science, Boston, pp. 385–397.
3. Pai, L. H. and Pastan, I. (1993) Immunotoxin therapy for cancer. *JAMA* **269,** 78–81.
4. Frankel, A. E., Tagge, E. P., and Willingham, M. C. (1995) Clinical trials of targeted toxins. *Semin. Cancer Biol.* **6,** 307–317.
5. Ghetie, M. A. and Vitetta, E. S. (1994) Recent developments in immunotoxin therapy. *Curr. Opin. Immunol.* **6,** 707–714.
6. Grossbard, M. and Nadler, L. M. (1994) Immunotoxin therapy of lymphoid neoplasms. *Semin. Hematol.* **31,** 88–97.
7. Wong, S. S. (1991) *Chemistry of Protein Conjugation and Cross-Linking.* CRC, Boca Raton, FL, pp. 267–294.
8. Vitetta, E. S., Thorpe, P. E., and Uhr, J. W. (1993) Immunotoxins: magic bullets or misguided missiles. *Trends Pharmacol. Sci.* **14,** 148–154.
9. Brinkmann, U. and Pastan, I. (1994) Immunotoxins against cancer. *Biochim. Biophys. Acta* **1198,** 27–45.
10. Kreitman, R. J. and Pastan, I. (1994) Recombinant toxins. *Adv. Pharmacol.* **28,** 193–219.
11. Carlsson, J., Drevin, H., and Axen, R. (1978) Protein thiolation and reversible protein–protein conjugation N-succinimidyl 3-(2-pyridyldithio)propionate, a new heterobifunctional reagent. *Biochem. J.* **173(3),** 723–737.
12. Brinkley, M. A. (1992) A survey of methods for preparing protein conjugates with dyes, haptens and crosslinking reagents. *Bioconjug. Chem.* **3,** 2–13.
13. Thorpe, P. E., Wallace, P. M., Knowles, P. P., Relf, M. G., Brown, A. N. F., Watson, G. J., et al. (1988) Improved anti-tumor effects of immunotoxins prepared with deglycosylated ricin A chain and hindered disulfide linkages. *Cancer Res.* **48,** 6396–6403.

14. FitzGerald, D., Idziorek, T., Batra, J. K., Willingham, M., and Pastan, I. (1990) Antitumor activity of a thioether-linked immunotoxin: OVB3-PE. *Bioconjug. Chem.* **1,** 264–268.
15. Lambert, J. M., Goldmacher, V. S., Collinson, A. R., Nadler, L. M., and Blattler, W. A. (1991) An immunotoxin prepared with blocked ricin: a natural plant toxin adapted for therapeutic use. *Cancer Res.* **51,** 6236–6242.
16. Harris, W. J. and Cunningham, C. (1995) *Antibody Therapeutics*. Landis , Austin, TX.
17. Goding, J. W. (1996) *Monoclonal Antibodies: Principles and Practices.* Academic, London, pp. 192–227.
18. Lamoyi, E. and Nisonoff, A. (1983) Preparation of $F(ab')_2$ fragments from mouse IgG of various subclasses. *J. Immunol. Methods* **50,** 234–243.
19. Parham, P. (1983) On the fragmentation of monoclonal IgG_1, IgG_{2a} and IgG_{2b} from BALB/c mice. *J. Immunol.* **131,** 2895–2902.
20. Ghetie, V., Ghetie, M., Uhr, J. W., and Vitetta, E. S. (1988) Large scale preparation of immunotoxins constructed with the Fab' fragment of IgG1 murine monoclonal antibodies and chemically deglycosylated ricin A chain. *J. Immunol. Methods* **112,** 267–277.
21. Thorpe, P. E., Wallace, P. M., Knowles, P. P., Relf, M. G., Brown, A. N. F., Watson, G. J., et al. (1987) New coupling agents for the synthesis of immunotoxins containing a hindered disulfide bond with improved stability in vivo. *Cancer Res.* **47,** 5924–5931.
22. Thorpe, P. E., Blakey, D. C., Brown, A. N., Knowles, P. P., Knyba, R. E., Wallace, P. M., et al. (1987) Comparison of two anti-Thy 1.1-abrin A-chain immunotoxins prepared with different cross-linking agents: antitumor effects, in vivo fate, and tumor cell mutants. *J. Natl. Cancer Inst.* **79,** 1101–1112.
23. Ghetie, V., Thorpe, P. E., Ghetie, M., Knowles, P., Uhr, J. W., and Vitetta, E. S. (1991) The GLP large scale preparation of immunotoxins containing deglycosylated ricin A chain and a hindered disulfide bond. *J. Immunol. Methods* **142,** 223–230.
24. Lambert, J. M., Blattler, W. A., McIntyre, G. D., Goldmacher, V. S., and Scott, C. F., Jr. (1988) Immunotoxins containing single chain ribosome-inactivating proteins, in *Immunotoxins* (Franker, A. E., ed.), Kluwer, Norwell, MA, pp. 175–213.
25. Duncan, R. J., Weston, P. D., and Wrigglesworth, R. (1983) A new reagent which may be used to introduce sulfhydryl groups into proteins, and its use in the preparation of conjugates for immunoassay. *Anal. Biochem.* **132,** 68–73.
26. Hashida, S., Imagawa, M., Inque, S., Ruan, K. H., and Ishikawa, E. (1983) More useful maleimide compounds for the conjugation of Fab to horseradish peroxidase through thiol groups in the hinge. *J. Appl. Biochem.* **6,** 56–63.
27. Lambert, J. M., McIntyre, G., Gauthier, M. N., Zullo, D., Rao, V., Steeves, R. M., et al. (1997) The galactose-binding sites of the cytotoxic lectin ricin can be chemically blocked in high yield with reactive ligands prepared by chemical modification of glycopeptides containing triantennary N-linked oligosaccharides. *Biochemistry* **30,** 3234–3247.
28. Thorpe, P. E., Detre, S. I., Foxwell, B. M. J., Brown, A. N. F., Skilleter, D. N., Wilson, G., et al. (1985) Modification of the carbohydrate in ricin with

metaperiodate-cyanoborohydride mixtures. Effects on toxicity and in vivo distribution. *Eur. J. Biochem.* **147,** 197–206.
29. Ghetie, M., May, R. D., Till, M., Uhr, J. W., Ghetie, V., Knowles, P. P., et al. (1988) Evaluation of ricin A chain-containing immunotoxins directed against CD19 and CD22 antigens on normal and malignant human B-cells as potential reagents for in vivo therapy. *Cancer Res.* **48,** 2610–2617.
30. Ghetie, V., Till, M. A., Ghetie, M., Tucker, T., Porter, J., Patzer, E. J., et al. (1990) Preparation and characterization of conjugates of recombinant CD4 and deglycosylated ricin A chain using different cross-linkers. *Bioconjug Chem.* **1,** 24–31.
31. Fulton, R. J., Blakey, D. C., Knowles, P. P., Uhr, J. W., Thorpe, P. E., and Vitetta, E. S. (1986) Production of ricin A_1, A_2, and B chains and characterization of their toxicity. *J. Biol. Chem.* **261,** 5314–5319.
32. Irvin, J. D. (1983) Pokeweed antiviral protein. *Pharmacol. Ther.* **21,** 371–387.
33. Irvin, J. D. and Uckun, F. M. (1997) Pokeweed antiviral protein: Ribosome inactivation and therapeutic applications. *Pharmacol. Ther.* **55,** 279–302.
34. Myers, D. E., Irvin, J. D., Smith, R. S., Kuebelbeck, V. M., and Uckun, F. M. (1991) Production of a pokeweed antiviral protein (PAP)-containing immunotoxin, B43-PAP, directed against the CD19 human B lineage lymphoid differentiation antigen in highly purified form for human clinical trials. *J. Immunol. Methods* **136,** 221–237.
35. Ogata, M., Chaudhary, V. K., Pastan, I., and Fitzgerald, D. J. (1997) Processing of pseudomonas exotoxin by a cellular protease results in the generation of a 37,000-Da toxin fragment that is translocated to the cytosol. *J. Biol. Chem.* **265,** 20,678–20,685.
36. Allured, V. S., Collier, R. J., Carroll, S. F., and McKay, D. B. (1986) Structure of exotoxin A of Pseudomonas aeruginosa at 3.0-Angstrom resolution. *Proc. Natl. Acad. Sci. USA* **83,** 1320–1324.
37. Hwang, J., FitzGerald, D. J., Adhya, S., and Pastan, I. (1987) Functional domains of Pseudomonas exotoxin identified by deletion analysis of the gene expressed in E. coli. *Cell* **48,** 129–136.
38. Kreitman, R. J., Hansen, H. J., Jones, A. L., FitzGerald, D. J. P., Goldenberg, D. M., and Pastan, I. (1993) Pseudomonas exotoxin-based immunotoxins containing the antibody LL2 or LL2-Fab' induce regression of subcutaneous human B-cell lymphoma in mice. *Cancer Res.* **53,** 819–825.
39. Mansfield, E., Pastan, I., FitzGerald, D. J. (1996) Characterization of RFB4—*Pseudomonas* exotoxin A immunotoxins targeted to CD22 on B-cell malignancies. *Bioconjug. Chem.* **7,** 557–563.
40. Ghetie, V., Swindell, E., Uhr, J. W., and Vitetta, E. S. (1993) Purification and properties of immunotoxins containing one vs two deglycosylated ricin A chain. *J. Immunol. Methods* **166,** 117–122.
41. Ghetie, V., Engert, A., Schnell, R., and Vitetta, E. S. (1995) The *in vivo* anti-tumor activity of immunotoxins containing two vs one deglycosylated ricin A chains. *Cancer Lett.* **98(1),** 97–101.

42. Fraker, P. J. and Speck, J. C., Jr. (1978) Protein and cell membrane iodinations with a sparingly soluble chloramide, 1,3,4,6-tetrachloro-3a,6a-diphenylglycoluril. *Biochem. Biophys. Res. Commun.* **80,** 849–857.
43. Ghetie, M. A., Richardson, J., Tucker, T., Jones, D., Uhr, J. W., and Vitetta, E. S. (1990) Disseminated or localized growth of a human B-cell tumor (Daudi) in SCID mice. *Int. Cancer* **45,** 481–485.
44. Ghetie, M. A., Richardson, J., Tucker, T., Jones, D., Uhr, J. W., and Vitetta, E. S. (1991) Antitumor activity of Fab' and IgG-anti-CD22 immunotoxins in disseminated human B lymphomas grown in mice with severe combined immunodeficiency disease: effect on tumor cells in extranodal sites. *Cancer Res.* **51,** 5876–5880.
45. Ghetie, M. A., Tucker, K., Richardson, J., Uhr, J. W., and Vitetta, E. S. (1992) The antitumor activity of an anti-CD22 immunotoxin in SCID mice with disseminated Daudi lymphoma is enhanced by either an anti-CD19 antibody or an anti-CD 19 immunotoxin. *Blood* **80,** 2315–2320.
46. Uckun, F. M., Ramakrishnan, S., and Houston, L. L. (1985) Immunotoxin-mediated elimination of clonogenic tumor cells in the presence of human bone marrow. *J. Immunol.* **134,** 2010–2016.

2

Construction of Ribonuclease–Antibody Conjugates for Selective Cytotoxicity

Dianne L. Newton and Susanna M. Rybak

1. Introduction

Immunotoxins based on human and humanized ribonuclease may have potential for cancer therapy while exhibiting less toxic side effects and stimulating less of an immune response in humans than immunotoxins based on plant and bacterial toxins ***(1)***. Both recombinant RNase fusion proteins (***2–4***; *see also* Chapter 6, this volume) and chemical RNase conjugates have been made and characterized. The cytotoxic potential of targeted ribonuclease was first demonstrated with bovine RNase conjugated to transferrin or an antibody directed against the human transferrin receptor ***(5)***. Antibody RNase conjugates have also been shown to have potent anti-tumor activity against human glioma cells in athymic mice ***(6)*** and to enhance the activity of vincristine in mdr1 multidrug-resistant colon cancer cells in vitro and in vivo ***(7)***. Recently, RNase chemically conjugated to an antibody against CD22 was found to specifically kill Daudi lymphoma cells in cell culture at picomolar concentrations (IC_{50}, 10–50 p*M*) and to exhibit potent antitumor activity in SCID mice with disseminated Daudi lymphoma (unpublished data). Methods for linking RNase to specific cell binding ligands are described.

2. Materials

2.1. Derivatization of RNase

1. RNase solution containing 3.2 mg at a concentration ≥3.2 mg/mL.
2. PD-10 columns (Sephadex G-25M) (Pharmacia LKB Biotechnology Inc., Piscataway, NJ).
3. Conjugation buffer: 84 mL 0.2 *M* Na_2HPO_4 (35.6 g/L Na_2HPO_4-$2H_2O$), 16 mL 0.2 *M* NaH_2PO_4 (27.6 g/L NaH_2PO_4-H_2O), 1.17 g NaCl + 100 mL H_2O (solution should be pH 7.5).

From: *Methods in Molecular Medicine, Vol. 25: Drug Targeting: Strategies, Principles, and Applications*
Edited by: G. E. Francis and C. Delgado

4. Centricon 3 and 30 microconcentrators (Amicon Inc., Beverly, MA).
5. *N*-Succinimidyl 3-(2-pyridyldithio) propionate (SPDP) (Pierce Chemical Co., Rockford, IL). Store over Drierite at 4°C.

2.2. Derivatization of Antibody for Disulfide Linkage

1. Antibody (2 mg) at a concentration ≥4 mg/mL.
2. 2-Iminothiolane (2-IT) (Pierce Chemical Co.). Store over Drierite at 4°C.
3. 0.78 *M* sodium borate buffer, pH 8.5: 29.8 g $Na_2B_4O_7 \cdot 10\ H_2O$. Adjust pH to 8.5 with 1 *M* NaOH and make up to a final volume of 0.1 L in distilled H_2O.
4. 5,5'dithiobis(2-nitrobenzoic acid) (DTNB) (Sigma, St. Louis, MO).

2.3. Derivatization of Antibody for Thioether Linkage

1. Dimethylformamide (DMF) (Sequenal grade, Pierce Chemical Co.). Store in vacuum desiccator over Drierite at 23°C.
2. *m*-Maleimidobenzoyl-*N*-hydroxysuccinimide ester (MBS) (Pierce Chemical Co.).

2.4. Conjugation of RNase to Antibody via a Disulfide Linkage

1. Dithiothreitol (DTT) (Sigma).

2.5. Conjugation of RNase to Antibody via a Thioether Linkage

1. 0.1 *M* sodium acetate, pH 4.5, containing 0.1 *M* NaCl; 2.72 g $CH_3COONa \cdot 3H_2O$; and 1.17 g NaCl, adjust to pH 4.5 with concentrated acetic acid. Adjust volume to 200 mL with distilled H_2O.

2.6. Purification of RNase–Antibody Mixture

1. High performance liquid chromatographic (HPLC) system equipped with a suitable high pressure pump, ultraviolet monitoring at 215 nm and a fraction collector.
2. Toyo Soda TSK 3000SW column, 7.5 × 600 mm (Toso Haas Corp., Montgomeryville, PA).
3. HPLC buffer: 0.1 *M* phosphate buffer, pH 7.5: 405 mL 0.2 *M* Na_2HPO_4 + 95 mL NaH_2PO_4 + 500 mL H_2O (*see* **Subheading 2.1., item 3** for formula of 0.2 *M* Na_2HPO_4 and 0.2 *M* NaH_2PO_4).
4. 4–20% sodium dodecyl (SDS)-polyacrylamide gels.

3. Methods

3.1. Derivatization of RNase

1. Apply the RNase solution (3.2–4.0 mg total in a volume ≤1.0 mL) to a PD-10 column equilibrated with conjugation buffer. Collect 0.5 mL fractions, read the absorbance at 280 nm, and pool the peak tubes (total volume 1.5–2.0 mL) (*see* **Note 1**).
2. Determine the concentration of the pooled RNase solution by measuring the optical density of the solution at 280 nm and using the appropriate extinction coefficient.

3. Concentrate the pooled RNase solution to 0.5 mL using a Centricon P-3 microconcentrator. Determine the final volume and concentration of the solution as described in **step 2** (*see* **Note 2**).
4. Prepare a fresh solution of SPDP at 20 µmol/mL in absolute ethanol (*see* **Note 3**).
5. To 3.2 mg RNase solution (a total of 0.23 µmol) (volume ≤0.5 mL) add 29 µL SPDP solution (a total of 0.58 µmol or a 2.5-fold molar excess of SPDP). Incubate the mixture for 30 min at room temperature (*see* **Note 4**).
6. Apply the mixture to a PD-10 column that has been equilibrated with the conjugation buffer to remove excess SPDP. Collect 0.5 mL fractions, read the absorbance at 280 nm, and pool the peak tubes (total volume 1.5–2.0 mL).
7. Remove 50 µL of the pooled modified RNase and determine the degree of substitution (mol of 2-pyridyl disulfide/mol RNase) (*see* **Note 5**).
8. Concentrate the remaining pooled derivatized RNase to 0.5 mL as described in **step 3** and store at 4ºC until needed for the reaction (*see* **Note 6**).

3.2. Derivatization of Antibody for Disulfide Linkage

1. Apply the antibody solution (2.5–3.0 mg total) to a PD-10 column equilibrated with conjugation buffer to remove any low-mol-wt materials that may interfere with the reaction. Collect 0.5-mL fractions, read the absorbance at 280 nm, and pool the peak tubes (total volume 1.5–2.0 mL) (*see* **Note 1**).
2. The concentration of the antibody solution should be at least 4 mg/mL. Concentration by Centricon P30 microconcentrator may be required to achieve this (*see* **Note 7**).
3. Just before use, prepare a stock 2-IT solution at 30 m*M* in 0.85 *M* borate buffer, pH 8.5, and DTNB at 10 m*M* in 0.1 *M* Tris, pH 8.0 (*see* **Note 8**).
4. Incubate 2 mg antibody (12.5 nmol) with 250 nmol 2-IT (20-fold molar excess) and 2.5 m*M* DTNB (final concentration) in 100 m*M* sodium borate, pH 8.5 at room temperature for 1 h in a final volume ≤0.5 mL (*see* **Notes 9** and **10**).
5. Apply the reaction mixture to a PD-10 column equilibrated with conjugation buffer to remove the excess 2-IT and DTNB. Collect 0.5-mL aliquots, determine the absorbance at 280 nm, and pool the peak fractions (total volume, 1.5–2.0 mL).

3.3. Derivatization of Antibody for Thioether Linkage

1. Apply the antibody solution (2.5–3.0 mg total) to a PD-10 column equilibrated with conjugation buffer to remove any low-mol-wt materials that may interfere with the reaction. Collect 0.5-mL fractions, read the absorbance at 280 nm, and pool the peak tubes (total volume 1.5–2.0 mL) (*see* **Note 1**).
2. The concentration of the antibody solution should be at least 4 mg/mL. Concentration by Centricon P30 microconcentrator may be required to achieve this (*see* **Note 7**).
3. Prepare a 30-m*M* solution of MBS in dry DMF just before use (*see* **Note 11**).
4. To 2 mg antibody (12.5 nmol) add 62.5 nmol MBS (fivefold molar excess).
5. Incubate at room temperature for 10 min.

6. Apply the reaction mixture to a PD-10 column equilibrated with conjugation buffer to remove excess MBS. Collect 0.5-mL fractions, read the absorbance at 280 nm, and pool the peak tubes (total volume 1.5–2.0 mL) (*see* **Note 12**).

3.4. Conjugation of RNase to Antibody via a Disulfide Linkage

1. Incubate the RNase-2-pyridyl disulfide derivative with 2 mM DTT (final concentration) for 1 h at room temperature to reduce the 2-pyridyl disulfide bond (*see* **Note 13**).
2. To remove excess DTT, apply the reduced RNase solution to a PD-10 column equilibrated with conjugation buffer. Collect 0.5-mL aliquots, determine absorbance at 280 nm, and pool the peak fractions (1.5–2.0 mL) (*see* **Note 14**).
3. Add the RNase solution, which now contains a free sulfhydryl group, to the modified antibody solution. Incubate at room temperature overnight or until the reaction has gone to completion (*see* **Note 15**). The RNase should be present at least as a 10-fold molar excess over antibody (*see* **Note 16**).

3.5. Conjugation of RNase to Antibody via a Thioether Linkage

1. Dialyze the SPDP-RNase against 0.1 *M* sodium acetate, pH 4.5, containing 0.1 *M* NaCl (*see* **Note 17**).
2. Add 0.5 *M* DTT to the SPDP-RNase in acetate buffer **(step 1)** to a final concentration of 25 m*M*. Incubate at room temperature for 30 min (*see* **Note 18**).
3. Apply the mixture to a PD-10 column equilibrated with conjugation buffer to separate the thiolated protein from the low-mol-wt material (*see* **Note 19**).
4. Add the thiolated RNase to the MBS-treated antibody and incubate at 4°C overnight (*see* **Note 20**). The RNase should be at least in a 10-fold molar excess over antibody (*see* **Note 16**).

3.6. Purification of RNase–Antibody Mixture

1. The reaction mixture is chromatographed on a Toyo Soda TSK 3000 SW column (7.5 × 600 mm) equilibrated in 100 m*M* phosphate buffer, pH 7.5, at 0.5 mL/min (*see* **Note 21**).
2. Collect 1 min fractions and determine the absorbance at 280 nm.
3. Several peaks will be observed in addition to the RNase–antibody conjugate (*see* **Note 22**). The predominant peak (retention time of 27–31 min) represents RNase–antibody conjugate (also some free antibody if the reaction did not go to completion; retention time, 31 min) (*see* **Note 23**) and that at 41–42 min represents SPDP-RNase. Pool the RNase–antibody conjugate (*see* **Note 24**).
4. The yield of conjugate is variable ranging from 30–60%. This will depend on how much of the very-high-mol-wt material is formed, the antibody, the ability of the antibody/RNase/conjugate to be concentrated, as well as the various reaction times and temperatures (*see* **Note 25**).
5. Determine the level of substitution by running a sample of the pooled RNase–antibody conjugate on an SDS-polyacrylamide reducing gel and comparing the density of the bands of the RNase and the heavy and light chains of the antibody with a standard curve of known concentrations of RNase and antibody.

4. Notes

4.1. Derivatization of RNase

1. It is advisable to chromatograph the RNase and antibody on a PD-10 column before use to remove any low-mol-wt materials that may interfere with the reaction between the RNase and SPDP or the antibody and 2-IT. Since SPDP and 2-IT react with free amino groups, the choice of buffer is also important. If the proteins are stable to dialysis, they may also be dialyzed against the conjugation buffer. Dialysis may be preferred over gel filtration since it will eliminate the need to concentrate the protein, as described in **Subheading 3.1., step 3** (*see* **Note 2**).
2. For some RNases, especially recombinant RNases, there can be a large loss of protein after concentration with a Centricon microconcentrator. Other methods of concentration, such as Diaflo ultrafiltration (Amicon Inc.) using a YM3 membrane, have not been successful in these cases. This concentration step can be avoided by either dialyzing as described in **Note 1** or by starting with more material, such as 1 mL of a 10–20 mg/mL RNase solution. The final protein concentration should be 6.4 mg/mL.
3. SPDP is a heterobifunctional cleavable crosslinker containing a *N*-hydroxysuccinimde residue and a pyridyl disulfide residue to react with primary amines and sulfhydryls, respectively ***(8)***. SPDP is stable as a solution in ethanol at room temperature as long as it is kept free of moisture; thus a 20-m*M* solution may be prepared and used for several days. The powder form of SPDP should be stored surrounded by silica gel (or another drying agent) because it is very unstable in water.
4. The ratio of SPDP to RNase (2.5 mol SPDP/mol RNase) consistently results in 0.9–1.1 mol 2-pyridyl disulfide groups/mol RNase for such RNases as bovine pancreatic RNase A ***(6)***, EDN (unpublished observations), human pancreatic RNase (unpublished observations), and Onconase ***(9,10)***. A higher level of substitution may result in complete inactivation of the protein or in multiples of antibody conjugated to the RNase.
5. To calculate the level of substitution of the RNase ***(8)***, remove 50 µL from the pooled derivatized RNase solution and adjust the volume to 0.5 mL with conjugation buffer. Determine the concentration of the modified RNase by measuring the optical density at 280 nm. Since the 2-pyridyl disulfide group also absorbs at 280 nm (molar extinction coefficient, 5.1×10^3 at 280 nm), its contribution to the optical density should be taken into account as follows; concentration of pyridine-2-thione $\times$ 5100 = A_{280} nm resulting from pyridine-2-thione. Add 25 µL of freshly prepared 50 m*M* DTT to the diluted RNase tube and determine the optical density at 343 nm. The mols of pyridine-2-thione released upon reduction can be calculated using the molar extinction coefficient for pyridine-2-thione at 343 nm (8.08×10^3). Do not recombine this sample with the original substituted RNase pool.
6. The SPDP-modified RNase is stable at 4°C for at least 1 wk.

4.2. Derivatization of Antibody for Disulfide Linkage

7. Applying more of a more concentrated solution of antibody will eliminate the need for this concentration step, i.e., 1 mL of 10 mg/mL solution.

8. 2-IT reacts with primary amines to introduce a sulfhydryl residue. It is stable in solution at acidic to neutral pH ***(11)***.
9. Before beginning a preparative conjugation, the optimal ratio of 2-IT to antibody should be determined. A pilot study in which the ratio of 2-IT to antibody varies between 10 and 40 mol 2-IT to 1 mol antibody should be performed and the reaction analyzed by HPLC as described in **Subheading 3.6.** The reaction conditions should be adjusted such that there is little remaining unreacted antibody and the level of high-mol-wt species of conjugate is minimal.
10. DTNB is employed in concert with 2-IT for three reasons: The number of thiol groups introduced onto the antibody can be followed by monitoring the absorbance at 412 nm (*see* **Note 15**), the 5-thio-2-nitrobenzoic acid is a very good leaving group in the formation of a disulfide linkage between the antibody and RNase, and the reaction between the antibody and RNase can be quantitated by following the absorbance at 412 nm (*see* **Note 15**) ***(12)***.

4.3. Derivatization of Antibody for Thioether Linkage

11. At a pH above neutrality, MBS hydrolyzes to maleamic acid and thus should be prepared just before use ***(13)***.
12. Studies by Liu et al. ***(13)*** show that the maleimide group on the protein is not stable at neutral pH. Also, the maleimide group reacts with both amino groups and sulfhydryl groups on the same or different molecules leading to dimerization/multimerization. Therefore, both the RNase and antibody should be prepared simultaneously so that both solutions are ready to be mixed immediately.

4.4. Conjugation of RNase to Antibody via a Disulfide Linkage

13. The disulfide bonds of the RNase are not affected by this concentration of DTT (2.0 m*M*) ***(14)***. If the RNase is stable to dialysis and concentration, the 2-pyridyl disulfide bond can be reduced under acidic conditions. At pH 4.5, the reduction of the protein-2-pyridyl disulfide is very specific. At this pH, the 2-thio-pyridine is a good leaving group ***(8)***. To perform the reduction under acidic conditions, follow **steps 1–3** in **Subheading 3.5.**
14. Do not let this reaction sit or the free sulfhydryl groups will interact with each other and form RNase dimers ***(8)***.
15. Follow the reaction between the RNase and antibody by observing the appearance of thionitrobenzoate (TNB) ***(12)***. TNB is released from the antibody as disulfide bonds between the RNase and antibody are formed. This can be observed spectrophotometrically at 412 nm using the molar extinction coefficient of TNB of 13,600. By comparing the number of mols of TNB released with the number of mols of antibody, the number of mols of RNase conjugated per mol of antibody can be determined.
16. The reaction must be driven to completion by a large excess of RNase, because it is very difficult to separate free unconjugated antibody from the RNase–antibody conjugate. The molecular weights of free antibody (160,000 kDa) and RNase-modified antibody differ only by 10–30 kDa (170,000–200,000 kDa) resulting in

retention times on the sizing column that differ by <1 min. Therefore, to minimize the interference that may result from any unreacted antibody, the reaction is driven to completion by a large excess of SPDP-modified RNase.

4.5. Conjugation of RNase to Antibody via a Thioether Linkage

17. The buffer may be exchanged by PD-10 chromatography on a column pre-equilibrated with 0.1 *M* sodium acetate, pH 4.5, containing 0.1 *M* NaCl. Before it can be used, the volume must be concentrated to 0.5 mL using a Centricon P3 microconcentrator. Another method of exchanging buffer is to dilute the SPDP modified-RNase with the sodium acetate buffer and concentrate via the Centricon P3 microconcentrator. Repeating this step several times will result in an exchange of buffers (*see* **Note 2**).
18. Reduction in the presence of acid pH will result in the reduction of the 2-pyridyl disulfide bond without affecting the disulfide bonds of the native protein.
19. The protein should be stored in the pyridyl disulfide-modified form until just before use. The thiol group is very reactive and unwanted conjugations will result if the thiol form is allowed to remain for any length of time in the absence of the antibody ***(8)***.
20. Incubation should be at 4°C because maleimide residues hydrolyze more slowly at lower temperatures.

4.6. Purification of RNase–Antibody Mixture

21. The reaction may be concentrated with a Centricon P30 microconcentrator before application to the sizing column to reduce the number of chromatographic columns that must be performed. Before concentration, however, an analytical run of the reaction before and after concentration should be performed to ensure that the concentration step does not result in an increase of higher-mol-wt aggregates. We find that some RNase–antibody conjugates can not be concentrated without a loss (in some cases up to 50%) of conjugate.
22. There may be some peaks appearing at the void volume of the column (19 min) and at 21–23 min. The material eluting at these retention times most likely includes multimers of at least two molecules of antibody and an unknown number of RNase molecules. This material should not be included in the pool of RNase–antibody conjugate.
23. Because there is such a small difference in molecular weight between unconjugated antibody (160,000) and conjugate (170,000–200,000), the conjugates are not cleanly separated from unconjugated antibody. When pooling the conjugate, pool narrowly on the downside of the peak in order to minimize any further contamination of the conjugate with free antibody. Similar results have been noted by Lambert and Blattler for antibody–gelonin conjugates ***(15)*** and Myers et al. for antibody–pokeweed antiviral protein ***(16)***. If the level of free antibody present in the conjugate solution interferes with the activity of the conjugate, several methods for further purification of the conjugate are described ***(15,16)***. RNases are very basic proteins ***(17)*** and therefore bind to CM Sephadex

C-50. In contrast to free RNase, at neutrality the RNase conjugates will not adhere to this resin. Decreasing the ionic strength and altering the pH of the conjugate to 5.0 allows some RNase conjugates to bind to CM-Sephadex C-50 while the unconjugated antibody passes through the column. The RNase conjugate can then be eluted by increasing the pH to 7.8 and increasing the NaCl concentration to 0.5 *M* (unpublished observation).

24. At this stage, the pooled RNase–antibody reaction may be concentrated on a Centricon P30 microconcentrator, however, the conjugate should be concentrated with caution because some RNase–antibody reactions will result in as much as a 50% loss of material as a result of aggregation.
25. To sterilize the RNase conjugate, use Millipore Millex-HV (Millipore Products Division, Bedford, MA) filters.

Abbreviations

SPDP, *N*-Succinimidyl 3-(2-pyridyldithio) propionate; 2-IT, 2-iminothiolane; DTNB, 5,5'dithiobis(2-nitrobenzoic acid); DMF, dimethlformamide; MBS, *m*-maleimidobenzoyl-*N*-hydroxysuccinimide ester; DTT, dithiothreitol.

References

1. Rybak, S. M., Newton, D. L., and Xue, Y. (1995) RNase and RNase immunofusions for cancer therapy. *Tumor Target.* **1,** 141–147.
2. Rybak, S. M., Hoogenboom, H. R., Meade, H., Raus, J. C. M., Schwartz, D., and Youle, R. J. (1992) Humanization of immuntoxins. *Proc. Natl. Acad. Sci. USA* **89,** 3165–3169.
3. Newton, D. L., Nicholls, P. J., Rybak, S. M., and Youle, R. J. (1994) Expression and characterization of recombinant human eosinophil-derived neurotoxin anti-transferrin sFv. *J. Biol. Chem.* **269,** 26,739–26,745.
4. Newton, D. L., Xue, Y., Olsen, K. A., Fett, J. W., and Rybak, S. M. (1996) Angiogenin single-chain immunofusions: influence of peptide linkers and spacers between fusion protein domains. *Biochemistry* **35,** 545–553.
5. Rybak, S. M., Saxena, S. K., Ackerman, E. J., and Youle, R. J. (1991) Cytotoxic potential of RNase and RNase hybrid proteins. *J. Biol. Chem.* **266,** 21,202–21,207.
6. Newton, D. L., Ilercil, O., Laske, D. W., Oldfield, E., Rybak, S. M., and Youle, R. J. (1992) Cytotoxic ribonuclease chimeras: targeted tumoricidal activity *in vitro* and *in vivo*. *J. Biol. Chem.* **267,** 19,572–19,578.
7. Rybak, S. M., Pearson, J. W., Fogler, W. F., Volker, K., Spence, S. E., Newton, D. L., Mikulski, S. M., Ardelt, W., Riggs, C. W., Kung, H. F., and Longo, D. L. (1996) Enhancement of vincristine cytotoxicity in drug-resistant cell by simultaneous treatment with Onconase, an anti-tumor ribonuclease. *J. Natl. Cancer Inst.* **88,** 747–753.
8. Carlsson, J., Drevin, H., and Axen, R. (1978) Protein thiolation and reversible protein–protein conjugation. *Biochem. J.* **173,** 723–737.
9. Rybak, S. M., Newton, D. L., Mikulski, S. M., Viera, A., and Youle, R. J. (1993) Cytotoxic Onconase and ribonuclease A chimeras: comparison and *in vitro* characterization. *Drug Delivery* **1,** 3–10.

10. Newton, D. L., Pearson, J. W., Xue, Y., Smith, M. R., Fogler, W. E., Mikulski, S. M., Alvord, W. G., Kung, H. F., Longo, D. L., and Rybak, S. M. (1996) Antitumor ribonuclease combined with or conjugated to monoclonal antibody MRK16, overcomes multidrug resistance to vincristine in vitro and in vivo. *Int. J. Oncol.* **8,** 1095–1104.
11. Jue, R., Lambert, J. M., Pierce, L. R., and Traut, R. R. (1978) Addition of sulfhydryl groups to *Escherichia coli* ribosomes by protein modification with 2-iminothiolane (methyl 4-mercaptobutyrimidate). *Biochemistry* **17,** 5399–5405.
12. Riddles, P., Blakeley, R., and Zerner, B. (1983) Reassessment of Ellman's reagent. *Methods Enzymol.* **91,** 49–60.
13. Liu, F. T., Zinnecker, M., Hamaoka, T., and Katz, D. H. (1979) New procedures for preparation and isolation of conjugates of proteins and a synthetic copolymer of D-amino acids and immunochemical characterization of such conjugates. *Biochemistry* **18,** 690–697.
14. Wearne, S. and Creighton, T. (1988) Further experimental studies of the disulfide folding transition of Ribonuclease A. *Prot. Struct. Funct. Genet.* **4,** 251–261.
15. Lambert, J. and Blattler, W. (1988) Purification and biochemical characterization of immunotoxins, in *Immunotoxins* (Frankel, A. E., ed.), Kluwer, Boston, MA, pp. 323–348.
16. Myers, D., Yanishevski, Y., Masson, E., Irvin, J., Evans, W., and Uckun, F. (1995) Favorable pharmacodynamic features and superior anti-leukemic activity of B43 (anti-CD19) immunotoxins containing two pokeweed antiviral protein molecules covalently linked to each monoclonal antibody molecule. *Leuk. Lymphoma* **18,** 93–102.
17. Beintema, J. J., Schuller, C., Irie, M., and Carsana, A. (1988) Molecular evolution of the ribonuclease superfamily. *Prog. Biophys. Mol. Biol.* **51,** 165–192.

3

Intracellular Targeting Using Bispecific Antibodies

Vic Raso

1. Introduction

The technological development and application of bispecific antibodies for biological research have advanced steadily since the idea of creating hybrid reagents with dual specificity was first promulgated by Nisonoff and Rivers *(1)*. It was realized that appropriately designed bispecific antibodies could provide a unique means for selectively delivering biologically active agents onto the surface of target cells so that they could ultimately be internalized *(2–7)*. Hybrid constructs developed in my laboratory used a specific antibody to reversibly bind the effector molecule within its combining site, whereas the second antibody or ligand component accurately targeted the complex to selected sites on the cell membrane **(Fig. 1)**. Those target receptor sites, along with the attached hybrid antibody complex, are subsequently taken inside the cell via receptor-mediated endocytosis. Cytotoxic drugs and toxins were chosen for delivery via the bispecific reagent because the entry of these potent molecules into target cells is signaled by an easily measured intracellular activity *(2–7)*.

One of the advantages to using this novel approach is that it allows for the delivery of sensitive bioactive molecules into cells in an unaltered state. No extraneous modification of their structure is required for carrier attachment since they are held within the antibody-combining site by noncovalent forces. The system circumvents any potential steric inactivation of delicate molecules that may result from directly coupling them to a carrier moiety by covalent linkage using either chemical means or genetically engineered fusion. Since spontaneous dissociation from the antibody-combining site frees the effector molecule, its structural integrity and full biologic potential are preserved. This automatic release obviates the need for subsequent enzymatic or chemical

From: *Methods in Molecular Medicine, Vol. 25: Drug Targeting: Strategies, Principles, and Applications*
Edited by: G. E. Francis and C. Delgado

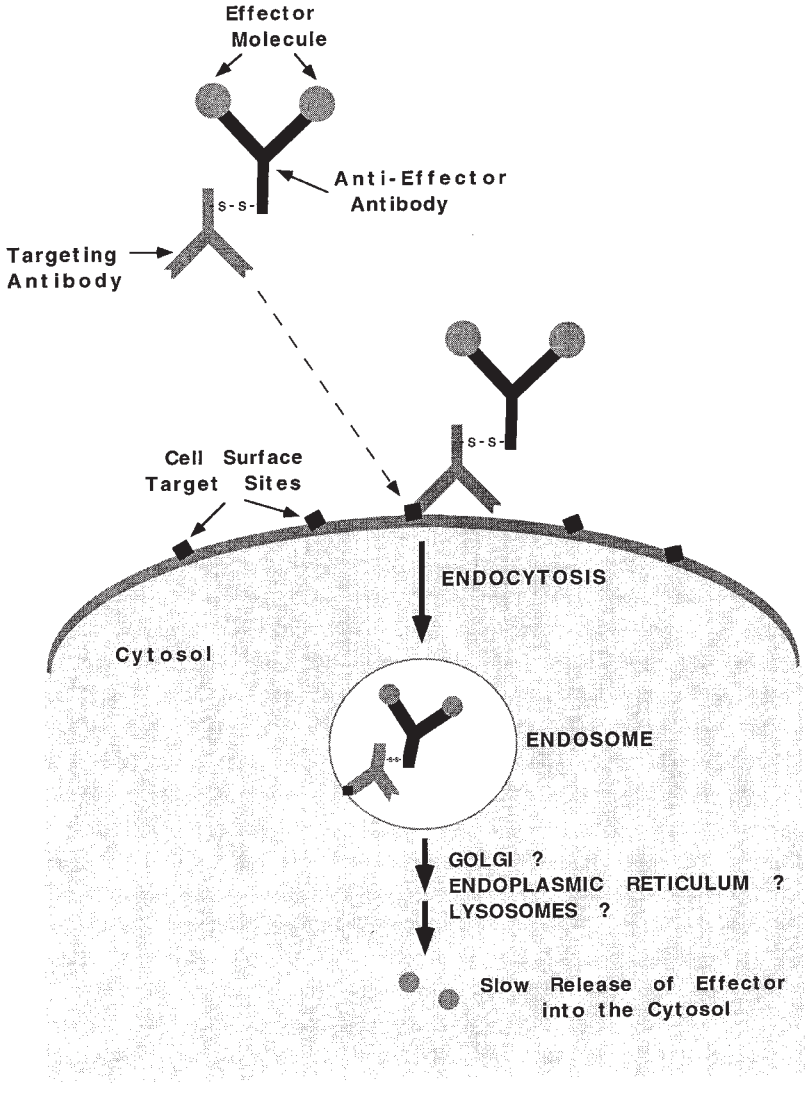

Fig. 1. Intracellular delivery of effector molecules using bispecific antibodies. A bifunctional carrier is constructed by linking a monoclonal anti-effector antibody to a monoclonal cell-targeting antibody. A noncovalent complex forms when the effector is added and binds to its specific antibody-combining sites. The targeting antibody directs this preformed complex to a distinct receptor site on the cell membrane. Alternatively, cells can be pretreated with the bispecific antibody, allowing the empty combining sites of the cell-bound reagent to be filled by subsequently added effector molecules. Surface-localized complexes quickly enter cells via a receptor-mediated endocytosis pathway. Escape of the effector from the cell vesicle system and passage into the cytosol is achieved but occurs slowly (~24 h).

cleavage from the carrier to restore activity inside of the cell. However, ligands that are bound to high-affinity antibodies may be relinquished slowly or could rebind to the antibody before exerting their effect inside the appropriate subcellular compartment. A novel mechanism was therefore devised to circumvent these potential problems for bispecific antibody-mediated delivery.

1.1. Acid-Triggered Release from Bispecific Antibodies

Initial studies on bispecific antibody delivery used the plant toxin ricin or its enzymatically active A chain as the bioactive agent for intracellular delivery ***(2–7)***, whereas subsequent work used saporin ***(8)*** or gelonin ***(9)***. Access to the cytosol was assured because these toxins shut down protein synthesis only if they reach and damage ribosomal RNA ***(10)***. Even though the bispecific antibody–toxin complexes were internalized and specifically killed target cells, neither the mechanism for antibody–toxin dissociation nor the intracellular compartment in which this release occured was known. The fact that it took 12–24 h to detect substantial inhibition of protein synthesis suggested that the transfer of the toxic moiety through these compartments and out into the cytosol was a slow rate-limiting step **(Fig. 1)**.

To overcome that restriction, new, second generation bispecific reagents were designed that allowed control of the mechanism, locus, and speed of effector release within the target cell. This was feasible because complexes that enter cells by endocytosis are quickly transported into endosomes that become acidic (pH 4.5–5.5) ***(11–13)*** because of the action of proton pumps ***(14)***. This perturbation in pH was exploited as a means for precisely triggering the rapid dissociation of active molecules from the bispecific antibody **(Fig. 2)**. The release mechanism is based on low pH-induced conformational changes, which molecules, such as diphtheria toxin (DT), undergo within acidic endosomal vesicles ***(15)***. Acid-triggered delivery was implemented by constructing bispecific reagents using select monoclonal antibodies (MAb) that bind the native toxin at neutral pH but rapidly release it as its conformation unfolds at mildly acidic conditions **(Fig. 2)**.

Monoclonal antibodies against acid-sensitive epitopes on DT were obtained by immunizing mice with sublethal doses of native toxin in complete Freund's adjuvant and then establishing hybridomas using standard methods ***(16)***. A solid-phase radioimmunoassay was developed so that antibodies in the hybridoma medium could be prebound to immobilized DT at neutral pH and then tested for release in response to the addition of an acidic buffer. This assay was used to identify several antibodies that recognized acid-sensitive epitopes on the three different functional/structural domains of DT ***(17)***. Those antibodies were covalently linked to a second, cell-reactive antibody or receptor ligand to form hybrid molecules with dual specificity. Like the original hybrid reagents,

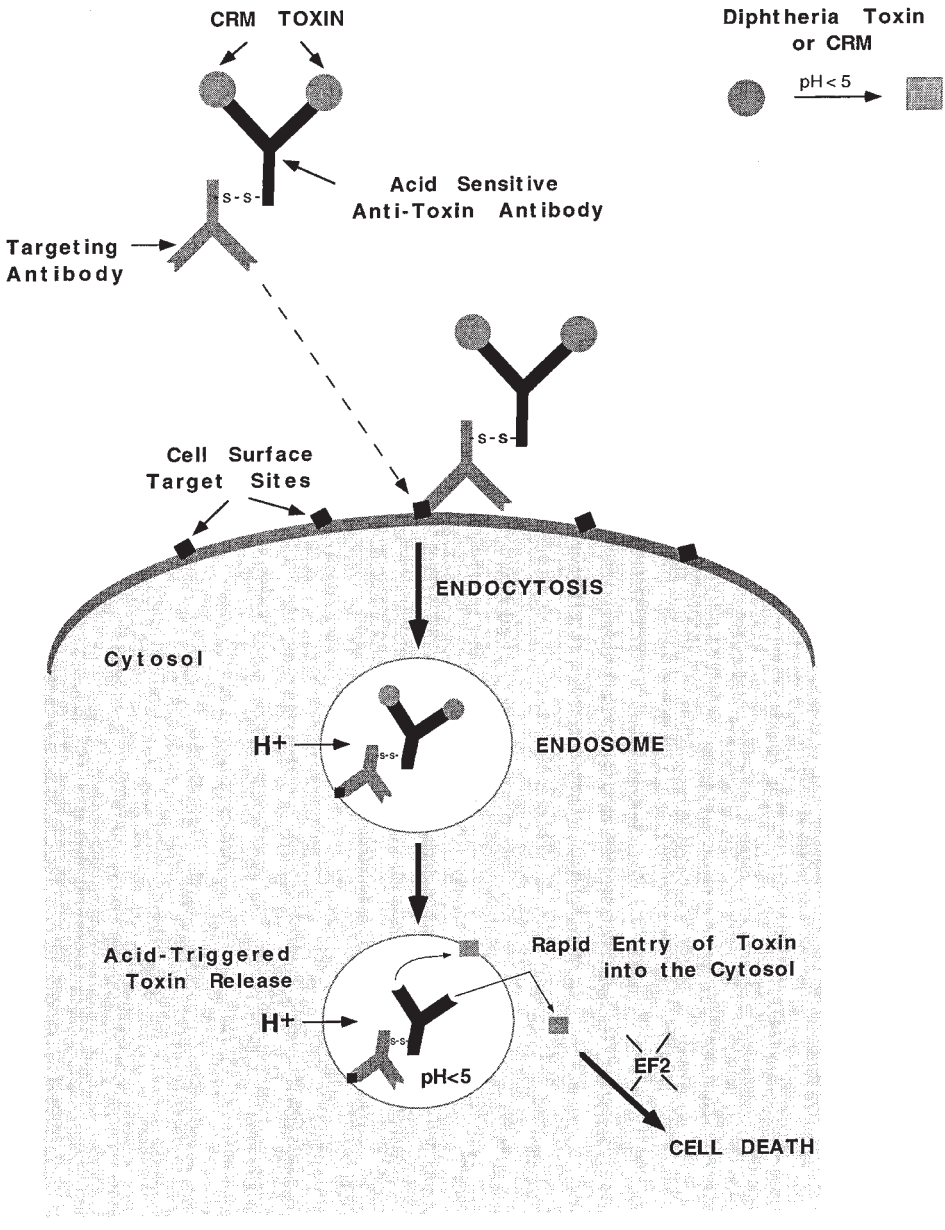

Fig. 2. Fast-acting acid-triggered bispecific antibody delivery systems. These new acid-triggered bispecific antibody carriers are similar to those shown in **Fig. 1**. However, the MAb that binds effector is directed against a conformational epitope that is altered by the mildly acidic conditions found in endosomes. Such pH-sensitive effector molecules are typified by diphtheria toxin and certain cell-binding defective mutant CRM forms of that toxin. This bispecific antibody–ligand complex spontaneously dis-

these carry antibody-bound toxin and selectively attach to the surface of cells bearing a chosen target site **(Fig. 2)**. However, now the toxin is immediately released in its lethal form when this bispecific antibody–toxin complex enters the cell and encounters a low pH within endosomes **(Fig. 2)**. The acid-induced conformational changes in DT also allow passage of its catalytic domain across vesicular membranes and into the cytosol ***(18,19)*** where it inactivates elongation factor 2 ***(20)***. This enzymatic action effectively terminates protein synthesis and kills the cell.

Special care must be taken to nullify the inherent receptor-binding capacity of effector molecules like DT when using them in cell-specific delivery systems. Only then will the chosen selectivity be strictly dictated by the targeting component of the bispecific antibody. Fortunately, there are many choices of receptor binding-defective DT molecules that retain full potency when delivered inside the cell by an appropriate bispecific antibody. For example, CRM107 and CRM45 which are obtained from the culture medium of mutant strains of *Corynebacterium diphtheriae* ***(21–24)***, have a single point mutation in the receptor-binding region and that entire domain deleted, respectively. In addition, genetically engineered constructs of DT and other effector molecules can be tailor-made for delivery via the bispecific antibody system. Using this approach researchers have produced minimal-sized, functional versions of both the catalytic and transmembrane domains of DT as well as molecules composed of the contiguous catalytic/transmembrane domains or the transmembrane/receptor-binding domains ***(25)***. Importantly, no extraneous linker region for attachment to carriers needed to be incorporated into those constructs since antibodies that bind to acid-sensitive epitopes on each of the three DT domains have been obtained.

Anti-transferrin receptor/anti-DT bispecific antibodies were used to deliver CRM107 into cells via the transferrin pathway and to demonstrate that the acid-release mechanism was functioning properly. This receptor was targeted because it normally cycles protein-bound iron through acidic endosomes where the Fe^{3+} is released by the low pH ***(26)***. The dual binding capacity of the bispecific antibodies was confirmed by their ability to specifically deliver [^{125}I]-diphtheria toxin to transferrin receptors present on intact human cells.

As predicted for a rapid, acid-triggered release, the bispecific antibody plus CRM107 combination reduced protein synthesis in target cells to 10% of the control level or less within only 2 h ***(5,6)***. Neither component alone had an

---

sociates when exposed to pH <5.0 in the endosome. The toxin is then rapidly translocated into the cytosol where it inactivates elongation factor 2 (EF2), shuts down protein synthesis, and kills the cell. The effects of acid-triggered bispecific antibody-delivered toxin on cellular protein synthesis are manifest within 2 h of treatment.

effect on the cells and neutralizing endosomal pH using NH_4Cl *(27)* protected them from the toxic action of hybrid antibody-delivered CRM107. Moreover, analogous bispecific antibodies were made with acid-stable anti-DT antibodies to serve as a control that does not release bound toxin inside the acidic endosomes. These hybrid reagents delivered CRM107 into the cell via the same transferrin receptor pathway but, as anticipated, failed to inhibit protein synthesis even after prolonged incubation *(6)*. The toxin was inactive because it remained complexed to the acid-stable antibody as it cycled through low pH compartments.

The acid-triggered bispecific antibodies mediated the cytotoxicity of CRM107, CRM45, and several genetically engineered DT constructs that are ordinarily inactive because they cannot bind to cells. The kinetics for inhibition of cellular protein synthesis was identical for the bispecific antibody/CRM107 complex and native DT, giving a $t_{1/2} = 20$ min for the rapid phase *(5)*. This implies both that the acid-induced release of CRM from the antibody carrier is fast and that translocation of its enzymatic domain into the cytosol is facilitated by its transmembrane domain in the same way as native DT.

1.2. Binary Mode of Delivery using Bispecific Antibodies

The acid-triggered hybrid antibodies are being used to develop a binary system for targeting toxins that could dramatically reduce nonspecific toxicity and substantially improve cell specificity. This scheme employs the segregated catalytic and transmembrane domains of DT produced by genetic engineering and two separate acid-releasable hybrid antibodies that bind to each of those component domains. Thus, the individual functional toxin parts can be independently delivered into the same cell to establish a binary delivery mode **(Fig. 3)**, which entails some important implications. Although either component alone is essentially nontoxic, the separate entities could cooperate to produce potent cytotoxicity when they are targeted into a cell and meet within the same acidified endosome. This possibility would allow each component to be directed at a different, distinguishing receptor site on the target cell **(Fig. 3)**, thereby greatly increasing selectivity for eliminating only that chosen cell type. Cells that have both determinants would be efficiently killed, whereas those possessing only one of the two target sites should remain unaffected. This basic strategy is generally applicable to any effector system that inherently requires or can be physically separated into two or more components needed to achieve full activity. Apart from the improved specificity, this binary delivery mode allows for the usage of attenuated effector moieties at very high concentrations without producing unwanted side effects. That feature would be especially important when bispecific antibodies are used in vivo since employing excess ligand should ensure a high occupancy of antibody-combining sites.

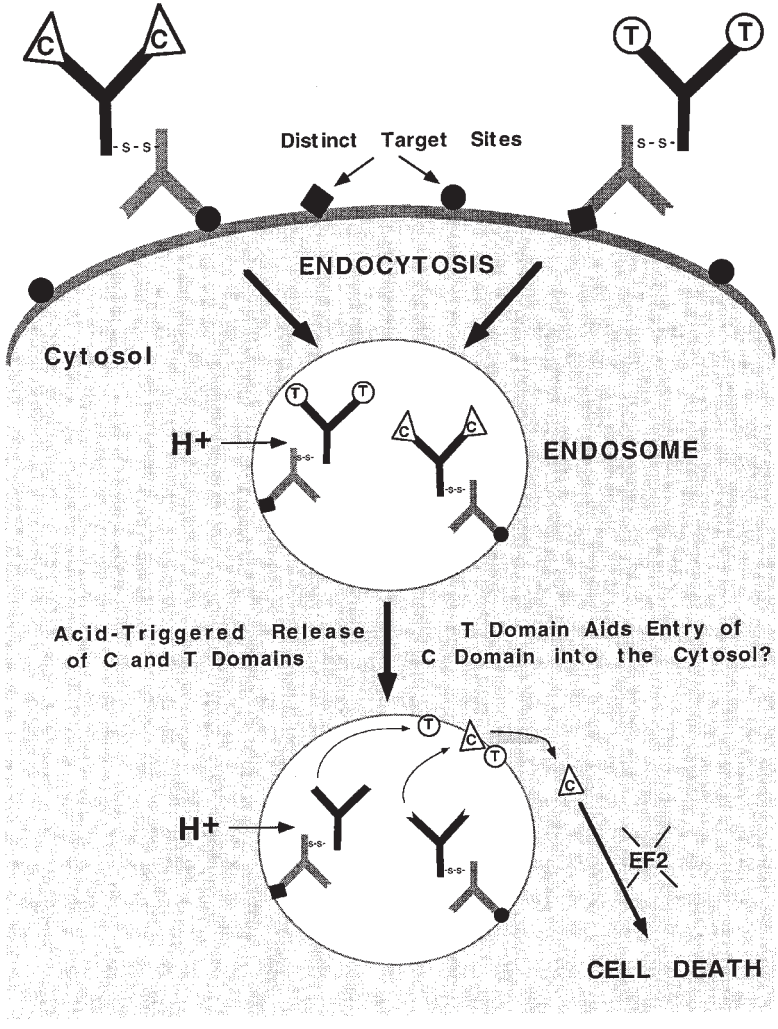

Fig. 3. Binary delivery mechanism. Bispecific antibodies can be used to deliver the complementary parts of an effector molecule to two distinct target sites on the same cell. In the example shown one acid-triggered bispecific antibody carries the catalytic domain (C) of DT to a selected receptor whereas the second carries its transmembrane domain (T) to a different receptor site. Cooperation between these functional units should occur when both complexes enter the same endosome and their bound toxin domains are released by the low pH conditions. Greatly improved specificity results from targeting two distinct sites on the cell and unwanted side effects are reduced by using attenuated effector moieties whose activity is restored intracellularly.

1.3. Refinement of Targeted Bispecific Antibodies

Whereas the initial bispecific antibodies (300 kDa) were assembled by unidirectionally linking two whole antibodies *(4)*, exclusively heterobispecific $F(ab')_2$ hybrid antibodies have also been made *(28)* using the targeting and acid-sensitive MAbs. These smaller $F(ab')_2$ reagents (100 kDa) have proven to be slightly superior delivery vehicles, on a molar basis, compared to the bivalent whole antibody constructs. Their effectiveness dispels the notion that cross-linking of two surface receptors is necessary for the cellular uptake of bispecific antibody-delivered toxins since these reagents are monovalent for both the toxin and the cell-surface epitope. The production of analogous bispecific single-chain Fv reagents (~50 kDa) for toxin delivery is feasible and the use of those smaller carriers might be advantageous for therapeutic purposes when penetration into target tissues is needed.

Additional effector molecules are suitable for the acid-triggered and binary modes of delivery using bispecific antibodies. For example, anthrax toxin operates through an acid-dependent mechanism that is similar to that used by DT *(29)*. One component of anthrax toxin undergoes a pH-induced conformational change and oligomerization to assist the translocation of its effector portion out of the endosome and into the cytosol *(30)*. Thus, this toxin or its complementary parts might also be targeted to cells and released inside low pH compartments by using an acid-triggered bispecific antibody approach analogous to the one developed for DT.

2. Materials

1. A partially purified preparation of DT is available from Connaught Laboratories (Willowdale, Ontario, Canada).
2. Na [^{125}I] (17 Ci/mg) and L-[3,4,5-^{3}H]-L-leucine (140 Ci/mmole) are available from New England Nuclear (Boston, MA).
3. Iodogen is available from Pierce (Rockford, IL). This can now be obtained precoated on tubes.
4. Sephadex G-25, SPDP, high resolution sephacryl S-300, phenyl-sepharose, and XK16 columns are available from Pharmacia (Uppsala, Sweden).
5. The human acute lymphoblastic leukemia CEM cell line and human colon adenocarcinoma LS 174T cell line are available from the American Type Culture Collection (Rockville, MD). The human mesothelioma H-Meso cell line *(32)* was used previously for cytotoxicity studies *(33,34)*.

3. Methods

3.1. Isolation of Toxins

1. Diphtheria toxin is isolated as previously described *(31)* using a partially purified preparation obtained from Connaught Laboratories as starting material. CRM107 and CRM45 *(21–23)* are obtained from cultures of the appropriate mutant strain

of *C. diphtheriae* as described earlier ***(21)***. Toxin is obtained from the culture supernatant either by $(NH_4)_2SO_4$ precipitation or by phenyl-sepharose chromatography ***(35)*** and purified further as described ***(31)***.

2. [^{125}I]-Diphtheria toxin (~4.5 µCi/µg) is produced by reaction with Na[^{125}I] using the iodogen method ***(36)***.

3.2. Generation and Characterization of Monoclonal Antibodies

1. BALB/c mice are immunized intraperitoneally over the course of 3 mo with progressively higher doses (1, 3, and 10 µg) of pure, biologically active DT emulsified in 0.25 mL complete Freund's adjuvant.
2. Hybridomas are generated 3 d following an iv booster injection of 10 µg of DT in phosphate-buffered saline (PBS) and selected using Hy medium with 10% fetal calf serum plus hypoxanthine, aminopterin, and thymidine (HAT) ***(6,16)***.
3. Supernatants from microtiter wells with clones are screened for the ability to bind [^{125}I]-DT, ~4.5 µCi/µg (diluted into 5% bovine serum albumin prior to use) ***(36)***, using a polyethylene glycol precipitation method ***(37)***. Antibody-positive supernatants bound ~25,000 cpm whereas negative clones and Hy medium alone have a background of ~4000 cpm. In a typical fusion, 35 positive antibody-producing clones are obtained from the spleen of a single animal.
3. A second assay was developed in order to examine the influence of pH on the interaction between DT and the different MAbs. DT (100 µL at 60 µg/mL in PBS) is adsorbed to polyvinyl chloride microtiter wells for 18 h and the plates are then blocked with 0.5% bovine serum albumin in PBS. Antibody or hybridoma culture medium is added to the washed wells in 100 µL of Hy medium and allowed to react for 2 h before washing the plate with PBS. Attached antibody is revealed by subsequent addition of ~3×10^4 cpm of an [^{125}I]-goat antimouse IgG reagent, ~2 µCi/µg ***(36)*** for 1 h followed by washing with PBS and measuring radioactivity in the wells using a Beckman model 5500 gamma counter. Negative controls with Hy medium alone had a background of ~100 cpm whereas antibody containing samples bound ~1000–4000 cpm. Disruption of the binding interaction between toxin and antibody is easily measured as a function of pH, temperature, and time with this rapid assay.
4. To test for the effects of pH on dissociation of the complex, MAb in 100 µL of Hy medium is bound to immobilized DT for 2 h in replicate wells, and 15 µL of 1 *M* sodium acetate buffer are then added to provide a final pH of 4.0, 4.5, 5.0, 5.5, or 7.0 (the control). Dissociation from the toxin is allowed to proceed for various time intervals at either 22 or 37°C. Released antibody is then quickly washed off the plates with PBS and the amount remaining is quantified using the [^{125}I]-goat antimouse IgG probe. Results are expressed as the percent bound or released compared to the final pH 7.0 control under identical conditions. This pH release assay gave better performance when carried out in Hy medium rather than PBS. Attempts to use a [^{125}I]-DT probe with immobilized antibody or in the polyethylene glycol precipitation method were not successful because at acid pH the [^{125}I]-DT stuck nonspecifically and irreversibly to surfaces.

5. Selected clones are injected into pristane-primed mice, ascites fluid is collected, and the 150 kDa anti-DT MAb is isolated by $(NH_4)_2SO_4$ precipitation and size fractionation on a high resolution Sephacryl S300 column. Specificity is further assessed by testing the immunoblot reactivity of each antibody for the A vs B fragment of nicked DT that had been separated by polyacrylamide gel electrophoresis (PAGE) under reducing conditions ***(10,38)***. Immunoblot analysis with CRM mutant proteins and genetically engineered diphtheria toxin constructs, $DT_{1–190}$, $DT_{201–370}$, and $DT_{201–535}$ is used to further characterize antibody specificity. Different antibodies recognized three distinct epitopes located on the receptor-binding domain of DT whereas others bound to separate sites on the transmembrane domains. Several additional antibodies interacted at different loci within the catalytic domain.
6. The attributes of the 7D3 MAb directed against the human transferrin receptor have been reported ***(33)***. Hybridoma clones are injected into pristane-primed BALB/c mice or Swiss nu/nu athymic mice (Taconic, Germantown, NY), ascites fluid is collected and the 150 kDa anti-DT MAb is isolated by $(NH_4)_2SO_4$ precipitation and size fractionation on a high resolution Sephacryl S-300 column. The antibodies were ~90% pure as judged by PAGE.

3.3. Production of Bispecific Antibodies

1. A method for unidirectionally disulfide-linking two MAbs has been described ***(4)***. The purified antibodies are each reacted with a sixfold molar excess of SPDP and the uncoupled reagent is removed by passage through a Sephadex G-25 column equilibrated with 0.1 *M* sodium acetate, 0.1 *M* NaCl, pH 4.5. This results in the addition of approx 3 moles of SPDP per mole of antibody. To produce an appropriate bispecific antibody combination, the SPDP-substituted anti-transferrin receptor antibody is reduced with 50 m*M* dithiothreitol for 30 min and the protein fraction is isolated by passage through a Sephadex G-25 column equilibrated with PBS. This thiolated antibody is then mixed with an SPDP-substituted anti-DT antibody and the combination is allowed to react overnight. The product, a 300,000 kDa disulfide-linked heterodimeric antibody with two binding sites for DT plus two sites directed against the transferrin receptor, is separated from unreacted antibody by chromatography on high resolution Sephacryl S-300. Fractions are analyzed by PAGE. No difference was seen when the bispecific antibody and its parent anti-DT were compared using ^{125}I-DT binding titrations, indicating that they retained full activity.

3.4. Binding of Toxin to Cells

1. Two different protocols were used to deliver [^{125}I]-DT to cells using the bispecific antibodies. In the first procedure, CEM cells (1×10^7) are removed from the culture medium and suspended in 100 µL PBS. Bispecific antibodies are added at $10^{-7}M$, incubated with the cells for 30 min at 2°C, and unbound reagent is then washed off with cold PBS. The bispecific antibody-coated cells are exposed to [^{125}I]-DT for 30 min at 2°C, washed with cold PBS, and analyzed for radioactivity to measure

the amount bound to cells. In some experiments, the 7D3 MAb is included at 10^{-5} *M* during the first step to block attachment of the bispecific antibody.

2. In the second method, [^{125}I]-DT was added either to 100 µL PBS or 100 µL PBS containing the designated hybrid antibody at 10^{-8} *M* and allowed to combine at 22°C for 15 min. CEM cells (1×10^7) are added to each preparation, incubated for 1 h at 2°C, washed with cold PBS, and then analyzed for radioactivity.

3.5. Cytotoxicity Assays

1. Human transferrin receptor-positive target cells are cultured at 37°C with 5% CO_2 in tissue culture flasks containing RPMI-1640 medium with 10% fetal calf serum, L-glutamine, and penicillin–streptomycin (GIBCO, Grand Island, NY). Adherent cells are released from the culture flask using 0.05% trypsin, and 0.02% EDTA for 10 min at 37°C, and then medium plus serum is added to inactivate the trypsin.
2. For cytotoxicity assays, culture medium is removed and the cells are resuspended at 5×10^5/mL in leucine-free minimal essential medium (GIBCO) supplemented with L-glutamine and penicillin–streptomycin. Aliquots are added to 96-well microtiter plates to give a final volume of 200 µL/well. Other additions made to the wells did not exceed a total volume of 20 µL. The bispecific antibody and CRM toxins are added either separately or mixed first so that the specified final concentration is achieved by diluting the preformed complex in the microtiter well. Both methods of treatment gave essentially identical results. After these components are delivered at room temperature, the cells are incubated for the designated time at 37°C in 5% CO_2. When the incubation is completed, 2.5 µCi of [^{3}H]-leucine are added to each well and the incubation is extended for 30 min at 37°C. The cells are then collected onto glass fiber filters using a Mash II cell harvester (GIBCO). Incorporation of [^{3}H]-leucine into cellular protein is measured by scintillation counting of the glass fiber disks. All of the cytotoxicity assay wells were set up in duplicate and the results were averaged. The standard deviation of the assay was <10%.

4. Notes

1. The bispecific antibody approach is very flexible since antibodies or ligands to virtually any membrane site can be easily coupled with the effector-bearing antibody to form a variety of highly specific delivery agents. Variations in potency are precluded since no modification of the effector molecule is needed for attachment to the carrier.
2. Endocytotic cycling through an acid compartment is required for successful deployment of the low pH-based release system, but that condition seems to be the rule rather than the exception for surface receptor sites.
3. Bispecific antibodies offer some potential advantages for therapeutic use because they can provide both the selective delivery of biological agents to target cells and a pH-controlled intracellular release mechanism.
4. They also allow for the design of binary delivery systems that enhance specificity by targeting the complementary parts of an effector molecule to two distinct receptor sites on the cell.

5. Furthermore, the hybrid antibody and active ligand can be administered either as separate components or as a single preloaded complex.
6. However, in order to maintain a high occupancy of antibody-combining sites in vivo, either high affinity antibodies or elevated levels of ligand would have to be used.

Acknowledgments

The mutant strains of *C. diphtheriae* that produced the CRM toxins were kindly provided by Drs. Neal Groman, John Murphy, and Richard Youle. This work was supported by National Institutes of Health Grants CA49856, CA49254, and GM58235.

Abbreviations

DT, diphtheria toxin; CRM, crossreacting material; SPDP, 3-(2-pyridyldithio)propionic acid *N*-hydroxysuccinimide ester; PBS, 0.14 *M* NaCl, 0.01 *M* sodium phosphate, pH 7.2; EDTA, ethylenediaminetetraacetic acid.

References

1. Nisonoff, A. and Rivers, M. M. (1961) Recombination of a mixture of univalent antibody fragments of different specificity. *Arch. Biochem. Biophys.* **93,** 460–467.
2. Raso, V. A. and Griffin, T. (1981) Hybrid antibodies with dual specificity for the delivery of ricin to immunoglobulin-bearing target cells. *Cancer Res.* **41,** 2073–2078.
3. Raso, V. A. (1982) Antibody mediated delivery of toxin molecules to antigen bearing target cells, in *Immunological Reviews: Antibody Carriers of Drugs and Toxins in Tumor Therapy*, vol. 62 (Moller, G., ed.), Munksgaard, Copenhagen, pp. 93–117.
4. Raso, V. A. and Basala, M. (1984) Monoclonal antibodies as cell targeted carriers of covalently and non-covalently attached toxins, in *Receptor Mediated Targeting of Drugs*, vol. 82 (Gregoriadis, G., Post, G., Senior, J., and Trouet, A., eds.), NATO Advanced Studies Institute, New York, pp. 119–138.
5. Raso, V. (1994) Immunotargeting intracellular compartments. *Anal. Biochem.* **222,** 297–304.
6. Raso, V., Brown, M., and McGrath, J. (1997) Intracellular targeting with low pH triggered bispecific antibodies. *J. Biol. Chem.* **272,** 27,623–27,628.
7. Raso, V., Brown, M., McGrath, J., Liu, S., and Stafford, W. (1997) Antibodies capable of releasing diphtheria toxin in response to the low pH found in endosomes. *J. Biol. Chem.* **272,** 27,618–27,622.
8. Glennie, M. J., Brennard, D. M., Bryden, F., McBride, H. M., Stirpe, F., Worth, A. T., and Stevenson, G. T. (1988) Bispecific F(AB')2 antibody for the delivery of saporin in the treatment of lymphoma. *J. Immunol.* **141,** 3662–3670.
9. Sforzini, S., Bolognesi, A., Meazza, R., Marciano, S., Casalini, P., Durkop, H., et al. (1995) Differential sensitivity of CD30+ neoplastic cells to gelonin delivered by anti-CD30/anti-gelonin bispecific antibodies. *Br. J. Haematol.* **90,** 572–577.
10. Endo, Y., Mitsui, K., Motizuki, M., and Tsurugi, K. (1987) The mechanism of action of ricin and related toxic lectins on eukaryotic ribosomes: The site and the

characteristics of the modification in 28 S ribosomal RNA caused by the toxins. *J. Biol. Chem.* **262(12),** 5908–5912.
11. Geisow, M. L. and Evans, W. H. (1984) pH in the endosome: measurements during pinocytosis and receptor-mediated endocytosis. *Exp. Cell Res.* **150,** 36–46.
12. Geisow, M. J. (1984) Fluorescein conjugates as indicators of subcellular pH: a critical evaluation. *Exp. Cell Res.* **150,** 29–35.
13. Overly, C. C., Lee, K. D., Berthiaume, E., and Hollenbeck, P. J. (1995) Quantitative measurement of intraorganelle pH in the endosomal-lysosomal pathway in neurons by using ratiometric imaging with pyranine. *Proc. Natl. Acad. Sci. USA* **92,** 3156–3160.
14. Nelson, N. (1992) The vacuolar H+-ATPase—one of the most fundamental ion pumps in nature. *J. Exp. Biol.* **172,** 19–27.
15. Blewitt, M. G., Chung, L. A., and London, E. (1985) Effect of pH on the conformation of diphtheria toxin and its implications for membrane penetration. *Biochemistry* **24,** 5458–5464.
16. Kennett, R. H. (1980) Monoclonal antibodies, in *Fusion Protocols* (Kennett, R. H., McKearn, T. J., and Bechtol, K. B., eds.), Plenum Press, New York, pp. 365–367.
17. Choe, S., Bennett, M. J., Fujii, G., Curmi, P. M. G., Kantardjieff, K. A., Collier, R. J., and Eisenberg, D. (1992) The crystal structure of diphtheria toxin. *Nature* **357,** 216–222.
18. Sandvig, K. and Olsnes, S. (1980) Diphtheria toxin entry into cells is facilitated by low pH. *J. Cell Biol.* **87,** 828–832.
19. Draper, R. K. and Simon, M. I. (1980) The entry of diphtheria toxin into the mammalian cell cytoplasm: evidence for lysosomal involvement. *J. Cell Biol.* **87,** 849–854.
20. Van Ness, B. G., Howard, J. B., and Bodley, J. W. (1980) ADP-ribosylation of elongation factor 2 by diphtheria toxin. NMR spectra and proposed structures of ribosyl-diphthamide and its hydrolysis products. *J. Biol. Chem.* **255,** 10,710–10,716.
21. Uchida, T., Pappenheimer, A. M. J., and Greany, R. (1973) Diphtheria toxin and related proteins: I. Isolation and properties of mutant proteins serologically related to diphtheria toxin. *J. Biol. Chem.* **248(11),** 3838–3844.
22. Laird, W. and Groman, N. (1976) Isolation and characterization of tox mutants of corynebacteriophage beta. *J. Virol.* **19,** 220–227.
23. Greenfield, L., Johnson, V. G., and Youle, R. J. (1987) Point mutations in diphtheria toxin separate binding from entry and amplify immunotoxin selectivity. *Science* **238,** 536–539.
24. Youle, R. J. (1991) Mutations in diphtheria toxin to improve immunotoxin selectivity and understand toxin entry into cells. *Cell Biol.* **2,** 39–45.
25. Raso, V., unpublished results.
26. Van Renswoude, J., Bridges, K. R., Harford, J. B., and Klausner, R. D. (1982) Receptor-mediated endocytosis of transferrin and the uptake of Fe in K562 cells: Identification of a nonlysosomal acidic compartment. *Proc. Natl. Acad. Sci. USA* **79,** 6186–6190.
27. Kim, K. and Groman, N. B. (1965) In vitro inhibition of diphtheria toxin action by ammonium salts and amines. *J. Bacteriol.* **90,** 1552–1556.

28. Brennan, M., Davison, P. F., and Paulus, H. (1985) Preparation of bispecific antibodies by chemical recombination of monoclonal immunoglobulin G1 fragments. *Science* **228,** 81–83.
29. Friedlander, A. M. (1986) Macrophages are sensitive to anthrax lethal toxin through an acid-dependent process. *J. Biol. Chem.* **261,** 7123–7126.
30. Milne, J. C., Furlong, D., Hanna, P. C., Wall, J. S., and Collier, R. J. (1994) Anthrax protective antigen forms oligomers during intoxication of mammalian cells. *J. Biol. Chem.* **269,** 20,607–20,612.
31. Carroll, S. F., Barbieri, J. T., and Collier, R. J. (1988) Diphtheria toxin: purification and properties. *Meth. Enzymol.* **165,** 68–76.
32. Reale, F. R., Griffin, T. W., Compton, J. M., Graham, S., Townes, P. L., and Bogden, A. (1987) Characterization of a human malignant mesothelioma cell line (H-MESO-1): A biphasic solid and ascitic tumor model. *Cancer Res.* **47,** 3199–3205.
33. Griffin, T. W., Richardson, C., Houston, L. L., LePage, D., Bogden, A., and Raso, V. (1987) Antitumor activity of intraperitoneal immunotoxins in a nude mouse model of human malignant mesothelioma. *Cancer Res.* **47,** 4266–4270.
34. Griffin, T., Rybak, M. E., Recht, L., Singh, M., Salimi, A., and Raso, V. A. (1993) Potentiation of antitumor immunotoxins by liposomal monensin. *J. Natl. Cancer Inst.* **85(4),** 292–298.
35. Rappuoli, R., Perugini, M., Marsili, I., and Fabbiani, S. (1983) Rapid purification of diphtheria toxin by phenyl sepharose and DEAE-cellulose chromatography. *J. Chromatog.* **268,** 543–548.
36. Fracker, P. J. and Speck, J. C. J. (1978) Protein and cell membrane iodinations with sparingly soluble chloroamide, 1,3,4,6,-tetrachloro-3a,6a-diphenylglycoluril. *Biochem. Biophys. Res. Comm.* **80,** 849–857.
37. Hayakawa, S., Uchida, T., Mekada, E., Moynihan, M. R., and Okada, Y. (1983) Monoclonal antibody against diphtheria toxin: effect on toxin binding and entry into cells. *J. Biol. Chem.* **258(7),** 4311–4317.
38. Zucker, D. R. and Murphy, J. R. (1984) Monoclonal antibody analysis of diphtheria toxin—I. Localization of epitopes and neutralization of cytotoxicity. *Mol. Immunol.* **21(9),** 785–793.

4

Antibody Conjugation Methods for Active Targeting of Liposomes

Steven M. Ansell, Troy O. Harasym, Paul G. Tardi, Susan S. Buchkowsky, Marcel B. Bally, and Pieter R. Cullis

1. Introduction

Liposomes are useful drug delivery vehicles since they may protect encapsulated drugs from enzymatic degradation and rapid clearance in vivo, or alter biodistribution, potentially leading to reduced toxicities ***(1,2)***. A major limitation to the development of many specialized applications is the problem of directing liposomes to tissues where they would not normally accumulate. Consequently, a great deal of effort has been made over the years to develop liposomes that have targeting vectors attached to the bilayer surface. These vectors have included ligands such as oligosaccharides ***(3,4)***, peptides ***(5,6)***, proteins ***(7,8)*** and vitamins ***(9)***. Most studies have focused on antibody conjugates since procedures for producing highly specific monoclonal antibodies (MAbs) are well established. In principle it should be possible to deliver liposomes to any cell type as long as the cells are accessible to the carrier. In practice it is usually not this simple since access to tissue, competition, and rapid clearance are formidable obstacles. It has also been shown that antibodies become immunogenic when coupled to liposomes ***(10,11)***, although in similar experiments with ovalbumin we have demonstrated that immunogenicity can be suppressed by formulating the liposomes with the cytotoxic drug doxorubicin ***(12)***. Such issues as these suggest that the development of antibody-targeted liposomes for in vivo applications will present difficult challenges.

In addition to addressing the challenges related to use of antibody-conjugated carriers, there must be a fundamental understanding regarding why a targeted ligand is being attached. The concept, in its simplest form, is to

From: *Methods in Molecular Medicine, Vol. 25: Drug Targeting: Strategies, Principles, and Applications*
Edited by: G. E. Francis and C. Delgado

enhance binding of the carrier to a defined cell population or a selected tissue element. It is essential, therefore, that the binding attributes of the targeting ligand be retained during the procedures that are used to prepare the targeted conjugate. Binding attributes can be determined in vitro using target cells in culture or in vivo by careful evaluation of the carrier's distribution characteristics. With respect to the latter, targeting should increase association of the carrier with a target cell, which may be reflected by enhanced delivery to the site where the cell is located, enhanced retention of the carrier within the site where the cell is located; a redistribution of the carrier within the site where the target cells are located, and/or target binding-mediated changes in the characteristics of the carrier.

Numerous procedures for the conjugation of antibodies to lipcsomes have been developed ***(13–16)***. These fall into four general categories defined by the particular functionality of the antibody being modified, namely amine modification, carbohydrate modification, disulfide modification, and noncovalent conjugation, each of which will be discussed below. These procedures are very similar to those used to prepare affinity columns ***(17)***, except for modifications made to accommodate the fact that the substrate is in the solution phase rather than the solid phase.

Antibodies consist of two pairs of light and heavy chains that are held together by intrachain disulfide bonds. There are two isoforms of the light chain and five of the heavy chain. The type of heavy chain defines the class of antibody, namely IgG, IgM, IgA, IgE, or IgD. Most liposome conjugates are produced using IgG and occasionally IgM. Various classes of antibodies exist as monomers or multimeric structures; for example, IgG exists as a monomer whereas the soluble form of IgM generally exists as a pentamer. These size differences may be significant when conjugating the antibody to liposomes, particularly when molecules, such as polyethylene glycol (PEG)-lipids, have been incorporated into the liposome membrane, affecting such parameters as conjugation efficiency and liposome aggregation. In order to illustrate potential sites of modification a schematic diagram of an IgG molecule is detailed in **Fig. 1**. Proteolytic degradation of antibodies can be used to generate smaller functional antigen-binding proteins. For example, treatment of IgG with papain or pepsin is used to generate Fab ***(18)*** and $F(ab')_2$ ***(19)*** fragments, respectively. Antibody fragments such as these are attractive for targeting purposes since they should not have the problems associated with the effector functions of the Fc chain, such as Fc receptor binding ***(20)*** and complement activation. It is also possible to generate chimeric antibodies to avoid problems associated with species differences in the conserved regions of the antibody ***(21)***.

Many chemistries have been used to conjugate antibodies to liposomes. The most useful of these involve modification of the antibody and a lipid in the

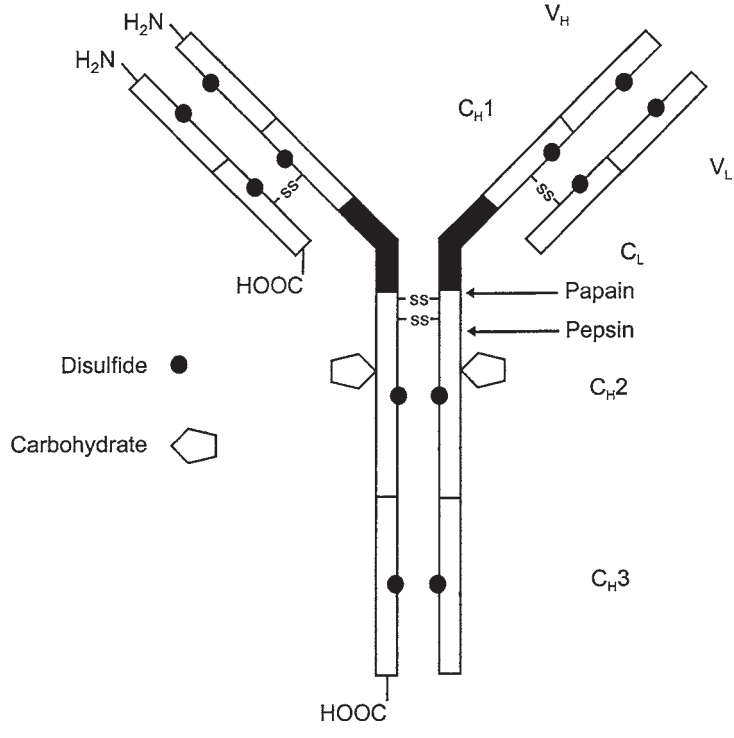

Fig. 1. A schematic representation of IgG depicting sites available for modification. Amino groups in the form of lysine residues may be scattered throughout the antibody. Arrows depict the sites of proteolytic lysis by papain and pepsin.

liposome with crosslinkers, which, when activated, react with each other to form a permanent covalent link. The most widely used approach has been the reaction of sulflhydryl groups with maleimide groups, as detailed in **Fig. 2A**. This reaction has the advantage of being relatively clean, fast, and efficient, and has been adapted to the modification of all of the antibody functional groups in the preparation of liposome conjugates. Selection of a particular chemistry and site of modification should be made depending on what procedures are compatible with the antibody in question. Different antibodies may be more sensitive to some procedures than others and it may be necessary to attempt a number of protocols. The recommended general procedure (because it is very well characterized) involves the thiolation of antibodies with 3-(2-pyridyldithio)propionic acid-*N*-hydroxysuccinimide ester (SPDP), followed by deprotection with dithiothreitol (DTT) and conjugation to liposomes containing maleimide-derivatized 1,2-distearoyl-sn-glycero-3-phosphoethanolamine (DSPE) or 1,2-dipalmitoyl-sn-glycero-3-phosphoethanolamine (DPPE).

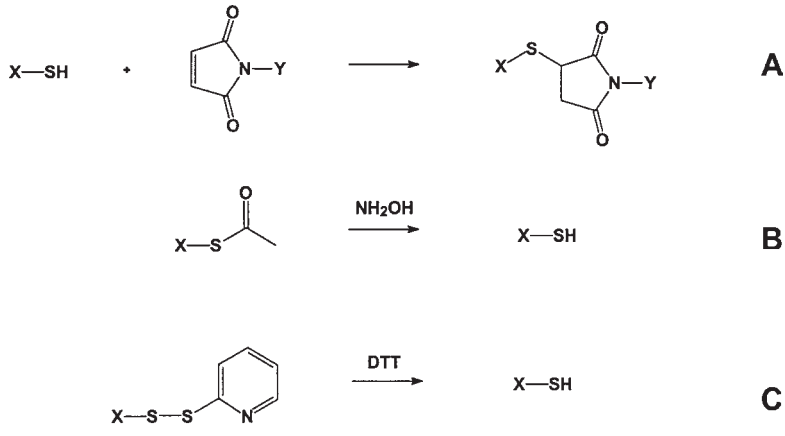

Fig. 2. Important reactions involved in the generation of thiol-maleimide links. All of these reactions proceed under neutral conditions. **(A)** Free sulfhydryl groups undergo additional reactions with maleimide groups. **(B)** Thioacetate protection groups may be hydrolyzed with hydroxylamine. **(C)** 2-Pyridyldisulfide protecting groups are reduced by DTT.

2. Materials

1. Crosslinkers are available from Molecular Probes, Inc. (P.O. Box 22010, Eugene, OR 97402-0469, Tel. 541-465-8300, Fax 541-344-6504, or Pierce (P.O. Box 117, Rockford, IL 61105, Tel. 815-968-0747, Fax 815-968-8148).
2. Lipids are available from Avanti Polar Lipids, Inc. (700 Industrial Park Drive, Alabaster, AL 35007, Tel. 800-227-0651, Fax 800-229-1004, or Northern Lipids, Inc. (2660 Oak Street, Vancouver, BC, V6H 3Z6, Canada, Tel. 604-875-4836, Fax 604-875-4979).
3. Extruders are available from Lipex Biomembranes Inc. (3550 W 11th Ave., Vancouver, BC, V6R 2K2, Canada, Tel. 604-734-8263, Fax 604-734-2390).
4. *N*-(2-hydroxyethyl)piperazine-*N'*-(2-ethanesulfonic acid) buffered saline (HBS): 20 m*M* HEPES, 150 m*M* NaCl, pH 7.4; sodium acetate buffered saline (SAS): 100 m*M* NaOAc, 50 m*M* NaCl, pH 4.4; phosphate-buffered saline (PBS): 20 m*M* Na_2HPO_4, 145 m*M* NaCl, pH 7.4.

3. Methods

3.1. Liposome Preparation

The most commonly used method of liposome preparation (*see* **Note 1**) involves hydration of a lipid mixture in buffer, followed by extrusion through a press of some description. A number of devices are commercially available for this purpose, the most widely used being the "Extruder" from Lipex Biomembranes. Homogenous lipid mixtures can be prepared by drying the

sample down from a chloroform solution, or by lyophilization from an organic solvent, such as benzene. We usually use the chloroform procedure when making liposomes, as follows:

1. Dissolve lipid mixture of the appropriate composition in chloroform (~1 mL per 50–100 µmole of lipid) in a glass tube. In some cases it may be necessary to add a minimum amount of methanol to dissolve all of the lipid.
2. Dry the lipid down to a thin film on the tube surface using a stream of nitrogen gas. It is advisable to use a reservoir of warm water to heat the solution during this process. This facilitates evaporation of the solvent and minimizes the possibility of lipid crystallizing or precipitating from the solution. The process should be repeated if there is any evidence that this has happened. It is important to produce as thin a film as possible since large lumps can be extremely difficult to hydrate.
3. Lightly cap the tube with tissue paper and dry the lipid overnight on a lyophilizer. Some foaming may occur because of residual solvent in the lipid film.
4. Add buffer to the tube and vortex until the lipid has fully dispersed. It may be necessary to warm the sample in a waterbath set at above the phase transition temperature of the primary lipid to facilitate this.
5. Transfer the suspension to a cryovial.
6. Freeze the suspension in liquid nitrogen for 5 min and then thaw it for 5 min in a water bath set above the phase transition temperature of the dominant lipid.
7. Repeat **step 6** four more times.
8. Pass the suspension though a stacked pair of polycarbonate 100-nm filters (Nuclepore) using an extruder. The suspension should be allowed to equilibrate for 5 min inside the extruder before pressure is applied in cases where the extrusion is performed above room temperature.
9. Repeat **step 8** nine more times. Equilibration is not usually required after the first pass.
10. Examine the filters when dismantling the extruder. Any sign of solids or gels indicates that some of the lipid has phase separated and consequently the lipid composition may have changed.
11. Analyze the lipid content using an incorporated label or by using a phosphate assay.
12. Dilute the lipid to the desired concentration with buffer.

3.2. Amine Modification

Modification of the protein amine groups is the procedure most frequently used to produce antibody–liposome conjugates. Early procedures used crosslinking agents, such as 1-ethyl-3-(3-dimethylaminopropyl)carbodiimide hydrochloride (EDC) ***(27,28)*** in the presence of preformed liposomes containing a lipophilic carboxylic acid. Condensing agents like these tend to form protein–protein polymers. Control of these reactions is typically difficult and complex, and as a result separation of the liposomes from protein polymers is a

major problem. Other early approaches involved direct modification of antibodies with activated fatty acids, such as the *N*-hydroxysuccinimide (NHS) ester of palmitic acid, prior to incorporation into a liposome membrane, typically by detergent dialysis procedures ***(29)***. Reagents, such as EDC, have been used in conjunction with NHS to activate acidic functions on liposomes, which were then conjugated to the amino groups on antibodies ***(30)***. Better control of the conjugation reaction can been achieved using hetereobifunctional crosslinkers, which efficiently introduce a unique and selective reactive function, such as a protected thiol or maleimide group. Examples of these crosslinkers are SPDP ***(31)***, *S*-acetylthioglycolic acid *N*-hydroxysuccinimide ester (SATA) ***(32,33)*** and 4-(p-maleimidophenyl)butyric acid *N*-hydroxy–succinimide ester (SMPB) ***(34)***. Antibodies which have been activated by these crosslinkers can, after deprotection where appropriate, react with activated lipids in liposome bilayers. Maleimide and protected thiol-derivatized lipids are available from commercial sources for this purpose.

Deprotection of 3-pyridyl disulfides is usually effected by DTT (**Fig. 2C**), and occasionally by some other mercaptan. Particular care should be exercised when removing these reagents after the reaction since they could potentially interfere in subsequent coupling reactions. Mercaptan-based deprotection reagents also damage the disulfide bonds in antibodies. This damage can be minimized by performing the deprotection at low pH ***(35)*** with short reaction times ***(36)***. Thioacetate-protected crosslinkers have been used less frequently. These reagents can be deprotected with hydroxylamine buffers (**Fig. 2B**) under conditions that do not damage the disulfide bonds. In theory this should allow better control of the thiolation process and simplify some of the workup steps.

Once deprotected, sulfhydryl groups can react with maleimide (for example, SMPB-modified conjugates) or iodo (for example, iodoacetic acid *N*-hydroxysuccinimide ester (SIAA)-modified conjugates) groups. Maleimide groups are recommended since iodo functions can react with amino groups in either of the substrates, leading to undesirable side products. Deprotection is not required for these reagents.

Liposomes containing excess maleimide or thiol groups after the conjugation reaction may exhibit undesirable qualities, such as aggregation, reactions in vitro and in vivo, and immunogenicity. In general, these aspects are not well studied and the effects of these groups on the liposome surface cannot therefore be predicted. It is possible to quench these reactive functions with reagents containing iodo, maleimide, or sulfhydryl groups where appropriate. This is likely to be a particularly serious problem for thiolated liposomes, consequently we recommend that the antibody be thiolated and that a maleimide modified lipid be incorporated into the liposomes in order to generate the appropriate reactive entities for the final conjugation reaction.

3.2.1. SPDP-Coupling Protocol

The most widely used procedure for generating protein–liposome conjugates involves modification of the protein with SPDP, followed by deprotection with DTT and conjugation to SMPB-derivatized liposomes. We use the following protocol to generate such conjugates using IgG (*see* **Note 2**).

1. Prepare liposomes incorporating 1% *N*-(4-(p-maleidophenyl)butyryl)-1,2-*sn*-distearoylphosphatidylethanolamine (MPB-DSPE) as described above. This should be done not more than 1 d prior to use.
2. Prepare a solution of IgG (10–20 mg/mL) in PBS or HBS at pH 7.4.
3. Prepare a 1 m*M* solution of SPDP in HBS by diluting 80 µL of an ethanol stock solution (3.9 mg SPDP/mL ethanol) with 920 µL HBS.
4. Add an aliquot of the SPDP (5 mol equivalents) solution to the IgG solution. Stir at room temperature for 20 min.
5. Pass the solution down a Sephadex G-50 column (10 mL gel/mL of solution) equilibrated in SAS (pH 4.4). Collect and combine fractions with an absorbance >1.0 at 280 nm.
6. Add DTT (3.8 mg/mL of solution) and stir at room temperature for 20 min.
7. Pass the solution down a Sephadex G-50 column (10 mL gel/mL of solution) equilibrated in HBS (pH 7.4). Collect and combine fractions with an absorbance >1.0 at 280 nm. In cases where the yield is low it may be necessary to collect fractions with lower absorbances as well.
8. Determine an approximate IgG concentration from the absorbance at 280 nm (mg/mL = A_{280}/1.35).
9. Add an aliquot of the IgG solution to an aliquot of the liposome solution (75 µg protein per µmol of lipid). Stir at room temperature for 16 h.
10. Pass the mixture down a Sepharose CL-4B column (10 mL gel/mL solution). Fractions containing liposomes are easily detected against a dark background because of the turbidity of the solution.
11. Determine the coupling efficiency using protein and lipid assays.
12. Determine the size of the conjugates using a particle sizer, if one is available.

3.3. Carbohydrate Modification

Oxidation of the carbohydrate functions on antibodies with sodium periodate generates aldehyde groups that can be used to conjugate the proteins to liposomes. This approach is attractive since it is known that procedures that derivatize antibody amino groups or disulfide bonds may damage some of the antigen-binding sites, whereas modification of the carbohydrate functions do not *(37)*. Glycosylation on antibodies occurs at various points on the structure depending on the antibody class. Most applications are likely to use IgG-type antibodies, which are glycosylated in the CH_2 region of the heavy chain. Modification of these functions therefore does not directly affect antigen binding, although it is known to affect the structure of the Fc chains and various effector functions of IgG, such as complement activation and Fc receptor binding.

Very few reports have been made using this approach to synthesize antibody–liposome conjugates. Early work ***(38)*** showed that simple acyl hydrazides in liposomes could be used to conjugate periodate-oxidized IgM in good yield. More recently, a lipid-PEG-hydrazide derivative has been reported that was used to couple oxidized IgG to liposomes ***(34)***, albeit in low yield. Subsequent work has reported optimized conditions that resolve these problems and minimize liposome–liposome crosslinking ***(10)***. We have recently reported a variation of these procedures in which a protected thiol-hydrazide crosslinker was used to thiolate oxidized IgG and subsequently to effect coupling to maleimide derivatized liposomes ***(36)***.

3.3.1. PDPH Coupling Protocol

The following is the procedure that we have developed to thiolate IgG through modification of the carbohydrate functions. The procedure is very similar to the SPDP protocol after the initial thiolation process (*see* **Note 3**).

1. Prepare liposomes incorporating 1% MPB-DSPE as described above. This should be done not more than 1 d prior to use.
2. Prepare a solution of IgG (10–20 mg/mL) in PBS or HBS at pH 7.4.
3. Prepare a 0.1 *M* suspension of 3-(2-pyridyldithio)propionic acid hydrazide (PDPH) in ethanol.
4. Dissolve sodium metaperiodate (1 mg/mL of final volume) in 0.3 mL distilled water.
5. Immediately add the antibody solution to the sodium periodate solution and stir at room temperature for 1 h.
6. Pass the solution down a Sephadex G-50 column (10 mL gel/mL of solution) equilibrated in SAS (pH 4.4). Collect and combine fractions with an absorbance >1.0 at 280 nm.
7. Add an aliquot of the PDPH suspension (vortex immediately prior to taking the aliquot)(40 µL PDPH stock per milliliter of IgG solution). Stir at room temperature for 5 h.
8. Pass the solution down a Sephadex G-50 column (10 mL gel/mL of solution) equilibrated in SAS (pH 4.4). Collect and combine fractions with an absorbance >1.0 at 280 nm.
9. Add DTT (3.8 mg/mL of solution) and centrifuge at 3000 rpm at room temperature for 20 min.
10. Pass the supernatant down a Sephadex G-50 column (10 mL gel/mL of solution) equilibrated in HBS (pH 7.4). Collect and combine fractions with an absorbance >1.0 at 280 nm. In cases where the yield is low it may be necessary to collect fractions with lower absorbances as well.
11. Determine an approximate IgG concentration from the absorbance at 280 nm (mg/mL = A_{280}/1.35).
12. Add an aliquot of the IgG solution to an aliquot of the liposome solution (75 µg protein per µmol of lipid). Stir the reaction mixture at room temperature for 16 h.

13. Pass the mixture down a Sepharose CL-4B column (10 mL gel/mL solution). Fractions containing liposomes are easily detected against a dark background because of the turbidity of the solution.
14. Determine the coupling efficiency using protein and lipid assays.
15. Determine the size of the conjugates using a particle sizer, if one is available.

3.4. Disulfide Modification

Treatment of antibodies, or abbreviated antibodies, such as Fab or $F(ab')_2$ fragments, with reducing agents, such as DTT or 2-mercaptoethylamine, cleaves disulfide bonds in the antibody. These sulfhydryl groups have been used to conjugate the antibodies to maleimide-derivatized liposomes ***(39–41)***. However, it is important to remember that some of the disulfide bonds are responsible for maintaining the structure of the variable region and damage to these by reducing agents may result in some loss of binding activity.

3.5. Indirect Methods

Liposomes may be targeted indirectly using antibodies if a secondary receptor–ligand system is used. For example, liposome–avidin conjugates have been shown to effectively target biotinylated antibodies ***(42,43)*** that have previously been bound to antigens on cells. A similar approach has frequently been used with protein A/G-liposome conjugates targeted to the Fc chain of antibodies ***(44,45)***. The latter approach is not suitable for in vivo applications because of competition from the general IgG population. These systems can be used to generate liposome–antibody conjugates before targeting ***(46)***, although these are likely to be more complex than direct conjugation procedures.

3.6. Analytical Protocols

Reliable lipid and protein analysis of the prepared antibody–liposome conjugate is essential for proper characterization and subsequent interpretation of results obtained in the application of the conjugates. In addition, we strongly advise that the liposome conjugate size be determined with a particle sizer, if one is available, since liposome size plays such an important role in the pharmacokinetics of the system in vivo.

3.6.1. Lipid Analysis

Lipid analysis is typically performed either by incorporating a nonexchangeable radiolabel marker, such as (^{14}C) or (^{3}H) cholesteryl hexadecyl ether (CHE), into the vesicle membrane, or by analyzing the phosphate content and extrapolating the result according to the original composition of the vesicles. Both approaches assume that the label concentration and vesicle composition do not change on vesicle preparation or subsequent manipulation. The phosphate assay is carried out as follows:

1. All glassware used in the assay should be washed with phosphate-free detergents.
2. Prepare a molybdate solution by dissolving 4.4 g of ammonium molybdate in 2000 mL of distilled water and 40 mL sulfuric acid.
3. Prepare Fiske reagent as follows: Dissolve 150 g sodium bisulfite and 5 g sodium sulfite in 1 L of distilled water. Add 2.5 g 1-amino-2-naphthol-4-sulfonic acid and warm to 40°C until the material has dissolved (keep the solution covered during this process). Allow to stand at room temperature overnight in the dark. Filter to remove the crystalline material formed and store in a dark bottle.
4. Prepare a 2 m*M* sodium phosphate standard solution.
5. Add aliquots (0, 25, 50, 100 µL) of the standard to 16 × 150-mm Pyrex test tubes.
6. Add aliquots in triplicate of the sample to be tested to 16 × 150-mm Pyrex test tubes. The aliquots should contain 100–200 nmol of phosphate. It may be necessary to dilute some of the sample prior to the assay.
7. Add 0.7 mL of perchloric acid to each tube.
8. Close the tube by placing a marble on the top. Digest the sample on heating blocks set at 180°C for 1 h (**Caution!** Hot perchloric acid is highly corrosive and potentially explosive. This procedure should be carried out in a suitable fumehood behind a blast shield).
9. Allow the tubes to cool. Add 7 mL of the molybdate solution followed by 0.7 mL of the Fiske reagent. Vortex to thoroughly mix the solutions.
10. Heat the tubes in a boiling water bath for 30 min. Cool to room temperature.
11. Assay the samples at 815 nm in a spectrometer using a standard curve (0, 50, 100, 200 nmol).

3.6.2. Sulfhydryl Analysis

Sulfhydryl content can be determined directly by using any thiol assay, typically by using Ellman's reagent, although other more sensitive procedures exist ***(47)***, or indirectly by release of some reporter molecule on deprotection of crosslinkers. For example, many reports use the absorbance of 2-thiopyridone at 343 nm after treatment of pyridyldithio-modified proteins with DTT. Extreme caution should be used when interpreting results from these indirect methods since in our experience treatment of antibodies with DTT, even under mild conditions, results in subtle changes in the baseline absorbance at 343 nm and consequent erroneous estimates of thiol content.

1. Add 60 µL Ellman's reagent (4 mg/mL solution in HBS) to 600 µL aliquots of a control and the samples.
2. Allow to stand at room temperature for 20 min.
3. Measure the absorbance at 280 nm in a spectrophotometer using the control to zero the instrument.
4. Determine the thiol content using the formula $SH = 1.1\ A_{412}/13{,}600\ C_p$, where A_{412} is the absorbance at 412 nm, C_p is the protein concentration, and SH is the number of thiol equivalents.

3.6.3. Protein Analysis

Protein is assayed using a modification of the protocol for the micro BCA protein assay kit from Pierce. Pierce claims that some lipids may interfere with the assay; therefore, it is advisable to periodically assay control liposomes to ensure that the protein assay is returning reliable results. This is particularly important when using new lipid formulations or buffers. Interference from lipids should not exceed 1 μg protein/μmol lipid.

1. Prepare a set of bovine serum albumin (BSA) standards containing 2.5, 5.0, 7.5, 10.0, 15.0, and 20.0 μg of protein in 5 mL tubes.
2. Add aliquots of the sample containing 0.333 μmol of lipid to 5-mL tubes in triplicate (if there is enough material).
3. Add 100 μL of 5% Triton X-100 solution to the standards and samples.
4. Dilute the standards and samples with distilled water to a final volume of 1.0 mL.
5. Prepare the assay reagent according to the instructions in the Pierce micro BCA assay kit.
6. Add 1.0 mL of the assay reagent to the standards and samples. Cap the tubes and vortex to ensure complete mixing.
7. Incubate the tubes in a water bath at 60°C for 1 h.
8. Cool the tubes to room temperature.
9. Determine the protein content of the samples using a standard curve obtained at 562 nm.

3.7. Application of Steric Barrier Molecules

A major problem in the preparation of protein–liposome conjugates is the tendency of the conjugates to crosslink, resulting in the formation of large aggregates that are cleared rapidly in vivo. The crosslinking effect is intrinsic to all reactions involving multivalent ligands and can be controlled by reducing the number of reactive functions on the liposome or antibody (for example, reducing the degree of thiolation when using SPDP, or by reducing the initial protein/lipid ratio). These approaches, however, generally require extensive optimization and result in lower coupling efficiencies. We have recently developed an alternative approach to this problem ***(48)***, where we use PEG-lipids to control the crosslinking reactions. PEG-lipids were originally developed to reduce liposome clearance in circulation ***(49,50)***, an effect that is achieved by reducing the absorption of serum proteins onto liposome surfaces. These proteins are believed in part to mediate clearance of the liposomes by the reticuloendothelial system ***(51,52)***. Access to the liposome surface in the presence of PEG-lipids is strongly affected by size; consequently, single antibodies may penetrate the polymer cloud and react at the surface but the much larger antibody-PEGylated liposome conjugates will not, because of steric interactions between the PEG-lipids incorporated into the membranes. Small size increases are typically observed when coupling

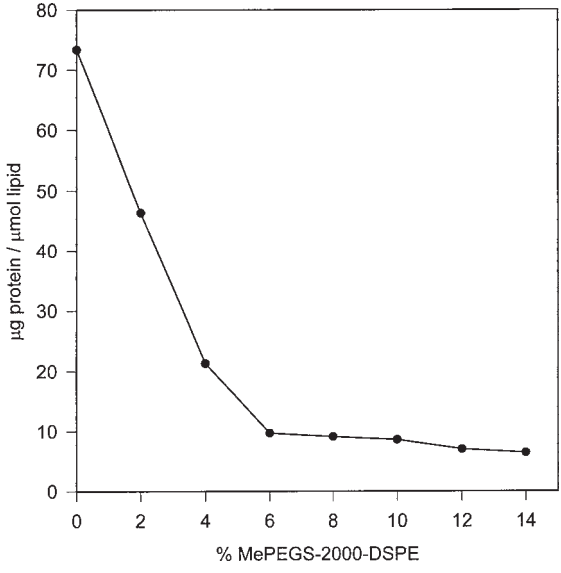

Fig. 3. The coupling efficiency of SPDP-modified human IgG to DSPC/Chol/MPB-DSPE/*N*-(2'-(ω-monomethoxypolyethyleneglycol$_{2000}$)succinoyl)-1,2-distearoyl-*sn*-glycero-3-phosphoethanolamine (MePEGS-2000-DSPE) (54-n:45:1:n) liposomes. The initial protein-to-lipid ratio was 150 µg protein/µmol lipid.

antibodies to PEGylated liposomes. In a typical case we see 100 nm vesicles increasing to ~120 nm in the presence of PEG. Similar 100 nm vesicles without PEG-lipids form aggregates with measured average diameters of 160 nm or larger.

Although this technique is a powerful method for preventing aggregation, it does have its drawbacks. First, since PEG-lipids reduce total protein binding at equilibration in vivo because of steric inhibition, they will also limit the amount of antibody that can be conjugated to the liposomes. The coupling efficiency is reduced in a manner dependent on PEG-lipid concentration and polymer size, typically reaching a base level at about 6% PEG-lipid (based on a PEG molecular weight of 2000) with 100 nm vesicles. The effect of PEG-lipid concentration is illustrated in **Fig. 3**. A second problem with the use of PEG-lipids in antibody targeting systems is the tendency of the polymer to act as a steric barrier, which inhibits interaction with the cellular target sites ***(53)***. Again, this is dependent on PEG-lipid concentration, with binding levels reaching control levels at 6% PEG-lipid.

We typically use 2% PEG-lipids (PEG molecular weight 2000) in our antibody-conjugated formulations in order to control aggregation but still retain reasonable binding and coupling efficiency.

More recently, PEG-lipids have been used as tethers between liposomes and antibodies ***(10,30,34)*** (*see* **Fig. 4**). The basic idea behind this approach has

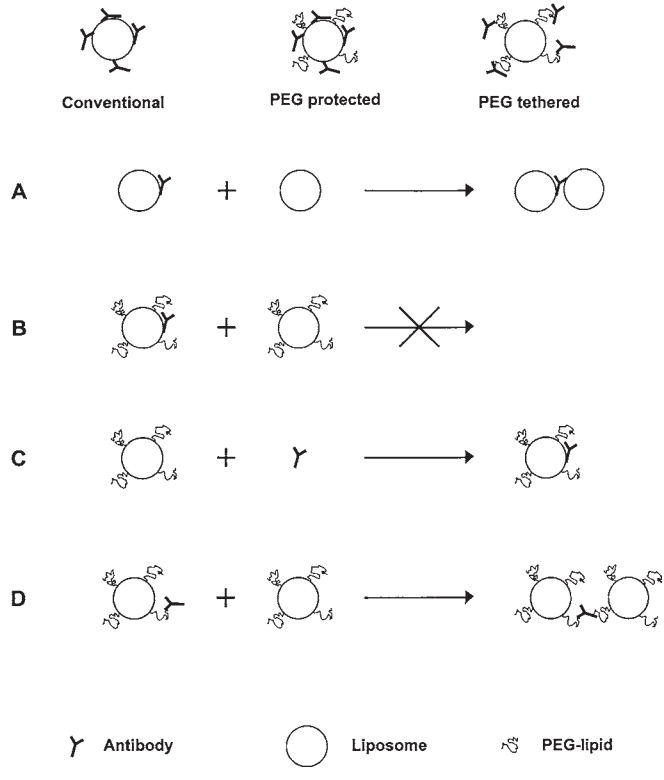

Fig. 4. Aggregation reactions associated with different classes of antibody–liposome conjugates. **(A)** Antibody–liposome conjugates may react further with other liposomes to form aggregates. **(B)** The presence of PEG-lipids prevents these crosslinking reactions through steric hindrance. **(C)** Individual proteins may penetrate the PEG cloud to react with the liposome surface. **(D)** Antibodies tethered on the distal end of PEG may react with the distal ends of PEG molecules on a second liposome, resulting in crosslinking.

been to remove the targeting vector from the surface to allow free access to binding sites but at the same time to retain the protection from serum proteins afforded by PEG lipids. Systems of this type are likely to suffer from the same crosslinking reactions as non-PEGylated systems, although not as severely since some steric inhibition will be effected by the PEG tether. Careful optimization has been shown in at least one case to minimize these problems ***(10)***.

4. Notes

1. Numerous techniques for the preparation of liposomes have been described. Typical procedures involve the hydration of lipid mixtures in buffer, resulting in the formation of large multilamellar vesicles (MLV). These are of limited use in

active targeting applications, particularly in vivo, because a strong correlation between size and clearance by the reticuloendothelial system exists. Larger vesicles tend to be cleared more rapidly than small vesicles. Unilamellar vesicles are prepared from MLVs in a number of ways. Sonication of MLVs results in the smallest thermodynamically stable vesicles, typically about 25 nm in size ***(22)***. These vesicles tend to be unstable and may not retain their contents, which is a significant problem when developing a drug-delivery system. Large unilamellar vesicles (LUV) can be prepared by extrusion of MLVs through sizing filters ***(23)***. Extrusion techniques result in narrow size distributions, which are determined primarily by the particular pore size of the filter used. Optimal formulation and clearance characteristics in vivo are typically observed with 100 nm vesicles, which are most conveniently prepared by extrusion methods. Other methods for liposome preparation include reverse-phase ***(24)*** and detergent dialysis ***(25)*** techniques.

Several important considerations should be addressed when coupling antibodies to liposomes. Activated lipids that are incorporated into liposomes often have limited stability and consequently the liposomes should be used as soon as possible after preparation. Suitable care should also be taken when selecting buffers, pH, and temperature to ensure compatibility with the lipids being used. Most applications of targeted systems are likely to involve liposomes that encapsulate some drug. In these situations it is important to select conditions that do not facilitate leakage or degradation of the drug. A commonly used method of drug encapsulation involves active loading of liposomes using pH gradients ***(26)***, typically with a low pH inside and neutral conditions outside the vesicle. Once drugs have been loaded in this manner it is important to maintain the pH gradient; consequently, the coupling reaction should be carried out before or after loading depending on the pH required for coupling.

2. It should be noted that in our experience the liposome conjugation efficiency varies for different MAbs; therefore, it is necessary to perform preliminary experiments to determine optimal initial antibody/lipid ratios. Other factors affecting conjugation efficiency include maleimide concentration, degree of thiolation, presence of PEG-lipids, and initial reagent concentration.
3. It is important to note that oxidation of IgG makes the protein more prone to aggregation and adhesion to surfaces. It is essential that the modified IgG be centrifuged prior to liposome coupling to ensure removal of aggregated IgG since this material is extremely difficult to remove after coupling and will interfere with assays used to characterize the final conjugate. Further, it appears important that the protein not be subjected to concentration procedures after the oxidation step since these often lead to the loss of large quantities of the antibody. The procedure is best suited for solutions with concentrations in the range 10–20 mg/mL, preferably 15 mg/mL, since this allows complete processing without the intervention of concentration steps.

References

1. Boman, N. L., Bally, M. B., Cullis, P. R., Mayer, L. D., and Webb, M. S. (1995) Encapsulation of vincristine in liposome reduces toxicity and improves anti-tumour efficacy. *J. Liposome Res.* **5,** 523–541.

2. Boman, N. L., Cullis, P. R., Bally, M. B., and Mayer, L. D. (1995) Preclinical and clinical activity of liposomal doxorubicin, in *Liposomes in Biomedical Applications*, HAP Academic Publishers, pp. 85–103.
3. Murohara, T., Margiotta, J., Phillips, L. M., Paulson, J. C., DeFrees, S., Zalipsky, S., Guo, L. S., and Lefer, A. M. (1995) Cardioprotection by liposome-conjugated sialyl Lewisx-oligosaccharide in myocardial ischaemia and reperfusion injury. *Cardiovas. Res.* **30,** 965–974.
4. Shimada, K., Kamps, J. A. A. M., Regts, J., Ikeda, K, Shiozawa, T., Hirota, S., and Scherphof, G. L. (1997) Biodistribution of liposomes containing synthetic galactose-terminated diacylglyceryl poly(ethyleneglycol)s. *Biochim. Biophys. Acta* **1326,** 329–341.
5. Hsu, M. J. and Juliano, R. L. (1982) Interactions of liposomes with the reticuloendothelial system. II: Nonspecific and receptor-mediated uptake of liposomes by mouse peritoneal macrophages. *Biochim. Biophys. Acta* **720,** 411–419.
6. Vidal, M., Saite-Marie, J., Philippot, J. R., and Bienevue, A. (1987) The influence of coupling transferrin to liposomes or minibeads on its uptake and fate in leukemic L2C cells. *FEBS Lett.* **216,** 159–163.
7. Nishiya, T. and Sloan, S. (1996) Interaction of RGD liposomes with platelets. *Biochem. Biophys. Res. Commun.* **224,** 242–245.
8. Zalipsky, S., Mullah, N., Harding, J. A., Gittleman, J., Guo, L., and DeFrees, S. A. (1997) Poly(ethylene glycol)-grafted liposomes with oligopeptide or oligosaccharide ligands appended to the termini of the polymer chains. *Bioconj. Chem.* **8,** 111–118.
9. Lee, R. J. and Low, P. S. (1994) Delivery of liposomes into cultured KB cells via folate receptor-mediated endocytosis. *J. Biol. Chem.* **2651,** 3198–3204.
10. Harding, J. A., Engbers, G. M., Newman, M. S., Goldstein, N. I., and Zalipsky, S. (1997) Immunogenicity and pharmacokinetic attributes of poly(ethylene glycol)-grafted immunoliposomes. *Biochim. Biophys. Acta* **1327,** 181–192.
11. Phillips, N. C. and Dahman, J. (1995) Immunogenicity of immunoliposomes: reactivity against species-specific IgG and liposomal phospholipids. *Immunology Letters* **45,** 149–152.
12. Tardi, P. G., Swartz, E. N., Harasym, T. O., Cullis, P. R., and Bally, M. B. (1999) An immune response to ovalbumin covalently coupled to liposomes is prevented when liposomes used contain doxorubicin. *J. Immun. Meth.*, submitted.
13. Heath, T. D. and Martin, F. J. (1986) The development and application of protein-liposome conjugation techniques. *Chem. Phys. Lipids* **40,** 347–358.
14. Hashimoto, Y., Endoh, H., and Sugawara, M. (1993) Chemical methods for the modification of liposomes with proteins or antibodies, in *Liposome Technology*, vol. 3, CRC, Boca Raton, FL, pp. 41–49.
15. Leserman, L. D., Machy, P., and Barbet, J. (1993) Covalent coupling of monoclonal antibodies and protein A to liposomes: specific interaction with cells in vitro and in vivo, in *Liposome Technology*, vol. 3, CRC, Boca Raton, FL, pp. 29–40.
16. Torchilin, V. P. (1993) Immobilization of specific proteins on liposome surface: systems for drug targeting, in *Liposome Technology*, vol. 3, CRC, Boca Raton, FL, pp. 75–90.

17. Hermanson, G. T., Mallia, A. K., and Smith, P. K. (1992) *Immobilized Affinity Ligand Techniques.* Academic, San Diego, CA.
18. Coulter, A. and Harris, R. (1983) Simplified preparation of rabbit Fab fragments *J. Immunol. Meth.* **59,** 199–203.
19. Rousseaux, J., Rousseaux-Prevost, R., and Bazin, H. (1983) Optimal conditions for the preparation of Fab and F(ab')2 fragments from monoclonal IgG of different rat IgG subclasses. *J. Immunol. Meth.* **64,** 141–146.
20. Aragonal, D. and Leserman, L. D. (1986) Immune clearance of liposomes inhibited by an anti-F_c receptor antibody in vivo. *Proc. Natl. Acad. Sci. USA* **83,** 2699–2703.
21. Winter, G. and Milstein, C. (1990) Man-made antibodies. *Nature* **349,** 293–299.
22. Huang, C. H. (1969) Studies on phosphatidylcholine vesicles: formation and physical characteristics. *Biochemistry* **8,** 344–352.
23. Hope, M. J., Nayar, R., Mayer, L. D., and Cullis, P. R. C. (1993) Reduction of liposome size and preparation of unilamellar vesicles by extrusion techniques, in *Liposome Technology*, vol. 1, CRC, Boca Raton, FL, pp. 123–139.
24. Szoka, F. and Papahadjopoulos, D. (1978) Procedure for preparation of liposomes with large internal aqueous space and high capture by reverse-phase evaporation. *Proc. Natl. Acad. Sci. USA* **75,** 4194–4198.
25. Szoka, F. and Papahadjopoulos, D. (1980) Comparative properties and methods of preparation of lipid vesicles (liposomes). *Ann. Rev. Biophys. Bioeng.* **9,** 467–508.
26. Mayer, L. D., Madden, T. M., Bally, M. B., and Cullis, P. R. (1993) pH gradient-mediated drug entrapment of liposomes, in *Liposome Technology*, vol. 2, CRC, Boca Raton, FL, pp. 27–44.
27. Endoh, H., Suzuki, Y., and Hashimoto, Y. (1981) Antibody coating of liposomes with l-ethyl-3-(3-dimethylaminopropyl)carbodiimide and the effect on target specificity. *J. Immun. Meth.* **44,** 79–85.
28. Dunnick, J. K., McDougall, I. R., Aragon, S., Goris, M. L., and Kriss, J. P. (1975) Vesicle interactions with polyamino acids and antibody: in vitro and in vivo studies. *J. Nuclear Med.* **16,** 483–487.
29. Huang, A., Huang, L., and Kennel S. J. (1980) Monoclonal antibody covalently coupled with fatty acid. A reagent for in vitro liposome targeting. *J. Biol. Chem.* **255,** 8015–8018.
30. Maruyama, K., Takizawa, T., Yuda, T., Kennel, S. J., Huang, L., and Iwatsuru, M. (1995) Targetability of novel immunoliposomes modified with amphipathic poly(ethylene glycol)s conjugated at their distal terminals to monoclonal antibodies. *Biochim. Biophys. Acta* **1234,** 74–80.
31. Barbet, J., Machy, P., and Leserman, L. O. (1981) Monoclonal antibody covalently coupled to liposomes: specific targeting to cells. *J. Supramolec. Struct. Cell. Biochem.* **16,** 243–258.
32. Jones, M. N. and Hudson, M. J. (1993) The targeting of immunoliposomes to tumour cells (A431) and the effects of encapsulated methotrexate. *Biochim. Biophys. Acta* **1152,** 231–242.
33. Schwendener, R. A., Trub, T., Schott, H., Langhals, H., Barth, R. F., Groscurth, P., and Hengartner, H. (1990) Comparative studies of the preparation of

immunoliposomes with the use of two bifunctional coupling agents and investigation of in vitro immunoliposome-target cell binding by cytofluorometry and electron microscopy. *Biochim. Biophys. Acta* **1026,** 69–79.
34. Hansen, C. B., Kao, G. Y., Moase, E. H., Zalipsky, S., and Allen, T. M. (1995) Attachment of antibodies to sterically stabilized liposomes: evaluation, comparison and optimization of coupling procedures. *Biochim. Biophys. Acta* **1239,** 133–144.
35. Carlsson, J., Drevin, H., and Axen, R. (1978) Protein thiolation and reversible protein–protein conjugation. *Biochem. J.* **173,** 723–737.
36. Ansell, S. M., Tardi, P. G., and Buchkowsky, S. S. (1996) 3-(2-pyridyldithio)-propionic acid hydrazide as a cross-linker in the formation of liposome-antibody conjugates. *Bioconj. Chem.* **7,** 490–496.
37. Domen, P. L., Nevens, J. R., Mallia, K., Hermanson, G. T., and Klenk, D. C. (1980) Site directed immobilization of proteins. *J. Chromatogr.* **510,** 293–302.
38. Chua, M. M, Fan, S. T., and Karush, F. (1984) Attachment of immunoglobulin to liposomal membrane via protein carbohydrate. *Biochim. Biophys. Acta* **800,** 291–300.
39. Shahinian, S. and Silvius J. R. (1995) A novel strategy affords high yield coupling of antibody Fab' fragments to liposomes. *Biochim. Biophys. Acta* **1239,** 157–167.
40. Kirpotin, D., Park, J. W., Hong, K., Zalipsky, S., Li W. L., Carter, P., Benz, C. C., and Papahadjopoulos, D. Sterically stabilized anti-HER2 immunoliposomes: design and targeting to human breast cancer cells in vitro. *Biochemistry* **36,** 66–75.
41. Martin, F. J. and Papahadjopoulos, D. (1982) Irreversible coupling of immunoglobulin fragments to preformed vesicles. An improved method for liposome targeting. *J. Biol. Chem.* **257,** 286–288.
42. Longman S. A., Cullis, P. R., and Bally, M. B. (1995) A model approach for assessing liposome targeting in vivo. *Drug Delivery* **2,** 156–165.
43. Longman, S. A., Cullis, P. R., Choi, L., de Jong, G., and Bally, M. (1995) A two step targeting approach for delivery of doxorubicin loaded liposomes to tumour cells in vivo. *Cancer Chem. Pharmacol.* **36,** 91–101.
44. Matthay, K. K., Heath, T. D., Badger, C. C., Bernstein, I. D., and Papahadjopoulos, D. (1986) Antibody-directed liposomes: comparison of various ligands for association, endocytosis, and drug delivery. *Cancer Res.* **46,** 4904–4910.
45. Machy, P. and Leserman, L. D. (1983) Small liposomes are better than large liposomes for specific drug delivery in vitro. *Biochim. Biophys. Acta* **730,** 313–320.
46. Lougrey, H. L., Bally, M. B., and Cullis, P. R. (1987) A novel-covalent method of attaching antibodies to liposomes. *Biochim. Biophys. Acta* **901,** 157–160.
47. Singh, R., Blattler, W. A., and Collinson, A. R. (1993) An amplified assay for thiols based on reactivation of papain. *Anal. Biochem.* **213,** 49–56.
48. Harasym, T. O., Tardi, P., Longman, S. A., Ansell, S. M., Bally, M. B., Cullis, P. R. C., and Choi, L. S. L. (1995) Poly(ethylene glycol)-modified phospholipids prevent aggregation during covalent conjugation of proteins to liposomes. *Bioconj. Chem.* **6,** 187–194.
49. Allen, T. M., Hansen, C., Martin, F., Redemann, C., and Yau-Young, A. (1991) Liposomes containing synthetic lipid derivatives of polyethylene glycol show prolonged circulation half-lives in vivo. *Biochim. Biophys. Acta* **1066,** 29–36.

50. Allen, T. M., Agrawal, A. K., Ahmad, I., I., Hansen, C. B., and Zalipsky, S. (1994) The use of glycolipids and hydrophilic polymers in avoiding rapid uptake of liposomes by the mononuclear phagocyte system. *J. Liposome Res.* **4,** 1–26.
51. Chonn, A. and Cullis, P. R. (1992) Ganglioside G_{MI} and hydrophilic polymers increase liposome circulation times by inhibiting the association of blood proteins. *J. Liposome Res.* **2,** 397–410.
52. Devine, D. V. and Marjan, J. M. (1997) The role of immunoproteins in the survival of liposomes in the circulation. *Crit. Rev. Ther. Drug Carrier Systems* **14,** 105–131.
53. Klibanov, A. L., Maruyama, K., Beckerleg, A. M., Torchilin, V. P., and Huang, L. (1991) Activity of amphipathic poly(ethylene glycol)5000 to prolong the circulation time of liposomes depends on the liposome size and is unfavourable for immunoliposome linking to target. *Biochim. Biophys. Acta* **1062,** 142–148.
54. Matthay, K. K., Abai, A. M., Cobb, S., Hong, K., Papahadjopoulos, D., and Straubinger R. M. (1989) Role of ligand in antibody-directed endocytosis of liposomes by human T-leukemia cells. *Cancer Res.* **49,** 4879–4886.

5

Folate as a Targeting Device for Proteins Utilizing Folate Receptor-Mediated Endocytosis

Robert J. Lee and Philip S. Low

1. Introduction

Folic acid (M_r = 441, **Fig. 1**) is a vitamin essential for *de novo* nucleotide synthesis and one-carbon metabolism. The ability to acquire folate, therefore, is important to the viability of proliferating cells.

The cellular transport of folate is mediated by the reduced folate carrier and/or the folate-binding protein, also known as the folate receptor. The folate receptor is a glycosyl-phosphatidylinositol (GPI)-anchored 38-kDa membrane glycoprotein with high affinity for folic acid ***(1)***. The receptor facilitates folate uptake via receptor-mediated endocytosis ***(2)***. Two membrane-associated isoforms of the folate receptor have been identified, type-α and type-β ***(3)***. These two receptor subtypes share approx 70% sequence homology, but exhibit different specificity for folates and folate analogs ***(3)***. Type-α receptors invariably have higher affinities for the various forms of folate than type-β, although both isoforms have very high affinity for folic acid itself (with K_d values for folic acid at 1 and 1.7 n*M*, respectively) ***(3)***.

1.1. Folate Receptor as a Tumor Marker

In humans, the type-α folate receptor is expressed in measurable quantities only in certain epithelial tissues ***(3)***. The same receptor, however, may be significantly overexpressed in malignant tissues of epithelial origin, including many types of carcinomas ***(3)***. In contrast, type-β folate receptor is found at very low levels in almost all types of normal tissues and is commonly elevated in malignancies of nonepithelial origin ***(3)***. In tissue culture, only the type-α receptor is usually detected, regardless of the tissue origin of the cell ***(3)***.

From: *Methods in Molecular Medicine, Vol. 25: Drug Targeting: Strategies, Principles, and Applications*
Edited by: G. E. Francis and C. Delgado

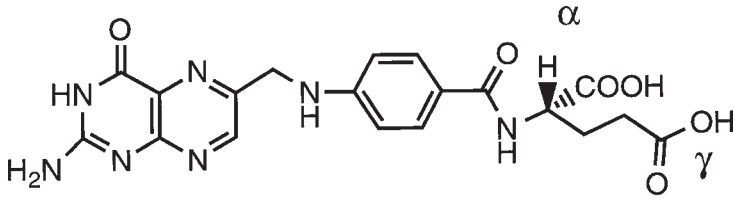

Fig. 1. Folic acid.

Weitman et al. showed by Northern blot analysis and immunoassays that the folate receptor (type-α) has a very restricted normal tissue distribution ***(4)***. Highly elevated receptor expression was only found in the choroid plexus and malignant tissues ***(4)***. Garin-Chesa et al. showed by immunohistochemical staining that 52 of 56 ovarian tumor samples displayed highly elevated folate receptor (type-α) expression ***(5)***. Receptor overexpression was also found in 10 of 11 endometrial, 6 of 27 colorectal, 11 of 53 breast, 6 of 18 lung, 9 of 18 renal cell, 4 of 5 brain metastases, and 3 of 21 neuroendocrine carcinomas ***(5)***.

1.2. Receptor-Mediated Endocytosis of Folate Conjugates

The folate receptor facilitates the cellular uptake of folate and 5-methyltetrahydrofolate via receptor-mediated endocytosis at caveolae (caveolae are plasma membrane invaginations distinct from the classical clathrin-coated pits) ***(6)***. It has been hypothesized that the folate receptor is functionally coupled to an anion transporter to mediate cytosolic folate delivery by a process defined as potocytosis ***(6)***. More recent studies suggest that folate receptor endocytosis also occurs at clathrin-coated pits ***(7)***. Studies by Low and coworkers at Purdue University have shown that folate conjugates are also taken up by the folate receptor ***(8–10)***, but not by the reduced folate carrier. **Figure 2** illustrates an endocytic pathway of the type envisioned for folate conjugates. Unfortunately, the subcellular transport pathway of the folate conjugates has been only partially characterized and may well be affected by the properties of the molecule attached to folate.

Because of its overexpression in many types of human tumors and its relative absence in most normal tissues, the folate receptor constitutes a promising target for tumor-specific drug delivery. Folate derivatization has been successfully exploited in the targeted delivery of proteins ***(8,11–13)***, liposomes ***(9,14)***, γ imaging agents ***(9,10,14–18)***, oligodeoxyribonucleotides ***(19)***, and gene transfer vectors ***(20)***. As a targeting ligand, folic acid has many important advantages compared to tumor-specific monoclonal antibodies (MAbs):

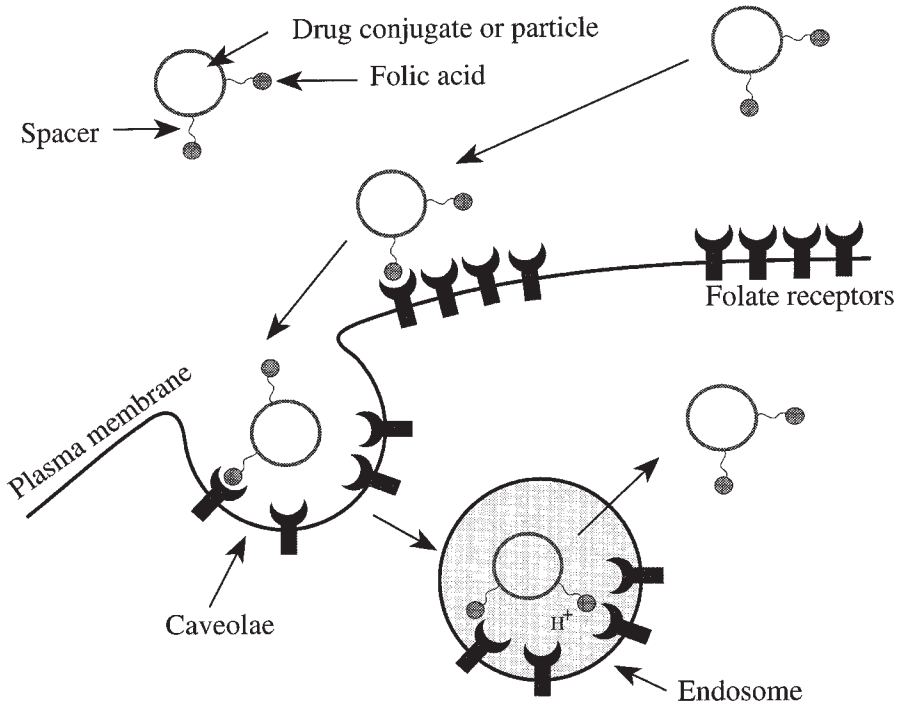

Fig. 2. Mechanism for receptor-mediated cellular uptake of folate conjugates.

1. Low immunogenicity (host immune responses against the MAbs or their fragments may prevent the repeated clinical use of antibody conjugates);
2. Rapid extravasation, tumor permeation, and systemic clearance (because of its low molecular weight, folate conjugates diffuse readily throughout a tumor mass, leading to improved tumor-to-background tissue target ratios);
3. Resistance to denaturation resulting from adverse storage and reaction conditions, such as exposure to organic solvents and repeated freezing and thawing;
4. Simple and defined conjugation chemistry, which leads to lower cost of conjugate production and easier quality control; and
5. High specificity for tumors, high occurrence of folate–receptor-positive tumors, and high receptor affinity.

In the remainder of this chapter, we will focus on the methods for using folate to target protein molecules to folate receptor-bearing cells. Proteins successfully delivered into tumor cells include bovine serum albumin, bovine immunogamma globulin, horseradish peroxidase, ribonuclease A, ferritin, the plant toxin momordin, diphtheria toxin catalytic domain, and a fragment of pseudonomous exotoxin. Protein–folate conjugates are usually synthesized by reacting activated folate with the amino groups on proteins to form an amide linkage, as described in the **Subheading 3.**

2. Materials

2.1. Preparation of Activated Folate

All chemicals should be reagent grade and can be obtained from major suppliers, e.g., Sigma Chemical Co. (St. Louis, MO).

1. Folic acid (light sensitive).
2. 1-Ethyl-3-(3-dimethylaminopropyl)carbodiimide (EDC) (moisture sensitive, store at –20°C).
3. Dicyclohexylcarbodiimide (DCC) (moisture sensitive).
4. *N*-Hydroxysuccinimide (NHS).
5. Dimethylsulfoxide (DMSO).
6. Triethylamine.
7. Acetone.
8. Diethylether.

2.2. Synthesis, Purification, and Characterization of Protein Conjugates

1. Conjugation buffer: 0.1 *M* Na_2HPO_4, 0.1 *M* boric acid, pH 8.5.
2. Phosphate-buffered saline (PBS): 136.9 m*M* NaCl, 2.68 m*M* KCl, 8.1 m*M* Na_2HPO_4, 1.47 m*M* KH_2PO_4, pH 7.4.
3. Size exclusion column: PD-10 desalting column can be obtained from Bio-Rad Laboratories (Hercules, CA). Alternatively, a Sephadex G-25 column from Pharmacia (Piscataway, NJ) may be used.

3. Methods

3.1. Preparation of Protein–Folate Conjugate

Folic acid (**Fig. 1**) must be conjugated to proteins via its γ carboxyl group in order to retain its receptor-binding activity. Whereas random activation of the two carboxyls (α and γ) leads to protein conjugation at both carboxyls, sufficient active (γ carboxyl) conjugates are usually produced to achieve efficient receptor-mediated targeting (*see* **Note 1**). For the preparation of protein conjugates, folate is usually attached to the ε-amino group of a lysine via an amide linkage. The folate carboxyl can either be activated by first reacting with EDC or converted to a more stable intermediate, i.e., the NHS-ester. The EDC-activated folic acid hydrolyzes rapidly in aqueous solution, especially at neutral or basic pH. Therefore, EDC–folate should be freshly prepared before use. Since the yield of the conjugation reaction is diminished by the hydrolysis of the activated folate, an excess of EDC–folate is usually required to achieve sufficient protein derivatization. The NHS-ester of folic acid (NHS-folate), however, is less sensitive to hydrolysis, has a higher pH optimum for protein derivatization, and is stable when stored as a dry powder.

3.1.1. Protein Conjugation Using EDC-Activated Folate

The following is a recommended procedure:

1. Dissolve folic acid in anhydrous DMSO.
2. Then add fivefold molar excess of EDC.
3. Shield the reaction mixture from light and allow it to incubate for 1 h at room temperature to generate EDC-activated folate.
4. Dissolve the desired protein in conjugation buffer.
5. Then add EDC-activated folate (in DMSO) to the protein solution under stirring.
6. The coupling reaction is complete in 30 min at room temperature.

The number of folates attached per protein depends on the size and lysine content of the protein. Usually, in order to achieve a conjugation number of 1–2 folates per protein, a five to eightfold molar excess of EDC-folate should be used in the coupling reaction. However, a test reaction is recommended to establish this ratio for any new protein (*see* **Note 2**).

3.1.2. Protein Conjugation Using NHS-Activated Folate

3.1.2.1. Synthesis of NHS-Activated Folate

An NHS-ester of folate can be synthesized as follows:

1. Dissolve 5 g folic acid and 2.5 g NHS in 100 mL DMSO and 2.5 mL triethylamine at 40°C with stirring.
2. Add 4.7 g DCC to the solution under stirring.
3. Stir the reaction mixture in the dark at room temperature overnight.
4. Remove the insoluble byproduct, dicyclohexylurea, by filtration of the reaction mixture through a glass wool plug.
5. Reduce the volume of the reaction mixture by ~60% by distillation at 40°C under vacuum generated by an oil pump.
6. Precipitate NHS–folate by addition of 10× volume of 30% acetone/70% diethylether.
7. Pellet the precipitate by centrifugation at 10,000*g* for 10 min and wash three times with 30% acetone/70% diethylether by resuspending the product and then collecting it by centrifugation.
8. Dry the pellet in air for 1 h followed by drying under vacuum.
9. The NHS–folate powder can be stored in the dark at 4°C for at least 6 mo without significant loss of activity.

3.1.2.2. Protein Derivatization Using NHS–Folate

The following is a typical procedure:

1. Dissolve the desired protein in the conjugation buffer, for example, at a concentration of 2 mg/mL (*see* **Subheading 2.**).
2. Dissolve NHS–folate at a concentration of ~1 mg/mL in DMSO and add 0.05 vol to the protein solution under stirring.
3. The coupling reaction is complete in 2 h under stirring at room temperature.

The protein coupling efficiency using NHS–folate is much higher than EDC-activated folate. Up to 80% of the folate may be attached to the protein. A test reaction should be performed to determine the coupling efficiency of any particular protein.

3.3. Purification and Characterization of the Conjugates

3.3.1. Purification of the Protein-Folate Conjugate

Because of its smaller molecular size, folic acid and any other byproducts generated during the protein coupling reaction can be conveniently removed from the protein–folate conjugates by size-exclusion chromatography (*see* **Note 3**). Either a PD-10 desalting column or a Sephadex G-25 column may be used for this purpose. The following is a sample procedure using a PD-10 column, a 10-mL prepacked polyacrylamide-based desalting column.

1. Pre-equilibrate a PD-10 column in PBS by passing 15 mL of the buffer through the column.
2. After the buffer has eluted from the column, load up to 2 mL of the crude reaction mixture containing the protein–folate conjugate onto the column.
3. When the sample has completely entered the column, layer 1.5 mL of PBS on the top of the column.
4. Discard the eluate up to this point.
5. Then add an additional 3.0 mL PBS to the column and elute the protein conjugate as a yellow band. The free folic acid appears as a more slowly moving yellow band.

3.3.2. Characterization of the Protein–Folate Conjugate

The protein content of the folate conjugate may be determined by a standard protein assay, e.g., using the bicinchoninic acid (BCA) assay (available from Pierce Chemical Co., Rockford, IL) ***(8)***. The number of folates attached to the protein can be determined by measuring ultraviolet absorption of the conjugate solution at 363 nm. The extinction coefficient for folate at that wavelength in PBS is 6197 ***(8)***. The number of folates per protein can, therefore, be calculated by the following equation:

$$\text{Folates/protein} = \frac{\text{(OD at 363 nm/6197) / [Protein concentration (mg/mL) / molecular weight of the protein]}}{} \quad (1)$$

Receptor-binding activity of the protein–folate conjugate can be determined by competitive displacement of a known quantity of [^{3}H]-labeled folic acid (available from NEN Life Science Products, Boston, MA) from receptor-expressing cells. Alternatively, if the protein can be labeled with a fluorescent probe (e.g., fluorescein isothiocyanate), its uptake by folate receptor-bearing cells can be monitored by fluorescence microscopy ***(8)***.

4. Notes

1. Because the preferred γ carboxyl is more sterically accessible, random carbodiimide activation of folic acid usually yields a ~70:30 ratio of γ carboxyl: α carboxyl-derivatized protein.
2. Usually, 1–2 folates per protein give good folate–receptor-targeting activity. Excessive folate derivatization may result in protein denaturation and/or loss of biological activity.
3. Folic acid has a tendency to form aggregates in aqueous solution that may elute from a gel-filtration column at a higher molecular weight. Furthermore, folate may associate noncovalently with lipid binding proteins, such as bovine serum albumin, and may compete with folate receptor-mediated uptake of the folate conjugates. Performing the column separation of the protein–folate conjugate at elevated pH, e.g., at pH 9.0–11.0, may facilitate the removal of free folate from the protein conjugate. Alternatively, a longer desalting column may be employed to eliminate all free folate from the protein preparation.
4. To avoid protein crosslinking, the protein concentration in the conjugation reaction should be kept below 50 mg/mL.

References

1. Antony, A. C. (1992) The biological chemistry of folate receptors. *Blood* **79,** 2807–2820.
2. Kamen, B. A., Wang, M. T., Streckfuss, A. J., Preyea, X., and Anderson, R. G. (1988) Delivery of folates to the cytoplasm of MA104 cells is mediated by a surface receptor that recycles. *J. Biol. Chem.* **263,** 13,602–13,609.
3. Ross, J. F., Chaudhuri, P. K., and Ratnam, M. (1994) Differential regulation of folate receptor isoforms in normal and malignant tissues in vivo and in established cell lines. *Cancer* **73,** 2432–2443.
4. Weitman, S. D., Lark, R. H., Coney, L. R., Fort, D. W., Frasca, V., Zurawski, V. R., Jr., and Kamen, B. A. (1992) Distribution of the folate receptor GP38 in normal and malignant cell lines and tissues. *Cancer Res.* **52,** 3396–3401.
5. Garin-Chesa, P., Campbell, I., Saigo, P. E., Lewis, J. L. J., Old, L. J., and Rettig, W. J. (1993) Trophoblast and ovarian cancer antigen LK26. Sensitivity and specificity in immunopathology and molecular identification as a folate-binding protein. *Am. J. Pathol.* **142,** 557–567.
6. Rothberg, K. G., Ying, Y. S., Kolhouse, J. F., Kamen, B. A., and Anderson, R. G. (1990) The glycophospholipid-linked folate receptor internalizes folate without entering the clathrin-coated pit edocytic pathway. *J. Cell Biol.* **110,** 637–649.
7. Rijnboutt, S., Jansen, G., Posthuma, G., Hynes, J. B., Schornagel, J. H., and Strous, G. J. (1996) Endocytosis of GPI-linked membrane folate receptor-α. *J. Cell Biol.* **132,** 35–47.
8. Leamon, C. P. and Low, P. S. (1991) Delivery of macromolecules into living cells: a method that exploits folate receptor endocytosis. *Proc. Natl. Acad. Sci. USA* **88,** 5572–5576.
9. Lee, R. J. and Low, P. S. (1994) Delivery of liposomes into cultured KB cells via folate receptor-mediated endocytosis. *J. Biol. Chem.* **269,** 3198–3204.

10. Wang, S., Lee, R. J., Mathias, C. J., Green, M. A., and Low, P. S. (1996) Synthesis, purification, and tumor cell uptake of Gallium-67–deferoxamine-folate, a potential radiopharmaceutical for tumor imaging. *Bioconj. Chem.* **7,** 56–62.
11. Leamon, C. P. and Low, P. S. (1992) Cytotoxicity of momordin-folate conjugates in cultured human cells. *J. Biol. Chem.* **267,** 24,966–24,971.
12. Leamon, C. P. and Low, P. S. (1993) Membrane folate-binding proteins are responsible for folate-protein conjugate endocytosis into cultured cells. *Biochem. J.* **291,** 855–860.
13. Leamon, C. P., Pastan, I., and Low, P. S. (1993) Cytotoxicity of folate-pseudonomas exotoxin conjugates towards tumor cells. Contribution of translocation domain. *J. Biol. Chem.* **25,** 24,847–24,854.
14. Lee, R. J. and Low, P. S. (1994) Folate-mediated tumor cell targeting of liposome-entrapped doxorubicin in vitro. *Biochim. Biophys. Acta* **1233,** 134–144.
15. Wang, S., Luo, J., Lantrip, D. A., Waters, D. J., Mathias, C. J., Green, M. A., Fuchs, P. L., and Low, P. S. (1997) Design and Synthesis of ^{111}In-DTPA-Folate for Use as a Tumor-Targeted Radiopharmaceutical. *Bioconj. Chem.*, submitted.
16. Mathias, C. J., Waters, D. J., Wang, S., Low, P. S., and Green, M. A. (1997) Indium-111 labeled Indium(III)-DTPA-folate as a radiopharmaceutical for targeting tumor-associated folate receptors: the effect of tumor size on targeting selectivity and radiochemical analysis of excreted tracer, in *12th International Symposium on Radiopharmaceutical Chemistry*, Uppsala, Sweden.
17. Mathias, C. J., Wang, S., Waters, D. J., Turek, J. J., Low, P. S., and Green, M. A. (1997) Indium-111–DTPA-folate as a radiopharmaceutical for targeting tumor-associated folate binding protein (FBP), in *Society of Nuclear Medicine 44th Annual Meeting*, San Antonio, Texas.
18. Mathias, C. J., Wang, S., Lee, R. J., Waters, D. J., Low, P. S., and Green, M. A. (1996) Tumor-selective radiopharmaceutical targeting via receptor-mediated endocytosis of gallium-67–deferoxamine-folate. *J. Nucleic Med.* **37,** 1003–1008.
19. Wang, S., Lee, R. J., Cauchon, G., Gorenstein, D. G., and Low, P. S. (1995) Delivery of antisense oligonucleotides against the human epidermal growth factor receptor into cultured KB cells with liposomes conjugated to folate via polyethyleneglycol. *Proc. Natl. Acad. Sci. USA* **92,** 13,318–13,322.
20. Lee, R. J. and Huang, L. (1996) Folate-targeted, anionic liposome-entrapped polylysine-condensed DNA for tumor cell-specific gene transfer. *J. Biol. Chem.* **271,** 8481-8487.

6

Preparation of Recombinant RNase Single-Chain Antibody Fusion Proteins

Dianne L. Newton and Susanna M. Rybak

1. Introduction

Selective cytotoxicity is an important goal of specific drug targeting. Toward this end, toxins isolated primarily from higher plants and bacteria have been coupled to monoclonal antibodies (MAbs) and evaluated for their clinical efficacy in cancer, AIDS, and immunological diseases ***(1,2)***. Immune responses against murine monoclonal antibodies MAbs ***(3,4)*** and antitoxin antibodies have been detected in both animals and humans treated with immunotoxins (ITs) ***(5–7)*** and present a major obstacle to the successful application of this technology. Although development of humanized antibodies have alleviated some of these effects (***8***, and references therein), the toxins themselves remain a problem. Consequently, the identification of human proteins to be used as components of immunoconjugates is highly desirable.

Some members of the human RNaseA superfamily of proteins are known to have host defense activities (reviewed in **ref. *9***). These include, for example, two of the eosinophil cytotoxic granular proteins, eosinophil cationic protein (ECP), and eosinophil-derived neurotoxin (EDN) ***(10)***. Angiogenin, a protein 65% homologous to pancreatic RNase ***(11,12)*** that was originally isolated on the basis of its angiogenic activity ***(13)***, is a potent inhibitor of protein synthesis in the rabbit reticulocyte lysate ***(14)*** and when injected into *Xenopus* oocytes ***(15)***. We have therefore sought to fuse RNases to MAbs to evaluate their usefulness as immunotoxins ***(16,17)***.

The genes for human angiogenin fused to a chimeric mouse/human antibody gene ***(18)*** and human EDN ***(19)*** or angiogenin ***(20)*** fused to a single-chain antibody (sFv) formed immunofusions directed against the human transferrin receptor that specifically killed human cells expressing that receptor. During the course of these studies, we found that both the enzymatic activ-

From: *Methods in Molecular Medicine, Vol. 25: Drug Targeting: Strategies, Principles, and Applications*
Edited by: G. E. Francis and C. Delgado

ity of the RNase as well as the binding affinity of the sFv must be considered in designing the fusion proteins. For the chimeras described here, the RNase is fused to the 5' end of the sFv. This configuration is effective for RNases, such as EDN ***(19)***, angiogenin ***(20)***, and human pancreatic RNase ***(21)***. The internal orientation of the sFv must also be considered, i.e., heavy chain variable region (V_H)-linker-light chain variable region (V_L) or V_L-linker-V_H. The nature of the linker connecting the V_H and V_L domains together can impact on the activity of the fusion protein. Linkers need to be long enough to span the distance between the V_L and V_H domains and still allow free association between the V_L and V_H domains without intercalating between them and interfering with binding. We have tried the rigid linker described by Bird et al. ***(22)*** and the more flexible Gly-Gly-Gly-Gly-Ser $(GGGGS)_3$ linker described by Houston et al. ***(23)*** and have found the $(GGGGS)_3$ linker to provide our sFv with the highest binding affinity for the receptor ***(20)***. Additionally, the activity and stability of the RNase-sFv fusion protein is substantially increased when there is a short (13 amino acid) spacer connecting the RNase to the sFv ***(20)***. The lack of an intervening sequence results in a fusion protein that is less stable and is less active in RNase activity, receptor binding activity, and cell kill activity. The materials, methods, and experimental details of constructing RNase-based immunoconjugates that may have applicablilty for cancer therapy are described.

2. Materials

2.1. Construction of the RNase-sFv Gene

1. Genes encoding the sFv and RNase of interest.
2. Oligonucleotides (primers) purified on oligonucleotide purification cartridges (OPC) (Cruachem, Inc., Dulles, VA) (*see* **Note 1**).
3. Vector, pET-11d, or appropriate pET vector (Novagen, Madison, WI) (*see* **Notes 2** and **6**).
4. Appropriate restriction enzymes.
5. Thermal cycling polymerase chain reaction (PCR) machine and reagents for performing PCR; GeneAmp PCR Reagent Kit (Perkin-Elmer, Foster City, CA).
6. Agarose and NuSieve 3:1 Agarose (FMC BioProducts, Rockland, ME) and appropriate gel electrophoresis apparatus.
7. GeneClean II (Bio 101 Inc., La Jolla CA).
8. Rapid DNA Ligation Kit (Boerhinger Mannheim, Indianapolis, IN).
9. Competent bacteria: XL1-Blue (Stratagene La Jolla, CA) (*see* **Note 13**), BL21(DE3) (Novagen, Madison, WI) (*see* **Note 19**).
10. Bacterial shaker, temperature 27° and 37°C.
11. DNA isolation kits: Wizard Plus Minipreps DNA Purification System (Promega, Madison, WI), Qiagen Plasmid Maxi kit (Qiagen, Chatsworth, CA).
12. Luria broth (LB): 10 g tryptone, 5 g yeast extract, and 5 g NaCl in 1 L; autoclave 20 min.

13. Ampicillin, 100 mg/mL in H_2O (Sigma, St. Louis, MO).
14. LB/amp plates: 10 g tryptone, 5 g yeast extract, 5 g NaCl, and 16 g agar in 1 L H_2O; autoclave 20 min, let cool to 55°C, and add 1 mL 100 mg/mL ampicillin. Pour 20–25 mL in a 100-mm Petri dish.

2.2. Analysis of RNase-sFv Protein Expression

1. 20 mg/mL Rifampicin in methanol (Sigma).
2. 120 mg/mL Isopropyl-β-D-thiogalactopyranoside (IPTG), (0.5 *M*) in H_2O (Gibco-BRL, Grand Island, NY).
3. 4–20% Sodium dodecyl (SDS)-polyacrylamide gels (Novex, San Diego, CA) or equivalent.

2.3. Sequence Analysis of the Plasmid That Expresses the RNase-sFv Gene

1. Sequenase II kit (US Biochemical Corp., Cleveland, OH) and sequencing apparatus.

2.4. Growth of RNase-sFv Recombinant Protein *in* Escherichia coli *Bacteria*

1. Superbroth: 12 g tryptone, 24 g yeast extract, 6.3 g glycerol, 12.5 g K_2HPO_4, 3.8 g KH_2PO_4 in 1 L H_2O; autoclave 20 min. After cooling, add 20 mL of 25% glucose (250 g/L H_2O, sterile filtered) and 10 mL 80 m*M* $MgSO_4$ (9.75 g $MgSO_4 \cdot 7\ H_2O$/500 mL H_2O, sterile filtered).

2.5. Preparation of Inclusion Bodies

1. Sucrose buffer: 30 m*M* Tris-HCl, pH 7.5, containing 20% sucrose (200 g/L H_2O) and 1 m*M* EDTA. This solution should be kept at 4°C.
2. Janke & Kunkel (KG Staufen, West Germany) polytron tissumizer or similar model with a 100 mm long × 10 mm OD shaft.
3. Tris-EDTA buffer; 50 m*M* Tris-HCl, pH 7.5, containing 20 m*M* EDTA.
4. Lysozyme (Sigma), 5 mg/mL in H_2O, prepared just before use.
5. Triton X-100 (Sigma), 25% solution in H_2O; use low heat to solubilize.
6. 292.25 g/L 5 *M* NaCl; use low heat to solubilize.

2.6. Solubilization of Inclusion Bodies

1. Solubilization buffer; 0.1 *M* Tris-HCl, pH 8.0, containing 6 *M* guanidine-HCl (573.2 g/L) and 2 m*M* EDTA.
2. Dithioerythritol (Sigma).
3. BCA protein assay reagent (Pierce Chemical Co., Rockford, IL).

2.7. Renaturation of Recombinant Protein

1. Renaturation buffer; 0.1 *M* Tris-HCl, pH 8.0, containing 0.5 *M* L-arginine-HCL (105 g/L) (Sigma), 8 m*M* glutathione, oxidized (GSSG) (Boehringer Mannheim) (4.9 g/L), and 2 m*M* EDTA, chilled to 10°C.

2. Dialysis buffer: 10× concentration containing 0.2 *M* Tris-HCl, pH 7.5, and 1 *M* urea (60 g/L) (**Note:** Do not make more than 2–3 h in advance; *see* **Note 42**); dilute to 1× just before needed.
3. 60 L Vat equipped with a lower valve for easy emptying.

2.8. Chromatography of the Refolded Recombinant Protein

1. Heparin-sepharose, CM-Sephadex C-50 (Pharmacia LKB Biotechnology Inc., Piscataway, NJ).
2. Ni^{2+}-NTA agarose (Qiagen).
3. Chromatography buffer: 20 m*M* Tris-HCl, pH 7.5, containing 10% glycerol and the same buffer containing 1 *M* NaCl or the same buffer containing the following concentrations of imidazole: 40, 50, 60, 100, 200, 300, 400, and 500 m*M*.
4. FPLC system consisting of program controller, two pumps (one for each of buffer A and B), a mixer, seven-port M-7 valve, assorted sample loops, UV monitor, and fraction collector (optional).
5. Mono S HR 5/5 cation exchange or Mono Q HR 5/5 anion exchange FPLC column (Pharmacia LKB Biotechnology) (optional).
6. Buffer A: 20 m*M* Tris-HCl, pH 7.5. Filter and degas before use.
7. Buffer B: 20 m*M* Tris-HCl, pH 7.5, 1 *M* NaCl. Filter and degas before use.

3. Methods

3.1. Construction of the RNase-sFv Gene

1. Design four oligonucleotide primers to incorporate the following (*see* **Note 1**):
   a. An appropriate restriction site at the 5' end of the RNase gene to facilitate cloning (**Fig. 1**, primer A) (*see* **Note 3**).
   b. A spacer (amino-acid residues 48–60 of fragment B of staphylococcal protein A) onto the 3' end of the RNase gene to separate the RNase and the sFv genes (**Fig. 1**, primer B) (*see* **Note 4**).
   c. The same spacer described in **step b** (amino-acid residues 48–60 of fragment B of staphylococcal protein A) onto the 5' end of the sFv gene (**Fig. 1**, primer C) (*see* **Note 5**).
   d. The termination signal, 3–6 histidyl residues for affinity purification and the appropriate restriction site (here described as a *Bam*HI site) to facilitate cloning at the 3' end of the sFv gene (**Fig. 1**, primer D) (*see* **Note 6**).
2. Set up two separate PCR amplifications for modification of the RNase gene and the sFv gene (**Fig. 1**, PCR#1 and PCR#2) (*see* **Note 7**). In the first reaction use the RNase gene and primers A and B; in the second reaction use the sFv gene and primers C and D. The reaction mixture should contain the following per 100 µL reaction volume:

   Final concentration

   1X reaction buffer (10 m*M* Tris-HCl, pH 8.3, 50 m*M* KCl, 1.5 m*M* $MgCl_2$).
   100 µ*M* of each of the nucleotides.
   0.5 µL AmpliTaq DNA polymerase.

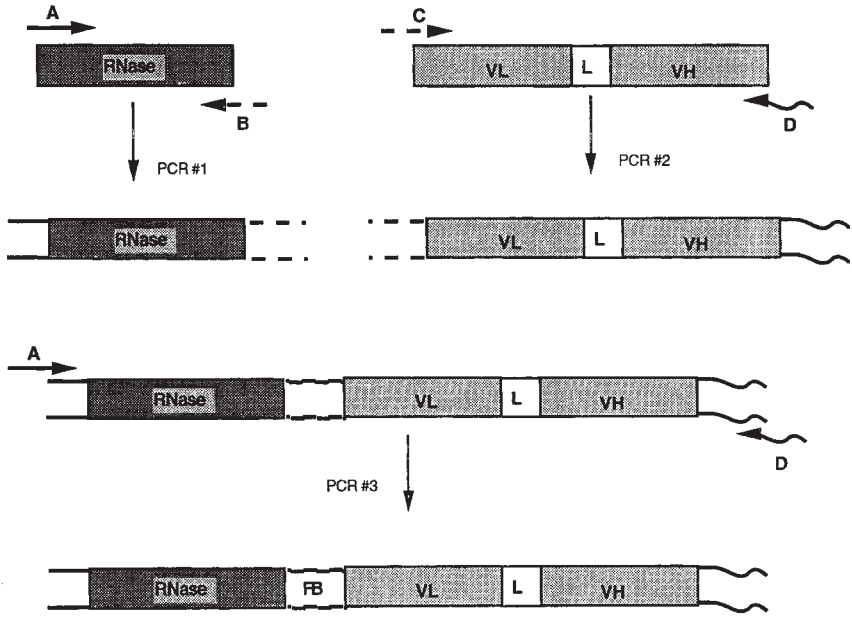

Fig. 1. Gene splicing by overlap extension. Primers A and D (5' end of the RNase gene and 3' end of the sFv gene, respectively) include restriction sites appropriate for cloning into the pET-11d vector. The gene for the RNase is fused to the gene for the sFv by attaching complementary sequences encoding the FB fragment of staphylococcal protein A (FB) to the 3' end of the RNase gene (primer B) and the 5' end of the sFv gene (primer C). This allows the two genes to be spliced together by overlap extension (SOEing, ***24***). The RNase and sFv genes were first amplified separately by PCR (PCR#1 and PCR#2, respectively) before they were purified, mixed, and subjected to a further 20 cycles of PCR (PCR#3) using primers A and D. The assembled gene was then cloned into the pET-11d vector. VL, light chain variable region; VH, heavy chain variable region; L, peptide linker $(GGGGS)_3$; FB, fragment B of staphylococcal protein A.

0.5 µ*M* primer A or C.
0.5 µ*M* primer B or D.
500 ng/mL DNA.

The following PCR conditions have been found to be optimal with many RNase genes: 94°C, 5 min before beginning the program; then 94°C, 1 min (denaturation); 55°C, 2 min (annealing); 72°C, 2 min (extension) for 20 cycles (*see* **Note 8**).

3. Analyze the PCR reaction by 1% agarose to determine the size of the amplified material (*see* **Note 9**).
4. Purify the DNA of interest to remove the primers and other components of the PCR reaction by using the GeneClean procedure according to the manufacturer's instructions, extracting the washed resin with 15 µL sterile H_2O.

5. The two genes that have been modified to share a segment of identical sequence or overlap sequence are now ready to be spliced together using the PCR technique of splicing by overlap extension (SOEing) ***(24)*** (*see* **Note 10** and PCR #3, **Fig. 1**). Use the original 5' primer from the RNase PCR reaction (primer A) and the 3' primer from the sFv PCR reaction (primer D). As discussed in **Note 10**, the FB gene segment added to the RNase gene and the sFv gene will hybridize together, allowing the two genes to be spliced together. One PCR tube is set up as described in **Subheading 3.1., step 2** using 1–2 µL of each of the purified genes from **Subheading 3.1., step 4** as the DNA source and primers A and D. Reaction conditions remain as described in **Subheading 3.1., step 2** (*see* **Note 11**).
6. Repeat **steps 3** and **4** above.
7. Restrict 7.5 µL of the spliced DNA (save the remaining DNA in case this step needs to be repeated) and 0.5 µg of vector using 1 µL of each of the restriction enzymes in the appropriate restriction enzyme buffers (final volume 100 µL). Incubate at 37°C overnight.
8. Purify the restricted DNA and vector using the GeneClean procedure according to the manufacturer's instructions. Extract the washed resin with 15 µL sterile H_2O.
9. Ligate the two restricted DNAs (RNase-sFv and vector) together using the Rapid DNA Ligation Kit according to manufacturer's instructions (*see* **Note 12**).
10. Transform XL1-Blue competent bacteria with 1–2 µL of the ligated DNA according to the manufacturer's instructions. Streak LB agar plates containing 100 µg/mL ampicillin with ≤100 µL reaction and incubate overnight at 37°C (*see* **Notes 13** and **14**).
11. Pick six individual colonies and inoculate each into 5 mL LB containing 100 µg/mL ampicillin. Incubate with shaking (225 rpm) overnight at 37°C (*see* **Note 15**).
12. Before isolating the plasmid, streak a fresh LB agar plate containing 100 µg/mL ampicillin with a streak of the bacterial solution from **Subheading 3.1., step 11** and incubate the plate overnight at 37°C (*see* **Note 16**). Centrifuge the remaining bacterial solution and isolate the plasmids containing the insert using the Wizard Plus Minipreps DNA Purification System or any other similar product following the manufacturer's instructions.
13. Restrict the miniplasmid preparations with the appropriate restriction enzyme and identify those plasmids containing inserts of the proper size by running the restriction digests on an agarose gel (*see* **Note 17**).

3.2. Analysis of RNase-sFv Protein Expression

1. Transform BL21(DE3)-competent bacteria with each of the plasmids that express an insert of the appropriate size (*see* **Notes 18** and **19**).
2. Streak the entire reaction (≤100 uL) onto LB agar plates containing 100 µg/mL ampicillin and incubate overnight at 37°C.
3. Place 2.5 mL LB containing 100 µg/mL ampicillin into 15 mL tubes. Add one colony from each plate and incubate shaking at 225 rpm at 37°C.
4. When the OD_{600} nm reaches 0.5–0.6, induce the bacteria with 0.4 m*M* IPTG and incubate for 30 min at 37°C with shaking (*see* **Note 20**).

5. Add 25 µL rifampicin to a final concentration of 200 µg/mL and continue incubation at 37°C, shaking for 90 min (*see* **Note 21**).
6. Remove 100 µL of the bacterial solution, centrifuge, aspirate the supernatant, add 25 µL protein denaturing dye, resuspend the pellet, boil 5 min, and analyze on a 4–20% SDS polyacrylamide gel (*see* **Note 22**).
7. Identify plasmids that express a protein of the appropriate molecular weight.

3.3. Sequence Analysis of the Plasmid that Expresses the RNase-sFv Gene

1. Inoculate 250–500 mL LB containing 100 µg/mL ampicillin with a streak of bacteria from the miniplate prepared in **step 12, Subheading 3.1.**
2. Grow the bacteria overnight with shaking at 37°C.
3. Isolate the plasmid using the Qiagen Plasmid Maxi kit or a similar product according to the manufacturer's instructions.
4. Restrict the purified plasmid with the appropriate restriction enzyme and analyze the digest by agarose gel electrophoresis (*see* **Note 23**).
5. Sequence the insert to ensure that no PCR errors occurred using Sequenase II or a similar product according to the manufacturer's instructions.

3.4. Growth of RNase-sFv Recombinant Protein in E. coli Bacteria

1. Transform BL21(DE3)-competent bacteria with the plasmid containing the RNase-sFv (*see* **Note 24**).
2. Streak the entire reaction (≤100 µL) onto LB agar plates containing 100 µg/mL ampicillin and incubate overnight at 37°C (*see* **Note 25**).
3. Prepare 1 L Superbroth as described in **Subheading 2.4.** into at least a 2-L Erlenmeyer or bacterial shake flask. Add 1 mL 100 mg/mL ampicillin (*see* **Note 26** and **27**).
4. Place 10 mL of the Superbroth onto the LB/amp plate containing the colonies. Using a tissue culture cell scraper, gently scrape the colonies off and add them to 1 L of Superbroth.
5. Grow overnight at 27°C, shaking at 225 rpm (*see* **Note 28**).
6. Raise the temperature to 37°C and induce with 0.8 m*M* IPTG for 1.5 to 3 h shaking at 225 rpm (*see* **Note 29**).
7. Centrifuge the bacteria at 8000*g* for 10–20 min at 4°C and store at –20°C if not ready to begin the extraction of the protein (*see* **Note 30**).

3.5. Preparation of Inclusion Bodies

1. Resuspend the pellet from a 1-L bacterial culture with 200 mL ice cold sucrose buffer and place on ice-for 10 min.
2. Centrifuge for 20 min at 8000*g* at 4°C.
3. Carefully pour off the supernatant and resuspend the pellet in 200 mL ice-cold H_2O. Place 25 mL into eight polypropylene tubes and place on ice for 10 min.
4. Centrifuge at 17,000*g* for 20 min at 4°C. Carefully pour off the supernatant (*see* **Note 31**).

5. Resuspend the pellet in each tube with 9 mL Tris-EDTA buffer using a Janke & Kunkel polytron tissumizer (or a similar model) equipped with a 100 mm long × 10 mm OD shaft and combine two tubes together such that each liter of original bacterial culture is now contained in four tubes.
6. Allow the tubes to stand at room temperature for 30 min.
7. Add 0.9 mL of 5 mg/mL lysozyme (final concentration 240 µg/mL)/18 mL tube and incubate at room temperature for 60 min, shaking occassionally.
8. Add 2.5 mL of 5 *M* NaCl and 2.5 mL of 25% Triton X-100 per tube, shaking after each addition (*see* **Note 32**). Incubate at room temperature for 30 min, shaking intermittently (*see* **Note 33**).
9. Centrifuge at 17,000*g* for 40 min at 4°C.
10. Carefully pour off the supernatant, resuspend the pellet in 15 mL Tris-EDTA buffer with the tissuemizer, and centrifuge again as in **step 9**. Repeat this three more times (*see* **Note 34**).
11. Store the washed inclusion body at –70°C until ready for solubilization.

3.6. Solubilization of Inclusion Bodies

1. Resuspend the inclusion body pellet using the tissumizer in a final volume of 10–20 mL solubilization buffer (*see* **Note 35**).
2. Incubate for 2 h or more at room temperature.
3. Centrifuge for 20 min at 4°C at 17,000*g* (*see* **Note 36**).
4. Determine the protein concentration of a 1:10 dilution of the supernatant (*see* **Note 37**).
5. Dilute the denatured protein with the solubilization buffer to a final concentration of 8 mg/mL (*see* **Note 38**).
6. Add dry DTE to a final concentration of 46.3 mg/mL (0.3 *M*) (*see* **Note 39**).
7. Incubate for 2 h or more at room temperature.

3.7. Renaturation of Recombinant Protein

1. Dilute the denatured sample 100 times with renaturation buffer that has been prechilled to 10°C (*see* **Note 40**).
2. Incubate the solution for 2–3 d at 10°C (*see* **Note 41**).
3. Dialyze the refolded protein extensively at 4°C against 10 times the volume of the renaturation solution. Change the dialysis buffer three times over a 24-h period (*see* **Note 42**).
4. Centrifuge the dialyzed solution for 20 min at 4°C at 8000*g* (*see* **Note 43**).

3.8. Chromatography of the Refolded Recombinant Protein

1. Apply the centrifuged renatured protein to a 4-mL CM-Sephadex C-50 or heparin sepharose column (*see* **Note 44**). Perform this step at 4°C.
2. Wash the column with 2 column volumes of chromatography buffer.
3. Elute the column with a 0–1.0 *M* NaCl gradient in the chromatography buffer (*see* **Note 45**).
4. Analyze 15–20 µL aliquots of the eluted protein on an SDS-polyacrylamide gel and pool the fractions containing the protein of interest.

5. At this stage, one of two different column chromatographic methods may be used. The best method for final purification needs to be determined for the protein of interest (*see* **Note 46**).

3.8.1. Method 1: Ni^{2+}-NTA Agarose

1. Prepare the sample by adding imidazole and Triton X-100 to final concentrations of 0.8 m*M* and 1%, respectively (*see* **Note 47**).
2. Apply the sample to 0.6 mL Ni^{2+}-agarose (per 320 mg of refolded protein as determined in **Subheading 3.6., step 4** (*see* **Note 48**).
3. Rotate the slurry end over end for ≥1 h at 4°C.
4. Collect the slurry as a column and wash with 10 mL 20 m*M* Tris-HCl, pH 7.5, containing 10% glycerol and 0.8 m*M* imidazole.
5. Step-elute the column with 2 column volumes of the same buffer made with 40, 50, 60, 100, 200, 300, 400, and 500 m*M* imidazole (*see* **Note 49**).
6. Analyze the fractions by SDS-gel electrophoresis and pool the appropriate tubes.
7. Determine the protein concentration using the BCA protein assay reagent (*see* **Notes 50** and **51**).

3.8.2. Method 2: Fast Protein Liquid Chromatography (FPLC)

1. Dialyze the sample against 20 m*M* Tris-HCl, pH 7.5, containing 10% glycerol overnight at 4°C.
2. Centrifuge the sample at 4°C for 10 min at 3000 rpm (*see* **Note 52**).
3. Apply the sample to a Mono S HR 5/5 column or Mono Q HR 5/5 column equilibrated with buffer A (*see* **Note 46**).
4. Elute the sample with a 30-min gradient between 0 and 80% buffer B with a final 10-min hold on 80% buffer B (*see* **Note 53**).
5. Analyze the fractions by SDS-gel electrophoresis and pool the appropriate tubes (*see* **Note 54**).
6. Determine the protein concentration either by using the BCA protein assay reagent (or equivalent) according to manufacturer's instructions or measuring the absorbance at 277 nm and assuming an extinction coefficient $E^{1\%}_{277} = 10.0$ (*see* **Notes 55** and **56**).

4. Notes

4.1. Construction of the RNase-sFv Gene

1. Primers should be purified before use to remove the short failure sequences. Neglecting to remove these sequences could result in incorrect priming or an error in the sequences being added to the gene. The disposable Oligo-Pak cartridges provide an effective and fast method for oligo purification.
2. The pET vector system designed by Studier et al. ***(25)*** is under the control of a T7 promoter. In the absence of T7 RNA polymerase, the target genes are maintained in a transcriptionally silent state, making these vectors ideal for the cloning of toxic genes. If some expression is detected, however; Novagen offers several bacterial hosts that will suppress basal expression levels even further (*see* **Note 19**).

3. Before incorporating the cloning restriction sites into the 5' and 3' primers, both the RNase and sFv should be analyzed for naturally occurring restriction sites within the genes. The use of two different restriction enzymes for cloning will facilitate the directional insertion of the gene into the vector and is preferred over a single restriction site. Several pET vectors are available for cloning. We chose the pET-11d vector because it contained the T7 *lac* promoter, which provides strong repression of any basal transcription of the target gene through the *lac* operator sequence, which is contained just downstream of the T7 promoter. This vector, however, contains an 11-amino-acid T7 tag sequence that would be fused to the N-terminus of the target gene. The tag sequence is provided to follow expression of the gene with an anti-T7 tag antibody. Because we did not want the tag sequence as part of our fusion protein, we rebuilt part of the vector, deleting those sequences coding for the tag. The modified vector sequence was incorporated into the 5' primer.The format for the 5' oligonucleotide (**Fig. 1**, primer A) is in the sense direction and is as follows:

   ATATA-**TCTAGA** -*AATAATTTTGTTTAACTTTAAGAAGGAGATATACAT*-ATG-first 21 bp of RNase gene, where the first 5 bp provide a clamp for the restriction enzyme, the bold sequence is an *Xba*I restriction site, and the italicized sequence is the modified vector sequence. The ATG before the RNase sequence provides the translation initiation site.
4. Design the oligonucleotide (**Fig. 1**, primer B) first in the sense direction and then convert it to the antisense direction. Sense direction 5' to 3': the last 21 bp of the RNase gene followed by the bp that codes for the spacer. The codons represent the FB spacer.

   21 bp RNase gene-GCCAAGAAACTGAACGACGCTCAGGCGCCGAAGAGTGAT Antisense direction from 5' to 3': ATCACTCTTCGGCGCCTGAGCGTCGT-TCAGTTTCTTGGC-21 bp RNase gene.
5. This oligonucleotide (**Fig. 1**, primer C) will contain the FB spacer complementary to that used in primer B (note **step 4**) followed by the first 21 bp of the sFv gene. It is made in the sense direction as follows: GCCAAGAAACTGAACGA-CGCTCAGGCGCCGAAGAGTGAT-21 bp sFv gene. The codons represent the FB spacer. Note that shorter primers may be made by splitting the overlap region such that there is a 17-bp overlap region between primers B and C. As reported by Horton ***(26)***, very short overlap regions can lead to inefficient SOEing reactions. This makes it necessary to increase the number of rounds of PCR, which then leads to an increase in the frequency of error.
6. Design the oligonucleotide in the sense direction and then convert it into the antisense direction. Sense direction: last 21 bp of the sFv gene-CATCACCAT (3 histidyl residues)-TAGTAG (2 termination codons)-GGATCC (*Bam*HI restriction site)-GCGCG (clamp).

   Antisense direction: CGCGCGGATCCCTACTAATGGTGATG-21 bp sFv gene. Two termination codons will ensure that there will be no readthrough of the gene into the vector. The histidyl residue tag will allow affinity purification by Ni^{2+}-NTA-agarose. Three histidines are routinely incorporated into the RNase-

sFv constructs described here. Some of the vectors available from Novagen have incorporated a histidine tag into the vector itself, which can be proteolytically cleaved from the purified protein. In our hands, the histidine tag serves two purposes; for final purification by affinity chromatography on Ni^{2+}- NTA-agarose and to stabilize the sFv. The sFvs lacking the His tag were less stable and degraded more readily than those containing the C-terminal His tail. For this reason, we chose to leave the three His residues on the 3' end of the sFv.

7. Qiagen-purified plasmids (or plasmids of equal or better purification) have been used with equal success.
8. The cycle number should be kept to a minimum (20 cycles) in order to avoid amplification of an error. High concentrations of template (approx 500 ng/100 µL) will help to minimize PCR error. The use of DNA polymerases, such as *Pfu* DNA polymerase (Stratagene), which exhibit low error rates, may obviate the need to sequence the final gene construct. However, if the fusion protein has low or no activity, the construct will need to be sequenced since no enzyme is totally error free.
9. Pancreatic RNase A type genes range between 300 and 400 base pairs. Small PCR products are best analyzed on a higher percentage of agarose, such as NuSieve:agarose in a 3:1 ratio.
10. Splicing by overlap extension is a simple method of fusing two genes together ***(24)***. It avoids needing correct or compatible restriction sites and eliminates one ligation reaction. In addition, it offers the advantage that new sequences of interest can be incorporated into the genes that are to be fused together. The FB spacer DNA sequence that was added onto the 3' end of the RNase gene and the 5' end of the sFv gene are complementary to each other, and thus will hybridize together in the SOEing reaction.
11. Occasionally, the reaction does not work well. The most common reason for not being able to SOE the two genes together is a mistake in the primer sequence itself or in the design of the primers. If the primers are correct, the starting DNA should be checked for yield to determine if there was a large loss resulting from the isolation procedure. We generally start with 10–12% of the volume of the DNA. This should be increased if the first reaction was poor. Higher concentrations of the DNA will help minimize the PCR error. In addition, 5–10 µL DMSO may be included in the PCR reaction to help in the amplification of the fusion gene. If this still does not improve the amplification, the PCR optimizer kit (Invitrogen, San Diego, CA) may be tried as well as varying the reaction times on the thermal cycler.
12. The optimal ratio of RNase-sFv DNA to vector DNA needs to be determined. If everything is performed as described above, 3 µL RNase-sFv to 0.5 µL vector is a good first approximation. If this does not result in any colonies, the ratio should be adjusted. If cloning into a single site, the vector should be dephosphorylated using calf intestinal phosphatase to prevent self-ligation.
13. Any host lacking the T7 RNA polymerase gene, such as XL1-Blue, JM109, HB101, and others, is suitable for generating the plasmid DNA.
14. The lack of colonies can result from the use of too little as well as too much of the ligation reaction. High concentrations of DNA can inhibit the transformation

reaction. Therefore, if no colonies result, the concentration of DNA should be both increased and decreased before deciding that the ligation reaction did not work. Perform the reaction as described by the manufacturer. The amount of bacteria used can be scaled down to 10 µL per reaction. When this is done, all the other components also need to be adjusted. The amount of ligated DNA (1–2 µL) is for a 25-µL reaction.

15. Place the plate containing the remaining colonies at 4°C for reuse if necessary.
16. This plate will contain a record of the miniprep DNA and is used to generate more DNA. One LB agar plate may be divided into six sections (one section for each miniprep).
17. Occassionally, the DNA containing the fusion gene will ligate into the vector destroying the restriction site. When repeated ligation and transformation of a good PCR product fails to yield any insert, other restriction enzymes should be used. PCR can also be used to check for the insert as follows: Pick a colony with a small tip. Touch the tip to a new LB plate containing 100 µg/mL ampicillin to have a record of the plasmid. Rinse the tip in 50 µL sterile H_2O, vortex, and boil for 5 min. Centrifuge the sample for 5 min in an eppifuge. Perform the PCR reaction as described in **Subheading 3.1., step 5**, except that the reaction volume is decreased to 50 µL. Use 10 µL of the colony mixture and 40 µL of the remaining reaction ingredients. Increase the cycle number to 35. Analyze the reaction by agarose gel.

4.2. Analysis of RNase-sFv Protein Expression

18. It is necessary to do a pilot protein expression using the plasmids that contain an insert of the correct size. Not all of these plasmids will express a protein of the appropriate size for such varied reasons as an inappropriate termination signal or a PCR error that results in an insertion or deletion of a base pair, resulting in a truncated or nonsense protein.
19. BL21(DE3) has been specifically engineered for the expression of toxic proteins ***(25)*** and is not used for DNA cloning (*see* **Note 13**). This strain carries the gene for T7 RNA polymerase, which is under the control of the *Lac* UV5 promoter. Expression is induced by the addition of IPTG. For extremely toxic proteins, any basal T7 RNA polymerase activity can be completely suppressed by expression in BL21(DE3)pLysS or pLysE, which contain the gene for lysozyme, an inhibitor of T7 RNA polymerase. The reaction is performed in Eppendorf tubes according to the manufacturer's directions. Total reaction volume can be decreased to 10.5 µL (10 µL bacteria and 0.5 µL DNA), adjusting the remaining components accordingly. Include a plasmid known to strongly express a protein of a different molecular weight as a positive control. If this is not possible, *see* **Note 20**.
20. If no control plasmid was included as described in **Note 19**, adjust the volume of the initial LB containing 100 µg/mL ampicillin to 5 mL and proceed as described until the induction step. At the induction step, remove 2.5 mL of the 5 mL and place into a separate tube so that the plasmid is now contained in two identical tubes. Induce one of the replicate tubes with IPTG and return both the induced

and uninduced tubes to the 37°C incubator and continue the experiment as described.

21. Rifampicin forms a very stable complex with bacterial RNA polymerases *(27)* and inhibits bacterial protein expression. Experiments by Studier et al. *(25)* demonstrate that BL21 is sensitive to rifampicin. Thus, in the presence of rifampicin proteins that may not express well can be detected with less interference by the bacterial proteins.
22. Compare those lanes expressing the protein of interest with lanes expressing the positive control plasmid or an uninduced control plasmid. If bacterial proteins migrate at the same molecular weight as the protein of interest, the density of the bands should be compared with the appropriate control.

4.3. Sequence Analysis of the Plasmid That Expresses the RNase-sFv Gene

23. Before sequencing, restrict the maxiprep DNA to ensure that the insert of the appropriate size is still contained in the plasmid. There is always a possibility that the initial streak contained additional plasmids that superceded the clone of interest.

4.4. Growth of RNase-sFv Recombinant Protein in E. coli Bacteria

24. As described in **Note 19**, the total reaction volume is 10.5 µL; 10 µL bacteria and 0.5 µL DNA. The reaction is performed in Eppendorf tubes per the manufacturer's directions and the remaining components are adjusted accordingly. Prepare one plate per desired liter of bacteria.
25. The plate should be almost confluent in colony density.
26. Superbroth is an enriched medium that will allow the cells to grow to a higher density than less rich broths, such as LB. Glucose is included to inhibit the activity of T7 RNA polymerase in the uninduced cells.
27. It is important to grow the bacteria in a large enough flask to allow for proper aeriation.
28. Growth may be carried out at 37°C, but must be monitored more closely because lysis can occur. When the OD_{600} nm reaches 1.0–1.2, the culture is ready for induction (usually within 4–5 h). Lysis is less of a problem when the bacteria are grown more slowly at 27°C. At 27°C, the bacteria are grown overnight before induction. An additional 0.5 mL 100 mg/mL ampicillin should be added to the flask before leaving for the day.
29. The optimal length of the induction period should be determined for each construct.
30. Freezing the bacterial pellet for long periods of time should be avoided. Pellets become harder to process and the yields of protein decrease as the storage time is increased (we like to process the pellet within 1 wk of growth). Frostfree freezers should be avoided.

4.5. Preparation of Inclusion Bodies

31. The pellet (spheroplast) may be frozen at this step at –70°C until ready to proceed. The supernatant contains the periplasm.

32. Solubility of the RNase-sFv in Triton X-100 needs to be determined before doing this step. Triton X-100 increases the purity of the inclusion bodies but it is important to first determine whether the RNase-sFv is also soluble in the detergent. If so, omit Triton X-100 and add only the NaCl.
33. The solution may become very viscous because of the presence of nucleic acids. We have found that using the tissumizer to homogenize the samples just prior to centrifugation results in a firm pellet. DNase 1 may also be used at 10 mg/mL in the presence of $MgCl_2$ ***(28)***.
34. The length of centrifugation time can be decreased as follows: centrifugation #1, 40 min; #2 and #3, 30 min; #4 and #5, 20 min. Washing the inclusion bodies results in removal of contaminating proteins. The pellet should begin to have translucent edges after the second centrifugation and translucency should increase with each successive centrifugation. A dark pellet indicates the presence of contaminating proteins. After the third or fourth resuspension with the Tris-EDTA buffer, 15 µL may be removed for analysis by SDS-PAGE. The protein of interest should be the major band and in some cases, the protein will be almost pure.

4.6. Solubilization of Inclusion Bodies

35. The pH of the solubilization buffer must be 8.0–8.5. The final volume will depend on the protein concentration and will be adjusted later. The solution should be free flowing and not too viscous. If it is very viscous, add more solubilization buffer. The amount of buffer required can reflect either how clean the inclusion bodies are or the amount of the recombinant protein present.
36. The supernatant can be stored at –70°C until ready to be renatured.
37. Dilute the sample 1:10 in the solubilization buffer. Solubilization buffer should be used as the diluent to avoid precipitation of the protein. Determine the protein concentration using the BCA protein assay reagent (or equivalent) according to the manufacturer's instructions. Be sure to include the same amount of the solubilization buffer in the standards because the buffer does affect the color reaction. When adding the solubilization buffer either alone or containing the recombinant protein, it is necessary to mix thoroughly and to work quickly.
38. The final concentration of protein in the renaturation buffer affects the yield of protein and should be optimized for each construct ***(29)***. We find that 80 µg/mL works well for many constructs.
39. The reducing agent DTE is required to promote correct disulfide bond formation.

4.7. Renaturation of Recombinant Protein

40. Each component of the buffer is important ***(29)***. L-arginine enhances correct folding. GSSG in the presence of DTE is partially reduced such that a redox system is established consisting of reduced and oxidized glutathione. To maintain the proper redox activity, the dilution must be exactly 100-fold. The optimal DTE-to-GSSG ratio has been carefully determined by Buchner et al. ***(29)***. Temperature also influences aggregation and yield of protein. Therefore, it is important that the buffer be chilled to 10°C before use. Have the buffer rapidly stirring and add

the denatured sample as a steady stream to the middle of the vortex. Do not add dropwise. Inhibitors of proteolysis may be included in the buffer if needed. The inhibitors are not needed when the proteins are in inclusion bodies.

41. The optimal length of refolding of the protein varies for each construct and needs to be determined. Studies by Brinkman et al. ***(30)*** demonstrate that the functional domains of the fusion proteins refold independently of each other and that peptides that connect the domains together influence both the refolding and the aggregation process. Starting the refolding on a Friday afternoon and allowing it to proceed over the weekend is convenient. Aggregation caused by incorrect folding of the fusion protein occurs during the renaturing process resulting in precipitation.
42. Before the recombinant protein can be purified, it is necessary to decrease the L-arginine concentration. This is done through extensive dialysis. Prepare a vat at 4°C containing dialysis buffer using 10 times the volume of the refolding solution (for example, 3 L of renatured protein requires 30 L dialysis buffer). Change the dialysis buffer three times over a 24-h period. A vat set on a stirrer containing a valve at the bottom with a hose that empties into a sink and a second hose attached to a 4°C distilled H_2O source to provide for easy filling makes this task fairly painless. Dialysis buffer concentrate (10×) is added and the H_2O level adjusted to the appropriate level. Do not prepare the 10× solution more than a few hours in advance because cyanate ions form, which can carbamylate amino groups.
43. The dialysis step results in a large loss of protein resulting from improper folding and aggregation. The presence of 100 m*M* urea will help limit precipitation ***(29)***. It is necessary, therefore, to centrifuge the protein before application to a chromatography column. The magnitude of loss varies from protein to protein. The supernatant should be carefully poured into a clean container because the precipitate does not tightly adhere to the sides of the centrifuge cup.

4.8. Chromatography of the Refolded Recombinant Protein

44. The appropriate column must be predetermined. This is most easily done by preparing the columns in tandem. The sample is first applied to a CM-Sephadex C-50 column and the flowthrough is allowed to flow onto a second column, such as heparin–sepharose. If the material of interest adheres to the CM-Sephadex C- 50, this column should be used since the majority of contaminating proteins will not stick to this resin. One 4-mL column is used per 2 L renatured protein (160 mg of protein). Although the manufacturer states that the denatured protein with a histidine tag will stick to a Ni^{2+}-NTA agarose column, we have not been able to bind the denatured RNase-sFv fusion proteins to the resin. Ni^{2+}-NTA agarose should not be the first column used in the purification procedure because of the interference of contaminating proteins. This column should be reserved for the final purification step.
45. It is very important that the buffer contain glycerol. The recombinant RNase-sFv will precipitate over time in the absence of glycerol. PBS as a buffer should also be avoided because of aggregation of sFvs in this buffer. We have consistently

found this buffer (20 m*M* Tris-HCl, pH 7.5, containing 10% glycerol) to be the best for many different RNase-fusion proteins.

46. Either method 1 or 2 should be tried to determine which results in the best yield and the most highly purified protein. If the FPLC is the method of choice, the sample should be chromatographed analytically to identify which column, Mono Q HR 5/5 anion exchange or Mono S HR 5/5 cation exchange, is the most appropriate for purification. Note that chromatography conditions for scaleup may have to be adjusted.
47. Without the low concentration of imidazole and Triton X-100, the protein eluted from the Ni^{2+}-NTA agarose column will contain other impurities. The imidazole and Triton X-100 help disrupt the binding of these impurities either to the fusion protein and/or to the resin of the column.
48. It is best to use the least amount of Ni^{2+}-NTA agarose possible to minimize the amount of nonspecific binding of other proteins to the column. Using a small column will maximize those proteins that contain multiples of contiguous histidyl residues, such as the fusion protein. According to the manufacturer (Qiagen), the binding capacity of Ni^{2+}-NTA agarose is 5–10 mg of His-tagged protein/mL resin.
49. For some RNase-sFvs a minor species elutes at the lower imidazole concentration (40–60 m*M* imidazole). This species is discarded because it is usually too low in concentration and there are other impurities present. This species most likely represents a slightly different folding (an isomer) of the fusion protein.
50. Determine the protein concentration using the BCA protein assay reagent (or equivalent) according to manufacturer's instructions. Be sure to include the same amount of the imidazole buffer in the standards because imidazole affects the color reaction.
51. Samples may be stored at 4°C for up to 1 yr without any loss in activity, although this may depend on the particular protein. Do not freeze the purified protein since this causes aggregation. NaCl and imidazole appear to prevent precipitation; thus, it is important that the final product is stored at 4°C in the presence of one of these salts. Samples should not be kept in the absence of these salts for any longer than necessary.
52. Even though the sample is in 10% glycerol, some material will precipitate (*see* **Note 51**). Before chromatography by FPLC, it is important to centrifuge the samples to avoid increasing the back pressure of the column.
53. The column conditions need to be adjusted for each recombinant protein. The %B can be varied over different time-points to create gradients of different degrees of shallowness. The conditions described here work for many different types of RNase-sFv fusion proteins.
54. If contaminants remain, the peak of interest will have to be rechromatographed. Dialyze the pooled tubes as noted in **Subheading 3.8.2., step 1** and reapply the sample to the same column using the same chromatography conditions. Contaminants are often purified away from the protein of interest. Note that the denaturation/renaturation procedure described here may result in different isomers of the

same protein. These forms may be visualized by FPLC or high performance liquid chromatography (HPLC).

55. It is important to achieve a concentration of protein as high as possible on the final purification step because we have not found a successful means of increasing the concentration of protein after this. Some RNase fusion proteins, but not all, can be concentrated by using a very small DEAE sepharose or CM-Sephadex C-50 column (0.2 mL) and strip eluting with multiple one-column aliquots and collecting each into separate tubes; however, this involves either dialysis or dilution of the sample prior to the concentration step, which usually results in some precipitation of the sample. Concentration by Centricon cartridges, Diaflo ultrafiltration (Amicon Inc., Beverly, MA) using a YM3 membrane, or placing the sample in a dialysis tube and packing it in G100 dry resin do not work.
56. To sterilize the RNase fusion proteins, use Millipore Millex-HV (Millipore Products Division, Bedford, MA) filters. Millex-GV low protein binding filters (Millipore Products) have been tried and result in a substantial loss of protein.

References

1. Vitetta, E. S., Thorpe, P. E., and Uhr, J. W. (1993) Immunotoxins: magic bullets or misguided missiles. *TIPS* **14,** 148–154.
2. Brinkmann, U. and Pastan, I. (1994) Immunotoxins against cancer. *Biochim. Biophys. Acta* **1198,** 27–45.
3. Sawler, D. L., Bartholomew, R. M., Smith, L. M., and Dillman, R. (1985) Human immune response to multiple injections of murine monoclonal IgG. *J. Immunol.* **135,** 1530–1535.
4. Schroff, R. W., Foon, K. A., Beatty, S. M., Oldham, R., and Morgan, A. (1985) Human anti-murine immunoglobulin response in patients receiving monoclonal antibody therapy. *Cancer Res.* **45,** 879–885.
5. Rybak, S. M. and Youle, R. J. (1991) Clinical use of immunotoxins: monoclonal antibodies conjugated to protein toxins. *Immunol. Allergy Clin. N. Am.* **11(2),** 359–380.
6. Harkonen, S., Stoudemire, J., Mischak, R., Spitler, L., Lopez, H., and Scannon, P. (1987) Toxicity and immunogenicity of monoclonal antimelanoma antibody-ricin A chain immunotoxins in rats. *Cancer Res.* **47,** 1377–1385.
7. Hertler, A. (1988) Human response to immunotoxins, in *Immunotoxins* (Frankel, A. E., ed.), Kluwer, Boston, MA, pp. 475–480.
8. Khazaeli, M. B., Conry, R. M., and LoBuglio, A. F. (1994) Human immune response to monoclonal antibodies. *J. Immunother.* **15,** 42–52.
9. Beintema, J. J., Schuller, C., Irie, M., and Carsana, A. (1988) Molecular evolution of the ribonuclease superfamily. *Prog. Biophys. Mol. Biol.* **51,** 165–192.
10. Gleich, G. J., Loegering, D. A., Bell, M. P., Checkel, J. L., Ackerman, S. J., and McKean, D. J. (1986) Biochemical and functional similarities between human eosinophil-derived neurotoxin and eosinophil cationic protein: homology with ribonuclease. *Proc. Natl. Acad. Sci. USA* **83,** 3146–3150.

11. Strydom, D. J., Fett, J. W., Lobb, R. R., Alderman, E. M., Bethune, J. L., Riordan, J. F., and Vallee, B. L. (1985) Amino acid sequence of human tumor derived angiogenin. *Biochemistry* **24,** 5486–5494.
12. Kurachi, K., Davie, E. W., Strydom, D. J., Riordan, J. F., and Vallee, B. L. (1985) Sequence of the cDNA and gene for angiogenin, a human angiogenesis factor. *Biochemistry* **24,** 5494–5499.
13. Fett, J. W., Strydom, D. J., Lobb, R. R., Alderman, E. M., Bethune, J. L., Riordan, J. F., and Vallee, B. L. (1985) Isolation and characterization of angiogenin, an angiogenic protein from human carcinoma cells. *Biochemistry* **24,** 5480–5486.
14. St. Clair, D. K., Rybak, S. M., Riordan, J. F., and Vallee, B. L. (1987) Angiogenin abolishes cell-free protein synthesis by specific ribonucleolytic inactivation of ribosomes. *Proc. Natl. Acad. Sci. USA* **84,** 8330–8334.
15. Saxena, S. K., Rybak, S. M., Winkler, G., Meade, H. M., McGray, P., Youle, R. J., and Ackerman, E. J. (1991) Comparison of RNases and toxins upon injection into Xenopus oocytes. *J. Biol. Chem.* **266,** 21,208–21,214.
16. Rybak, S. M., Saxena, S. K., Ackerman, E. J., and Youle, R. J. (1991) Cytotoxic potential of RNase and RNase hybrid proteins. *J. Biol. Chem.* **266,** 21,202–21,207.
17. Newton, D. L., Ilercil, O., Laske, D. W., Oldfield, E., Rybak, S. M., and Youle, R. J. (1992) Cytotoxic ribonuclease chimeras: targeted tumoricidal activity in vitro and in vivo. *J. Biol. Chem.* **267,** 19,572–19,578.
18. Rybak, S. M., Hoogenboom, H. R., Meade, H., Raus, J. C. M., Schwartz, D., and Youle, R. J. (1992) Humanization of immuntoxins. *Proc. Natl. Acad. Sci. USA* **89,** 3165–3169.
19. Newton, D. L., Nicholls, P. J., Rybak, S. M., and Youle, R. J. (1994) Expression and characterization of recombinant human eosinophil-derived neurotoxin anti-transferrin sFv. *J. Biol. Chem.* **269,** 26,739–26,745.
20. Newton, D. L., Xue, Y., Olsen, K. A., Fett, J. W., and Rybak, S. M. (1996) Angiogenin single-chain immunofusions: influence of peptide linkers and spacers between fusion protein domains. *Biochemistry* **35,** 545–553.
21. Zewe, M., Rybak, S., Dubel, S., Coy, J., Welschof, M., Newton, D., and Little, M. (1997) Cytotoxicity of a human pancreatic RNase A immunotoxin. *Immunotechnology* **3,** 127–136.
22. Bird, R. E., Hardman, K. D., Jacobson, J. W., Johnson, S., Kaufman, B. M., Lee, S. M., Lee, T., Pope, S. H., Riordan, G. S., and Whitlow, M. (1988) Single-chain antigen- binding proteins. *Science* **242,** 423–426.
23. Huston, J. S., Mudgett-Hunter, M., Tai, M. S., McCartny, J., Warren, F., Haber, E., and Oppermann, H. (1991) Protein engineering of single-chain Fv analogs and fusion proteins. *Methods Enzymol.* **203,** 46–88.
24. Horten, R. M., Cai, Z., Ho, S. N., and Pease, L. R. (1990) Gene splicing by overlay extension: tailor made genes using the polymerase chain reaction. *BioTechniques* **8,** 528–535.
25. Studier, F. W., Rosenberg, A. H., Dunn, J. J., and Dubendorff, J. W. (1990) Use of T7 RNA polymerase to direct expression of cloned genes. *Methods Enzymol.* **185,** 60–89.

26. Horton, R. (1993) In vitro recombination and mutagenesis of DNA; SOEing together tailor-made genes, in *Methods in Molecular Biology*, *vol. 15: PCR Protocols: Current Methods and Applications* (White, B. A., ed.), Humana, Totowa, NJ, pp. 251–261.
27. Wehrli, W., Knusel, F., Schmid, K., and Staehelin, M. (1968) Interaction of rifamycin with bacterial RNA polymerase. *Proc. Natl. Acad. Sci. USA* **61,** 667–673.
28. Worrall, D. M. (1994) Extraction of recombinant protein from bacteria, in *Methods in Molecular Biology*, *vol. 59: cDNA Library Protocols* (Cowell, I. G. and Austin, C. A., eds.), Totowa, NJ, pp. 31–37.
29. Buchner, J., Pastan, I., and Brinkmann, U. (1992) A method for increasing the yield of properly folded recombinant fusion proteins: single chain immunotoxins from renaturation of bacterial inclusion bodies. *Anal. Biochem.* **205,** 263–270.
30. Brinkmann, U., Buchner, J., and Pastan, I. (1992) Independent domain folding of Pseudomonas exotoxin and single-chain immunotoxins: influence of interdomain connections. *Proc. Natl. Acad. Sci. USA* **89,** 3075–3079.

7

Practical Considerations in the Exploitation of Passive Tumor Targeting

Gillian D. Thomas

1. Substances Found to Localize in Tumors

Specific targeting of radioisotopes or toxic drugs to tumors for cancer detection and treatment is an enticing but elusive goal. It has proved difficult to achieve adequate concentration ratios between tumor and normal tissues to improve on standard diagnostic and therapeutic methods.

Many substances are concentrated in tumor tissues to some extent after iv injection, by means of nonspecific trapping in tumor interstitium or other more effective mechanisms in special tumor types. Iodine, in particular, achieves high tumor:normal tissue concentration ratios by active uptake and is established in routine use as ^{131}I for the diagnosis and curative treatment of thyroid carcinoma, with excellent results ***(1)***. Metaiodo-benzylguanidine (MIBG), taken up and stored like noradrenaline in neuronal tissue, now has a role in diagnosis and anal palliative treatment of neuroblastoma and pheochromocytoma ***(2)***.

Large molecules may become 'trapped' in tumors because of the lack of normal lymphatic drainage and their slow rate of diffusion. Nonspecific localization in tumor interstitium and/or cells after iv injection has been noted with many substances, including albumin ***(3)***, ferritin, gallium ***(4)***, hematoporphyrin ***(5)***, flavone-acetic acid ***(6)***, lipiodol ***(7)***, and liposomes ***(8)***, and can be achieved by magnetizing microspheres for injection and applying external magnets over the tumor ***(9)***. These agents, though with potentially wide application, have been of limited practical value because of lack of specificity and sensitivity. More attractive are those that bind specifically to tumor cell components, such as peptide hormones or analogues ***(10)***, or the most adaptable and extensively studied targeting agents, antibodies.

From: *Methods in Molecular Medicine, Vol. 25: Drug Targeting: Strategies, Principles, and Applications*
Edited by: G. E. Francis and C. Delgado

Table 1
Experimental Approaches to the Problem of Low Tumor:Normal Tissue Concentration Ratios of Targeting Molecules

Problem with targeting substance	Experimental approach
1. Loss of radio label or toxin	Modify labeling methods and try different labels
2. Long half-life in plasma	Image manipulation in radiodetection
	Use antibody to clear background
	Fragment larger molecules or find small ones
	Two-stage (pre-) targeting
3. Low concentration in tumor	Regional administration
	Increase dose
	Fragments or small molecules
	Exploit abnormal tumor microenvironment
4. Immune reaction	Humanization of antibody
	Immunosuppression
	Plasmapheresis
5. Low receptor availability	Try increasing expression by cells
	Use more than one targeting molecule
6. Modulation of cellular receptors	Use nonmodulating receptors
	Use univalent antibodies
7. Nontumor receptors targeted	Block peripheral binding sites
	Increase dose of targeting agent

2. Limiting Factors in Tumor Accumulation

Problems that have prevented successful targeting are outlined in **Table 1**, along with strategies used to try to overcome them. These factors have been studied mainly in relation to antibodies but also apply to other agents.

3. Theoretical Strategies to Maximize Tumor:Normal Tissue Uptake Ratios

3.1. Loss of Radiolabel: Radiolabeling Methods and Different Isotopes

Isotopes of iodine have been used most for antibody labeling because of the ease of protein iodination methods, but ^{131}I scans can be relatively difficult to interpret because of the low count rate ($t_{1/2}$ = 8.4 d) and high energy (364 kV) of the gamma radiation. High efficacy labeling techniques, which give many ^{131}I molecules per antibody molecule, have been developed for use in radioimmunotherapy ***(11)***. However, a high-energy gamma radiation and short half-life is undesirable for high-dose localized therapy. Other disadvantages include dissociation of iodine from antibody resulting from unstable labeling

reactions ***(12)***, and/or enzymic attack in the body by the deiodinases active in thyroid hormone metabolism ***(13)***. Internalization into tumor cells after binding to cell membrane components ***(14)*** can also lead to rapid degradation of antibodies used for targeting and loss of iodine. Labeling with the short-range, long-lived β emitter ^{90}Yttrium was developed ***(12,15)*** with a view to therapy, and ^{90}Y-antibody conjugates have been studied in vivo ***(16,17)***.

Indium-111 was first used as an antibody label in 1982 ***(18)*** for its shorter half-life (68 h) and lesser gamma energies (171 and 245 kV) compared with ^{131}Iodine. Uptake of ^{111}I into the liver and prolonged retention there proved to be a problem, but was reduced by further modifications, using different chelating agents ***(19)***, or modifying the antibody ***(20)***. Animal and patient studies showed superior imaging with ^{111}In compared with ^{125}I ***(21)***. Other isotopes with suitable properties have been investigated but not widely used because of expense, technical difficulties, and lack of major advantages. These included ^{123}I ***(22)***, 188 Re ***(23)***, ^{67}Copper, and ^{57}Cobalt ***(24)***.

Technetium-99m was thought desirable as an antibody label for diagnostic scanning because of its very high count rate ($t_{1/2}$ = 6.5 h) and ideal gamma energy (140 kV). It is widely used in nuclear medicine and is inexpensive. Methods for protein labeling with ^{99m}Tc were very time-consuming and complex until fast and simple labeling was developed in 1987 ***(25)***, and good resolution of small lesions has since been reported using this method ***(26)***.

3.2. Long Half-Life of Large Targeting Molecules in Plasma

3.2.1. Image Manipulation

Scans with ^{131}I or ^{111}In as the antibody label can be improved by giving ^{99m}Tc-labeled albumin 20 min before the antibody scan to represent the blood pool. Computer subtraction of counts in the energy range appropriate to ^{99m}Tc reduces background activity, but has disadvantages in that it reduces the signal:noise ratio by adding noise and may produce false hot spots resulting from artifacts ***(27)***. Further statistical manipulations ,described as thresholding, kinetic analysis, and probability mapping ***(28,29)*** remove areas of activity not significantly different from background, theoretically leaving only tumor activity on the scan.

Single photon emission computed tomography (SPECT) imaging allows visualization of transverse slices, useful where tumors might be hidden behind a hot liver or bladder on the planar scan. No major advantage over planar imaging was demonstrated in a large comparative study ***(30)***.

3.2.2. Second Antibody to Clear Background

The administration of a second antibody directed against the first can clear excess circulating antibody to the liver, spleen, and bone marrow via immune

cells with Fc receptors ***(31,32)***. Counts of radioactivity in the blood fall more than twice as quickly as in control subjects, yet tumor counts are maintained. However, since the second antibody removes little unbound first antibody from the extravascular space, the effect is limited to an increase of only about 50% in the uptake ratio. The dose of second antibody required may be five times that of the first, increasing the likelihood of severe immune responses.

3.2.3. Fragments or Small Molecules

Preparation of antibody fragments is a logical approach to the problems of long plasma half-life and immunogenicity. Removal of the Fc end of foreign immunoglobulins to produce a $F(ab')_2$ fragment reduces reticuloendothelial uptake. The still smaller Fab' fragments extravasate faster and diffuse through ECF more rapidly, as shown by local clearance after sc injection ***(33)***. They also penetrate more easily into tumor tissue than $(Fab')_2$ fragments or whole immunoglobulin, as shown by studies with multicellular spheroid tumor models ***(34)***, although their urinary excretion is correspondingly faster. Slightly higher uptake ratios are achieved with fragments down to Fv compared with intact antibodies ***(35–37)***, but the absolute concentration of fragments in the tumors is lower. One animal study using either intact affinity-purified goat polyclonal antibody or its Fab' fragments, or murine monoclonals for anti-CEA imaging in humans, showed no difference in the proportion of known lesions detected ***(38)***. Clinical studies with anti-CEA showed no obvious advantage for fragments vs the intact molecule; Goldenberg et al. ***(39)*** in a large overview concluded that 1 mg of Fab fragments should be optimal. Any small molecule might be engineered chemically or genetically to bind to tumors in theory, but lack of specificity, toxicity, metabolic degradation, and rapid excretion could present practical difficulties with such a hypothetical substance. Perhaps it could be kept in circulation by reversible plasma protein binding, like many hormones, but there needs to be an optimal balance between clearing the plasma and losing too much of the targeting molecule. Linkage to polyethylene glycol (PEGylation) can extend the half-life of smaller proteins and peptides without altering their biological properties and can reduce immunogenicity, which can result in enhanced tumor specificity of antibody fragments ***(40)***.

3.2.4. Two-Stage or Pretargeting

The size of the labeled targeting molecules can be effectively reduced by first injecting antitumor antibody without any label, and following this much later with a small labeled substance that binds to the antibody (pretargeting). Background activity should clear rapidly, thus reducing the large normal tissue dose otherwise received during the gradual localization of antibodies. Binding of a small ligand to antibody can be arranged by creating a bifunctional

molecule that binds both antigen and the chosen labeled molecule ***(41)***. Linking the antibody to avidin (mol wt 60,000) prior to injection allows targeting with labeled biotin (mol wt 244), which binds to avidin with extremely high affinity (10^{-5} M^{-1}) ***(42)***. The system has been tried in animals and shown to speed up tumor localization of the label even with biotinylated antibody and labeled avidin ***(43,44)***, which seems less logical, since avidin is larger than a Fab' fragment.

Another innovation based on a similar concept is to link the pretargeted antibody to an inactive cytotoxic drug that is later switched on by injecting an enzyme ***(45)***. This has been called antibody-dependent enzyme prodrug therapy (ADEPT), and may be an advance on simply attaching cytotoxics to antibodies, in which case their efficacy is reduced and toxicity increased ***(46)***.

Small labeled molecules that can bind specifically and with high affinity to the antibody once it has accumulated in the tumor should reduce the normal tissue integral dose, thus increasing the therapeutic ratio, but tumor residence time and thus total dose would still depend on antibody localization. Since no increase in the maximal uptake ratio could be achieved, there would be little advantage for diagnostic purposes. These principles apply to drugs as well as radioisotopes; the problem of binding to antibody in normal tissue must remain, even if the drug is only activated when bound, and substantial increases in uptake ratio are still required.

3.3. Low Concentration of Targeting Agent in Tumor

3.3.1. Regional Administration

Local administration of antibody has been tried by several workers using different routes appropriate to the antigen of interest. Thus, to image tumor-bearing lymph nodes, antibody was given subcutaneously in the area drained by the nodes but false positive results were a problem ***(47)***. Rates of clearance from the injection site were inversely related to the size of the antibody molecule (Fab > IgG > IgM) ***(33)***. Intra-arterial injection was tried for tumors in the brain ***(48)*** without any major advantage over iv injection. Intrathecal ***(49)***, intrapleural, intrapericardial ***(50)***, intraperitoneal ***(16,51,52)***, and intraventricular ***(53)*** administration were all used in attempts to overcome the systemic sequestering and slow extravasation found with the iv route. However, uptake ratios were not significantly improved, and these studies failed to show advantages over conventional treatment.

3.3.2. Increase Dose of Targeting Agent

Studies comparing different dose levels and schedules in patients have almost always compared tumor uptake in different patients. Press et al. ***(54)*** compared different dose levels in the same patients by infusing escalating doses

of cold antibody with a tracer dose of radioactivity. Integral dose ratios were calculated by following the distribution of the tracer on daily whole-body scans over the week following each dose. Optimal ratios were found using the highest doses. Other studies in patients and in animals have given conflicting results, but a computer model analyzing the effect of dose predicts that it must be optimized in relation to tumor and nontumor receptor quantities to maximize uptake ratios (*see* Chapter 8).

3.3.3. Fragments or Small Molecules

Smaller molecules diffuse faster through intersititial fluid and do not circulate long in plasma, so theoretically it should be possible to get higher concentrations to tumors, using fragments of antibody or other small tumor-binding molecules if possible. However partly because of low binding affinity, they are also quickly lost from the tumor and excreted. *See also* **Subheading 3.2.3.**

3.3.4. Exploiting the Abnormal Tumor Microenvironment

The tumor microenvironment differs from normal tissue, largely because of abnormal vasculature and disorganized cell growth, and it has been shown by Jain ***(55)*** that the interstitial pressure around tumor cells is abnormally high, slowing diffusion of all targeting molecules in the interstitium, particularly larger ones, toward tumor cell surfaces. To counteract this, molecules arriving via the tumor's own blood vessels will be more easily extravasated since the abnormal vessels are relatively leaky, so the engineering of larger molecules can exploit this "enhanced permeability and retention," or EPR ***(56)***. However, tumor cells in underperfused and necrotic areas (those typically resistant to chemo- and radiotherapy) might be relatively inaccessible to any circulating molecules, particularly large ones.

Corticosteroids are used in clinical practice to relieve pressure symptoms caused by many tumor types, notably intracerebral tumors but also those causing airway or central venous obstruction. Their mode of action has been studied in animals ***(57)*** and humans ***(58)***, and is thought to involve first constriction of tumor vascular volume and then a reduction in water content. Reduced interstitial pressure should increase perfusion and extravascular diffusion rates, and high doses of steroids have been shown to increase blood flow in human colonic tumors transplanted into mice. Uptake of antibody into tumors has been assessed before and after administration of high-dose dexamethasone to decrease tumor interstitial pressure and thus increase antigen accessibility. Three patients with recurrent colorectal carcinoma had two antibody scans each, 72 h apart, and the injected dose was the same for all scans (20 mg). Dexamethasone was started 24 h before the second dose of antibody, with an initial iv dose of 10 mg followed by 4 mg four times daily orally for 48 h.

Dexamethasone significantly increased uptake ratios in seven of eight tumor sites ***(59)***. To achieve adequate tumor targeting, high affinity and the correct dose might need to be combined with maneuvers to increase antigen or receptor accessibility. Reducing the high interstitial pressure in tumors by prior treatment with dexamethasone or with chemotherapy or radiotherapy might increase uptake of any targeting substance in this way ***(60)***. Alternatively, tumor (and whole body) permeability could be increased to facilitate extravasation of large molecules, such as antibodies. Interleukin 2 has been shown to improve tumor localization of antibody in mice by this mechanism ***(61)***. However, in humans the toxicity of this approach, resulting from generalized protein leakage from capillaries, would probably preclude its use.

Relative concentrations of CEA in tumor and normal tissues are such that targeting each molecule would result in very high tumor:normal tissue ratios adequate for radioimmunotherapy. In practice, most of the tumor CEA is unbound because of inhomogeneities in the microenvironment and raised interstitial pressure, as well as inadequate antibody dose (normal tissues unsaturated) and low binding affinity.

3.4. Immune Reactions: Humanization, Immunosuppression, and Plasmapheresis

The smallest functional unit of antibody is the complementarity-determining region (CDR), but the intact Fab' molecule is required to maintain the conformational structure of the CDR necessary for antigen binding. However, to reduce immunogenicity the CDR can be genetically recombined with human IgG to produce chimeric human–mouse antibodies ***(62)***, which have been used in repeated large doses with no development of antimouse antibody ***(63)***. It is also possible to make human monoclonals ***(64)***. Immunosuppression with cyclosporin has been successful in suppressing antimouse responses in patients ***(65)***, but large doses were required, with concomitant side effects. Plasmapheresis has also been used in patients for this purpose ***(66)***. Linking Fab molecules with PEG can reduce their immunogenicity ***(40)***. Although all these approaches are rational, none would be expected to improve antibody localization on first injection.

3.5. Low Receptor or Antigen Availability

3.5.1. Increasing Cellular Expression

Expression of CEA at the cell surface has been shown to be variable ***(67)***, and some workers have examined the possibility of increasing tumor concentrations of CEA and other antigens. Thus, interferons have been shown to increase expression of a breast tumor antigen in vitro ***(68)*** and to improve tumor uptake in mice with HLA-antigen-expressing tumors in vivo ***(69)***. Hyperthermia also enhances CEA expression in cell lines ***(70)***.

Antigen concentration has not been considered limiting for tumor detection with antibodies: CEA molecules, for example, number 10^5–10^6 per tumor cell ***(71)***, although it is not known how much of this can be reached by antibody in a given tumor. Antibody uptake at different tumor sites in the same subject might vary because of differences in mass, antigen concentration, degree of differentiation, or vascularity of different tumor deposits. It may not be valid to compare antibody localization in different subjects without taking at least tumor volume and antigen density into account. Intracellular antigens might be considered irrelevant for localization, but have been successfully targeted ***(72,73)***.

3.5.2. Targeting with More than One Agent

Two or more antibodies targeted to different tumor-associated antigens, or different epitopes on the same antigen, have been tried in a variety of tumors to maximize the amount of antibody at the tumor site and overcome the problems of modulation and antigenic heterogeneity ***(74,75)***, but the tumor:normal tissue ratios were not obviously increased by this strategy. Tumor antigen density per cell has been measured accurately with flow cytometry to select the best single antigen to use ***(76)***.

3.6. Modulation of Cellular Receptors

Some cell surface receptors may be recycled, effectively increasing the numbers available for binding ***(77)***, or rapidly shed along with any bound antibody. Antibody binding may itself reduce antigen availability by causing modulation. Not all intact antibodies do this, but Fab' fragments do not ***(78)***.

3.7. Nontumor Receptors

3.7.1. Blocking of Peripheral Binding Sites

Intravenously injected antibody may bind to any soluble antigen present in plasma, reducing the amount available to tumor binding sites ***(79,80)***, and also, in the case of polyclonal antibodies, possibly resulting in the formation of large antigen–antibody complexes with rapid uptake into the reticuloendothelial system. However, circulating CEA does not seem to interfere with imaging of colonic tumors by polyclonal antibodies ***(81)***, and Bosslet et al. ***(82)*** found that binding of monoclonal anti-CEA to colonic tumor cells in vitro was not easily inhibited by excess soluble CEA. Although the majority of antigens are found on normal tissue cell surfaces as well as tumors and thus are tumor-associated rather than -specific, the exception is antigen, which itself is an immunoglobulin, with a unique CDR region. Such antigens, called idiotypes, may be found in B-cell lymphomas. Anti-idiotype antibodies must be prepared for each tumor but they have been used as targets for serotherapy, although without any obvi-

ous improvement compared with other antigens ***(63,83)***. Some circulating antigens may bind antibody at lower affinity than cell surface antigen ***(84)*** and/or be present at low concentration, and thus have little effect.

Normal tissue binding has been suggested as the cause of improved tumor uptake of antiferritin at higher doses ***(85)***. Others have suggested that preliminary injection of cold antibody saturates nonspecific binding sites in the liver, spleen, or bone marrow ***(86,87)***, or that coinjection of cold antibody can enhance tumor localization of radiolabeled antibody in patients ***(88)***. The proportion of the antitumor agent flavone-8-acetic acid in tumor tissue increases sharply once plasma protein-binding sites are saturated ***(89)***, and uptake of liposomes into hepatic parenchymal cells is increased at doses above that required to saturate phagocytic uptake ***(90)***. Separate hepatic blocking agents have been tried to enhance uptake of ricin-antibody conjugates; this is a different approach, effectively removing one normal-tissue compartment ***(91)***. Most patient studies demonstrating enhanced uptake with increasing dose have used an indium label, and here there may be saturable uptake of the free isotope in the liver.

If peripheral binding sites are filled before tumor sites, it might be possible to block these prior to injection of any labeled substance, to increase specificity. Very high binding affinity might make this blocking essentially irreversible. A small labeled tumor-binding substance might be best used second for rapid tumor penetration and a larger unlabeled molecule used first to avoid occupation of tumor sites.

3.7.2. Increase Dose of Targeting Agent

The tumor antigens or receptors being targeted are in general not specific to tumors, but also found on normal tissues and often in circulation. The normal tissue content will be less concentrated but more widely dispersed around the body, and may mop up the injected targeting molecule before much of it can reach the tumor. The immune system may also mo up injected foreign protein through circulating antibodies or cells in the liver. All these processes may be saturable, so that above a certain dose no more of the targeting substance will be lost to them and tumor uptake will rise. *See also* **Subheading 3.3.2.** and Chapter 8.

4. Models of Tumor Targeting

Modeling can be used to explore the effects of altering basic parameters, including tumor-binding affinity, injected dose, molecular size, and normal tissue receptor quantity, and to predict the optimal combination of values of a host of factors that are difficult to alter independently in practice. It can also predict the effects of novel strategies, such as two-stage targeting,

and of untried, theoretical approaches, such as a tumor-binding ligand with a plasma protein carrier, and modes of tumor uptake other than reversible receptor binding.

Models of tumor targeting have used pharmacokinetic data and scintigraphy or tissue measurements to calculate rate constants for transfer between body compartments ***(86,92)***. Bound and free molecules can be modelled as if in separate compartments, transferring between them on association to or dissociation from the receptor or binding protein ***(93,94)***. "Movement" between such conceptual compartments is described by the kinetics of the binding reaction rather than blood flow rates or crossing of physical barriers. In such linear models the alteration of any parameter produces a proportional, predictable effect (this is the meaning of linearity), but unpredictable effects caused by reversible, saturable binding are not demonstrable. Some models have included saturable compartments ***(87)***, usually representing hepatic binding. These have excluded any reversibility or receptor-binding kinetics to avoid computational problems in simulating very widely-varying rate constants (*see* Chapter 8).

In models of chemical reaction systems, which do incorporate binding kinetics, it is usual to consider a state of equilibrium to exist and to ignore extremely small values to simplify the analysis ***(95,96)***. In the gradual process of tumor targeting, the tumor concentration of the injected substance gradually rises and falls so no equilibrium exists, and the proportion of the injected dose bound to tumor is very small, but of central importance, so may not be ignored. The model described in Chapter 8 overcomes these problems to ask questions about tumor targeting that would be very difficult to address experimentally or with simpler models.

References

1. Bierwaltes, W. H. (1982) The treatment of thyroid carcinoma with radioactive iodine. *Semin. Nucl. Med.* **23,** 43.
2. Hofnagel, C. A. and Lewington, V. J. (1994) MIBG therapy, in *Nuclear Medicine in Clinical Diagnosis and Treatment* (Murray and Ell, eds.), Churchill Livingstone, Edinburgh, Scotland.
3. Bauer, F. K., Tubis, M., and Thomas, H. B. (1955) Accumulation of homologous radioiodinated albumin in experimental tumours. *Proc. Soc. Exper. Biol. Med.* **90,** 140–142.
4. Hoffer, P. P. and Gottschalk A. (1974) Tumour scanning agents. *Semin. Nucl. Med.* **4,** 305–316.
5. Quastel, M. R., Richter, A. M., and Levy, J. G. (1990) Tumour scanning with Indium-111 dihaematoporphyrin ether. *Br. J. Cancer* **62,** 885–890.
6. Zwi, L. J., Baguley, B. C., Gain, J. B., and Wilson, W. R. (1990) Necrosis in non-tumour tissues caused by flavone acetic acid and 5,6-dimethyl xanthenone acetic acid. *Br. J. Cancer* **62,** 932–934.

7. Nakajo, M., Kobayashi, H., Shimabukuro, K., Shirono, K., Sakata, H., Taguchi, M., Uchiyama, N., Sonoda, T., and Shinohara, S. (1988) Biodistribution of in vivo kinetics of Iodine-131 lipiodol infused via the hepatic artery of patients with hepatic cancer. *J. Nucl. Med.* **29,** 1066–1077.
8. Briele, B., Hotze, A., Oehr, P., Biersack, H. J., Rosanowski, F., Gorgulla, W., and Herberhold, C. (1990) Tumour imaging with labelled liposomes. *Lancet* **336,** 875–876.
9. Widder, K. J., Morris, R. M., Poore, G. A., Howard, D. P., and Senyei, A. E. (1983) Selective targeting of magnetic albumin microspheres containing low-dose doxorubicin: total remission in Yoshida sarcoma-bearing rats. *Eur. J. Cancer Clin. Oncol.* **19,** 135–139.
10. Evers, B. M., Parekh, D., Townsend, C. M., Jr., and Thompson, J. C. (1991) Somatostatin and analogues in the treatment of cancer. *Ann. Surg.* **213,** 190–198.
11. Mather, S. J. and Ward, B. G. (1987) High efficiency iodination of monoclonal antibodies for radiotherapy. *J. Nucl. Med.* **28,** 1034–1036.
12. Anderson, W. T., and Strand, M. (1978) Radiolabelled antibody: iodine versus radiometal chelates. *NCI Monogr.* **3,** 149–151.
13. Hillier, A. P. (1972) Deiodination of thyroid hormones by the perfused rat liver. *J. Physiol.* **222,** 475–485.
14. Pernis, B. (1985) Internalisation of lymphocyte membrane components. *Immunol. Today* **6,** 45–49.
15. Hnatowich, D. J., Virxi, F., and Doherty, P. W. (1985) DTPA-coupled antibodies labeled with yttrium-90. *J. Nucl. Med.* **26,** 503–509.
16. Stewart, J. S., Hird, V., Snook D., Sullivan, M., Myers, M. J., and Epenetos, A. A. (1988) Intraperitoneal 131I- and 90Y-labelled monoclonal antibodies for ovarian cancer: pharmacokinetics and normal tissue dosimetry. *Int. J. Cancer* **(Suppl. 3),** 71–76.
17. Vriesendorp, H. M., Herpst, J. M., Leichner, P. K., Klein, J. L., and Order, S. E. (1989) Polyclonal 90Yttrium labeled antiferritin for refractory Hodgkin's disease. *Int. J. Rad. Oncol. Biol. Phys.* **17,** 815–821.
18. Rainsbury, R. and Westwood, J. (1982) Tumour localisation with monoclonal antibody radioactivity labelled with metal chelate rather than iodine. *Lancet* II: 1347–1348.
19. Meares, C. F., Moi, M. K., Diril, H., Kukis, D. L., McCall, M. J., Deshpande, S. V., DeNardo, S. J., Snook, D., and Epenetos, A. A. (1990) Macrocyclic chelates of radiometals for diagnosis and therapy. *Br. J. Cancer* **62(Suppl. X),** 21–26.
20. Alvarez, V. L., Wen, M. L., Lee, C., Lopes, A. D., Rodwell, J. D., and McKearn, T. J. (1986) Site-specifically modified ^{III}Indium labeled antibodies give low liver backgrounds and improved radioimmunoscintigraphy. *Int. J. Rad. Appl. Instrum. [B]* **13,** 347–352.
21. Otsuka, F. L. and Fleishman, J. B. (1986) Comparative studies using ^{125}I- and ^{III}Inlabeled monoclonal antibodies. *Eur. J. Nucl. Med.* **II,** 295–299.
22. Epenetos, A. A., Britton, K. E., Mather, S., Shepherd, J., Granowska, M., Taylor-Papadimitriou, J., Nimmon, C. C., Durbin, H., Hawkins, L. R., Malpas, J. S., and

Bodmer, W. F. (1982) Targeting of Iodine-123-labelled tumour-associated monoclonal antibodies to ovarian, breast, and gastrointestinal tumours. *Lancet* **II,** 999–1004.

23. Zamora, P. O., Bender, H., Knapp, F. F. (R.) Jr., and Biersack, H. J. (1996) Radiotherapy of intrathoracic carcinoma xenografts with ^{188}Re-RC-160, a somatostatin analogue. *Tumor Targeting* **2,** 49–59.
24. Cole, W. C., DeNardo, S. J., Meares, C. F., McCall, M. J., DeNardo, G. L., Epstein, A. L., O'Brien, H. A., and Moi, M. K. (1987) Comparative serum stability of radiochelates for antibody radiopharmaceuticals. *J. Nucl. Med.* **28,** 83–90.
25. Schwarz, A., Streinstrasser, A., and Hoechst, A. G. (1987) A novel approach to Tc99m-labelled monodonal antibodies. *J. Nucl. Med.* **28,** 721.
26. Baum, R. P., Hertel, A., Lorenz, M., Schwarz, A., Encke, A., and Hor, G. (1989) ^{99m}Tc-labelled anti-CEA monoclonal antibody for tumour immunoscintigraphy: first clinical results. *Nucl. Med. Commun.* **10,** 345–352.
27. Ott, R. J., Grey, L. J., Zivanovic, M. A., Flower, M. A., Trott, N. G., Moshakis, V., Coombes, R. C., Omerod, M. C., Westwood, J. H., and McCready, V. R. (1983) The limitations of the dual radionuclide subtraction technique for the external detection of tumour by radioiodine-labelled antibodies. *Br. J. Radiol.* **56,** 101–108.
28. Chandler, S. T. and Anderson, P. (1987) A method for thresholding subtracted images in radiolabelled-antibody imaging. *Br. J. Radiol.* **60,** 881–886.
29. Granowska, M., Nimmon, C. C., Britton, K. E., Crowther, M., Mather, S. J., Slevin, M. L., and Shepherd, J. H. (1988) Kinetic analysis and probability mapping applied to the detection of ovarian cancer by radioimmunoscintigraphy. *J. Nucl. Med.* **29,** 599–607.
30. Serafini, A. N., Goldenberg, D. M., Higinbotham-Ford, E. A., Silberstein, E. B., Van Heertum, R. L., Kotler, J. A., Balasubramanian, N., Garty, I., and Wlodkowski, T. (1989) A multicenter trial of cancer imaging with fragments of CEA monoclonal antibodies. *J. Nucl. Med.* **82,** 748.
31. Goodwin, D., Meares, C., Diamanti, C., McCall, M., Lai, X., Torti, F., McTigue, M., and Martin, B. (1984) Use of specific antibody for rapid clearance of circulating blood background from radiolabelled tumour imaging proteins. *Eur. J. Nucl. Med.* **9,** 209–215.
32. Pedley, P. B., Dale, R., Boden, J. A., Begent, R. H., Keep, P. A., and Green, A. J. (1989) The effect of second antibody clearance on the distribution and dosimetry of radiolabelled anti-CEA antibody in a human colonic tumor xenograft model. *Int. J. Cancer* **43,** 713–718.
33. Wahl, R. L., Geatti, O., Liebert, M., Wilson, B., Shreve, P., and Beers, B. A. (1987) Kinetics of interstitially administered monoclonal antibodies for purposes of lymphoscintigraphy. *J. Nucl. Med.* **28,** 1736–1744.
34. Sutherland, R. M., Buchegger, F., Schreyer, M., Vacca, A., and Mach, J. P. (1987) Penetration and binding of radiolabeled anti-carcinoembryonic antigen monoclonal antibodies and their antigen binding fragments in human colon multicellular spheroids. *Cancer Res.* **47,** 1627–1633.

35. Searle, F., Adam, T., and Boden, J. A. (1986) Distribution of intact and Fab_2 fragments of anti-human chorionic gonadotrophin antibodies in nude mice bearing human choriocarcinoma xenografts. *Cancer Immunol. Immunother.* **21,** 205–208.
36. Burraggi, G. L., Callegaro, L., Marianari, G., Turrin, A., Cascinelli, N., Attili, A., Bombardieri, E., Terno, G., Plassio, G., Dovis, M, Mazzuca, N., Natali, P. G., Scassallati, G. A., Rosa, U., and Ferrone, S. (1985) Imaging with ^{131}I-labelled monoclonal antibodies to a high molecular weight melanoma-associated antigen in patients with melanoma: efficiency of whole immunoglobulin and its $F(ab)_2$ fragments. *Cancer Res.* **45,** 3378–3387.
37. Rowlinson-Busza, G., Deonarain, M. P., and Epenetos, A. A. (1996) Comparison of intact monoclonal antibody, its $F(ab')_2$ and Fab fragments and recombinant single chain Fv in a human tumour xenograft model. *Tumour Targeting* **2,** 37–48.
38. Sharkey, R. M., Primus, F. J., Shochat, D., and Goldenberg, D. M. (1988) Comparison of tumour targeting of mouse monoclonal and goat polyclonal antibodies to carcinoembryonic antigen in the GW-39 human tumour–hamster host model. *Cancer Res.* **48,** 1823–1828
39. Goldenberg, D. M., Goldenberg, H., Sharkey, R. M., Lee, R. E., Higginbotham-Ford, E., Horowitz, J. A., Hall, T. C., Pinsky, C. M., and Hansen, H. J. (1989) Imaging of colorectal carcinoma with radiolabeled antibodies. *Semin. Nucl. Med.* **19,** 262–281.
40. Delgado, C., Pedley, B., Herraez, A., Boden, R., Boden, J. A., Keep, P. A., Chester, K. A., Fisher, D., Begent, R. H., and Francis, G. E. (1996) Enhanced tumour specificity of an anti-carcinoembryonic antigen Fab' fragment by poly(ethylene glycol) (PEG) modification. *Br. J. Cancer* **73,** 175–182.
41. Neri, D., de Lalla, C., Petrul, H., Soldani, P., di Stefano, A., Lozzi, L., Neri, G., and Neri, P. (1995) Engineering recombinant bifunctional antibodies. *Tumour Targeting* **1,** 189–194.
42. Green, N. M. (1963) Avidin. The nature of the biotin-binding site. *Biochem. J.* **89,** 599–609.
43. Hnatowich, D. J., Virzi, F., and Rusckowski, M. (1987) Investigations of avidin and biotin for imaging applications. *J. Nucl. Med.* **28,** 1294–1302.
44. Pimm, M. V., Fells, H. F., Perkins, A. C., and Baldwin, R. W. (1988) Iodine-131 and indium-111 labelled avidin and streptavidin for pre-targeted immunoscintigraphy with biotinylated antitumour monoclonal antibody. *Nucl. Med. Commun.* **9,** 931–941.
45. Bagshawe, K. D., Sharma, S. K., Springer, C. J., and Antoniw, P. (1995) Antibody directed enzyme prodrug therapy: a pilot-scale clinical trial. *Tumour Targeting* **1,** 17–30.
46. Pimm, M. V. (1988) Drug—antibody conjugates for cancer therapy: potentials and limitations. *Crit. Rev. Ther. Drug Carrier Syst.* **5,** 189–227.
47. Weinstein, J. N., Steller, M. A., Keenan, A. M., Covell, D. G., Kay, M. E., Sieber, S. M., Oldham, R. K., Hwang, K. M., and Parker, R. J. (1983) Monoclonal antibodies in the lymphatics: selective delivery to lymph node metastases of a solid tumor. *Science* **222,** 423–426.

48. Epenetos, A. A., Courtenay-Luck N., Pickering, D., Hooker, G., Durbin, H., Lavender, J. P., and McKenzie, C. G. (1985) Antibody guided irradiation of brain glioma by arterial infusion of radioactive monoclonal antibody against epidermal growth factor receptor and blood group A antigen. *Br. Med. J.* **290,** 1463–1466.
49. Coakham, H. B., Richardson, R. B., Davies, A. G., Boume, A. P., Moseley, R. P., Kemshead, J. T., and Lashford, L. (1986) Antibody-guided radiation therapy via the CSF for malignant meningitis. *Lancet* **II,** 860,861.
50. Pectasides, D., Stewart, S., Courtenay-Luck N., Rampling, R., Munro, A. J., Krausz, T., Dhokia, B., Snook D., Hooker, G., Durbin, H., Taylor-Papadimitriou, J., Bodmer, W. F., and Epenetos, A. A. (1986) Antibody-guided irradiation of malignant pleural and pericardial effusions. *Br. J. Cancer* **53,** 727–732.
51. Hnatowich, D. J., Chinol, M., Siebecker, D. A., Gionet, M., Griffin, T., Doherty, P. W., Hunter, R., and Kase, K. R. (1988) Patient distribution of intraperitoneally administered yttrium-90-labeled antibody. *J. Nucl. Med.* **29,** 1428–1434.
52. Wahl, R. L., Barrett, J., Geatti, O., Liebert, M., Wilson, B. S., Fisher, S., and Wagner, J. G. (1988) The intraperitoneal delivery of radiolabeled monoclonal antibodies: studies on the regional delivery advantage. *Cancer Immunol. Immunother.* **26,** 187–201.
53. Smith, D. B., Mosely, R. P., Begent, R. H. J., Coakham, H. B., Glaser, M. G., Dewhurst, S., Kelly, A., and Bagshawe, K. D. (1990) Quantitative distribution of ^{131}I-labelled monoclonal antibodies administered by the intraventricular route. *Eur. J. Cancer* **26,** 129–136.
54. Press, O. W., Eary, J. F., Badger, C. C., Martin, P. J., Appelbaum, F. R., Levy, R., Miller, R., Brown, S., Nelp, W. B., Krohn, K. A., Fisher, D., DeSantes, K., Porter, B., Kidd, P., Thomas, E. D., and Bernstein, I. D. (1989) Treatment of refractory non-Hodgkin's lymphoma with radiolabeled MB-1 (anti-CD37) antibody. *J. Clin. Oncol.* **7,** 1027–1038.
55. Jain, R. K. and Baxter, L. T. (1988) Mechanisms of heterogeneous distribution of monoclonal antibodies and other macromolecules in tumours: significance of raised interstitial pressure. *Cancer Res.* **48,** 7022–7032.
56. Maeda, H. (1991) SMANCS and polymer-conjugated macromolecular drugs: advantages in cancer chemotherapy. *Adv. Drug Delivery Rev.* **6,** 181–202.
57. Braunschweiger, P. G. and Schiffer, L. M. (1986) Effect of dexamethasone on vascular function in RIF-1 tumors. *Cancer Res.* **46,** 3299–3303.
58. Leenders, K. L., Beaney, R. P., Brooks, D. J., Lammertsma, A. A., Heather, J. D., and McKenzie, C. G. (1985) Dexamethasone treatment of brain tumour patients: effects on regional cerebral blood flow, blood volume, and oxygen utilisation. *Neurology* **35,** 1610–1616.
59. Attard, A. R., Thomas, G. D., Chappell, M. J., Taylor, D. N., Baum, R. P., Dykes, P. W., Godfrey, K. R., Fraser, I. A., and Bradwell, A. R. (1991) Effect of high dose, high affinity antibody and dexamethasone on antibody uptake by colorectal cancer: results of a pilot study. *Antibody, Immunoconj. Radiopharmaceut.* **4,** 871–876.
60. Curti, B. D., Urba, W. J., Alvord, W. G., et al. (1993) Interstitial pressure of subcutaneous nodules in melanoma and lymphoma patients: changes during treatment. *Cancer Res.* **53,** 2204.

61. Schultz, K. R., Badger, C. C., Dombi, G. W., Greenberg, P. P., and Bernstein, I. D. (1992) Effect of interleukin-2 on biodistribution of monoclonal antibody in tumour and normal tissues in mice bearing SL-2 thymoma. *J. Natl. Cancer Inst.* **15,** 109–112.
62. Jones, P. T., Dear, P. H., Foote, J., Neuberger, M. S., and Winter, G. (1986) Replacing the complementarily-determining regions in a human antibody with those from a mouse. *Nature* **321,** 522–525.
63. Hamblin, T. J., Cattan, A. R., Glennie, M. J., Mackenzie, M. R., Stevenson, F. K., Watts, H. F., and Stevenson, G. T. (1987) Initial experience in treating human lymphoma with a chimeric univalent derivative of monoclonal anti-idiotype antibody. *Blood* **69,** 790–797.
64. McCabe, R. P., Peters, L. C., Haspel, M. V., Pomato, N., Carrasquillo, J. A., and Hanna, M. G., Jr. (1988) Preclinical studies on the pharmacokinetic properties of human monoclonal antibodies to colorectal cancer and their use for detection of tumors. *Cancer Res.* **48,** 4348–4353.
65. Ledermann, J. A., Begent, R. H. J., Bagshawe, K. D., Riggs, S. J., Searle, F., Glaser, M. G., Green, A. J., and Dale, R. G. (1988) Repeated antitumour antibody therapy in man with suppression of the host response by Cyclosporin A. *Br. J. Cancer* **58,** 654–657.
66. Zimma, A. M., Rosen, S. T., Spies, S. M., Golman-Leilin, R., Kazikiewicz, J. M., Silverstein, E. A., and Kaplan, E. H. (1988) Radioimmunotherapy of patients with cutaneous T-cell lymphoma using an iodine-131-labeled monoclonal antibody: analysis of retreatment following plasmapheresis. *J. Nucl. Med.* **19,** 174–180.
67. Rosenthal, K. C., Tompkins, W. A. F., and Rawls, W. E. (1980) Factors affecting the expression of carcinoembryonic antigen at the surface of cultured human colon carcinoma cells. *Cancer Res.* **40,** 4774–4750.
68. Iacobelli, S., Scambia, G., Natoli, C., Benedetti Panici, P., Baiocchi, G., Perone, L., and Mancuso, S. (1988) Recombinant human leucocyte interferon-α 2b stimulates the synthesis and release of a 90K tumor-associated antigen in human breast cancer cells. *Int. J. Cancer* **42,**182–184.
69. Rowlinson, G., Balkwill, F., Snook, D., Hooker, G., and Epenetos, A. A. (1986) Enhancement by gamma-interferon of in vivo tumour radiolocalization by a monoclonal antibody against HLA-DR antigen. *Cancer Res.* **46,** 6413–6417.
70. Wong, J. Y. C., Mivechi, N. F., Paxton, R. J., Williams, L. E., Beatty, B. G., Beatty, J. D., and Shively, J. E. (1989) The effects of hyperthermia on tumor carcinoembryonic antigen expression. *Int. J. Radiol. Biol. Phys.* **17,** 803–808.
71. Shi, Z. R., Tsao, D., and Kim, Y. S. (1983) Subcellular distribution, synthesis, and release of carcinoembryonic antigen in cultured human colon adenoma cell lines. *Cancer Res.* **43,** 4045–4049.
72. Goldenberg, D. M., Kim, E. E., DeLand, F. H., Spremulli, E., Nelson, M. O., Cockerman, J. P., Primus, F. J., Corgan, R. L., and Alpert, E. (1980) Clinical studies on the radioimmunodetection of tumours containing alpha-fetoprotein. *Cancer* **45,** 2500–2505.
73. Katoh, Y., Nakata, K., Kohno, K., Shima, M., Satoh, A., Kusumoto, Y., Ishii, N., Kohji, T., Shiku, H., and Nagataki, S. (1990) Immunoscintigraphy of human

tumors transplanted in nude mice with radiolabeled anti-ras p21 monoclonal antibodies. *J. Nucl. Med.* **31,** 1520–1526.
74. Krizan, Z., Murray, J. L., Hersh, E. M., Rosenblum, M. G., Glenn, H. J., Gschwind, C. R., and Carlo, D. J. (1985) Increased labeling of human melanoma cells in vitro using combinations of monoclonal antibodies recognising separate cell surface antigenic determinants. *Cancer Res.* **45,** 4904–4909.
75. Baum, R. P, Lorenz, M., Hottenrott, C., Albrecht, M., Senekowitch, R., Happ, J., Hertel, A., Spitz, J., and Hor, G. (1988) Radioimmunoscintigraphy using monoclonal antibodies to CEA, CA 19-9 and CA 125. *Int. J. Biol. Markers* **3,** 177–184.
76. Durrant, L. G., Robins, R. A., and Baldwin, R. W. (1989) Flow cytometric screening of monoclonal antibodies for drug or toxin targeting to human cancer. *J. Natl. Cancer Inst.* **9,** 688–696.
77. Brown, M. S., Anderson, R. G. W., and Goldstein, J. L. (1983) Recycling receptors: the round-trip itinerary of migrant membrane proteins. *Cell* **32,** 663–667.
78. Glennie, M. J. and Stevenson, G. T. (1982) Univalent antibodies kill tumour cells in vitro and in vivo. *Nature* **295,** 712–714.
79. Nadler, L. M., Stashenko, P., Hardy, R., Kaplan, W. D., Burton, L. N., Kufe, D. W., Antman, K. H., and Schlossman, S. F. (1980) Serotherapy of a patient with a monoclonal antibody directed against a human lymphoma-associated antigen. *Cancer Res.* **40,** 3147–3154.
80. Miller, R. A., Maloney, D. G., McKillop, J., and Levy, R. (1981) In vivo effects of murine hybridoma monoclonal antibody in a patient with T cell leukaemia. *Blood* **58,** 78–86.
81. Primus, F. J., Bennett, S. J., Kim, E. E., DeLand, F. H., Zahn, M. C., and Goldenberg, D. M. (1980) Circulating immune complexes in cancer patients receiving goat radiolocalising antibodies to carcinoembryonic antigen. *Cancer Res.* **40,** 497–501.
82. Bosslet, K., Steinstrasser, A., Schwarz, A., Harthus, H. P., Luben, G., Kuhlmann, L., and Sedlacek, H. H. (1988) Quantitative considerations supporting the irrelevance of circulating serum CEA for the immunoscintigraphic visualization of CEA expressing carcinomas. *Eur. J. Nucl. Med.* **14,** 523–528.
83. Stevenson, G. T., Glennie, M. J., Hamblin, T. J., Lane, A. C., and Stevenson, F. K. (1988) Problems and prospects in the use of lymphoma idiotypes as therapeutic targets. *Int. J. Cancer* **Suppl. 3,** 9–12.
84. Mason, D. W. and Williams, A. F. (1980) The kinetics of antibody binding to membrane antigens in solution and at the cell surface. *Biochem. J.* **187,** 1–20.
85. Rostock, R. A., Klein, J. L., Kopher, K. A., and Order, S. E. (1984) Variables affecting the tumor localization of 131 I-anti-ferritin in experimental hepatoma. *Am. Clin. Oncol*. **6,** 9–18.
86. Eger, R. R., Covell, D. G., Carrasquillo, J. A., Abrams, P. G., Foon, K. A., Reynolds, J. C., Schroff, R. W., Morgan, A. C., Larson, S. M., and Weinstein, J. N. (1987) Kinetic model for the biodistribution of an 111Indium-labeled monoclonal antibody in humans. *Cancer Res.* **47,** 3328–3336.
87. Murray, J. L., Lamki, L. M., Shanken, L. J., Blake, M. E., Plager, C. E., Benjamin, R. S., Schweighardt, S., Unger, M. W., and Rosenblum, M. G. (1988) Immuno-

specific saturable clearance mechanisms for Indium-111-labeled anti-melanoma monoclonal antibody 96. 5 in humans. *Cancer Res.* **48,** 4417–4422.

88. Carrasquillo, J. A., Abrams, P. G., Schroff, R. W., Reynolds, J. C., Woodhouse, C. S., Morgan, A. C., Keenan, A. M., Foon, K. A., Perentis, P., Marshall, S., Horowitz, M., Szymendera, J., Englert, J., Oldham, R. K., and Larson, S. M. (1988) Effect of antibody dose on the imaging and biodistribution of Indium-111 9.2.27 anti-melanoma monoclonal antibody. *Nucl. Med.* **29,** 39–47.
89. Chabot, G. G., Bissery, M.-C., Corbett, T. H., Rutkowski, K., and Baker, L. H. (1989) Pharmacodynamics and causes of dose-dependent pharmacokinetics of flavone-8-acetic acid (LM-975; NSC-347512) in mice. *Cancer Chemother. Pharmacol.* **24,** 15–22.
90. Chow, D. D., Essien, H. E., Padki, M. M., and Hwary, K. J. (1989) Targeting small unilamellar liposomes to hepatic parenchymal cells by dose effect. *J. Pharmacol. Exp. Ther.* **248,** 506–513.
91. Byers, V. S., Pimm, M. V., Pawluczyk, I. Z., Lee, H. M., Scannon, P. J., and Baldwin, R. W. (1987) Biodistribution of ricin-antibody conjugates and influence of hepatic blocking agents. *Cancer Res.* **47,** 5277–5283.
92. Covell, D. G., Barbet, J., Holton, O. D., Black, C. D. V., Parker, R. J., and Weinstein J. N. (1986) Pharmacokinetics of monoclonal immunoglobulin G1, $F(ab')_2$, and Fab' in mice. *Cancer Res.* **46,** 3969–3978.
93. Oie, S. and Tozer, T. N. (1979) Effect of altered plasma protein binding on apparent volume of distribution. *J. Pharm. Sci.* **68,** 1203–1205.
94. Rowland, M. (1984) Physiologic pharmacokinetic models: relevance, experience and future trends. *Drug Metab. Rev.* **15,** 55–74.
95. DiStefano, J. J. and Chang, R. F. (1971) Computer simulation of thyroid hormone binding, distribution, and disposal dynamics in man. *Am. J. Physiol.* **221,** 1529–1544.
96. Ishikawa, H., Maeda, T., Hikita, H., and Miyatake, K. (1988) The computerised derivation of rate equations for enzyme reactions on the basis of the pseudo-steady-state assumption and the rapid-equilibrium assumption. *Biochem. J.* **251,** 175–181.

8

Effect of Dose, Molecular Size, and Binding Affinity on Uptake of Antibodies

Gillian D. Thomas

1. Analysis of the Process of Antibody Targeting

1.1. Extravasation: Molecular Size of Antibody

The huge molecular radius of immunoglobulins would seem to be a major drawback for the targeting of solid tumors, because of slow extravasation into tumor interstitium and a long plasma half-life. The permeability of normal continuous capillary endothelia to intravascular solutes of different molecular sizes has been determined in animals, mainly for macromolecules, and different sources give data consistent with the graph in **Fig. 1** ***(1–3)***. The position of whole antibodies (IgG, mol wt 150 kDa and effective molecular radius 5.5 nm) is well to the right of albumen (66 kDa and 3.5 nm), and they are therefore very slowly extravasated in normal tissues. A $F(ab')_2$ fragment (100 kDa, 5.06 nm) should not extravasate much faster than the intact molecule on this basis and a monomeric Fab' fragment (50 kDa, 3.48 nm) still has quite a high molecular radius ***(4)***, so a much smaller molecule would be necessary to equilibrate very quickly with extracellular fluid (ECF).

Studies in xenografts and spheroids have shown that the smallest antibody fragments do localize fastest and penetrate farthest into tumor tissue ***(5–7)***. They are also less immunogenic because they lose the Fc portion. It is therefore surprising that the use of fragments for radioimmunodetection has not proved to be a worthwhile advance. This might be because of their lower affinity ***(8)***: if antibody fragments or even smaller, nonimmunological binding molecules could be engineered to have high affinity, their tumor content and uptake ratio might be much higher than could be achieved with intact antibodies. Alternatively, affinity might be more important than size, so that an intact

From: *Methods in Molecular Medicine, Vol. 25: Drug Targeting: Strategies, Principles, and Applications*
Edited by: G. E. Francis and C. Delgado

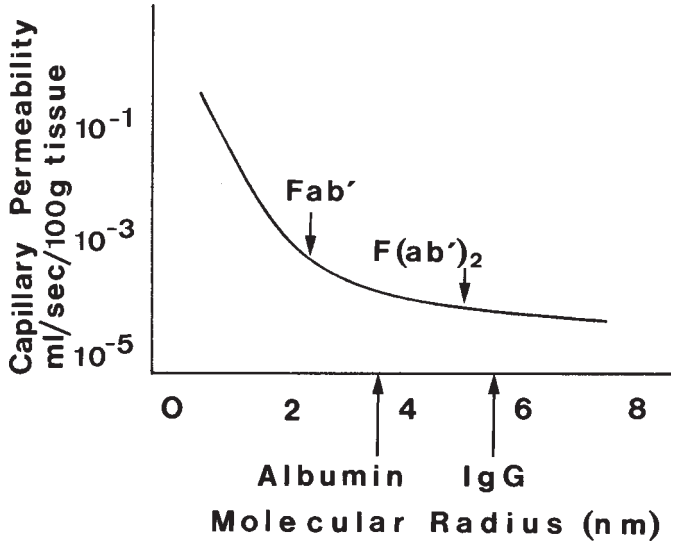

Fig. 1. Relationship between molecular radius and permeability/surface area product for intact capillaries.

antibody of very high affinity would be a significant advance and its fragmentation would not improve results further. It is also possible that the rapid urinary excretion of small molecules would offset any advantage. Animal studies suggest that the vascular endothelium in tumors may be up to 10 times more permeable than in normal tissues **(Table 1)**.

1.2. Concentration at the Tumor Site: Injected Dose of Antibody

Several patient and animal studies have examined the effect on uptake ratios of increasing antibody dose. Results are conflicting, showing improved localization, inferior results, or no difference with increasing dose **(Table 2)**.

1.3. Localization in Tumor: Antibody–Antigen Binding Affinity

Adequate binding affinity for tumor localization has not been defined, although the importance of high affinity for maximal cell binding and for sensitive in vitro radioimmunoassay has been shown ***(41–43)***. It has, however, also been suggested that low affinity is preferable in vivo to allow more tissue penetration and avoid trapping of tightly bound antibody at the tumor surface ***(44)***. One study of xenograft targeting using different antibodies to carcinoembryonic antigen (CEA) showed no correlation of localization with affinity ***(45)***, but the affinity required to show improvement may be very high, and their highest value was in a polyclonal antiserum in which nonspecific anti-

Table 1
Experimentally Determined Tumor:Normal Tissue Permeability Ratios[a]

Tumor	Normal tissue	Solute radius (nm)	Tumor:normal permeability	Ref.
Walker carcinosarcoma	Muscle	3.5	7.2	***(9)***
	Liver	<1	1.8	***(10)***
Chondrosarcoma	Muscle	3.5	2	***(9)***
Sarcoma Rd/3	Liver	3.5	1.1	***(11)***
	Kidney	3.5	1.4	
Fibrosarcoma	Connective tissue	<1	1	***(12)***
Sarcoma	Gut	3.5	2	***(13)***
	Gut	5.5	3.7	***(13)***
	Muscle	3.5	3.2	***(13)***
	Muscle	5.5	10	***(13)***
VX2 carcinoma	Mature granulation tissue	8.2	8	***(14)***

[a]From animal studies of the extravasation of test solutes: blue dyes (<1 nm), albumin (3.5 nm), IgG (5.5 nm) and fluorescent dextrans (up to 8.2 nm). All animals were rats except the VX2 carcinoma (rabbit).

body can lower uptake ratios. Also, CEA was targeted and is known to be heterogeneous ***(46)*** and affinity studies were not performed using CEA from the xenografts themselves.

A single-binding site, reversible antibody–antigen (or ligand-receptor) binding reaction is represented at equilibrium by the equation:

$$k_a[Ab][Ag] = k_d[Ab\text{-}Ag] \quad (1)$$

with equilibrium constant $K_{eq} = k_a/k_d$, where k_a = association rate constant; k_d = dissociation rate constant; [Ab] = concentration of free antibody [Ag] = concentration of free antigen; and [Ab–Ag] = concentration of bound antibody–antigen complex.

Values of k_a are very large; thus, binding happens almost instantaneously and is only limited by diffusion. Values of k_d are variable ***(8,47)*** and determine length of binding time. The half-time of binding is inversely proportional to the log of the dissociation rate constant. To maintain appreciable binding for several days, which would be necessary to deliver a curative dose of radiation

Table 2
Studies on the Effect of Antibody Dose on Tumor:Normal Tissue Uptake Ratios

Subjects	Label	Dose (mg)	Effect	Measured by	Ref.
Rats	I	1–5 mg	+	Tissue counts	***(15)***
Rats	In	2.5–500 µg	+	Tissue counts	***(16)***
Mice	I	To 16/kg	0	Tissue counts	***(17)***
Mice	In	To 6.25	0	Tissue counts	***(18)***
Mice	I	To 0.4	–	Tissue counts	***(19)***
Mice	Y	To 0.2	+	Tissue counts	***(20)***
Hamsters	I	0.1–10/kg	0	Tissue counts	***(21)***
Mice	I	To 0.5	0	Tissue counts	***(22)***
Mice	I	1 µg–1 mg	–	Tissue counts	***(23)***
Patients	In	1–11	+	% +ve scans	***(24)***
	In	0.5–0	+	% +ve scans	***(25)***
	In	1–50	0	% +ve scans	***(26)***
	In	1–100	+	% +ve scans	***(27)***
	In	1–20	+	% +ve scans	***(28)***
	In	1–20	+ (ab 1)		***(29)***
			– (ab 2)	% +ve scans	***(29)***
	In	5–80	+	% +ve scans	***(30)***
	In	1–41	+	% +ve scans	***(31)***
	In	20 vs 40	0	% +ve scans	***(32)***
	In	2.5–80	+	% +ve scans	***(33)***
	In	1–100	+	% +ve scans	***(34)***
	I	0.3–19	0	% +ve scans	***(35)***
	In	2.5–80	+ (40 mg)		***(36)***
			– (80 mg)	% +ve scans	***(36)***
	In	10–40	+	% +ve scans	***(28)***
	I	0.5–10/kg	+	Serial scans	***(37)***
	In	1 vs 30	+	Blood/liver UR	***(38)***
	I	1 vs 10	0	% +ve scans	***(39)***
	I	0.1–40	0	Biopsies	***(40)***

[a]In, ^{111}Indium; I, ^{131}Iodine or ^{125}I; Y, ^{90}Yttrium; +, increased uptake ratio or %ID/g at higher dose; –, decreased 0, no effect of increasing dose.

via a radioisotope label, a k_d of 10^{-6}/s or lower would be required. At least one antibody has been reported with such a low k_d ***(48)***, in addition to many enzyme inhibitors ***(49)***, and the binding of hem to hemopexin, iron to transferrin, and classically avidin to biotin are essentially irreversible ***(50,51)***.

Measures of affinity are very seldom quoted in reports of targeting studies and may be relatively low for a monoclonal antibody (MAb) e.g., $K_{eq} = 10^8/M$,

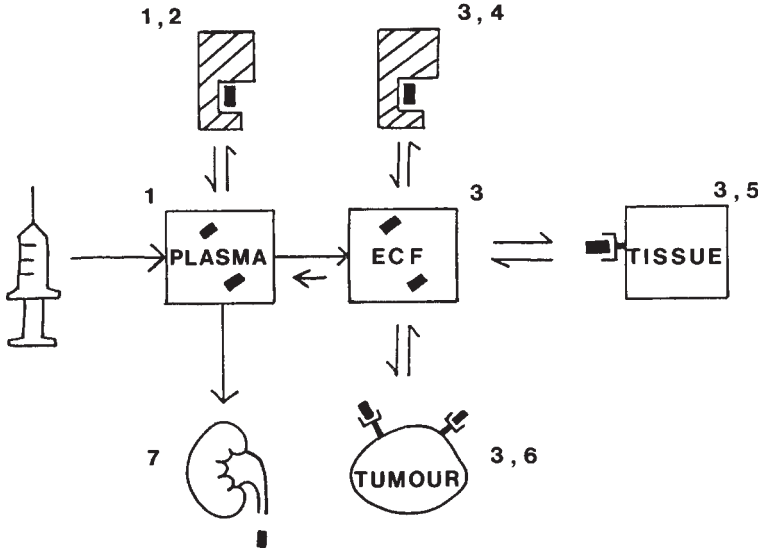

Fig. 2. Model of the disposition of antibody (or smaller molecule) shown free in plasma (1) and ECF (3), or reversibly bound to identical normal tissue (3,5) and tumor (3,6) antigens or receptors and to soluble antigen (1,2 and 3,4). Urinary excretion is also indicated (7).

compared to polyclonal antibody affinities ranging up to $10^{12}/M$. Very few antibody affinities have been determined at human body temperature, although dissociation constants may be increased by an order of magnitude relative to those measured at 20°C ***(8)*** so that binding time will be shortened. Conversely, for some antibodies an increase in temperature prolongs binding ***(52)***. In the absence of accurate measurements the role of affinity remains unclear and difficult to study experimentally. Computer modeling can be helpful in analyzing such interdependent parameters as molecular size, dose, and affinity.

2. Modeling the Process of Antibody Targeting

2.1. Designing the Model Structure

This model of antibody uptake (***53***; *see* **Fig. 2**) includes compartments that are physically separate (plasma, ECF) and those that are not (bound and free compartments within plasma and ECF). It does not consider forward blood flow around the body, but only diffusion from plasma to ECF. Since the reasons for differential antibody uptake in normal tissues are complex and vary with the particular antibody and antigen, normal tissue content is averaged over the whole body for calculation of predicted tumor:normal tissue uptake ratios.

Entry of the targeting substance is by iv bolus injection, although infusion could be simulated, and exit via plasma into urine. After extravasation the substance enters a "bound compartment" from which it returns to the "free in ECF" compartment on dissociation. Few absolutely tumor-specific cell components have been identified to date, so the model has separate tumor-bound and other-tissue-bound compartments, the latter postulated to exist homogeneously throughout ECF. Extra compartments represent binding to soluble antigen in plasma or ECF. Disposition of the injected dose depends on the concentrations of targeted and targeting molecules and on rates of transfer between compartments. Metabolic degradation, reticuloendothelial uptake, and dissociation of attached radiolabels or drugs are ignored. These would each reduce both the tumor content (TC) and uptake ratio (UR) of the label, by effectively reducing its concentration in the tumor vicinity. Thus, predicted TC and UR results are likely to be overestimates.

Only some of the antibody in ECF can be available to bind to tumor antigen at any instant since the tumor is localized to one site in the body. If antibody in an ECF volume equal to the tumor volume is presumed to be available, this would give tumor-binding sites the same accessibility as "normal tissue" sites. The increased permeability can be allowed for in a model by effectively multiplying the available antibody at the tumor site by a "permeability factor" of 5.

The tumor microenvironment is assumed to be homogeneous, whereas in reality, receptor/antigen expression, blood flow, vascularity, and capillary permeability may vary from one part of the tumor to another ***(44)***, reducing the accessibility of tumor receptors to the injected substance. Thus, measured antigen quantities from tumor samples would also likely be overestimates. Rate constants representing extravasation, recirculation, and excretion are approximations. Rates of transfer of different molecules out of intact capillaries are established ***(1,2)***, though these would not apply in liver, spleen, and bone marrow, where cells are bathed in blood, or in brain, where there are tight junctions between capillary cells. If a single rate constant can describe back-diffusion into plasma from ECF, its value is unknown. With regard to excretion, other factors affect urinary loss besides molecular size (charge, shape, renal catabolism) so the assumption of (extravasation through intact capillaries) = (glomerular filtration rate) for all molecular sizes is a rough estimate.

2.2. Expression of the Model by Equations

The model has up to six compartments with transfer of the injected substance between them depending on both first- and second-order reactions (representing rates of movement and reversible binding, respectively). Strictly, there are four more compartments representing unoccupied binding sites, but their inclusion as separate entities does not alter the equations because the extra expressions cancel out ***(54)***.

Binding affinity is often described in terms of the equilibrium constant K_{eq}, defined as the ratio of the association and dissociation rate constants k_a and k_d. Typically, antibodies have very large k_a values (10^5–10^8/*M*/s) and lower, more variable values of k_d (10^{-5}–10^3/s). According to the law of mass action, if *A* = antibody or ligand, *B* = receptor, and *AB* = bound antibody or ligand:

$$A + B \underset{k_d}{\overset{k_a}{\rightleftharpoons}} AB; \tag{2}$$

this gives rise to the simultaneous nonlinear differential equations ***(55)***

$$d/dt\ [A] \text{ or } [B] = k_d[AB] - k_a[A][B]; \tag{3}$$

and

$$d/dt\ [AB] = k_a[A][B] - k_d[AB] \tag{4}$$

Expressions in this form describe all nonlinear transfers between compartments (those resulting from reversible saturable binding rather than diffusion or excretion, where the rate is simply the rate constant times the concentration).

In practice, injected antibody does not all arrive at the tumor binding sites at once because of its molecular size and circulation time. Thus, though the rate constant k_a is large, the rate $k_a[A][B]$ of binding is likely to be slow because of the small value of [*A*], the local ECF concentration of antibody. Dissociating antibody can rebind instead of diffusing away from the tumor, so the slower diffusion of larger molecules might prolong tumor residence time by promoting rebinding, and it will also be replenished by the slow arrival of more antibody with time. Because there is concurrent elimination from the body, no state of equilibrium is reached (the term "equilibrium constant" is still valid, determined from equilibrium conditions in vitro).

2.3. Mathematics and Computer Software

The set of equations combined with realistic parameter values **(Table 3)** constitute what is described mathematically as a stiff system, which initially undergoes very rapid changes but then gradually smoothes out to give slowly varying changes ***(56,57)***. This is caused in this model by the very large differences (several orders of magnitude) between the values of the rate constants operating in the different compartments and the initial bolus injection or "impulsive initial input." As a test for stiffness ***(57)***, a factor can be calculated for a typical set of initial parameter values and is found to be of the order of 10^8 ***(58)***. A factor of 10^2 is considered stiff. Very stiff systems are difficult to solve ***(56)***, and computer programs that can deal with nonstiff systems cannot give solutions beyond the initial rapidly changing period without yielding negative and/or wildly improbable values, because the set of equations describing the model must be solved at

Table 3
Standard Parameters for Model Simulation

Injected dose at time 0	$= 6 \times 10^{-8}$ moles
Plasma volume	= 2.51
ECF volume	= 121
Tumor volume	= 0.011
Whole body volume	= 701
Plasma binding association constant	= 0
Plasma-binding dissociation constant	= 0
Rate constant from plasma to ECF	$= 10^{-5}$ s^{-1}
ECF to plasma	$= 2 \times 10^{-6}$ s^{-1}
Tissue binding association constant	$= 10^{7}$ M^{-1} s^{-1}
Tissue binding dissociation constant	$= 10^{-3}$ s^{-1}
Excretion rate constant	$= 10^{5}$ s^{1}
Tumor receptor concentration	$= 2 \times 10^{-8}$ $M1^{-1}$
Tissue receptor concentration	$= 2 \times 10^{-10}$ $M1^{-1}$
Plasma receptor concentration	= 0
ECF receptor concentration	= 0

extremely short intervals during the initial phase, which becomes inappropriate at a later stage when change is more gradual. Algorithms for solving very stiff systems have variable intervals between calculations, adjusted by internal feedback according to the momentary rates of change within the system. This is how the FACSIMILE/CHEKMAT package ***(59)*** is able to handle the model parameters.

Sensitivity analysis is a mathematical technique that can then be used to determine which factors are the most important in achieving the desired result. The inverse problem is to identify unknown factors, for which values have been estimated, if the experimental value of one or more is known. To do this the system must be identifiable, i.e., there must be a mathematical solution to the puzzle. In an experimental setting such unknowns might include the true in vivo binding affinity of antibody to cell surfaces, or the total antigen in normal tissues throughout the body.

The effects of individual parameters on tumor:background uptake ratios were assessed by comparing the tumor:background UR and TC of the injected substance. Unless stated, values were standardized as in **Table 3**, and the effects of altering the model variables were then assessed by inserting different values in sequential simulations.

3. Model Predictions

3.1. Molecular Size

In the absence of any binding to tumor, normal tissue, or circulating receptors, the model predicts whole body half-times of 36, 4.7, and 1.4 h for plasma

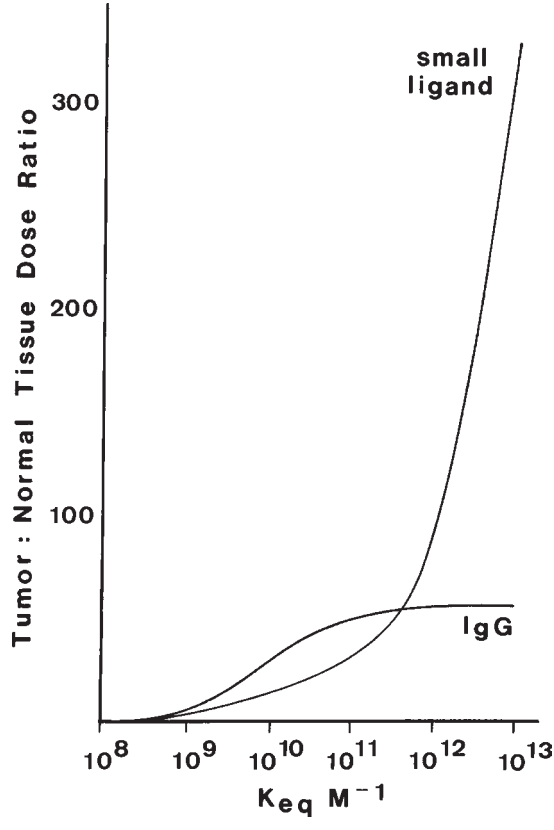

Fig. 3. Integral dose ratios for whole antibody (IgG) and a small tumor-binding ligand at increasing affinities (K_{eq}).

to ECF values of 10^{-5}, 10^{-4}, and 10^{-3} s^{-1} respectively, consistent with molecular sizes of IgG, Fab' fragments, and a small ligand.

The maximal TC and maximal tumor:normal UR achieved do not differ significantly among molecular sizes but occur later with increasing molecular size. The peak TC occurs earlier than the peak UR for a given size. For the smallest molecule, peak values of TC and UR occur almost simultaneously, very early, and fall again rapidly. Thus, the area under the TC curve and hence the cumulative or integral tumor dose is small, whereas for an "IgG" molecule there is a greater dose-to-tumor than for the small molecule, but during this time the low UR indicates a large dose to the rest of the body. The effect of increasing affinity is greatest for the smallest molecule **(Fig. 3)**. It should be difficult to achieve adequate TC and UR values together, and this separation of TC and UR peaks is one of the fundamental problems of tumor targeting.

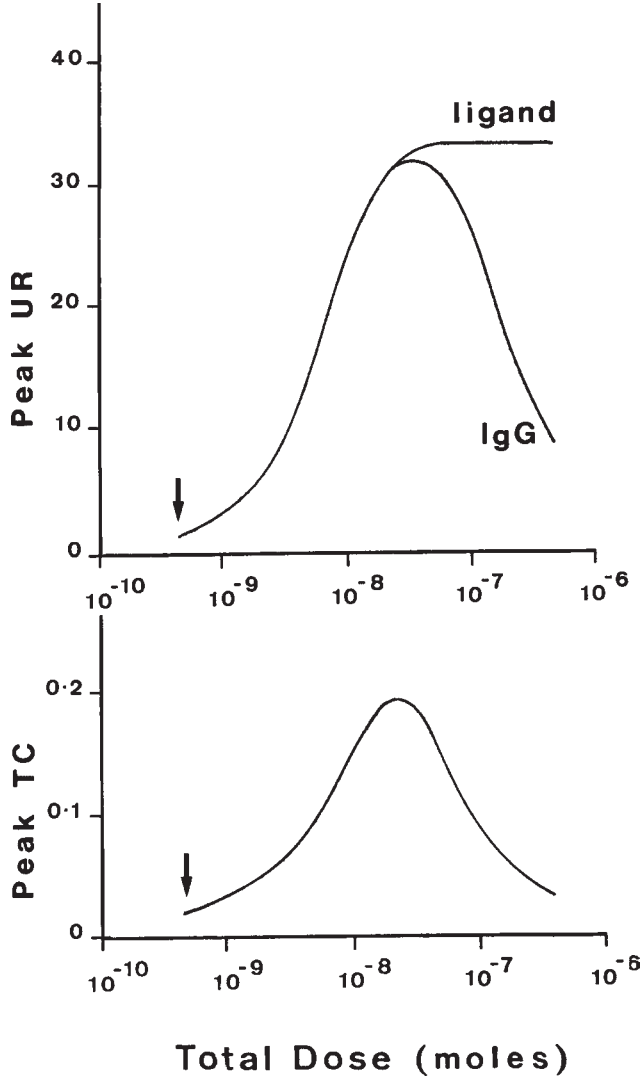

Fig. 4. Effect of injected dose on (top) peak tumor:normal tissue UR for whole antibody (IgG) and a small tumor-binding ligand, and (bottom) peak tumor content as a percentage of injected dose for all molecular sizes. Affinity in all cases (K_{eq}) = $10^{10}/M$. Arrows show the typical doses used in antibody scanning.

3.2. Injected Dose

Initially, and unexpectedly, as the dose is increased a greater proportion of the injected dose becomes bound to tumor, so that the UR is increased **(Fig. 4)**. With further increases this proportion falls again, although the total amount

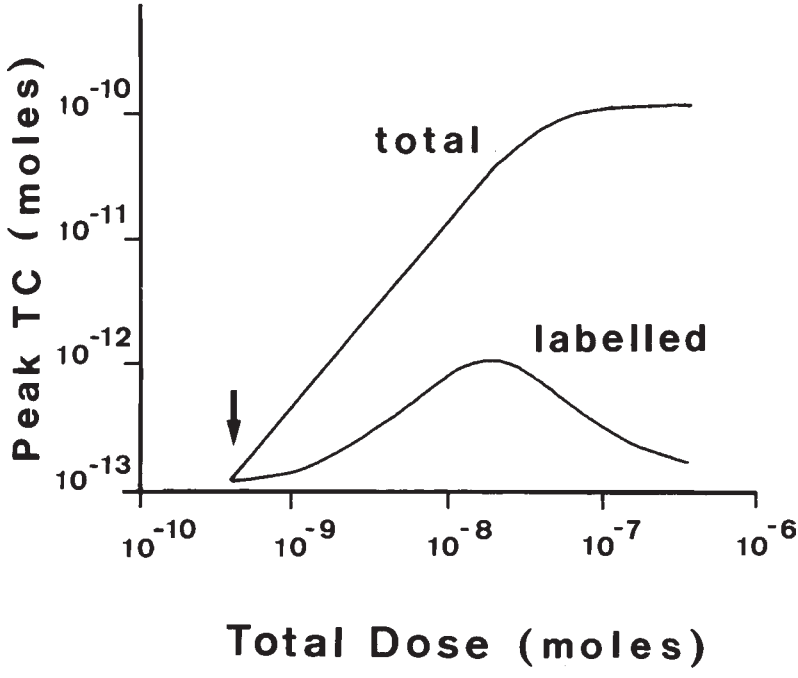

Fig. 5. Effect of injected dose on peak TC of injected substance (all molecular sizes). Curves represent total and labeled molecules bound to tumor given a fixed number of labeled molecules (6×10^{10} mol) at all dose levels. Arrow shows the typical dose used in antibody scanning.

reaching the tumor steadily increases to a plateau, consistent with saturation of all tumor receptors. For a very small injected molecule the UR reaches a plateau as excess molecules are excreted, whereas for large sizes typical of antibody molecules the UR is lowered by excess molecules contributing to "background" concentration resulting from slow excretion.

If the labeled dose is assumed constant and the dose increased by adding unlabeled molecules, the absolute amount of labeled substance is seen to rise and fall with increasing dose **(Fig. 5)**. Thus, adding the correct proportion of unlabeled molecules, to achieve optimal binding without any excess, increases the TC of the label.

3.3. Combined Effects of Injected Dose, Molecular Size, and Binding Affinity

The effects of dose, size, and affinity are evidently interdependent **(Fig. 6)**. High affinity is essential, but the dose must be optimized to achieve the best results. The values of TC and UR are continuously changing and can be predicted for any dose/affinity combination at any instant.

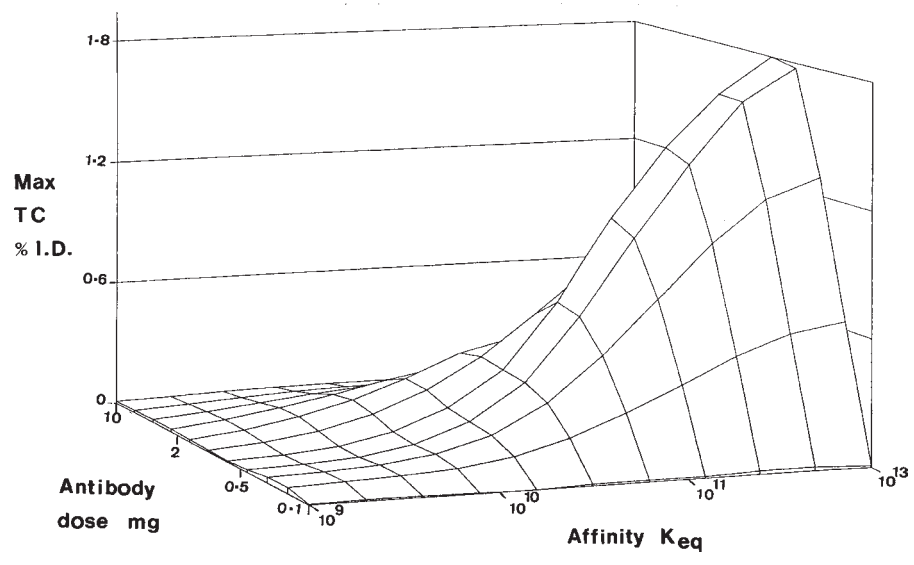

Fig. 6. Combined effect of injected dose and binding affinity K_{eq} on TC as a percentage of injected dose for a large (antibody) molecule. Curves for UR are similar.

4. Discussion

The "optimal dose" effect on UR is predicted only in model simulations that include tumor-associated receptors at nontumor sites, i.e., on normal tissue cells and in circulation. This is because of the initial predominance of nontumor binding, with an increase in UR beginning at the dose at which nontumor sites are approx 95% saturated. Conversely, in a tumor bearing a completely tumor-specific receptor or antigen (such as a xenograft), UR will not change with dose until tumor saturation is approached, when it begins to fall. These model predictions could partly explain the higher UR and TC (as percentage of injected dose) values shown in animal studies generally. In practice, normal tissue receptors in humans may well be more accessible than tumor receptors, and thus occupied first, being more widespread (trapping antibody away from the tumor site) and in better-vascularized tissues. This model was validated in a clinical study using anti-CEA and data from scanning and biopsy material ***(60,61)***. Unique values could be found for all the unknown parameters in each patient studied, within reasonably narrow confidence intervals, to fit with the observed tumor:normal tissue URs, provided that the amount of tumor antigen available for binding to antibody was reduced substantially from the actual measured concentration in biopsies. No other alteration in any single parameter could give close correlation of observed and predicted URs.

A decrease in UR with increasing dose can be explained by saturation of receptors. Exceeding the saturation dose is less detrimental to the UR of small than of large molecules since clearance of unbound small molecules is rapid, but the proportion of the injected dose reaching the tumor still tends to zero with further increments in dose. The absence of any dose effect in some studies may be explained by tumor-specific receptors in animals, a small range of doses studied, variability of antigen quantity in relation to dose in different subjects, or antibody of too low an affinity.

From computer simulation of antibody targeting, high affinity is of overriding importance to maximize UR and TC, but the dose must be optimized or the effect of high affinity is not seen. Dose is more critical for large molecules because UR values fall as soon as tumor binding is saturated, whereas for small, rapidly cleared molecules, a minimum optimal dose is seen beyond which UR is maintained. Low doses give low UR and TC values for all molecules because of normal-tissue binding. Much higher integral dose ratios are seen with small molecules, and the ideal targeting substance would be small with very high affinity.

It might be possible to achieve "supernatural" binding by molecular modeling and chemical or genetic engineering of existing antibody-binding sites. Study of the structure of known high-affinity binding sites and of antibody–antigen interfaces, using crystallographic data and computer modeling, should suggest structural modifications likely to improve affinity. It may ultimately be possible to design small tumor-binding molecules by computer modeling of tumor-associated substances that are structurally well-defined. The techniques involved are complex and good theoretical evidence of the likely benefits is important. Also, prediction of affinity may be difficult based on the structures of free molecules since variable domains have been shown to alter on binding, i.e., an induced fit rather than lock-and-key mechanism ***(62)***. This mechanism may be responsible for the 17-fold increase in affinity observed using bispecific antibodies binding to two epitopes at once ***(63)***. Increased affinity has also been found to result from the use of two different antibodies, either binding to opposing epitopes on the antigen to form stable, circular complexes ***(64,65)*** or binding to adjacent epitopes allowing the Fc ends to interact ***(64)***.

Currently available targeting substances, of which antibodies have the broadest potential application in clinical practice, do not have high enough binding affinities to give consistently reliable results in diagnostic studies or to be safe for effective therapy. Further studies should address this fundamental problem and aim to identify or create targeting substances with very high affinity and ideally specificity. All nonspecific agents need dose optimization to maximize their uptake, which can rationally be approached using a computer model interactively with all measurable patient data to predict individual optimal doses.

References

1. Garlick, D. G. and Renkin, E. M. (1970) Transport of large molecules from plasma to interstitial fluid and lymph in dogs. *Am. J. Physiol.* **219,** 1595–1605.
2. Arfors, K.-E., Rutili, G., and Svensjo, E. (1979) Microvascular transport of macromolecules in normal and inflammatory conditions. *Acta. Physiol. Scand. Suppl.* **463,** 93–103.
3. Taylor, A. E. and Granger, D. N. (1984) Exchange of macromolecules across the microcirculation, in *Handbook of Physiology*, 4th ed. (Eugene, M. and Rekin, C., eds.), Waverly, Baltimore, MD, pp. 467–520.
4. Pilz, I., Kratky, O., Licht, A., and Sela, M. (1975) Shape and volume of fragments Fab' and $F(ab')_2$ of anti-poly(D-alanyl) antibodies in the presence and absence of tetra-D-alanine as determined by small-angle x-ray scattering. *Biochemistry* **14,** 1326–1333.
5. Covell, D. G., Barbet, J., Holton, O. D., Black, C. D. V., Parker, R. J., and Weinstein J. N. (1986) Pharmacokinetics of monoclonal immunoglobulin G1, $F(ab')_2$, and Fab' in mice. *Cancer Res.* **46,** 3969–3978.
6. Sutherland, R. M., Buchegger, F., Schreyer, M., Vacca, A., and Mach, J. P. (1987) Penetration and binding of radiolabeled anti-carcinoembryonic antigen monoclonal antibodies and their antigen binding fragments in human colon multicellular spheroids. *Cancer Res.* **47,** 1627–1633.
7. Rowlinson-Busza, G., Deonarain, M. P., and Epenetos, A. A. (1996) Comparison of intact monoclonal antibody, its $F(ab')_2$ and Fab fragments and recombinant single chain Fv in a human tumor xenograft model. *Tumor Target.* **2,** 37–48.
8. Mason, D. W. and Williams, A. F. (1980) The kinetics of antibody binding to membrane antigens in solution and at the cell surface. *Biochem. J.* **187,** 1–20.
9. Heuser, L. S. and Miller, F. N. (1986) Differential macromolecular leakage from the vasculature of tumors. *Cancer* **57,** 461–464.
10. Ackerman, N. B. and Hechmer, P. A. (1978) Studies on the capillary permeability of experimental liver metastases. *Surg. Gyn. Obstet.* **146,** 884–888.
11. Underwood, J. C. E. and Carr, I. (1972) The ultrastructure and permeability characteristics of a transplantable rat sarcoma. *J. Pathol.* **107,** 157–166.
12. Papadimitriou, J. M. and Woods, A. E. (1975) Structural and functional characteristics of the microcirculation in neoplasms. *J. Pathol.* **116,** 65–72.
13. Peterson, H.-I., Appelgren, L., Lundborg, G., and Rosengren, B. (1973) Capillary permeability of two transplantable rat tumours as compared with various normal organs of the rat. *Bibl. Anat.* **12,** 511–518.
14. Gerlowski, L. E. and Jain, R. K. (1986) Microvascular permeability of normal and neoplastic tissues. *Microvasc. Res.* **31,** 288–305.
15. Rostock, R. A., Klein, J. L., Kopher, K. A., and Order, S. E. (1984) Variables affecting the tumor localization of 131I-anti-ferritin in experimental hepatoma. *Amer. J. Clin. Oncol.* **6,** 9–18.
16. Otsuka, F. L. and Fleishman, J. B. (1986) Comparative studies using ^{125}I-and ^{111}In-labeled monoclonal antibodies. *Eur. J. Nucl. Med.* **11,** 295–299.
17. Badger, C. C., Krohn, K. A., Peterson, A. V., Shulman, H., and Bernstein, I. D. (1985) Experimental radiotherapy of murine lymphoma with 131I-labeled anti-Thy 1. 1 monoclonal antibody. *Cancer Res.* **45,** 1536–1544.

18. Jakowatz, J. G., Beatty, B. G., Vlahos, W. G., Porudominsky, D., Philben, V. J., Williams, L. E., Paxton, R. J., Shively, J. E., and Beatty, J. D. (1985) High specific activity 111In-labeled anticarcinoembryonic antigen monoclonal antibody: biodistribution and imaging in nude mice bearing human colon cancer xenografts. *Cancer Res.* **45,** 5700–5706.
19. Rogers, G. T., Harwood, P. J., Pedley, R. B., Boden, J., and Bagshawe, K. D. (1986) Dose-dependent localisation and potential for therapy of $F(ab')_2$ fragments against CEA studied in a human tumour xenograft model. *Br. J. Cancer* **54,** 341–344.
20. Washburn, L. C., Sun, T. T., Lee, Y. C., Byrd, B. L., Crook, J. E., and Steplewski, Z. (1987) Y-90-labeled monoclonal antitumour antibodies: effect of purification method and coinjection of unlabeled antibody. *J. Nucl. Med.* **28,** 721.
21. Sharkey, R. M., Primus, F. J., and Goldenberg, D. M. (1987) Antibody protein dose and radioimmunodetection of GW-39 human colon tumor xenografts. *Int. J. Cancer* **39(9),** 611–617.
22. Kennel, S. J., Falcioni, R., and Wesley, J. W. (1991) Microdistribution of specific rat monoclonal antibodies to mouse tissues and human tumour xenografts. *Cancer Res.* **51,** 1529–1536.
23. Boerman, O. C., Sharkey, R. M., Wong, G. Y., Blumenthal, R. D., Aninipot, R. L., and Goldenberg, D. M. (1992) Influence of antibody protein dose on therapeutic efficacy of radioiodinated antibodies in nude mice bearing GW-39 human tumor. *Cancer Immunol. Immunother.* **35,** 127–134.
24. Halpern, S. E., Dillman, R. O., Witztum, M. D., Shega, J. F., Hagan, P. L., Burrows, W. M., Dillman, J. B., Clutter, M. L., Sobol, R. E., Frincke, J. M., Bartholomew, R. M., David, G. S., and Carlo, D. J. (1985) Radioimmunodetection of melanoma utilising In-111 96.5 monoclonal antibody: a preliminary report. *Radiology* **155,** 493–499.
25. Murray, J. L., Rosenblum, M. G., Sobol, R. E., Bartholomew, R. M., Plager, C. E., Haynie, T. P., Jahns, M. F., Glenn, H. J., Lamki, L., Benjamin, R. S., Papadopoulos, N., Boddie, A. W., Frincke, J. M., David, G. S., Carlo, D. J., and Hersh, E. M. (1985) Radioimmunoimaging in malignant melanoma with 111Indium labeled monoclonal antibody 96.5. *Cancer Res.* **45,** 2376–2381.
26. Carrasquillo, J. A., Bunn, P. A., Keenan, A. M., Reynolds, J. C., Schroff, R. W., Foon, K. A., Ming-Hsu, S., Gazdar, A. F., Mulshine, J. L., Oldham, R. K., Parentesis, P., Horowitz, M., Eddy, J., James, P., and Larson, S. M. (1986) Radioimmunodetection of cutaneous T-cell lymphoma with 111In-labeled T101 monoclonal antibody. *N. Engl. J. Med.* **315,** 673–680.
27. Eger, R. R., Covell, D. G., Carrasquillo, J. A., Abrams, P. G., Foon, K. A., Reynolds, J. C., Schroff, R. W., Morgan, A. C., Larson, S. M., and Weinstein, J. N. (1987) Kinetic model for the biodistribution of an 111Indium-labeled monoclonal antibody in humans. *Cancer Res.* **47,** 3328–3336.
28. Murray, J. L., Lamki, L. M., Shanken, L. J., Blake, M. E., Plager, C. E., Benjamin, R. S., Schweighardt, S., Unger, M. W., and Rosenblum, M. G. (1988) Immunospecific saturable clearance mechanisms for Indium-111–labeled anti-melanoma monoclonal antibody 96. 5 in humans. *Cancer Res.* **48,** 4417–4422.

29. Rosenblum, M. G., Murray, J. L., Lamki, L., David, G., and Carlo, D. (1987) Comparative clinical pharmacology of [111In]-labeled murine monoclonal antibodies. *Cancer Chemother. Pharmacol.* **20,** 41–47.
30. Babaian, R. J., Murray, J. L., Lamki, L. M., Haynie, T. P., Hersh, E. M., Rosenblum, M. G., Glenn, H. J., Unger, M. W., Carlo, D. J., and Von Eschenbach, A. C. (1987) Radioimmunological imaging of metastatic prostate cancer with 111indium-labeled monoclonal antibody PAY 276. *J. Urol.* **137,** 439–443.
31. Kirkwood, J. M., Neumann, R. D., Zoghbi, S. S., Ernstoff, M. S., Cornelius, E. A., Shaw, C., Ziyadeh, T., Fine, J. A., and Unger, M. W. (1987) Scintigraphic detection of metastatic melanoma using indium 111/DTPA conjugated anti-gp 240 antibody (ZME-018). *J. Clin. Oncol.* **5,** 1247–1255.
32. Abdel-Nabi, H. H., Schwartz, A. N., Goldfogel, G., Ortman-Nabi, J. A., Matsuoka, D. M., Unger, M. W., and Wechter, D. G. (1988) Colorectal tumours: scintigraphy with In-111 anti-CEA monoclonal antibody and correlation with surgical, histopathologic, and immunohistochemical findings. *Radiology* **166,** 747–752.
33. Patt, Y. Z., Lamki, L. M., Haynie, T. P., Unger, M. W., Rosenblum, M. G., Shirkhoda, A., and Murray, J. L. (1988) Improved tumour localisation with increasing dose of Indium-111-labeled anti-CEA monoclonal antibody ZCE-025 in metastatic colorectal cancer. *J. Clin. Oncol.* **6,** 1220–1230.
34. Carrasquillo, J. A., Abrams, P. G., Schroff, R. W., Reynolds, J. C., Woodhouse, C. S., Morgan, A. C., Keenan, A. M., Foon, K. A., Perentis, P., Marshall, S., Horowitz, M., Szymendera, J., Englert, J., Oldham, R. K., and Larson, S. M. (1988) Effect of antibody dose on the imaging and biodistribution of Indium-111 9.2.27 anti-melanoma monoclonal antibody. *J. Nucleic Med.* **29,** 39–47.
35. Carrasquillo, J. A., Sugarbaker, P., Colcher, D., Reynolds, J. C., Esteban, J., Bryant, G., Keenan, A. M., Perentis, P., Yakoyama, K., Simpson, D. E., Ferroni, P., Farkas, R., Schlom, J., and Larson, S. M. (1988) Radioscintigraphy of colon cancer with iodine-131–labeled B72. 3 monoclonal antibodies. *J. Nucleic Med.* **29,** 1022–1030.
36. Lamki, L. M., Murray, J. L., Rosenblum, M. G., Patt, Y. Z., Babaian, R., and Unger, M. W. (1988) Effect of unlabeled monoclonal antibody (Moab) on biodistribution of 111indium labeled (Moab). *Nucleic Med. Commun.* **9,** 553–564.
37. Press, O. W., Eary, J. F., Badger, C. C., Martin, P. J., Appelbaum, F. R., Levy, R., Miller, R., Brown, S., Nelp, W. B., Krohn, K. A., Fisher, D., DeSantes, K., Porter, B., Kidd, P., Thomas, E. D., and Bernstein, I. D. (1989) Treatment of refractory non-Hodgkin's lymphoma with radiolabeled MB-1 (anti-CD37) antibody. *J. Clin. Oncol.* **7,** 1027–1038.
38. Griffin, T. W., Bokhari, F., Collino, J., Stochl, M., Bernier, M., Gionet, M., Siebecker, D., Wertheimer, M., Giroves, E. S., Greenfield, L., Houston, L. L., Doherty, P. W., and Wilson, J. (1989) A preliminary pharmacokinetic study of 111In-labeled 260F9 anti-(breast cancer) antibody in patients. *Cancer Immunol. Immunother.* **29,** 43–50.
39. Serafini, A. N., Goldenberg, D. M., Higinbotham-Ford, E. A., Silberstein, E. B., Van Heertum, R. L., Kotler, J. A., Balasubramanian, N., Garty, I., and

Wlodkowski, T. (1989) A multicenter trial of cancer imaging with fragments of CEA monoclonal antibodies. *J. Nucl. Med.* **82,** 748.

40. Scheinberg, D. A., Straus, D. J., Yeh, S. D., Divgi, C., Gavin-Chesa, P., Graham, M., Pentlow, K., Coit, D., Oettgen, H. F., and Old, L. J. (1990) A phase I toxicity, pharmacology, and dosimetry trial of monoclonal antibody OKB7 in patients with non-Hodgkins lymphoma: effects of tumor burden and antigen expression. *J. Clin. Oncol.* **8,** 792–803.
41. Steward, M. W. and Steensgaard, J. (1983) *Antibody Affinity: Thermodynamic Aspects and Biological Significance*. CRC, Boca Raton, FL.
42. Kennel, S. J., Foote, L. J., Lanford, P. K., Johnson, M., Mitchell, T., and Braslawsky, G. R. (1983) Direct binding of radio-iodinated monoclonal antibody to tumour cells: significance of antibody purity and affinity for drug targeting or tumour imaging. *Hybridoma* **2,** 297–310.
43. Devey, M. E. and Steward, M. W. (1988) The role of antibody affinity in the performance of solid phase assays, in *Elisa and Other Solid Phase Immunoassays* (Kemeny, D. M. and Chollacombe, S. J., eds.), Wiley, UK, pp. 135–153.
44. Weinstein, J. N., Covell, D. G., Barbet, J., Eger, R. R., Holton, O. D., Talley, M. J., Parker, R. J., and Black, C. D. V. (1987) Local and cellular factors in the pharmacology of monoclonal antibodies, in *Membrane Mediated Cytotoxicity* (Bonavida, B. and Collier, R. J., eds.), Liss, New York, pp. 279–289.
45. Sharkey, R. M., Primus, F. J., Shochat, D., and Goldenberg, D. M. (1988) Comparison of tumour targeting of mouse monoclonal and goat polyclonal antibodies to carcinoembryonic antigen in the GW-39 human tumour-hamster host model. *Cancer Res.* **48,** 1823–1828.
46. Wang, A.-C., Banjo, C., Fuks, A., Shuster, J., and Gold, P. (1976) Heterogeneity of the protein moiety of carcinoembryonic antigens. *Immunol. Commun.* **5,** 205–210.
47. Olson, W. C., Spitznagel, T. M., and Yarmush, M. L. (1989) Dissociation kinetics of antigen-antibody interactions: studies on a panel of anti-albumin monoclonal antibodies. *Mol. Immunol.* **26,** 129–136.
48. Watt, R. M., Herron, J. M., and Voss, E. W. (1980) First order dissociation rates between a subpopulation of high-affinity rabbit anti-fluorescyl IgG antibody and homologous ligand. *Mol. Immunol.* **17,** 1237–1243.
49. Morrison, J. F. and Walsh, C. T. (1988) The behaviour and significance of slow-binding enzyme inhibitors. *Adv. Enzymol.* **61,** 201–301.
50. Aisen, P. and Leibman, A. (1978) Thermodynamic and accessibility factors in the specific binding of iron to human transferrin, in *Transport by Proteins* (Blauer, G. and Sund, H., eds.), Walter de Gruyter, Berlin, pp. 277–294.
51. Green, N. M. (1963) Avidin. The nature of the biotin-binding site. *Biochem. J.* **89,** 599–609.
52. Absolom, D. R. and van Oss, C. J. (1986) The nature of the antigen-antibody bond and the factors affecting its association and dissociation. *CRC Crit. Rev. Immunol.* **6,** 1–46.
53. Thomas, G. D., Chappell, M. J., Dykes, P. W., Ramsden, D. B., Godfrey, K. R., Ellis, J. R. M., and Bradwell, A. R. (1989) Effect of dose, molecular size, affinity,

and protein binding on tumour uptake of antibody or ligand: a biomathematical model. *Cancer Res.* **49,** 3290–3296.
54. Chappell, M. J., Thomas, G. D., Godfrey, K. R., and Bradwell, A. R. (1991) Optimal tumour targeting by antibodies: development of a mathematical model. *J. Pharmacokin Biopharm.* **19,** 227–260.
55. Jacquez, J. A. (1985) *Compartmental Analysis in Biology and Medicine*, University of Michigan Press, Ann Arbor, MI.
56. Shampine, L. F. and Gear, C. W. (1979) A user's view of solving stiff differential equations. *SIAM Rev.* **21,** 1–17.
57. Fatunla, S. O. (1988) *Numerical Methods for Initial Value Problems in Ordinary Differential Equations*. Academic, New York.
58. Chappell, M. J. and Godfrey, K. R. (1990) Structural identifiability of a model developed for optimal tumour targeting by antibodies using the similarity transformation approach. University of Warwick Control and Instrument Systems Centre, Report No. 7.
59. Curtis, A. R. and Sweetenham, W. P. (1987) FACSIMILE/CHEKMAT User's Manual. Harwell Laboratory Report, UK Atomic Energy Authority, Atomic Energy Research Establishment, Computer Science and Systems Division, 12805.
60. Attard, A. R., Chappell, M. J., Bennett, J., Thomas, G. D., Godfrey, K. R., Dykes, P. W., and Bradwell, A. R. (1991) Optimal tumor targeting by antibodies: Validation of a mathematical model. *Antibody Immunoconj. Radiopharmaceu.* **4,** 435–441.
61. Thomas, G. D. (1995) Development of a model of tumour targeting to predict optimal conditions for therapy. MD Thesis, University of London, London.
62. Bhat, T. N., Bentley, G. A., Fischmann, T. O., Boulot, G., and Poljak, R. J. (1990) Small rearrangements in structures of Fv and Fab fragments of antibody D1. 3 on antigen binding. *Nature* **347,** 483–485.
63. Cheong, H. S., Chang, J. S., Park, J. M., and Byun, S. M. (1990) Affinity enhancement of bispecific antibody against two different epitopes in the same antigen. *Biochem. Biophys. Res. Commun.* **173,** 795–800.
64. Ehrlich, P. H., Moyle, W. R., Moustafa, Z. A., and Canfield, R. E. (1982) Mixing two monoclonal antibodies yields enhanced affinity for antigen. *J. Immunol.* **128,** 2709–2713.
65. Holmes, N. J. and Parham, P. (1983) Enhancement of monoclonal antibodies against HLA-A2 is due to antibody bivalency. *J. Biol. Chem.* **258,** 1580–1586.

9

Inhibition of Tumor Blood Flow

Lai-Ming Ching, William R. Wilson, and Bruce C. Baguley

1. Introduction

Research into the treatment of cancer has often been driven by the idea that a common biochemical pathway might exist in all tumors, providing an ideal target for therapy. However, it is now clear that a great variety of genetic changes contributes to the development of individual cancers, and that no two cancers are identical. Nevertheless, a common feature in solid tumors is the disorganized way in which the blood vessels develop. Networks of tumor capillaries, linked to the blood supply by arterioles and venules, are necessary for tumors to grow but, in contrast to capillaries supplying normal tissue, are haphazard in both their structure and their dynamics. It may be possible to use this common feature as a basis for selective therapy. In this chapter we provide a short review of the vasculature of solid tumors, then describe methods by which drugs might be used to inhibit tumor blood flow. Finally, we review some of the methods available for measurement of tumor blood flow.

1.1. Tumor Vasculature

Although the architecture of tumor blood vessels has been studied using a number of techniques, one of the most fascinating involves the use of acrylic resin casts. This is exemplified by the work of Skinner et al ***(1)***, who studied a series of chemically induced tumors in rats. A resin solution was injected intra-arterially into the anesthetized rat, the animal was killed, and the blood vessels to the tissue, were clamped while the resin set. Tissue was digested with alkali and the cast coated with gold and examined by electron microscopy. Whereas normal colon mucosa showed a consistent regular pattern, tissue from tumors showed considerable disorganization with marked dilation and tortuosity of capillaries. For small tumors it was possible to discern areas in the tumor that

From: *Methods in Molecular Medicine, Vol. 25: Drug Targeting: Strategies, Principles, and Applications*
Edited by: G. E. Francis and C. Delgado

had a regular, normal vascular appearance. These areas were thought to arise from tumor invasion of pre-existing blood vessels. The remaining areas were thought to arise from tumor-induced formation of new capillaries (angiogenesis) ***(2)***.

1.2. Hypoxia and Necrosis

The disorganized vasculature of solid tumors has a number of consequences for the physiological state of the tumor cells. The lack of coordinated development of exchange vessels means that some tumor cells will be growing at positions comparatively distant from the nearest blood vessel. When this distance exceeds a few cell diameters, the supply of oxygen is compromised by oxygen consumption of the intervening cells. Such cells are referred to as chronically hypoxic and exhibit altered behavior as a result of this stress. They are comparatively resistant to ionizing radiation because oxygen is a radiosensitizing agent ***(3)***. They have an increased tendency to undergo apoptosis ***(4,5)*** and may also show genetic instability, leading to tumor progression and drug resistance ***(6,7)***. Cells at a distance from the vasculature are deprived of nutrients as well as oxygen. They may become unable to sustain their production of adenosine triphosphate (ATP), which is essential for maintaining the integrity of the plasma membrane as well as of internal membranes, such as the mitochondrial membrane. As a result, calcium ions leak into the cell, the mitochondria swell, and the cell dies by necrosis. Both necrosis and apoptosis are commonly observed in solid tumors ***(4).***

Hypoxia and necrosis may also arise from the dynamics of tumor blood flow. Because the network of tumor capillaries is disorganized, blood flow rates and even flow directions are not constant. This is accentuated by the high interstitial pressure in tumors, itself a consequence of fluid leakage from capillaries ***(8)***. As a result, blood flow in some capillaries may slow or cease entirely for varying periods of time, leading to acute stress, hypoxia, and sometimes necrosis. Furthermore, the resumption of tumor blood flow following a period of cessation can lead to tissue damage by a process known as "reperfusion" injury. This process is well known in cardiac tissue as a result of heart attacks and in brain tissue as a result of stroke ***(9)***. It has been studied in tumors by means of physical clamping of subcutaneous tumors (to halt the blood supply) for various periods of time ***(10)***. The mechanism of reperfusion injury involves overproduction of oxygen radicals in response to re-establishment of the blood supply. These radicals cause tissue damage and consequent necrosis.

1.3. Tumor Blood Flow and Cancer Therapy

The inefficient blood supply in tumor tissue has important implications for cancer therapy. Cells poorly supplied with oxygen and nutrients tend to be resistant not only to radiotherapy, as noted in **Subheading 1.2.**, but also to

most chemotherapeutic agents. However, the inefficient vascular system of tumors may also be an "Achilles heel" that can be attacked for therapeutic benefit. If tumor blood flow can be selectively inhibited for prolonged periods, extensive additional cell killing would be expected. Even transient increases in hypoxia resulting from blood flow inhibition might be therapeutically useful, thanks to the development of "bioreductive" drugs that are activated selectively by metabolic reduction under hypoxic conditions ***(11,12)***. Increased hypoxia as a result of selective inhibition of tumor blood flow does appear to improve the tumor selectivity of bioreductive drugs, as noted in **Subheading 2**. Inhibition of tumor blood flow can also result in entrapment of a therapeutic agent within the tumors, thereby increasing its therapeutic effect ***(13–15)***.

In the same way that diffusion of oxygen and nutrients to tumor cells is limited by both diffusion distance and intermittent blood flow changes, diffusion of cancer chemotherapeutic drugs is limited, with consequent reduction of chemotherapeutic effect. Although some steps can be taken to minimize this effect, for instance by continuous drug infusion and by the use of pharmacological agents to increase tumor blood flow, an alternative approach is to exploit these properties of solid tumors. Selective reduction of tumor blood flow will lead to increased hypoxia, providing a target for selective chemotherapy ***(6,11,12,16,17)***. A combination of agents reducing tumor blood flow with those killing hypoxic cells therefore represents a promising therapeutic approach. Since reduction of blood flow is likely to kill tumor cells distant from blood vessels by ischemic injury, whereas cytotoxic agents are likely to kill cells close to blood vessels, a combination of blood-flow suppression techniques with conventional cytotoxic therapy provides a second approach. A third approach involves the use of blood-flow modifying agents to cause entrapment of a therapeutic agent within the tumor, thereby increasing its effect ***(13–15)***.

2. Selective Inhibitors of Tumor Blood Flow

A wide variety of exogenously administered compounds has been shown to modify tumor blood flow, including inhibitors of nitric oxide production ***(18)***, nicotinamide ***(19)***, catecholamine agonists and antagonists ***(20)***, angiotensin ***(21)***, pentoxifylline ***(22)***, flavone acetic and its analogs, and the *Vinca* alkaloids. An exhaustive review of these agents is beyond the scope of this chapter, but key findings with five important classes of tumor blood flow inhibitors (chemical structures of some of these are shown in **Fig. 1**) are outlined below.

2.1. Serotonin

Serotonin (5-hydroxytryptamine, 5-HT), a neurotransmitter with a number of other physiological effects, selectively decreases tumor blood flow ***(23,24)***. It induced tumor necrosis similar to that observed with tumor necrosis factor

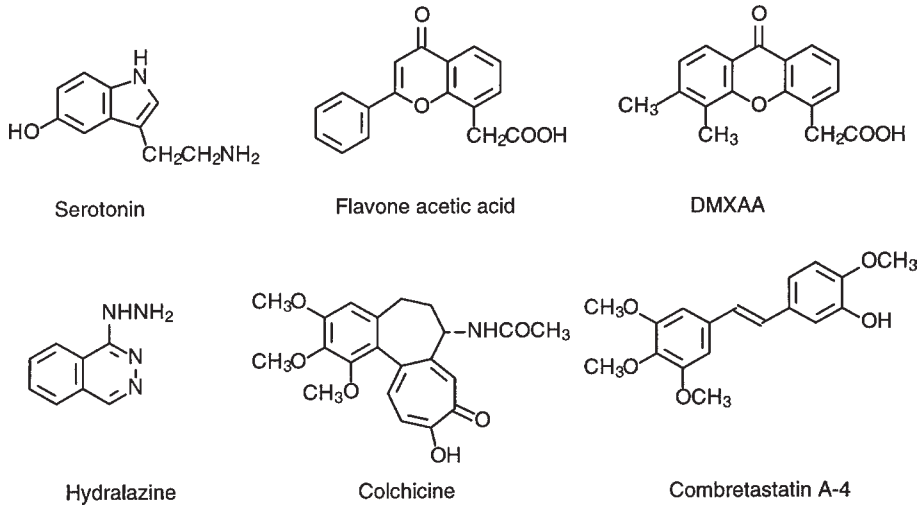

Fig. 1. Chemical structures of examples of compounds that decrease tumor blood flow. *See text* for details.

(25,26) and with some cases a tumor growth delay ***(24)***. Thus, serotonin alone may be useful as a tumor blood flow modifier either alone or in combination therapy. Coadministration of serotonin increased the antitumor response of the murine Colon 38 tumor to the drug DMXAA ***(25)***. Similar results were obtained with a human colon xenograft ***(27)*** and with the MDAH-MCa-4 murine mammary tumor ***(28).***

Serotonin interacts with type 2 (5-HT_2) serotonin receptors on smooth muscle cells underlying vascular endothelial cells to cause vasoconstriction. In normal tissues this effect is balanced with its capacity to cause vascular endothelial cells to release nitric oxide, a vascular relaxing factor ***(29)***. Serotonin appears to induce selective vasoconstriction of the arterioles supplying tumors, leading to a selective decrease in tumor blood flow ***(24)***. Serotonin has the potential to be used clinically, particularly because unwanted side effects may be reduced with specific antagonists of other types of serotonin receptors. Alternatively, specific agonists of 5-HT_2 receptors may be useful in this approach.

2.2. Hydralazine

Hydralazine, a vasodilator in clinical use, has been the most intensively studied of the vasoactive agents in targeting tumor blood flow as an approach for cancer therapy. Hydralazine inhibits tumor blood flow in a number of murine tumors, giving a maximum inhibition of 80–90% at doses between 2.5 and 5 mg/kg ***(30,31)***. However, at doses of <1 mg/kg, hydralazine increases tumor blood flow ***(31)***. Effects were seen within 15 min of administration, were main-

tained for at least 30 min postinjection ***(31)*** and persisted for 4–6 h ***(32)***. By itself, hydralazine caused tumor necrosis ***(33)*** but the growth delay elicited with hydralazine alone in experimental tumors was minimal ***(34)***. However, through its ability to reduce tumor blood flow, and thus tumor oxygenation and pH, a significant therapeutic gain was obtained when hydralazine was combined with bioreductive drugs designed to selectively target hypoxic cells ***(35)***. Potentiation of hyperthermia of experimental tumors was also observed using hydralazine ***(36)*** since inhibition of tumor perfusion reduces heat dissipation, leading to more pronounced selective heating of the tumor. It is the synergistic responses obtained when hydralazine is combined with bioreductive agents and hyperthermia that has promoted its investigations as an agent for targeting tumor blood flow.

The mechanism by which hydralazine reduces tumor blood flow is widely regarded to be a consequence of the "steal effect" ***(37)***. Since tumor blood vessels lack smooth muscle and do not respond to changes in perfusion pressure ***(38)***, dilation of normal blood vessels diverts blood flow away from tumor vessels. Using the double-labeling technique (*see* **Subheading 3.3.**), which allows quantitation of functional tumor vasculature before and after administration of the drug, Trotter and coworkers ***(39)*** showed that a substantial proportion of the vasculature in SCCVII murine tumors experienced complete cessation of flow following hydralazine administration. The response was highly heterogeneous, because not all vessels were rendered nonfunctional, and those that were nonfunctional were not uniformly distributed throughout the tumor mass. The number of nonperfused vessels was critically dose-related.

One of the disadvantages of hydralazine is that its blood flow effects are not specific to tumors ***(32)***. Hydralazine, although dramatically reducing tumor perfusion, also reduced relative perfusion to kidney, liver, lung, and spleen ***(32)***. The time course of the reduction in kidney and liver was similar to that for tumor. Nor was it possible to select a dose or schedule that achieved a reduction in tumor blood flow while leaving renal and hepatic functions intact. The pharmacokinetic profile of any drug given at the same time as hydralazine would be altered. Despite its systemic effects, hydralazine potentiated the response of Lewis Lung murine tumors to the hypoxic cell cytotoxin RSU-1069 ***(34)*** and to melphalan ***(40)***. Studies using a mouse fibrosarcoma showed hydralazine to be effective and safe for the potentiation of the response of the tumor to hyperthermia ***(36)***.

2.3. Flavone Acetic Acid

Flavone acetic acid (FAA, structure shown in **Fig. 1**), developed originally for its anti-inflammatory properties ***(41)***, has been shown to be a very effective agent against murine tumors ***(42)***. It appears to mediate its antitumor action in

mice indirectly ***(43)*** through modification of tumor vasculature ***(44–47)***. Several studies showed FAA to inhibit tumor blood flow as early as 10–15 min post treatment, with maximal inhibition achieved after 4–6 h ***(44–47)***. The fraction of nonperfused vessels increased with time after FAA treatment, and nonperfused vessels were not randomly distributed, but rather appear as foci ***(45)***. FAA treated tumors developed extensive hemorrhagic necrosis by 12–24 h ***(48,49)***, consistent with an effect on tumor blood flow. In contrast to hydralazine, tumor vascular collapse induced by FAA was sustained, leading to ischemia, necrosis, and growth inhibition ***(50)***. The vascular effects induced with FAA correlated with the antitumor response in a panel of murine tumors with differing sensitivities to FAA ***(51)***. These studies indicate that tumor vascular effects of FAA play a major role in the antitumor action of this agent.

An advantage of FAA over hydralazine is that FAA acts more selectively on tumor vasculature. FAA had no effect on blood flow in normal tissues apart from a transient reduction in the spleen 1–3 h after administration ***(52)***. The basis for this selectivity has not been established, but the biological effects of FAA have been attributed to its ability to induce a number of cytokines, most notably tumor necrosis factor-a (TNF) and the interferons ***(53)***. Whereas TNF production appears to be important for the blood flow effects, interferons elevate natural killer and T-cell mediated antitumor responses and may be necessary for long-term tumor responses ***(54)***. Pretreatment with antibodies to TNF completely abolished FAA-induced tumor vascular collapse ***(55)***, providing compelling evidence that TNF plays a critical role in mediating the vascular effects of FAA. The observations with FAA are consistent with those on the vascular effects of exogenously administered TNF, which induced tumor vascular collapse ***(13)***, leading to haemorrhagic necrosis ***(56)***. Histological examination of murine tumors from mice treated with TNF showed hemorrhage and congestion after 1–2 h, consistent with a progressive loss of blood flow ***(57)***. These effects were associated with an increase in clotting time induced only in tumor-bearing mice 4–6 h after FAA administration ***(58)***. The histological appearance, as well as the rate of induction of haemorrhagic necrosis of FAA-treated tumors, was similar to that of TNF-treated tumors ***(49)***, further suggesting that FAA-induced vascular effects are mediated by TNF. In culture, TNF increased endothelial cell permeability and leakage, partially through destabilization of cytoskeletal connections of cell adhesion molecules ***(59)***.

Although FAA has significant antitumor action on its own, it can augment the activity of bioreductive agents ***(60,61)*** and of hyperthermia ***(62)***. However, FAA has failed to demonstrate clinical activity when tested either as a single agent ***(63)*** or in combination with other cytokines ***(64)***. FAA upregulates cytokine production effectively in murine splenocytes but not in human blood cells ***(65)***, suggesting that a species difference might explain this discrepancy.

Thus, although FAA has failed to demonstrate activity in human systems, its impressive activity against murine tumors warrants its regard as a lead for antivascular therapies.

2.4. Xanthenone Analogs of FAA

A large number of chemical analogs of FAA were screened in this laboratory in a search for agents that could overcome the species selectivity of FAA, and compounds based on xanthenone-4-acetic acid (XAA) were found to have similar activity to FAA against murine tumors ***(66)***. Synthesis and biological testing of XAA derivatives led to the identification of 5,6-dimethylxanthenone-4-acetic acid (DMXAA, chemical structure shown in **Fig. 1**), which demonstrated superior (curative) antitumor activity and 12-fold higher dose potency than FAA against a murine colon carcinoma ***(67)***. FAA and DMXAA have been compared for immune stimulation ***(68)***, inhibition of tumor blood flow ***(69)***, and the induction of TNF ***(70)***, nitric oxide ***(71)***, and serotonin ***(72)***. In all cases DMXAA showed equal or greater activity at a 10-fold lower dose.

The action of DMXAA in mice, like that of FAA, appears to be mediated by the induction of synthesis of cytokines, in particular TNF ***(70)***. A significant step toward the selection of DMXAA as a clinical candidate occurred when it was shown that DMXAA could upregulate TNF mRNA in human HL-60 cell lines while FAA was inactive ***(73)***. In addition, DMXAA, but not FAA, has been found to stimulate human peripheral blood leukocytes to produce TNF in culture. The responsiveness of leucocytes has been found to vary among individuals ***(74)***. These studies demonstrate that DMXAA, but not FAA, can stimulate TNF production in blood leukocytes from the majority of the population.

DMXAA has been found to potentiate the response of two bioreductive agents, again at 10-fold lower doses than those used with FAA ***(61)***, and thus represents one of the most promising low mol-wt tumor blood flow inhibitors available. Results from the current clinical trial may indicate whether DMXAA will also have potential as an inhibitor of tumor blood flow in humans.

2.5. Vinca *Alkaloids and Other Antimitotic Agents*

Vinca alkaloids are best known for their tubulin binding activity and consequent arrest of cells in mitosis ***(75)***. Discovered by screening of plant products against murine leukemias, vincristine, vinblastine, and the semisynthetic vindesine are now in clinical use for the treatment of hematological malignancies. Baguley et al ***(76)*** demonstrated induction of tumor necrosis by vincristine, vinblastine, colchicine, and podophyllotoxin. Vincristine at a dose of 5 mg/kg was shown using a fluorescent dye technique to reduce tumor blood flow after 4 h by 73%. Leukemia sublines that were resistant to vincristine and vinblastine were refractory when grown as in an ascitic form, but were sensi-

tive to the induction of hemorrhagic necrosis by vinblastine when grown as subcutaneous tumors ***(76)***. Interestingly, paclitaxel, which induces tumor necrosis factor in vitro ***(77)*** and exerts its antimitotic action by stabilising microtubules, did not induce hemorrhagic necrosis ***(72)***. Hill and coworkers ***(78)***, using the CaNT murine carcinoma, showed that following the maximum tolerated doses of vincristine or vinblastine tumor blood flow was reduced to 10% of pretreatment value after 2 h and remained low for 24 h. Reductions to blood flow in skin, kidney, liver, and muscle were also observed, but these did not exceed 40% and had fully recovered by 6 h ***(79)***.

The tumor necrosis obtained using *Vinca* alkaloids and colchicine had a similar appearance to that induced using TNF or FAA ***(76,78)***. However, in contrast to FAA-treated mice, plasma TNF was not increased in tumor bearing mice treated with vinblastine ***(70,80)***. The results suggested that these structurally diverse agents inhibited tumor blood flow by different mechanisms. Combination of the two agents lead to synergistic growth delays, provided FAA administration followed that of vinblastine by 15 min to 24 h ***(80)***.

The *Vinca* alkaloids and some other antimitotic agents thus represent another class of agents that can selectively inhibit tumor blood flow by a mechanism that is distinct from that of TNF or TNF inducers such as FAA and DMXAA. Combretastatin A4, another antimitotic agent, appears to have a vascular basis for its action ***(81)*** and is currently a candidate for clinical trial. The mechanism of action of mitotic inhibitors is not well understood, but may result from their effects on vascular endothelial cells ***(82)***.

3. Methods for Assessing Drug-Induced Inhibition of Tumor Blood Flow

3.1. Introduction

A wide variety of different methods are available for measuring blood flow in experimental tumors, and some have recently been applied to investigation of human tumors. The following overview outlines the principles, advantages, and limitations of the most commonly used methods. The available techniques differ widely in the type of information they provide, in the extent to which they are invasive or destructive, in their spatial and temporal resolution, and in the sophistication of the technology required. There is no single preferred method for measuring tumor blood flow; the most appropriate technique will depend on the nature of the question to be addressed in each case. In this chapter we will not discuss nuclear medicine imaging methods, such as positron emission tomography (PET), single photon emission computed tomography (SPECT), and magnetic resonance imaging (MRI), since they have limited application in most experimental studies at this time. However, they will have obvious future applications.

Some general methodological issues warrant comment. As with any physiological measurement, the health and welfare of experimental animals is of paramount concern, not only for ethical reasons but because stressed animals do not give reliable information about the unstressed state. The possibility that the measurement technique might perturb blood flow must always be considered. It is well known that anesthetics generally depress respiration and heart rate and lower blood pressure. Core body temperature can fall by several degrees unless deliberately maintained, and the relative cardiac output to different organs changes. These cardiovascular effects can markedly alter blood flow in tumors ***(83,84)***. The use of anesthetics is unavoidable with some blood flow techniques and with appropriate controls these may still yield useful information, but considerable caution is needed in interpreting such data. Restraint without anesthesia is generally considered preferable for methods requiring immobilization but not surgery, but the restraint of animals can itself suppress tumor blood flow ***(85,86)***. The consequences of restraint on tumor radiation response are well documented ***(84,87,88)***. Joiner et al ***(86)*** have shown that acclimatization of mice to a restraining jig can overcome the effect of restraint on tumor blood flow, suggesting that the effect of restraint may be largely caused by stress.

A further potential problem is that volume loading can alter hemodynamics and tumor blood flow ***(89)***, and controls must always be employed to check for this or other effects of the vehicle used for drug administration. Finally, the difficulty of extrapolating findings from any particular experimental tumor system to primary tumors in humans must always be borne in mind. An interesting case in point is the finding ***(90)*** that whereas radiation-induced primary tumors in mice were not responsive to the blood flow effects of hydralazine, when one of the nonresponsive primary tumors was transplanted in isogenic mice the resulting tumors were then sensitive.

3.2. Measurement of Erythrocyte Velocity

One of the most direct and conceptually simple methods for assessing blood flow is by determining the velocity and flux of erythrocytes in exchange vessels. Two methods with quite different spatial resolution are available. Erythrocyte velocity can be measured in tumor "window" preparations in which tumors are grown between transparent windows so that the microvasculature can be examined directly, in real time, by microscopy ***(91)***. In some studies ***(92)*** fluorescently labeled erythrocytes are administered and visualized by fluorescence microscopy to facilitate enumeration and determination of flux. Such techniques can readily demonstrate changes in blood flow at the microregional level, but are somewhat restrictive in that few regions can be sampled and the required technology is not widely available. The suitability of window prepa-

rations as models for tumors in other anatomical sites is also unclear. Confocal laser scanning microscopy has recently allowed extension of these methods to provide real-time flow visualization of fluorescently labeled erythrocytes without using window preparations ***(93)***.

An alternative method for assessing erythrocyte velocity is based on the Doppler shift of infrared laser light when scattered by moving erythrocytes in tissue ***(94,95)***. The technique is minimally invasive since the infrared light has sufficient tissue penetrance that the probe can be placed on the surface of the tumor. Flow can then be examined in the periphery of superficial tumors after making only a small incision to expose the tumor surface. However, strict immobilization of tumors is essential. A number of laser Doppler flowmeters are now commercially available. Earlier probes sampled a tissue volume of 1–2 mm^3, but instruments providing multiple probes with sensing volumes of about 0.01 mm^3 each are now available ***(96)***. These have been used to demonstrate marked spatial and temporal heterogeneity of flow in murine and human tumors ***(97)***.

3.3. Tracer Uptake

Many methods for measurement of tumor blood flow are based on quantifying the tumor uptake of a systemically administered tracer. Such uptake will obviously be a function of regional blood flow, but it will also depend on the arterial input function and the efficiency with which the tracer is extracted from the blood during passage through the microvasculature. The latter parameter is defined as the extraction ratio (ER):

$$\text{ER} = (\text{arterial concentration} - \text{venous concentration})/(\text{arterial concentration}) \quad (1)$$

In principle, any tracer that is strongly extracted by tissue can be used to assess regional blood flow. After a single intravenous administration, the initial distribution of such a tracer to the organs will be in proportion to the fraction of the cardiac output that each receives. Provided that subsequent recirculation is minimal (i.e., ER = 1.0, or if less than unity is uniform for all tissues so that there is no net redistribution), the concentration of tracer in each tissue provides a convenient measure of the fractional cardiac output to that tissue.

The K^+ analog Rb^+, available as the gamma-emitting nuclide ^{86}Rb, is widely used as a convenient tracer for such uptake studies. Like KCl, RbCl is rapidly taken up by all mammalian cells; the uptake has the characteristics of a high-capacity exchange reaction (resulting from the large intracellular K^+ reservoir), providing a large distribution volume and high ER. Sapirstein ***(98)*** first showed that ^{86}Rb concentrations in rodent organs (except brain) are constant between 9 and 60 ss after iv administration, indicating that little redistribution occurs (ER

is less than unity but is similar for all tissues and close to the mean for the whole body). Zanelli and Fowler ***(99)*** confirmed this constancy for mouse tumors. Changes in relative cardiac output to tumor and other organs can thus readily be determined by sacrifice of mice approx 1 min after an iv bolus injection of ^{86}RbCl into a tail vein, with subsequent gamma counting of dissected organs. It is usual to measure residual radioactivity in the tail also, and to reject any animals with high counts (>10% of the injected activity) because these are indicative of extravasation during iv injection. Although this technique is very convenient, it must be remembered that it is a measure of fractional cardiac output, not absolute flow. If a test drug causes cardiac output to decease, but does not alter the fraction that flows to tumor, the decrease in absolute blood flow to tumor will not be detected by this method.

An alternative uptake method is to inject radiolabeled microspheres (typically 15–25 μm in diameter) into the systemic circulation and to count tissues after these have become trapped in the microcirculation ***(100)***. This requires direct administration of the tracer into the arterial supply (to avoid entrapment in the lungs), usually by catherization of the left ventricle, and thus requires significant surgical preparation of the animals. Absolute blood flow can be determined by this technique if blood is withdrawn from the femoral artery to allow determination of the arterial input function. A wide variety of different gamma-emitting nuclides have been used in microsphere studies. In one investigation three different sets of labeled microspheres (^{141}Ce, ^{85}Se, and ^{51}Cr, which have gamma energies sufficiently different to distinguish them) were administered before and 30 or 60 min after the test agent to examine time-dependent changes in flow ***(101)***.

Limitations of the above methods include their low spatial resolution (essentially being restricted to determining an average for a whole organ) and the need for termination of the animals (providing only a single time point from each animal). It would be highly desirable to have noninvasive imaging methods capable of quantitating tracer uptake with high temporal and spatial resolution. This is an active area of research, particularly in relation to MRI.

The fluorescent DNA-binding drug Hoechst 33342 (Seroa Fine Chemicals, Westbury, NY) is an important tracer in studies of tumor perfusion microscopic resolution. H33342 is cleared very rapidly from blood (half-life 2 min) after iv administration (it is poorly absorbed intraperitoneally), and is tightly bound in tissue with little recirculation over 2–4 h ***(102)***. Its uptake can be quantitated on a whole-tumor basis by flow cytometry ***(95)***, providing information broadly similar to ^{86}RbCl uptake. However, the important advantage of H33342 is that it stains perivascular cells, thereby allowing identification of functional exchange vessels in frozen sections by fluorescence microscopy. Used in this way, H33342 provides information on tumor blood flow at the microregional

level. This technique is more informative with tumors than with normal tissues since the latter are usually so well perfused that individual vessels are difficult to distinguish. H33342 fluorescence microscopy is thus not the method of choice if the objective is to compare vascular responses in tumor and normal tissues.

A number of studies have investigated changes in tumor perfusion by intravenous injection of H33342 at various times after the test agent, with sacrifice of the animals approx 5 min later ***(81)***. Change in perfusion can be quantitated using point counting (or image analysis) methods, with scoring of either the area inside H33342-stained vessels or the total stained area. The latter is more useful as it is sensitive to quantitative flow changes within a vessel (changing the thickness of the stained perivascular zone), whereas counting of a stained vessel lumenal area is sensitive only to complete collapse of the vessel. Counting the stained area does require selection of a staining threshold, but the fluorescence intensity gradient is usually steep enough that this is not a major source of error. With the development of low-magnification image analysis methods for whole tumor sections, H33342 staining is now a powerful method for mapping perfusion and perfusion changes at the microregional level in tumors.

A very sensitive variant of this technique is to combine H33342 with a second fluorescent dye to provide a double-label method for detecting changes in flow in individual vessels. Trotter et al ***(103)*** used this approach to demonstrate spontaneous opening and closing of vessels in murine tumors, using the carbocyanine dye 3,3-diheptyloxacarbocyanine ($DiOC_7(3)$) (Molecular Probes, Inc., Eugene, OR) as a second vascular marker. The same technique has been used to demonstrate drug-induced vessel closure following FAA treatment, as illustrated in **Fig. 2**. H33342 was administered first to define the functional vasculature, followed by the test agent, then $DiOC_7(3)$ up to 4 h later ***(45)***. $DiOC_7(3)$ has very poor water solubility, requiring (iv) administration in 75% DMSO, and causes large blood flow effects itself as demonstrated by laser Doppler flowmetry ***(103)***. It is also not as stably retained in tissue, as is H33342. Thus, it is only suitable for use as the second marker (immediately before sacrifice). Zwi et al ***(69)*** reported the use of an alternative fluorescence dye, the mitochondrial stain 10-nonyl acridine orange (Molecular Probes), as the second label. This has superior water solubility and lower toxicity than $DiOC_7(3)$, but is also suitable only as the second marker because of limited tissue retention. Whereas these dual-label methods provide very sensitive detection of flow changes, H33342 can itself have vascular effects at high dose ***(104)***. Its use prior to the test agent could therefore influence the measured response.

3.4. Tracer Washout

The rate of clearance of a tracer following its injection into a tissue provides an alternative strategy for measuring blood flow. The rate of clearance gives a

measure of local blood flow if the rate-limiting step is the removal of the tracer by the blood (i.e., the rate of transfer of the tracer through the tissue to the blood is fast relative to tracer washout by blood flow). The relationship between blood flow, *BF*, and the half-life of clearance of the tracer from the injection site $\tau_{1/2}$ is given by ***(105),***

$$BF = P(\ln 2^{y}\ \tau_{1/2}) \quad (2)$$

where *P* is the tissue/blood partition coefficient (tissue/blood concentration ratio at equilibrium). Thus, the determination of absolute blood flows requires separate measurement of the partition coefficient of the tracer for each tissue of interest. One example of such determination is given by Brown et al. ***(106),*** who determined partition coefficients for plasma vs blood cells, and plasma vs tumor cells by equilibrating in vitro, and from these ratios derived the tumor/blood partition coefficients for the tracers of interest. Tracer washout methods have an advantage over tracer uptake methods in that they provide a more direct measure of changes in absolute flow (rather than fractional cardiac output), assuming, of course, that the partition coefficient is not altered by the test agent. In addition, they are less destructive, and subsequent tumor growth can be reliably quantitated in the same animals. Washout methods present, however, their own set of problems. The technique is only suitable with relatively accessible tissues, the volume of tissue that is sampled is quite low, and its position in the tumor is not well defined. The sampling problems can be reduced by making 2–3 injections (typically in a total volume of 5–20 μL in 0.5 g murine tumors) at different sites in the same tumor, but quite large groups of animals are usually required for reliable determination of blood flow changes. Frequently if two injections are made into a single tumor, the clearance from the two sites is sufficiently different that the two exponentials can easily be resolved. In such cases it is appropriate to use a weighted average of the two rates ***(61)***.

A widely used tracer for "washout" studies is ^{133}Xe. As a noble gas, xenon is removed rapidly from the circulation in the lungs, which ensures that activity remains low in the blood pool. Xe clearance underestimates blood flow in muscle by about one-half, but is consistent over a wide range of absolute flows ***(107)***. It has been widely used to assess blood flow in tumors ***(108)*** and gives reasonably consistent data when the same tumor is injected 1.5–24 h later ***(83)***.

^{133}Xe is expensive and is difficult to handle because of its volatility. The pertechnetate ion ($^{99m}TcO_4^-$), which is readily available in nuclear medicine departments, is a convenient alternative tracer for blood flow studies. Like ^{133}Xe, ^{99m}Tc (technetium) has convenient physical characteristics, with a photon energy (140 kEV) very suitable for external counting or scintigraphic imaging. Although it is not cleared from the body as rapidly as is xenon, its short radioactive half-life (6 h) helps to make repeat injections possible the

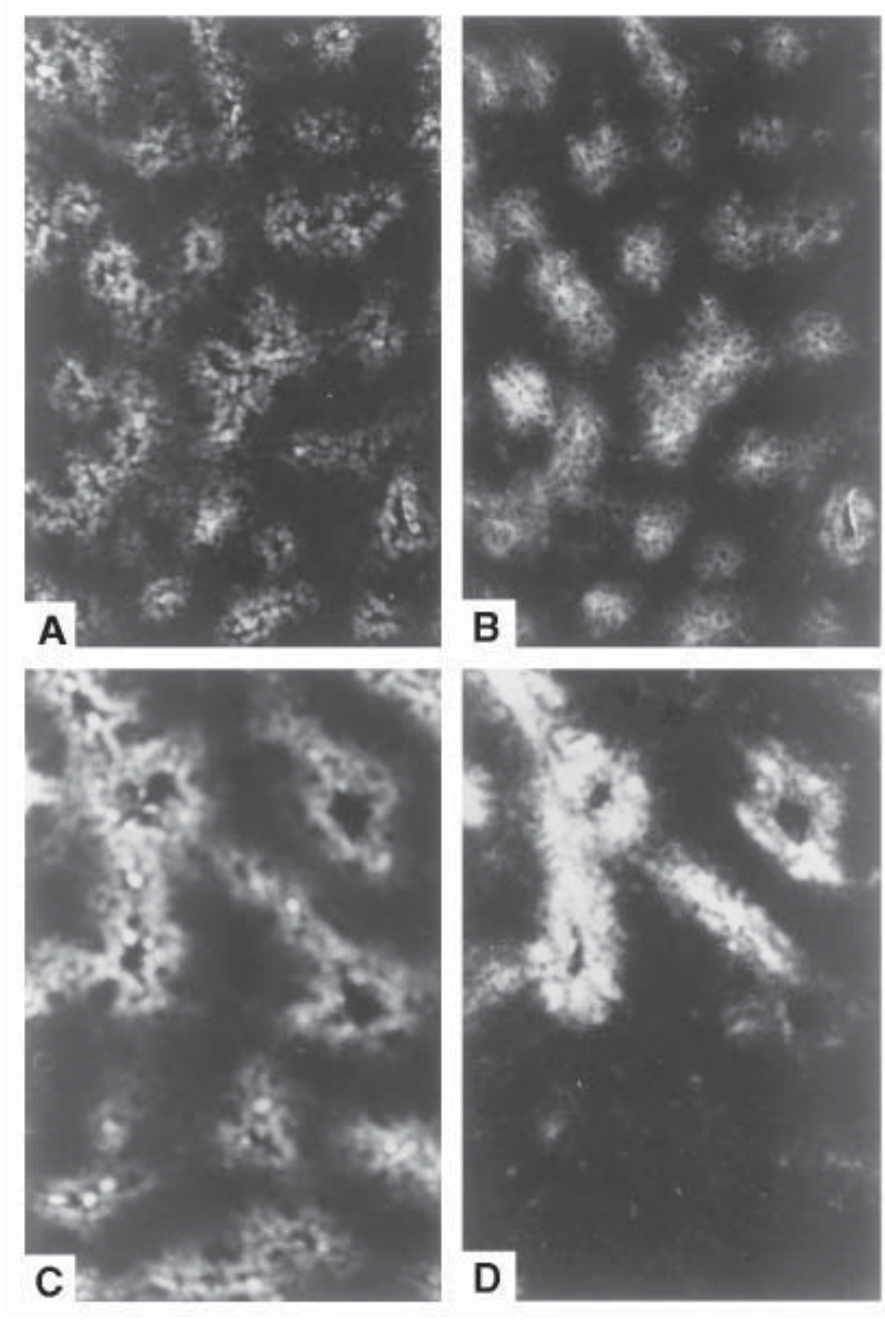

Fig. 2. Demonstration of tumor blood flow inhibition with fluorescent perfusion markers, using a double-label method ***(118)***. The fluorescence photomicrographs show two areas of the same colon 38 tumors in BDF1mice. H33342 (15 mg/kg) was admin-

following day. A potential difficulty is that this ionic species would be expected to diffuse less rapidly in tissue than xenon, and blood flow may therefore not always be rate limiting for its local clearance. The washout of $^{99m}TcO_4^-$ and ^{133}Xe has been compared directly following co-injection of both tracers into murine tumors and normal muscle ***(106)***. Clearance half times were longer for $^{99m}TcO_4^-$, but when corrected for the difference in partition coefficient the two markers gave estimates of blood flow that were in good agreement except in very large tumors. The pertechnetate clearance method has been used to demonstrate inhibition of tumor blood flow by FAA and DMXAA ***(61)***, and by serotonin/DMXAA combinations ***(28)***, as illustrated in **Fig. 3**.

3.5. Indirect Methods

Metabolic changes in tumors are readily demonstrable and can provide indirect evidence for blood flow inhibition. Thus, alterations in concentrations of phosphorous-containing metabolites (decrease in phosphocreatine and nucleoside triphosphates, and increase in inorganic phosphate) can be detected by ^{31}P magnetic resonance spectroscopy (MRS). Lowering of intracellular pH can also be detected from the Pi chemical shift. These changes have been widely used to demonstrate ischemic damage to tumor tissue as a result of blood flow inhibition ***(109–112)***. ^{31}P-MRS has the advantage of being completely noninvasive, but has low spatial resolution and care is required to ensure that normal tissue does not contribute to the signal elicited by the surface coils. ^{1}H-NMR offers much higher spatial resolution, and the determination of ^{1}H-NMR spectroscopic images of lactate, accumulated in RIF-1 tumors after hydralazine treatment, has recently been reported ***(113)***.

The importance of hypoxia in tumor biology and tumor treatment has stimulated much interest in developing methods for assessing hypoxia in human tumors ***(114,115)***. These same methods may be useful for detecting additional hypoxia induced by inhibition of tumor blood flow. At present, the clinically available hypoxia methods are invasive (e.g., polarographic O_2 probes-***[116]***) but a variety of minimally invasive or noninvasive methods are under development ***(117)*** and may prove valuable for monitoring blood flow changes during treatment with antivascular agents.

---

istered intravenously to define the functional exchange vessels, simultaneously with FAA (1.2 mmol/kg). A second fluorescence marker DiOC7(3) was administered intravenously (0.25 mg/kg) 15 min later. Plates show staining of the same fields with H33324 (left, excited at 400 nm to give blue fluorescence) and with DiOC7(3) (right, excited at 510 nm to give green fluorescence). The upper pair (**A** and **B**) show a similar pattern of functional vessels with both stains, whereas the lower pair (**C** and **D**) from a less vascular region show loss of blood flow in the lower part of the field.

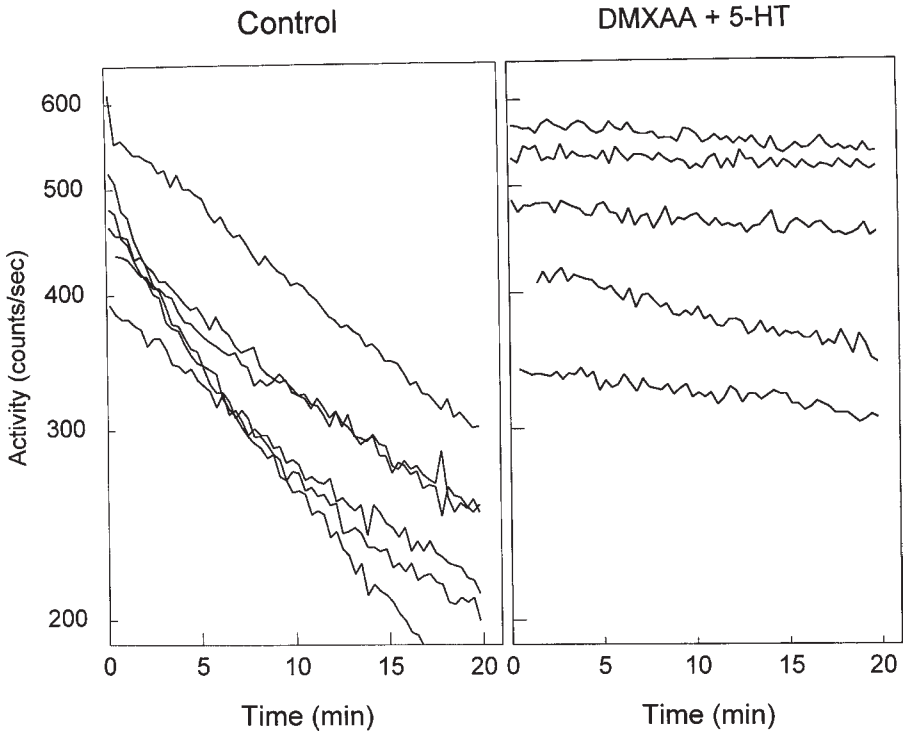

Fig. 3. Demonstration of tumor blood flow inhibition using the pertechnetate washout method. C3H/HeN mice with MDAH-MCa-4 mammary tumors (0.5 g) in the gastronemius muscle were restrained without anesthesia, and tumors were injected with 99mTcO4 (2×5 μL in saline, 10 MBq) using a 30-gauge needle. Activity in the tumor-bearing region (ordinate, log scale) was subsequently monitored using a GE Starcam 3000 gamma camera that allows recording from six animals simultaneously. Each trace is for an individual tumor. Washout from control tumors (**left**) is approximately exponential and is faster than from tumors treated 4 h previously by simultaneous ip administration of DMXAA (40 μmol/kg) and 5-HT (700 μmol/kg)(**right**).

4. Perspective

Selective inhibition of tumor blood flow is now becoming increasingly recognized as having potential application in cancer therapy. It can result in the induction of tumor necrosis, in increases in tumor hypoxia and in altered tumor pharmacokinetics of cytotoxic drugs. Since the effects of tumor blood flow modifiers are generally greatest in tissue remote from tumor vasculature whereas those from most other types of antitumor treatment are greatest for tumor cells close to blood vessels, combination therapy offers a number of advantages. Results obtained so far indicate that inhibition of blood flow can

synergize with radiotherapy, cytotoxic chemotherapy, hypoxia-selective cytotoxins, and hyperthermia. Of the five classes of agents reviewed in this chapter, drugs acting on serotonin (5-HT) type 2 receptors, certain mitotic poisons, and, in particular, cytokine inducers, such as DMXAA, offer much potential for the future. Clinical trials of such agents present particular challenges in the monitoring of tumor blood flow in individual patients, but newer noninvasive methods may be able to answer these challenges. Although successful clinical trials are the goal for research in this area, there are still many possibilities for innovative preclinical research.

References

1. Skinner, S. A., Tutton, P. J., and O'Brien, P. E. (1990) Microvascular architecture of experimental colon tumors in the rat. *Cancer Res.* **50,** 2411–2417.
2. Folkman, J. (1986) How is blood vessel growth regulated in normal and neoplastic tissue? – GHA Clowes memorial award lecture. *Cancer Res.* **46,** 467–473.
3. Siemann, D. W., Bronskill, M. J., Hill, R. P., and Bush, R. S. (1975) The relationship between mouse arterial partial pressure of oxygen (PaO2) and the effectiveness of localized tumour irradiation. *Br. J. Radiol.* **48,** 662–667.
4. Shimizu, S., Eguchi, Y., Kamiike, W., Itoh, Y., Hasegawa, J., Yamabe, K., Otsuki, Y., Matsuda, H., and Tsujimoto, Y. (1996) Induction of apoptosis as well as necrosis by hypoxia and predominant prevention of apoptosis by Bcl-2 and Bcl-XL. *Cancer Res.* **56,** 2161–2166.
5. Alarcon, R. M., Rupnow, B. A., Graeber, T. G., Knox, S. J., and Giaccia, A. J. (1996) Modulation of c-Myc activity and apoptosis in vivo. *Cancer Res.* **56,** 4315–4319.
6. Teicher, B. A. (1994) Hypoxia and drug resistance. *Cancer Metastasis Rev.* **13,** 139–168.
7. Reynolds, T. Y., Rockwell, S., and Glazer, P. M. (1996) Genetic instability induced by the tumor microenvironment. *Cancer Res.* **56,** 5754–5757.
8. Boucher, Y. and Jain, R. K. (1992) Microvascular pressure is the principal driving force for interstitial hypertension in solid tumors: implications for vascular collapse. *Cancer Res.* **52,** 5110–5114.
9. Lefer, A. M. and Lefer, D. J. (1993) Pharmacology of the endothelium in ische–mia-reperfusion and circulatory shock. *Annu. Rev. Pharmacol. Toxi–col.* **33,** 71–90.
10. Parkins, C. S., Dennis, M. F., Stratford, M. R., Hill, S. A., and Chaplin, D. J. (1995) Ischemia reperfusion injury in tumors: the role of oxygen radicals and nitric oxide. *Cancer Res.* **55,** 6026–6029.
11. Wilson, W. R. (1992) Tumour hypoxia: challenges for cancer chemotherapy, in *Cancer Biology and Medicine, 3, The Search for New Anticancer Drugs* (Waring, M. J. and Ponder, B. A. J., eds.), Kluwer Academic Publishers, Lancaster, PA, pp. 87–131.
12. Brown, J. M. (1993) SR-4233 (tirapazamine)—a new anticancer drug exploiting hypoxia in solid tumours. *Br. J. Cancer* **67,** 1163–1170.

13. Naredi, P. L. J., Lindner, P. G., Holmberg, S. B., Stenram, U., Peterson, A., and Hafstrom, L. R. (1993) The effects of tumour necrosis factor-alpha on the vascular bed and blood flow in an experimental rat hepatoma. *Intl. J. Cancer* **54,** 645–649.
14. Pedley, R. B., Begent, R. H., Boden, J. A., Boxer, G. M., Boden, R., and Keep, P. A. (1994) Enhancement of radioimmunotherapy by drugs modifying tumour blood flow in a colonic xenograft model. *Intl. J. Cancer* **57,** 830–835.
15. Pruijn, F. B., van Daalen, M., Holford, N. H. G., and Wilson, W. R. (1997) Mechanisms of enhancement of the antitumour activity of melphalan by the tumour blood flow inhibitor 5,6-dimethylxanthenone-4-acetic acid. *Cancer Chemother. Pharmacol.* **39,** 541–546.
16. Coleman, C. N. (1988) Hypoxia in tumors: a paradigm for the approach to biochemical and physiologic heterogeneity. *J. Natl. Cancer. Inst.* **80,** 310–317.
17. Vaupel, P., Kallinowski, F., and Okunieff, P. (1989) Blood flow, oxygen and nutrient supply, and metabolic microenvironment of human tumors: a review. *Cancer Res.* **49,** 6449–6465.
18. Andrade, S. P., Hart, I. R., and Piper, P. J. (1992) Inhibitors of nitric oxide synthase selectively reduce flow in tumour-associated neovasculature. *Br. J. Pharmacol.* **107,** 1092–1095.
19. Stone, H. B., Minchinton, A. I., Lemmon, M., Menke, D., and Brown, J. M. (1992) Pharmacological modification of tumor blood flow: lack of correlation between alteration of mean arterial blood pressure and changes in tumor perfusion. *Intl. J. Radiat. Oncol. Biol. Phys.* **22,** 79–86.
20. Mattsson, J., Lilja, J., and Peterson, H. I. (1982) Influence of vasoactive drugs on local tumor blood flow. *Eur. J. Cancer Clin. Oncol.* **18,** 677–684.
21. Hori, K., Zhang, Q. H., Saito, S., Tanda, S., Li, H. C., and Suzuki, M. (1993) Microvascular mechanisms of change in tumor blood flow due to angiotensin-II, epinephrine, and methoxamine: a functional morphometric study. *Cancer Res.* **53,** 5528–5534.
22. Lee, I., Boucher, Y., Demhartner, T. J., and Jain, R. K. (1994) Changes in tumour blood flow, oxygenation and interstitial fluid pressure induced by pentoxifylline. *Br. J. Cancer* **69,** 492–496.
23. Cater, D. B., Petrie, A., and Watkinson, D. A. (1965) Effect of 5-hydroxytryptamine and cyproheptadine on tumour blood flow. *Acta Radiolog. Ther. Phys. Biol.* **3,** 109–128.
24. Stücker, O., Vicaut, E., and Teisseire, B. (1992) Specific response to 5-HT2 agonists by arterioles linked to Meth A tumors in mice. *Am. J. Physiol.* **262 (Pt 2),** H704–H709.
25. Baguley, B. C., Cole, G., Thomsen, L. L., and Zhuang, L. (1993) Serotonin involvement in the antitumour and host effects of flavone-8-acetic acid and 5,6-dimethylxanthenone-4-acetic acid. *Cancer Chemother. Pharmacol.* **33,** 77–81.
26. Manda, T., Nishigaki, F., Mori, J., and Shimomura, K. (1988) Important role of serotonin in the antitumor effects of tumor necrosis factor-alpha in mice. *Cancer Res.* **48,** 4250–4255.

27. Pedley, R. B., Boden, J. A., Boden, R., Boxer, G. M., Flynn, A. A., Keep, P. A., and Begent, R. H. J. (1996) Ablation of colorectal xenografts with combined radioimmunotherapy and tumor blood flow-modifying agents. *Cancer Res.* **56,** 3293–3300.
28. Lash, C. J., Li, A. E., Ruthland, M., Baguley, B. C., Zwi, L. J., and Wilson, W. R. (1998) Enhancement of the antitumour effects of the antivascular agent 5,6-dimethylxanethenone-4-acetic acid (DMXAA) by combination with 5-hydroxytryptamine and bioreductive drugs. *Br. J. Cancer* **78,** 439–445.
29. Vanhoutte, P. M. (1991) Serotonin, hypertension and vascular disease. Netherlands *J. Med*. **38,** 35–42.
30. Peters, C. E. and Chaplin, D. J. (1992) Blood flow modification in the SCCVII tumor: effects of 5-hydroxytryptamine, hydralazine and propranolol. *Intl. J. Radiat. Oncol. Biol. Phys*. **22,** 463–465.
31. Horsman, M. R., Christensen, K. L., and Overgaard, J. (1992) Relationship between the hydralazine-induced changes in murine tumor blood supply and mouse blood pressure. *Intl. J. Radiat. Oncol. Biol. Phys*. **22,** 455–458.
32. Honess, D. J. and Bleehen, N. M. (1992) Comparative effects of hydralazine on perfusion of KHT tumor, kidney and liver and on renal function in mice. *Intl. J. Radiat. Oncol. Biol. Phys*. **22,** 953–961.
33. Jones, G. R., Ellis, R., and Frohn, M. J. (1981) Drug-induced interference with energy metabolism in the S180 sarcoma: a new principle in the production of selective tumor injury. *Oncodev. Biol. Med*. **2,** 155–164.
34. Chaplin, D. J. and Acker, B. (1987) The effect of hydralazine on the tumor cytotoxicity of the hypoxic cell cytotoxin RSU-1069. Evidence for therapeutic gain. *Int. J. Radiat. Oncol. Biol. Phys*. **13,** 579–585.
35. Chaplin, D. J. (1986) Potentiation of RSU-1069 tumour cytotoxicity by 5-hydroxytryptamine (5-HT). *Br. J. Cancer* **54,** 727–731.
36. Kalmus, J., Okunieff, P., and Vaupel, P. (1990) Dose-dependent effects of hydralazine on microcirculatory function and hyperthermic response of murine FSall tumors. *Cancer Res*. **50,** 15–19.
37. Belfi, C. A., Paul, C. R., Shan, S., and Ngo, F. Q. (1994) Comparison of the effects of hydralazine on tumor and normal tissue blood perfusion by MRI. *Intl. J. Radiat. Oncol. Biol. Phys*. **29,** 473–479.
38. Vaupel, P. (1975) Interrelationship between mean arterial blood pressure, blood flow, and vascular resistance in solid tumor tissue of DS-carcinosarcoma. *Experientia* **31,** 587–589.
39. Trotter, M. J., Acker, B. D., and Chaplin, D. J. (1989) Histological evidence for nonperfused vasculature in a murine tumor following hydralazine administration. *Intl. J. Radiat. Oncol. Biol. Phys*. **17,** 785–789.
40. Chaplin, D. J., Acker, B., and Olive, P. L. (1989) Potentiation of the tumor cytotoxicity of melphalan by vasodilating drugs. *Intl. J. Radiat. Oncol. Biol. Phys*. **16,** 1131–1135.
41. Atassi, G., Briet, P., Berthelon, J.-J., and Collonges, F. (1985) Synthesis and antitumor activity of some 8-substituted 4-oxo-4H-1-benzopyrans. *Eur. J. Med. Chem*. **5,** 393–402.

42. Plowman, J., Narayanan, V. L., Dykes, D., Szarvasi, E., Briet, P., Yoder, O. C., and Paull, K. D. (1986) Flavone acetic acid: a novel agent with preclinical antitumor activity against colon adenocarcinoma 38 in mice. *Cancer. Treat. Rep*. **70,** 631–638.
43. Finlay, G. J., Smith, G. P., Fray, L. M., and Baguley, B. C. (1988) Effect of flavone acetic acid (NSC 347512) on Lewis lung carcinoma: evidence for an indirect effect. *J. Natl. Cancer Inst*. **80,** 241–245.
44. Evelhoch, J. L., Bissery, M.-C., Chabot, G. G., Simpson, N. E., McCoy, C. L., Heilbrun, L. K., and Corbett, T. H. (1988) Flavone acetic acid (NSC 347512)-induced modulation of murine tumor physiology monitored by in vivo nuclear magnetic resonance spectroscopy. *Cancer Res*. **48,** 4749–4755.
45. Zwi, L. J., Baguley, B. C., Gavin, J. B., and Wilson, W. R. (1989) Blood flow failure as a major determinant in the antitumor action of flavone acetic acid (NSC 347512). *J. Natl. Cancer Inst*. **81,** 1005–1013.
46. Hill, S., Williams, K. B., and Denekamp, J. (1989) Vascular collapse after flavone acetic acid. A possible machanism of its antitumour action. *Eur. J. Cancer Clin. Oncol*. **25,** 1419–1423.
47. Bibby, M. C., Double, J. A., Loadman, P. M., and Duke, C. V. (1989) Reduction of tumor blood flow by flavone acetic acid: a possible component of therapy. *J. Natl. Cancer Inst*. **81,** 216–220.
48. Smith, G. P., Calveley, S. B., Smith, M. J., and Baguley, B. C. (1987) Flavone acetic acid (NSC 347512) induces haemorrhagic necrosis of mouse colon 26 and 38 tumours. *Eur. J. Cancer Clin. Oncol*. **23,** 1209–1212.
49. Baguley, B. C., Calveley, S. B., Crowe, K. K., Fray, L. M., O'Rourke, S. A., and Smith, G. P. (1989) Comparison of the effects of flavone acetic acid, fostriecin, homoharringtonine and tumour necrosis factor alpha on Colon 38 tumors in mice. *Eur. J. Cancer Clin. Oncol*. **25,** 263–269.
50. Zwi, L. J., Baguley, B. C., Gavin, J. B., and Wilson, W. R. (1994) The morphological effects of the anti-tumour agents flavone acetic acid and 5,6-dimethylxanthenone acetic acid on the colon 38 mouse tumour. *Pathology* **26,** 161–169.
51. Hill, S. A., Williams, K. B., and Denekamp, J. (1992) A comparison of vascular-mediated tumor cell death by the necrotizing agents GR63178 and flavone acetic acid. *Intl. J. Radiat. Oncol. Biol. Phys*. **22,** 437–441.
52. Honess, D. J. and Bleehen, N. M. (1991) Effects of two tumour blood flow modifiers, hydralazine and flavone acetic acid, on KHT tumours and normal tissues in mice. *Intl. J. Radiat. Biol*. **60,** 249–253.
53. Mace, K. F., Hornung, R. L., Wiltrout, R. H., and Young, H. A. (1990) Correlation between in vivo induction of cytokine gene expression by flavone acetic acid and strict dose dependency and therapeutic efficacy against murine renal cancer. *Cancer Res*. **50,** 1742–1747.
54. Hornung, R. L., Back, T. C., Zaharto, D. S., Urba, W. J., Longo, D. L., and Wiltrout, R. H. (1988) Augmentation of natural killer (NK) activity, induction of interferon and development of tumor immunity during the successful treatment of established murine renal cancer using flavone acetic acid (FAA) and interleukin 2. *J. Immunol*. **141,** 3671–3679.

55. Mahadevan, V., Malik, S. T. A., Meager, A., Fiers, W., Lewis, G. P., and Hart, I. R. (1990) Role of tumor necrosis factor in flavone acetic acid-induced tumor vasculature shutdown. *Cancer Res.* **50,** 5537–5542.
56. North, R. J. and Havell, E. A. (1988) The antitumour function of tumour necrosis factor (TNF) II. Analysis of the role of endogenous TNF in endotoxin-induced hemorrhagic necrosis and regression of an established sarcoma. *J. Exp. Med.* **167,** 1086–1099.
57. Watanabe, N., Yoshiro, N., Umeno, H., Kuriyama, H., Neda, H., Yamauchi, N., Maeda, M., and Urushizaki I. (1988) Toxic effect of tumor necrosis factor on tumor vasculature. *Cancer Res.* **48,** 2179–2183.
58. Murray, J. C., Smith, K. A., and Thurston, G. (1989) Flavone acetic acid induces a coagulopathy in mice. *Br. J. Cancer* **60,** 729–733.
59. Ferrero, E., Villa, A., Ferrero, M. E., Toninelli, E., Bender, J. R., Pardi, R., and Zocchi, M. R. (1996) Tumor necrosis factor alpha-induced vascular leakage involves PECAM1 phosphorylation. *Cancer Res.* **56,** 3211–3215.
60. Sun, J. R. and Brown, J. M. (1989) Enhancement of the antitumor effect of flavone acetic acid by the bioreductive cytotoxic drug SR 4233 in a murine carcinoma. *Cancer Res.* **49,** 5664–5670.
61. Cliffe, S., Taylor, M. L., Rutland, M., Baguley, B. C., Hill, R. P., and Wilson, W. R. (1994) Combining bioreductive drugs (SR 4233 or SN 23862) with the vasoactive agents flavone acetic acid or 5,6-dimethylxanthenone acetic acid. *Intl. J. Radiat. Oncol. Biol. Phys.* **29,** 373–377.
62. Sakaguchi, Y., Maehara, Y., Baba, H., Kusumoto, T., Sugimachi, K., and Newman, R. A. (1992) Flavone acetic acid increases the antitumor effect of hyperthermia in mice. *Cancer Res.* **52,** 3306–3309.
63. Kerr, D. J. and Kaye, S. B. (1989) Flavone acetic acid—preclinical and clinical activity. *Eur. J. Cancer Clin. Oncol.* **25,** 1271,1272.
64. O'Reilly, S. M., Rustin, G. J. S., Farmer, K., Burke, M., Hill, S., and Denekamp, J. (1993) Flavone acetic acid (FAA) with recombinant interleukin-2 (rIL-2) in advanced malignant melanoma.1. Clinical and vascular studies. *Br. J. Cancer* **67,** 1342–1345.
65. Futami, H., Eader, L. A., Komschlies, K. L., Bull, R., Gruys, M. E., Ortaldo, J. R., Young, H. A., and Wiltrout, R. H. (1991) Flavone acetic acid directly induces expression of cytokine genes in mouse splenic leukocytes but not in human peripheral blood leukocytes. *Cancer Res.* **51,** 6596–6602.
66. Rewcastle, G. W., Atwell, G. J., Baguley, B. C., Calveley, S. B., and Denny, W. A. (1989) Potential antitumor agents. 58. Synthesis and structure-activity relationships of substituted xanthenone-4-acetic acids active against the Colon 38 tumor in vivo. *J. Med. Chem.* **32,** 793–799.
67. Rewcastle, G. W., Atwell, G. J., Zhuang, L., Baguley, B. C., and Denny, W. A. (1991) Potential antitumor agents. 61. Structure-activity relationships for in vivo colon-38 activity among disubstituted 9-oxo-9H-xanthene-4-acetic acids. *J. Med. Chem.* **34,** 217–222.
68. Ching, L.-M., Joseph, W. R., Zhuang, L., Atwell, G. J., Rewcastle, G. R., Denny, W. A., and Baguley, B. C. (1991) Induction of natural killer activity by

xanthenone analogues of flavone acetic acid: relation with antitumour activity. *Eur. J. Cancer*. **27,** 79–83.
69. Zwi, L. J., Baguley, B. C., Gavin, J. B., and Wilson, W. R. (1994) Correlation between immune and vascular activities of xanthenone acetic acid antitumor agents. *Oncol. Res*. **6,** 79–85.
70. Philpott, M., Baguley, B. C., and Ching, L.-M. (1995) Induction of tumour necrosis factor-alpha by single and repeated doses of the antitumour agent 5,6-dimethylxanthenone-4-acetic acid. *Cancer Chemother. Pharmacol*. **36,** 143–148.
71. Thomsen, L. L., Ching, L. M., Zhuang, L., Gavin, J. B., and Baguley, B. C. (1991) Tumor-dependent increased plasma nitrate concentrations as an indication of the antitumor effect of flavone-8-acetic acid and analogues in mice. *Cancer Res*. **51,** 77–81.
72. Baguley, B. C., Zhuang, L., and Kestell, P. (1997) Increased plasma serotonin following treatment with flavone-8-acetic acid, 5,6-dimethylxanthenone-4-acetic acid, vinblastine, and colchicine—relation to vascular effects. *Oncol. Res*. **9,** 55–60.
73. Ching, L. M., Joseph, W. R., Crosier, K. E., and Baguley, B. C. (1994) Induction of tumor necrosis factor-alpha messenger RNA in human and murine cells by the flavone acetic acid analogue 5,6-dimethylxanthenone-4-acetic acid (NSC 640488). *Cancer Res*. **54,** 870–872.
74. Philpott, M., Joseph, W. R., Crosier, K. E., Baguley, B. C., and Ching, L.-M. (1997) Production of tumour necrosis factor-alpha by cultured human peripheral blood leucocytes in response to the antitumour agent 5,6-dimethylxanthenone-4-acetic acid (NSC 640488). Br. J. Cancer, in press.
75. Jordan, M. A., Thrower, D., and Wilson, L. (1991) Mechanism of inhibition of cell proliferation by Vinca alkaloids. *Cancer Res*. **51,** 2212–2222.
76. Baguley, B. C., Holdaway, K. M., Thomsen, L. L., Zhuang, L., and Zwi, L. J. (1991) Inhibition of growth of colon-38 adenocarcinoma by vinblastine and colchicine: evidence for a vascular mechanism. *Eur. J. Cancer* **27,** 482–487.
77. Bogdan, C. and Ding, A. (1992) Taxol, a microtubule-stabilizing antineoplastic agent, induces expression of tumor necrosis factor alpha and interleukin-1 in macrophages. *J. Leukocyte Biol.* **52,** 119–121.
78. Hill, S. A., Lonergan, S. J., Denekamp, J., and Chaplin, D. J. (1993) Vinca alkaloids—anti-vascular effects in a murine tumour. *Eur. J. Cancer* **29A,** 1320–1324.
79. Hill, S. A., Lonergan, S. J., Denekamp, J., and Chaplin, D. J. (1994) The effect of Vinca alkaloids on tumour blood flow. *Adv. Exp. Med. Biol*. **345,** 417–422.
80. Hill, S. A., Sampson, L. E., and Chaplin, D. J. (1995) Anti-vascular approaches to solid tumour therapy: evaluation of vinblastine and flavone acetic acid. *Intl. J. Cancer* **63,** 119–123.
81. Dark, G. G., Hill, S. A., Prise, V. E., Tozer, G. M., Pettit, G. R., and Chaplin, D. J. (1997) Combretastatin A-4, an agent that displays potent and selective toxicity toward tumor vasculature. *Cancer Res*. **57,** 1829–1834.
82. Watts, M. E., Woodcock, M., Arnold, S., and Chaplin, D. J. (1997) Effects of novel and conventional anti-cancer agents on human endothelial permeability: influence of tumour secreted factors. *Anticancer Res*. **17,** 71–75.

83. Pallavicini, M. G. and Hill, R. P. (1983) Effect of tumor blood flow manipulations on radiation response. *Intl. J. Radiat. Oncol. Biol. Phys*. **9,** 1321–1325.
84. Cullen, B. M. and Walker, H. C. (1985) The effect of several anaesthetics on the blood pressure and heart rate of the mouse and on the radiation response of the mouse sarcoma RIF-1. *Intl. J. Radiat. Biol*. **48,** 761–771.
85. Zanelli, G. D. and Lucas, P. B. (1976) Effect of stress on blood perfusion and vascular space in transplanted mouse tumors. *Br. J. Radiol*. **49,** 382,383.
86. Joiner, B., Hirst, V. K., McKeown, S. R., McAleer, J. J. A., and Hirst, D. G. (1993) The effect of recombinant human erythropoietin on tumour radiosensitivity and cancer-associated anaemia in the mouse. *Br. J. Cancer* **68,** 720–726.
87. Penhaligon, M. (1984) Radioprotection of mouse skin vasculature and the RIF-1 fibrosarcoma by WR-2721. *Intl. J. Radiat. Oncol. Biol. Phys*. **10,** 1541–1544.
88. Shibamoto, Y., Sasai, K., and Abe, M. (1987) The radiation response of SCCVII tumor cells in C3H/He mice varies with the irradiation conditions. *Radiat. Res*. **109,** 352–354.
89. Trotter, M. J., Chaplin, D. J., and Olive, P. L. (1991) Effect of angiotensin II on intermittent tumour blood flow and acute hypoxia in the murine SCCVII carcinoma. *Eur. J. Cancer Clin. Oncol*. **27,** 887–893.
90. Field, S. B., Needham, S., Burney, I. A., Maxwell, R. J., Coggle, J. E., and Griffiths, J. R. (1991) Differences in vascular response between primary and transplanted tumours. *Br. J. Cancer* **63,** 723–726.
91. Ward-Hartley, K. A. and Jain, R. K. (1987) Effect of glucose and galactose on microcirculatory flow in normal and neoplastic tissues in rabbits. *Cancer Res*. **47,** 371–377.
92. Kimura, H., Braun, R. D., Ong, E. T., Hsu, R., Secomb, T. W., Papahadjopoulos, D., Hong, K., and Dewhirst, M. W. (1996) Fluctuations in red cell flux in tumor microvessels can lead to transient hypoxia and reoxygenation in tumor parenchyma. *Cancer Res*. **56,** 5522–5528.
93. Suzuki, T., Yanagi, K., Ookawa, K., Hatakeyama, K., and Ohshima, N. (1996) Flow visualisation of microcirculation in solid tumor tissues: intravital microscopic observation of blood circulation by use of a confocal laser scanning microscope. *Front. Med. Biol. Engineer* **7,** 253–263.
94. Vaupel, P. W. and Okunieff, P. G. (1988) Role of hypovolemic hemoconcentration in dose-dependent flow decline observed in murine tumors after intraperitoneal administration of glucose or mannitol. *Cancer Res*. **48,** 7102–7106.
95. Guichard, M., Lespinasse, F., Trotter, M., Durand, R., and Chaplin, D. (1991) The effect of hydralazine on blood flow and misonidazole toxicity in human tumour xenografts. *Radiother. Oncol*. **20,** 117–123.
96. Chaplin, D. J. and Hill, S. A. (1995) Temporal heterogeneity in microregional erythrocyte flux in experimental solid tumours. *Br. J. Cancer* **71,** 1210–1213.
97. Pigott, K. H., Hill, S. A., Chaplin, D. J., and Saunders, M. I. (1996) Microregional fluctuations in perfusion within human tumours detected using laser *Doppler flowmetry. Radiother. Oncol*. **40,** 45–50.
98. Sapirstein, L. A. (1958) Regional blood flow by fractional distribution of indicators. *Am. J. Physiol*. **193,** 161–168.

99. Zanelli, G. D. and Fowler, J. F. (1974) The measurement of blood perfusion in experimental tumors by uptake of 86Rb1. *Cancer Res*. **34,** 1451–1456.
100. Kaelin, W. G., Jr., Shrivastav, S., and Jirtle, R. L. (1984) Blood flow to primary tumors and lymph node metastases in SMT-2A tumor-bearing rats following intravenous flunarizine. *Cancer Res*. **44,** 896–899.
101. DiPette, D. J., Ward-Hartley, K. A., and Jain, R. K. (1986) Effect of glucose on systemic hemodynamics and blood flow rate in normal and tumor tissues in rats. *Cancer Res*. **46,** 6299–6304.
102. Olive, P. L., Chaplin, D. J., and Durand, R. E. (1985) Pharmacokinetics, binding and distribution of Hoechst 33342 in spheroids and murine tumours. *Br. J. Cancer* **52,** 739–746.
103. Trotter, M. J., Chaplin, D. J., and Olive, P. L. (1989) Use of a carbocyanine dye as a marker of function vasculature in murine tumours. *Br. J. Cancer* **59,** 706–709.
104. Smith, K. A., Hill, S. A., Begg, A. C., and Denekamp, J. (1988) Validation of the fluorescent dye Hoechst 33342 as a vascular space marker in tumours. *Br. J. Cancer* **57,** 247–253.
105. Lassen, N. A., Lindberg, J., and Munck, O. (1964) Measurement of blood flow through skeletal muscle by intramuscular injection of xenon-133. *Lancet*, **1,** 686–689.
106. Brown, S. L., Hunt, J. W., and Hill, R. P. (1988) A comparison of the rate of clearance of xenon (133Xe) and pertechnetate ion (99mTcO-4) in murine tumors and normal leg muscles. *Nuclear Med. Biol*. **15,** 381–390.
107. Cerretelli, P., Marconi, C., Pendergast, D., Meyer, M., Heisler, N., and Piiper, J. (1984) Blood flow in exercising muscles by xenon clearance and by microsphere trapping. *J. Appl. Physiol*. **56,** 24–30.
108. Kallman, R. F., Denardo, G., and Stasch, M. (1972) Blood flow in irradiated mouse sarcoma as determined by the clearance of xenon-133. *Cancer Res*. **32,** 483–490.
109. Evelhoch, J. L., Sapareto, S. A., Nussbaum, G. H., and Ackman, J. J. H. (1986) Correlation between 31P NMR spectroscopy and 15O perfusion measurements in the RIF-1 murine tumor in vivo. *Radiat. Res*. **106,** 122–131.
110. Rofstad, E. K., DeMuth, P., Fenton, B. M., Ceckler, T. L., and Sutherland, R. M. (1989) 31P NMR spectroscopy and HbO2 cryospectrophotometry in prediction of tumor radioresistance caused by hypoxia. *Intl. J. Radiat. Oncol. Biol. Phys*. **16,** 919–923.
111. Okunieff, P., Kallinowski, F., Vaupel, P., and Neuringer, L. J. (1988) Effects of hydralazine-induced vasodilation on the energy metabolism of murine tumors studied by in vivo 31P-nuclear magnetic resonance spectroscopy. *J. Natl. Cancer. Inst*. **80,** 745–750.
112. Burney, I. A., Maxwell, R. J., Griffiths, J. R., and Field, S. B. (1991) The potential for prazosin and calcitonin gene-related peptide (CGRP) in causing hypoxia in tumours. *Br. J. Cancer* **64,** 683–688.
113. Bhujwalla, Z. M., Shungu, D. C., and Glickson, J. D. (1996) Effects of blood flow modifiers on tumor metabolism observed in vivo by proton magnetic resonance spectroscopic imaging. *Magnetic Resonance Med*. **36,** 204–211.

114. Stone, H. B., Brown, J. M., Phillips, T. L., and Sutherland, R. M. (1993) Oxygen in human tumors: Correlations between methods of measurement and response to therapy. *Radiat. Res*. **136,** 422–434.
115. Raleigh, J. A., Dewhirst, M. W., and Thrall, D. E. (1996) Measuring tumor hypoxia. S*eminars Rad. Oncol*. **6,** 37–45.
116. Vaupel, P. W. and Hockel, M. (1995) Oxygenation status of human tumors: a reappraisal using computerized pO2 histography, in *Tumor Oxygenation* (Vaupel, P. W., Kelleher, D. K., and Gunderoth, M., eds.), Fischer-Verlag, Stuttgart, Germany, pp. 219–232.
117. Chapman, J. D., Coia, L. R., Stobbe, C. C., Engelhardt, E. L., Fenning, M. C., and Schneider, R. F. (1996) Prediction of tumour hypoxia and radioresistance with nuclear medicine markers. *Br. J. Cancer* **74XXVII,** S204–S208.
118. Zwi, L. J. (1992) The mechanism of the anti-tumour action of flavone acetic acid and its xanthenone acetic acid analogs. Thesis, The University of Auckland, New Zealand.

10

Targeting in Myocardial Infarction

Ban An Khaw and Vladimir P. Torchilin

1. Introduction

Targeting pharmaceuticals to the infarcted myocardium has two primary objectives: the diagnostic imaging of the infarcted myocardium and the delivery of therapeutic agents to compromised myocardial areas. Various diagnostic and therapeutic agents (such as radiolabeled compounds, thrombolytic enzymes, proteolytic drugs, and antioxidants) have been proposed for visualization or treatment of the infarcted myocardium. However, none of these reagents has the specificity for targeting the compromised myocardium. Therefore, the availability of a target-specific delivery system should increase the efficacy of diagnosis and therapy. Furthermore, the existence of such a targeted delivery system may pave the way for the use of new pharmaceuticals that by themselves can be harmful to normal tissues.

1.1. Monoclonal Antibodies in Targeting Myocardial Infarction

Monoclonal antibodies (MAbs) provide an effective method for noninvasive detection and visualization of different cardiac disorders, acute myocardial infarction (MI) being among them. Taking into account the high frequency of this disease and the limited time window for optimal therapy, fast and specific diagnosis become matters of primary importance. The overview of myocardial infarct visualization with MAb has been reported recently ***(1)***. This approach is based on the theory that following myocardial cell death as a result of ischemia or other causes, an antibody against an intracellular antigen will bind to the homologous antigen only when the antibody could enter the intracellular space via the cell membrane lesions. Normal cells with intact cell membrane will prevent the antibody from interacting with the intracellular antigen. This enables one to differentiate viable cells with intact membranes from necrotic

From: *Methods in Molecular Medicine, Vol. 25: Drug Targeting: Strategies, Principles, and Applications*
Edited by: G. E. Francis and C. Delgado

cells with disrupted membranes. If the antibody were appropriately radiolabeled, then the areas of irreversible myocardial damage could be recognized by a method to determine the accumulation of antibody-bound radioactivity in the target organ. Cardiac myosin, which is a highly insoluble contractile protein that is not washed away following cell disintegration, was chosen as the target antigen for the development of a targeting strategy for the infarcted myocardium ***(2–4)***.

The efficacy of antimyosin (AM) antibodies labeled with ^{131}I, ^{111}In, and ^{99m}Tc for gamma-scintigraphic visualization of MI was demonstrated in rabbit and canine experiments ***(5–7)***. Moreover, radiolabeled Fab fragment of murine monoclonal AM antibody, designated R11D10 (Myoscint, Centocor, Malvern, PA), has already been used successfully in clinical trials ***(8,9)*** and has been approved for clinical commercialization in Europe and the United States. Clinical trials demonstrated high sensitivity (90–98%) and specificity of this method for detection of acute left ventricular MI (*see* review in **ref. *1***). In most studies, almost all anterior myocardial infarcts were detected, however, some inferior MIs were not detected possibly because of the smaller size of inferior MIs ***(10,11)***. In patients with equivocal electrocardiogram, serum enzyme levels, or clinical symptoms for acute MI, radiolabeled AM is highly effective for definitive diagnosis of MI ***(9)***. Johnson et al. also demonstrated the diagnostic ability of AM for right ventricular infarction in 12 patients. Only 3 of these 12 had diagnostically significant electrocardiographic changes for right ventricular infarction ***(9)***. Other applications of radiolabeled AM antibody include estimation of myocardial damage following coronary bypass open heart surgery ***(12,13)***.

Other MAbs with potential value for diagnosis of acute MI include antibodies specific for cardiac troponin-I and mitochondria ***(14)***. These antibodies have been shown to accumulate in the infarcted regions of the myocardium in experimental canine studies.

1.1.1. Antibodies Labeled with Metals via Chelating Polymers

A wide range of radioisotopes is now available for labeling antibodies. Transition metals constitute a majority. For rapid and firm attachment of the metal radiolabel to a protein molecule, chelating residues are routinely chemically attached to antibody molecules. Use of radiolabeled antibodies for in vivo targeting should meet several important criteria:

1. The attachment of the chelating moiety as well as metal binding should not affect the affinity and specificity of the antibody.
2. The chelating group used should not permit metal detachment (transchelation) or rechelating.
3. High specific radiolabeling should be achievable to provide a good in vivo signal.
4. The removal of nonbound radiolabel should be fast enough to decrease the background signal and thereby provide high target-to-normal ratios.

The optimal results of radiolabeling with metal-chelate complexes can be obtained using an indirect method of antibody modification with chelating groups ***(15)***. Synthetic polymers containing numerous chelate residues and a single-terminal protein-reactive group ***(15–18)*** have been developed (*see* **ref. *19*** for review). The ability of a polymer to carry a large number of chelating moieties and bind to an antibody via a single point attachment provides a major advancement toward increasing the amount of heavy-metal binding sites per antibody molecule. Thus, using chelate-derived polylysines of different molecular weights, several dozen reporter metal atoms have been bound to the monoclonal AM antibody R11D10 ***(20)***; the principle of the method and its efficacy are shown in **Fig. 1**. The polymer moiety can be additionally modified to alter the biodistribution of the modified antibody, thus decreasing the nonspecific blood radioactivity ***(21)***. As a consequence of the modification of the antibody, clearly defined myocardial infarct images were obtained in experimental animals within minutes after injection of the polymer-modified radiolabeled antibody (*see* typical images in **Fig. 2**), which was impossible using traditional "direct" labeling.

It was also demonstrated that the chemistry of attachment of the chelating polymer to the antibody exerts a strong influence on biodistribution and infarct accumulation ***(22)***; the reaction schemes and biodistribution of various derivatives are shown in **Fig. 3**. It follows from **Fig. 3** that only "actively" adsorbing organs (like target infarct area and reticolu-endothelial system [RES] organs) exhibited differences in the uptake of conjugates. Target/nontarget accumulation ratio (which may be as high as 25 for SMCC-based conjugate) is determined exclusively by high-infarct tissue uptake, which should permit optimization of radiolabeling as well as in vivo targeting for noninvasive diagnostic applications.

1.2. Liposomes in Targeting MI

1.2.1. Spontaneous Accumulation of Liposomes in Infarct

Spontaneous accumulation of positively charged liposomes in regions of experimental MI was described by Caride as early as 1977 ***(23)***. This observation was later partially confirmed by other researchers ***(24)***, who found predominant accumulation of positively charged liposomes in perfused nonischemic isolated rabbit hearts compared to negatively charged or neutral liposomes. It was also observed that liposomes concentrated in depolarized myocardial cells ***(25)***. Additional animal experiments ***(26–28)*** implicated liposome accumulation in ischemic tissues as a general phenomenon. Liposome accumulation in the infarcted myocardium was the result of impaired filtration in ischemic areas that resulted in the trapping of liposomes in these areas ***(29)***. This observation lead to a conclusion that drug-loaded liposomes

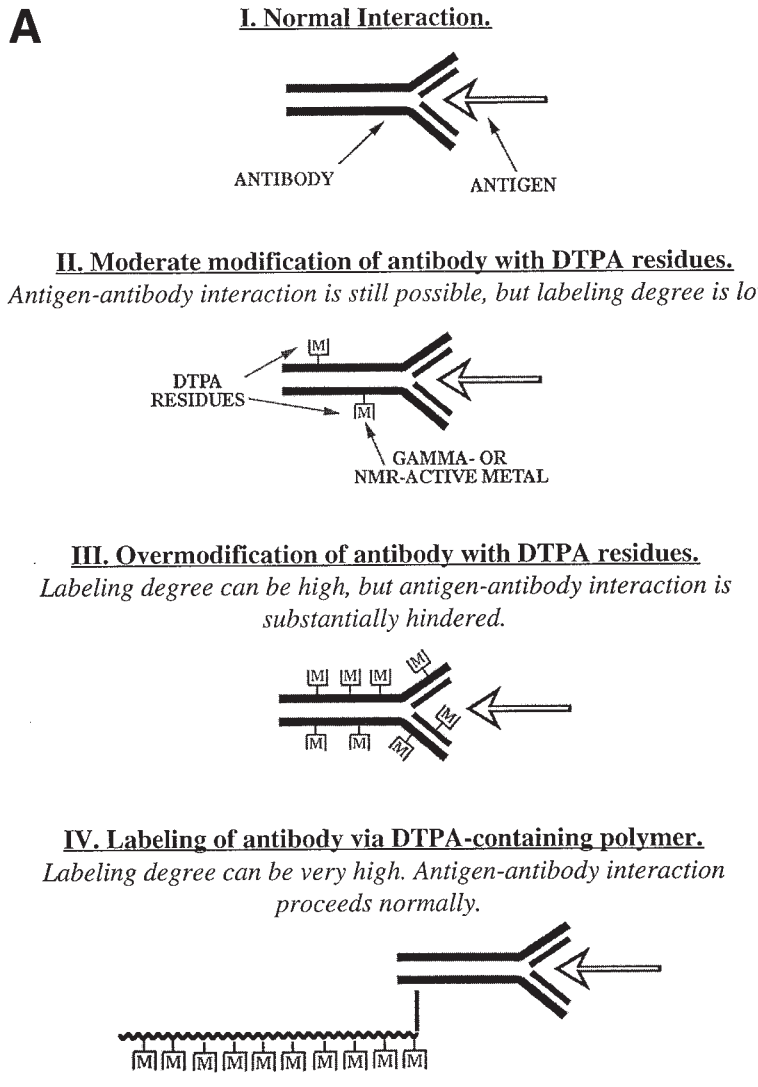

Fig. 1. **(A)** Possible of labeling antibody with a reporter metal via a chelating group. Single-point attachment of a polymeric chelate provides the maximum metal load without affecting antibody immunologic properties.

can be used for "passive" delivery into the ischemic tissues (i.e., into the infarcted myocardium) ***(30,31)***.

Thus, liposomes loaded with thrombolytic enzyme streptokinase achieved accelerated thrombolysis and reperfusion in a canine model of MI ***(32)***. Fur-

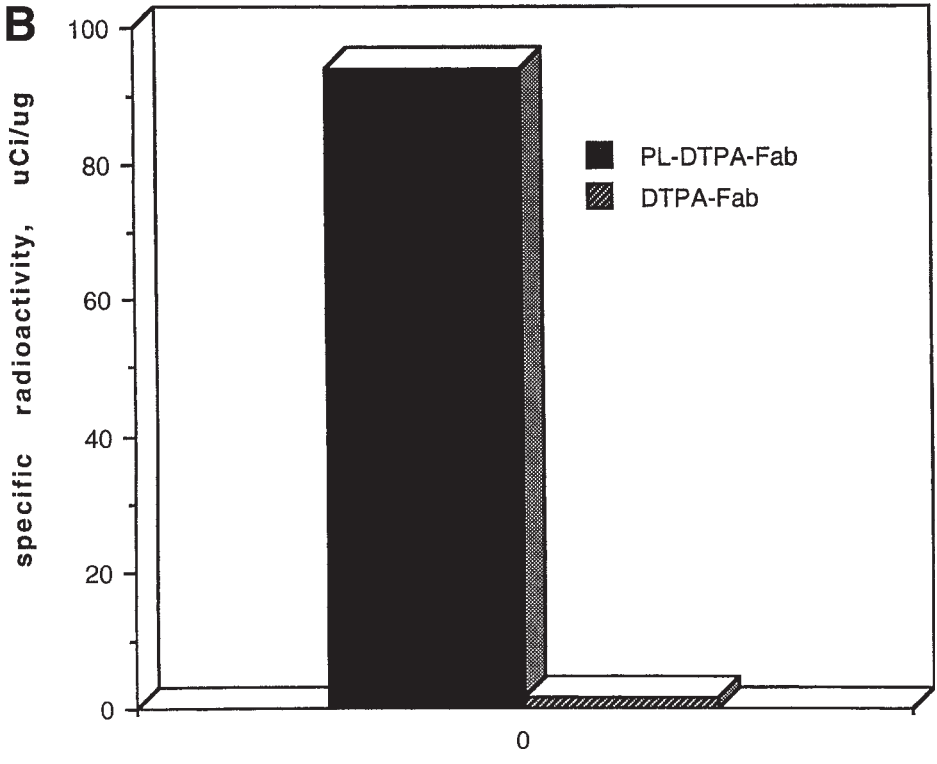

Fig. 1. *(continued)* **(B)** Radioactivity (^{111}In) bound to an antibody Fab fragment directly modified with a limited number of chelating groups (DTPA), and to the same Fab fragment via single-site attached polymeric chelate (DTPA-PL); *see* corresponding cases II and IV in (A).

thermore, studies with isolated rat cardiomyocytes, as well as isolated perfused rat and rabbit hearts, demonstrated that perfusion with high Ca^{2+} (4.5 m*M*), high K^+ (8.7 m*M*), or a free radical-generating system significantly increased myocardial uptake of positively charged liposomes ***(33,34)***. Additionally, liposomes with superoxide dismutase (SOD) were more effective than native enzyme treatment in the treatment of reperfusion injury of the myocardium. The efficacy of liposomal SOD in the treatment of ischemia-reperfusion damage in different organs, including the myocardium, has been amply reported ***(35–37)***. Experiments with cultured heart cells of chicken embryos showed that liposomes loaded with sodium or calcium ions were able to influence electrical activity of those cells ***(38)***, whereas liposomes with entrapped adenosine triphosphate (ATP) were able to normalize ischemic conditions in certain tissues ***(39)***.

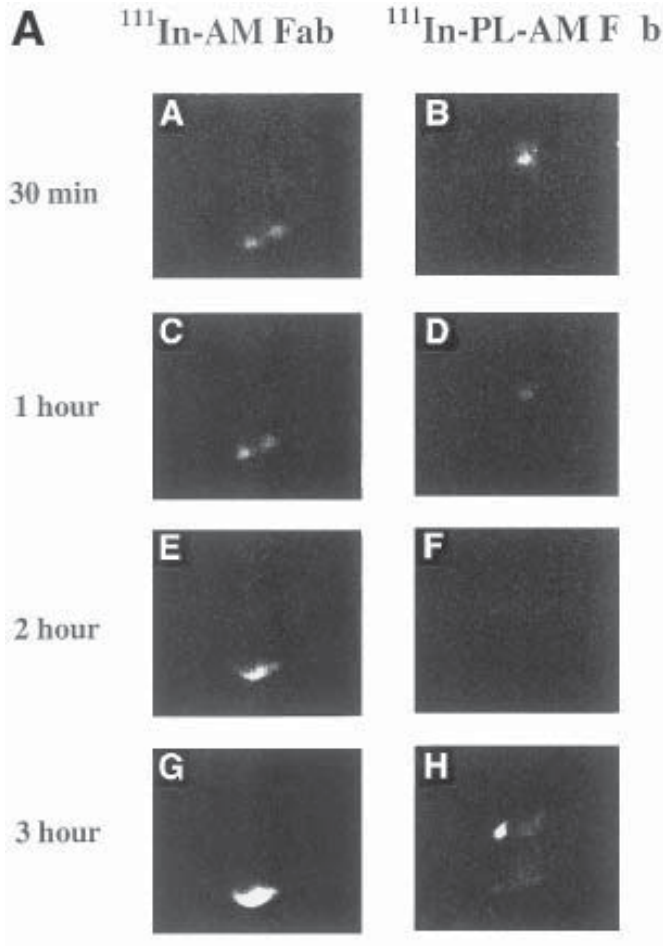

Fig. 2. **(A)** Left lateral gamma images of dogs with acute experimental MI. Images a, c, e, and g were obtained after iv administration of conventionally modified ^{111}In-DTPA-antimyosin Fab (AM-Fab); images b, d, f, and h were obtained after administration of AM-Fab modified with ^{111}In-loaded chelating polymer (PL-AM Fab). The heavy load of chelating polymer-modified AM Fab with reporter radiometal permits one to obtain a clear infarct image in the left lateral oblique position only in 3 h (bright spot on image *h*). Whereas the use of traditionally labeled antibody requires ≤24 h to yield images of a comparable quality. From **ref. *21***.

1.2.2. Immunoliposome (IL) Targeting to MI

To target liposomes to the infarcted myocardium, attempts have also been made to utilize AM antibody with liposomes ***(40)***. Antimyosin antibody (*see*

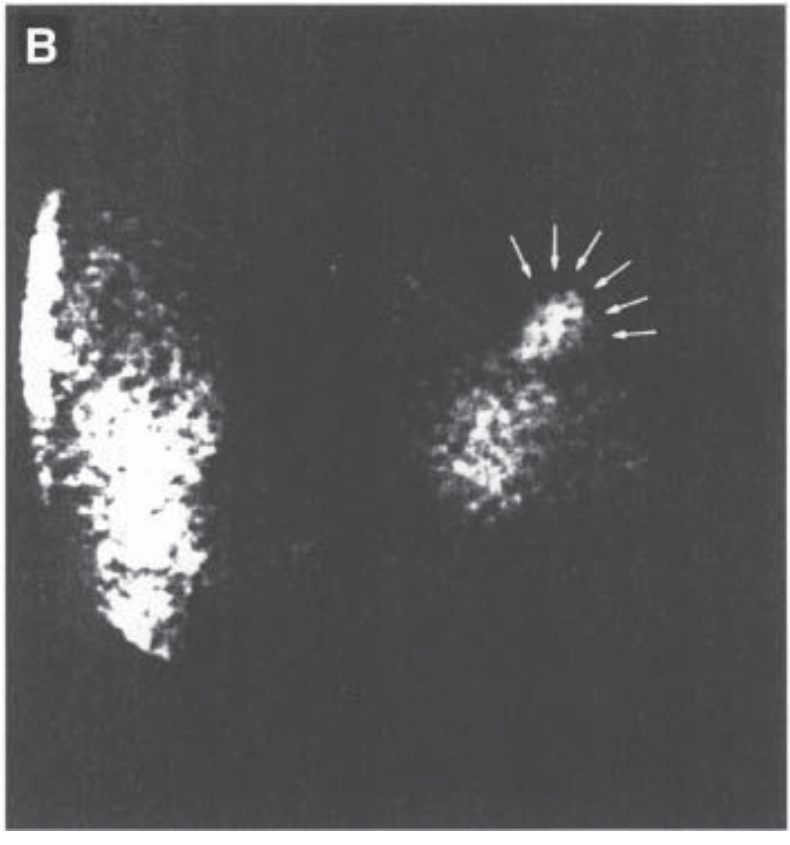

Fig. 2. *(continued)* **(B)** Gamma-visualization of experimental MI in rabbit. The image was obtained 2 h after iv administration of ^{111}In-labeled conjugate of AM Fab with a chelating polymer (DTPA-polylysine).

Subheading 1.1.) should enable these modified liposomes to home in on the sites of exposed myosin through cell membrane lesions of the infarcted myocardium. Antibody to canine cardiac myosin was covalently coupled via glutaraldehyde to liposomes prepared by sonication of a mixture of egg lecithin, cholesterol, and phosphatidyl ethanolamine. Preservation of AM antibody activity after covalent coupling to liposomes was confirmed by in vitro binding of AM-liposomes to ^{125}I-labeled canine cardiac myosin, which remained the same as that of the native AM antibody. In vivo studies in dogs with reperfused experimental MI injected intravenously with AM-liposomes radiolabeled intravesicularly with $^{111}InCl_3$ accumulated in the infarcts. These studies attested to the feasibility of the using of ILs for targeting the necrotic myocardium in vivo.

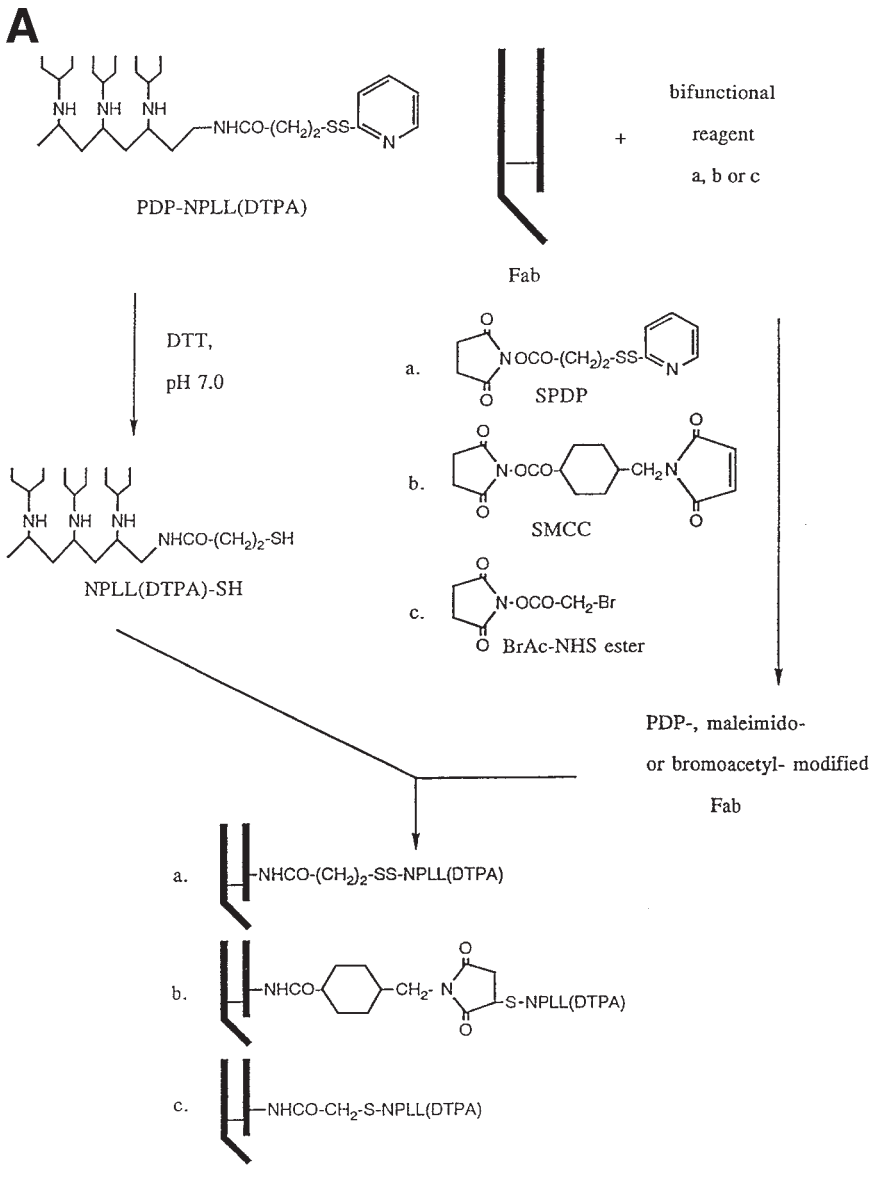

Fig. 3. **(A)** Possible synthetic methods of preparing conjugates between antibody Fab fragment and DTPA-PL with a different covalent bond between the antibody and chelating polymer. From **ref. *22***.

1.2.3. Poly(Ethylene Glycol) (PEG)-Liposomes and PEG-ILs

Conventional ILs can not demonstrate high accumulation in the areas of infarction with limited blood supply because enhanced sequestering of the ILs

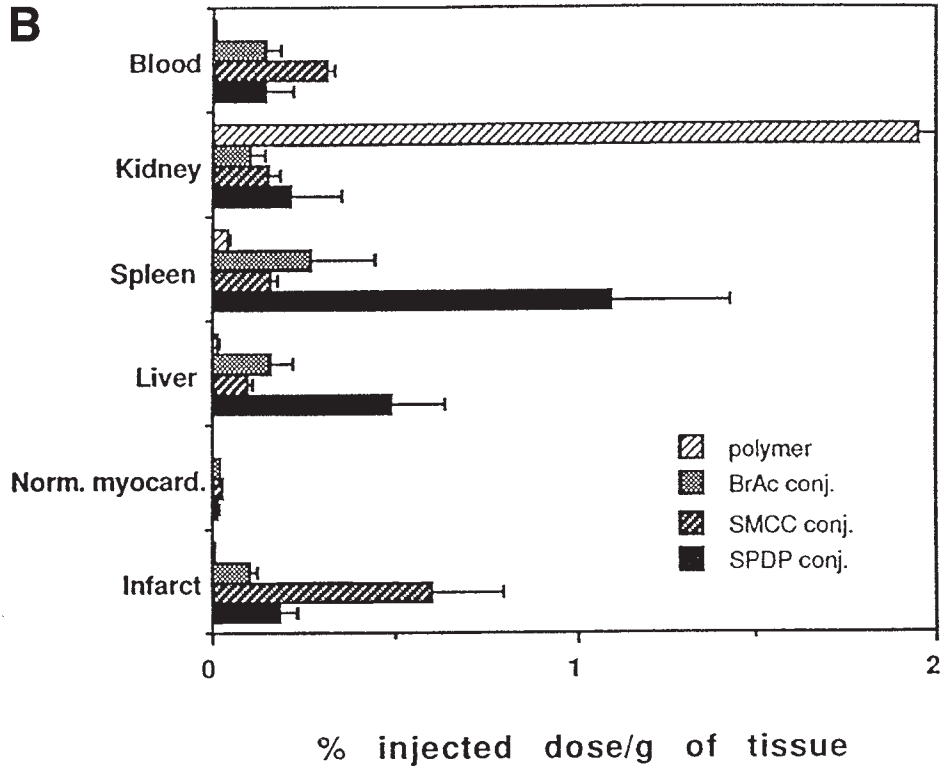

Fig. 3. *(continued)* **(B)** Biodistribution of 111In-DTPA-PL and different ^{111}In-DTPA-PL-AM Fab conjugates (A) in rabbits with experimental MI (5 h postinjection, 3–5 animals per group). Different chemical properties of conjugates result in different biodistribution and infarct accumulation patterns. From **ref. *22***.

by the reticuloendothelial system resulting in insufficient time for contact with the target. One of the most promising approaches to increase the circulation time of the ILs is to coat the IL surface with PEG. This modification decreases the opsonization rate and recognition by liver cells for clearance, thereby sharply increasing the half-life of the ILs in the blood ***(41,42)***. We ***(43)*** showed that under certain antibody-to-PEG ratio, the liposome surface contained both AM and PEG, enabling it to recognize and bind to the target as well as circulate long enough to provide high target accumulation for in vivo visualization.

Such liposomes were prepared by detergent dialysis from a mixture of phosphatidyl choline and cholesterol. Antibody modified with *N*-glutaryl phosphatidyl ethanolamine (NGPA) ***(44)*** was incorporated into the liposomal membrane in the process of liposome preparation. PEG modified with NGPA was also

incorporated by the same mechanism. These long-circulating ILs were labeled with trace amounts of ^{111}In via a liposome-incorporated membranothropic chelating compound (diethylenetriamine pentaacetic acid stearylamide). Studies in rabbits with experimental MI induced by temporary coronary artery occlusion with subsequent reperfusion after 30–60 min were injected intravenously with ^{111}In-labeled liposomes 1 h after reperfusion of the ligated coronary artery. Three hours after liposome injection, animals were killed by an overdose of pentobarbital. The hearts were excised and cut into 5-mm-slices, then stained with 2% triphenyl tetrazolium chloride for histochemical infarct delineation. Each slice was further divided into smaller sections and samples of normal and necrotic myocardium were weighed and counted in the a gamma-counter ***(43)***. The blood-clearance study at 180 min demonstrated prolonged circulation of PEG-coated ILs with increased accumulation in the target areas. The areas of increased radioactivity in the myocardium coincide with the histochemical infarct-positive stained regions. Thus, PEG-coated liposomes are specific and long-circulating. Such long-circulating ILs can deliver more materials into the target zone than conventional ILs because of their prolonged availability in the circulatory system (*see* **Fig. 4**).

The relative importance of the presence of PEG and AM antibody (AM) on the surface of liposome for infarct accumulation has also been studied ***(45,46)***. It was observed that in the infarcted myocardium, accumulation depended significantly on the presence or absence of both the PEG coating ($p = 0.0013$) and the AM antibody ($p = 0.005$). Presence of both in liposomal coatings markedly increased the mean infarct accumulation of the reagents. Plain liposomes, on the other hand, had a marginally higher liposome accumulation in the infarcted myocardium relative to the remote normal myocardium. Such nonspecific localization of liposomes in the injured myocardium has been discussed previously ***(23–27)***. Interestingly, PEG liposomes and AM liposomes accumulated in the necrotic myocardial areas almost identically (0.13 and 0.14% injected dose/g, respectively). This indicated the involvement of two different mechanisms of liposome accumulation: first, the involvement of a specific mechanism requiring the presence of antibodies on the surface of short-circulating liposomes, which permitted selectively intense targeting of necrotic myocardium even after few passages over the area of interest ***(40)***, and second, a nonspecific mechanism that taps the long-circulating liposomes resulting from leaky vascular endothelium and impaired filtration mechanisms in the affected tissues. The second mechanism requires repeated passage of liposomes through the target, i.e., prolonged circulation (**Table 1**). The phenomenon of accumulation of long-circulating liposomes has been reported previously in tumors with highly a permeable endothelial layer ***(47,48)***, where the necrotic zone (if any) may also suffer from impaired drainage, facilitating liposome accumulation.

Although the absolute accumulation of AM liposomes and PEG liposomes in the infarcts is similar, the infarct-to-normal ratio (or relative targeting) is higher for AM liposomes than PEG liposomes (22.70 ± 2.38 vs 8.05 ± 5.03, respectively). This difference in the uptake ratios is probably caused by low nonspecific accumulation of AM liposomes in normal tissues resulting from the short duration of AM liposome residence in the blood, whereas long-circulating PEG liposomes with very slow clearance suffer from higher nonspecifically accumulation in normal tissues. Therefore, PEG liposomes demonstrated lower target-to-normal tissue uptake ratios relative to AM liposomes, even though both types of liposome preparation showed equivalent target accumulation.

The combination of AM and PEG (PEG-AM liposomes) on the liposome surface adversely affected target-to-normal ratio. This ratio is lower than that of AM-liposomes because of higher nonspecific capture of PEG-AM liposomes in normal tissue. However, absolute uptake in the infarct of this combination was excellent (0.25 ± 0.14% injected dose/g); it was twofold higher than that of short-circulating AM liposomes. The intense PEG-AM liposome accumulation in the infarcted tissue resulted from the synergistic accumulation of both specific and nonspecific mechanisms.

1.3. Targeting of Ischemic Cardiocytes with ILs

Various pathological conditions, including hypoxia and inflammation, induce cell membrane lesions. The presence of these lesions which represent microscopic holes in the sarcolemma, permits washout of intracellular macromolecules into the circulation. On the other hand, certain intracellular proteins of the cytoskeleton (myosin, vimentin) become exposed through these holes to the extracellular milieu. Appropriately radiolabeled antibodies against intracellular cytoskeletal antigens have been described to delineate cell-membrane lesions. Moreover, if these antibodies are coupled to liposomes, such reagents acquire the ability to target delivery of these phospholipid vesicles to the sites of membrane lesions of the affected cells and anchor ("plug") them directly into (over) the holes (lesions); the principal scheme of the approach is shown in **Fig. 5**.

We have hypothesized and then experimentally demonstrated that antibody-directed liposomes specific for an intracellular cytoskeletal antigen can have two important medical applications: prevention of hypoxia-induced release of intracellular contents and subsequent cell death by sealing (plugging) membrane lesions with such ILs, and use of ILs for the targeted intracellular delivery of pharmacologically important substances, such as drugs or genetic constructs.

1.3.1. Targeted Sealing of Damaged Cardiomyocytes with Immunoliposomes

The hallmark of necrotic cell death is the loss of cell membrane integrity as evidenced by the presence of cell membrane lesions. Antimyosin antibody, a

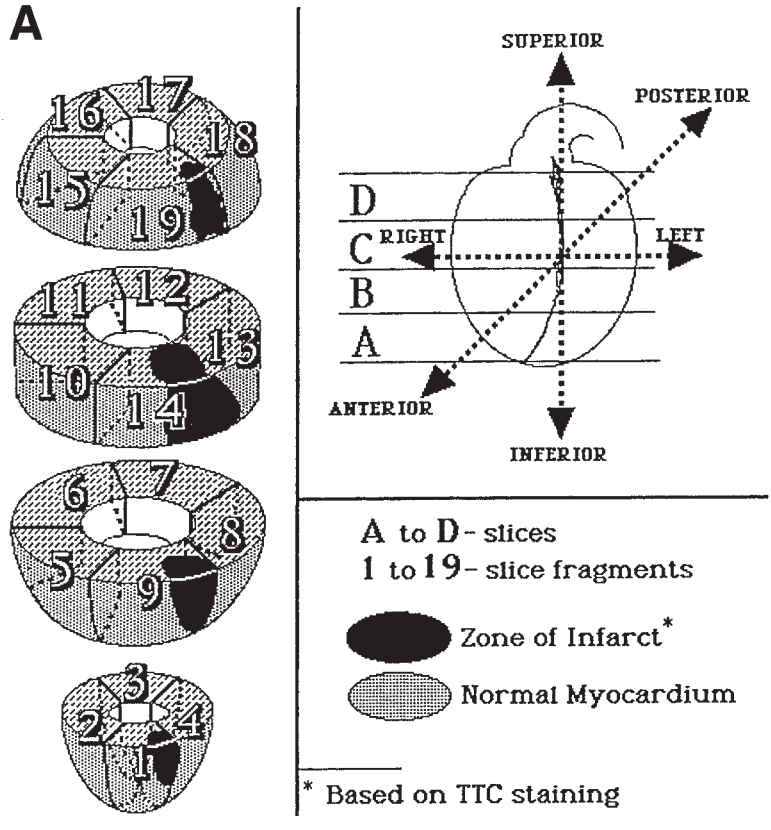

Fig. 4. **(A)** Diagrammatic representation of sample preparation in experiments on liposome accumulation in the area of experimental MI in rabbits. The postmortem heart was cut into 5-mm slices (I–IV), stained with TTC (dark areas show infarct zone), and each slice was further cut into numbered sections (1–19) that were then counted for ^{111}In radioactivity. The numbers of slices and sections in the diagram are shown only as examples. The actual number of slices and sections from each heart varied, depending on the size of the heart and the infarct volume; for example, *see* **(B)** where in different experiments the number of sections varies from 26 to 35. From ***(43)***. **(B)** The accumulation of liposomes in infarcted myocardium 6 h after iv of ^{111}In-labeled liposomes in rabbits. Typical patterns of radioisotope distribution in the left ventricle (LV) fragments for individual animals are presented as an infarct-to-normal ratio. **(a)** Liposomes contain 4 mol% PEG and no immunoglobulin; **(b)** liposomes contain AM antibody and no PEG; **(c)** Liposomes contain both, AM antibody and 4 mol% PEG. It is clearly seen that PEG-liposomes give no substantial infarct accumulation, and ILs accumulate well only in heavily infarcted areas, whereas PEG-immunoliposomes demonstrate excellent accumulation in both heavily and moderately infarcted areas (as confirmed by TTC staining), supporting the advantage of combining specificity and prolonged circulation. Modified from **ref. *43***. **(C)** Radioimmunoscintigraphy of

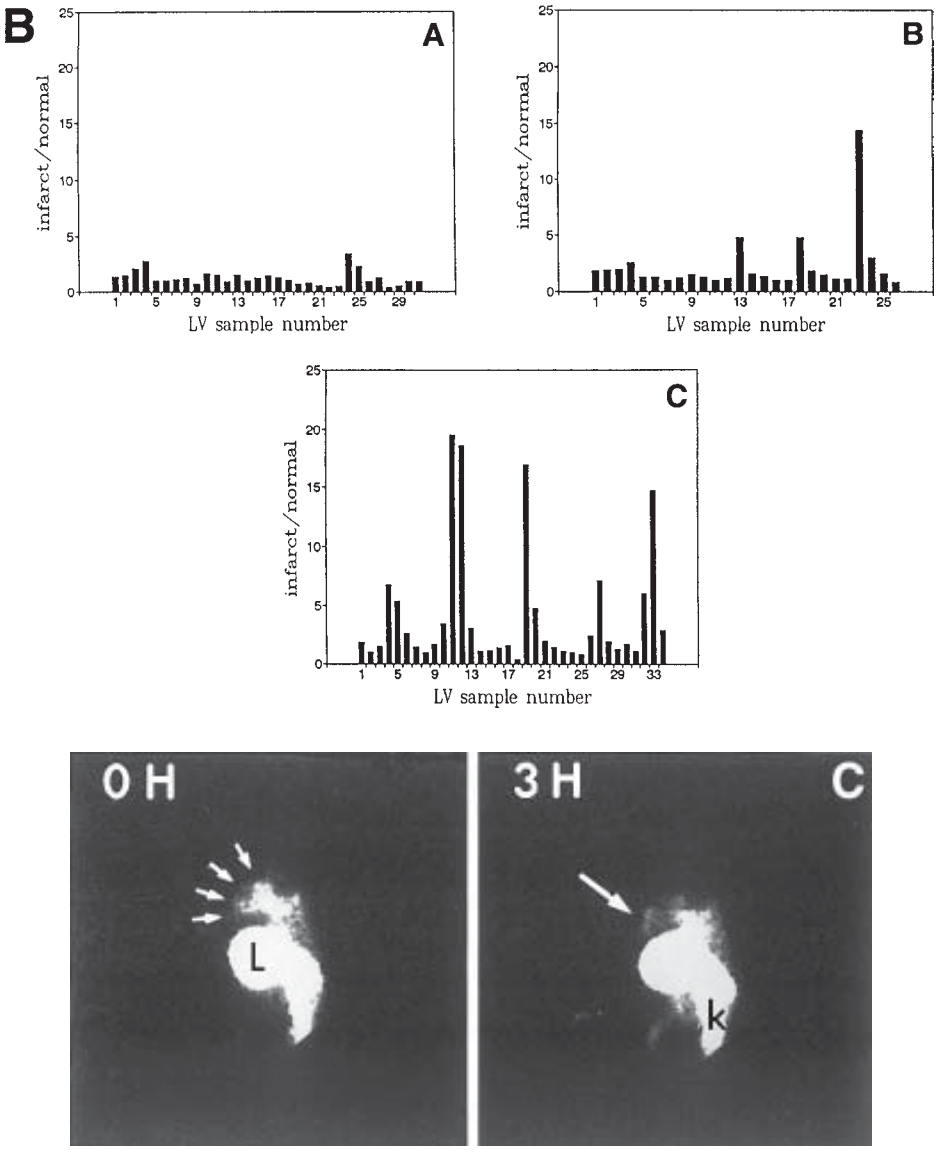

experimental MI in a dog with ^{111}In-PEG-AM-liposomes. Multiple arrows on the left icon show the area of the initial blood flow pattern in the heart area. Infarct can be clearly seen already after 3 h postinjection (single arrow on the right icon). L–liver; K–kidney.

marker of an intracellular cytoskeletal antigen, has been used to demonstrate sacrolemmal lesions indicative of necrotic myocyte damage ***(2,3)***. Hypoxia-provoked membrane disruption cannot be reversed by simple restoration of

Table 1
Liposome Targeting to Infarcted Myocardium

Liposome type	Accumulation, % dose/g	Comments
Plain liposomes	0.02	Very low accumulation
Liposomes with antimyosin	0.14	Both types of liposomes demonstrate good and similar accumulation. Two mechanisms work: (a) specific binding of antibody-liposomes, and (b) nonspecific accumulation of long-circulating liposomes resulting from impaired filtration. Relative targeting (target-to-normal ratio) is much better for immunoliposomes (22) than for PEG-liposomes (8) because of low accumulation of immunoliposomes in normal tissues (fast clearance) and high accumulation of PEG-liposomes (slow clearance).
Liposomes with PEG	0.13	
Liposomes with both antibody and PEG	0.25	Maximum absolute accumulation: both above mentioned mechanisms work synergistically. Relative targeting is intermediate (14) because of relatively high liposome accumulation in normal tissue (slow clearance).

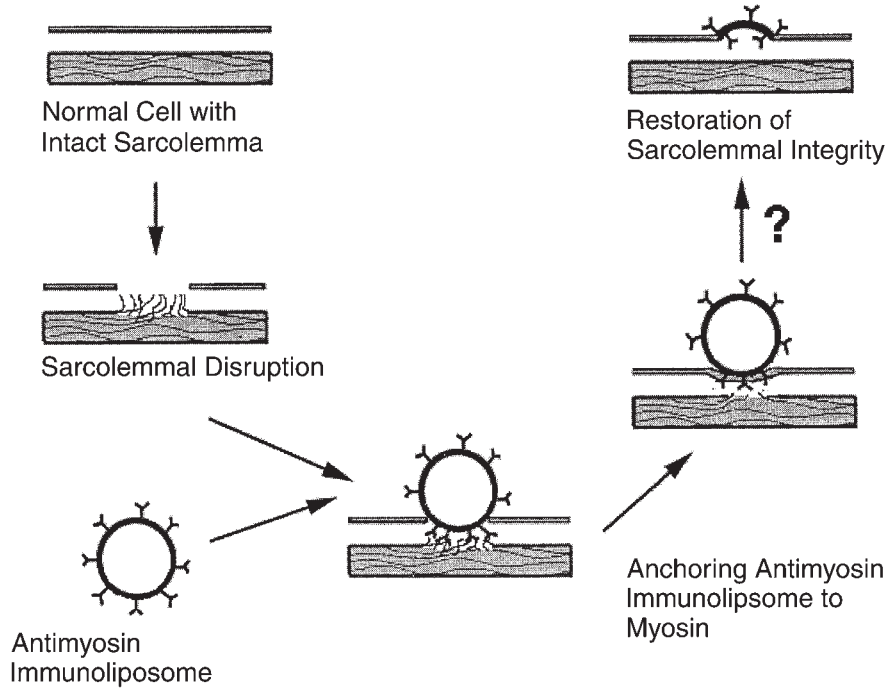

Fig. 5. Diagrammatic representation of the hypothesized mechanism of cell membrane sealing and salvage by AM-liposomes. Modified from **ref. *51***.

blood flow to the myocardium at risk. Moreover, reperfusion may even accentuate irreversible cell death by reperfusion-free radical injury, greater washout of intracellular contents, and explosive cell swelling ***(49,50)***. To minimize cell death and preserve the viability of the compromised myocardium, we hypothesized that if the membrane lesions could be sealed to prevent loss of intracellular contents, the treated cells should recover and remain viable. To achieve this result, we proposed the use of antibody-targeted liposome plugs ***(51)***. A cytoskeletal antigen exposed via a membrane lesion can be used to anchor the IL plug to provide the initial seal and prevent washout of the intracellular macromolecules.

The phenomenon of plug and seal to prevent necrotic cell death was demonstrated using myosin as the cytoskeletal target antigen and the corresponding AM antibody as the anchoring device incorporated in the liposomes, and tested in a hypoxic model of injury of H9C2 rat embryonic cardiocytes ***(51)***. H9C2 cardiocytes in hypoxic culture conditions were incubated with AM-ILs (IL), plain liposomes (PL), and control nonspecific IgG liposomes immunoglobulin (IgL). Hypoxic (HC) and normoxic cardiocytes (NC) without liposome treatment were used as additional controls.

Table 2
Assessment of Cell Viability by ^{3}H-Thymidine Uptake

Cells and treatment conditions	Viability by ^{3}H-thymidine, (% of control)
NC (control)	100
HC	3.21 ± 4.22
HC + PL	30.99 ± 15.7
HC + IL	88.59 ± 13.02

Assessment of the viability of the cells was performed after 24 h of hypoxia by Trypan-blue exclusion or by immediate further incubation of the cells with [^{3}H]-thymidine (3HT). According to the trypan-blue dye exclusion data, almost all control HSs were nonviable. Plain liposomes provided some protection from hypoxic injury, probably, by nonspecifically sticking to cell surfaces and fortuitously 'sealing' some of the cell membrane breaches. ILs completely prevented cell death, with a cell viability similar to that of normoxic cells. Hypoxic cells treated with nonspecific IgG liposomes demonstrated viability at the level of PL-treated cells.

3HT uptake studies indicative of DNA replication and cell viability demonstrated a similar pattern. If the mean 3HT uptake in control NCs was assigned a 100% value, uptake in untreated hypoxic controls was only approx 3% after 24 h of hypoxia. Uptake in IL-treated hypoxic cells was almost 90% of normoxic cells and significantly greater than PL-treated hypoxic controls (approx 30%); *see* **Table 2**.

Cell salvage may be caused by fusion of the IL lipid bilayer with the cell membrane promoted by the anchoring of the IL plug to the underlying cytoskeletal myofilaments with AM on the IL surface. The mechanism of cell salvage may also be by simple plugging of the sarcolemmal lesions with the IL kept in place by the antibody anchors. Whatever the exact mechanism, this model of intervention provided a novel approach to preservation of cell viability.

Further studies have demonstrated that IL-treated hypoxic cells were growing normally for more than 7 d after the hypoxic event when subsequently cultured under normoxic conditions. These treated cells were able to replicate normally. Prevention of cell death by cell-membrane-lesion sealing as described above could have significant clinical utility.

It is also important to determine how long this protective effect can last. Therefore, we undertook to determine whether AM-IL could protect severely injured cardiocytes cultured under hypoxic conditions for 1–5 d ***(52)***. Cell viability was assessed for cell replication by 3HT uptake and observed by confocal microscopy. Untreated HC, NC, and cardiocytes treated with plain PL were used as controls.

Survival of NCs as assessed by 3HT uptake, increased from 100% (the mean 3HT uptake in control NC was assigned 100%) to approx 254% after 24 h normal cell replication, whereas virtually no survival of HCs was registered after the same time period. Plain liposomes added to HC provided some protection, as evidenced by a decrease in viability after 24 h (approx 78%), of to approx 4% after 2 d of hypoxia, and essentially 0% after 3 d or more. When hypoxic cells were treated with IL, not only did IL confer protection, but it also permitted cell replication. This is evidenced by the similarity in the increase of 3HT uptake after 24 h of incubation between NCs (254%) and IL-treated HC (225%). After 48 h or more of hypoxia, replication in IL-treated HCs was decreased, but the viability of cells was maintained on the level of approx 90, 48, 15, and 7.8% after 2, 3, 4, and 5 d of hypoxia, respectively. These data show that the protective effect imposed by IL on hypoxic cells leads to a long-term preservation of cardiocyte viability, which might be especially important from a practical point of view for long-term preservation of myocardial viability.

1.3.2. Delivery of Drugs and DNA into HCs

In an attempt to learn more about the exact mechanism of IL interaction with HCs, we performed ultrastructural studies of HCs treated with silver grain-loaded electron-dense ILs or plain liposomes ***(51,53,54)***.

Electron microscopy of hypoxic cells incubated with silver oxide-loaded ILs demonstrated internalization of the silver grains and localization in the cytoplasmic compartment, denoting possible fusion of the ILs with the cell membrane followed by release of the intraliposomal contents into the cytoplasm ***(54)***. This finding led us to conclude that artificially imposed hypoxia may be used to facilitate intracellular delivery of various drugs, including DNA constructs, by cytoskeleton-specific ILs.

We hypothesize that if the target cells for drug and/or gene delivery are under naturally or artificially imposed stress, stress-induced small membrane lesions will allow intracellular trafficking of liposomes rendered specific for an intracellular antigen. Such liposomes may simultaneously plug and seal stress-induced cell-membrane lesions and provide intracellular drug (gene) release and delivery. Proof of this new technology was demonstrated in our experiments with silver oxide-loaded AM ILs ***(55)***. Further confirmational studies were provided by enhanced transfection and expression of a plasmid pEScFv 2G42D7 vector in H9C2 embryonic cardiocytes using ILs as plasmid carriers ***(56)***.

Plasmid pEScFv is a eukariotic expression vector containing an AM single-chain Fv (ScFv) fragment linked with domain B of protein A of *Staphylococcus aureus*. Sp2/O myeloma cells transfected with pEScFv 2G42D7 secreted

Table 3
Expression of ScFv in Transfected Cardiocytes

Cells and liposomes	ScFv concentration by ELISA, μg/mL antibody concentration
NC + PL	0.090 ± 0.001
HC + PL	0.212 ± 0.016
HC + IL	0.484 ± 0.023

ScFv into the culture media. *Escherichia coli* strain XL1/Blue was transformed with pEScFv 2G42D7 plasmid, and plasmid DNA was obtained by alkaline lysis ***(57)*** from the ampicillin-resistant line.

H9C2 cells were subjected to hypoxic stress in the presence of IL-plasmid complex and were kept under hypoxia for 6 h. After that, cells were washed and incubated for another 48 h under normoxic conditions. Enzyme-linked immunosorbent assays (ELISAs) assays with rat cardiac myosin were performed to assess the expression of 2G42D7 ScFv.

It follows from the data obtained that the transfection efficiency of hypoxic cells with ILs was 3.5 times higher than for PL with hypoxic cells and 5.5 times higher than for PL with normoxic cells; *see* **Table 3**. (Better expression in PL-treated hypoxic cells than in PL-treated normoxic cells can be explained by increased plasmid delivery in hypoxic cells nonspecifically sealed with PL).

2. Materials

2.1. Antibody-Related Experiments

1. Diethylaminoethyl (DEAE)-cellulose, DEAE-Sephadex A-25, Sephadex G-25, Sephadex G-50, and protein A-Sepharose are available from Pharmacia (Piscataway, NJ).
2. Immobilized papain and other components for antibody fragment preparation and Iodogen are available from Pierce (Rockford, IL).
3. All salts and buffer components, as well as poly-D,L-lysine (PL), CBZ-protected PL, diethylene triamine penta-acetic acid (DTPA) and its anhydrides, water-soluble carbodiimide (1-ethyl-3-(dimethylaminopropyl)-carbodiimide, EDC), (SPDP), SMCC, dithiothreithol, succinic anhydride, trinitrobenzene sulfonic acid, triethylamine, bovine serum albumin (BSA), and *N*-hydroxy sulfosuccinimide (HSSI) are available from Sigma (St. Louis, MO).
4. Dimethylformamide, HBr, and glacial acetic acid were from Aldrich (Milwaukee, WI).
5. Only freshly prepared buffers were used.
6. Commercial antibodies were purchased from ICN. Radioisotopes (Costa Mesa, CA), such as ^{111}In and ^{125}I, were obtained from Amersham (Piscataway, NJ).

2.2. Liposome-Related Experiments

1. Monomethoxy polyethylene glycol succinimidyl succinate (PEG-OSu), mol wt approx 5000, octyl glucoside (OG), cholesterol, stearyl amine (SA), and buffers, such as HEPES and MES, are available from Sigma (St. Louis, MO).
2. Dioleoyl phosphatidyl ethanolamine (PE), egg yolk phosphatidyl choline (PC), and *N*-glutaryl phosphatidyl ethanolamine (NGPE) are available from Avanti Polar Lipids (Hercules, CA).
3. Bio-Gel A1.5M is available from Bio-Rad (Alabaster, AL).
4. Polycarbonate filters are available from Osmonics (Livermore, CA).
5. Liposome size measurements were performed using a Coulter N4 MD Submicron Particle Size Analyzer Beckman Coulter (Fullerton, CA).

2.3. Cell-Related Experiments

1. All culture media and plasma components are available from Gibco (Gaithersburg, MD).
2. ^{3}H-thymidine (3HT) is available from Amersham.

2.4. In Vivo Experiments

1. Triphenyl tetrasolium chloride (TTC) is available from Sigma.
2. ^{201}Tl and ^{123}I are available from Amersham.

3. Methods

3.1. In Vitro Protocols

3.1.1. Antibody-Related Protocols

3.1.1.1. Preparation of Antibodies and Their Fragments

1. MAbs, such as mouse MAb R11D10 or 2G42D7 specific for cardiac myosin heavy chains, are purified according to the standard methods from the corresponding murine ascites by ammonium sulfate precipitation, DEAE-cellulose anion exchange chromatography, and affinity chromatography ***(6)***.
2. Antibody preparations are characterized by polyacrylamide gel electrophoresis and high-performance liquid chromatography (HPLC).
3. Fab fragments are used instead of whole antibodies when appropriate in order to decrease Fc-mediated uptake of liposome-whole antibody conjugates by cells of the reticuloendothelial system (RES).
4. Digestion of IgG and purification of Fab are as follows:
   a. 0.5 mL of the 50% slurry of immobilized papain (Pierce) are washed two times with 4 mL of digestion buffer (42 mg of cystein/12 mL of phosphate buffer, pH 7.0) for equilibration, and then suspended in 0.5 mL of the same buffer;
   b. 0.5 mL of IgG sample (10–20 mg protein/mL) are diluted with 0.5 mL of the digestion buffer and added to the tube with immobilized papain suspension;
   c. Incubation at 37°C proceeded for up until overnight with constant stirring; the extent of digestion is monitored by HPLC;

d. Digested Fab and Fc fragments and nondigested IgG are separated from papain gel;
e. A column with 5 mL of protein A-Sepharose (Pharmacia) is equilibrated with phosphate-buffered saline (PBS), pH 8.0, and digested IgG sample is applied;
f. The column is washed with PBS and Fab fragment is collected (purity is checked by HPLC);
g. The Fc fragment is washed away with 0.1 *M* glycine, pH 3.0, to regenerate the column.

3.1.1.2. Modification of Polylysine with Multiple Chelating Groups and Coupling of DTPA-Polylysine with an Antibody (*See* **Note 1**)

3.1.1.2.1. Preparation of a Modified Polylysine with Pendant Chelating Groups of DTPA. DTPA was covalently linked to a PL of required molecular weight by the mixed anhydride method of Krejcarek and Tucker ***(58)***.

1. To an aliquot of 10–20 mg PL/mL in 0.1 *M* $NaHCO_3$, aliquots of 10% by volume of mixed anhydride of DTPA (50 mg/mL) are added with continuous stirring. For optimal substitution with DTPA, five additions of the anhydride are applied. With each addition of DTPA anhydride, the pH of the reaction is monitored with pH paper, and the pH is maintained above 7.0 without precipitation of the modified polylysine. It appears that when substantial number of lysine residues have been covalently linked with DTPA, the polymers tend to form precipitates, probably because of polymerization by ionic interaction. Lowering the pH resolublized the precipitate.
2. A 10-fold molar excess of succinic anhydride, relative to the total number of moles of lysine in the polylysine, is then added to completely block unreacted amino-groups of PL (DTPA normally modifies up to 95 of amino groups). The reaction is stirred for at least 1 h at room temperature, after which the reaction is allowed to incubate at 4°C overnight.
3. DTPA-succinylated polylysine (DTPA-PL) of various molecular weights is separated from free DTPA and free succinic acid by column chromatography on a 1.5 × 45 cm Sephadex G-50 column. The modified polylysine is eluted in the void volume, whereas the free DTPA and succinic acids are eluted in the salt volume. The column is equilibrated and developed in deionized distilled water. The elution is monitored by spectrophotometric reading at 230 nm.
4. The completion of the substitution is followed by reaction of an aliquot of the polymer with trinitrobenzene-sulfonic acid ***(59)***. No color reaction was achieved with completely succinylated PL. The modified polylysine is then concentrated by lyophilization.

3.1.1.2.2. Covalent Coupling of Modified PL to an Antibody. Covalent coupling of the DTPA-PL to AM-Fab is achieved by modification of the water-soluble carbodiimide protocol previously described by using an intermediary carrier, *n*-hydroxy sulfosuccinimide (HSSI).

1. DTPA-PL at 8.33×10^{-5} m*M* in 250 µL distilled deionized H_2O (pH adjusted to 4.0) is mixed with 14-fold molar excess (1.15×10^{-3} m*M*) of *n*-HSSI (250 µg/250 µL) in deionized distilled H_2O.

2. To this, approx 400 µg/40 µL EDC (9.4 mg/mL) were added and immediately followed by another aliquot of HSSI.
3. The reaction is allowed to proceed at room temperature for 5 min.
4. Free HSSI and EDC are separated from sulfosuccinylated-DTPA-PL by Sephadex-G25 column centrifugation. The smaller HSSI and free EDC remain in the column, whereas the sulfosuccinylated DTPA-PL is directly eluted into receptacles containing 1 mg AM-Fab in 1 mL of 0.1 *M* borate (pH 8.3). This procedure reduced the amount of denaturation that might be affected by the reaction of excess free EDC with AM Fab.

3.1.1.2.3. Purification of DTPA-PL-AM-Fab from Free DTPA-PL and AM-Fab. DTPA-PL-AM-Fab is purified from free DTPA-PL and AM-Fab by DEAE Sephadex A-25 anion-exchange column chromatography.

1. A 5- to 10-mL column of DEAE-Sephadex A-25 was equilibrated in 0.05 *M* phosphate buffer (pH 6.0).
2. The reaction mixture containing all three species of molecules is loaded on the column and eluted with 3 column volumes of equilibrating buffer.
3. Free Fab is eluted in the wash.
4. DTPA-PL-AM-Fab is eluted from the column with 0.35–0.45 *M* NaCl step gradient, whereas free DTPA-PL is retained by the anion-exchanger. The DTPA-PL can be eluted from the column by a 0.95 *M* NaCl step gradient.
5. The peak tubes containing DTPA-PL-AM-Fab are pooled, and the antibody concentration is estimated from its optical density reading at 280 nm utilizing an extinction coefficient of 1.5 for Fab.

3.1.1.2.4. Alternative Methods of PL Modification with DTPA and DTPA-PL Coupling to an Antibody. Alternatively, to ensure a single-point attachment of DTPA-PL to an antibody, DTPA-PL bearing a PDP on its N-terminal is synthesized ***(22)***, see the scheme in **Fig. 3A**. For this purpose,

1. ε,*N*-carbobenzoxy-protected poly-D,L-lysine (5 mg), SPDP (2.5 mg), and triethylamine (5 µL) were mixed in 0.5 mL of dimethylformamide and incubated overnight at room temperature.
2. The water-washed and lyophilized precipitate are deprotected with a 30% solution of HBr in glacial acetic acid (2 mL).
3. The deprotected polymer is washed with dry diethyl ether and lyophilized.
4. Chelating residues were introduced into the polymer as described in **Subheading 3.1.1.2.1.**

SPDP, SMCC, and Br-Ac-NHS (*see* **Fig. 3A**) are used as bifunctional modifiers to react with aminogroups of an antibody for subsequent antibody coupling with DTPA-PL-PDP. The reaction mixture typically consists of 200 µg of antibody Fab and 10 µg of a bifunctional reagent in 100 µL HBS. The reaction is allowed to proceed for 1 h at room temperature and then terminated by dialysis against HBS at 4°C.

Just prior to the reaction with modified Fab, PDP-containing DTPA-PL is activated by the treatment with 2.5 m*M* dithiotreithol in HBS for 20 min at 37°C. Dithiotreithol

is separated from the polymer using a Sephadex G-25 spin column equilibrated with HBS. Modified Fab is mixed with reduced DTPA-PL in a 1:1 weight ratio and the reaction mixture is incubated overnight at 4°C. The conjugate is separated from unmodified Fab and free polymer as described in **Subheading 3.1.1.2.3.**

3.1.1.3. Determination of Immunoreactivity

Immunoreactivity of the various preparations of DTPA-PL-modified AM-Fab are determined by solid-phase radioimmunoassay. Serial dilutions of the modified AM are compared to serial dilutions of unmodified and conventionally DTPA-modified AM Fab.

1. Cook's microtiter wells are coated with 50 µL of 10 µg/mL solution of human cardiac myosin, then the plates are blocked and washed 12 times with 1% horse serum in 0.15 *M* phosphate-buffered saline (pH 7.4).
2. Duplicate samples of 50-µL aliquots of the serial dilutions of the AM preparations are then added to each well and incubated either at room temperature for 3 h or at 4°C overnight. Serial dilutions of antibody concentration ranged from 0.1 ng to 100 µg.
3. The antibody is then removed, and the wells were again washed 12 times with 1% horse serum in 0.15 *M* PBS. The 50 µL aliquots of 50,000 cpm of ^{125}I-labeled goat antimurine IgG Fab (GAM-Fab) are added to the wells and incubated at room temperature for 1–2 h.
5. The excess radioactivity is removed from each well by aspiration into a radioactive waste container, followed by washing 12 times with 1% HS-PBS.
6. The wells are cut out and counted in a gamma scintillation counter for the 30 and 60 keV peaks of ^{125}I (Micromedics gamma counter) to determine the antibody activity.
7. The binding activities of the antibody preparations are compared to intact AM. When Fab is used, a comparison is made to the binding of AM-Fab fragments.

3.1.1.4. Radiolabeling

3.1.1.4.1. Radioiodination

1. GAM-Fab is labeled with ^{125}I by the chloramine-T method (a standard procedure used to radiolabel the secondary antibody for in vitro assays) ***(60)***.
2. Free and bound ^{125}I is separated by column chromatography using a 10-mL Spehadex-G25 column.
3. ^{125}I-labeled GAM-Fab eluted in the void volume is pooled and stored frozen in 1% bovine serum albumin until used.

Antimyosin Fab was labeled with ^{125}I and ^{123}I by the Iodogen iodination method ***(61)*** because of its gentler nature of compared to chloramine T. Free and AM-bound radioactivity were separated as described above.

*3.1.1.4.2. ^{111}In Labeling (*See **Note 2***)*

1. DTPA-PL-coupled AM Fab is labeled with ^{111}In by transchelation utilizing 0.1–0.5 *M* citrate (pH 5.5) as the weak transchelator ***(62)***.

2. 1 mCi $^{111}InCl_3$ was added to equivolumes of 1 *M* citrate (pH 5.5), then 10–15 µg of DTPA-PL (PL of molecular weight between 1000 and 10,000 and can be used) AM Fab in 0.05 *M* PBS are added to the ^{111}In citrate solution.
3. Transchelation is allowed to proceed for 15 min, then bound and free ^{111}In are separated by Sephadex-G25 column chromatography.

In the labeling of DTPA-PL-AM-Fab, the antibody sample was mixed with 1 mg carrier BSA prior to addition of ^{111}In-citrate to minimize denaturation and loss through adsorption to test tube surfaces and column matrix of a very dilute solution of the antibody.

*3.1.2. Liposome-Related Protocols (*See **Note 3***)*

3.1.2.1. Antibody Modification with Lipid Derivative

For the incorporation of AM antibody into the liposomal membrane, AM-Fab is initially modified with a hydrophobic anchor, NGPE, as described in **ref. *44***.

1. An aliquot (0.3 mg) of NGPE in chloroform is dried with argon and then solubilized with 0.5 mL of 0.016 *M* octylglucoside (OG) in 50 m*M* MES.
2. The solution is supplemented with 12 mg EDC and 15 mg of HSSI.
3. The mixture is incubated for 5 min and then added to the solution of 2 mg of Fab in 0.1 *M* HEPES, pH 7.6.
4. The pH is adjusted to 8.0 with 1 *M* NaOH, and the mixture is incubated overnight at 4°C.
5. The modified antibody is purified by dialysis against HBS.

3.1.2.2. Synthesis of PEG-PE

PEG-PE can be acquired commercially, or the synthesis of PEG-PE can be performed as described in **ref. *41***.

1. An aliquot of PEG-OSu is added to a solution of PE in chloroform, followed by addition of triethylamine (PEG-OSu:PE:triethylamine = 3:1:3.5, mol/mol).
2. The reaction mixture is incubated overnight at room temperature and the chloroform is evaporated with a stream of nitrogen gas.
3. The reaction mixture is then redissolved in 0.145 *M* NaCl.
4. Unreacted PEG-OSu is rapidly hydrolyzed in the aqueous media.
5. The resulting mixture in saline is applied to a Bio-Gel A1.5M column equilibrated with saline.
6. Peak fractions containing PEG-PE micelles eluted in the void volume are pooled, dialyzed against water, and lyophilized.

3.1.2.3. Preparation of Liposomes, ILs, and PEG-Liposomes (*See* **Note 3**)

1. Liposomes are prepared by detergent (OG) dialysis from a mixture of PC and cholesterol (7:3 molar ratio).

2. When necessary, 6 mol% of PEG-PE and 1 mol% of DTPA-SA are added to the lipid mixture, which is then dried with argon, further dried under vacuum, then solubilized with OG in HEPES-buffered saline (HBS), pH 7.4 (final total lipid concentration may vary from 5 to 20 mg/mL), and dialyzed overnight against HBS at 4°C.
3. When preparing AM-ILs, 0.01 mol% NGPE-AM Fab is added to OG-solubilized lipid mixture.

Modification with NGPE allows binding of several hundred protein molecules per 250 nm diameter liposome ***(44)***. Using ^{125}I-labeled antibody, the efficacy of protein binding varied between 65 and 75% and did not depend on the presence of PEG-PE in the lipid mixture. The unbound antibody is separated on a Bio-Gel A15M column. Liposomes obtained are serially filtered through polycarbonate filters with pore sizes of 0.6, 0.4, and 0.2 μm. The actual size (normally 160–190 nm) and distribution of the liposomes are determined with a particle size analyzer.

3.1.2.4. Radiolabeling of Liposomes

For biodistribution studies, liposomes are radioactively labeled with ^{111}In via amphophilic chelating agent DTPA-SA incorporated into the liposomal membranes.

1. To prepare DTPA-SA, 1.55 g SA and 2.5 g DTPA cyclic anhydride are mixed with 250 mL dry chloroform.
2. The mixture is refluxed for 1 h, the top outlet of the system being coated with foil. Then, 3 mL of triethylamine are added and the mixture is refluxed for an additional 48 h.
3. The chloroform is evaporated using a rotary evaporator and traces of residual chloroform are removed by incubating the flask in a water bath at 50°C.
4. 100 mL of 0.1 *N* HCl are added to the dry product, and the mixture is stirred with heating at 80°C for 10 min and stored overnight at room temperature.
5. The precipitate was separated by centrifugation, washed 3 times with 100 mL of 0.1 *N* HCl with stirring, and then lyophilized. The lyophilized product is washed twice with 100 mL of methanol, and then recrystallized twice from boiling methanol and dried.
6. Loading DTPA-SA with ^{111}In is performed after DTPA-SA has been incorporated into the liposomes by transchelation. Briefly, the liposome suspension (normally 2 mL) is supplemented with 30 μL of 1.0 *M* citrate, pH 5.0–6.0 and incubated for 1 h with the required quantity of ^{111}In-citrate at room temperature, then dialyzed overnight against HBS at 4°C to remove free label (*see* **Note 2**).

3.1.2.5. Determination of Antibody-Liposome Immunoreactivity by Direct Binding of Radiolabeled Antibody-Liposome and Antibody-Liposome-Polymer Conjugates

1. Microtiter plates are coated with 50 mL of 10–50 mg/mL dog cardiac myosin and incubated at 4°C for 12–18 h.

2. The antigen solution is removed and the wells are blocked with 1% horse serum in 0.15 *M* PBS (pH 7.4) to saturate the remaining nonspecific binding surfaces of the microtiter wells.
3. The solution is removed after a 4-h incubation at room temperature and the wells are washed extensively with standard washing solution.
4. To the antigen-coated wells prepared as described in **Subheading 3.1.1.3.**, serial dilutions of ^{111}In-labeled antibody-polymer-liposome preparation are added. The maximum count used per 50 mL aliquot is 2×10^5 cpm. Half dilutions were made until the aliquots contained approx 10,000 cpm/50 mL.
5. The reaction is allowed to proceed until equilibrium is reached at 4 h at room temperature or overnight at 4°C.
6. The wells are extensively washed to remove nonspecifically bound radioactivity, then the wells are cut and counted in a gamma-scintillation counter for ^{111}In activity.
7. Binding of ^{111}In-labeled antibody-polymer-liposome conjugates was compared with the binding of corresponding antibody directly labeled with ^{111}In via covalently attached DTPA.

3.1.3. Cell-Related Protocols

3.1.3.1. Cell Cultivation under Normal and Hypoxic Conditions and Cell Survival in the Presence of Liposomes

1. Two million H9C2 cardiocytes are incubated in 25-mL culture flasks with 10% fetal calf serum in DMEM at 37°C, 5% CO_2.
2. After overnight incubation, the cells are washed in PBS (0.02 *M* phosphate, pH 7.4; 0.13 *M* NaCl) and recultured in 3 mL fresh medium with (7.2 mg total lipids) or without liposomes (PL, IL, or IgL; for liposome preparation *see* **Subheading 3.1.2.**). Sterile nitrogen gas is bubbled through the medium vigorously for 4 min, dislodging all cells (>95%) from the bottom of the flasks. The flasks are then closed tightly to maintain hypoxia through overnight incubation at 37°C. All studies are performed in triplicate.
3. Assessment of cell viability is performed after 24 h of incubation by Trypan blue exclusion or by immediate further incubation with 3HT for an additional 24 h of normoxic culture conditions.
4. For 3HT uptake studies, an aliquot of 5 µCi 3HT (4.5×10^6 cpm) is added to each flask for 24 h at 37°C. The medium is then aspirated, and each flask is washed with ice-cold PBS.
5. The DNA is then precipitated by a standard method ***(63)*** and beta-counting performed in a liquid scintillation counter.

3.1.3.2. Intracellular Delivery of DNA by Immunoliposomes

The used plasmid pEScFv is a eukaryotic expression vector containing an AM single-chain Fv (ScFv) fragment linked with domain B of a protein A of *S. aureus*. Sp2/O myeloma cells transfected with pEScFv 2G42D7 secreted ScFv into the culture media. *E. coli* strain XL1/Blue is transformed with plasmid pEScFv

2G42D7. Plasmid DNA is obtained by standard alkaline lysis from an ampicillin-resistant line. Purified plasmid is checked by agarose electrophoresis.

1. To prepare DNA-loaded liposomes, plasmid pEScFv 2G42D7 is added to OG-solubilized liposomal lipids before final detergent removal by dialysis (when necessary, together with modified AM antibody). The quantity of the plasmid used is 50 μg/mL. Other steps of liposome preparation are described in **Subheading 3.1.2.**
2. For transfection, H9C2 cells (5×10^5) are placed in six-well culture plates together with fetal calf serum in DMEM at 37°C, 5% CO_2, and incubated overnight. Then the cells are washed with PBS and recultured in 1 mL of serum-free medium (SFM)/liposome mixture (0.5 mL SFM + 0.5 mL PL or IL in PBS at lipid concentration of 7–10 mg/mL). Nitrogen gas is passed through the medium for 1 min, and wells are covered tightly with Parafilm and incubated for 6 h (these conditions result in mild hypoxia). Normoxic cells are kept under normal conditions for 6 h.
3. Media is removed after 6 h and cells are washed with PBS. FCS-containing medium is then added to each well, and cells are incubated further for 48 h at 37°C, 5% CO_2. After this incubation period is completed, media is removed and concentrated (by 5–10-fold).
4. Standard ELISA assays with porcine (10 μg/mL) and rat (50 μg/mL) cardiac myosin are performed to assess the expression of 2G42D7 ScFV.

3.2. In Vivo Protocols

*3.2.1. Experimental MI in Dogs and Imaging of Infarct with Radiolabeled Antibodies (*See **Note 4***)*

1. Dogs are anesthetized by iv administration of 30 mg/kg sodium pentobarbitol, and respiration is maintained on room air using a Harvard Respirator.
2. A left thoracotomy is performed through the fifth intercostal space, and the heart is suspended in a pericardial cradle.
3. A segment of the left anterior descending coronary artery (LAD), approximately two-thirds the distance from apex to base, is isolated and a silk ligature is placed around the segment.
4. The right femoral artery is also isolated and a pressure transducer is attached to monitor arterial pressure.
5. The femoral vein is cannulated for taking blood samples. Intravenous lines are established in the brachial vein of the right foreleg.
6. For subsequent histochemical confirmation of acute MI, an atrial line for the administration of triphenyltetrazolium chloride is inserted into the left atrial appendage.
7. The LAD is occluded for 3 h, before blood flow is restored by removal of the occlusive ligature ***(64)***.
8. Fifteen minutes after reperfusion, 600 μCi of ^{201}Tl is administered intravenously, and after another 15 min ^{201}Tl distribution images (at the 80 keV photopeak with a 20% window) are obtained in the left lateral position to confirm myocardial perfusion deficit.

9. Immediately after ^{201}Tl imaging, a bolus of a mixture of approx 800 µCi ^{111}In-labeled DTPA-PL-AM-Fab or 400 µCi ^{123}I- or ^{125}I-labeled AM Fab in lactate Ringer's solution is injected intravenously.
10. A series of 60-s acquisition images is obtained for the next 64 min (at the 247 keV, higher energy peak of ^{111}In, with a 20% window). Hourly images were obtained for the next 4 h. Blood samples were also obtained at 1, 2, 3, 5, 10, 15, 30, 45, 60, 75, 90, 120, 150, 180, 210, and 240 min after administration of the ^{111}In-labeled reagents. The 1-min blood sample served as the 100% blood activity reference standard.
11. After gamma imaging at 4 h, the animals are killed by an overdose of pentobarbitol and intra-atrial infusion of warm (~40°C) 2% triphenyltetrazolium chloride (TTC, 200 mL). The heart, lungs, liver, spleen, kidneys (cortex and medulla), abdominal skeletal muscles, and intestine are excised and weighed, and organ pieces of approx 1 g are counted in a gamma counter for ^{201}Tl, ^{111}In, and radioiodine distributions.
12. The heart is imaged whole and as 1-cm bread-loaf slices for ^{201}Tl, ^{111}In, and radioiodine activities. When ^{123}I-labeled AM-Fab is used in the study, a photopeak of 159 keV with a 20% window is employed. However, when ^{125}I-labeled AM-Fab is used, the X-ray peak of ^{125}I was used to image the iodine distribution.
13. Following imaging, the heart slices are cut into endocardial and epicardial pieces of approx 1 g, weighed, and counted in a gamma-counter (Compugamma, LKB) for radioiodine, ^{111}In, and ^{201}Tl activities.
14. Aliquots (10 µL) of each radiolabeled reagent are retained and counted with the tissue samples for subsequent calculation of percent injected dose per gram of the tissue samples.

To demonstrate that ^{111}In-DTPA-PL alone is not an infarct avid imaging agent, we injected approx 0.5 mCi of ^{111}In-DTPA-PL 3.3 kDa into three dogs with experimental MI. The experimental protocol was the same as that described directly above.

3.2.2. Experimental Myocardial Infarction in Rabbits and Targeting of Infarct with Liposomes

1. Rabbits (New Zealand White rabbits, 2–3 kg) are anesthetized with Ketamine (70–75 mg/kg) and Xylazine (7-7.5 mg/kg).
2. Right femoral artery cut-down is performed to establish a blood pressure line and for arterial blood sampling.
3. The right femoral vein is catheterized to allow iv medication.
4. A tracheostomy is performed and ventilation is instituted through an endotracheal tube with a Harvard Rodent Ventilator (model 683).
5. After the establishment of ventilator-assisted respiration, anesthesia is switched to 3 mL (19.5 mg) pentobarbital infusion/h.
6. A left thoracotomy is performed and the anterior descending coronary artery is occluded with a silk suture placed through the myocardium with an SH-needle.

7. After 40 min, the snare is released to allow reperfusion.
8. A radiolabeled liposome preparation (2–3 mL in HBS, up to 30 mg of total lipids and 200–500 μCi of ^{111}In) is injected intravenously within 30 min of reperfusion.
9. Blood samples are taken serially at 1, 3, 5, 10, 20, 30, 45, 60, 90, 120, 150, 180, 240, and 300 min after injection of liposomes to measure blood radioactivity (liposomal clearance). $T_{1/2}$ the time of 50% reduction of the blood activity of the injected dose is determined.
10. Five hours after liposome injection, animals are euthanized by an overdose of pentobarbital.
11. The heart is excised and cut into 5-mm slices, and stained with 2% triphenyl tetrazolium chloride to histochemically identify the necrotic areas ***(65)***. Each slice is further divided into smaller segments for biodistribution studies following a standard protocol ***(21,43)***.
12. Samples of normal and infarcted myocardium and other organs of interest are blotted dry of excess blood, weighed, and counted in a gamma counter.
13. Liposome accumulation in the heart is expressed as an infarct-to-normal myocardium radioactivity ratio. Biodistribution of liposomes in nontarget organs (such as liver, spleen, kidneys, and lung), is expressed as % injected dose/g tissue.

4. Notes

1. Antibody modification. Depending on the particular type and source of an antibody, its modification according to any of the described protocols might cause some activity decrease or even complete antibody inactivation. To escape this, immunological activity of modified and/or liposome-incorporated antibodies must be checked in a simple ELISA assay after each modification step and upon storage. If a chosen method results in antibody inactivation, and alternative protocol must be used.
2. ^{111}In labeling of chelating polymers, modified antibodies, or liposomes. The presence of citrate in the reaction medium for ^{111}In labeling is crucial, since under neutral pH in the absence of an intermediate weak chelate, such as citrate, In instantly precipitates as an insoluble oxide and no labeling proceeds.
3. Liposomes. To escape undesirable liposome aggregation and widening size distribution, only fresh liposome preparation (1–2 d old) should be used in biodistribution and targeting experiments.
4. Animal experiments. When ligating LAD, the danger of ventricular fibrillation often exists (up to 20% of animals might demonstrate certain cardiac rhythm abnormalities). This should be closely followed by electrocardiogram.

References

1. Khaw, B. A. (1994) Antimyosin antibody for the diagnosis of acute myocardial infarction: experimental validation, in *Monoclonal Antibodies in Cardiovascular Diseases* (Khaw, B. A., Narula, J., and Strauss, H. W., eds.), Lea and Febiger, Malvern, PA, pp. 15–29.
2. Khaw, B. A., Beller, G. A., Haber, E., and Smith, T. W. (1976) Localization of cardiac myosin-specific antibody in myocardial infarction. *J. Clin. Invest.* **58,** 439–446.

3. Khaw, B. A., Fallon, J. T., Beller, G. A., and Haber, E. (1979) Specificity of localization of myosin specific antibody fragments in experimental myocardial infarction: histologic, histochemical, autoradiographic and scintigraphic studies. *Circulation* **60,** 1527–1531.
4. Khaw, B. A., Scott, J., Fallon, J. T., Haber, E., and Homcy, C. (1982) Myocardial injury: quantitation by cell sorting initiated with antimyosin fluorescent spheres. *Science* **217,** 1050–1053.
5. Khaw, B. A., Beller, G. A., and Haber, E. (1978) Experimental myocardial infarct imaging following intravenous administration of iodine-131 labeled antibody $(Fab')_2$ fragments specific for cardiac myosin. *Circulation* **57,** 743–750.
6. Khaw, B. A., Mattis, J. A., Melincoff, G., Strauss, H. W., Gold, H. K., and Haber, E. (1984) Monoclonal antibody to cardiac myosin: scintigraphic imaging of experimental myocardial infarction. *Hybridoma* **3,** 11–23.
7. Khaw, B. A., Strauss, H. W., Carvalho, A., Locke, E., Gold, H. K., and Haber, E. (1982) Technetium-99m labeling of antibodies to cardiac myosin Fab and to human fibrinogen. *J. Nucl. Med.* **23,** 1011–1019.
8. Strauss, H. W., Narula, J., and Khaw, B. A. (1994) Acute myocardial infarct imaging with technetium-99m and indium-111 antimyosin Fab, in *Monoclonal Antibodies in Cardiovascular Diseases* (Khaw, B. A., Narula, J., and Strauss, H. W., eds.), Lea and Febiger, Malvern, PA, pp. 30–42.
9. Johnson, L. L., Seldin, D. W., Becker, L. C., LaFrance, N. D., Liberman, H. A., James, C., Mattis, J. A., Dean, R. T., Brown, J., Reiter, A., Arneson, V., Cannon, P. J., and Berger, H. J. (1989) Antimyosin imaging in acute transmural myocardial infarction: results of a multicenter clinical trial. *J. Am. Coll. Cardiol.* **13,** 27–35.
10. Hendel, R. C., McSherry, B. A., and Leppo, J. A. (1990) Myocardial uptake of indium-111-labeled antimyosin in acute subendocardial infarction: clinical, histochemical and autoradiographic correlation of myocardial necrosis. *J. Nucl. Med.* **31,** 1851–1853.
11. Nakata, T., Sakakibara, T., Noto, T., Shoji, T., Tsuda, T., Kubota, M., Hattori, A., and Iimura, O. (1991) Myocardial distribution of indium-111 antimyosin Fab in acute inferior and right ventricular infarction: comparison with Tc-99m pyrophosphate imaging and histological examination. *J. Nucleic Med.* **32,** 865–867.
12. van Vlies, B., van Royen, E. A., Visser, C. A., Meyne, N. G., van Buul, M. M., Peter, R. T., and Dunning, A. J. (1990) Frequency of myocardial indium-111 antimyosin uptake after uncomplicated coronary artery bypass surgery. *Am. J. Cardiol.* **66,** 1191–1195.
13. van Vlies, B., Koch, K. T., and van Royen, E. A. (1994) Perioperative myocardial damage assessed with indium-111 antimyosin scintigraphy, in *Monoclonal Antibodies in Cardiovascular Diseases* (Khaw, B. A., Narula, J., and Strauss, H. W., eds.), Lea and Febiger, Malvern, PA, pp. 56–63.
14. Cummins, B., Russell, G. J., Chandler, S. T., Pears, D. J., and Cummins, P. (1990) Uptake of radioiodinated cardiac specific troponin-I antibodies in myocardial infarction. *Cardiovasc. Res.* **24,** 317–327.

15. Torchilin, V. P., Trubetskoy, V. S., Narula, J., Khaw, B. A., Klibanov, A. L., and Slinkin, M. A. (1993) Chelating polymer modified monoclonal antibodies for radioimmunodiagnostics and radioimmunotherapy. *J. Contr. Release* **24,** 111–118.
16. Torchilin, V. P., Klibanov, A. L., Slinkin, M. A., Danilov, S. M., Levitsky, D. O., and Khaw, B. A. (1989) Antibody-linked chelating polymers for immunoimaging in vivo. *J. Contr. Release* **11,** 297–303.
17. Slinkin, M. A., Klibanov, A. L., and Torchilin, V. P. (1991) Terminal-modified polylysine-based chelating polymers: highly efficient coupling to antibody with minimal loss in immunoreactivity. *Bioconj. Chem.* **2,** 342–348.
18. Trubetskoy, V. S., Narula, J., Khaw, B. A., and Torchilin, V. P. (1993) Chemically optimized antimyosin Fab conjugate with chelating polymers: importance of the nature of the protein-polymer single site covalent bond for biodistribution and infarction localization. *Bioconj. Chem.* **4,** 251–255.
19. Torchilin, V. P. and Klibanov, A. L. (1991) The antibody-linked chelating polymers for nuclear therapy and diagnostics. *CRC Crit. Rev. Ther. Drug Carrier Syst.* **7,** 275–308.
20. Torchilin, V. P., Klibanov, A. L., Nossiff, N. D., Slinkin, M. A., Strauss, H. W., Haber, E., Smirnov, V. N., and Khaw, B. A. (1987) Monoclonal antibody modification with chelate-linked high-molecular-weight polymers: major increase in polyvalent cation binding without loss of antigen binding. *Hybridoma* **6,** 229–240.
21. Khaw, B. A., Klibanov, A. L., O'Donnell, S. M., Saito, T., Nossiff, N., Slinkin, M. A., Newell, J. B., Strauss, H. W., and Torchilin, V. P. (1991) Gamma imaging with negatively charge-modified monoclonal antibody: modification with synthetic polymers. *J. Nucl. Med.* **32,** 1742–1751.
22. Trubetskoy, V. S., Narula, J., Khaw, B. A., and Torchilin, V. P. (1993) Chemically optimized antimyosin Fab conjugates with chelating polymers: Importance of the nature of the protein-polymer single site covalent bond for biodistribution and infarct localization. *Bioconj. Chem.* **4,** 251–255.
23. Caride, V. J. and Zaret, B. L. (1977) Liposome accumulation in regions of experimental myocardial infarction. *Science* **198,** 735–738.
24. Kayawake, S. and Kako, K. J. (1982) Association of liposomes with the isolated perfused rabbit heart. *Basic Res. Cardiol.* **77,** 668–681.
25. Mueller, T. M., Marcus, M. L., Mayer, H. E., Williams, J. K., and Hermsmeyer, K. (1981) Liposome concentration in canine ischemic myocardium and depolarized myocardial cells. *Circ. Res.* **49,** 405–415.
26. Cole, A. W., Kingaby, R. O., Lab, M. J., and Palmer, T. N. (1982) Myocardial liposome uptake in the early stages of myocardial infarction. *Cardiovasc. Res.* **16,** 516–523.
27. Caride, V. J., Twickler, J., and Zaret, B. L. (1984) Liposome kinetics in infarcted canine myocardium. *J. Cardiovasc. Pharmacol.* **6,** 996–1005.
28. Palmer, T. N., Caride, V. J., Fernandez, L. A., and Twickler, J. (1981) Liposome accumulation in ischaemic intestine following experimental mesenteric occlusion. *Biosci. Rep.* **1,** 337–344.

29. Palmer, T. N., Caride, V. J., Caldecourt, M. A., Twicjler, J., and Abdullah, V. (1984) The mechanism of liposome accumulation in infarction. *Biochim. Biophys. Acta* **797,** 363–368.
30. Palmer, T. N., Caldercourt, M. A., and Kingaby, R. O. (1984) Liposome drug delivery in chronic ischemia. *Biochem. Soc. Trans.* **12,** 344–345.
31. Baldeschweiler, J. D. (1990) Liposomal targeting of ischemic tissue. Intl. Patent 9012595.
32. Nguen, P. D., Orear, E. A., Johnson, A. E., Patterson, E., Whitsett, T. L., and Bhakta, R. (1990) Accelerated thrombolysis and reperfusion in a canine model of myocardial infarction by liposomal incapsulation of streptokinase. *Circ. Res.* **66,** 875–878.
33. Tang, C. S., Su, J. Y., Li, Z. P., Zhang, L. Z., Yang, J., Qi, M., Liu, F. A., and Tang, J. (1993) Possibility of targeting treatment for ischemic heart disease with liposome (I). *Sci. China. B.* **36,** 590–598.
34. Tang, C. S., Su, J. Y., Li, Z. P., Zhang, L. Z., Yang, J., Qi, M., Liu, F. A., and Tang, J. (1993) Possibility of targeting treatment for ischemic heart disease with liposome (II). *Sci. China. B.* **36,** 809–816.
35. Jadot, G. and Michelson, A. M. (1987) Comparative anti-inflammatory activity of different superoxide dismutases and liposomal SOD in ischemia. *Free Radical Res. Commun.* **3,** 389–394.
36. Suzuki, S., Miyachi, Y., Niwa, Y., and Isshiki, N. (1989) Significance of reactive oxygen species in distal flap necrosis and its salvage with liposomal SOD. *Br. J. Plastic Surg.* **42,** 559–564.
37. Phelan, A. M. and Lange, D. G. (1991) Ischemia-reperfusion-induced changes in membrane fluidity characteristics of brain capillary endothelial cells and its prevention by liposomal-incorporated superoxide dismutase. *Biochim. Biophys. Acta* **1067,** 97–102.
38. Bkaily, G., Sperelakis, N., Elishalom, Y., and Barenholz, Y. (1983) Effect of Na^+- or Ca^{2+}-filled liposomes on electrical activity of cultured heart cells. *Am. J. Physiol.* **245** (*Heart Circ. Physiol.* **14**), H756–H761.
39. Laham, A., Claperon, N., Durussel, J. J., Fattal, E., Delattre, J., Puisieux, F., Couvreur, P., and Rossignol, P. (1988) Liposomally entrapped adenosine triphosphate inproved efficiency against experimental brain ischaemia in the rat. *J. Chromatogr.* **440,** 455–458.
40. Torchilin, V. P., Khaw, B. A., Smirnov, V. N., and Haber, E. (1979) Preservation of antimyosin antibody activity after covalent coupling to liposomes. *Biochem. Biophys. Res. Commun.* **89,** 1114–1119.
41. Klibanov, A. L., Maruyama, K., Torchilin, V. P., and Huang, L. (1990) Amphipathic polyethyleneglycols effectively prolong the circulation time of liposomes. *FEBS Lett.* **268,** 235–237.
42. Mori, A., Klibanov, A. L., Torchilin, V. P., and Huang, L. (1991) Influence of the steric barrier activity of amphipathic poly(ethyleneglycol) and ganglioside GM1 on the circulation time of liposomes and on the target binding of immunoliposomes in vivo. *FEBS Lett.* **284,** 263–266.

43. Torchilin, V. P., Klibanov, A. L., Huang, L., O'Donnell, S., Nossiff, N. D., and Khaw, B. A. (1992) Targeted accumulation of polyethylene glycol-coated immunoliposomes in infarcted rabbit myocardium. *FASEB J.* **6,** 2716–2719.
44. Weissig, V., Lasch, J., Klibanov, A. L., and Torchilin, V. P. (1986) A new hydrophobic anchor for the attachment of proteins to liposomal membranes. *FEBS Lett.* **202,** 86–90.
45. Torchilin, V. P., Narula, J., Halpern, E., and Khaw, B. A. (1996) Poly(ethylene glycol)-coated anti-cardiac myosin immunoliposomes: factors influencing targeted accumulation in the infarcted myocardium. *Biochim. Biophys. Acta* **1279,** 75–83.
46. Torchilin, V. P., Narula, J., and Khaw, B. A. (1994) Delivery of pharmaceuticals by long-circulating immunoliposomes: factors influencing longevity and target accumulation. Proceedings of the 21st International Symposium on Controlled Release of Bioactive Materials, Nice, France. Controlled Release Society, pp. 222–223.
47. Gabizon, A. A. (1995) Liposome circulation time and tumor targeting: implications for cancer chemotherapy. *Adv. Drug Deliv. Rev.* **16,** 285–294.
48. Gabizon, A. A. (1992) Selective tumor localization and improved therapeutic index of anthracyclines encapsulated in long-circulating liposomes. *Cancer Res.* **52,** 891–896.
49. Reimer, K. A., Jennings, R. B., and Tatum, A. H. (1983) Pathobiology of acute myocardial ischemia: Metabolic, functional and ultrastructural studies. *Am. J. Cardiol.* **52,** 72A–82A.
50. Braunwald, E. and Kloner, R. A. (1985) Myocardial reperfusion: a double edged sword? *J. Clin. Invest.* **76,** 1713–1719.
51. Khaw, B. A., Torchilin, V. P., Vural, I., and Narula, J. (1995) Plug and seal: prevention of hypoxic cardiocyte death by sealing membrane lesions with antimyosin-liposomes. Nature Med. **1,** 1195–1198.
52. Khaw, B. A., Vural, I., Narula, J., Haider, N., and Torchilin, V. P. (1996) Preservation of cardiocyte viability by immunoliposome-cell membrane sealing at 1, 2, 3, 4 and 5 days of hypoxia. Proceedings of the 23d International Symposium on Controlled Release of Bioactive Materials, Kyoto, Japan. Controlled Release Society, pp. 617,618.
53. Khaw, B. A., Vural, I., Narula, J., and Torchilin, V. P. (1995) Targeted sealing of cell membrane lesions: model of preservations of cell viability by immunoliposome therapy. Proceedings of the 22nd International Symposium on Controlled Release of Bioactive Materials, Seattle, WA. Controlled Release Society, pp. 184–185.
54. Torchilin, V. P., Ivanov, N. N., Klibanov, A. L., Papisov, M. I., and Chebanov, S. M. (1988) On the mechanism of electron-dense liposome internalization by macrophages in vitro, in *Liposomes as Drug Carriers* (Gregoriadis, G., ed.), Wiley, Avon, UK, pp. 63–74.
55. Vural, I., Narula, J., Torchilin, V. P., and Khaw, B. A. (1995) A method for targeted intracellular delivery of drugs and genes: a novel utilization of immuno-

liposomes. Proceedings of the 22nd International Symposium on Controlled Release of Bioactive Materials, Seattle, WA. Controlled Release Society, pp. 450,451.

56. Khaw, B. A., Vural, I., Torchilin, V. P., Haider, N., and Narula, J. (1996) Expression of antimyosin sFv gene in cardiocytes: use of cytoskeleton-specific immunoliposomes for transfection. Proceedings of the 23d International Symposium on Controlled Release of Bioactive Materials, Kyoto, Japan. Controlled Release Society, pp. 135,136.
57. Sambrook, D., Fritsch, E. F., and Maniatis, T. (1989) *Molecular Cloning: A Laboratory Manual*, 2nd ed., Cold Spring Harbor Laboratory Press, Cold Spring Harbor, New York.
58. Krejcarek, G. E. and Tucker, K. L. (1977) Covalent attachment of chelating groups to macromolecules. *Biochem. Biophys. Res. Commun.* **77,** 581–585.
59. Habeeb, A. F. S. A. (1966) Determination of free amino groups in proteins by trinitrobenzene sulfonic acid. *Anal. Biochem.* **14,** 328–336.
60. Greenwood, F. C. and Hunter, W. M. (1963) The preparation of ^{131}I-labeled human growth hormone of high specific radioactivity. *Biochem. J.* **89,** 114–123.
61. Salacinski, P. R. P., McLean, C., Sykes, J. E. C., Clement-Jones, V. V., and Lowry, P. J. (1981) Iodination of proteins, glycoproteins, and peptides using a solid phase oxidizing agent, 1,3,4,6-tetrachloro-3a,6a-diphnyl glycoluril (Iodogen). *Anal. Biochem.* **117,** 136–146.
62. Khaw, B. A., Strauss, H. W., Cahill, S. L., Soule, H. R. Edgington, T., and Cooney, J. (1984) Sequential imaging of indium-111-labeled monoclonal antibody in human mammary tumors hosted in nude mice. *J. Nucl. Med.* **25,** 592–603.
63. Tandan, R., Robinson, S. H., Munzer, J. S., and Bradley, W. G. (1987) Deficient DNA repair in amyotropic lateral sclerosis. *J. Neurol.* **79,** 189–203.
64. Khaw, B. A., Strauss, H. W., Moore, R., Fallon, J. T., Yasuda, T., Gold, H. K., and Haber, E. (1987) Myocardial damage delineated with In-111 antimyosin FAb and Tc-99m pyrophosphate. *J. Nucl. Med.* **28,** 76–82.
65. Lie, J. T., Pairolero, P. C., Holley, K. E., and Titus, J. (1975) Macroscopic enzyme-mapping verification of large, homogenous, experimental myocardia infarcts of predictable size and location in dogs. *J. Thorac. Cardiovasc. Surg.* **69,** 599–605.

11

Targeting HIV-Infected Cells

Seth H. Pincus

1. Introduction

This chapter will describe methods that may be used to deliver agents to HIV-infected cells. These materials may be used for therapeutic or experimental purposes. There are several general approaches to delivering compounds to human immunodeficiency cells (HIV)-infected cells. All cells may be exposed to materials that only have an effect or become activated in HIV-infected cells. Examples include drugs that are specific for HIV-encoded enzymes, such as reverse transcriptase or protease, or genes that are expressed under the control of the HIV-LTR. Lack of specificity is a major limitation to this approach; for example, reverse transcriptase inhibitors also inhibit cellular DNA polymerases and cellular transcription factors clan initiate low-level-transcription off the HIV-LTR, even in the absence of *tat*. The alternative approach, which is the subject of this chapter, is to target the materials specifically to the infected cells. We have used monoclonal antibodies (MAbs) to deliver toxins to HIV-infected cells, but others have used this approach to deliver antiviral agents, liposomes, and even genes.

Specific delivery of agents to HIV infected cells may be accomplished in two ways: delivery via HIV-encoded structures on infected cells, whereby the HIV envelope proteins (gp160 precursor, gp120 extracellular, and gp41 transmembrane, collectively referred to as Env) are the sole virus-encoded structures found on the surface of HIV-infected cells; or delivery to cellular subsets where HIV is known to replicate. Activated T cells, bearing the interleukin-2 (IL-2) receptor, are the primary cellular sites of HIV replication.

At the present time, it is only possible to target actively infected cells, those secreting virions. Cells that are latently infected, with a transcriptionally silent provirus, cannot be distinguished from uninfected cells. Because cellular activa-

From: *Methods in Molecular Medicine, Vol. 25: Drug Targeting: Strategies, Principles, and Applications*
Edited by: G. E. Francis and C. Delgado

tion also results in the activation of the provirus, latently infected cells will not express the activation markers that distinguish the subset of T cells secreting HIV.

In the pages that follow, we will discuss how HIV-infected cells may be targeted, what has been targeted to infected cells, how one may assess the efficacy of targeting, and the experimental and therapeutic uses for this technology.

1.1. Modes of Targeting

HIV-infected cells may be targeted either by the expression of viral antigens on the cell surface or by cell-surface markers that define the subset of activated CD4+ cells to which the majority of actively infected cells belong. These molecules may be identified with antibodies antibody fragments, or by the natural ligand for the cell-surface structures, e.g., by CD4 for gp120 or by IL-2 for the IL-2 receptor. Details are described in **Subheadings 1.1.1.** and **1.1.2.**

1.1.1. HIV-Encoded Structures on Cell Surface

The expression of HIV-1 antigens on the surface of productively-infected cells has been studied intensively. The presence of Env is well established ***(1)***. Although cell-surface expression of core (Gag) proteins has been demonstrated in other retroviruses, including murine leukemia viruses ***(2,3)***, it is a matter of some controversy with regard to HIV-1. Whereas there have been some reports of both p17 and p24 expression on infected cells ***(4,5)*** and of neutralizing anti-p17 antibodies ***(6)***, most others have failed to find any evidence of cell-surface Gag. HIV-infected cells have been successfully targeted with agents that bind Env, but not with anti-Gag ***(7)***.

1.1.1.1. Targeting with MAbs

Although the HIV-envelope proteins display a high degree of variability, both gp120 and gp41 have well-conserved regions that are accessible to MAbs (reviewed in **ref. *1***). These epitopes have been the targets of anti-HIV immunotoxins ***(1,7–11)***. Although gp120 and gp41 are found on the cell surface, they are also secreted on infected cells in the form of virions. These free virions can prevent the binding of antibodies to target cells by acting as an immunological smoke screen," which may lead to the paradoxical finding that cells with the greatest amount of HIV protein on the cell surface (a consequence of a high rate of virus secretion) may be the least sensitive to immunotoxin effects ***(9)***.

Targeting directed to gp41 may be more effective than to gp120. Gp41 is an integral membrane protein, whereas soluble gp120 can be found in serum and cell supernatants. It has been shown with immunotoxins directed against well-defined structures that greater entry is obtained with epitopes more proximal to the cell surface ***(12)***. Most importantly, however, it has been shown that the

addition of soluble CD4 can enhance, by 30–100-fold, the internalization of antibodies directed against gp41 but not against gp120. This remarkable effect is a result of both increased antigen exposure and more rapid turnover of cell-surface Env ***(10)***.

1.1.1.2. Targeting with CD4

CD4 is the receptor by which HIV binds to and infects cells. There is a high affinity interaction between CD4 and gp120, and the CD4-binding site is well conserved on all infectious isolates of HIV-1 and HIV-2. Soluble CD4 molecules have been constructed and bind to virion-associated and cell-surface Env with varying affinities, highest for laboratory strains of HIV and somewhat lower for primary clinical isolates ***(13–16)***. In vitro studies show that soluble CD4 molecules effectively neutralize HIV infectivity. CD4 has also been used to target immunotoxins to HIV-infected cells ***(17–27)***. These immunotoxins function extremely well in vitro, killing different cell types infected with a variety of HIV isolates and working in synergy with reverse transcriptase inhibitors so that HIV has been eliminated from tissue culture. The clinical effects of both soluble CD4 and CD4-based immunotoxins when tested in acquired immune deficiency syndrome (AIDS) patients has been disappointing ***(17,28)***. However new forms of soluble CD4 that utilize multivalent attachments have shown greater in vitro efficacy against clinical isolates of HIV and are now undergoing testing in patients ***(29)***.

1.1.1.3. Targeting with Coreceptors

It has recently been discovered that HIV requires a coreceptor to infect cells, and that chemokine receptors serve this function ***(30–33)***. HIV that are tropic for T cells utilize the receptor CXCR4. These that grow in macrophages and are usually the form transmitted from person to person utilize the receptor CCR5. People with mutations in the CCR5 receptor have been found to be resistant to HIV infection, despite repeated exposures ***(34)***. These chemokine receptors belong to the seven-transmembrane G protein-coupled family. Although the chemokines that bind these receptors block HIV infection, neither the actual sites on the receptors bound by HIV nor the mechanism of HIV binding have been fully defined, although it appears that the interaction is with gp120. It may be possible that these coreceptors or derivatives of them can be used to target agents to HIV-infected cells, either alone or in combination with soluble CD4.

1.1.2. Targeting Cell Populations Containing the Pool of HIV-Infected Cells

An alternative to using virus structures to target HIV-infected cells is to use cell-surface markers that define subsets of cells containing those cells in which

HIV replicates. Because this approach may target many cells that are not HIV-infected, it is best used when the agent to be delivered is virus specific.

1.1.2.1. Targeting to IL-2 Receptor

Using immunotoxins it has been shown that the majority, if not all, of HIV replication in peripheral blood mononuclear cells takes place within the subset of activated CD4+ lymphocytes ***(35,36)***. Although this has not been shown to be the case in AIDS patients, it seems likely that a significant amount of HIV replication takes place within this cellular subset. Activated T cells express the IL-2 receptor, and this structure may be targeted with IL-2 or with MAbs to one of the receptor chains (CD25) ***(35–40)***. A fusion toxin consisting of a chimeric IL-2-diphtheria toxin molecule is currently in a clinical trial for the treatment of AIDS ***(40)***. The concurrent use of anti-IL-2 immunotoxins and immunosuppressive drugs that prevent T-cell activation, such as cyclosporine, enhances the anti-HIV activity of IL-2-targeted immunotoxins ***(35,37–39)***. Although there have been concerns that eliminating activated T cells in patients who are already immunodeficient may worsen the disease, this has not been proven in clinical trial. Whether the immunotoxin will be effective in lowering viral replication remains to be determined.

1.1.2.2. Other Cell-Surface Markers

HIV may infect CD4+ T cells as well as macrophages. These cells express a number of markers that have been used to target antiviral agents either in the form of immunoconjugates or drug-containing liposomes. Cell-surface structures that have been used include CD3, CD4, CD14, CD38, and Fc receptors ***(41–44)***. Because the cellular expression of these markers is broad and includes many cells that would not be infected with HIV, antiviral rather than cytotoxic agents have been delivered to the cells, including pokeweed antiviral protein, anti-sense RNA, and reverse transcriptase inhibitors.

1.2. Materials That May Be Targeted

The agents that affect HIV production by infected cells may be considered in several classes. In the first group are materials that alter cellular functions and inhibit the production of HIV as a secondary effect. Included in this group are toxins and cytotoxic drugs, which kill the cells producing HIV. The second group are HIV-specific drugs, which have little or no effect on the normal cellular functions. Examples are drugs that act by inhibiting HIV-encoded enzymes, such as reverse transcriptase or protease, or HIV-specific gene therapies. There may be a third group of drugs that may inhibit HIV production by targeting very specific cellular processes important in HIV secretion, but that do not cause significant alterations or damage to normal cellular functioning. Cyclosporine may have such properties.

Most drugs do not require any specific targeting; the specificity of action determines the functions affected by the drug. As the nonspecific effects of a pharmaceutical agent increase, so does the need for targeting that agent to a particular cell. The most obvious examples of this are the toxins used in immunotoxins, which would kill any cell without specific targeting. Most HIV antivirals are reasonably specific, although each has a number of unwanted toxicities. Another reason for targeting an agent may be to avoid problems associated with rapid degradation or elimination. For example, antisense oligonucleotides have very short in vivo residence times and therapeutic concentrations have been difficult to obtain. Packaging these into liposomes targeted with MAbs has been shown to be an effective method of delivering these materials ***(41,44)***.

In the following sections we will briefly describe the materials that have been targeted to HIV-infected cells and shown to have an effect on virus production.

1.2.1. Toxins

Immunotoxins have been targeted to HIV antigens with CD4 ***(17–27)*** and MAbs to both gp120 and gp41 ***(1,7–11,45–49)***, and to the IL-2 receptor ***(35–40)***. The goal is to eliminate cells that are actively secreting HIV and halt the spread of infection to uninfected cells. Among the toxins that have been used are ricin A chain and truncated forms of pseudomonas exotoxin A and diphtheria toxin. In each case the toxins have been modified to remove the cell-binding domain of the native toxin and replace it with the targeting agent. One of the immunotoxins directed against HIV, a chimeric CD4-pseudomonas exotoxin, has undergone a clinical trial. No anti-HIV effect was seen ***(17,28)***. However, this compound was found to be extremely toxic (even for an immunotoxin), have a short serum half-life, and was probably targeted to the wrong portion of Env: gp120 rather than gp41. An IL-2-diphtheria toxin fusion is also undergoing clinical trials.

1.2.2. Antivirals

Both in vitro and clinical studies have shown that antivirals, encapsulated within liposomes, may be delivered to specific cells using MAbs. Whether there is a benefit to this procedure, in terms of decreased nonspecific toxicity or increased therapeutic efficacy, has not been shown. As more effective AIDS antivirals are developed and successfully used in combinations, the rationale for specific targeting of these agents diminishes. However, it is possible that a highly effective antiviral may be developed that is found to have such high nonspecific toxicity that targeting may be necessary.

1.2.3. Nucleic Acids

A number of "gene therapy" approaches have been applied to HIV infection. These include antisense ***(41,50)***, ribozyme ***(50)***, intracellular expression

of antibodies that bind to HIV proteins ***(51,52)***, suicide genes that are activated at the same time as HIV ***(53)***, and the production of specific inhibitors of HIV-gene expression. Although all of these approaches have specificity for HIV, targeting may still be useful to increase the efficiency of gene expression in the appropriate cells or to minimize degradation and elimination of the administered nucleic acids. Thus, liposomes targeted by MAbs have been used to deliver antisense oligonucleotides and suicide genes ***(41,53)***. A novel approach to targeting gene therapies involves the use of viral gene transfer vectors that not only encode the gene that will be expressed, but also contain a chimeric envelope protein fused to an antibody fragment that directs the virus to the desired target cell ***(54)***.

1.2.4. Viruses

Viruses may be constructed that express the HIV-receptor CD4 and coreceptor on the viral surface, either as part of the virus itself, or as the result of viral pseudotyping ***(55,56)***. These molecules then define the target-cell specificity of the virions, and they bind to and infect target cells expressing the HIV envelope on the cell surface (i.e., HIV-infected cells). If the virus itself is cytopathic, then it may kill the target cell ***(55)***. Alternatively, these viruses may be used to package nucleic acids for gene therapy, toxins, or other anti-HIV materials.

2. Materials

2.1. Targeted Agents

The agents used to target HIV-infected cells are extremely diverse, but all share two functions. The first is a method to deliver the agent to the infected cells. This may consist of an antibody or some other molecule capable of recognizing cell-surface structures that identify HIV-infected cells. The second function allows the targeted agent to cause some effect, e.g., kill the cell, label the cell, or inhibit virus production. Because of the diversity of materials that may accomplish these functions, it is not feasible to discuss details of their construction. The reader is referred to the literature cited in the discussion in **Subheading 1.**

2.2. Cellular Targets

In this section we will discuss the in vitro methodology that can be used to determine whether one is effectively targeting HIV-infected cells. Translation of this information to therapeutic applications may be problematic, since relevant animal models of HIV infection are limited.

Any discussion of the evaluation of HIV function must include mention of two facets: laboratory adaptation of HIV and cellular tropism. It has been found

that laboratory-adapted HIV differ from primary clinical isolates in important ways, including susceptibility to neutralization with antibodies and CD4 ***(13,57,58)***. Laboratory-adapted HIVs are easier to work with because they may be propagated within tissue culture cell lines, whereas clinical isolates may only be passaged a limited number of times within cultures of peripheral blood mononuclear cells activated with a mitogen (e.g., PHA) and/or IL-2 before losing their nonadapted characteristics. Initial targeting studies may be performed with laboratory-adapted viruses and persistently infected cell lines, but the relevance of the findings will not be accepted by most investigators until the studies are replicated with clinical isolates in PHA-blast cultures.

The molecular basis of HIV tropism has recently been discovered. The two major classes of cells that HIV may infect are macrophages and T cells. Generally, the virus will grow in one or the other of these cell types, although occasional dual-tropic HIVs have been identified. In most cases, the form of HIV that is transmitted from person to person is macrophage-tropic. As the disease develops there is a switch to the T-cell-tropic form, which eventually results in depletion of CD4+ T cells and immunodeficiency. The structure of gp120, particularly within the immunodominant V3 loop, is a major determinant of cellular tropism. Both forms of HIV utilize CD4 as the primary receptor, but utilize different coreceptors, as described in **Subheading 1.1.3.** Because these different isolates of HIV infect different cell types, the modes of targeting and the effects on the targeted cells may be very different.

HIV may be grown in a variety of cells, ranging from well established cell lines to primary lymphocyte and macrophage cultures;. As noted above, the characteristics of the virus will vary depending on how it is cultured. In addition, the biology of the cells will greatly influence the efficacy of the targeting agent as well as that of the targeted moiety.

2.2.1. Cell Lines

HIV can be cultivated in CD4+ T-cell lines and in cells that have been transfected with the appropriate receptors and coreceptors. To date, no macrophage-derived cell line has proven suitable for culturing HIV. Some neuronal cell lines and intestinal epithelial cells have also been reported to support transient infection with HIV ***(59,60)***. Infection of cell lines may either be acute or persistent. Acute infection usually results in a high degree of cytopathic effect, with the majority of cells dying during the first week or two of infection. Subsequently, the outgrowth of cells resistant to the cytopathic effect occurs. This may result from either a cellular or a viral adaptation. These persistently infected cells may either continue to express high levels of HIV infection for long periods of time, or more commonly will “burn out,” with the majority of cells ceasing to secrete HIV and needing periodic replenishment with

uninfected cells. Although cell lines may be infected with either laboratory-adapted or primary HIV isolates, once these strains of HIV grow well within cell lines, they have taken the characteristics of laboratory-adapted viruses ***(58)***.

The major advantage of working with HIV-infected cell lines is that it is possible to work with populations in which the large majority, if not all, of the cells are productively infected with HIV. In this regard, we have found H9/NL4-3, a cell line we established many years ago ***(61)***, to be an optimal target cell ***(7,9,10)***. H9/NL4-3 was produced by infecting the human CD4+ lymphoma cell line H9 with the molecularly cloned HIV NL4-3. Through many years of repetitive culture H9/NL4-3 has remained virtually 100% infected, with all cells expressing high levels of HIV antigens on the cell surface, secreting infectious HIV, and susceptible to killing with anti-HIV immunotoxins. We have found that immunotoxin-resistant variant cells arise at a frequency of $<10^{-4}$ ***(62,63)***. This cell line does not require replenishment with uninfected cells. The advantage of working with a cell line in which all cells are productively infected is that one can assay effects on cell viability, protein synthesis, or cell division rather than examining HIV production, a more difficult and tedious process (*see* **Subheading 3.2.**).

2.2.2. Primary Cell Cultures

It is generally agreed among workers in the field that the in vitro assay with the greatest relevance to the disease state is the use of clinical isolates of HIV cultured in primary cell cultures, usually PHA blasts. Clinical isolates retain their unique characteristics when cultured in primary cell cultures. PHA-blast cultures support the growth of both T cell and macrophage-tropic HIV.

Cultures of PHA blasts are initiated by purifying peripheral blood mononuclear cells, usually by Hypaque-Ficoll density gradient centrifugation. These cells are then incubated with 10 µg/mL of the plant lectin phytohemagglutinin (PHA), which activates T cells. After 48 h, the medium is removed and fresh medium, supplemented with IL-2, is added. The cells are replenished with fresh medium and IL-2 every 3 d. These cells may be infected with either cell-free virus or with HIV-infected cells. Peak infection usually occurs anywhere from 7–28 d postinfection, depending on the size of the inoculum and the characteristics of the virus. In general, at the peak of infection, <5% of the cells in the culture are actually infected. However if extreme care is taken and the T-cell blasts are separated from nonactivated cells, it is possible to obtain infection in the majority of the cells in the culture ***(58)***.

Experiments have also been performed with primary macrophage and dendritic cell cultures ***(64)***. However, these have only been performed when it is necessary to show that the virus will only grow in macrophages and not in T cells. Since macrophage-tropic HIVs grow well in PHA blasts, and culturing

PHA blasts is considerably easier than culturing primary macrophages, there is little need for primary macrophage cultures when testing the delivery of agents to macrophage-tropic HIV. Experiments have also show that HIVs grow in primary bone marrow and brain astrocyte cultures, but because of the difficulty in obtaining such material this is rarely performed.

3. Methods

The method used to detect the effect of an agent delivered to HIV-infected cells depends on the cells used, the degree of infection, and the type of agent delivered. The assays range from measures of cellular cytotoxicity which may be used when the large majority of cells are HIV infected, to indirect assays indicating the spread of viral infection within a tissue culture (such as the presence of viral proteins or RNA), to direct measure of the production of infectious virus.

3.1. Cytotoxicity

Cell killing may be assayed when the agent delivered to the HIV-infected cell is a toxic material, such as a toxin or antimetabolite. We have measured cytotoxic effects when testing anti-HIV immunotoxins on H9/NL4-3 cells ***(7,9,10)***. When cytotoxicity was compared to a direct measure of the production of infectious virus in these cells, the same IC_{50} of immunotoxin was obtained ***(45)***. This indicates that cell killing does not result in the release of infectious virus, which is consistent with our understanding of the mechanism of retrovirus budding. Cytotoxicity may be assayed by measuring protein synthesis (incorporation of ^{35}S-methionine into cellular proteins), DNA or RNA synthesis (incorporation of ^{3}H-thymidine or uridine), or MTT dye reduction. These assays are considerably easier than measuring the production of virus (**Subheading 2.**). With anti-HIV immunotoxins, the cytotoxic effect may be seen within 30 min of the administration of immunotoxin ***(45)***. In primary cell cultures or during acute infection of cell lines, cytotoxicity is not an indicator of antiviral effect. Only a small fraction of cells may be infected and acute infection itself results in a high degree of cellular cytotoxicity. **Figure 1** shows the cytotoxic effect of two different anti-HIV immunotoxins on uninfected and persistently infected cells.

The incorporation of ^{35}S-methionine into cellular proteins is a straightforward method to measure cellular protein synthesis and, consequently, viability. We perform the assay by culturing 3×10^4 H9/NL4-3 cells per well of 96-well flat-bottom culture plates in a total volume of 20 µL. Immunotoxin is added to the desired concentration. Depending on the immunotoxin, IC_{50}s range from 1 to <0.03 µg/mL. The cells and immunotoxin are cultured in a humidified 37°C incubator for 48 h, and then the wells pulsed with 0.5 µCi

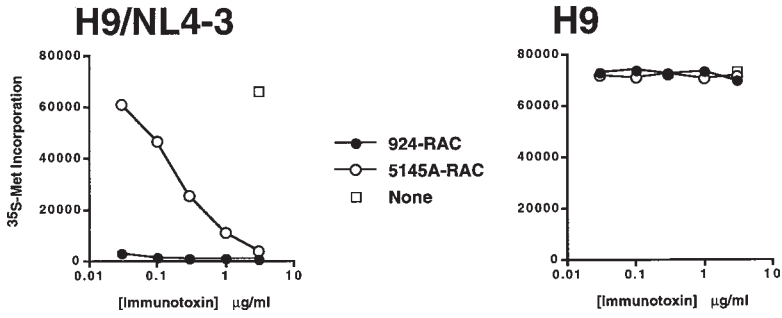

Fig. 1. Cytotoxic effects of anti-HIV immunotoxins on HIV-infected and uninfected cells. Persistently infected H9/NL4-3 cells and the uninfected parental H9 cells were incubated in the presence of varying concentrations of immunotoxin. Two different immunotoxins were used, each consisting of an anti-gp120 MAb conjugated to ricin A chain. Antibody 924 is directed against the immunodominant V3 loop, whereas 5145A blocks gp120-CD4 binding. Cells and immunotoxins were incubated for 48 h and then pulsed with ^{35}S-methionine for the final 20 h of culture. Cytotoxicity was measured as the failure to incorporate ^{35}S-methionine into cellular proteins. 924-RAC is considerably more active as an immunotoxin than 5145A-RAC, perhaps indicating that the V3 loop is closer to the cell membrane than the CD4-binding site (*see* **Subheading 4.1.3.**).

of ^{35}S-methionine. After an additional 24 h of culture, the wells are harvested onto membrane filters and washed with 95% ethanol to decontaminate any viable HIV. ^{35}S-methionine incorporation is quantified using liquid scintillation counting.

3.2. Inhibition of Virus Production

The best measure of the efficacy of an antiviral agent targeted to an HIV-infected cell is to assay virus production. This may be done either by measuring parts of the virus, e.g., antigens or RNA, or by measuring the production of infectious virus. Because all components of the virion must be functioning to produce an infectious virus, the latter assays are best, but often the most difficult to perform. Infectivity assays are preferred because it is possible that an antiviral agent will inhibit one function of the virus, rendering it noninfectious, but other functions, such as the production of a particular antigen, may be unhindered. In addition, infectivity assays measure the function of greatest relevance to antiviral therapy, i.e., the ability to produce virus that can infect other cells.

Virus production may be measured in either a stable or a kinetic situation. An example of the former would be the use of persistently infected cell lines, such as H9/NL4-3, in which virus production by the cells is in a steady state. A

kinetic situation is one in which the spread of virus infection through a tissue culture is measured as a function of time. The advantage of measuring spread of infection is that it provides information regarding the production of infectious virus, even if one is only monitoring the production of viral products. However, persistently infected cell lines may be more amenable to mechanistic studies to determine how an agent is actually causing an effect.

3.2.1. Measurement of Virus Products

The two HIV products most commonly assayed are reverse transcriptase and the Gag protein, p24. Reverse transcriptase is assayed via a functional assay in which a template, primer, and radiolabeled nucleotides are provided ***(65)***. The synthesis of radiolabeled DNA is then measured. p24 is detected via an antigen capture assay. A number of commercial kits are available for this purpose. The sensitivity of the assay is on the order of 5–10 pg/mL of p24, whereas the production of p24 in infected cultures is often measured in ng/mL. Although the use of the kits is easy, sensitive, and quantitative, their cost (approx $5/sample) may be a limiting factor. Reagents and instructions for constructing an antigen capture enzyme-linked immunosorbent assay (ELISA) are available through the National Institutes of Health (NIH) AIDS Research and Reference Reagent Program (685 Lofstrand Lane, Rockville, MD 20850, telephone [301] 340-0245). The sensitivity of this assay is somewhat less (50 pg/mL), but usually well within the range of utility for analyzing in vitro cultures. As noted above, an important drawback to measuring either reverse transcriptase or p24 is that these products may be made at normal levels in the presence of an agent that interferes with some other aspect of HIV function, causing false conclusions regarding the antiviral efficacy of that agent. This may be avoided if reverse transcriptase or p24 is monitored in a kinetic situation, because infectious virus needs to be produced to get spread of infection, and an increase in these products, with time.

3.2.2. Nucleic Acid Quantitation

The polymerase chain reaction (PCR), branched-DNA analyses, and related techniques are highly sensitive methods to quantify both viral RNA and proviral DNA. Proviral DNA is a measure of the number of cells infected, whereas viral RNA reflects production of virions. As with the measurement of viral products, one cannot easily determine whether the nucleic acids measured represent infectious viruses. A number of commercially available technologies, exist for the measurement of HIV nucleic acids, since this methodology is now the standard of care for AIDS patients. Laboratories performing their own quantitative analyses have generally used a modification of the quantitative competitive (QC)-PCR ***(66)***.

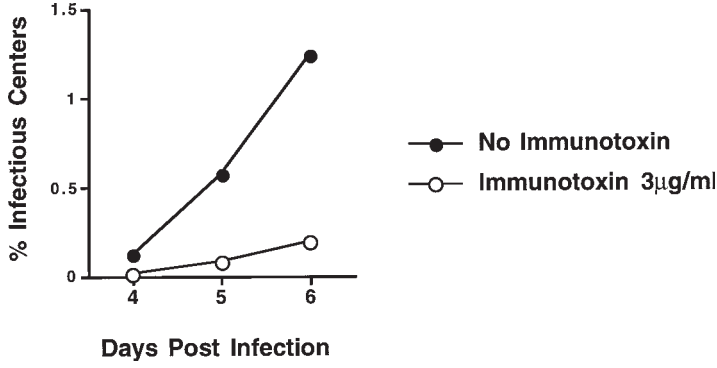

Fig. 2. Inhibition of spread of infection by immunotoxins. A kinetic analysis of the effect of an anti-gp120 immunotoxin is shown. PHA blast cells were infected with a primary clinical isolate of HIV in the presence or absence of immunotoxin. Beginning 4 d after infection, an aliquot of cells was taken and plated onto a monolayer of H1-J cells. The cells were washed off the monolayer 1 d later and 2 d later the cells were stained for HIV foci. The percent of cells secreting infectious HIV was determined by dividing the number of foci by the number of input cells. Note both the small proportion of cells that were infected and the increase in infectious centers with time postinfection.

3.2.3. Focal Infectivity Assay

The focal infectivity assay (FIA) is a highly sensitive method to detect and quantify infectious HIV, rather than viral proteins or nucleic acids. This is an advantage because it is possible that an antiviral agent will inhibit one function of the virus, rendering it noninfectious, but other functions, such as the production of RT or viral RNA, may be unhindered. In addition, infectivity assays measure the function of greatest relevance to antiviral therapy, i.e., the ability to produce virus that can infect other cells. Thus, the effect of the drug on the production of infectious virus (the critical parameter) can be studied directly. **Figure 2** shows the effects of an immunotoxin on the spread of infection in PHA blast cultures infected with a primary clinical isolate of HIV.

Cell-free virus or infected cells (infectious centers, ICs) can be measured at frequencies as low as 10^{-6}. The sensitivity of the FIA rivals that of PCR, where examining the input from 10^6 cells is an upper limit. The FIA detects all strains of HIV, including primary isolates from patients ***(9,57,61,64,67–69)***. ICs may be detected in tissue culture cell lines and PHA blast cultures infected in vitro. The assay has also been used to quantify infectious HIV in AIDS patients ***(69)***. The assay is performed by plating either infected cells or cell-free virus on a monolayer of HeLa cells expressing CD4, CXCR4, and CCR5. Detection of clinical isolates is highly dependent on the HeLa-CD4 cell line used and is a

function of the degree of CD4 expression ***(57)***. We use a cell line, designated H1-J.C53, which has a high level of CD4 expression. Serial dilutions of the infectious inoculum are plated on the monolayer for several hours, then washed off, and the monolayer cultured for 3 d. After the culture period, the cells are fixed and immunoperoxidase stained with anti-HIV antisera. Viral foci are detected both by the immunoperoxidase staining as well as the characteristic syncytia that form. The number of foci reflect the number of infectious events. The FIA has been used to study the effects of different anti-HIV therapeutics. We showed that α-interferon and AZT work by different mechanisms in acute and persistent infection ***(61)***. We have used the assay in a number of different forms to study the in vitro effects of anti-HIV immunotoxins ***(7,9,10)*** and to measure antibody-mediated neutralization following infection or immunization ***(70–72)***.

The FIA may be performed in 24-, 48-, or 96-well formats. In 48-well plates, we culture 3.5×10^4 H1-J.C53 cells in 0.5 mL RPMI-1640 medium containing 10% fetal calf serum (FCS). The cells are infected the next day. If we will be using cell-free virus, the wells are washed with serum-free medium and then incubated for 15 min with serum-free medium containing 8 µg/mL of DEAE-dextran. The DEAE-dextran is washed off following the incubation and serial dilutions of input virus in serum-free medium are plated onto the monolayer cells. The virus is incubated with the cells for 3 h, washed out, and the cells cultured for 3 d in medium containing 10% FCS. To infect the monolayer with HIV-infected cells, it is not necessary to pretreat the monolayer with DEAE-dextran. Graded numbers of HIV-infected cells are plated onto 24-h-old monolayers and incubated. One day later, the input cells are washed off the monolayer and the monolayer cultured for an additional 2 d. Three days following the infection of the monolayer, the cells are fixed with 95% ethanol for 15–30 min and then stored in phosphate-buffered saline (PBS), 1% bovine serum albumin, and 0.01% sodium azide until they are ready to be stained. It is crucial that the monolayer not be allowed to dry out during the staining process. The cells are first incubated with an anti-HIV antibody. We use human HIV immune globulin (available from the AIDS research and Reference Reagent Program) at a 1:3000 dilution. Following this step, the monolayer cells are washed three times in PBS and incubated with horseradish peroxidase-conjugated antihuman Ig. The peroxidase substrate aminoethyl-carbazol is used to detect antibody binding. HIV foci can be identified by their characteristic multinucleated appearance and the red immunoperoxidase staining.

4. Discussion

The ability to target HIV-infected cells has both experimental and therapeutic utility. We originally produced anti-HIV immunotoxins as potential thera-

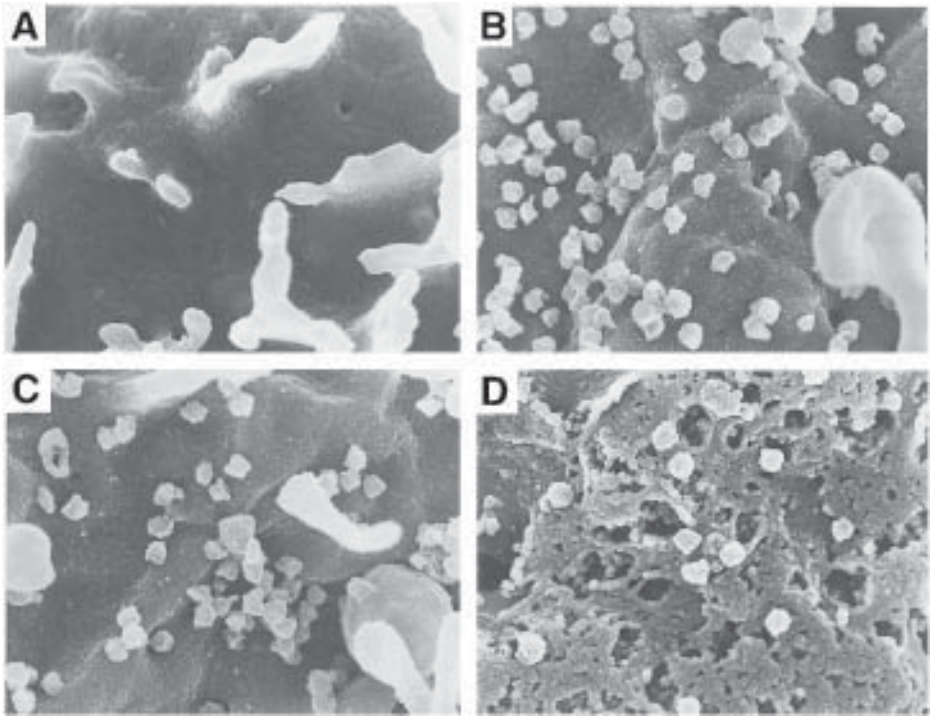

Fig. 3. Effect of immunotoxin treatment on cell morphology. Scanning electron micrographs (80,000×) were made of uninfected H9 cells **(A)**, persistently infected H9/NL4-3 cells **(B)**, H9/NL4-3 cells following treatment with antibody **(C)**, and H9/NL4-3 following immunotoxin treatment **(D)**. Budding virions are plainly evident on H9/NL4-3 cells. Antibody has no effect on the cells; immunotoxin results in massive disruption of the cell membrane. Interestingly, remains of budding virions can be seen following immunotoxin treatment, but these are no longer infectious. From **ref. *7***, courtesy of Mary Ann Liebert Publishers.

pies for AIDS, but have also found them to be useful tools to study the cell biology of HIV infection. **Figure 3** shows the morphological effects of an anti-HIV immunotoxin on HIV-infected cells.

4.1. Experimental Uses

Immunotoxins must be internalized before they can function to kill a cell ***(1)***. We have targeted immunotoxins to the HIV-envelope proteins because they are the only virus-encoded structures on the surface of productively infected cells. Most virologists consider that retroviral-envelope proteins found on the cell surface are in the process of leaving the cell via viral budding.

However, the efficacy of immunotoxins targeted to these proteins indicates that at least a portion of the cell-surface envelope protein is reinternalized. This is not a function of crosslinking, since even monomeric CD4-based immunotoxins are effective. Our studies with anti-HIV immunotoxins not only demonstrate that there is a recirculating pool of envelope protein, but that the rates of internalization are subject to regulatory influences.

4.1.1. Measurement of Env Internalization

The efficacy of anti-HIV immunotoxins demonstrates that HIV-envelope proteins are internalized from the cell surface. We have demonstrated that soluble CD4, the ligand for gp120, can markedly enhance the efficacy of anti-gp41, but not anti-gp120 immunotoxins ***(10)***. This is the result of two different mechanisms. The first is "CD4-stripping" ***(73)***, whereby the binding of gp120 to CD4 causes a disruption of the noncovalent association between gp120 and gp41, resulting in enhanced exposure of gp41 epitopes on the cell surface and a decrease in cell-surface gp120. The second effect, which occurs equally for both gp120 and gp41, is that there are increased rates of internalization of the envelope proteins when CD4 is present ***(10)***. Thus, cell-surface envelope behaves as a cellular receptor, showing enhanced rates of internalization in the presence of its ligand. Since the soluble CD4 used in these experiments was monomeric, the enhanced internalization was not a result of crosslinking. This behavior indicates that the internalization of cell-surface envelope is not simply an accidental process resulting from the mechanics of retroviral budding, but that it is an integral part of the cell's biology and is subject to regulatory influences.

4.1.2. Immunotoxin-Resistant Variants

We have used immunotoxins to select for variant cells in persistently infected cell lines. These studies have been informative regarding HIV variation as well as the processing of the HIV-envelope proteins (***62,63,65)***. We found that variants arose at a very low frequency ($<10^{-4}$) in the cell line we were studying. Variants fell into two classes, one in which the expression of all HIV proteins was downregulated and the other that was the result of altered envelope processing. Surprisingly, none of the variants were the result of a mutation within the epitope recognized by the targeting moiety, even though at least one of the immunotoxins used was directed against a hypervariable region of gp120. Among the variants with altered envelope processing, we described one with a mutation causing a truncation in gp41. This not only caused the production of noninfectious HIV (with normal levels of viral proteins and nucleic acids) but also altered the entire secretory pathway, resulting in the collection of virions within intracellular vesicles rather than budding from the

cell surface ***(65)***. Another variant failed to cleave the precursor gp160 into gp120 and gp41. Studies showed that this mutation was not the result of a mutation within the virus, but rather an alteration of the cell ***(63)***. These studies demonstrate the utility of an undirected approach to studying HIV-envelope processing. Rather than induce specific mutations and then study the cell that results, we chose to let nature perform the mutagenesis and then applied a powerful selection. In each case, the results were unanticipated and contributed to our knowledge of the cell biology of HIV infection.

4.1.3. Cell-Surface Topology of HIV Protein

The three-dimensional structure of the HIV-envelope protein has recently been demonstrated ***(74–76)***. Some of our studies with immunotoxins directed against different epitopes on gp120 and gp41 allow us to draw some inferences about the location of these epitopes relative to the cell surface. We have found that some immunotoxins bind well to infected cells, but that they function poorly as immunotoxins ***(9)***. This paradoxical finding may be explained in the context of other studies with immunotoxins directed against well-defined structures of cell-surface immunoglobulin ***(12)***. These studies found that the toxicity of the immunotoxins was a function of the proximity of the epitope to the cell surface. Consistent with this result, we have found that anti-gp41 immunotoxins are generally more efficacious than anti-gp120 ***(7)***. Within the group of anti-gp120 immunotoxins tested, there was a wide range of variability in efficacy. These differences may indicate that the epitopes that are less effective targets may be more distant from the cell surface than the others.

4.2. Therapeutic Applications

The therapeutic utility of anti-HIV immunotoxins remains an open question ***(46)***. Their anti-HIV effect would result from elimination of cells that are actively secreting infectious HIV. In vitro, these agents have been found to be the most effective anti-HIV agents tested, with a therapeutic index of $>10^4$ ***(10)***. Yet a clinical trial with CD4-PE40, a chimeric protein consisting of CD4 fused to the toxic and translocation domains of pseudomonas exotoxin A, resulted in no demonstration of clinical efficacy ***(17,28)***. In many ways, CD4-PE40 was a flawed immunotoxin. It is 10–30-fold more nonspecifically toxic than ricin-based immunotoxins, it has a very short plasma residence time compared to antibody immunotoxins, and it is not subject to the remarkable enhancement of activity seen with anti-gp41 immunotoxins in the presence of soluble CD4 ***(46)***. Thus, the failure of CD4-PE40 may say more about the shortcomings of this particular immunotoxin than about the potential therapeutic efficacy of anti-HIV immunotoxins. Unfortunately, these results have markedly diminished the enthusiasm for the development and clinical testing of

other anti-HIV immunotoxins. We are currently studying the in vivo efficacy of immunotoxins made with anti-gp41 MAbs conjugated to deglycosylated ricin A chain. These immunotoxins are being studied in SCID mice injected with HIV-infected human cells. The efficacy of anti-gp41 immunotoxins, with and without soluble CD4, is being compared to that of CD4. If we can convincingly demonstrate that anti-gp41 + CD4 is more efficacious than CD4-PE40 in vivo, then we may have an opportunity to test these immunotoxins against AIDS.

References

1. Pincus, S. H. and Tolstikov, V. V. (1995) Anti-human immunodeficiency virus immunoconjugates. *Adv. Pharmacol.* **32,** 205–242.
2. Tung, J. S., Yoshiki, T., and Fleissner, E. (1976) A core polyprotein of murine leukemia virus on the surface of mouse leukemia cells. *Cell* **9,** 573–578.
3. Pincus, S. H., Cole, R., Ireland, R., MacAtee, F., Fujisawa, R., and Portis, J. (1995) Protective efficacy of non-neutralizing monoclonal antibodies in acute infection with murine leukemia virus. *J. Virol.* **69,** 7152–7158.
4. Shang, F., Huang, H., Revesz, K., Chen, H.-C., Herz, R., and Pinter, A. (1991) Characterization of monoclonal antibodies against the human immunodeficiency virus matrix protein p17: identification of epitopes exposed at the surfaces of infected cells. *J. Virol.* **65,** 4798–4804.
5. Laurent, A. G., Krust, B., Rey, M.-A., Montagnier, L., and Hovanessian, A. G. (1989) *Cell* surface expression of several species of human immunodeficiency virus type 1 major core protein. *J. Virol.* **63,** 4074–4078.
6. Papsidero, L. D., Sheu, M., and Ruscetti, F. W. (1989) HIV-1 neutralizing monoclonal antibodies that react with the p17 core protein: characterization and epitope mapping. *J. Virol.* **63,** 267–272.
7. Pincus, S. H., Wehrly, K., Cole, R., Fang, H., Lewis, G. K., McClure, J., Conley, A. J., Wahren, B., Posner, M. R., Notkins, A. L., Tilley, S. A., Pinter, A., Eiden, L., Teintze, M., Dorward, D., and Tolstikov, V. V. (1996) In vitro effects of anti-HIV immunotoxins directed against multiple epitopes on the HIV-1 envelope glycoprotein gp160. AIDS *Res. Hum. Retrovirus* **12,** 1041–1051.
8. Till, M. A., Zolla-Pazner, S., Gorny, M. K., Patton, J. S., Uhr, J. W., and Vitetta, E. S. (1989) Human immunodeficiency virus-infected T cells and rnonocytes are killed by monoclonal human anti-gp41 antibodies coupled to ricin A chain. *Proc. Natl. Acad. Sci. USA* **86,** 1987–1991.
9. Pincus, S. H., Cole, R. L., Hersh, E. M., Lake, D., Masulho, Y., Durda, P. J., and McClure, J. (1991) In vitro efficacy of anti-HIV immunotoxins targeted by various antibodies to the envelope protein. *J. Immunol.* **146,** 4315–4324.
10. Pincus, S. H. and McClure, J. (1993) Soluble CD4 enhances the efficacy of immunotoxins directed against gp41 of the human immunodeficiency virus. *Proc. Natl. Acad. Sci. USA* **90,** 332–336.
11. Kim, Y.-W., Fung, M. S. C., Sun, N.-C., Sun, C. R. Y., Chang, N. T., and Chang, T. W. (1990) Immunoconjugates that neutralize HIV virions kill T cells inferted with diverse strains of HIV-1. *J. Immunol.* **144,** 1257–1262.

12. May, R. D., Finkelman, F. D., Wheeler, H. T., Uhr, J. W., and Vitetta, E. S. (1990) Evaluation of ricin A chain-containing immunotoxins directed against different epitopes on the delta-chain of cell surface-associated igD on murine B cells. *J. Immunol.* **144,** 3637–3642.
13. Moore, J. P., McKeating, J. A., Huang, Y., Ashkenazi, A., and Ho, D. D. (1992) Virions of primary human immunodeficiency virus type 1 isolates resistant to soluble CD4 (sCD4) neutralization differ in sCD4 binding and glycoprotein gp120 retention from sCD4-sensitive isolates. *J. Virol.* **66,** 235–243.
14. Clapham, P. R., Weber, J. N., Whitby, D., Mcintosh, K., Dalgleish, A. G., Maddon, P. J., Deen, K. C., Sweet, R. W., and Weiss, R. A. (1989) Soluble CD4 blocks the infectivity of diverse strains of HIV and SIV for T cells and monocytes but not for brarin and muscle cells. *Nature* **337,** 368–370.
15. Capon, D. J., Chamow, S. M., Mordenti, J., Marsters, S. A., Gregory, T., Mitsuya, H., Byrn, R. A., Lucas, C., Wurm, F. M., Groopman, J. E., Broder, S., and Smith, D. H. (1989) Designing CD4 immunoadhesins for AIDS therapy. *Nature* **337,** 525–531.
16. Traunecker, A., Schneider, J., Kieler, H., and Karjalainen, K. (1989) Highly efficient neutralization of HIV with recombinant CD4-immunoglobulin molecules. *Nature* **339,** 68–70.
17. Davey, R. T., Boenning, C. M., Herpin, B. R., Batts, D. H., Metcalf, J. A., Wathen, L., Cox, S. R., Polis, M. A., Kovacs, J. A., Falloon, J., Walker, R. E., Salzrnan, N., Masur, H., and Lane, H. C. (1994) Recombinant soluble CD4-pseudomonas exotoxin, a novel immunotoxin, in the treatment of individuals infected with HIV. *J. Infect. Dis.* **170,** 1180–1188.
18. Ashorn, P., Englund, G., Martin, M. A., Moss, B., and Berger, E. A. (1991) Anti-HIV activity of CD4-*Pseudomonas* exotoxin on infected primary human lymphocytes and monocyte/macrophages. *J. Infect. Dis.* **163,** 703–709.
19. Ashorn, P., Moss, B., and Berger, E. A. (1992) Activity of CD4-*Pseudomonas* exotoxin against cells expressing diverse forms of the HIV and SIV envelope glycoproteins. *J. AIDS* **5,** 70–77.
20. Berger, E. A., Chaudhary, V. K., Clouse, K. A., Jaraquemada, D., Nicholas, J. A., and Rubino, K. L. (1990) Recombinant CD4-*Pseudomonas* exotoxin hybrid protein displays HIV-specific cytotoxicity without affecting MHC class 11-dependent functions. *AIDS Res. Hum. Retroviruses* **6,** 795–804.
21. Winters, M. A. and Merigan, T. C. (1993) Continuous presence of CD4-PE40 is required for antiviral activity against single passage HIV isolates and infected peripheral blood mononuclear cells. *AIDS Res. Hum. Retroviruses* **9,** 1091–1096.
22. Zverev, V., Sidorov, A., Zdanovsky, A., Malushova, V., Zdanovska, N., Shukhmina, N., Anjaparidze, O., Pille, E., and Melnikova, N. (1992) Inhibition of the infectivity of HIV by different forms of CD4-diphtheria recombinant immunotoxins. VIII International Conference on AIDS, Amsterdam, The Netherlands, p. 45.
23. Kennedy, P. E., Moss, B., and Berger, E. A. (1993) Primary HIV-1 refractory to neutralization by soluble CD4 are potently inhibited by CD4-*Pseudomonas* exotoxin. *Virology* **192,** 375–379.

24. Aullo, P., Alcami, J., Popoff, M. R., Klatzmann, D. R., Murphy, J. R., and Boquet, P. (1992) A recombinant diphtheria toxin related human CD4 fusion protein specifically kills HIV infected cells which express gp120 but selects fusion toxin resistant cells which carry HIV. *EMBO J.* **11,** 575–583.
25. Till, M. A., Ghetie, V., Gregory, T., Patzer, E. J., Porter, J. P., Uhr, J. W., Capon, D. J., and Vitetta, E. S. (1988) HIV-infected cells are killed by rCD4-ricin A chain. *Science* **242,** 1166–1168.
26. Chaudhary, V. K., Mizukami, T., Fuerst, T. R., FitzGerald, D. J., Moss, B., Pastan, I., and Berger, E. A. (1988) Selective killing of HIV-infected cells by recombinant human CD4 *Pseudomonas* exotoxin hybrid protein. *Nature* **335,** 369–372.
27. Berger, E. A., Clouse, K. A., Chaudhary, V. K., Chakrabarti, S., FitzGerald, D. J., Pastan, I., and Moss, B. (1989) CD4-*Pseudomonas* exotoxin hybrid protein blocks the spread of human immunodeficiency virus infection in vitro and is active against cells expressing the envelope glycoproteins from diverse primate immunodeficiency retroviruses. *Proc. Natl. Acad. Sci. USA* **86,** 9539–9543.
28. Ramachandran, R. V., Katzensteln, D. A., Wood, R., Batts, D. H., and Merigan, T. C. (1994) Failure of short-term CD4-PE40 infusions to reduce viral load in HIV infected individuals. *J. Infect. Dis.* **170,** 1009–1013.
29. Allaway, G. P., Davis-Bruno, K. L., Beaudry, G. A., Garcia, E. B., Wong, E. L., Ryder, A. M., Hasel, K. W., Gauduin, M.-C., Koup, R. A., McDougal, S., and Maddon, P. J. (1995) Expression and characterization of CD4-IgG**2,** a novel heteroteramer that neutralizes primary HIV-1 isolates. *AIDS Res. Hum. Retroviruses* **11,** 533–539.
30. Alkhatib, G., Combadiere, C., Broder, C. C., Feng, Y., Kennedy, P. E., Murphy, P. M., and Berger, E. A. (1996) CC CKR5: a RANTES, MIP-1 receptor as a fusion cofactor for macrophage-tropic HIV-1. *Science* **272,** 1955–1958.
31. Feng. Y., Broder, C. C., Kennedy, P. E., and Berger, E. A. (1996) HIV-1 entry cofactor: functional cDNA cloning of a seven transmembrane G protein-coupled receptor. *Science* **272,** 872 –877.
32. Choe, H., Farzan, M., Sun, Y., Sullivan, N., Rollins, B., Ponath, P. D., Wu, L., Mackay, C. R., LaRosa, G., Newman, W., Gerard, N., Gerard, C., and Sodroski, J. (1996) The B-chemokine receptors CCR3 and CCR5 facilitate infection by primary HIV-1 isolates. *Cell* **85,** 1135–1148.
33. Dragic, T., Litwin, V., Allaway, G. P., Martin, S. R., Huang, Y., Nagashima, K. A., Cayanan, C., Maddon, P. J., Koup, R. A., Moore, J. P., and Paxton, W. A. (1996) HIV-1 entry into CD4+ cells is mediated by the chemokine receptor CC-CKR-5. *Nature* **381,** 667–673.
34. Liu, R., Paxton, W. A., Choe, S., Ceradini, D., Martin, S. R., Horuk, R., MacDonald, M. E., Stuhimann, H., Koup, R. A., and Landau, N. R. (1996) Homozygous defect in HIV-1 coreceptor accounts for resistance of some multiply-exposed individuals to HIV-1 infection. *Cell* **86,** 367–377.
35. Ramilo, O., Bell, K. D., Uhr, J. W., and Vitetta, E. S. (1993) Role of $CD25^+$ and CD25-T cells in acute HIV infection in vitro. *J. Immunol.* **150,** 5202–5208.

36. Finberg, R. W., Wahl, S. M., Allen, J. B., Soman, G., Strom, T. B., Murphy, J. R., and Nichols, J. C. (1991) Selective elimination of HIV-1-infected cells with an interleukin-2 receptor-specific cytotoxin. *Science* **252,** 1703–1705.
37. Borvak, J., Chou, C.-S., Bell, K., Van Dyke, G., Zola, H., Ramilio, O., and Vitetta, E. S. (1995) Expression of CD25 defines peripheral blood mononuclear cells with productive versus latent HIV infection. *J. Immunol.* **155,** 3196–3204.
38. Borvak, J., Chou, C. S., Van Dyke, G., Rosenwirth, B., Vitetta, E. S., and Ramilo, O. (1996) The use of cyclosporine, FK**506,** and SDZ NIM811 to prevent CD25-quiescent peripheral blood mononuclear cells from producing human immunodeficiency virus. *J. Infect. Dis.* **174,** 850–853.
39. Bell, K. D., Ramilo, O., and Vitetta, E. S. (1993) Combined use of an immunotoxin and cyclosporine to prevent both activated and quiescent peripheral blood T cells from producing type 1 human immunodeficiency virus. *Proc. Natl. Acad. Sci. USA* **90,** 1411–1415.
40. Zhang, L. J., Waters, C. A., Poisson, L. R., Estis, L. F., and Crumpacker, C. S. (1997) The interleukin-2 fusion protein, DAB(389)1L-**2,** inhibits the development of infectious virus in human immunodeficiency virus type 1-infected human peripheral blood mononuclear cells. *J. Infect. Dis.* **175,** 790–794.
41. Renneisen, K., Leserman, L., Matthes, E., Schroder, H. C., and Muller, W. E. (1990) Inhibition of expression of human immunodeficiency virus-1 in vitro by antibody-targeted liposomes containing antisense RNA to the env region. *J. Biol. Chem.* **265,** 16,337–16,342.
42. Zarling, J. M., Moran, P. A., Haffar, O., Sias, J., Richrnan, D. D., Spina, C. A., Myers, D. E., Kuebelbeck, V., Ledbetter, J. A., and Uckun, F. M. (1990) Inhibition of HIV replication by pokeweed antiviral protein targeted to $CD4^+$ cells by monoclonal antibodies (letter). *Nature* **347,** 92–95.
43. Erice, A., Balfour, H. H., Jr., Myers, D. E., Leske, V. L., Sannerud, K. J., Kuebelbeck, V., Irvin, J. D., and Uckun, F. M. (1993) Anti-human immunodeficiency virus type 1 activity of an anti-CD4 immunoconjugate containing pokeweeci antiviral protein. *Antimicrob. Agents Chemother.* **37,** 835–338.
44. Rombi, G., Piu, G., Piro, S., Pautasso, M., Garau, G., and Palomba, A. (1992) MAB labelled liposomes as vehicles for AZT: choice of specific monoclonal antibodies for infected cells. VIII International Conference on AIDS, Amsterdam, The Netherlands, p. 129.
45. Pincus, S. H., Wehrly, K., and Chesebro, B. (1989) Treatment of HIV tissue culture infection with monoclonal antibody-ricin A chain conjugates. *J. Immunol.* **142,** 3070–3075.
46. Pincus, S. H. (1996) Therapeutic potential of anti-HIIV immunotoxins. *Antiviral Res.* **33,** 1–9.
47. Zarling, J. M., Moran, P. A., Grosmaire, L. S., McClure, J., Shriver, K., and Ledbetter, J. A. (1988) Lysis of cells infected with HIV-1 by human lymphocytes targeted with monoclonal antibody heteroconjugates. *J. Immunol.* **140,** 2609–2613.
48. Till, M. A., Ghetie, V., May, R. D., Auerbach, P. C., Zolla-Pazner, S., Gorny, M. K., Gregory, T., Uhr, J. W., and Vitetta, E. S. (1990) Immunoconjugates containing ricin

A chain and either human anti-gp41 or CD4 kill H9 cells infected with different isolates of HIV, but do not inhibit normal T or B cell function. *J. AIDS* **3,** 609–614.

49. Matsushita, S., Koito, A., Maeda, Y., Hattori, T., and Takatsuki, K. (1990) Selective killing of HIV-infected cells by anti-gp 120 immunotoxins. *AIDS Res. Hum. Retroviruses* **6,** 193–203.
50. Lo, K. M. S., Biasolo, M. A., Dehni, G., Palu, G., and Haseltine, W. A. (1992) Inhibition of replication of HIV-1 by retroviral vectors expressing *tat*-antisense and anti-*tat* ribozyme RNA. *Virology* **190,** 176–183.
51. Levy-Mintz, P., Duan, L. X., Zhang, H. Z., Hu, B. C., Dornadula, G., Zhu, M. H., Kulkosky, J., Bizub-Bender, D., Skalka, A. M., and Pomerantz, R. J. (1996) Intracellular expression of single-chain variable fragments to inhibit early stages of the viral life cycle by targeting human immunodeficiency virus type 1 integrase. *J. Virol.* **70,** 8821–8832.
52. Chen, S.-Y., Zani, C., Khouri, Y., and Marasco, W. A. (1995) Design of a genetic immunotoxin to eliminate toxin immunogenicity. *Gene Therapy* **2,** 116–123.
53. Konopka, K., Harrison, G. S., Felqner, P. L., and Duzgunes, N. (1997) Cationic liposome-mediated expression of HIV-regulated luciferase and diphtheria toxin a genes in HeLa cells infected with or expressing HIV. *Biochim. Biophys. Acta* **1356,** 185–197.
54. Chu, T. H. T. and Dornburg, R. (1997) Toward highlly efficient cell-type-specific gene transfer with retroviral vectors displaying single-chain antibodies. *J. Virol.* **71,** 720–725.
55. Schnell, M. J., Johnson, J. E., Buonocore, L., and Rose, J. K. (1997) Construction of a novel virus that targets HIV–1-infected cells and controls HIV-1 infection. *Cell* **90,** 849–857.
56. Mebatsion, T., Finke, S., Weiland, F., and Conzelmann, K. K. (1997) A CXCR4/CD4 pseudotype rhabdovirus that selectively infects HIV-1 envelope protein-expressing cells. *Cell* **90,** 841–847.
57. Kabat, D., Kozak, S. L., Wehrly, K., and Chesebro, B. (1994) Differences in CD4 dependence for infectivity of laboratory-adapted and primary patient isolates of HIV. *J. Virol.* **68,** 2570–2577.
58. Wrin, T., Loh, T. P., Vennari, J. C., Schuitemaker, H., and Nunberg, J. H. (1995) Adaptation to persistent growth in the H9 cell line renders a primary isolate of HIV-1 sensitive to neutralization by vaccine sera. *J. Virol.* **63,** 39–48.
59. Harouse, J. M., Bhat, S., Spitalnik, S. L., Laughlin, M., Stefano, K., Silberberg, D. H., and Gonzales-Scarano, F. (1991) Inhibition of entry of HIV-1 in neural cell lines by antibodies against galactosyl ceramide. *Science* **253,** 320–323.
60. Fantini, J., Cook, D. G., Nathanson, N., Spitaloik, S. L., and Gonzalez-Scarano, F. (1993) Infection of colonic epithelial cell lines by type 1 human immunodeficiency virus is associateo with cell surface expression of galactosylceramide, a potential alternative gp120 receptor. *Proc. Natl. Acad. Sci. USA* **90,** 2700–2704.
61. Pincus, S. H. and Wehrly, K. (1990) AZT demonstrates anti-HIV-1 activity in persistently infected cell lines: implications for combination chemotherapy and immunotherapy. *J. Infect. Dis.* **162,** 1233–1238.

62. Fang, H. and Pincus, S. H. (1995) Unique insertion sequence and pattern of CD4 expression in variants selected with immunotoxins from human immunodeficiency virus type 1-infected T cells. *J. Virol.* **69,** 75–81.
63. Duensing, T. D., Fang, H., Dorward, D. W., and Pincus, S. H. (1995) Processing of the envelope glycoprotein gp160 in immunotoxin-resistant cell lines chronically infected with HIV-1. *J. Virol.* **69,** 7122–7131.
64. Chesebro, B., Wehrly, K., Nishio, J., and Perryman, S. (1992) Macrophage-tropic HIV isolates from different patients exhibit unusual V3 envelope sequence homogeneity in comparison with T-cell-tropic isolates: definition of critical amino acids involved in cell tropism. *J. Virol.* **66,** 6547–6554.
65. Pincus, S. H., Wehrly, K., Tschachler, E., Hayes, S. F., Buller, R. S., and Reitz, M. (1990) Variants selected by treatment of human immunodeficiency virus-infected cells with an immunotoxin. *J. Exp. Med.* **172,** 745–757.
66. Zimmerman, K. and Mannhalter, J. W. (1996) Technical aspects of quantitative competitive PCR. *BioTechniques* **21,** 268–273.
67. Chesebro, B. and Wehrly, K. (1988) Development of a sensitive quantitative focal assay for human immunodeficiency virus infectivity. *J. Virol.* **62,** 3779–3788.
68. Pincus, S. H., Wehrly, K., and Chesebro, B. (1991) Use of a focal infectivity assay for testing susceptibility of HIV to antiviral agents. *BioTechniques* **10,** 336–342.
69. Chesebro, B., Wehrly, K., Metcalf, J., and Griffin, D. E. (1991) Use of a new CD4-positive HeLa cell clone for direct quantitation of infectious human immunodeficiency virus from blood cells of AIDS patients. *J. Infect. Dis.* **163,** 64–70.
70. Pincus, S. H., Messer, K. G., Schwartz, D. H., Lewis, G. K., Graham, B. S., Blattner, W. A., and Fisher, G. (1993) Differences in the antibody response to human immunodeficiency virus 1 envelope glycoprotein (gp160) in infected laboratory workers and vaccinees. *J. Clin. Invest.* **91,** 1987–1996.
71. Pincus, S. H., Messer, K. G., and Hu, S.-L. (1994) Effect of nonprotective vaccination on antibody response to subsequent human imrnunodeficiency virus infection. *J. Clin. Invest.* **93,** 140–146.
72. Pincus, S. H., Messer, K. G., Nara, P. L., Blattner, W. A., Colclough, G., and Reitz, M. (1994) Temporal analysis of the antibody response to HIV envelope protein in HIV-infected laboratory workers. *J. Clin. Invest.* **93,** 2505–2513.
73. Moore, J. P., McKeating, J. A., Weiss, R. A., and Sattentau, Q. J. (1990) Dissociation of gp120 from HIV-1 virions induced by soluble CD4. *Science* **250,** 1139–1142.
74. Chan, D. C., Fass, D., Berger, J. M., and Kim, P. S. (1997) Core structure of gp41 from the HIV envelope glycoproteih. *Cell* **89,** 263–273.
75. Rizzuto, D. D., Wyatt, R., Hernandez-Ramos, N., Sun, Y., Kwong, P. D., Hendrickson, W. A., and Sodroski, J. (1998) A conserved HIV gp120 glycoprotein structure involved in chemokine receptor binding. *Science* **280,** 1949–1953.
76. Wyatt, R., Kwong, P. D., Desjardins, E., Sweet, R. W., Robinson, J., Hendrickson, W. A., and Sodroski, J. G. (1998) The antigenic structure of the HIV gp120 envelope glycoprotein. *Nature* **393,** 705–711.

12

Making Fusion Toxins to Target Leukemia and Lymphoma

Robert J. Kreitman and Ira Pastan

1. Introduction

Recombinant toxins are cytotoxic proteins that are encoded by DNA sequences that can be expressed in prokaryotic or eukaryotic cells. The proteins contain both a ligand, for binding to cells, and a toxin, for killing the cells. In recombinant toxins the connection between the toxin and ligand is encoded by the DNA and not produced by chemical conjugation. Since recombinant toxins must bind specifically to cell surface molecules to kill cells, the number of possible recombinant toxin molecules that can bind to a cell is in the hundreds or thousands; hence, the toxins must be very potent.

Molecules most useful for producing recombinant toxins are derived from *Pseudomonas* exotoxin (PE) or diphtheria toxin (DT), One or a few molecules of either toxin is sufficient to kill cells if the toxin gains entry to the cytosol ***(1)***. These bacterial toxins are each composed of a cell-binding domain at one end, an enzymatic domain, which ADP ribosylates elongation factor 2 (EF-2) at the other end, and a translocation domain in the middle that transports the enzymatic domain into the cytosol, where it can interact with EF-2 ***(2–6)***. In PE the binding domain is near the amino terminus and the catalytic domain is near the carboxyl terminus, whereas in DT the orientation is reversed. In recombinant toxins, cell-binding ligands replace the toxin's binding domain at the amino terminus of PE or at the carboxyl terminus of DT. The truncated form of PE, which is missing the binding domain, is termed PE40 and is composed of amino acids 253–613 of PE. PE40 is truncated further to PE38 by removal of a disulfide loop just prior to the catalytic domain, and hence is composed of amino acids 253–364 and 381–613 of PE. DAB_{486} contains the first 485 amino acids

From: *Methods in Molecular Medicine, Vol. 25: Drug Targeting: Strategies, Principles, and Applications*
Edited by: G. E. Francis and C. Delgado

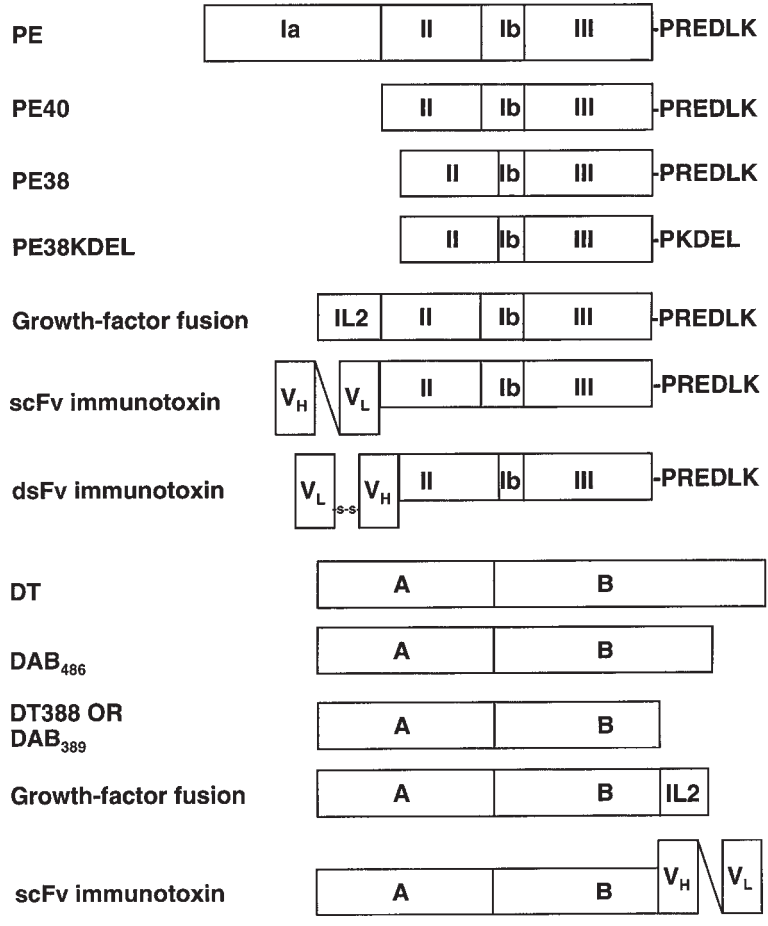

Fig. 1. Schematic diagram of recombinant toxins. Ia, II, Ib, and III indicate domains Ia (amino acids 1–252), II (amino acids 253–364), Ib (amino acids 365–399), and III (amino acids 400–607) of PE. Amino acids 608–613, the carboxyl terminus of PE, is listed as PREDLK. IL2 and GM-CSF represent human ligands. V_H and V_L represent the heavy and light variable domains of an MAb. DAB_{486} represents the first 485 amino acids of DT, not counting the initiator methionine. DAB_{389} or DT_{388} represents the first 388 amino acids of DT.

of DT, whereas either DAB_{389} or DT_{388} contain the first 388 amino acids of DT *(7–10)*. To increase activity, the 5-carboxyl terminal amino acids of PE can be converted from REDLK to KDEL *(8,11,12)*.

Figure 1 depicts the schematic structures for several different types of recombinant toxins. In proteins composed of growth factors fused to toxins, a ligand, such as interleukin 2, is fused to the amino terminus of truncated PE or

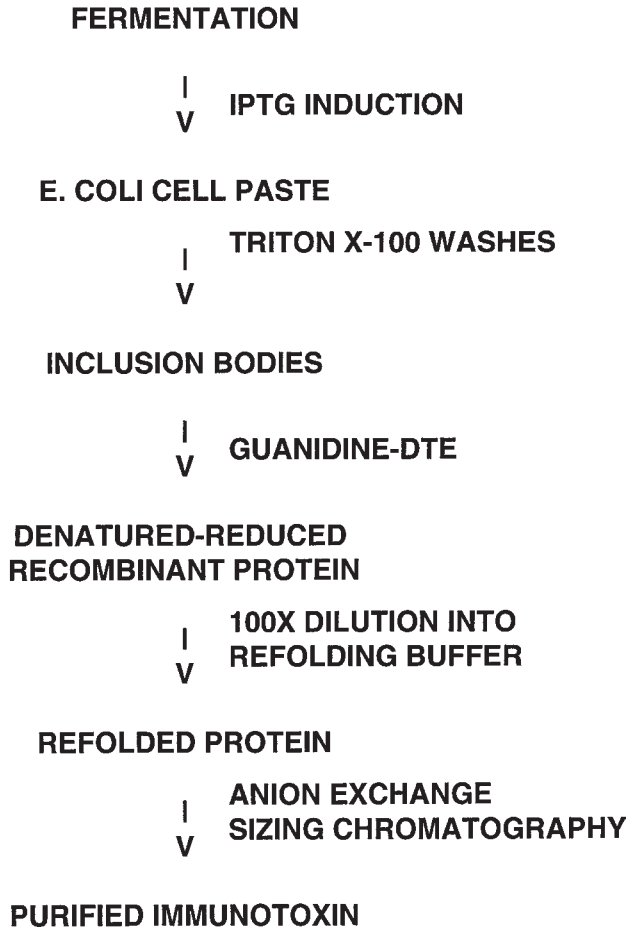

Fig. 2. Overview for the purification of recombinant toxin.

the carboxyl terminus of DT. Recombinant immunotoxins contain the variable domains of monoclonal antibodies (MAbs) fused to truncated toxin. In single-chain Fv (scFv) recombinant immunotoxins, one variable domain is attached to the other variable domain through a peptide linker, typically 15 amino acids long, and the other variable domain in turn is fused to the toxin. In disulfide-stabilized Fv (dsFv) recombinant immunotoxins, the two variable domains are connected via cysteine residues engineered into the framework regions, and one of the variable domains is fused to the toxin.

An overview of the methods involved in producing recombinant toxins is shown in the flow chart in **Fig. 2**. Purified recombinant toxins are produced by isolating insoluble inclusion body protein from the paste of *Escherichia coli*

cells, which express the protein, and then by renaturing the solubilized, denatured, and reduced protein in a redox refolding buffer. The refolded protein is then purified by ion exchange and sizing chromatography. The following is a detailed description of how to purify a typical recombinant toxin. Very few modifications of the protocol are needed for individual differences between recombinant toxins; these modifications discussed in **Subheading 4.** The scale discussed here involves the production of 3.7 mg purified recombinant toxin from 1 L of bacteria fermented in shake flasks. The results regarding chromatograms and yield are typical of recombinant toxins purified in this manner, and were taken from the preparation of the recombinant toxin GM-CSF-PE38KDEL, which has been described briefly ***(13)***.

2. Materials

2.1. Plasmids

Plasmids contain the DNA encoding the recombinant toxin under control of the T7 promoter ***(14)***, and contain an ampicillin or chloramphenicol resistance gene. The latter is preferred for the preparation of proteins for clinical use, since patients allergic to penicillin might react to recombinant proteins purified from bacteria grown in the presence of ampicillin. Plasmids are stored at a concentration of 1 mg/mL in 0.01 *M* Tris-HCl, pH 8.0, and 1 m*M* EDTA at 4°C.

2.2. Transformation and Fermentation

1. Competent bacteria: BL21/DE3 ***(14)***.
2. SOC medium.
3. LB plates containing 100 µg/mL ampicillin or 15 µg/mL chloramphenicol.
4. Superbroth containing added glucose (0.5%), MgSO4 (1.6 m*M*) and ampicillin (100 µg/mL) or chloramphenicol (15 µg/mL).
5. 100 m*M* Isopropyl-β-D-thiogalactopyranoside in water.

2.3. Washing Inclusion Bodies

1. Triton X-100 (25%) in water.
2. TES buffer: 50 m*M* Tris-HCl, pH 8.0, 100 m*M* NaCl, and 20 m*M* EDTA.
3. Lysozyme 5 mg/mL solution in TES.

2.4. Solubilization and Reducing Agents and Buffers

1. Denaturation buffer: 7 *M* guanidine-HCl, 0.1 *M* Tris-HCl, pH 8.0, and 5 m*M* EDTA.
2. 100 mg/mL Dithioerythritol (DTE) in denaturation buffer.
3. 2 mg/mL Bovine serum albumin (BSA) standard.
4. Refolding buffer: 0.1 *M* Tris-HCl, pH 8.0, 0.5 *M* arginine-HCl, 2 m*M* EDTA, 0.9 m*M* Oxidized glutathione (GSSG).
5. Dialysis buffer: 0.02 *M* Tris, pH 7.4, and 0.1 *M* urea.

2.5. Anion Exchange Columns and Buffers

1. Buffer A: 0.02 *M* Tris-HCl, pH 7.4.
2. Buffer B: 1.0 *M* NaCl in buffer A.
3. QSepharose Fast Flow anion exchange resin (Pharmacia, Piscataway, NJ).
4. MonoQ anion exchange resin (Pharmacia).

2.6. Sizing Chromatography

1. TSK G2000SW column (TosoHaas, Philadelphia, PA).
2. Equilibration and running buffer: phosphate-buffered saline (PBS) containing 0.35 *M* additional NaCl (final 0.5 *M* NaCl).

3. Method

3.1. Plasmid Preparation

This chapter will not focus on the recombinant DNA techniques used to construct plasmids encoding recombinant toxins, since such methods are not unique to recombinant toxins. The method described for plasmid expression in *E. coli* BL21/λDE3 cells is applicable for plasmids containing the T7 promoter ***(14)*** and the ampicillin resistance gene.

3.2. Transformation (see Notes 1 and 2)

1. Competent *E. coli* BL21/λDE3 cells, stored at –70–80°C, are thawed on ice.
2. Bacteria (200 µL) is mixed with 4 µg of plasmid on ice for 30–45 min (*see* **Note 3**).
3. The suspension is incubated at 42°C for 1 min and placed back on ice.
4. SOC (1.8 mL) is added and the mixture shaken at 37°C for 1 h (*see* **Note 4**).
5. The SOC-bacterial mixture is plated on 10 LMB-AMP plates (200 µL/plate) and incubated at 37°C for 14–18 h.
6. Bacteria scraped from the 10 plates are resuspended in 1 L superbroth (with ampicillin, $MgSO_4$, and glucose) divided into two 2 L shake flasks, (500 mL/flask) which are shaken vigorously at 275 rpm at 37°C to ensure good aeration.
7. Samples of culture are tested for absorbance at 650 nm.
8. When the diluted OD_{650} becomes ~2.4, IPTG (10 mL of 100 m*M*) is added to give a final concentration of 1 m*M*.
9. After 90 min of continued shaking at 37°C, the cells are centrifuged at 3000*g* for 20 min at 4°C.

3.3. Isolation of Inclusion Body Protein

1. The cell paste is resuspended with a homogenizer in 160 mL of TES buffer.
2. The cell paste is added to a centrifuge bottle containing 6.5 mL of lysozyme solution (5 mg/mL).
3. The cell paste is homogenized in lysozyme and incubated at room temperature for 1 h.
4. The cell paste is rehomogenized and centrifuged at 25,000*g* for 45 min at 4°C.
5. The pellet is homogenized in 160 mL TES with 20 mL of 25% Triton X-100.

6. The homogenized paste is incubated at room temperature for 30 min.
7. After rehomogenizing, the mixture is centrifuged at 25,000*g* for 30 min at 4°C.
8. **Steps 5–7** are repeated one to three more times, decreasing the incubation time in **step 6** to 5 min and decreasing the centrifugation time in **step 7** to 20 min (*see* **Note 5**).
9. **Steps 5–7** are repeated four more times with TES alone to remove Triton X-100, without incubating prior to centrifuging, and centrifuging for 15–20 min.

3.4. Solubilization and Reduction of Inclusion Bodies

1. Using a spatula, the inclusion body pellet is transferred to a 40–50-mL centrifuge tube. Alternatively, the pellet is homogenized in <40 mL of TES and poured into the 40–50-mL tube, where it is centrifuged at 40,000*g* for 5 min at 4°C.
2. Using a homogenizer with a small homogenizer tip, the inclusion bodies are resuspended in ~4 mL of denaturation solution (see **Note 6**).
3. Protein concentration is determined by diluting 10 µL of the denatured and solubilized protein 20-fold with denaturation buffer, and then adding 5–10 µL to cuvets (*see* **Note 7**). The standard to be used is 2 mg/mL BSA diluted to 400 µg/mL with denaturation buffer. Pierce Coomassie Plus Protein Assay Reagent is used (Pierce, Rockford, IL).
4. The protein to be renatured is added to a centrifuged tube along with an equal weight in milligrams of DTE from the 100 mg/mL solution. For example, to renature 37 mg of recombinant protein add 37 mg of DTE (0.37 of the 100 mg/mL solution).
5. The protein is diluted with denaturation solution if necessary to reach a protein concentration of 10 mg/mL.
6. The concentrated denatured protein is incubated at room temperature for 4–24 h to allow complete reduction of disulfide bonds.

3.5. Refolding

1. To remove small amounts of undissolved material, the reduced, denatured, and solubilized recombinant protein is centrifuged at 40,000*g* for 20–40 min at 4°C.
2. The supernatant is pipetted over 20–30 s into cold stirring refolding buffer to a final protein concentration of 100 µg/mL. After several min of stirring the protein is stored at 10°C for 36–72 h (*see* **Note 8**).

3.6. Reducing Ionic Strength Prior to Ion Exchange

Reducing ion strength prior to ion exchange can be accomplished by one of the following four methods (*see* **Note 9**).

1. The protein is filtered through a 0.45-µ filter and diluted eightfold in water.
2. The protein is dialyzed against 0.02 *M* Tris, pH 7.4, containing 0.1 *M* Urea. After the ionic strength of the protein decreases below that of 0.055 *M* NaCl (Some recombinant proteins require even lower ionic strength to bind to an ion exchange column, as described in **Note 9**), the protein is filtered through a 0.45-µ filter.

3. The protein can be concentrated using large capacity concentrators, such as the CH2 system from Amicon (Beverly, MA) or the TFF concentrator from Millipore (Bedford, MA). With these concentrators the buffer is removed from the protein by ultrafiltration through a membrane having a 30-kDa cutoff. The protein is concentrated to 10–20% of its original volume and dialysis buffer is added at the same rate as buffer is removed by ultrafiltration. In some cases the dialysis buffer should contain up to 0.075 *M* NaCl to prevent aggregation of the concentrated protein. After the ionic strength is reduced to this level, the protein is quantitatively removed from the ultrafiltration device and with washings of buffer A the protein is diluted below an ionic strength of 0.05 *M* NaCl.
4. An alternate refolding buffer may occasionally be used in **step 2**, **Subheading 3.5.**, which contains 2.0 *M* urea, 10 m*M* Tris-HCl, pH 8.0, and 0.9 m*M* GSSG. After renaturing for 36–72 h, the protein is then filtered through a 0.45-µ filter.

3.7. Ion Exchange Chromatography

All chromatography steps are performed at 4°C.

1. The filtered protein is loaded on a 5–8-mL QSepharose column previously washed with 100 mL of buffer A, 200 mL of buffer B, and then 100 mL of buffer A.
2. After loading the protein over 1–3 h the column is washed with buffer A and eluted in 5-mL fractions with 30% buffer B in buffer A.
3. The peak fractions (usually #3–8), determined by protein assay, are diluted five-fold with buffer A. In GM-CSF-PE38KDEL the yield at this point was 12.3 mg from 37 mg of total protein renatured in **step 2**, **Subheading 3.5.** ***(13)***.
4. The protein is loaded on a 1-mL high resolution anion exchange column, such as monoQ (Pharmacia). This requires a high-pressure pump.
5. The column is washed with ~20 mL of buffer A and eluted with a linear gradient of buffer B in buffer A with a 1% increase in buffer B per 1 mL of elution. A typical chromatogram is shown in **Fig. 3A**.
6. The peak fractions of protein eluting at ~0.2 *M* NaCl are individually evaluated by sodium dodecyl sulfate-polyacrylamide gel electrophoresis (SDS-PAGE) under reducing conditions (*see* **Note 10**). Pooled fractions should be >90% pure and not be contaminated with proteins of similar molecular weight. Otherwise, the contaminants will still be present after sizing chromatography.

3.8. Sizing Chromatography

1. The pooled protein purified by anion-exchange chromatography is concentrated by centricon 30 (Amicon) to a volume of 0.5–1 mL (*see* **Note 11**).
2. The protein is loaded on a 7.5 × 600-mm TSK G2000SW (see **Note 12**) column, equilibrated and eluted with PBS containing a total of 0.5 *M* NaCl. As shown in **Fig. 3B**, the protein elutes at 15–18 mL.
3. The fractions from the sizing column are analyzed by reducing SDS-PAGE, pooled, and stored at –80°C. A typical yield is 5–10% of total recombinant protein renatured in **step 2**, **Subheading 3.5.**

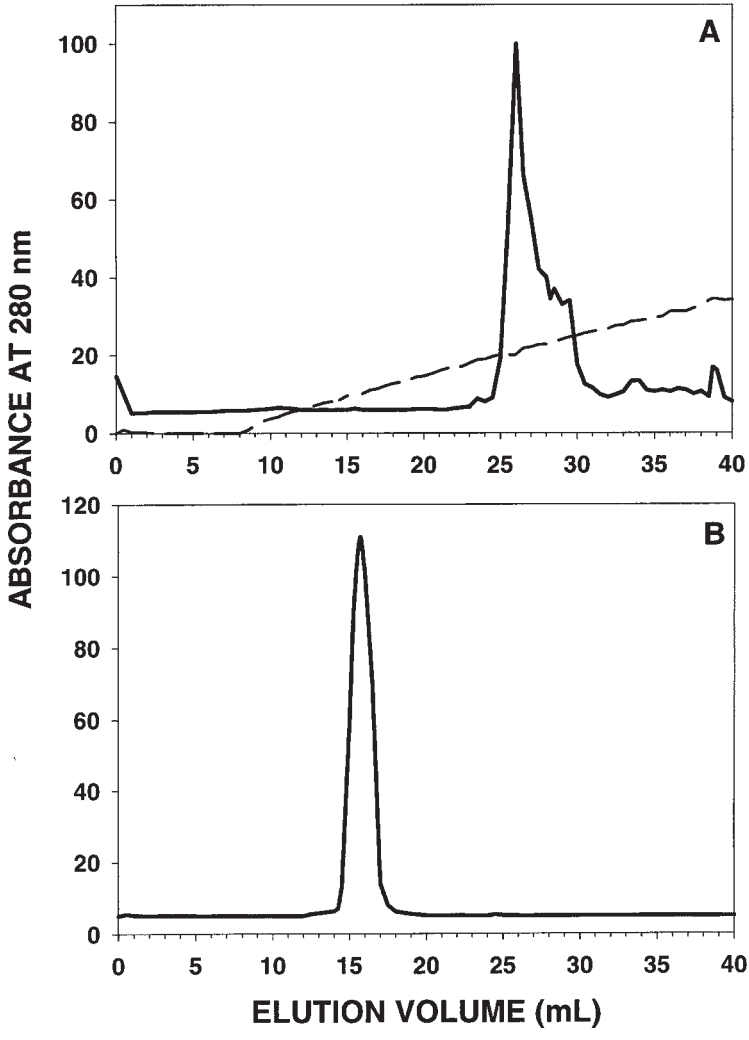

Fig. 3. Chromatography in the purification of a recombinant toxin. **(A)** A 1-mL monoQ column is loaded with recombinant protein, washed with 5 mL of buffer A, and eluted with a linear gradient of buffer B in buffer A. The solid line shows the A_{280} of the eluted protein. The dotted line shows the output from the electroconductivity meter, where buffer A is set to 0 and buffer B is set to 100. **(B)** Concentrated protein is loaded on a 7.5 × 600-mm TSK G3000SW sizing column.

3.9. Characterization of the Pure Protein

1. The protein concentration is assayed by the Pierce Coomassie Plus assay using BSA as a standard. This assay gives results similar to those of amino acid analysis

(11). The BCA protein assay gives inaccurate results. If 10 µg of BSA in 0.5 mL water is mixed with 0.5 mL of Pierce Coomassie Plus protein assay reagent in a cuvet of 1 cm path-length, the absorbance at 595 nm should be ~0.5. When the reagent becomes old, the absorbance may decrease to ~0.3, and this decrease may not be proportional to that seen with the recombinant protein. Thus, using old assay reagent will lead to inaccurate results even if a fresh standard is used.

2. The protein concentration can be determined by measuring absorbance at 280 nm. The extinction coefficient should be redetermined based on the Coomassie assay for all new proteins.
3. Nonreducing and reducing SDS-PAGE can be performed on the pooled protein.
4. Cytotoxicity assay: To test the cytotoxicity of the recombinant toxin on adherent cell lines, 1.5×10^4 cells/well are plated in 96-well plates, and 24 h later toxin or control molecules are added and incubated for 16–48 h in final volumes of 200 µL. The medium to use varies with the cell type, but 5–20% fetal bovine serum (FBS) is typically used because calf serum can sometimes contain antibodies against the recombinant toxin. The cells are then pulsed for 4–6 h with 1 µCi [^{3}H]-leucine/well. After freezing and thawing to liberate the cells from the plastic, the protein is harvested onto glass-fiber filters and counted in a scintillation counter. To test cytotoxicity on nonadherent cell lines, $1–4 \times 10^4$ cells/well are plated in 96-well plates in volumes of 50 or 150 µL, and 50 µL aliquots of toxin or control molecules are added. If the cells do not adhere at all to the plastic during the 1–2 d incubation prior to pulsing, they do not require freezing and thawing prior to harvesting. To test cytotoxicity on fresh patient bone marrow, lymph node, or peripheral blood malignant cells, the malignant mononuclear cells are partially purified by Ficoll centrifugation and plated as nonadherent cells using medium that contains only ~1 µg/mL of leucine, just 2% of the leucine content in normal media. After incubating with toxins for 2–4 d, the cells are frozen and thawed, harvested, and counted. The IC_{50} is the concentration of toxin necessary for 50% inhibition of protein synthesis.
5. Binding assay: To determine binding affinity of the recombinant toxin, the ligand (growth factor or antibody not connected to a toxin) is radiolabeled. In a standard displacement assay, increasing concentrations of either cold ligand or recombinant toxin are added to a constant concentration of radiolabeled ligand, and the amount of bound radiolabeled ligand determined. The EC_{50} is the concentration of protein required to displace 50% of the radiolabeled ligand from binding to its receptor. The EC_{50}s of the ligand and the ligand–toxin fusion are compared to determine the extent to which fusion of the toxin to the ligand prevents its binding. The displacement assay gives more accurate data than if the recombinant toxin is radiolabeled and its affinity determined directly by a Scatchard plot, since radiolabeling of small proteins may damage them and decrease or abolish their binding.
6. Endotoxin assay: The endotoxin assay may be performed using a variety of different kits (LAL assay, Sigma, St. Louis, MO). An acceptable level of endotoxin is <1 EU/mg of protein, which can be obtained without the use of additional

techniques to remove endotoxin, because most of the endotoxin is removed by washing the inclusion bodies with detergent.

4. Notes

1. For best results, the transformation should not precede the fermentation by >18 h, since leakiness of the expression system can result in protein expression and bacterial lysis prior to induction with IPTG. This results in reduced growth and viability of the bacteria during culture and poor expression after induction with IPTG. In some cases premature protein expression occurs while the bacteria are growing on the LB-AMP plates, leading to smaller than normal colonies. To decrease the leakiness of the expression system, an episome containing a repressor can be added to the BL21/λDE3 cells. In addition, protein expression may be poor because the eukaryotic DNA to be expressed in bacteria contains codons that are rare for gram negative bacteria, such as AGA and AGG. This problem can be solved using a plasmid encoding tRNA for these codons as well as a *lac* repressor ***(15)***. The BL21/λDE3 cells are simply transformed with the episome, which contains a kanamycin resistance gene, and competent cells prepared for transformation with plasmid-encoding recombinant toxin.
2. An alternative to transformation each time a protein is to be produced is to prepare a master cell bank. To produce a master cell bank, a single colony obtained from the transformation in **step 5**, **Subheading 3.2.**, is cultured in a shake-flask with 200 mL of superbroth containing 100 µg/mL ampicillin (or 15 µg/mL chloramphenicol). When the culture reaches an OD_{650} of ~3, the cells are placed on ice, mixed with a 50% volume of 86% glycerol in water, and frozen at –80°C in 1.5 mL aliquots. Future fermentations can be started from a single aliquot for more reproducible results.
3. The amount of plasmid DNA needed for transformations depends on the competence, and the 4 µg quantity is to ensure a maximal number of colonies even when the competence is low, as is usually the case with BL21/λDE3. If the competence is high, lower quantities of plasmid DNA can be used.
4. If desired, the shaking time can be shortened or eliminated. If the bacterial cells were very competent, the maximal number of colonies will still be obtained.
5. A major problem with some recombinant proteins, particularly those <50 kDa, is that their inclusion bodies often dissolve in detergents, such as Triton X-100. In these cases the number of washes with detergent must be minimized. Alternatively, a different detergent (such as Brij 35, Sigma) may be tried. Extra washes with detergent may help to remove endotoxin from the inclusion bodies.
6. Some foaming is inevitable at this step, and it should not be completely prevented by homogenizing slowly, since the inclusion bodies are more difficult to dissolve the longer they are allowed to remain as large chunks in the denaturation solution. After several min the foaming should disappear and a clear brown (sometimes hazy) solution remains. The inclusion bodies should dissolve even if the 7 *M* guanidine buffer is diluted to 5–6 *M*. Therefore, a cloudy mixture after the foam clears usually indicates that the inclusion bodies contain other bacterial products, and not that additional denaturation solution needs to be added.

7. The protein concentration in the denaturing solution must be measured accurately if a proper protein concentration during renaturation is to be obtained. The protein in the denaturing solutions should be diluted 20-fold in denaturing solution rather than water prior to adding to a cuvet, since precipitation of protein will occur after dilution in water, leading to an inadequate addition of protein to the cuvet. Measuring protein concentration in the renaturation solution is difficult because of the presence of L-arginine, but it can be measured accurately after dialysis.
8. Stirring during the entire 36–72 h incubation at 10°C should not be done because it leads to severe aggregation of the protein.
9. Some proteins, particularly those containing truncated DT, may require a very low ionic strength for binding to an anion exchange resin.
10. Recombinant proteins after monoQ need to be evaluated by reducing SDS-PAGE to rule out contamination with disulfide-bonded impurities that might comigrate with the recombinant toxin on a nonreducing gel but appear as lower-mol-wt impurities on a reducing gel. The protein may be contaminated with dimeric or multimeric recombinant toxin, which will not be apparent on a reducing gel, but these multimers can be removed by the sizing column.
11. Alternatively, the protein can be concentrated first by diluting it 5–10-fold with buffer A and then loading the protein on a QSepharose column (25–50 mg protein/mL resin). The protein is then eluted in a small volume with buffer A containing 50% buffer B.
12. A TSK G3000SW column can also be used, particularly if the molecular weight of the protein is >80 kDa. A large capacity, low pressure disposable column effective for clinical grade preparations is the Sephacryl S200 column (Pharmacia).

References

1. Yamaizumi, M., Mekada, E., Uchida, T., and Okada, Y. (1978) One molecule of diphtheria toxin fragment A introduced into a cell can kill the cell. *Cell* **15,** 245–250.
2. Carroll, S. F. and Collier, R. J. (1987) Active site of *Pseudomonas aeruginosa* exotoxin A. Glutamic acid 553 is photolabeled by NAD and shows functional homology with glutamic acid 148 of diphtheria toxin. *J. Biol. Chem.* **262,** 8707–8711.
3. Uchida, T., Pappenheimer, A. M., Jr., and Harper, A. A. (1972) Reconstitution of diphtheria toxin from two nontoxic cross-reacting mutant proteins. *Science* **175,** 901–903.
4. Uchida, T., Pappenheimer, A. M., Jr., and Greany, R. (1973) Diphtheria toxin and related proteins I. Isolation and properties of mutant proteins serologically related to diphtheria toxin. *J. Biol. Chem.* **248,** 3838–3844.
5. Rolf, J. M., Gaudin, H. M., and Eidels, L. (1990) Localization of the diphtheria toxin receptor-binding domain to the carboxyl-terminal M_r ~ 6000 region of the toxin. *J. Biol. Chem.* **265,** 7331–7337.
6. Choe, S., Bennett, M. J., Fujii, G., Curmi, P. M. G., Kantardjieff, K. A., Collier, R. J., and Eisenberg, D. (1992) The crystal structure of diphtheria toxin. *Science* **357,** 216–222.

7. Siegall, C. B., Chaudhary, V. K., FitzGerald, D. J., and Pastan, I. (1989) Functional analysis of domains II, Ib, and III of *Pseudomonas* exotoxin. *J. Biol. Chem.* **264,** 14,256–14,261.
8. Kreitman, R. J., Batra, J. K., Seetharam, S., Chaudhary, V. K., FitzGerald, D. J., and Pastan, I. (1993) Single-chain immunotoxin fusions between anti-Tac and *Pseudomonas* exotoxin: relative importance of the two toxin disulfide bonds. *Bioconj. Chem.* **4,** 112–120.
9. Williams, D. P., Snider, C. E., Strom, T. B., and Murphy, J. R. (1990) Structure/function analysis of interleukin-2-toxin (DAB_{486}-IL-2). Fragment B sequences required for the delivery of fragment A to the cytosol of target cells. *J. Biol. Chem.* **265,** 11,885–11,889.
10. Chaudhary, V. K., FitzGerald, D. J., and Pastan, I. (1991) A proper amino terminus of diphtheria toxin is important for cytotoxicity. *Biochem. Biophys. Res. Commun.* **180,** 545–551.
11. Seetharam, S., Chaudhary, V. K., FitzGerald, D., and Pastan, I. (1991) Increased cytotoxic activity of *Pseudomonas* exotoxin and two chimeric toxins ending in KDEL. *J. Biol. Chem.* **266,** 17,376–17,381.
12. Kreitman, R. J. and Pastan, I. (1995) Importance of the glutamate residue of KDEL in increasing the cytotoxicity of *Pseudomonas* exotoxin derivatives and for increased binding to the KDEL receptor. *Biochem. J.* **307,** 29–37.
13. Kreitman, R. J. and Pastan, I. (1997) Recombinant toxins containing human GM-CSF and either *Pseudomonas* exotoxin or diphtheria toxin kill gastrointestinal cancer and leukemia cells. *Blood* **90,** 252–259.
14. Studier, F. W. and Moffatt, B. A. (1986) Use of bacteriophage T7 polymerase to direct selective expression of cloned genes. *J. Mol. Biol.* **189,** 113–130.
15. Brinkmann, U., Mattes, R. E., and Buckel, P. (1989) High-level expression of recombinant genes in Escherichia coli is dependent on the availability of the dnaY gene product. *Gene* **85,** 109–114.

13

Antibody-Bearing Liposomes as Chloroquine Vehicles in Treatment of Murine Malaria

Ajay K. Agrawal and Chhitar M. Gupta

1. Introduction

Malaria is a serious public health problem that affects about 300–500 million people and claims 1.5–2.7 million deaths every year. One-third of all humans live in zones where they risk catching it ***(1)***. The situation is aggravated because the malarial parasites are rapidly developing resistance to the existing antimalarial drugs, like chloroquine ***(2)***, when given in classical pharmaceutical forms. Studies on the molecular basis of chloroquine resistance suggest that enhanced active efflux of the drug from the cells infected with resistant parasite strain prevents drug accumulation to toxic levels within the cytosol of the infected erythrocytes ***(3–5)***. It has been shown that erythrocytes infected with chloroquine-resistant parasite accumulate less chloroquine than those with sensitive parasites ***(6,7)***. Furthermore, inhibiting the chloroquine efflux by Ca^{2+}-channel blockers render the resistant cells fully sensitive to chloroquine ***(8)***, indicating that the antimalarial activity of the chloroquine is directly related to its concentration within the parasite food vacuole ***(9)***. The mechanism by which this concentration effect is achieved is unclear, but it is believed to involve binding to a putative chloroquine receptor ***(10)***.

Development of new, more selective drugs is usually very expensive, time-consuming, and often uncertain. Consequently, much attention is being given to an alternative approach, namely the use of drug delivery systems in order to optimize the action of the drugs already in existence by transporting or facilitating their release where they are needed. A large number of macromolecular, cellular, and synthetic carriers have been explored as new drug delivery systems ***(11–14)*** but among these, liposomes bearing cell-specific recognition

From: *Methods in Molecular Medicine, Vol. 25: Drug Targeting: Strategies, Principles, and Applications*
Edited by: G. E. Francis and C. Delgado

molecules (i.e., antibody, lectin, sugar) on their surface have received wide consideration as vehicles for site-specific delivery of drugs and enzymes in vivo ***(15–17)***. Of the cell-specific ligand-bearing liposomes, a significant number, but not all of the liposomes has been shown to bind the target cells. Only a fraction of the bound liposomes deliver their contents to the cells because delivery depends on the mode of liposome interaction with cells ***(18,19)***.

We have previously shown that binding of the liposomes to red cells can considerably be enhanced (20–25-fold) by covalently attaching $F(ab')_2$ fragments of a mouse polyclonal antibody, raised against the erythrocytes membrane, to their surface ***(20,21)***. We further demonstrated that at least 20–30% of the cell-bound liposomes delivered their contents to the target cells, presumably by membrane-membrane fusion ***(21)*** and this amounts to only 2.5% of the initially injected dose of liposomes.

To examine whether this method of drug targeting had any functional significance in the treatment of a pathologic condition of erythrocytes, i.e., erythrocytes infected with the malarial parasites, we encapsulated an antimalarial drug, chloroquine, to which the malarial parasites rapidly develop resistance ***(2)*** in the antibody-targeted liposomes and examined the therapeutic efficacy of the liposomized drug against chloroquine-susceptible *Plasmodium berghei* infections in mice ***(22)***. The therapeutic response after injection of chloroquine-loaded immunoliposomes was compared with the response after intravenous administration of chloroquine containing plain liposome (without a specific homing device) or free chloroquine. Results of these studies indicated that ability of the chloroquine to control malarial infection was significantly enhanced when delivered in antimouse erythrocytes $F(ab')_2$ bearing liposomes ***(22)***.

Then we evaluated the viability of this approach in controlling chloroquine-resistant *P. berghei* infections in mice ***(23)***. The results of these studies revealed that liposomized chloroquine was very effective in suppressing the disease both in terms of reduction in parasitemia and prolongation in the survival times of the liposome-treated mice, as compared to the appropriate control mice ***(23)***. It was also reported that liposomization of chloroquine increased its maximal tolerable dose as well as efficiency against chloroquine-resistant malarial infection ***(24)***.

In continuation of our studies, we further explored the possibility of the treatment of malaria by covalently attaching $F(ab')_2$ fragments of a mouse monoclonal MAb F_{10}, raised against the erythrocyte membrane isolated from the *P. berghei*-infected mice rather than the polyclonal antibody, to chloroquine-containing liposomes ***(25)***. These liposomes specifically recognized the *P. berghei*-infected mouse erythrocytes under both in vitro and in vivo conditions (*see* **Note 1**). No such specific binding of the liposomes with the infected cells was observed when a specific monoclonal antibody, MAb F_{10} was

replaced by another mouse monoclonal antibody, MAb D_2. It has been shown that the intracellular malarial parasite modifies the host erythrocyte membrane protein composition ***(26)***. Not only does it structurally alter the native erythrocyte membrane proteins ***(27)***, but it also inserts some new proteins in the plasma membrane of the host cell ***(28,29)***. This prompted us to speculate that MAb F_{10} might have been directed against some new protein(s) of parasite origin. Results of this study indicated that these immunoliposomes were more effective and chloroquine-susceptible, and that resistant malarial infection can be cured with chloroquine by delivering this drug in target-specific liposomes ***(25)***.

From these results it appears that the MAb F_{10} recognizes some surface antigen that is unique to the *P. berghei*-infected erythrocytes. In addition, the efficient internalization of the cell-bound MAb F_{10}-liposomes and/or the specific binding of these liposomes to the free parasites could also be attributed to the enhanced drug efficiency observed here. These immunoliposomes, with increased specificity for infected red blood cells, led to a reduction of at least 80 times the dose (assuming that the average weight of the mouse is approx 20 g) required for effective treatment as previously published by Peeters et al. ***(24)*** for chloroquine-resistant *P. berghei* infections (*see* **Note 2**).

2. Materials

Solutions and reagents are stored at room temperature and buffers, antibody solutions, and $F(ab')_2$ fragments are stored at 4°C unless specified otherwise. All chemicals used are of analytical grade.

2.1. Liposomes

1. Egg phosphatidylcholine (PC) and gangliosides: In our laboratory, we routinely isolate and purify egg PC and gangliosides from their natural sources (egg yolk ***[30]*** and buffalo brain ***[20]***, respectively). They are commercially available from a number of companies. However, it is important to check the egg PC by TLC (*see* **Note 3**) to make sure that no lyso PC is formed. Store at –4°C under nitrogen atmosphere.
2. Chloroform: methanol (2:1; v/v).
3. Cholesterol: Centron Research Laboratory (Bombay, India) (*see* **Note 4**).
4. Borate-buffered saline: 10 m*M* borate, 60 m*M* NaCl, pH 8.4.
5. Chloroquine: a gift from Walter Reed Army Institute, Washington DC.
6. Sephadex G-50: Pharmacia, Uppsala, Sweden.
7. Triton X-100: Sigma Chemical Company (St. Louis, MO).
8. Sonicator and ultracentrifuge.

2.2. Preparation of MAb F_{10}

1. Normal and *P. berghei* infected BALB/c mice.
2. PAI-0: a myeloma cell line ***(31)***.

3. Polyethylene glycol (mol wt 1500) (BDH Chemicals Ltd., Poole, UK).
4. Isotype-specific antibody: Sigma.
5. 20 m*M* phosphate containing 0.1 m*M* EDTA.

2.3. Preparation of F(ab')$_2$ Fragments

1. Pepsin: Sigma. Store at –4°C.
2. 100 m*M*, Acetate buffer: pH 4.5.
3. 10 m*M* Tris-HCl, 150 m*M* NaCl, pH 7.4.
4. Glycine buffer: 100 m*M*, pH 8.0 and 2.5.
5. Amicon Centriflo CF-25 cone (Millipore, Watford, UK).

2.4. Preparation of ^{125}I Labeled Fragments

1. Lactoperoxidase: Sigma. Store at –4°C.
2. β-mercaptoethanol: Sigma.
3. 0.1 m*M* Sodium iodide: Sigma.
4. Sodium phosphate: Sigma.
5. Hydrogen peroxide: Sigma.
6. [^{125}I]Sodium iodide (carrier-free): Amersham (Buckinghamshire, UK).
7. [^{14}C]inulin: Amersham.
8. 20 m*M* Tris-HCl buffer, pH 7.4.

2.5. Covalent Coupling of Liposomes to Antimouse Erythrocytes F(ab')$_2$

1. Sodium metaperiodate: Centron Research Laboratory.
2. Sodium cyanoborohydride: Sigma.
3. Sepharose 6B and Sephadex G-50: Pharmacia, Uppsala, Sweden. Store at 4°C.
4. Millipore filter 0.22 μm (Millipore).
5. Sucrose-supplemented Tris-buffered saline: 10 m*M* Tris-HCl, 44 m*M* sucrose, 150 m*M* NaCl, and 5 m*M* EDTA, pH 7.4.
6. 10 m*M* borate buffer containing 60 m*M* NaCl, pH 8.4.
7. 20 m*M* borate buffer containing 120 m*M* NaCl, pH 8.4.

2.6. Development of Chloroquine Resistance

1. Animals: Randomly bred 8–10-wk-old male Swiss mice of 20 ± 2 g average weight. The animals are kept in plastic cages and given pellet diet (Hindustan Lever Ltd., India) and water ad libitum.
2. Parasites: *P. berghei* parasites are obtained from National Institute of Communicable Diseases (New Delhi, India) and maintained in Swiss mice through serial blood passage. The strain is fully susceptible to chloroquine; the ED_{90} being 15 mg/kg × 4 d intraperitoneally.

2.7. Tissue Distribution of Liposomes

1. Healthy and infected (50–60% parasitemia) BALB/c mice.
2. Heparinized capillary pipets.

3. Sucrose-supplemented Tris-buffered saline: 10 m*M* Tris containing 44 m*M* sucrose, 150 m*M* NaCl, and 5 m*M* EDTA, pH 7.4.

2.8. Liposome Binding In Vitro

1. Healthy and infected (50–60% parasitemia) BALB/c mice.
2. Heparinized glass tubes.
3. Phosphate-buffered saline: 10 m*M* phosphate, 150 m*M* NaCl, pH 7.4.
4. CF-11 column (5 mL).
5. Conray 33% (w/v) solution in water.
6. 9% solution of Ficoll 400 in normal saline.
7. Tris-buffered saline: 10 m*M* Tris-HCl, 50 m*M* NaCl, pH 7.4.
8. Sucrose-supplemented Tris-buffered saline: 10 m*M* Tris-HCl containing 44 m*M* sucrose, 150 m*M* NaCl, 5 m*M* EDTA, pH 7.4.

3. Methods

3.1. Liposomes

1. Dissolve egg PC (20 µmol), cholesterol (20 µmol), and gangliosides (4 µmol) in 2.0 mL of chloroform:methanol (2:1; v/v) mixture in a thick glass tube.
2. Remove the solvents under a slow jet of nitrogen gas to produce a thin film of lipid on the wall of the tube.
3. Remove any traces of solvents by leaving the tube overnight under *vacuo*.
4. The lipid is then dispersed in 0.8 mL borate-buffered saline (10 m*M* borate, 60 m*M* NaCl, pH 8.4) containing chloroquine (350 µmol) or traces of [^{14}C]inulin by vortexing for binding studies.
5. Sonicate (*see* **Note 5**) the dispersion with a probe-type sonicator for 30 min (*see* **Note 6**) under nitrogen atmosphere (*see* **Note 7**) at 4°C (*see* **Notes 8** and **9**).
6. Centrifuge the sonicated preparation at 105,000*g* for 1 h at 5°C to effect the removal of titanium particles as well as poorly dispersed lipids. Use only the top two-thirds of the supernatant (*see* **Note 10**).
7. Separate free chloroquine from liposomized chloroquine by gel filtration over Sephadex G-50.
8. Measure the size of the liposomes (*see* **Note 11**).

3.1.1. Chloroquine Estimation

1. Lyse appropriate aliquots of chloroquine containing liposomes with Triton X-100 (1%, w/v) (*see* **Note 12**).
2. Estimate the chloroquine by measuring its absorbance at 342 nm (*see* **Notes 13–15**).

3.2. Preparation of MAb F_{10}

1. Immunize BALB/c mice intraperitoneally at 3-wk intervals with the erythrocyte membranes isolated from approx 1.5×10^7 mouse erythrocytes infected predominantly with the trophozoite stage of *P. berghei*.

2. Isolation of the membranes from the infected cells is carried out as follows:
   a. Lyse the infected cells with 20 m*M* phosphate containing 0.1 m*M* EDTA at 4°C.
   b. Centrifuge the lysate immediately at 750*g* for 2 min at 4°C.
   c. Aspirate off the supernatant carefully, leaving behind a pellet containing parasites and few unlysed cells.
   d. Further purify the membrane from parasites by centrifugation of the supernatant again at 2250*g* for 3 min at 4°C.
   e. Isolate the membranes by centrifuging the second supernatant at 20,000*g* for 45 min at 4°C.
3. After four to six immunizations, fuse spleen cells with PAI-0, a myeloma cell line, by using polyethylene glycol.
4. Screen hybridoma supernatants by immunofluorescence assay with infected erythrocytes (*see* **Note 16**).
5. After cloning by limiting dilutions, select two clones of interest, F_{10} and D_2, on the basis of their Western blotting patterns by using erythrocyte membranes isolated from the infected cells for ascitic fluid generation.
6. Further purify the antibodies from the ascitic fluids by affinity chromatography with Protein A-Sepharose at pH 8.0.
7. Determine the type of these antibodies by enzyme-linked immunosorbent assay (ELISA) with isotype-specific antibodies.
8. Examine the purity of the antibodies by sodium dodecyl sulfate-polyacrylamide gel electrophoresis (SDS-PAGE).

3.3. Preparation of F(ab')$_2$ Fragments

1. Add pepsin (final concentration 250 µg/mL) in 100 m*M* acetate buffer, pH .5.0, to protein solution (10 mg/mL).
2. Incubate the mixture at 37°C overnight.
3. Remove the pepsin and other insoluble materials by centrifugation, dialyze the supernatant against Tris-buffered saline (10 m*M* Tris containing 150 m*M* NaCl, pH 7.4) for 46 h, and remove undigested immunogamma globulin (IgG) by passage through a protein A-Sepharose column.
3. Elute the F(ab')$_2$ fragments with 100 m*M* glycine buffer, pH 8.0, and IgG with low pH glycine buffer (100 m*M*, pH 2.5).
4. Pool together the F(ab')$_2$ fragments and concentrate to 5–6 mg/mL protein using Amicon centriflo CF-25 cone.
5. Examine the purity of these fragments by 5.6% polyacrylamide gel electrophoresis.

3.4. Preparation of ^{125}I Labeled Fragments

1. Add lactoperoxidase (7.5 µg), carrier-free sodium [^{125}I] iodide (0.25 mCi), and cold sodium iodide (0.1 m*M*, 30 µL) to protein solution (2.0 mg/mL in Tris buffer, pH 7.4) at 6°C.
2. Gently shake the reaction mixture and add H_2O_2 (0.8 m*M*, 75 µL) in five aliquots at 2 min intervals.

3. Stop the reaction by adding β-mercaptoethanol (final concentration 10 m*M*).
4. Dialyze the reaction mixture extensively against sodium phosphate (2 m*M*, pH 7.0). The first dialyzing medium should also contains NaI (2 m*M*) (*see* **Notes 17** and **18**).

3.5. Covalent Coupling of Liposomes to Antimouse Erythrocytes F(ab')$_2$

1. Mix equal volumes (1.5 mL each) of sodium metaperiodate solution, freshly made in borate-buffered saline (10 m*M* borate containing 60 m*M* NaCl, pH 8.4, 16 m*M*) in the dark to liposomes suspension to attain a final concentration of sodium metaperiodate as 8 m*M*.
2. Incubate this mixture at 25°C in the dark for 2 h.
3. Remove excess periodate by gel filtration on a Sephadex G-50 column (20 × 1.5 cm) using borate-buffered saline (20 m*M* borate containing 120 m*M* NaCl, pH 8.4) as the eluent.
4. Pool the liposome-rich fractions together and concentrate using an Amicon centriflo CF-25 cone.
5. Mix these liposomes (10 μmol P/mL buffer) with protein (approx 2 mg in borate-buffered saline [500 μL]).
6. Add sodium cyanoborohydride (2 *M*, 15 μL) to the mixture and allow to proceed for approx 16 h at 30°C.
7. Separate the liposomes from the uncoupled protein on the Sepharose 6B column (35 × 1.4 cm) using sucrose-supplemented Tris-buffered saline (10 m*M* Tris containing 44 m*M* sucrose, 150 m*M* NaCl, and 5 m*M* EDTA, pH 7.4).
8. Pool the liposomes eluting in the void volume together, concentrate, and pass through a Millipore filter (pore size 0.22 μm) prior to their use in animal experiments (*see* **Notes 19** and **20**).

3.5.1. Leakage of Chloroquine

1. Incubate the chloroquine containing liposomes with buffer at 37°C for 12 h.
2. Separate free drug from the liposomized drug by gel filtration over Sephadex G-50 column.
3. Assay the fractions for the amount of chloroquine as done in **Subheading 3.1.1.** (*see* **Note 20**).

3.6. Development of Chloroquine Resistance

1. Infect the Swiss mice with approx 10^7 *P. berghei*-infected red cells and on the same day administer a single dose of chloroquine (60 mg/kg; intraperitoneally).
2. Once the animals develop about 2% parasitemia, transfuse the infected blood from these animals into the healthy animals, which are also given chloroquine (60 mg/kg, intraperitoneally) simultaneously.
3. Repeat the above treatment several times until it becomes resistant to chloroquine (50 mg/kg × 4 d; intraperitoneally) (*see* **Notes 21–24**).

3.7. Drug Treatment

1. Infect Swiss mice (5–6 animals/group) on d 0 with approx 10^6 erythrocytes infected with chloroquine-susceptible or resistant *P. berghei* strains.
2. Administer in these animals different treatments, e.g., free chloroquine, chloroquine loaded in nontargeted [free of $F(ab')_2$ liposomes, or targeted liposomes [bearing $F(ab')]_2$ on d 4 postinfection when the parasitemia reaches 0.1–0.5% (*see* **Note 22**).
3. Keep the animals under observation on various days to record parasitemia and mortality (*see* **Note 22**).

3.8. Tissue Distribution of Liposomes

1. Inject liposomes (0.60–1.25 µmol lipid phosphate, 200 µL) intravenously to healthy and infected (50–60% parasitemia) in BALB/c mice.
2. Draw 20 µL blood immediately (≤2 min) after the injection by retro-orbital puncture in heparinized capillary pipets and transfer to preweighed scintillation vials. Reweigh the vials and count for radioactivity (*see* **Notes 25–27**).
3. For measuring the binding of liposomes to blood cells, draw blood at specified times and centrifuge at 1000*g* for 5 min. Remove plasma and analyze for radioactivity (*see* **Note 27**).
4. From the pellet, remove buffy coat and wash erythrocyte pellet with sucrose-supplemented Tris-buffered saline (10 m*M* Tris containing 44 m*M* sucrose, 150 m*M* NaCl, and 5 m*M* EDTA, pH 7.4) profusely and analyze for radioactivity (*see* **Note 27**).
5. After drawing the final time-point blood, sacrifice the animals and remove the various organs (liver, kidney, heart, spleen, lung).
6. Wash, blot, and weigh the organs and prepare 10% homogenate (w/v) in the aforesaid buffer.
7. Centrifuge the homogenate at 5000*g* and determine the radioactivity in the measured aliquots of supernatant (*see* **Note 27**).

3.9. Liposome Binding In Vitro

1. Draw 5 mL blood from infected and healthy uninfected mice in heparinized glass tubes containing phosphate-buffered saline (10 m*M* NaCl, pH 7.4).
2. Pass it through CF-11 column (5 mL) to remove leukocytes.
3. Separate infected and normal erythrocytes by Ficoll-Conray gradient.
4. Ficoll-Conray gradient is prepared as follows: mix Conray 420 (33% [w/v] solution in water on the basis of sodium iothalamate content) to a 9% solution of Ficoll 400 in normal saline until the density of the mixture is 1.08 g/mL
5. Layer a total of 1 mL of the cell suspension (50% hematocrit) carefully on top of the 2 mL of gradient in the glass tube (5 mL).
6. Centrifuge at 300*g* for 10 min at 20 ± 2°C.
7. Aspirate off the infected cells from the top and wash several times with Tris-buffered saline (10 m*M* Tris-HCl containing a 50 m*M* NaCl, pH 7.4) (*see* **Note 28**).

8. Incubate approx 65×10^6 erythrocytes with doubly radiolabeled liposomes (100–500 nmol of lipid P) at 37°C for 30 min.
9. After incubation, pellet the cells and wash extensively with ice-cold, sucrose-supplemented TBS and count for radioactivity (*see* **Note 27**).

4. Notes

1. It is important to ascertain the specific binding of the $F(ab')_2$ liposomes both in vitro and in vivo before examining their therapeutic efficacies.
2. The demonstrated biologic response of chloroquine-laden targeted liposomes may further be enhanced by doing one or a combination of the following variations:
   a. Use antibody-bearing long-circulatory liposomes ***(33–35)*** rather than conventional liposomes.
   b. Enhance nonspecific host resistance to infections caused by a variety of organisms ***(36,37)***. In one of our studies ***(38)***, we have shown that in *P. berghei* infections, the mortality rate and parasitemias were significantly reduced and the mean survival time was considerably enhanced by pretreating the mice with tuftsin-bearing liposomes.
   c. The concentration of chloroquine in erythrocytes infected with chloroquine-resistant malaria can be increased by encapsulating an appropriate Ca^{2+}-channel blocker along with the chloroquine, which in turn should increase the antimalarial activity ***(6)***.
   d. Finally, change the route of administration ***(24)***.
3. The plate is developed in chloroform:methanol:water (65:25:4; v/v) and the lipid spots are identified by staining them with iodine vapor followed by phosphate-specific molybdenum-blue spray.
4. Recrystallize the cholesterol three times from methanol.
5. In our original papers ***(22,23,25)***, we used sonicated liposomes, but if your laboratory is equipped with an extruder we see no reason why you can not use extruded liposomes as long as they are approx 60 nm in diameter.
6. For the most efficient sonication, it is advisable to hold the liposomal suspension in the sonication vial and immerse the probe in suspension approx 3.0 mm below the surface.
7. In order to have nitrogen free of oxygen and moisture, it should be passed through three traps, attached in series, containing pyrogallol solution (20%, w/v), nothing, and sulfuric acid respectively.
8. Since a large amount of heat is generated in the sonication process, the sonication vial containing the material should be immersed in a cooling bath (temperature approx 4°C).
9. Wear earplugs while doing sonication.
10. Great care must be taken not to leave any titanium particles from the preparation because they are very toxic.
11. In our laboratory, we routinely measure the size of the liposomes by negative stain electron microscopy but if you have the access to a particle size you will get the results quickly.

12. The chloroquine absorbance at 342 nm is unaffected by the presence of liposomes and detergent, and is linear at least up to 100 µg quantity of chloroquine.
13. Since protein absorbance interferes with accurately determining the amount of chloroquine entrapped in antibody-bearing liposomes, i.e., the chloroquine should be measured prior to the liposome coupling to $F(ab')_2$ fragments.
14. It is important to know the position of drug in the liposomes, i.e., whether the drug is entrapped in the liposome aqueous core or intercalated within the membrane because in the later case it can cause marked changes in the physical properties of the liposome membranes. Polar drugs are released from the liposomes when the bilayer membrane is breached, whereas nonpolar drugs remain affiliated with the liposomes unless there is a gross disruption of the membrane structure. In the case of chloroquine it resides in the internal aqueous phase rather than the lipid bilayer.
15. In our typical preparation, we get approx 140 µg of chloroquine/µmol of lipid P.
16. The description is beyond the scope of this chapter; *see* **ref. *32***.
17. In our original papers ***(22,23,25)*** we used lactoperoxidase-catalyzed radioiodination. If you prefer to use another method of iodination then we strongly recommend comparing the biological activity, before and after the radioiodination of the $F(ab')_2$ fragments, by hemagglutination ***(39)***.
18. We use dialysis because it works quite satisfactorily but if you prefer to use gel filtration we do not see any reason why you should not. However, it is a good idea to check the biological activity.
19. In our typical coupling experiment we obtain a protein-to-lipid ratio of approx 85 µg protein/µmol lipid P.
20. It is important to check the status of chloroquine in liposomized preparation before injecting into the animals. No leakage of the chloroquine from the liposomes is detected under these conditions.
21. We adapted this method from **ref. *40***.
22. Parasitemia is determined by counting 10^3 parasitized red cells in a thin blood smear stained with Giemsa and expressed as number of parasitized cells/100 erythrocytes.
23. It is important to keep the mice under constant drug pressure and check the resistant character of chloroquine from time to time.
24. The strain used in our original papers ***(23,25)*** retained chloroquine-resistant character even after withdrawing the drug pressure for a year.
25. The liposomes are doubly radiolabeled by attaching ^{125}I- labeled $F(ab')_2$ fragments to the surface and entrapping [^{14}C]inulin in the aqueous compartment.
26. The total amount of radioactivity injected in animals is calculated from the 2 min values by assuming total blood volume as 8% of the body weight ***(21)***.
27. The amount of cell-associated ^{125}I is determined without disrupting the cells, whereas for measuring ^{14}C the cells are lysed with Triton X-100 (1%). It is important to duly correct the ^{14}C counts for quenching by hemoglobin.
28. We usually get the infected erythrocyte preparation contaminated with ≤3% normal erythrocytes.

Acknowledgments

We thank Drs. M. Owais, A. Choudhury, G. C. Varshney, A. Singhal, and S. Chandra for their help in the work and Walter Reed Army Institute, Washington DC, for kindly providing us chloroquine diphosphate.

References

1. Butler, D., Maurice, J., and O'Brien, C. (1997) Time to put malaria control on the global agenda. *Nature* **386,** 535–540.
2. Schapira, A., Beales, P. F., and Halloran, M. E. (1993) Malaria: living with drug resistance. *Parasitol. Today* **9,** 168–174.
3. Ward, S. A. (1988) Mechanisms of the chloroquine resistance in malaria chemotherapy. *Trends Pharmacol.* Sci. **9,** 241–246.
4. Cowman, A. F. (1991) The P-glycoprotein homologues of *Plasmodium falciparum*: are they involved in chloroquine resistance? *Parasitol. Today* **7,** 70–76.
5. Martin, S. K. (1993) Chloroquine-resistance *Plasmodium falciparum* and the MDR phenotype. *Parasitol. Today* **9,** 278,279.
6. Macomber, P. B., O'Brien, R. L., and Hahn, F. E. (1966) chloroquine: physiological basis of drug resistance in *Plasmodium berghei*. *Science* **152,** 1374.
7. Verdier, F., Le Bras, J., Clavier, F., Hatin, I., and Blayo, M. (1985) Chloroquine uptake by *Plasmodium falciparum*-infected human erythrocytes during *in vitro* culture and its relationship to chloroquine resistance. *Antimicrob. Agents Chemother.* **27(4),** 561–564.
8. Martin, S. K., Oduola, A. M. J., and Milhous, W. K. (1987) Reversal of chloroquine resistance in *Plasmodium falciparum* by verapamil *Science* **235,** 899–901.
9. Fitch, C. D. (1969) Chloroquine resistance in malaria: a deficiency of chloroquine binding. *Proc. Natl. Acad. Sci. USA* **64(4),** 1181–1187.
10. Chan, A. C., Chevli, R., and Fitch, C. D. (1980) Ferriprotoporphyrin IX fulfils the criteria for identification as the chloroquine receptor of malaria parasites. *Biochemistry* **19,** 1543–1549.
11. Green, R. and Widder, K. J. (1987) *Methods in Enzymology, Drug and Enzyme Targeting*, Vol. 149, Academic, San Diego, CA, pp. 51–213.
12. Ram, B. P. and Tyle, P. (1987) Immunoconjugates: applications in targeted drug delivery for cancer therapy. *Pharm. Res.* **4(3),** 181–188.
13. Ranade, V. V. (1991) Drug delivery systems. 6. Transdermal drug delivery. *J. Clin. Pharmacol.* **31(5),** 401–418.
14. Agarwal, A., Kandpal, H., Gupta, H. P., Singh, N. B., and Gupta, C. M. (1994) Tuftsin-bearing liposomes as refampin vehicles in treatment of tuberculosis in mice. *Antimicrob. Agents Chemother.* **38,** 588–593.
15. Gregoriadis, G., ed. (1988) *Liposomes as Drug Carriers: Recent Trends and Progress.* Wiley, Chichester, UK.
16. Wang, C. Y. and Huang, L. (1989) Highly efficient DNA delivery mediated by pH-sensitive immunoliposomes. *Biochemistry* **28(24),** 9508–9514.
17. Ghosh, P. C. and Bachhawat, B. K. (1991) Targeting of liposomes to hepatocytes, in *Liver Diseases: Diagnosis and Therapy Using Specific Receptor and Ligands* (Wu, G. Y. and Wu, C. H., eds.), Marcel Dekker, New York, pp. 87–103.

18. Pagano, R. E. and Weinstein, J. N. (1978) Interactions of liposomes with mammalian cells. *Annu. Rev. Biophys. Bioeng.* **7,** 435–468.
19. Eytan, G. D., Broza, R., Notsani, B., Dachir, D. and Gad, A. E. (1982) Interaction of acidic liposomes with red blood cells. Induction of endocytosis and shedding of particles. *Biochim. Biophys. Acta* **689,** 464–474.
20. Singhal, A., Bali. A, and Gupta, C. M. (1986) Antibody-mediated targeting of liposomes to erythrocytes in whole blood. *Biochim. Biophys. Acta* **880,** 72–77.
21. Singhal, A. and Gupta, C. M. (1986) Antibody-mediated targeting of liposomes to red cells in vivo. *FEBS Lett.* **201,** 321–326.
22. Agrawal, A. K., Singhal, A., and Gupta, C. M. (1987) Functional drug targeting to erythrocytes in vivo using antibody-bearing liposomes as drug vehicles. *Biochem. Biophys. Res. Commun.* **148,** 357–361
23. Chandra, S., Agrawal, A. K., and Gupta, C. M. (1991) Chloroquine delivery to erythrocytes in *Plasmodium berghei*-infected mice using antibody-bearing liposomes as drug vehicles. *J. Biosci.* **16,** 137–144.
24. Peeters, P. A. M., Huiskamp, C. W. E. M., Eling, W. M. C., and Crommelin, D. J. A. (1989) Chloroquine containing liposomes in the chemotherpaty of murine malaria. *Parasitology* **98,** 381–386.
25. Owais, M., Varshney, G. C., Choudhury, A., Chandra, S., and Gupta, C. M. (1995) Chloroquine encapsulated in malaria-infected erythrocytes-specific antibody-bearing liposomes effectively controls chloroquine-resistant *Plasmodium berghei* infections in mice. *Antimicrob. Agents Chemother.* **39,** 180–184.
26. Sherman, I. W. (1985) Membrane structure and function of malaria parasites and the infected erythrocytes. *Parasitology* **91,** 609–645.
27. Sherman, I. W. and Winogard, E. (1990) Antigens on *Plasmodium falciparum* infected erythrocytes are not parasite derived. *Parasitol. Today* **6,** 317–320.
28. Howard, R. J. and Pasloske, B. L. (1993) Target antigens for asexual malaria vaccine development. *Parasitol. Today* **9,** 369–372.
29. Newbold, C. I. and Marsh, K. (1990) Antigens on the *Plasmodium falciparum* infected erythrocytes surface are parasite derived. A reply. *Parasitol. Today* **6,** 320–322.
30. Gupta, C. M. and Bali, A. (1981) Carbamyl analogs of phosphatidylcholines: synthesis, interaction with phospholipases and permeability behaviour of their liposomes. *Biochim. Biophys. Acta* **663,** 506–515.
31. Stocker, J. W., Forstes, H. K., Miggiano, V., Stahli, C., Straiger, G., Takacs, B., and Staechelin, T. (1982) Generation of two mouse myeloma cell lines "PAI" and "PAI-O" for hybridroma production. *Res. Disclosure* **217,** 155–157.
32. Perlman, H., Berzins, K., Wahlgren, M., Carlsson, J., Bjorkmin, A., Patarroyo, M. E., and Perlmaann, P. (1984) Antibodies in malarial sera to parasite antigens in the membrane of erythrocytes infected with early asexual stages of *Plasmodium falciparum J. Exp. Med.* **159,** 1686–1704.
33. Agrawal A. K. and Allen, T. M. (1992) Attachment of antibodies to pegylated liposomes by the biotin-avidin method. *Biophys. J.* **61,** A493.
34. Allen, T. M., Agrawal A. K., Ahmad, I., Hansen, C. B., and Zalipsky, S. (1994) Antibody-mediated targeting of long-circulating (StealthR) liposomes. *J. Lipos. Res.* **4(1),** 1–25.

35. Francis, G. E., Delgado, C., Fisher, D., Malik, F., and Agrawal, A. K. (1996) Polyethylene glycol modification: relevance of improved methodology to tumour targeting. *J. Drug Targeting* **3,** 321–340.
36. Coune, A. (1988) Liposomes as drug delivery system in the treatment of infectious diseases. Potential applications and clinical experience. *Infection* **16,** 141–147.
37. Guru, P. Y., Agrawal, A. K., Singha, U. K., Singhal, A., and Gupta, C. M. (1989) Drug targeting in *Leishmania donovani* infections using tuftsin-bearing liposomes as drug vehicles. *FEBS Lett.* **245,** 204–208.
38. Gupta, C. M., Puri, A., Jain, R. K., Bali, A., and Anand, N. (1986) Protection of mice against *Plasmodium berghei* infection by a tuftsin derivative. *FEBS Lett.* **205,** 351–354.
39. Garvey, J. S., Natalie, E. C., and Sussadoff, D. H. (1981) Hemagglutination in *Methods in Immunology*. Benjamin/Cummings Publishing Co., Menlo Park, CA, pp. 347–371.
40. Warhurst, D. C. and Folwell, R. O. (1968) Measurement of growth rate of the erythrocytes stages of the *Plasmodium berghei* and comparisons of the potency of inocula after various treatments. *Ann. Trop. Med. Parasitol.* **62,** 349–360.

14

Immunotargeting of Catalase to the Pulmonary Vascular Endothelium

Vladimir R. Muzykantov

1. Introduction

Hydrogen peroxide formed in the lung tissue in ischemia/reperfusion or released from activated leukocytes causes oxidative injury of the vascular endothelial cells ***(1–3)***. H_2O_2-degrading enzyme, catalase, has been extensively explored in order to protect cells and tissues against H_2O_2-mediated injury ***(4)***. Catalase, however, has short lifetime in the bloodstream and provides only marginal protective effect after intravascular administration in animals ***(5)***. Catalase modification (conjugation with polyethylene glycol ***(6)*** or encapsulation in liposomes ***[7]***), prolongs catalase lifetime in the circulation and facilitate its cellular uptake. These modifications, however, do not provide it with an affinity to the endothelial cells. In order to provide catalase with such an affinity, catalase could be chemically conjugated with a carrier antibodies recognizing the surface endothelial antigens ***(8)***. A monoclonal antibody (MAb) against such an antigen, angiotensin-converting enzyme (anti-ACE MAb 9B9, produced by Dr. Sergei M. Danilov ***[9]***), accumulates in the pulmonary endothelium after systemic injection ***(10)***. Therefore, MAb 9B9 may serve as an affinity carrier for targeting of catalase to the pulmonary endothelial cells, for specific augmentation of their antioxidative defense.

Streptavidin–biotin crosslinker seems to be an appropriate tool for the conjugation of catalase with MAb 9B9 (and other potentially appropriate carriers). Streptavidin, a 60-kDa protein, possesses four high affinity binding sites for vitamin biotin ***(11)***. Proteins, sugars, nucleic acids, and other biomolecules can be biotinylated using a variety of biotin derivatives and thus the streptavidin/biotin pair gained a high profile in biomedicine as a universal crosslinking agent ***(12)***. During the last decade the streptavidin/biotin pair has been suc-

From: *Methods in Molecular Medicine, Vol. 25: Drug Targeting: Strategies, Principles, and Applications*
Edited by: G. E. Francis and C. Delgado

cessfully utilized for various in vivo applications, such as gamma-immunoscintigraphy ***(13)***, blood clearance ***(14)***, and drug targeting ***(15,16)***. Streptavidin is a nontoxic protein and causes no harmful reactions in laboratory animals or in human patients ***(13)***. In previous studies we have documented that both biotinylated anti-ACE MAb 9B9 (b-MAb 9B9) and radiolabeled streptavidin conjugated with b-MAb 9B9 accumulate in the rat lungs after systemic injection ***(17,18)***.

This chapter summarizes results reported in our recent publications ***(17–20)*** and describes the methodology for catalase conjugation to a carrier antibody, evaluation of the antigen-binding and H_2O_2-degrading capacity of the antibody–catalase conjugate in vitro, and characterization of biodistribution, pulmonary uptake, and blood clearance of the conjugate after intravascular administration in rats.

Both catalase and antibody were biotinylated with 6-biotinylaminocaproic acid *N*-hydroxysuccinimide ester. Biotinylated catalase (b-catalase) was conjugated with biotinylated antibody (b-Ab) via streptavidin (SA). Neither biotinylation nor conjugation with SA markedly reduced enzymatic activity of catalase and antigen-binding capacity of b-Ab. Antibody-conjugated radiolabeled b-catalase specifically bound to the antigen-coated plastic wells. Substitution of b-Ab with control b-IgG abrogated the binding. H_2O_2 was degraded specifically in the antigen-coated wells preincubated with antibody–catalase conjugate. Results of in vivo experiments demonstrate that MAb 9B9-catalase conjugate accumulates in the rat lungs. These results imply that the described methodology is useful for the development of a novel strategy for the targeting of antioxidants to the pulmonary vascular endothelium.

2. Materials

1. Buffer solutions: Components of buffer solutions are available from Sigma (St. Louis, MO). Phosphate-buffered saline (PBS) contains 20 m*M* NaH_2PO_4 and has pH 7.4 (PBS); borate-buffered saline (BBS) contains 20 m*M* boric acid, pH 8.1. Where indicated, either buffer contained 2 mg/mL bovine serum albumin (PBS-BSA or BBS-BSA).
2. Catalase: There are several commercially available preparations of catalase, with specific activity ranging from 2000 U/mg to 60,000 U/mg. In the present study we have used lyophilized catalase purified from bovine liver (20,000 U/mg) from Fluka (Ronkonkoma, NY). Stock solution of catalase in BBS (10 mg/mL) is stable for several weeks at 4°C. Freezing/thawing, however, leads to precipitation of catalase and loss of enzymatic activity.
3. Antibodies and immunoglobulins: Goat polyclonal antibody against mouse IgG and mouse IgG are available from Calbiochem (San Diego, CA). Preparation and properties of mouse MAb against angiotensin-converting enzyme (anti-ACE MAb 9B9) were described previously ***(9,10,17)***. Briefly, MAb 9B9 is a mouse

IgG_1 type MAb crossreacting with human and rat ACE. This MAb does not inhibit ACE enzymatic activity and does not induce endothelial injury either in cell culture or in vivo ***(21,22)***. Preparations of immunoglobulins and antibodies are stable in BBS for several months at –20°C (without freezing/thawing recycling) or for several weeks at 4°C.

4. Streptavidin (SA) and biotin ester: Streptavidin and 6-biotinylaminocaproic acid *N*-hydroxysuccinimide ester (BxNHS) are available from Calbiochem. Streptavidin (SA) stock solution (10 mg/mL in BBS) is stable for several months at –20°C or for several weeks at 4°C. BxNHS provides covalent coupling of biotin residue(s) to amino group(s) of proteins ***(11)***. Stock solution of 0.1 *M* BxNHS in anhydrous dimethyl formamide must be used fresh.
5. Miscellaneous reagents. Sodium [^{125}I]iodine was from Amersham (Arlington Heights, IL).
6. Iodogen is available from Pierce (Rockford, IL).
7. Sephacryl S-200HR is available from Pharmacia-LKB.
8. Dimethyl formamide (DMF), bovine serum albumin (BSA), and trichloroacetic acid (TCA) are available from Sigma (St. Louis, MO).
9. Protein concentration was determined by Bio-Rad protein microassay kit (Hercules, CA).

3. Methods

3.1. Biotinylation of Proteins

The procedure for biotinylation of antibodies and catalase, as well as the analysis of streptavidin-binding properties of biotinylated proteins have been described in detail in recent publications ***(17,20)***.

1. Prepare solutions of an antibody, IgG, or catalase (2 mg/mL in BBS).
2. Add 10 µL of fresh 10 m*M* BxNHS to 1 mL of immunoglobulin solution.
3. Add 15 µL of fresh 10 m*M* BxNHS to 1 mL of catalase solution.
4. After 1 h incubation on ice, dialyze proteins against BBS.

3.2. Determination of Catalase Activity

Determine catalase activity by measuring the rate of hydrogen peroxide decomposition.

1. Prepare 50 mL of fresh 10 m*M* H_2O_2 solution in water, make a serial dilution to cover in the range of 0.1–10 m*M*, and determine the calibration curve of H_2O_2 optical density at 234 nm against water. Keep the stock solution of 10 m*M* H_2O_2 on ice.
2. Add catalase, biotinylated catalase, or b-catalase conjugated with streptavidin (0.5–5 µg of catalase per 10 µL sample) into a cuvet containing 3 mL of a 10 m*M* solution of H_2O_2, mix well and measure the optical density in the cuvet at 234 nm for 3 min after catalase addition.
3. From the linear part of the curve calculate catalase activity as units per milligram of protein (1 U decomposes 1 µ*M* of H_2O_2/min).

3.3. Radiolabeling of Proteins

Use iodogen-coated tubes for radioiodination of streptavidin and b-catalase. The iodo-beads technique, described in the recommendations of the manufacturer (Pierce) is also suitable and offers similar results.

1. Dissolve 1 mg of iodogen in 1 mL of anhydrous chloroform, add 100 µL of this solution to a 5-mL glass tube, and evaporate chloroform under nitrogen gas.
2. Add 100 µL of 1 mg/mL protein solution in BBS and 100 µCi of Na[^{125}I] in the iodogen-coated glass tube.
3. Incubate for 20 min on ice with periodic gentle shaking.
4. Dialyze radiolabeled protein against BBS.
5. The procedure yields radioiodinated proteins with a specific radioactivity of approx 500 cpm/ng of streptavidin and 50 cpm/ng of catalase.
6. To assess free iodine and/or degraded protein, add 1 µL of radiolabeled protein to 1 mL of PBS-BSA.
7. Add 200 µL of 100% TCA to the sample, vortex the sample, incubate 30 min on ice, and centrifuge 15 min at 2500 rpm (1300*g*).
8. Count the supernatant and pellet separately and calculate the percentage of TCA-precipitable radioactivity. More than 95% of radiolabeled proteins should be precipitable by TCA.

3.4. Immobilization of Proteins in Plastic Wells and Binding Assay

For the determination of binding properties of biotinylated proteins and conjugates, use flexible 96-wells microplates (Nunc). The general design of the method is similar to classical enzyme-linked immunosorbent assay (ELISA) and RIA methods. Use the described procedure for immobilization of streptavidin, antigen, biotinylated or nonmodified antibody, or catalase.

1. Add 100 µL of BBS containing 10 µg/mL of a protein per well and incubate overnight at 4°C. Protein-coated wells may be stored for 1 wk at 4°C.
2. Before the binding assay, eliminate an excess of nonbound protein by washing with water.
3. Block nonspecific binding sites by 1 h incubation with 200 µL BBS-BSA in the wells. Use these wells to determine binding of radiolabeled ligand(s) in direct radioimmunoassay. For example, to determine streptavidin-binding ability of biotinylated proteins (b-catalase or b-antibody), use SA-coated plastic wells.
4. Add 100 µL of BBS-BSA containing serial dilutions of radiolabeled biotinylated protein (1–1000 ng/well) in the SA-coated wells. To control the specificity of binding, use SA-free wells coated with albumin.
5. After 1 h incubation at room temperature eliminate nonbound radiolabeled protein by extensive washing with distilled water.
6. Cut the wells and determine radioactivity bound in the wells in a gamma-counter.

3.5. Conjugation of b-Catalase to b-Antibody via Streptavidin and Determination of Binding Capacity of the Conjugate

To conjugate b-catalase with b-antibody we recommend using a two-step procedure, described in our recent publications ***(19,20)***. The purpose of the first step is to conjugate b-catalase with streptavidin, to form bimolecular complex SA/b-catalase possessing high residual biotin-binding capacity useful for attachment of b-antibody (*see* **Notes 1** and **2**).

1. Mix 2 mg radiolabeled b-catalase with 5 mg streptavidin in 2 mL BBS and incubate 1 h on ice.
2. Any excess of free streptavidin is removed by gel-filtration using a Sephacryl S-200 HR column (60 mL). Collect the void volume peak (approx 22–25 mL fractions). This peak contains the SA/b-catalase complex.
3. To determine the biotin-binding capacity of the complex, prepare b-IgG-coated wells as described in **Subheading 3.4.**
4. Incubate 100 µL of the initial SA:b-catalase mixture or 100 µL of gel-filtration fractions containing 1–1000 ng SA/b-catalase in the b-IgG-coated wells or in albumin-coated wells for 1 h at room temperature.
5. Eliminate nonbound material by washing with distilled water and measure ^{125}I bound in the wells in a gamma-counter.
6. Select fractions possessing the highest b-IgG-binding ability for the resulting conjugation with biotinylated antibody.

The purpose of the second step of the conjugation procedure is to conjugate the bimolecular complex ^{125}I-labeled SA/b-catalase to b-Ab or control b-IgG utilizing residual biotin-binding sites of SA/b-catalase complex.

1. Mix 100 µL of BBS-BSA containing 50 µg of b-Ab or b-IgG with an equal volume of SA/b-catalase complex containing 25 µg of radiolabeled b-catalase.
2. One hour incubation on ice provides b-Ab/SA/b-catalase conjugates stable for several days at 4°C.

3.6. In Vitro Assessment of Antigen-Binding Ability and H_2O_2-Degrading Activity of b-Antibody/SA/b-Catalase Conjugate

To determine antigen-binding and H_2O_2-degrading properties of the b-Ab/SA/b-catalase conjugate, use the plastic wells of 24-well "Multiwell" cultural plates (Nunc) coated with an antigen (*see* **Note 3**). To control the specificity of binding, use albumin-coated wells.

1. Add 1 µg of b-Ab/SA/b-catalase or b-IgG/SA/b-catalase conjugates containing radiolabeled catalase in 0.5 mL of BBS-BSA per well.
2. After 1 h incubation at room temperature eliminate nonbound conjugates by washing.

3. Add 1 mL of 10 m*M* H_2O_2 solution per well and incubate for 5 min at room temperature. Each minute withdraw a sample of H_2O_2 solution from the well and measure absorbance at (A234 nm), to determine the rate of H_2O_2 decomposition by the antigen-bound catalase as detailed above (*see* **Subheading 3.2**.).
4. Thereafter eliminate solution from the wells, add 1 mL of 1 *N* NaOH, and measure radioactivity in the eluates by gamma-counting to quantitate binding of catalase to the immobilized antigen.

3.7. Intravenous Injection of b-MAb 9B9/SA/b-Catalase Conjugate in Rats and Characterization of Its Biodistribution, Pulmonary Uptake, and Blood Clearance

Use male Wistar or Sprague-Dowley rats. Results are more reproducible in young (200–250 g) e.g., animals. It is important to use pathogen-free animals, since pulmonary disorders (pneumonia) markedly affect the pulmonary uptake of radiolabeled anti-ACE MAb 9B9 ***(10)***. Devote at least four animals in each experimental group (*see* **Note 4**).

1. Inject 200 µL of pentobarbital solution intraperitoneally and wait 10–20 min to obtain sufficient anesthesia.
2. Inject via the tail vein 0.3–0.5 mL of PBS-BSA containing 1–5 µg of catalase, b-catalase, SA/b-catalase, b-MAb 9B9/SA/b-catalase, or b-IgG/SA/b-catalase. These preparations must contain radiolabeled catalase (or b-catalase) as a tracer. Total radioactivity of injected catalase (i.e., injected dose, ID) should be in the range 5×10^5–5×10^6 cpm per rat.
3. One hour after injection (or at an otherwise indicated time) open the peritoneal cavity and add 0.5 mL of heparin solution into the cavity.
4. Cut the descending aorta and collect 5 mL of blood from the cavity.
5. Harvest the internal organs (kidney, spleen, liver, heart, lungs, and other organs of interest).
6. Rinse organs with saline and gently blot with a filter paper.
7. Count ^{125}I radioactivity of 1 mL blood and plasma, as well as of tissue pieces (about 1 g each) in a gamma-counter and weigh the tissue samples to calculate radioactivity per gram of tissue.

3.8. Conclusion

This chapter describes the methodology for conjugation of catalase to a carrier antibody and properties of the conjugate in vitro and in vivo. Our results indicate that streptavidin/biotin crosslinker offers an antibody–catalase conjugate possessing antigen-binding and hydrogen peroxide degrading activities. Catalase conjugated with an MAb against angiotensin-converting enzyme accumulates in the rat lungs after iv injection. The specificity of the pulmonary targeting of anti-ACE/catalase is extremely high; immunospecificity (i.e., ratio between pulmonary uptake of immune and nonimmune conjugates) is equal to

100. Such a high specificity, prolonged pulmonary retention of the targeted catalase and high effectiveness of the targeting (up to 10% of injected dose accumulates in the lung) provide a valid background for the assessment of the functional (therapeutic) effects of the targeting. Our recent results document that other monoclonal antibodies against the surface endothelial antigens also are capable of pulmonary delivery of catalase. For example, catalase conjugated with a MAb against intercellular adhesion molecule-1 (anti-ICAM-1) also accumulates in the rat lungs after iv injection ***(23)***. Our recent data show that anti-ACE MAb 9B9-catalase and anti-ICAM-1-catalase both afford significant augmentation of antioxidant defense in the lung and protect perfused rat lungs against oxidative insult ***(24)***. Therefore, conjugation of catalase to a carrier antibody and pulmonary targeting of the antibody-conjugated catalase represent a background for the exploration of a novel strategy for specific protection of the pulmonary vasculature against oxidative stress.

4. Notes

1. Modification of proteins with streptavidin-biotin crosslinker: Both avidin and streptavidin possess four high-affinity biotin-binding sites ***(11)***. Avidin, however, is a positively charged glycoprotein; both charge and sugar moiety mediate its high nonspecific binding ***(12)***. For this reason, streptavidin, a neutral protein of bacterial origin, is more widely used as a crosslinker for biotinylated compounds ***(12)***.

   There are several commercially available biotin derivatives for biotinylation of proteins. In this study we used 6-biotinylaminocaproic acid *N*-hydroxysuccinimide ester (BxNHS). BxNHS provides covalent coupling of biotin residue(s) to amino group(s) of proteins ***(12)***. Biotin binding sites of streptavidin are located in the invaginations of the streptavidin molecule and, therefore, the protein-coupled biotin residue(s) interacts with the streptavidin biotin-binding site less effectively than noncoupled biotin ***(11)***. BxNHS provides a spacer between the modified amino group and biotin residue and thus enhances steric accessibility of the protein-coupled biotin residue(s) for interaction with biotin-binding sites of streptavidin ***(12)***. This is important in the context of strong steric and stoichiometric limitations imposed on the formation of an active b-antibody/SA/b-catalase conjugate and its interaction with the target antigen.

   There are several methods to assess degree of protein biotinylation. For example, titration of protein amino groups with TNBS before and after biotinylation allows estimation of the total number of biotin residues coupled per protein molecule ***(12)***. However, only streptavidin-accessible biotin residues localized on the surface of biotinylated protein contribute to its conjugation with streptavidin. To determine such accessible biotin residues we utilize direct solid-phase radioassay of binding of radiolabeled streptavidin to immobilized biotinylated protein (or vice versa) ***(17)***.

   Modification with BxNHS provides both MAb 9B9 and catalase with streptavidin-binding ability ***(17,20)***. Biotinylation at high BxNHS:protein ratio,

however, leads to marked loss of catalase enzymatic activity and antigen-binding ability of MAb 9B9. Importantly, biotinylation of either protein at BxNHS:protein molar ratios in the range of 1–20 does not lead to significant inactivation of either catalase or the antibody. Binding of streptavidin to b-catalase does not affect the enzymatic activity. This result implies that either biotin residues are localized remotely from the catalase active center or that attachment of streptavidin does not inhibit interaction of catalase with its small substrate, hydrogen peroxide. Enzymatic activity of b-catalase was indistinguishable from that of nonmodified catalase (19,900 U/mg) and conjugation with streptavidin did not affect enzymatic activity of b-catalase.

2. Conjugation of biotinylated catalase with biotinylated antibody via streptavidin: At the first step of the conjugation, we generate SA/b-catalase complex possessing residual biotin-binding sites. Those sites will be further used for SA/b-catalase conjugation with a biotinylated carrier antibody. SA/b-catalase complexes formed at low SA:b-catalase ratio display low residual biotin-binding capacity, presumably because of the occupation of most of biotin-binding sites of streptavidin with biotin residues of b-catalase ***(20)***. In contrast, at high SA:b-catalase ratios, nonconjugated streptavidin competes with SA/b-catalase for binding with b-IgG. To eliminate nonconjugated streptavidin, we performed a Sephacryl S-200HR gel filtration of the SA/b-catalase complex formed at SA:b-catalase molar ratios equal to 10. After the conjugation with streptavidin, the major portion of ^{125}I-labeled b-catalase elutes as a single high-mol-wt peak containing SA/b-catalase bimolecular complex in the excluded volume of the column. This result implies that effectiveness of the conjugation at these conditions is high and the product contains a minor amount of free b-catalase. Elimination of free streptavidin by gel filtration allows one to obtain SA/b-catalase complex capable of interaction with biotinylated antibodies. Therefore, incubation of SA/b-catalase with b-antibody or b-IgG (the second step of the conjugation) provides a trimolecular complex b-Ab/SA/b-catalase (or b-IgG/SA/b-catalase).
3. In vitro properties of the b-Ab/SA/b-catalase conjugate: Potentially biomedical important antigens (e.g., purified human angiotensin-converting enzyme) are often unavailable or too expensive for preparation of the antigen-coated plastic wells. To determine the antigen-binding properties of a b-Ab/SA/b-catalase conjugate in vitro, we utilized b-catalase conjugated with commercially available biotinylated goat antibody against mouse IgG. Therefore, this antibody and mouse IgG were utilized in this part of the study as a "generic" antibody/antigen pair. Accordingly, we used plastic wells of 24-well cultured plastic "Multiwell" (Nunc) coated with nonmodified mouse IgG as a model antigen coating. To assess the formation of a trimolecular b-Ab/SA/b-catalase conjugate and its antigen-binding capacity, we determined its binding to mouse IgG-coated plastic wells by measuring the radioactivity of b-catalase bound in the wells. **Table 1** shows that b-Ab/SA/b-catalase conjugate binds specifically to the antigen-coated wells, but does not bind to the albumin-coated wells. When b-antibody was substituted with control b-IgG, the conjugate bound to neither antigen-coated nor albumin-coated

Table 1
Binding of the Antibody-Conjugated Catalase to the Immobilized Antigen[a]

	Antigen	Albumin
Antibody-catalase	14.7 ± 0.3 ng/well	0.4 ± 0.3 ng/well
IgG-catalase	0.4 ± 0.2 ng/well	0.2 ± 0.1 ng/well

[a]Radiolabeled b-catalase has been conjugated to b-antibody against mouse IgG (antibody–catalase) or to b-IgG (IgG-catalase), using streptavidin as a crosslinker as described in **Subheading 3.5.** Plastic wells were coated with the antigen (mouse IgG) or with albumin as described in **Subheading 3.4.** The conjugates were incubated in the wells for 1 h at room temperature. After extensive washing of the nonbound conjugates, radioactivity bound in the wells has been determined in a gamma-counter. The data are shown as M ± SD, $n = 3$. *See* **Subheading 3.6.** for a complete description of the procedure.

wells. Therefore, conjugation of b-antibody with SA/b-catalase complex does not eliminate antigen-binding ability of b-antibody and streptavidin-mediated conjugation of b-catalase to b-antibody provides the enzyme with an affinity to the immobilized antigen. Presumably, interaction of the antibody–catalase conjugate with immobilized antigen is under stronger steric limitations than interaction with soluble antigen. Therefore, the experimental design described in this section is specifically important in terms of in vitro evaluation of the conjugate affinity to cellular or tissue antigens possessing limited steric accessibility for the antibodies.

In order to test H_2O_2-degrading activity of the antigen-bound b-Ab/SA/b-catalase, we incubated H_2O_2 in the antigen-coated wells preincubated with the conjugate. **Table 2** shows that antigen-bound complex degrades H_2O_2 in the wells. There was no detectable degradation of H_2O_2 in the antigen-coated wells preincubated with nonimmune counterpart (b-IgG/SA/b-catalase), because of the lack of binding of this preparation to either antigen-coated or albumin-coated wells (*see* **Table 1**).

4. Pulmonary targeting of catalase conjugated with anti-ACE MAb 9B9: We recommend calculating the following indices of the tissue distribution of the radiolabeled catalase: percentage of injected radioactivity per gram of tissue (% ID/g), ratio of radioactivity per gram of tissue to that of blood (localization ratio), or ratio of radioactivity per gram of tissue after injection of antibody-conjugated catalase to that after injection of IgG-conjugated catalase (immunospecificity index). These three indices characterize effectiveness, tissue selectivity, and specificity of the targeting.

   As rapidly as 1 h after iv injection of radiolabeled catalase, the blood level of radioactivity was equal to 0.5 ± 0.02% ID/g of blood. Assuming that the total blood weight in rat is equal to about 15 g (i.e., 7% of the total body weight, 250 g), this result means that <10% of injected catalase circulates in the bloodstream 1 h

Table 2
Decomposition of Hydrogen Peroxide in the Antigen-Coated Wells by Antibody-Conjugated Catalase[a]

Time of H_2O_2 incubation	0 min	5 min
Antibody-catalase	9.7 ± 0.1	7.8 ± 0.3[b]
IgG-catalase	9.8 ± 0.2	9.7 ± 0.1

[a]Experimental protocol described in **Subheading 3.6.** IgG-catalase conjugate or antibody-conjugated catalase were incubated in the antigen-coated wells for 1 h. After elimination of nonbound conjugate, 10 mm H_2O_2 was incubated in the wells for 5 min. Numbers show m*M* concentrations of H2O2 in the wells at zero time and after 5 min incubation in the wells. The data are shown as M ± SD, $n = 3$. Note that the antibody–catalase conjugate bound to the immobilized antigen decomposes H_2O_2 in the wells. The difference between 0 and 5 min is statistically significant for immune conjugate.

[b]$p < 0.05$.

after injection. This result corroborates with literature data that the enzyme undergoes fast elimination from the bloodstream ***(4,5)***. Modification of catalase with biotin and conjugation with streptavidin significantly prolong its lifetime in the bloodstream: 1.4+0.25% and 2.1 ± 0.13% ID/g of b-catalase or SA/b-catalase were found in the blood 1 h after injection. None of the preparations, however, demonstrated pulmonary uptake. Pulmonary radioactivity was equal to 0.25 ± 0.03, 0.61 ± 0.05, and 0.62 ± 0.01% ID/g 1 h after injection of catalase, b-catalase, or SA/b-catalase, respectively. Localization ratio, i.e., ratio of radioactivity in the lung and blood, allows quantitation of the tissue selectivity of the pulmonary uptake of these preparations. Lung/blood ratio was equal to 0.5, 0.43 and 0.28 1 h after injection of catalase, b-catalase, and SA/b-catalase, respectively. Therefore, an apparent increase in the pulmonary uptake of b-catalase and SA/b-catalase compared with the initial preparation of the enzyme (approx 0.6 vs 0.25% ID/g) reflects rather an elevation of the blood level of the circulating enzyme, but not specific accumulation in the lung.

Figure 1 shows the distribution of radiolabeled catalase conjugated with MAb 9B9 or with control IgG in rat tissues 1 h after iv injection. Both preparations display similar tissue uptake in all inspected tissues, except the lungs. Relatively high splenic uptake of both immune and nonimmune conjugates (approx 5% ID/g) might be explained by phagocytosis of the circulating conjugates via Fc-receptor-mediated pathway. The same mechanism also explains significant acceleration of the blood clearance of both conjugates, as compared with SA/b-catalase (down to 0.5–0.7% ID/g in the blood vs 2.1% ID/g). The most important result, however, is that MAb 9B9-catalase conjugate accumulates in the rat lungs. One hour after injection, pulmonary uptake of catalase conjugated with MAb 9B9 was equal to 7.5 ± 0.5% ID/g. It is noteworthy that IgG-catalase conjugate does

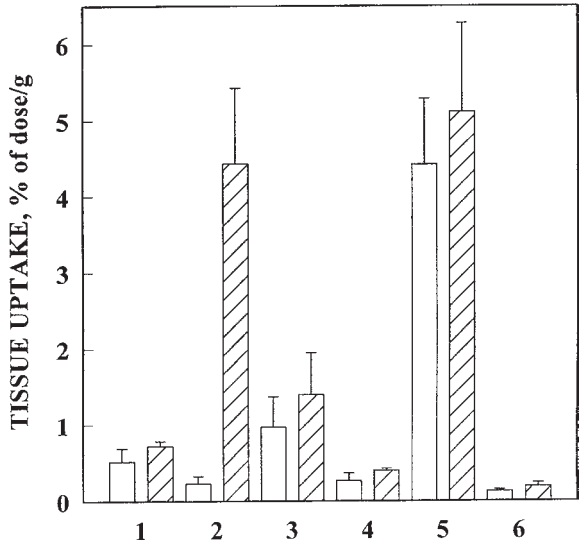

Fig. 1. Biodistribution of radiolabeled catalase conjugated with anti-ACE MAb 9B9 (hatched bars) or with control mouse IgG (open bars) 1 h after iv injection in rats. The data are shown as M ± SD, $n = 3$. The tissues are indicated as: 1, blood; 2, lung; 3, liver; 4, kidney; 5, spleen; 6, heart. Note that both conjugates demonstrate a similar biodistribution pattern in all inspected tissues, except the lung, where antibody–catalase conjugate displays about ten times higher accumulation than nonimmune counterpart.

not accumulate in the lung (0.23 ± 0.2% ID/g). Therefore, immunospecificity index (ratio of radioactivity per gram of the lung tissue after injection of immune and nonimmune conjugates) is more than 30. This result clearly indicates that pulmonary targeting of catalase occurs due to its conjugation to anti-ACE antibody and reflects specific interaction of the conjugate with ACE localized on the luminal surface of the pulmonary vascular endothelium.

Figure 2 shows the kinetics of blood clearance and pulmonary uptake of various preparations of catalase. During the entire period of the study (5 min–24 h after injection) b-catalase and SA/b-catalase do not accumulate in the lung; the pulmonary level of radioactivity is consistently lower than blood level and does not exceed 1% ID/g. In contrast, MAb 9B9-catalase conjugate demonstrates fast (4.2 ± 0.1% ID/g 5 min after injection) and prolonged (2.9 ± 0.6% ID/g 24 h after injection) pulmonary uptake. The lung/blood ratio was equal to 10 1 h after injection and reached the value 25.6 ± 2.7 1 d after injection. This time-dependent elevation of the lung/blood ratio can be explained by elimination of the conjugate from the bloodstream. In contrast, the lung/blood ratio was 0.22 1 d after injection of IgG-conjugated catalase. The calculation of lung/blood ratio allows compensation for the difference in the blood level of the conjugates. Therefore, comparison of lung/blood ratios 1 d after injection of immune and nonimmune

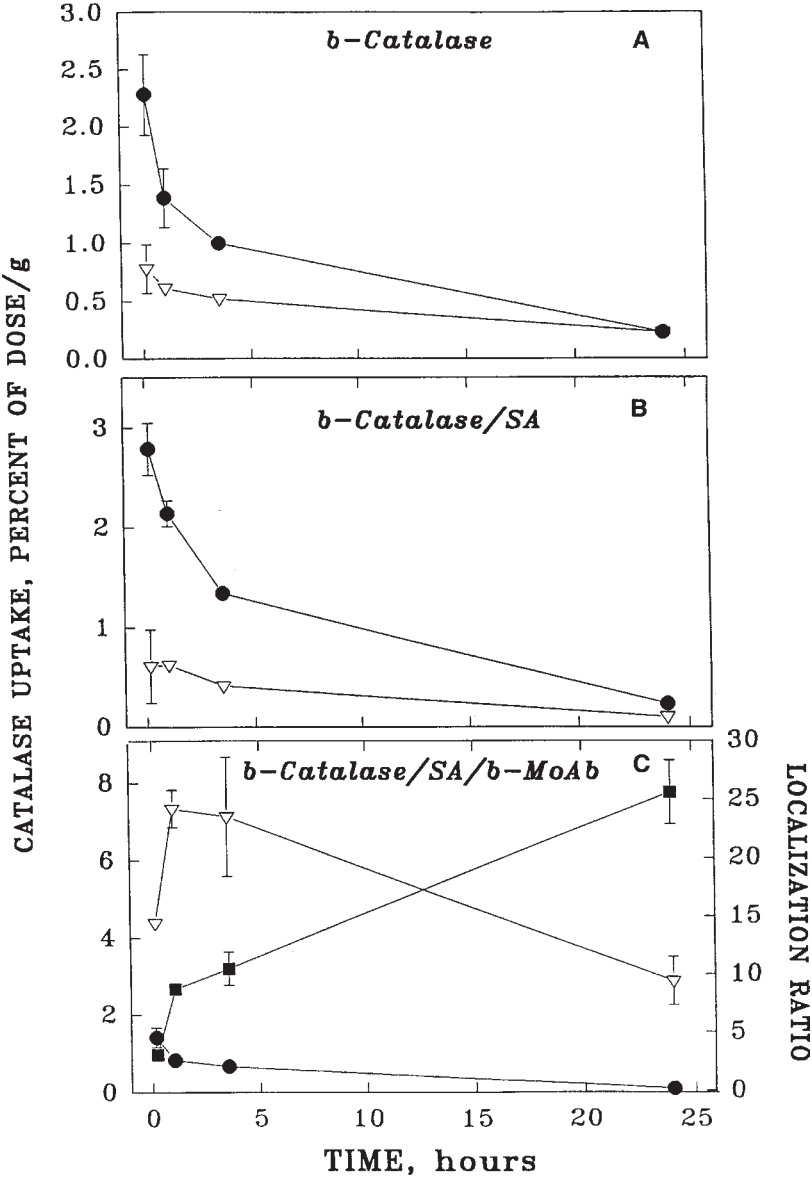

Fig. 2. Kinetics of blood clearance and pulmonary uptake of radiolabeled catalase preparations after iv injection in rats. Circles show blood level of radioactivity, and triangles show pulmonary level of radioactivity, both expressed as a percent of injected dose per gram of tissue (%ID/g). Squares show lung/blood ratio (localization ratio) of antibody–catalase conjugate (right scale, C). The data are shown as M ± SD, n = 3. Note fast and prolonged uptake of the antibody–catalase conjugate in the rat lungs. (Adapted with permission from **ref. *19***.)

conjugates shows that anti-ACE MAb 9B9-catalase displays about 100 times higher pulmonary uptake than IgG-catalase.

Acknowledgments

This study is supported by the Established Investigator Grant #9640204 from the American Heart Association. The author thanks Drs. Sergei M. Danilov (University of Illinois at Chicago), Elena N. Atochina, and Aron B. Fisher (University of Pennsylvania) for a long-term collaboration, invaluable experimental help, and stimulating discussions as well as coauthorship of previous publications that provided a background for the present chapter.

References

1. Fantone, J. C. and Ward, P. A. (1982) Role of oxygen-derived free radicals and metabolites in leukocytes-dependent inflammatory reactions. *Am. J. Pathol.* **107,** 397–424.
2. Fisher, A. B., Dodia, C., Tan, Z., Ayene, I., and Eckenhoff, R. G. (1991) Oxygen-dependent lipid peroxidation during lung ischemia. *J. Clin. Invest.* **88,** 674–679.
3. Schraufstatter, I., Revack, S., and Cochrane, C. (1984). Proteases and oxidants in experimental pulmonary inflammatory injury. *J. Clin. Invest.* **73,** 1175–1184.
4. Greenwald, E. (1990) Superoxide dismutase and catalase as therapeutic agents for human diseases. *Free Rad. Biol. Med.* **8,** 201–209.
5. Turrens, J. F., Crapo, J. D., and Freeman, B. A. (1984) Protection against oxygen toxicity by intravenous injection of liposome-entrapped catalase and superoxide dismutase. *J. Clin. Invest.* **73,** 87–95.
6. Beckman, J. S., Minor, R. L., White, C. W., Repine, J. E., Rosen, G. M., and Freeman, B. A. (1988) Superoxide dismutase and catalase conjugated with polyethylene glycole increase endothelial enzyme activity and oxidant resistance. *J. Biol. Chem.* **263,** 6884–6892.
7. Freeman, B. A., Young, S. L., and Crapo, J. D. (1983) Liposome-mediated augmentation of superoxide dismutase in endothelial cells prevents oxygen injury. *J. Biol. Chem.* **258,** 12,534–12,542.
8. Sakharov, D. V., Muzykantov, V. R., Domogatsky, S. P., and Danilov, S. M. (1987) Protection of cultured endothelial cells from hydrogen peroxide by antibody-conjugated catalase. *Biochim. Biophys. Acta* **930,** 140–144.
9. Danilov S., Allikmets, E., Sakharov, I., Dukhanina, E., and Trakht, I. (1987) Monoclonal antibodies against ACE. *Biotechnol. Appl. Biochem.* **9,** 312–322.
10. Muzykantov V. and Danilov, S. (1995) Targeting of radiolabeled monoclonal antibody against ACE to the pulmonary endothelium, in *Targeted Delivery of Imaging Agents* (Torchilin, V., ed.), CRC, Boca Ration, FL, pp. 465–485.
11. Green, M. (1975) Avidin, in *Advances in Protein Chemistry* (Afunsen, C., Edsall, J., and Richards, F., eds.), Academic, New York, pp. 85–133.
12. Wilchek, M. and Bayer, E. (1988) The avidin-biotin complex in bioanalytical research. *Anal. Biochem.* **171,** 1–32.

13. Paganelli, G., Magnani, P., Belloni, C., Siccardi, A., and Fazio, F. (1992) Two-step tumor targeting in ovarian cancer patients using biotinylated monoclonal antibodies and radioactive streptavidin. *Eur. J. Nucl. Med.* **19,** 322–329.
14. Taylor, R., Sutherland, W., Reist, C., Webb, D. J., Wright, S., and Labunguen, R. (1991) Use of heteropolymeric monoclonal antibodies to attach antigens to the C3b receptor of human erythrocytes: a potential therapeutic treatment. *Proc. Natl. Acad. Sci. USA* **88,** 3305–3309.
15. Bickel, U., Yoshikawa, T., Landaw, E., Faul, K., and Pardridge, W. (1993) Pharmacological effects in vivo in brain by vector-mediated peptide drug delivery. *Proc. Natl. Acad. Sci. USA* **90,** 2618–2622.
16. Wu, D., Boado, R., and Pardridge, W. (1996) Complete inactivation of target mRNA by biotinylated antisense oligonucleotide-avidin conjugates. *J. Pharm. Exp. Therap.* **276,** 206–211.
17. Muzykantov, V., Gavriljuk, V., Reinecke, A., Atochina, E., Kuo, A., Barnathan, E., and Fisher, A. (1995) The functional effects of biotinylation of anti-AEC monoclonal antibody in terms of targeting *in vivo*. *Anal. Biochem.* **226,** 279–287.
18. Muzykantov, V., Atochina, E., Gavriljuk, V., Danilov, S., and Fisher, A. (1994) Immunotargeting of streptavidin to the pulmonary endothelium. *J. Nucl. Med.* **35,** 1358–1365.
19. Muzykantov, V., Atochina, E., Ischiropoulos, H., Danilov, S., and Fisher, A. (1996) Immunotargeting of antioxidant enzymes to the pulmonary endothelium. *Proc. Natl. Acad. Sci. USA* **93,** 5213–5218.
20. Muzykantov, V. (1997) Conjugation of catalase to a carrier antibody via streptavidin-biotin cross-linker. *Biotechnol. Appl. Biochem.* **26,** 103–109.
21. Danilov S., Muzykantov, V., Martynov, A., Atochina, E., Sakharov, I., Trakht, I., and Smirnov, V. (1991) Lung is the target organ for a monoclonal antibody to angiotensin-converting enzyme. *Lab. Invest.* **64,** 118–124.
22. Danilov, S., Atochina, E., Hiemish, H., Churakova T., Moldobayeva, A., Sakharov, I., Deichman, G., Ryan, U., and Muzykantov, V. (1994) Interaction of monoclonal antibody to ACE with antigen in vitro and in vivo. *Int. Immunol.* **6,** 1153–1160.
23. Muzykantov, V., Atochina, E., Granger, D., and Fisher, A. (1997) ICAM–1-directed delivery of catalase to the pulmonary vasculature. *Am. J. Resp. Crit. Care Med.* 155(4), A192.
24. Atochina, E., Balyasnikova, I., Danilov, S., Granger, D., Fisher, A., and Muzykantov, V. (1998) Immunotargeting of catalase ACE and ICAM–1 protects perfused rat lungs against oxidative stress. *Am. J. Physiol.* **275,** (Lung Cell. Mol. Physiol. 19) L806–L817.

15

Targeted Gene Transfer

A Practical Guide Based on Experience with Lipid-Based Plasmid Delivery Systems

Ellen K. Wasan, Dorothy L. Reimer, Pierrot Harvie, Spencer Kong, Frances M. P. Wong, and Marcel B. Bally

1. Introduction

The overall goal of gene therapy is to cure or stabilize a disease process that results from the production of a mutant protein (for example, the chloride channel protein important in cystic fibrosis) or overproduction of a normal protein (such as the products of certain oncogenes). We can achieve this goal by replacing the defective gene or by reducing the overexpression of the target gene using an antisense strategy, thus reducing the production of the disease-promoting protein ***(1,2)***. For either method, it is critical to transfer DNA into target cells in a concentration high enough to be effective in modifying the disease. DNA must be delivered to the desired cell population in an intact state, whereby it can be efficiently transcribed and ultimately translated. The method of gene transfer must be highly efficient and nontoxic, and the delivery system must be relatively easy to prepare and administer ***(3)***. There is a great deal of optimism surrounding the development of gene therapy as an effective strategy for management of many different human diseases. The active agent used to procure gene therapy is likely to consist of oligonucleotides, ribozymes, or a DNA sequence that can be transcribed into a message capable of eliciting a therapeutic response. Unlike conventional small-molecule therapeutics however, gene therapy requires the use of a carrier system to deliver the active agent directly into the target cell population.

Viruses, which have the ability to gain access to cells very efficiently, are the most common gene-therapy vectors. Most clinical gene therapy trials to

From: *Methods in Molecular Medicine, Vol. 25: Drug Targeting: Strategies, Principles, and Applications*
Edited by: G. E. Francis and C. Delgado

date utilize viruses to deliver DNA. Nonviral DNA delivery methods, however, are growing in popularity because they have several distinct advantages. The DNA used for nonviral-mediated gene transfer is usually in plasmid form, for which the size restrictions are much less limiting than for most viral-based systems. Plasmids do not integrate into the host genome, but rather remain episomal, eliminating the potential for insertional mutagenesis. Plasmids are not potentially infectious agents, unlike viruses, which could become infectious if complementation in the host occurs ***(4–6)***. For effective DNA uptake into most tissues by nonviral delivery methods, plasmid requires the use of carrier molecules, such as cationic lipids ***(7–9)*** or cationic polymers, which have the advantage of low antigenicity ***(10,11)***, permitting multiple administrations if necessary. Targeting molecules can be incorporated into the DNA/carrier complex to improve specificity of delivery. Numerous approaches are available to prepare effective lipid-based DNA delivery systems. In general, however, the formations rely on formation of either a liposome– or lipid–DNA complex. Complex formation, in turn, rely, on the use of charged lipids that can bind DNA directly (cationic lipid binding to the anionic DNA molecule) or indirectly (anionic lipid binding to a cationic peptide/protein–DNA complex). Lipid-based carriers are proving to be a versatile and pharmaceutically viable technology. A practical guide to some of the methods used in the preparation and characterization of these DNA transfer formulations is presented here. The actual DNA transfer process is likely to be a consequence of the physical and chemical attributes of the complex, which insure that DNA is maintained in a form that is protected from enzymatic hydrolysis and readily taken into a cell. These are, however, rather nonspecific functions that can be fulfilled by many DNA binding molecules or structures. We believe that bound lipids may play a more active role in gene transfer as well as gene expression. The former may involve the well-established role of lipids in membrane fusion, whereas the latter concerns the role of lipids in destabilization of condensed DNA structures.

Regardless of the strategy, it is imperative to understand the mechanism(s) involved in the delivery process. Targeting of DNA to a specific cell population by any method can only be optimized when the components of the delivery system are fully characterized. This will ultimately enable researchers to effectively assess the efficiency of DNA delivery and cellular uptake, critical parameters in gene transfection. It is important to determine how cells handle exogenously administered DNA and to determine where the rate-limiting step is in the transfection process. This chapter will address many of the current issues related to the development and analysis of nonviral-mediated DNA delivery methods, with emphasis on the lipid-based carrier systems.

1.1. An Overview of Nonviral DNA Delivery Systems

Although the specific physicochemical properties of nonviral plasmid carrier formulations will vary, the goal is the same: to produce stable particles in a highly reproducible manner that promote efficient cellular uptake of the DNA. Small particle size (<200 nm) is required for effective systemic biodistribution. The DNA also must be protected from rapid degradation, either in vitro or in vivo, yet must be released from the carrier at the appropriate time within the cell for it to be actively transcribed. The inclusion of targeting moieties on the surface of the carrier, although potentially improving the specificity of delivery, also increases the complexity. Consideration must be made when designing a carrier for in vivo use because the route of administration and the physiological attributes of the tissue in which one wishes to achieve DNA expression are important parameters. A number of pharmaceutical factors, such as carrier aggregation state and stability, reproducibility of preparation, sterilization, and scale-up of the production for manufacturing purposes, are also ongoing challenges.

The carriers for DNA in the nonviral delivery systems currently include cationic liposomes ***(12–15)***, lipid/DNA particles ***(16,17)***, lipopolyamines ***(18)*** and other polycations ***(19–21)***, including polylysine ***(22–25)***, various dendrimers ***(26–28)***, cationic or amphipathic peptides ***(29,30)***, and combinations of these ***(31)***. (**Table 1**) The most frequently cited method of nonviral DNA transfer is that employing cationic lipid carriers This idea was based originally on experience with liposomal delivery of conventional small-molecule drugs and on the need to improve the interaction of the DNA with the cell ***(32)***. Plasmids, however, do not encapsulate well into liposomes because of their size and charge, but they can be efficiently bound to cationic liposomes through electrostatic interactions ***(33)***. Cationic liposome/DNA complexes have been used for gene transfer for a wide variety of tissues and cell types ***(34–37)***. They have been administered intravenously ***(38,39)***, intraperitoneally ***(40,41)***, intratracheally ***(42–44)***, intraocularly ***(45)***, and locally into tumors ***(46–48)*** or solid organs ***(49)*** of several animal species and humans ***(50)***. Transfection tends to be inefficient, transient, and variable for most tissues as compared to viral vectors, but considerably greater than plasmid in the absence of the carrier. To address this inefficiency, many groups have spent considerable effort developing new cationic lipids ***(51–54)*** and exploring the effect of "helper lipids," such as dioleoylphosphatidylethanolamine (DOPE). DOPE enhances the transfection ability of some cationic lipids, supposedly by improving the fusogenicity or endosomolytic activity of the liposome component ***(55)***. Despite their usefulness for transfection in vitro or local administration in vivo, cationic liposome/DNA complexes, are not always suitable for iv use because they have a tendency to undergo aggregation, resulting in large, heterogeneous particle sizes (>1 μm) ***(56)***. This is particularly true in solutions of moderate to high ionic

Table 1
Examples of Nonviral DNA-Delivery Systems

DNA delivery system	Structural features	Positive attributes	Negative attributes
Cationic liposome/DNA complex	Ill-defined, heterogeneous aggregates in sheets, balls, or strands	Most effective nonviral carrier; wide variety of lipids available; easy to prepare; may allow for targeting	Difficult to control complex formation; variable, inefficient transfection
Cationic lipid/DNA particle	Dense small particles; DNA may be condensed	Particle formation can be controlled; targeting molecules may be attached	Transfection ≤liposome/DNA complex; aggregation sometimes occurs
Polylysine/DNA complex	Toroid or cochleate particles; DNA is condensed	Well-defined structure; targeting possible	Low efficiency; toxicity
Starburst dendrimer/DNA complex	Dendrimers—highly branched spheroids	Surface properties modifiable; transfection similar to DNA/liposome complexes	Toxicity? availability limited; may require the use of transfection enhancers

strength (i.e., >10 m*M* NaCl). More recently, small homogeneous lipid/DNA particles have been produced by detergent dialysis methods, which have different physical properties than liposome/DNA complexes, such as improved stability, but with at least equivalent transfection ability ***(16,17)***.

Polymers such as polylysine ***(22,25,57)*** and dendrimers ***(26–28)***, have been shown to promote transfection at least as well as the cationic lipid-delivery systems. Polylysine, like other polycations, condenses plasmid DNA ***(58,59)***, which may impart a protective effect against nucleases and possibly improve its eventual activity within the cell. Polylysine can be covalently coupled to targeting peptides, as discussed later, to achieve improved specificity of uptake. Antigenicity of polylysine is not anticipated to be a concern, evidenced by the use of polylysine as a component of the microencapsulation system used to protect live cells in allogeneic transplantation from immune attack ***(60–62)***.

Dendrimers, highly branched synthetic polymers with a spherical shape, are currently under development for a variety of applications, from computers to drug delivery. The size, shape, and surface features of these macromolecules can be readily controlled ***(63,64)***. Polyamidoamines, also known as Starburst dendrimers (Dendritech, Detroit, MI) or PAMAM, in particular have been used as gene-transfer vehicles ***(26–28)***. They have a high positive charge density because of their terminal amine groups, which makes them amenable to DNA complexation. Dendrimers have been demonstrated to be at least as efficient as cationic liposomes or polylysine in enhancing transfection of a variety of cell types, and they have been reported to be less toxic ***(27,28)***. Transfection efficiency is affected by the size of the polymer sphere and the ratio of polymer to DNA ***(28)***. The current hypothesis about their mode of action is that following endocytosis, the titratable amines of the polymer act as a buffering agent in the acidic environment of the endosome preventing degradation. Furthermore, if enough flexibility is present in the polymer molecule, such as when it is pretreated with heat, it will also swell in the endosome, disrupting the organelle and promoting DNA escape ***(26)***.

Cationic peptides have also been used as DNA carriers. For example, gramicidin S and tyrocidine are cationic peptides that will bind to plasmid DNA. When combined with DOPE, the peptide/DNA complex has been shown to transfect cells in vitro. The efficiency of the peptide compared to liposome/DNA complexes varies by cell type, but the toxicity is equally low ***(65)***. Other types of cationic peptides have also been utilized for gene transfer, and they are most effective in combination with molecules that exhibit pH-dependent membrane perturbation effects ***(30,66)***. Presumably these helper components promote endocytic escape after cellular uptake. Cationic peptide-type carriers are not in wide usage at this time, particularly in vivo. It will be interesting to see if these peptides induce any immune response when administered to animals.

1.1.1. Targeting of Nonviral Delivery Systems

In an effort to improve the specificity of uptake of DNA/carrier complexes, several methods have been developed that utilize the natural receptor-mediated uptake mechanisms of the cell. These methodologies are largely based on experience with other types of targeted delivery systems for conventional drugs, as discussed elsewhere in this volume. Transferrin ***(23–25,67)*** and asialoorosomucoid (ASO) ***(68–70)*** are molecules that have been especially useful as model ligands for the development of cell type-specific gene therapy constructs. Both transferrin and ASO receptors are highly upregulated on hepatocytes. Transferrin receptors are also upregulated on some kinds of cancer cells. For targeting, polylysine is chemically coupled to transferrin, then used to bind DNA. Uptake of the complex can be enhanced by means that upregulate the transferrin receptor, such as by depleting cellular iron, blocking the synthesis of heme, or promoting the degradation of heme. Successful transfection may require treatment with the lysosomotropic agent chloroquine ***(23)***. This process has been demonstrated to involve only receptor-mediated uptake ***(67)***.

Antibody-mediated methods are also in use, in which the antibody is chemically coupled to the polylysine prior to DNA complexation ***(67,71)***. Even more complicated methods have been developed in which a quaternary complex is formed among DNA, polylysine, the targeting ligand, and replication-defective adenoviral particles ***(72–75)***. The polylysine binds and condenses the DNA, the targeting molecule promotes specificity of cellular delivery, and the adenoviral particles induce endosomolysis after uptake. Other fusion peptides, such as INF5 from influenza virus ***(76)*** or hemagglutinating virus ***(77,78)***, have been used similarly in DNA-polylysine complexes to promote endosomal escape. Targeting of liposomal gene carriers can also be achieved, such as by the sterically stabilized immunoliposomes (SIL) recently developed by Papahadjopoulos and coworkers to induce high levels of uptake in human breast cancer cells expressing the HER-2 receptor. Fab' fragments of anti-HER2 monoclonal antibody (MAb) were covalently attached to poly(ethylene glycol) (PEG-lipids). The modified PEG-lipids, cholesterol, and cationic lipids then were formulated into liposomes used to make the DNA complex for transfection. Further work is ongoing to develop the SIL into programmable fusogenic liposomes, in which a modified PEG-lipid conjugate portion can be induced to detach, rendering the liposome more prone to fusion, presumably with target cells ***(79)***.

The following sections will focus exclusively on the lipid-based carriers, which are the most widely used vehicles for nonviral DNA transfer. Discussion will center on the preparation and analysis of the DNA and carrier components as well as the analysis of uptake, distribution, and efficacy in vitro and in vivo.

2. Materials

2.1. Plasmid Preparation

1. Luria broth (LB) is available from Bio101 (La Jolla, CA).
2. Plasmid purification by anion exchange chromatography may be performed using the Qiagen (Chatsworth, CA) kit.
3. An alternative plasmid purification kit is available from Machery-Nagel (Nucleobond, Duren, Germany).
4. For removal of both cesium chloride and ethidium bromide a desalting column may be used (Econo-Pac 10GD, Bio-Rad) prepacked with Bio-Gel P-6DG gel (Bio-Rad).
5. Endotoxin removal by ligand binding can be performed using DNA Etox resin (Sterogene Separations, Calsbad, CA).
6. Gel filtration to separate plasmid from RNA may be done using Sephacryl S-1000 Superfine matrix (Pharmacia, Uppsala, Sweden), or by precipitation with PEG_{6000} (Fisher, Fair Lawn, NJ).
7. Dialysis of plasmid preparations is done with cellulose dialysis membranes with a mol wt cutoff of ≤12,000 (Spectropor, Spectrum Medical Industries, Houston, TX).
8. For preparation of radiolabeled plasmid, tritiated thymidine is available from DuPont/NEN (Markham, Ontario, Canada), with a specific activity of approx 6–7 Ci/mmol and a purity >95%.
9. The DNA-intercalating fluorescent dyes TO-PRO and YO-YO can be purchased from Molecular Probes (Eugene, OR).

2.2. Lipids

2.2.1. Cationic Lipids

1. *N*-[1-(2,3 Dioleyloxy)-propyl]-*n,n,n*-trimethylammonium chloride (DOTMA) is available in combination with the neutral helper lipid dioleoylphosphatidyl-ethanolamine (DOPE) in Lipofectin reagent (Gibco-BRL, Grand Island, NY).
2. 2,3-Dioleyloxy-*N*[2(sperminecarboxyamido)ethyl]-*N*,*N*-dimethyl-1-propanaminium trifluoroacetate (DOSPA) is available with DOPE in LipofectAmine reagent (Gibco-BRL).
3. Dioleoyl-1,2-diacyl-3-trimethylammonium propane (DOTAP) can be obtained from Avanti Polar Lipids (Alabaster, AL) or as methyl sulfate salt from Sigma (St. Louis, MO).
4. Dimethyldioctadecyl ammonium bromide (DDAB) can be purchased from Sigma or Avanti Polar Lipids, or formulated with DOPE in Lipofectace reagent (Gibco-BRL).
5. Dimyristyloxypropyl-3-dimethyl-hydroxyethyl ammonium (DMRIE) (Gibco-BRL) and cholesteryl 3,β-[*N*-dimethylaminoethyl] carbamate (DC-Chol) are also available from Sigma.
6. Dioctadecylamidoglycyl spermidine (DOGS) (Transfectam) can be purchased from Promega (Madison, WI).

7. Dioleyldimethylammonium chloride (DODAC) is provided by custom synthesis (Inex Pharmaceuticals, Vancouver, BC, Canada).

2.2.2. Radiolabeled, Fluorescent, and Anionic Lipids

1. Radiolabeled cholesteryl hexadecyl ether (CHDE) (^{3}H and ^{14}C) may be obtained from DuPont/NEN.
2. Radiolabeled (^{14}C) DOPE can be purchased from Amersham (Oakville, Ontario, Canada).
3. ^{3}H-DODAC is provided to us by custom synthesis (Inex Pharmaceuticals).
4. The fluorescently labeled lipids *N*-(7-nitrobenz-2-oxa-l ,3-diazol-4-yl)-modified phosphatidylethanolamine (NBD-PE) and lissamine-rhodamine-modified phosphatidylethanolamine (rhodamine-PE) can be bought from Molecular Probes.
5. Dioleoylphosphatidylcholine (DOPC) and dioleoylphosphatidylserine (DOPS) are available from Avanti Polar Lipids.

2.3. Liposome Preparation

1. The extrusion device used to prepare the liposomes (the Extruder) is available from Lipex Biomembranes (Vancouver, BC, Canada).
2. The polycarbonate membranes used with the Extruder to limit the size of the liposomes are obtained from Poretics (Mississauga, Ontario, Canada).
3. Assessment of the mean diameter of the liposomes is performed under ambient conditions on a Nicomp submicron particle sizer (Model 270, Pacific Scientific, Santa Barbara, CA) with the laser operating at 200 kHz and a wavelength of 632.8 nm, and the external and scattering angle fixed at 90°.
4. Chloroform and methanol should be high-performance liquid chromatography (HPLC) grade (Fisher).

2.4. Analysis of DNA Protection, Delivery, and Transfection

1. For DNA extractions, phenol (Gibco-BRL) is first equilibrated with Tris-HC1 (pH 8.0).
2. Electrophoresis is done in 0.8% agarose gel (Sigma, St. Louis, MO) using a Bio-Rad (Richmond, CA) Model 3000xi programmable power supply, operating at 80–100 V.
3. Fetal bovine serum may be obtained from Gibco-BRL, and mouse serum from Cedar Lane (Hornby, Ontario, Canada).
4. Dissolution of gel slices is done with Solvable (Dupont/NEN, Boston, MA).
5. DNA extraction from cells or tissues may be done using DNAzol (Gibco-BRL).
6. Southern blotting is done using the digoxigenin chemiluminescence kit from Boerhinger Mannheim (Mannheim, Germany).
7. A computerized imager for digitization and analysis directly from blots or gels is available from Molecular Dynamics (Storm PhosphoImager, Sunnydale, CA).
8. Analysis of transfection using the luciferase reporter gene is done using a luciferase kit from Promega.

All other chemicals or reagents not specified otherwise above are from Sigma.

3. Methods

3.1. The Active Components

3.1.1. Plasmids

Gene transfection experiments often require large quantities of plasmid of high purity. Large amounts of DNA can be obtained by transforming a host cell, such as the bacteria *Escherichia coli*, with these small extrachromosomal pieces of circular DNA (the plasmids). Although a discussion about the construction of plasmid expression vectors is beyond the scope of this chapter, it is important that the plasmid contain a gene that encodes for antibiotic resistance (such as ampicillin or tetracycline) which is used to ensure that the bacteria growing in the presence of the drug retain the plasmid of interest. Following growth of the bacterial culture and subsequent amplification of the plasmid, the bacteria are lysed and the plasmid recovered by routine isolation techniques.

3.1.1.1. Plasmid Isolation and Purification

The techniques for culturing bacteria-carrying plasmid are now routine and can be found in standard manuals ***(80,81)***. Many strains of bacteria are now available, that have been genetically characterized for specific uses, and culture conditions may vary depending on the strain chosen.

1. Transformed *E. coli* containing the plasmid of interest are grown from a glycerol stock (0.85 mL bacterial culture + 0.15 mL glycerol, stored at –70°C) and plated on a semisolid matrix containing Luria Broth (LB), agar, and the selection antibiotic.
2. The bacteria are grown overnight at 37°C.
3. A single bacterial colony is picked from the plate, introduced into 10 mL LB with antibiotic, and incubated overnight in a shaker incubator at 37°C (*see* **Note 1**).
4. From the 10 mL overnight culture, 5 mL is added to each of two 4 L flasks containing 1 L of LB with selection antibiotic and the bacteria are grown to saturation, usually overnight, in a shaker incubator at 37°C ***(80)***.
5. The optical density at 550 nm (OD_{550}) of the culture should be about 1.0–1.5, but may vary depending on the bacterial strain and the type of plasmid used.
6. Plasmid is routinely recovered from bacteria by an alkaline lysis procedure, which lyses the bacterial cell while maintaining bacterial DNA attachment to the cell wall. This procedure enables subsequent precipitation of bacterial DNA and cellular debris, leaving a crude preparation enriched in plasmid. We routinely use a plasmid DNA purification kit provided by Qiagen that utilizes the alkaline lysis method for harvesting, and anion exchange column chromatography for rapid purification. We refer the reader to the detailed instructions provided in the kit by the manufacturer, which we have not found necessary to modify for purification of laboratory-use plasmid DNA.

Table 2
Plasmid Can Be Purified by Several Methods

Purification method	Problems	References
Alkaline lysis	Crude, requires further purification	***(80,81)***
Anion exchange	Endotoxin contamination	***(162,164)***
Cesium chloride	CsCl and/or ethidium bromide contamination; time consuming; not readily scaled up	***(80,161)***
Size exclusion	Time consuming; dilution of product	***(163,166,167)***
PEG precipitation	May require further purification to remove PEG; efficiency low if DNA concentration low	***(169)***

7. Once the bacterial cells have been lysed and a crude preparation of plasmid has been obtained, several other methods are available for purification of plasmid from the crude nucleic acid preparation, such as cesium chloride ultracentrifugation, gel filtration/size exclusion chromatography, anion exchange (used in the Qiagen kit mentioned above), and HPLC (**Table 2**) (*see* **Note 2**).
8. When the purified plasmid has been obtained, it is necessary to evaluate the level of purity of the sample and to determine the quantity and concentration obtained from the extraction procedure. Using a spectrophotometer, an optical density profile should be performed (between 230 and 340 nm). The profile should generate a peak at OD_{260} where DNA absorbs maximally (*see* **Note 3**).
9. To determine the concentration of the DNA sample, an OD reading at 260 nm is taken and the concentration determined (1 OD_{260} = 50 µg/mL DNA) ***(80)***.
10. Following quantification, the sample is dialyzed to remove impurities, such as salts and other contaminants, that can affect the behavior of the DNA in its interaction with the carrier and its transfection efficiency. The entire DNA sample is dialyzed against 4 L sterile distilled water overnight at 4°C.
11. One hour after the start of dialysis 1 L of the water is replaced with fresh sterile water.
12. After the overnight dialysis, the dialysis bag is transferred to a fresh beaker of sterile water and dialyzed another 1 h at 4°C.
13. The OD_{260} of the postdialysis sample at an appropriate dilution in water is checked and concentration and recovery are calculated.
14. For laboratory use, such as in vitro transfection, it is convenient to dilute this stock DNA solution to 1 mg/1 mL aliquots, which may be stored frozen until use.

15. As an additional precaution, it is important to ensure that the plasmid that has been isolated contains the expected insert. The plasmid should be digested with restriction enzymes known to excise the insert and the resulting fragments evaluated following agarose gel electrophoresis.

3.1.1.2. Preparation of Radiolabeled Plasmid

Radiolabeled plasmid can be utilized for studies involving animal pharmacokinetics, subcellular distribution during transfection, or biochemical/biophysical analyses in which one wishes to follow the fate of the plasmid DNA. For these purposes, ^{32}P or ^{3}H-labeled plasmid may be used. Although ^{32}P provides excellent sensitivity, the ^{32}P-labeled plasmid is more susceptible to radiation-induced damage, and, if prepared by nick translation, to exonuclease attack. ^{3}H-labeling of the plasmid provides a safer alternative with a high degree of sensitivity for detection. The preparation of tritiated plasmid, described here in **steps 1–8**, is modified from standard protocols because of the need to induce the bacteria to incorporate large quantities of radiolabeled nucleotide (for example, tritiated thymidine) during log-phase growth. The radioactive nucleotide is incorporated not only into the plasmid, but also into the host genome, the latter of which is a larger percentage of the total radiolabeled DNA. The following procedure outlines a fairly simple method to obtain tritiated plasmid on a laboratory scale.

1. *E. coli* containing the plasmid of interest are taken from a glycerol stock ***(80)*** (*see* **Note 4**) and plated onto an M9 (minimal media) plate (M9: 10 g M9 salts in 1 L autoclaved, distilled water, or 15 g M9 salts/L, of bacto agar to prepare plates) with appropriate antibiotics for selection.
2. To each 100 mL of media, 5 mL 20% glucose, 0.1 mL 1 *M* $MgSO_4$, 10 µL 1 *M* $CaCl_2$, and 1.0 mL 0.1% thiamine HCl are added, plus the desired selection antibiotic.
3. Incubation proceeds at 37°C, for no longer than 16 h or the antibiotic may be depleted and bacteria without plasmid may grow. A lawn of white opaque colonies will result.
4. Fresh M9 media (10–20 mL) is added and the colonies dislodged with a bent glass stirring rod.
5. The liquid containing the bacteria is transferred to 100 mL M9 and the OD_{550} is measured. It should be approx 0.1. If the OD is <0.05, initial growth may be slow (*see* **Note 5**).
6. The 100 mL M9 culture is allowed to grow in a 37°C shaker until the OD_{550} is about 0.2–0.3, which can take as little as 5 h.
7. Next, 1 mCi tritiated thymidine, or sufficient quantity to reach the desired final specific activity, is added to the culture (*see* **Note 6**).
8. Incubation proceeds overnight at 37°C, and a diluted sample is checked the next day prior to harvesting the bacteria, ensuring that the bacteria have grown to saturation (OD_{550} is about 1.5).
9. We use the Qiagen kit, discussed in **Subheading 2.1.1.**, to harvest and purify the plasmid, following the manufacturer's instructions.

10. For transfection-grade radiolabeled plasmid, the final step is dialysis against several changes of water at 4°C overnight.
11. The $OD_{230–340}$ profile is generated as described above and the final concentration and specific activity are determined following liquid scintillation counting of a known volume. From 50 µL of starting glycerol stock of *E. coli* carrying pCMVβ-galactosidase, typical yield from this procedure is 200 µg plasmid, with a specific activity of 80,000 dpm/µg.
12. The ^{3}H-plasmid should be stored at –70°C to minimize radiation-induced breaks. It may be used for up to 1 yr, providing that the quality of the plasmid is checked regularly (e.g., approx every 2 mo) by agarose gel electrophoresis.

3.1.1.3. Preparation of Fluorescently Labeled Plasmid (*see* **Note 7**)

1. YO-YO is supplied as a 1 m*M* solution in DMSO, which is added to the plasmid at approx 1:100 dye:base pair ratio. At this ratio, sensitivity is high and DNA/liposome complex formation is compromised very little.
2. After incubation of plasmid and YO-YO dye at 50°C for 2–4 h, the plasmid is dialyzed against sterile distilled water at 4°C for 4–5 h with several changes of the water, or overnight. Dialysis removes the DMSO and any potential unbound YO-YO dye (P. Joshi, Inex Pharmaceuticals, personal communication).
3. After requantification of DNA concentration as described in **Subheading 3.1.1.1.**, **steps 8–9**, the plasmid is ready for use.
4. Fluorescence can be read with excitation at 491 nm and emission at 509 nm ***(82)***. It is important to note, however, that it is not yet established whether YO-YO is readily displaced from the DNA during preparation of lipid-based DNA delivery systems or following cellular interactions.

*3.1.2. Cationic Liposomes for Gene Transfer (*see ***Note 8****)*

3.1.2.1. Preparation of Cationic Liposomes

Prepared, quality-control tested liposomes are available from commercial sources, as listed in **Subheading 2.**, but they remain quite expensive. We describe here a method for the preparation of cationic liposomes by extrusion, a process that can be performed reproducibly in the laboratory with a minimum of equipment (a vortex mixer, a source of vacuum, and an extrusion device).

1. High-purity lipids in the desired proportions are dissolved in HPLC-grade chloroform (5–20 mg/mL), and may be radiolabeled with trace amounts (~1 µCi/mL) of [^{3}H]- or [^{14}C]-CHDE (*see* **Note 9**).
2. The lipid solution is reduced in volume under a stream of N_2 gas and dried to a thin film for several hours under vacuum.
3. The lipid films are hydrated by adding an aqueous solution while agitating, such as with a vortex mixer, to produce multilamellar vesicles (MLVs) (*see* **Note 10**).
4. The hydrated lipid suspension is then passed 10 times at room temperature through an extrusion device containing three 0.08-µm polycarbonate membranes stacked together.

5. The resulting large unilamellar vesicles (LUVs) have a mean diameter of 100–140 nm as determined by quasielastic light scattering (QELS). This diameter can be modified by using membranes of different pore size.
6. Final lipid concentration may be determined by use of the radiolabeled lipid or by an assay of phospholipid phosphorous.
7. Liposomes should be stored at 4°C and used within 1 mo. Extruded vesicles should not be frozen. Vesicles will naturally begin to coalesce within 6 mo to 1 yr.

3.1.2.2. Formation of Liposome/DNA Complexes

Although there are ongoing advances in the development of nonviral delivery systems for gene transfer, liposome/DNA complexes are still the most common and best studied.

1. Plasmid to be used for liposome/DNA complexes is prepared in deionized water.
2. Liposomes and plasmid DNA should be centrifuged (7000–10,000*g* for 2 min) prior to use to pellet any debris or aggregates (*see* **Note 11**).
3. Complexes are prepared with plasmid DNA and liposome components cooled on ice.
4. Liposomes and DNA are diluted separately in dust-free tubes using the same type of solution that was used to prepare the liposomes. We often use liposomes at a final dilution of 0.5–1 m*M* total lipid, and DNA concentrations of 5–500 µg/mL in a total volume of 0.2–1 mL.
5. Diluted plasmid DNA is pipeted gently into an equal volume of diluted liposomes, keeping the mixture on ice.
6. Complex formation is rapid; typically complexes are allowed to form for about 30 min ***(33)***.
7. The particle size of the resultant complexes varies with the ratio of lipid to DNA, however, the minimum diameter is usually 200–400 mn, a size which is two to five times larger than the original liposomes prior to DNA addition. The greatest aggregation occurs when the complex is approximately charge-neutral ***(56)***.
8. Complexes should be used within a few hours of preparation because transfection efficiency is reduced if complexes are stored ***(83)*** and further aggregation can occur over time.

3.1.3. Lipid/DNA Particles for Gene Transfer

Lipid/DNA particles represent a nonliposomal but lipid-based delivery system for gene transfer. Monomeric or micellar lipids are allowed to interact with DNA in the presence of detergent or some other surface-active agent that is then removed by dialysis. As the surface-active agent diffuses out, solid, condensed particles of lipid and DNA form ***(17)***. These can be prepared such that they are smaller and more homogeneous than liposome/DNA complexes yet transfect cells equally well (F. Wong, unpublished observations).

1. A lipid film consisting of cationic and neutral lipids is prepared as described in **Subheading 3.1.2.1.**, **steps 1–2** for liposome/DNA complexes, except the lipids are dissolved in chloroform:methanol 1:1 in dust-free test tubes.

2. After the film is dried under vacuum to remove residual solvent, hydration is performed with 35 m*M* *n*-octyl β-D-glucopyranoside (OGP), a nonionic detergent, which is added at a concentration known to cause solubilization of the lipid components used. To ensure that this critical step is complete, the lipid mixture is heated at 50°C in a water bath.
3. The solution should be clear and colorless on visual inspection and the mean micellar diameter should be ≤50 nm, as measured by QELS. Additional OGP may be added if solubilization is incomplete.
4. The lipid solution is then kept on ice until use.
5. Equal volumes of plasmid DNA (5–150 μg DNA/mL) and the mixed detergent/lipid micelles at the desired charge ratio are mixed followed by vortex mixing. Particle formation will occur spontaneously under these conditions.
6. The mixture is dialyzed against sterile distilled water for 72 h at 4°C to remove OGP, with replacement of the water every 12 h.
7. Particle size distribution and homogeneity are evaluated by QELS as solid particles (rather than vesicles). There should be minimal changes in particle size after dialysis.
8. Typically, lipid/DNA particles prepared in our laboratory have a mean diameter by Gaussian analysis of 110–120 mn, but particles as small as 50 nm can also be prepared by this method, depending on the lipid composition and the detergent used ***(17)***. Aggregation can be a problem if the lipids are not fully dispersed in the OGP initially or if the charge ratio of lipid:DNA is close to 1:1. Controlling the temperature during dialysis (4°C) also helps prevent aggregation (*see* **Note 13**).

3.1.4. Other Formulation Strategies and Incorporation of Targeting Molecules

In order to incorporate targeting molecules in the DNA/carrier complex, usually the ligand is chemically coupled to polylysine, such as by treatment with 3-mercaptopropionate or succinimidyl 3-(2-pyridyldithio)proprionate (SPDP) to form a disulfide linkage, followed by purification by column chromatography and dialysis ***(67)*** (*see* **Note 14**).

1. The ligand–polylysine complex can then be mixed with plasmid DNA (1:1 w:w), or with adenoviral particles then plasmid DNA.
2. For example, the approximate ratios useful for transfection in a report using this particular quaternary complex are 2×10^{10} adenoviral particles: 1.25 μg antibody–polylysine complex: 6 μg plasmid DNA, added to 6 μg polylysine or 8 μg polylysine–transferrin complex ***(74)***. Simple mixing of the components results tin rapid and spontaneous formation of the macrocomplex. Carbohydrates have also been used as targeting ligands ***(84,85)***.

In another strategy developed by Legendre and Szoka ***(65)***, the cationic peptides gramicidin S and tyrocidine are combined with DOPE (5:1 lipid:peptide ratio). Complex formation was promoted by simple mixing of the peptide (2 mg/mL) with DNA (20 μg in 300 μL) in 30 m*M* Tris-HCl (pH 8.5), followed by addition

of 175 nmoles DOPE in 175 µL. For transfection the optimal molar ratio of DOPE:peptide was approx 4.5:1 ***(65)***. In another study, cationic peptides were made more lipophilic by chemically attaching a fatty acyl group to one of the amino groups. This molecule was used to prepare peptide/DNA particles similar to liposome/DNA complexes. *N*,*N*-dihexadecyl-*N* α-[6-(trimethylamino)-hexanoyl]-L-alaninamide bromide was used to make sonicated liposomes that formed a complex with plasmid DNA. COS-7 cells were transfected with this complex in vitro with greater efficiency and less toxicity than conventional cationic liposome/DNA complexes ***(29)***. Other strategies are summarized in **Note 15**.

3.2. Characterization of Lipid-Based Gene Transfer Formulations

3.2.1. Measuring Particle Size and Aggregation State (See **Note 16**)

1. The particle size of lipid carriers can be measured by a number of techniques, such as dynamic light scattering (quasi-elastic light scattering [QELS]) ***(86,87)***.
2. In our laboratory we use the QELS method with a Nicomp Submicron Particle Sizer, for which accurate measures of vesicle or solid particle diameters can be made in the range of 20–1000 nm.
3. In QELS analysis it is possible to measure particles that exhibit a normal (Gaussian) distribution of mean diameters or several subpopulations of different diameters. As aggregation progresses, the analysis will show an increase in polydispersity. Diameters >1 µm are not accurately measured with this particle sizer, which impedes somewhat the study of highly aggregated complexes.
4. Particle size can also be estimated by electron microscopy (EM). Freeze-fracture EM requires fairly high lipid concentrations (preferably ≥10 m*M*), which may not be what is used in actual working gene therapy formulations. Additionally, the use of glycerol in sample preparation can induce vesicle shrinkage as a result of osmotic forces. Electron microscopy can provide further structural information. An interesting variety of structures, such as long strands or globules or sheets, has been described using this technique ***(88–90)***. Freeze-fracture EM of lipid/DNA particles has not been very informative, presumably because the lipid in the particles is not in a typical bilayer configuration. Negative staining EM of lipid/DNA particles yields an image of spherical particles ***(17)***. Another microscopy technique that has been applied to lipid carriers with plasmid DNA is cryogenic transmission EM (CTEM) ***(91)***, which has the advantages of rapid sample freezing and a lack of additional staining molecules foreign to the sample ***(92,93)***.
5. Aggregation state can also be assessed visually, since cloudiness increases slightly as particle size increases, until flocculent white flaky masses, chunks, or threadlike particulates appear in the suspension.
6. Similarly, turbidity can be measured, for example by measuring absorbance at 450 nm of small samples in a 96-well tissue culture plate in a plate reader. This is limited by the fact that the absorbance will decrease once flocculation begins.
7. A simple method to assess the degree of excess aggregation is to subject the sample to centrifugation (10,000*g*). Small liposome/DNA complexes, liposomes,

or plasmid DNA alone will not pellet under these conditions, but large aggregates (>1 μm) will pellet ***(94)***. The centrifugation conditions required will vary according to the cationic lipid used. For example, DDAB-containing liposome/DNA aggregated complexes will pellet within 5 min at room temperature but DODAC-containing aggregates require 30 min of centrifugation at 4°C (E. K. Wasan, unpublished observations). If the lipid and/or DNA have been radiolabeled, then the supernatant can be sampled for scintillation counting and the percentage remaining unpelleted may be calculated.

*3.2.2. Fusogenic Potential (*See ***Note 17****)*

The assessment of the fusogenic character of lipid–DNA carriers is based on lipid-mixing assays developed for use with liposomes as model membranes ***(95)***. Most frequently used is the resonance energy transfer (RET) technique. Fluorescently labeled lipids, such as NBD-PE and rhodamine-PE, are incorporated into the lipid mixture used to make the liposomes or lipid/DNA particles. NBD-PE fluorescence is quenched when it is molecularly close to rhodamine-PE due to resonance energy transfer from NBD to rhodamine ***(96,97)***. When lipid mixing occurs, the rhodamine component is physically moved away from the NBD by lipid dilution, and the NBD then spontaneously emits its energy as fluorescence. NBD-PE and rhodamine-PE are used in low concentrations in the lipid formulation (0.5–1% each), to minimize functional changes in the lipid membrane or particle to be studied. The fluorescent liposomes are mixed with nonfluorescent liposomes of otherwise identical composition in a ratio of l:l to 1:10. A ratio as high as 1:1 gives a strong fluorescence signal, which is useful when the effects of light scattering produce a noisy background. However, a ratio as low as 1:10 may be more sensitive because the dilution of the fluorescent lipids will be greater upon membrane fusion, producing a bigger percent change in the fluorescence signal.

1. To begin the assay, the baseline fluorescence (T_o) of a dilute suspension of liposomes or lipid/DNA particles (0.5–1 m*M*) is measured over time with a fluorometer (for the NBD/rhodamine system, excitation 465, emission 535 ***[82]***, using a cutoff filter at about 530 nm). An emission wavelength cutoff filter is valuable because it minimizes the effects of light scattering, which can be significant. If no cutoff filter is available, controls must be included in which the experimental conditions are exactly the same except no fluorescent lipids are used ***(98)***. These control values can then be subtracted from the experimental values as background.
2. The next step is to add the fusion-inducing component, such as a salt solution, DNA, or another kind of liposome/membrane/cell, while continuously recording the fluorescence (T_f). The ratio of this component to the lipid vesicles or particles will vary according to the experimental goals. Similar to anionic liposomes, such as phosphatidylserine/phosphatidylcholine (PS/PC) which fuse rapidly in the

presence of 1 m*M* Ca_2Cl ***(99)***, cationic liposomes, such as DODAC/DOPE or DODAC/DOPC, when mixed with DNA undergo rapid lipid mixing with the reaction complete within a few minutes ***(100,101)***. Lipid/DNA particles or cationic liposomes containing DOPE also undergo rapid fusion with model membranes, such as DOPS/DOPC ***(102,103)***.

3. Finally, complete lipid mixing is simulated by the addition of a nonionic detergent solution, such as 0.1–3% Triton X-100 or 35 m*M* OGP, to completely disperse the lipids.
4. The fluorescence reading at this point is taken to be the maximal fluorescence (T_{max}). It can be difficult to solubilize DNA/liposome aggregates with Triton X-100, but heating the samples to the cloud point of the detergent (about 100°C) ***(104)*** followed by vortex mixing helps.
5. The average fluorescence readings at each step are then converted to percent of maximal lipid mixing by the following formula: $(T_f - T_o)/(T_{max} - T_o)$. The initial fluorescence is subtracted from both T_{max} and T_f to account for the variability in the actual fluorescence readings from sample to sample and between different batches of liposomes (*see* **Note 18**).

3.2.3. Carrier-Membrane Fusion

Studies of the interaction between cationic liposomes with or without added DNA and model membranes have been used in an attempt to understand what factors are important in carrier-cell interactions. Vesicle aggregation, aqueous contents mixing, or leakage and lipid mixing assays in the presence and absence of the fusion promoter (such as ions or DNA) are the most frequently examined phenomena. Contents mixing demonstrates more clearly than lipid mixing that actual complete fusion of liposomes has occurred. Liposomal aqueous-contents mixing assays are difficult to perform for DOPE-containing; cationic liposomes because the combination of fluorescent molecules used are salts of strong acids, such as 8-aminonaphthalene-3,6,8-trisulfonic acid/*N*,*N*'-r-xylylene bis(pyridinium bromide) (ANTS/DPX) ***(105,106)*** or ($TbCl_3$/DPA) terbium chloride/dipicolinic acid ***(107)***. These compounds induce H_{II} phase formation of DOPE, resulting in the inability of the liposome to maintain a bilayer configuration. The lipid-mixing behavior of cationic liposomes, however, is currently the subject of intense study. For example, the effects of the lipid composition of the target membrane have been considered. The density of negative charge and the degree of lipid-chain saturation on the target membrane appear to be critical factors ***(108)***. The effect of anionic model membranes (DOPC/DOPS) on the release of DNA from the lipid carrier has been investigated in an attempt to elucidate the mechanism of DNA escape from cationic liposome/DNA complexes ***(102)*** or DNA/lipid particles ***(103)***. These analyses are accomplished through the use of the lipid mixing assay, as described above, using anionic model membranes as the fusion promoter.

3.2.4. DNA Protection (See **Note 19**)

3.2.4.1. Fluorescent Dye Labeling of Plasmid

1. DNA accessibility can be determined by how well the DNA binds fluorescent intercalating dyes. TO-PRO-1 is a cyanine dye that fluoresces only when bound to nucleic acid ***(82)***. It is more sensitive for fluorescence detection than ethidium bromide and binds stably to the DNA. The relative degree of protection of the DNA can be quantified.
2. TO-PRO-1 (final concentration 1 μ*M*) is added to formed complexes or particles containing 1 μg plasmid in 0.6 mL.
3. A reference standard consisting of 1 μg DNA in water is also prepared and TO-PRO-1 added.
4. Spectrofluorometric readings are taken after 5 min incubation of the experimental samples and the reference standard with TO-PRO (excitation 509, emission 533 nm) ***(82)***. TO-PRO-1 is light sensitive, so all experiments using this dye should be carried out under reduced light conditions.
5. A value for comparison between samples can be calculated, called the "condensation index," CI = $(I_o - I) / I_o$ where I is fluorescence of the sample in the presence of TO-PRO-1 and I_o is flourescence of the DNA reference ***(17)***. Under conditions in which DNA is fully condensed, such as when bound to polylysine, the CI index approaches 1.0. TO-PRO-1 is reported to be membrane impermeant; therefore, the DNA could be protected from dye binding by the lipids and yet still not be condensed in the rigorous sense of the term ***(109–111)***.
6. As an alternative, the "dye exclusion index," DEI = $(I_f - I_j)/I_f \times 100\%$, may be calculated, where I_j is the fluorescence of the lipid/DNA complexes or particles in the presence of TO-PRO-1 and I_f is the fluorescence of the sample after solubilization with 35 m*M* OGP. The DEI is the percentage of the dye excluded from binding that potentially could bind.

3.2.4.2. DNase I Sensitivity

DNase I is now routinely used to evaluate the stability of DNA against enzymatic degradation in the context of a carrier system to provide an indication of the potential in vivo usefulness of the carrier. The more protected and/or condensed the plasmid DNA is by the components of the carrier, the less effect incubation with DNase I will have ***(103,112)***.

1. Liposome/DNA complexes or lipid/DNA particles containing 1 μg plasmid (we have used plasmids that are 4–7.5 kb) are mixed with 0.33 U DNase I and incubated at 37°C for 10 min. This should be sufficient to degrade naked DNA into small fragments, which should be included as a control. Incubation times or DNase I concentrations may have to be adjusted by the investigator.
2. The reaction is terminated by the addition of ethylenediaminetetra-acetic acid (EDTA) to a final concentration of 25 m*M*.
3. The DNA may then be extracted by the method of Bligh and Dyer ***(113)***. The sample is mixed with 1 part chloroform and 2.1 parts methanol, forming a monophase upon vortex mixing.

4. An additional 1 part chloroform and 1 part water are then mixed thoroughly with the monophase, forming a two-phase system.
5. The upper, aqueous phase is removed by pipet and the DNA is ethanol:precipitated by standard techniques.
6. Phenol/chloroform extraction of the DNA may also be used ***(80)***.
7. Electrophoresis of the DNA sample on a 0.8% agarose gel will then reveal the amount of degradation that has occurred.
8. Well-protected DNA will appear in a banding pattern that is similar to untreated plasmid, although a slightly higher proportion of the relaxed form is consistently observed. Degraded control plasmid will appear as a smear of low mol-wt fragments.

3.2.4.3. Serum Stability

Serum contains proteins and nucleases that can interact with extracellular DNA and promote degradation. It has been demonstrated that in vitro transfection efficiency using most cationic lipids is reduced in the presence of fetal bovine serum (5–10%) ***(114)***. The stability of DNA in serum therefore indicates the degree of protection afforded to the DNA by the lipid carrier.

1. DNA/liposome complexes or DNA/lipid particles (40 µg DNA/mL and 100 nmoles lipid/mL) containing 2 µg DNA total in 35–50 µL are added to 2 vol sterile water or 2 vol serum (such as normal mouse serum).
2. The serum is centrifuged at 600*g* for 2 min prior to use to settle any precipitates.
3. After mixing, incubation proceeds for 2 h at 37°C, sufficient time to fragment naked plasmid to small pieces, which can be detected by gel electrophoresis. For ease of handling, sample volumes are brought up to 300 µL with water.
4. One volume of Tris-buffered phenol is added followed by vigorous vortex mixing.
5. Centrifugation at 600*g* for 15 min enhances separation of the sample into two phases.
6. The upper aqueous phase containing the DNA is removed to a clean tube, avoiding the protein precipitate at the interface.
7. The DNA is ethanol precipitated by standard techniques and evaluated by 0.8% agarose gel electrophoresis ***(80)***.
8. The results are typically similar to those of the DNase I stability assay, where protected plasmid appears with its characteristic bands and degraded plasmid is seen as a low-mol-wt smear.

3.3. Analysis of Cell Delivery

3.3.1. Overview

The process by which the transgene is taken up into a cell and the gene product is expressed is complicated and not fully understood. Understanding the mechanisms involved in this process is imperative for the development of nonviral DNA delivery systems with high transfection efficiency. This has recently become the subject of intensive investigation and a number of critical

barriers to transfection have now been identified ***(115,116)***, including entry across the cell membrane, escape from the endosomal/lysosomal system, and nuclear entry. Endocytosis is believed to be the primary mode of cellular internalization of lipid/DNA carrier complexes. Receptor-mediated uptake is thought to be the major route of cellular entry, with targeted vectors bearing peptide ligands ***(23–25,117)***, carbohydrate ligands ***(84,118)*** or antibodies ***(67,71)*** (*see* **Note 20**).

3.3.2. Plasmid and Lipid Delivery

To achieve successful transfection, it is important that the DNA and the carrier are taken up by the target cells. Assessing the delivery process will help determine whether uptake of a particular lipid/DNA formulation is a limiting factor in the transfection process. Analysis of DNA and lipid delivery will also help in understanding whether internalization is a limiting factor for a cell line which is difficult to transfect (*see* **Note 21**).

3.3.2.1. Quantification of Plasmid Isolated from Transfected Cells

There are several ways to determine the quantity of plasmid in cells following transfection. We present here a fairly simple procedure in which radiolabeled plasmid complexed to cationic lipids is used to transfect cells, followed by quantification of the plasmid at various timepoints ***(119)***.

1. Cells are grown at an appropriate concentration such that they will be 70–80% confluent at the time of transfection.
2. The serum-containing medium is removed and replaced with serum-free medium (80 µL in the case of 48 well plates).
3. Liposome/DNA complexes or lipid-DNA particles in which the plasmid is radiolabeled (*see* **Subheading 2.1.2.**) are added to the cells at the desired concentration, usually 0.5–1 µg DNA/well in 20 µL of complexes.
4. Incubation proceeds at 37°C for 1, 2, 3, or 4 h, at which time the experiment is terminated. It is important to include a parallel control at 4°C, where cellular metabolism and DNA uptake are inhibited. This serves as a valuable control to evaluate DNA internalization.
5. The supernatant is removed and the cells are washed with serum-free medium which is pooled with supernatants, to determine the amount of plasmid which is not associated with the cells.
6. The cells are then lysed in 300 µL 10 µ*M* Tris-HCl (pH 8.0) containing 0.5% sodium dodecyl sulfate (SDS), 3 m*M* $MgCl_2$, and 10 m*M* NaCl.
7. The lysate is transferred to clean tubes and the wells rinsed with 300 µL lysis buffer, which is pooled with the corresponding samples.
8. The amount of tritium in each sample is determined by scintillation counting and the amount of cell-associated DNA is calculated by subtracting the amount of DNA associated with the cells at 4°C from that obtained at 37°C (*see* **Note 22**).

Other methods for quantifying the amount of DNA delivered to cells often require the use of DNA isolation procedures. Radiolabeled plasmid can be isolated from transfected cells using a modified Hirt lysis procedure ***(120)***. This procedure selectively precipitates host genomic DNA using high-salt and cold SDS precipitation, leaving plasmid in the supernatant for further purification and analysis.

1. In the modified Hirt procedure NaCl is added to the cell lysates (0.6% SDS, 10 m*M* EDTA) to a final concentration of 1 *M*.
2. The samples are incubated at 4°C overnight to promote precipitation.
3. Centrifugation at 10,000*g* for 15 min settles out a pellet of crosslinked genomic DNA and cell debris.
4. The supernatant containing the plasmid is extracted using equal volumes of phenol/chloroform (1:1).
5. The purified plasmid DNA is precipitated with 2 vol ethanol and 0.1 mL 3 *M* sodium acetate, pH 5.0, or 0.7 vol isopropanol by standard procedures, centrifuged (10,000*g* for 30 min), and the resulting pellet dissolved in TE buffer (10 m*M* Tris-HCl, 1 m*M* EDTA, pH 8.0).
6. The plasmid is then subjected to agarose gel electrophoresis.
7. Since the plasmid has been radiolabeled, the bands on the gel can be excised and radioactivity measured by liquid scintillation counting.
8. After transferring the gel slices to scintillation vials, the gel is melted in 500 µL of water or tissue solubilizer in a boiling waterbath.
9. The samples are mixed with the scintillation fluid and radioactivity counted.

If the plasmid has not been radiolabeled, the amount of DNA taken up following transfection can be evaluated using "dot-blot" analysis (*see* **Note 23**).

Following administration of a carrier/DNA complex to animals, plasmid can be quantified as described above. The distribution, half-life, and other pharmacokinetic parameters of the plasmid can then be calculated if recovery is adequate. The simplest method to follow DNA in vivo is to utilize radiolabeled DNA and to assess radioactivity in tissue homogenates after transfection ***(39,121–123)***. One must be careful to account for the total dose in order to make analysis of the data meaningful. Upon systemic administration, for example, larger organs, such as the liver, may take up more of the total dose, but may not account for the largest proportion when normalized to tissue weight ***(124)***.

3.3.2.2. Analysis of Plasmid DNA Integrity

Delivery of the plasmid to the target cells is only useful if the plasmid remains intact during the process and it is in a transcription-ready form after cellular internalization. As indicated earlier, it is not clear yet which plasmid conformation(s) can be defined as the "active species." Any analysis of plasmids isolated from cells or tissues should take this into consideration; bearing

in mind that the extraction procedure itself could possibly affect DNA topology. In addition, it is unknown what quantity of DNA must reach the nucleus intact in order for transfection to be successful.

The most widely used approach for the detection and analysis of DNA is Southern analysis ***(80,81,125)***, which is useful because it not only allows detection of the specific plasmid, but also assessment of degradation and conformation of the transfected plasmid. The method can be applied to DNA samples from in vitro or in vivo transfection. Southern analysis is sensitive enough to detect small amounts of plasmid DNA against a large background of genomic DNA.

1. Total DNA is isolated from washed cells or frozen-powdered tissues by standard techniques, such as with Tris/EDTA/SDS extraction (10 m*M* Tris-HCI, 0.1 m*M* EDTA, pH 8.0, 20 µg/mL pancreatic RNase, 0.5% SDS), followed by proteinase K treatment (100 µg/mL) and phenol extraction of the DNA. An alternative method involves lysing the cells with 7.5 vol 6 *M* guanidine, 0.1 *M* sodium acetate, followed by ethanol precipitation then rehydration in TE buffer ***(80)***.
2. Following DNA extraction, a restriction digest is performed using one or more restriction enzymes that will not cleave the plasmid. This digestion will result in a uniform smear of genomic DNA upon gel electrophoresis and thus uninterrupted migration of the plasmid.
3. After gel electrophoresis, the DNA fragments are transferred to a charged nylon membrane.
4. DNA probes complementary to the sequence of interest are hybridized to the DNA on the membrane. The probes can be radioactively labeled or bound to other molecules that can be easily detected, such as digoxigenin. Radiolabeled probes can detect as little as 0.1 µg of DNA on a Southern blot.
5. The digoxigenin chemiluminescence system, available in kit form, has the advantage of not requiring radioactive materials and it can detect as little as 10 ng of plasmid. These high levels of sensitivity are important to detect low levels of DNA delivered to cells or tissues. If even greater sensitivity is required, PCR ***(80,81)*** can be used to amplify plasmid from transfected cells or tissues ***(126–128)*** for a qualitative assessment of the presence of the transfected plasmid. PCR, like Southern analysis, requires specific intact DNA sequences for detection of the plasmid, so these methods may be more appropriate than analyzing for the presence of radiolabeled DNA. PCR, however, can also amplify degraded plasmid; Southern blotting provides a more thorough analysis (DNA quality as well as quantity).

3.3.2.3. Analysis of Lipid Delivery

The interaction of carrier lipid molecules and cellular components is a key factor in the delivery and release of the plasmid DNA prior to transcription. The carriers' physicochemical properties that promote optimal transfection are still being investigated. An analysis of carrier lipid disposition within the cell,

however, coupled with plasmid analysis and transfection data will provide valuable information. Assessment of lipid delivery to transfected cells or tissues can be accomplished in several ways, all of which should be pursued with caution. The lipid components of the carrier system can be fluorescently or radioactively labeled. Fluorescently labeled lipid taken up by cells can be visualized by microscopy ***(129)*** or quantified by flow cytometry ***(130,131)***. Radioactivity resulting from the labeled lipid in transfected tissue cultured cells can be assessed directly by scintillation counting. It should be noted that the distribution of labeled lipid components, whether tagged by a radioisotope or a fluorescent marker, may not necessarily be representative of the liposome/DNA complex or lipid/DNA particle. When these systems are mixed with serum (in vitro or following iv injection) or are in contact with other membranes (cell plasma membrane) or lipid-rich proteins (lipoproteins) there is the potential for the lipid component to exchange. The problem is compounded by issues related to metabolism and degradation. As indicated in **Subheading 2.2.**, these problems have been well-addressed for liposomes used as carriers of small molecules in which CHE has proven to be a nonexchangeable, nonmetabolizable liposomal lipid marker. Importantly, the lipid marker only tracks the fate of the liposome, not the associated small molecule. For these reasons we always attempt to measure both lipid component as well as associated active agents ***(132)***.

In the case of cationic lipid/DNA complexes, the lipid markers that have been used are often the same as those used for conventional liposomes (i.e., CHE). This may not be appropriate. Therefore, we believe it is best to use a radiolabeled form of the lipids used to prepare the carrier system ***(133)***. Ideally, carrier cationic lipid and plasmid DNA quantification should be performed on the same tissues within in the same experiment. It may also be useful to analyze the fate of the neutral lipid components of the carrier. Radiolabeled DOPE is available, for example. It may also be useful, in certain types of analyses, such as pharmacokinetic and biodistribution studies, to label both the cationic and neutral components of the lipid carrier. Without some kind of tag, however, the process of detection may be more complex because of the need to efficiently extract the carrier lipid(s) from cells or tissues prior to analysis. The presence of endogenous lipids may make this difficult. For cationic lipids, such as DOTAP or DODAC, for example, it may be recommended that quantification of tissue levels, such as by HPLC analysis, be performed by those specializing in lipid analysis (Northern Lipids, Vancouver, BC, Canada).

3.3.3. Expression of the Transgene

The ultimate endpoint of any gene therapy strategy is expression of the transgene in the tissue of interest. Following successful cellular uptake of the

gene carrier system, the cell's transcription and translation machinery produces messenger RNA and subsequently the protein product from the transgene. The number and specificity of the interactions that must occur among the gene carrier, the exogenous plasmid DNA, and components of the target cell in order for the gene product to be expressed is staggering. Control over the specificity, onset, and duration of this expression is still a major hurdle, largely resulting from the many variables involved. For example, without integration into the genome, which is currently achievable with retroviruses, expression will necessarily be transient. Loss of the transgene will inevitably occur as cell division progresses. However, if one is treating a disease, such as cancer, or administering a vaccine, transient expression is in fact desirable. Restriction of expression can be achieved with tissue-specific gene promoters, but currently those in use for gene therapy applications are few in number ***(134–136)***. Inducible promoters are also an attractive option, giving the investigator the ability to turn expression of the gene on and off as desired ***(137–140)***. These promoters, however, may not generate the high level of expression achievable with nonspecific promoters, such as the cytomegalovirus (CMV), simian virus (SV-40), or Rous sarcoma virus (RSV) promoters commonly in use today.

3.3.3.1. Evaluation of Transfection Using Reporter Genes

We often use "reporter genes" to evaluate the ability of a gene carrier system to deliver exogenous DNA or for a given plasmid construct to achieve expression in vitro or in vivo ***(141,142)***. These genes encode protein products, usually enzymes, for which there are simple biochemical assays, such as β-galactosidase, chloramphenicol acetyltransferase (CAT), and luciferase. These three are currently the most commonly used reporter genes. They share the advantage of providing a simple, quantitative measure of the effectiveness of a gene therapy vector in terms of expression of a product. Using any reporter gene, however, the actual level of expression may vary greatly between experiments, between cells on a tissue culture plate, or between animals within the same experiment. One must be cautious about how to make comparisons between groups or between different gene therapy studies that are utilizing reporter gene expression as a measure of success. The reporter genes are not completely interchangeable in, a given vector; i.e., the level of expression driven by a particular promoter may vary according to the reporter gene ***(143)***. Another consideration to bear in mind is that all three of these reporter gene products remain cytoplasmic, and may not be representative of the efficacy of a secreted therapeutic gene product, which could produce a "bystander effect."

3.3.3.1.1. β-*Galactosidase.* (EC 3.2.1.23) is an enzyme found in many bacterial and eukaryotic cell types that converts *o*-nitrophenyl β-D-galactoside to *o*-nitrophenol and D-galactose. It will also convert 5-bromo-4-chloro-3-indoyl

β-D-galactoside ("X-gal") to form a blue-colored substance that can be assayed spectrophotometrically. The assay for the final product is reasonably rapid and simple to perform. The main advantage and use of β-galactosidase as a reporter gene is that individual transfected cells can be seen under a light microscope because of the deposition of the blue product in the cytoplasm. X-gal can be added to the cells during histochemical analysis or it can be incorporated into agar tissue culture plates ***(144)*** for easy visualization of the transfected (blue) cells. Transfection efficiency and the percentage of cells expressing the transgene can be calculated from counting the blue vs clear cells. Fluorescence-activated cell-sorting (FACS) analysis can also be adapted for analysis of cells transfected with β-galactosidase ***(145,146)***. The disadvantage of β-galactosidase is that quantitation of the blue product, based on the optical density of cell lysates at 570 nm, is not very accurate or sensitive. There is also the concern that endogenous β-galactosidase may interfere with interpretation of transfection results ***(147)***. In an in vivo transfection setting, typically one will use β-galactosidase as the reporter gene to determine the cell types being transfected and to estimate efficiency. This is coupled with the use of a different reporter gene, such as luciferase or CAT, as described in **Subheading 3.3.3.1.2.**, to perform the actual quantitation of the amount of transgene product produced ***(148–150)***. When using β-galactosidase as a histological marker it is important to control for the background by including tissues obtained from animals injected with a β-galactosidase-null plasmid.

3.3.3.1.2. Chloramphenicol Acetyltransferase (CAT). Chloramphenicol acetyltransferase (EC 2.3.1.28) is a plasmid-localized bacterial enzyme that catalyzes acetylation of chloramphenicol with the use of acetyl-*S*-Coenzyme A. When the bacterial gene is inserted into a plasmid expression vector appropriate for transfecting eukaryotic cells, the CAT enzyme can be quantified by measuring its activity ***(151)***. One assay for enzyme activity on cell or tissue homogenates employs a radioactive substrate, either ^{14}C-chloramphenicol or ^{14}C-acetyl, from labeled acetyl CoA ***(152)***. Tissues must first be heat-inactivated and treated with paraoxon (diethyl ρ-nitrophenyl phosphate) to avoid contributions from other acetylating enzymes present in the tissue. Analysis is performed by liquid scintillation counting of the radioactive product after extraction. The activity of the cells or tissue expressing CAT is compared to the known activity of a CAT standard. This assay provides better sensitivity than β-galactosidase; however, it involves the use of radioactive materials and the assay procedure is lengthy and labor-intensive. When reporting CAT activity, one should convert the transferred cpm of radioactivity to units of CAT activity based on the standard. It has also been argued that units should be converted into milligrams of product to obtain a value that can be compared among research laboratories.

3.3.3.1.3. Luciferase. Luciferase (EC 1.13.12.7) is a light-producing enzyme from the American firefly *Photinus pyralis*. The luciferase gene has been cloned and inserted into vectors for expression in bacterial or eukaryotic cells ***(153)***. Luciferase has no mammalian endogenous counterpart, so there is no background interference ***(154)***. Luciferase utilizes ATP as a substrate to produce light, which can then be measured in a simple luminometer ***(155,156)***. Less accurately, the light emission can be measured by scintillation counting or by exposure to photographic film ***(157)***. The assay to measure luciferase activity is extremely simple, basically involving adding the substrate ATP to the prepared cell or tissue homogenates and measuring light production within a specific time frame. Light emission increases rapidly for the first 10 s after substrate addition, then emits at steady state for about 5 min. After 5 min, light production is reduced with a half-life of about 5 min; thus, it is important to take the reading during the steady-state phase. The more sophisticated luminometers can analyze the kinetics of the reaction and assess luciferase activity based on the integrated area of the steady-state phase of light emission over time.

3.3.4. Gene vs Message vs Product

Although we are necessarily most interested in the final expression of the transgene, its time of onset, and duration of action, it may be necessary to perform more fundamental investigations when expression is less than optimal. We have addressed the importance of assessing DNA delivery to the target cell population (*see* **Subheading 3.3.2.1.**). It has also been noted that although plasmid delivery is necessary for transfection, it is not sufficient in itself ***(119,158)***. The interaction between the carrier and the plasmid DNA is important not only for delivery and protection of the DNA, but also for release within the appropriate intracellular compartment. Thus, the study of the intracellular uptake, distribution, and degradation of both plasmid and carrier are useful in the effort to improve our understanding of nonviral DNA transfection of cells. Although the discussion here has focused on lipid carriers, the same principles apply to other types of nonviral carriers. Analysis of the disposition of targeted vectors and multicomponent delivery systems may be more complex, but no less worthwhile.

Another issue is the transcription of the delivered gene into mRNA, in particular the time of its appearance in the target cells and the stability of the message. This may be influenced not only by the properties of the transfected cell, but also by the sequence itself. Northern blot analysis ***(80,81)*** can reveal when transcription of the transferred gene is beginning and how long it continues, whether <24 h or for months. Analysis of the gene product, the marker or therapeutic protein of interest, is the ultimate step and care must be taken to

Table 3
Characterization of Nonviral DNA-Delivery Systems

Component	Characteristic	Technique	Subheading
Lipid	Particle size	QELS, turbidity	**3.2.1.**
	Fusion	RET	**3.2.2.–3.2.3.**
	Biodistribution	Radiolabel or fluorescent label	**3.3.2.3.**
DNA	Condensation	Dye-binding	**3.2.4.1.**
	Protection	DNase I stability	**3.2.4.2.**
		Serum stability	**3.2.4.3.**
	Integrity	Gel electrophoresis/ Southern blotting	**3.3.2.2.**
	Structure	Electron microscopy	**3.2.1.**
	Biodistribution	Fluorescent label; Radiolabel; Southern blotting; PCR	**3.3.2.1.–3.3.2.2.**
Cell/tissue	DNA delivery	Lipid and DNA uptake	**3.3.**
	Transfection	Reporter genes	**3.3.3.–3.3.4.**

chose a detection method that is both sensitive and free of background. When DNA delivery, carrier delivery and stability, mRNA expression, and protein expression data are examined together, this can give information about which steps in the cellular process leading to expression are rate-limiting. The greatest limitation to improving nonviral DNA delivery systems may be in not knowing where the bottleneck is in the process from plasmid uptake to functional protein production.

4. Notes

1. It is important to ensure that the plasmid of interest is present before continuing. This can be done by checking for the presence of the desired plasmid using any standard miniprep method ***(80,81)*** followed by enzyme digestion and analysis by gel electrophoresis.
2. Plasmid purification methods vary in the time, expense, and equipment required and in the purity of the plasmid produced. Purity is important to generate high levels of transfection in a reproducible manner. Potential contaminants include bacterial genomic DNA, RNA, protein, endotoxin, chemical residues, trace metals, and undesirable counterions ***(159)***. Depending on the user's endpoint, concern regarding any of these contaminants will vary. For example, if the plasmid product is intended for human clinical trials, strict quality control over of all these factors, among others, must be addressed. Lesser concern is warranted for

use in molecular biology studies; however, one should bear in mind that even cell culture transfection assays may be strongly affected by the quality of the DNA ***(160)***. The cesium chloride gradient method using ultracentrifugation ***(80)*** yields high-quality DNA but requires considerable time to perform, is more difficult to scale up, and requires the use of ethidium bromide, a carcinogen. The ethidium bromide is typically removed from the purified plasmid by solvent extraction and the cesium chloride by dialysis. Techniques have been developed in which the cesium chloride and ethidium bromide can be removed from the DNA in one rapid step on a desalting column (*see* **Subheading 2.**). The impure DNA is first pretreated with 5 *M* guanidine thiocyanate and 5% β-mercaptoethanol, and briefly heated at 65°C for 5 min, which allows complete removal of the CsCl upon column chromatography ***(161)***.

Anion exchange chromatography takes advantage of the difference in affinity of plasmid DNA vs proteinaceous cellular debris for the column matrix. A recent study comparing plasmid purified by anion exchange chromatography vs CsCl density gradient showed that the two methods produced plasmid that was equivalent in transfection ability. Clearly, both methods yielded highly purified DNA. This report did show, however, that the anion exchange method yielded plasmid with significantly higher levels of endotoxin ***(162)***.

Endotoxin is bacterial cell-wall lipopolysaccharide that is toxic to cells and may have an impact on the transfection of some cell lines. Its presence is also unacceptable in human gene therapy products because of the potential for anaphylactic reactions. It behaves much like large plasmid on a size exclusion or anion exchange column because of its physical and chemical characteristics, which makes it difficult to separate from the DNA ***(163)***. Endotoxin removal can be accomplished by several methods, such as treatment with Triton X-114 or polymixin B chromatographic resin. Triton X-114, when brought to its cloud point temperature of 20°C, will solubilize the highly lipophilic endotoxin but not plasmid. Polymixin B, which binds with high affinity to endotoxin but not to DNA, is available bound to a polymer, which is used as a slurry to perform the extraction, usually by mixing with the crude DNA extract overnight. Alternatively, it can be used in a column. Unfortunately, these two methods are reported to not work well in the presence of CsCl ***(162)***. The anion exchange columns used in the Qiagen and Nucleobond plasmid preparation kits also remove some endotoxin, but not as much as by the aforementioned methods ***(164)***. Commercial sources of regeneratable resin-immobilized ligand can be used to remove endotoxin to trace levels; however, if clinical use of the DNA is intended, methods must be in place to quantitate levels of released ligand in the final product.

Gel filtration or size exclusion isolation of plasmid from the crude nucleic acid preparation offers the advantages of good separation of plasmid from genomic DNA and RNA and a simple, inexpensive procedure ***(165,166)***. The use of Sephacryl S-1000 Superfine matrix allows excellent separation of plasmid from RNA. When this separation is optimal, the use of RNase can be omitted from the isolation procedure, which is important for clinical considerations. This

method of purification isolates predominantly supercoiled DNA (covalently closed circular DNA) ***(167)***, and may be quite useful for studies investigating which conformation of the DNA is the most effective in transfecting cells; some studies have suggested that supercoiled DNA may be the most effective conformation ***(168)***. A disadvantage of using large exclusion columns to effect complete separation of supercoiled DNA is that the sample may become quite diluted in the process, requiring an additional precipitation step and subsequent loss of product (S. S.-Y. Wong, unpublished observations).

Differential separation of plasmid forms (supercoiled, relaxed, linear) can also be accomplished using PEG_{6000} as the precipitating agent rather than ethanol or isopropanol. The technique is based on the fact that a certain threshold concentration of PEC, is required to precipitate nucleic acid of a given size. RNA and genomic DNA, therefore, can also be removed. Lower molecular weight nucleic acids require higher PEG concentrations to precipitate. To isolate plasmid, PEG (5–12%) is added to the crude nucleic acid preparation and incubated overnight, followed by centrifugation at 8000*g* for 5 min. Recovery is reduced if the initial DNA concentration is low. Removal of the PEG, if required, can be accomplished by DEAE cellulose chromatography, gel electrophoresis, or CsCl density gradient ***(169)***.

3. A simple measure of DNA purity is to determine the ratio of OD_{260}/OD_{280}. A pure DNA sample will have a ratio of 1.8–2.0 ***(80,81)***. A ratio lower than 1.8 raises concerns about high levels of contamination with RNA or protein. A spectrophotometric scan (absorbance 230–340 nm) is also useful to evaluate protein contamination since protein scatters light much more effectively at 230 nm and the presence of protein may shift the absorbance of DNA to slightly greater than 260 nm ***(170)***.
4. The quantity of glycerol stock to start with may have to be adjusted to ensure that enough bacteria are present to reach this OD within a reasonable period of time.
5. This procedure avoids starting the liquid culture from a LB plate, which may result in slower growth of the bacterial culture. Picking a single colony from a LB plate and growing it up in M9 media is often unsuccessful for the same reasons: growth will be too slow.
6. Adding radioactive thymidine before the OD_{550} reaches 0.5 results in a higher final specific activity.
7. Fluorescently labeled plasmid can be quite useful for cellular uptake and distribution studies ***(112)***. The main concern with fluorescently tagged DNA is that the presence of the dye molecules may interfere with the interactions between the DNA and the carrier, or the DNA and cellular components. Of equal importance, the binding of the dye to the DNA must be irreversible, so that the dye molecules do not dissociate from the DNA once internalized by the cell. A number of fluorescent DNA-intercalating dyes are available for DNA labeling, such as ethidium bromide, ethidium monoazide, the TO-PRO series, various other cyanine dyes, and many others ***(82)***. For example, the membrane-impermeable compound YO-YO

labels plasmid extremely well, giving a strong signal for direct fluorescence measurements ***(171)***, FACS ***(172)***, or microscopy of cells that have taken up the labeled plasmid DNA ***(173)***. This dye binds to DNA by intercalation (high affinity) and by ionic interactions (low affinity).

8. Cationic liposome/DNA complexes are taken up by most cells in vitro or in vivo much more efficiently than naked DNA. For preparation of gene transfer vehicles the liposomes are preformed, then mixed in a defined ratio with the nucleic acid for rapid, spontaneous formation of liposome/DNA complexes. Several methods are available for the preparation of liposomes, such as reverse-phase evaporation ***(174)***, sonication ***(175)***, French press ***(176)***, and extrusion ***(177)***. We prefer to use extrusion because of its ease and its ability to produce homogenous vesicles of defined size. Cationic lipids that are typically used derive their positive charge from a modified amine or amide headgroup. Those useful for transfection include, but are not limited to, DOTMA, DOSPA, DOTAP, DDAB, DMRIE, DC-Chol, DOGS, DODAC, and an ever-increasing number of variants of these older lipids. Helper lipids, such as DOPE, are often included with certain cationic lipids in liposome formulations, generally at 50/50 mol% with the cationic lipid. Theoretically, DOPE acts to promote endosomolysis upon transfection through its ability to promote membrane fusion ***(54,55)***, although the exact mechanism remains controversial. Some cationic lipids do not seem to require DOPE to achieve transfection ***(53,54)***. The lipid to be used for a given transfection experiment remains somewhat an empirical choice at this time because the differences between the effective cationic lipids overall appears to be slight. Derivatives of the older cationic lipids continue to be synthesized, with reports of improved transfection efficiency in a few cell lines, but further investigation is required to determine if these derivatives offer any significant benefit over the parent compounds in a wide variety of cell types and experimental conditions.
9. Although it is well-established that CHE is an excellent lipid marker for following the fate of liposomes in vivo because it is nonexchangeable and nonmetabolizable, it is not clear whether this lipid marker is adequate for following the fate of cationic liposomes used for gene transfer. For this reason, we often use radiolabeled DOPE as a marker for DOPE-containing formulations. Where possible, we employ radiolabeled cationic lipid. The latter two options are considerably more expensive than using CHDE.
10. The hydrating solution should be of very low ionic strength or nonionic and 0.22 μm-filtered. High concentration salt solutions tend to cause rapid aggregation of DOPE-containing liposomes, or may prevent proper hydration of the lipid film, required for liposome formation. This step should be performed at a temperature above the gel-to-liquid crystalline transition temperature of the lipids, but below the DOPE bilayer-to-hexagonal phase-transition temperature ***(178,179)***, meaning hydration is performed in the range of 2°C to room temperature. Keeping the hydrating solution on ice is beneficial.
11. Large unilamellar liposomes (LUVs, as described in **Note 8**) and plasmid DNA will not be pelleted by this procedure ***(94)***.

12. There has been considerable debate in the field about the relative importance of the mixing rate during liposome/DNA complex preparation, but to our knowledge no study with a rigorous test of the effect of this parameter on complex formation and transfection has been published. We have found that flocculent aggregation is less likely when DNA is added slowly to the liposomes and mixed immediately by gentle pipeting rather than by rapid vortex mixing. Dust and debris in the components, easily acquired from room air, must also be scrupulously avoided. Flocculent aggregation may also be related to the presence of impurities in the plasmid DNA, which can be avoided by careful, standardized DNA purifications procedures and quality-control testing prior to use (*see* **Subheading 2.1.1.**).
13. An alternative method developed by L. Huang and coworkers ***(118)*** involves the formation of an emulsion, utilizing DC-Chol, DOPE, and Tween 80 (0.75:0.25:0.125 w/w/w ratio). The presence of Tween 80 presumably stabilizes the emulsion and prevents aggregation. Interestingly, this particular formulation was not sensitive to the presence of serum, which reduces transfection efficiency for most cationic liposome formulations.
14. Polylysine of 300 repeat units has been found to be the most useful for coupling. Some authors have stated that residual uncoupled polylysine can reduce the efficiency of specific receptor-mediated transfection in the final preparation unless more extensive purification is done, such as preparative acid-urea gel electrophoresis followed by cation-exchange HPLC ***(69)***.
15. A great deal of effort has been directed toward development of targeted liposomes, and it can be suggested that many of the approaches used can be applied to both liposome/DNA complexes as well as lipid/DNA particles. It is well established that many of the approaches involving covalent attachment of proteins onto liposomes can result in liposome–liposome crosslinking ***(85,180)***. It is anticipated, therefore, that such procedures (described elsewhere in this volume) will not be suitable for use with liposome/DNA complexes. Coupling techniques may be useful for attaching protein-based targeting ligands onto lipid/DNA particles, provided that reactive lipids can be incorporated stably in the outermost lipid monolayer. We believe that targeting strategies based on incorporation of low-mol-wt targeting ligands covalently attached to appropriate lipid anchors is best for achieving cell targeting. An excellent example of this approach is that described by Lee et al. involving folate-modified lipids ***(181)***. Folate-modified PEG has also been used in the preparation of polylysine/DNA/cationic lipid/PEG complexes for transfection, which showed folate-receptor-specific uptake at high lipid-to-DNA ratios ***(182)***.
16. The particle diameter and homogeneity of the sample is an important parameter with regard to both cellular uptake and biodistribution. In vitro, larger particles theoretically can settle more readily onto a cell monolayer than very small particles. On the other hand, if the particles are too large (μm range) endocytosis may be impaired. In the in vivo setting, if large particles are administered intravenously, the potential exists for emboli formation ***(183)***. The particles can

become lodged in the very small capillary beds, such as in the lung, limiting distribution to other sites. Gross flocculation also makes administration of a well-defined dose difficult. From studies involving the biodistribution of liposomally encapsulated drugs ***(184–186)*** and other microparticulate systems ***(187,188)***, it has been demonstrated that particles larger than 200 nm are avidly taken up by cells, of the reticuloendothelial system, such as macrophages, which will prevent distribution to other cell types. This is also something to bear in mind if the target cells are macrophages.

17. For lipid carriers to be taken up by cells, there must be interaction between the cellular membrane and the particle. DNA/liposome complexes are believed to be taken up primarily by endocytosis, with direct membrane fusion as a potential alternative route ***(90)***. Once inside the cell, the particle is thought to interact with anionic endocytic membranes to escape the endosome and avoid degradation ***(129)***, and for the DNA to reach either the cytoplasm or the nucleus for activation. These processes imply that the particle itself must possess a certain critical degree of "fusogenic potential," or ability to fuse with these cellular membranes. This property can be measured with model membrane systems, as described in **Subheading 3.2.2.** One should bear in mind, in the case of liposome/DNA complexes, that the initial fusogenic potential of the liposome itself may be significantly reduced once it has complexed with the plasmid DNA.

    Fusion of the cationic liposomes with each other is a result of several factors. Charge neutralization and aggregation reactions mediated by addition of DNA to the cationic liposomes fosters close contact between membranes and may lead to local dehydration at the membrane interfaces. Another important component is the presence of a fusogenic lipid, such as DOPE, which in isolation prefers to adopt a hexagonal rather than bilayer configuration. DOPE is stabilized in a bilayer phase by addition of the cationic lipid; however, charge neutralization and/or phase separation of the cationic lipid will result in bilayer destabilization. Formation of H_{II} phase or inverted micellar intermediate structures has been correlated to initiation of membrane fusion ***(189–191)***. For those cationic lipids that require combination with DOPE :for optimal transection, DOPE may be working by increasing the fusogenic potential of the carrier complex ***(192)***. Perhaps those cationic lipids that do not require DOPE for transfection ***(53,54)*** already possess significant fusogenic properties, although this is speculation. We would predict that there is a balance between a minimal fusogenic potential that optimizes cellular uptake and endosomal escape, and a fusogenic potential that results in excessive aggregation of the particles amongst themselves, thereby reducing cellular uptake. The role of promoting fusion has been emphasized more recently by studies demonstrating enhanced transfection when using fusogenic peptides, such as peptides from influenza virus ***(77,78)***. The relationship between fusogenic potential (as measured by lipid-mixing behavior) and transfection mediated by lipid-based DNA carriers, however, is unclear ***(193)***.

18. Some researchers prepare a mock fusion control, in which 1/10 of the usual fluorescent lipid (i.e., 0.05–0.1%) is included in the liposome preparation ***(98)***.

Theoretically, the fluorescence of the mock fusion control should be the same as fluorescent plus nonfluorescent liposomes in a 1:10 ratio that are 100% fused (and thus this value could be used as T_{max} or factored into the equation provided in **Subheading 3.2.2.**, **step 5**). However, in practical application, the efficiency of fluorescent lipid incorporation tends to be variable, and the distribution of the fluorescent lipid in the two faces of the liposomal bilayer may not be equivalent. An additional concern is that lipid exchange may occur. These factors are difficult to control.

19. For gene transfer to be effective, the DNA must reach its site of action intact. One reason that naked DNA is ineffective for gene transfer to most tissues ***(34–50)*** (except muscle ***[194–196]***) is because it is rapidly degraded by nucleases in the plasma compartment and interstitial spaces. Once taken up by the cells, DNA can also be degraded by intracellular nucleases in lysosomes, the terminal, degradative component of the endosomal system ***(197)*** into which transfected DNA is transported after gaining access to the cell ***(129)***. Intracellular nuclease-mediated degradation is detrimental to both in vitro and in vivo transfection efforts. It is therefore essential that the DNA be protected. This can be achieved by binding the DNA to cationic liposomes, by lipid-DNA particle formation, or by DNA condensation, such as with the cation polylysine, thus preventing accessibility of nucleases to labile bonds of the DNA structure. In **Subheading 3.2.4.**, three complementary assays for determining the level of DNA protection that are useful for comparing formulations are described. Relatively greater protection, however, does not necessarily correlate directly to increased competency in transfection ***(103)***. For example, lipid/DNA particles prepared using cationic lipid and phosphatidylethanolamine (PE) are less stable than formulations prepared with phosphatidylcholine (PC), however, PE-containing lipid/DNA particles are more effective for in vitro transfection of cells than PC-containing lipid/DNA particles. The more important factor in the difference in the effectiveness of these two formulations in transfection may be the relative fusogenicity of PE vs PC, as discussed in **Subheading 3.2.** The PE headgroup may allow dissociation of the cationic lipid from DNA more effectively than PC. We speculate that if the DNA is too tightly bound, it cannot escape the carrier and reach the nucleus for transcription.
20. The first intracellular destination of the complex is the endosomal system. For DNA to be an effective transfection agent, it must escape the endocytic pathway, or it will eventually be degraded by lysosomes (which contain nucleases and lipases). An event that has been recently recognized to be of fundamental importance is that the plasmid DNA must dissociate from the carrier once it is internalized by the cell for transcription to occur. It generally believed that this event occurs within the endosome itself, releasing the DNA in an unbound form into the cytoplasm ***(116)***, although some investigators have proposed that the complex is directly delivered to the nucleus ***(198)***. We believe the biochemical characteristics of the carrier play a critical role in the timing and efficiency of that release process. It is also likely that there are cell-type-specific properties that may have an impact on both the uptake and the breakdown of the carrier/DNA

complex intracellularly ***(158)***. Regardless, the plasmid DNA must gain entry to the nucleus in an intact form, where the cell's own machinery can eventually produce a functional protein.

The mechanism by which plasmid enters the nucleus, whether by active transport or by diffusion ***(115)***, is not clear but it is believed to be a major barrier to transfection. To avoid this problem, carrier systems have been designed in which the vector is transcribed in the cytoplasm without the use of the host cell's transcription machinery, avoiding the limiting step of nuclear entry ***(199,200)***. Alternatively, other groups have utilized nuclear localization signal peptides (NLS) to facilitate nuclear targeting ***(201,202)***. To elucidate the mechanism of gene transfer and expression, studies must be done to track the tissue, cellular, and subcellular localization of both the active agent, in this ease DNA, and the carrier components (cationic and associated helper lipids). In **Subheading 3.3.**, we describe some of the techniques we have used to gain a better understanding of the mechanisms of delivery of plasmid and carrier lipids. Many of the methods described herein can yield valuable information; however, they have limitations. New approaches to evaluate the pharmacokinetic and pharmacodynamic behavior of "gene medicines" must be developed.

21. A nontransfecting cell line may exhibit DNA uptake, but no transfection ***(119,158)***. One type of carrier may work very well in transfecting cells and a similar one not at all ***(51–53,108)***. Moreover, the study of intracellular pharmacokinetics can reveal important characteristics about the carrier and the DNA and how these elements behave during the transfection process. Although several methods are available to evaluate DNA and lipid delivery, caution should be exercised in choosing the approach to be used. For example, many researchers have used plasmid that is bound to gold particles or tagged by fluorescent molecules. Although this approach is convenient for microscopy studies, the potential exists for the tagging molecules themselves to interfere with the interaction between the DNA and the carrier, or the carrier/DNA complex and cellular components. Radioactive tags can provide excellent sensitivity for following the fate of plasmid or lipid through the cell, but they must be nonexchangeable and located on chemically unreactive parts of the molecule. The DNA/carrier complex is processed in the endosomes; therefore, analysis of delivery to subcellular components may be required which involves cellular fractionation. In addition, nuclear isolation, which may be simpler to perform than subcellular fractionation, may be helpful in the study of the intracellular processing of plasmid/carrier complexes. These procedures must be executed under well-controlled conditions to avoid contaminating the fractions in order to accurately determine the intracellular distribution of the carrier and DNA ***(203)***. A combination of techniques is best employed to ensure an accurate assessment of intracellular distribution.
22. One of the concerns with this method is that it is difficult to determine whether the plasmid associated with the cells is in fact internalized or associated externally with the cell membrane, or is simply adhering nonspecifically to the tissue culture plate. To address this problem the cells can also be briefly protease-treated

prior to collection. Adherent cells are subjected to trypsin (0.25% trypsin for 2 min at 4°C) and diluted with 400 µL HEPES-buffered saline (HBS, 25 m*M* HEPES, 150 m*M* NaCl). Cell-associated DNA is separated from nonassociated by centrifugation at 400*g* for 30 min at ambient temperature in a density gradient between 1.077 and 1.022 (NycoPrep, Sigma). Cells are collected at the interface and cell-associated DNA evaluated for radioactivity.

23. Total DNA (genomic and plasmid) can be isolated from cells following transfection in vitro and in vivo using standard techniques ***(80,81)***. Alternatively, total DNA can be extracted from cells or tissue homogenates using DNAzol following the manufacturer's instructions, or by the modified Hirt lysis procedure described in **Subheading 3.3.2.1.** Following isolation and purification of DNA, the resolubilized DNA is applied to a dot-blot apparatus. Plasmid DNA bound to the nylon membrane used in this procedure can be detected using ^{32}P, ^{35}S, or digoxigenin random-prime labeled plasmid ***(80,81)***. Plasmid is quantified by comparison with known standards after X-ray film exposure or directly using a phosphoimager. Although the dot-blot technique is excellent for quantification of plasmid, a concern is that the probe will hybridize to degraded fragments of the plasmid as well as intact plasmid, so that one cannot distinguish between the two. The polymerase chain reaction (PCR) is another routinely used option that eliminates concerns about using radiolabeled plasmid. PCR allows detection of very low levels of transfected DNA after in vivo administration ***(122)***, and it can be adapted to the analysis of histological sections of tissues ***(123)***. Limitations to this technique include difficulty in controlling contamination and the inability to evaluate plasmid integrity.

In summary, gene therapy strategies are being aggressively tested in the clinic, an indication of the immense hope being placed on this treatment approach. It is clear, however, that the pharmaceutical development of drugs consisting of oligonucleotides or plasmids has not yet been fully realized. Furthermore, our understanding of these agents as therapeutic molecules is very limited. It is believed that carriers will be required to facilitate efficient DNA delivery to target cells. Issues that must be addressed in the development of DNA as a drug are not dissimilar to those encountered in the development of small molecules. Interest may arise from a novel mechanism of action and/or an activity that is better than that achieved with drugs already known to be active in the particular target disease. A pharmaceutically viable formulation must be defined, one that is amenable to manufacturing processes that can be validated, resulting in a product that is suitable for use in humans. It is anticipated that Phase I studies, designed to assess toxicity, and Phase II studies, designed to assess efficacy, will progress in the absence of established mechanism(s) of action. However, it will be critical to the pharmaceutical development of DNA as a drug to define the pharmacokinetic and pharmacodynamic characteristics of the DNA. It is likely that the carrier formulations

used to deliver the DNA will also be considered active drug components; therefore, methodologies must be further developed to accurately and reproducibly measure the biological fate of DNA delivery systems.

Acknowledgment

This work was supported by the Medical Research Council of Canada and Inex Pharmacouticals Corp. D. L. Reimer was an MRC Postdoctoral Fellow at the time of this work. E. K. Wasan is supported through a B.C. Science Council Graduate Research, Engineering and Technology fellowship. F.M.P. Wong is a recipient of a fellowship from the Science Council of British Columbia and the Cancer Research Society, Inc. P. Harvie is a FRSQ post-doctoral fellow.

References

1. Sokol, D. L. and Gewirtz, A. M. (1996) Gene therapy: basic concepts and recent advances. *Crit. Rev. Euk. Gene Express.* **6(1),** 29–57.
2. Roth, J. A. and Cristiano, R. J. (1991) Gene therapy for cancer: what have we done and where are we going? *J. Natl. Cancer Inst.* **89(1),** 21–39.
3. Bertling, W. A., Gareis, M., Paspaleeva, V., Zimmer, A., Kreuter, J., Numberg, E., and Harrer, P. (1991) Use of liposomes, viral capsids and nanoparticles as DNA carriers. *Biotech. Appl. Biochem.* **13,** 390–405.
4. Cooper, M. J. (1996) Noninfectious gene transfer and expression systems for cancer gene therapy. *Sem. Oncol.* **23(1),** 172–187.
5. Ledley, F. D. (1995) Nonviral gene therapy: the promise of genes as pharmaceutical products. *Hum. Gene Ther.* **6,** 1129–1144.
6. Tomlinson, E. and Rolland, A. P. (1996) Controllable gene therapy: pharmaceutics of non-viral gene delivery systems. *J. Contr. Rel.* **39,** 357–372.
7. Nabel, E. G., Gordon, D., Yang, Z. Y., Xu, L., San, H., Plautz, G. E., Wu, B. Y., Gao, X., Huang L., and Nabel, G. J. (1992) Gene transfer in vivo with DNA-liposome complexes: lack of autoimmunity and gonadal localization. *Hum. Gene Ther.* **3,** 649–656.
8. Nabel, G. J., Nabel, E. G., Yang, Z. Y., Fox, B. A., Plautz, G. E., Gao, X., Huang, L., Shu, S., Gordon, D., and Chang, A. E. (1992) Direct gene transfer with DNA-liposome complexes in melanoma: expression, biologic activity, and lack of toxicity in humans. *Proc. Natl. Acad. Sci. USA* **90,** 11,307–11,311.
9. Canonico, A. E., Plitman, J. D., Conary, J. T., Meyrick, B. O., and Brigham, K. L. (1994) No lung toxicity after repeated aerosol or intravenous delivery of plasmid-cationic liposome complexes. *J. Appl. Phys.* **77(1),** 415–419.
10. Bogdanov, A. A., Jr., Weissleder, R., Frank, H. W., Bogdanova, A. V., Nossif, N., Schaffer, B. K., Tsai, E., Papisov, M. I., and Brady, T. J. (1993) A new macromolecule as a contrast agent for MR angiography: preparation, properties, and animal studies. *Radiol.* **187(3),** 701–706.
11. Chancerelle, Y., Mathieu, J., Viret-Soropogui, R., Tosetti, F., Alban, C., and Kergonou, J. F. (1993) Immunization of rabbits with proteins reacted with mal-

onic dialdehyde (MDA): kinetics and specificity ofthe immune response. *Biochem. Molec. Biol. Intl.* **29(1),** 141–148.
12. Felgner, P. L., Gadek, T. R., Holm, M., Roman, R., Chan, H. W., Wenz, M., Northrop, J. P., Ringold, G. M., and Danielsen, M. (1987) Lipofection: a highly efficient, lipid-mediated DNA-transfeGtion procedure. *Proc. Natl. Acad. Sci. USA* **84,** 7413–7417.
13. Felgner, P. L. and Ringold, G. M. (1989) Cationic liposome-mediated transfection. *Nature* **337(6205),** 387,388.
14. Farhood, H., Gao, X., Son, K., Yang, Y.-Y., Lazo, J. S., Huang, L., Barsoum, J., Bottega, R., and Epand, R. (1994) Cationic liposomes for direct gene transfer in therapy of cancer and other diseases. *Ann. NY Acad. Sci.* **716,** 23–35.
15. Caplen, N. J., Kinrade, E., Sorgi, F., Gao, X., Gruenert, D., Geddes, D., Coutelle, C., Huang, L., Alton, E. W., and Williamson, R. (1995) In vitro liposome-mediated DNA transfection of epithelial cell lines using the cationic liposome DC-Chol/DOPE. *Gene Ther.* **2,** 603–613.
16. Gao, X. and Huang, L. (1996) Potentiation of cationic liposome-mediated gene delivery by polycations. *Biochemistry* **35(3),** 1027–1036.
17. Zhang, Y.-P., Reimer, D. L., Zhang, G., Lee, P. H., and Bally, M. B. (1996) Self-assembling DNA-lipid particles for gene transfer. *Pharmaceut. Res.* **14(2),** 190–196.
18. Behr, J. P., Demeneix, B., Loeffler, J.-P., and Perez-Mutul, J. (1989) Efficient gene transfer into mammalian primary endocrine cells with lipopolyamine-coated DNA. *Proc. Natl. Acad Sci USA* **86,** 6982–6986.
19. Wolfert, M. A., Schacht, E. J., Toncheva, V., Illbrich, K., Nazarova, O., and Seymour L. W. (1996) Characterization of vectors for gene therapy formed by self assembly of DNA with synthetic block co-polymers. *Hum. Gene Ther.* **7(17),** 2123–2133.
20. Barthel, F., Remy, J.-S., Loeffler, J.-P., and Behr, J.-P. (1993) Gene transfer optimization with liposperrnine:coated DNA. *DNA Cell Biol.* **12(6),** 553–560.
21. Kabanov, A. V. and Kabanov, V. A. (1995) DNA complexes with polycations for the delivery of genetic material into cells. *Bioconj. Chem.* **6,** 7–20.
22. Zhou, X, Klibanov, A., and Huang, L. (1991) Lipophile polylysines mediate efficient DNA transfection in mammalian cells. *Biochim. Biophys. Acta* **1065,** 8–14.
23. Cotten, M., Langle-Rouault, F., Kirlappos, H., Wagner, E., Mechtler, K., Zenke, M., Beug, H., and Birnstiel, M. L. (1990) Transferrin-polycation-mediated introduction of DNA into human leukemic cells: stimulation by agents that affect the survival of transfected DNA or modulate transferrin receptor levels. *Proc. Natl. Acad. Sci. USA* **87(11),** 4033–4037.
24. Wagner, E., Zenke, M., Cotten, M., Beug, H., and Birnstiel, M. L. (1990) Transferrin-polycation conjugates as carriers for DNA uptake into cells. *Proc. Natl. Acad. Sci. USA* **87(9),** 3410–3414.
25. Zenke, M., Steinlein, P., Wagner, E., Cotten, M., Beug, H., and Birnstiel, M. L. (1990) Receptormediated endocytosis of transferrin-polycation conjugates: an

efficient way to introduce DNA into hematopoietic cells. *Proc. Natl. Acad. Sci. USA* **87(10),** 3655–3659.
26. Tang, M. X., Redemann, C. T., and Szoka, F. C. (1996) In vitro gene delivery by degraded polyamidoamine dendrimers. *Bioconj. Chem.* **7,** 703–714.
27. Bielinska, A., Kukowska-Latallo, J. F., Johnson, J., Tomalia, D. A., and Baker, J. R. (1996) Regulation of in vitro gene expression using; antisense oligonucleotides or antisense expression plasmids transfected using starburst PAMAM dendrimers. *Nucl. Acids Res.* **24(11),** 2176–2182.
28. Haensler, J. and Szoka, F. C. (1993) Polyamidoamine cascade polymers mediate efficient transfection of cells in culture. *Bioconj. Chem.* **4(5),** 372–379.
29. Kato, T., Iwamoto, K., Ando, H., Asakawa, N., Tanaka, I., Kikuchi, J., and Murakami, Y. (1996) Synthetic cationic amphiphile for liposome-mediated DNA transfection with less cytotoxicity. *Biol. Pharmaceut. Bull.* **19(6),** 860–863.
30. Legendre, J. Y., Trzeciak, A., Bohrmann, B., Deuschle, U., Kitas, E., and Supersaxo, A. (1997) Dioleoylmelittin as a novel serum-insensitive reagent for efficient transfection of mammalian cells. *Bioconj. Chem.* **8(1),** 57–63.
31. Hong, K., Zheng, W., Baker, A., and Papahadjopoulos, D. (1997) Stabilization of cationic liposome-plasmid DNA complexes by polyamines and poly(ethylene glycol)-phospholipid conjugates for efficient in vivo gene delivery. *FEBS Lett.* **400(2),** 233–237.
32. Felgner, P. L. (1997) Nonviral strategies for gene therapy. *Scientific Am.* **276(6),** 102–106.
33. Wong, F. M. P., Reimer, D. L., and Bally, M. B. (1996) Cationic lipid binding to DNA: characterization of complex formation. *Biochemistry* **35,** 5756–5763.
34. Canonico, A. E., Conary, J. T., Meyrick, B. O., and Brigham, K. L. (1994) Aerosol and intravenous transfection of human alpha-1 antitrypsin gene to lungs of rabbits. *Am. J. Resp. Cell Mol. Biol.* **10(1),** 24–29.
35. Leibiger, I., Leibiger, B., Sarrach, D., Walter, R., and Zuhlke, H. (1990) Genetic manipulation of rat hepatocytes in vivo. Implications for a therapy model of type-1 diabetes. *Biomed. Biochim. Acta* **49(12),** 1193–1200.
36. Thierry, A. R., Lunardi-Iskandar, Y., Bryant, J. L., Rabinovich, P., Gallo, R. C., and Mahan, L. C. (1996) Systemic gene therapy: biodistribution and long-term expression of a transgene in mice. *Proc. Natl. Acad Sci. USA* **92,** 9742–9746.
37. Schmid, R. M., Weidenbach, H., Draenert, G. F, Lerch, M. M., Liptay, S., Schorr J., Beckh, K. H., and Adler, G. (1994) Liposome-mediated in vivo gene transfer into different tissues of the gastrointestinal tract. *Z. Gastroenterol.* **32(12),** 665–670.
38. Lesoon-Wood, L. A., Kirn, W. H., Kleinman, H. K., Weintraub, B. D., and Mixson, A. J. (1995) Systemic gene therapy with p53 reduces growth and metastases of a malignant human breast cancer in nude mice. *Hum. Gene Ther.* **6,** 395–405.
39. Lew, D., Parker, S. E., Latimer, T., Abai, A. M., Kuwahara-Rundell, A., Doh, S. G., Yang, Z.-Y., Laface, D., Gromkowski, S. H., Nabel, G. J., Manthrope, M., and Norman, J. (1995) Cancer gene therapy using plasmid

DNA: pharmacokinetic study of DNA fallowing injection in mice. *Hum. Gene Ther.* **6,** 553–564.

40. Xing, X., Matin, A., Yu, D., Xia, W., Sorgi, F., Huang, L., and Hung, M. C. (1996) Mutant SV40 large T antigen as a therapeutic agent for HER-2/neu-overexpressing ovarian cancer. *Cancer Gene Ther.* **3(3),** 168–174.
41. Yu, D., Matin, A., Xia, W., Sorgi, F., Huang, L., and Hung, M. C. (1995) Liposome-mediated in vivo gene transfer suppressed dissemination of ovarian cancer cells that overexpress HER-2/neu. *Oncogene* **11(7),** 1383–1388.
42. Meyer, K. B., Thompson, M. M., Levy, M. Y., Barron, L. G., and Szoka, F. C. (1995) Intratracheal gene delivery to the mouse airway: characterization of plasmid DNA expression and pharmacokinetics. *Gene Ther.* **2,** 450–460.
43. McLachlan, G., Ho, L. P., Davidson-Smith, H., Samways, J., Davidson, H., Stevenson, B. J., Cathothers, A. D., Alton, E. W., Middleton, P. G., Smith S. N., Kallmeyer, G., Michaelis, U., Seeber, S., Nanjoks, K., Greening, A. P., Innes, J. A., Oorin, J. R., and Porteous, D. J. (1996) Laboratory and clinical studies in support of cystic fibrosis gene therapy using pCMV-CFTR-DOTAP. *Gene Ther.* **3(12),** 1113–1123.
44. Hyde, S. C., Gill, D. R., Higgins, C. F., Trezise, A. E., MacVinish, L. J., Cutherbert, A. W., Ratcliff, R., Evans, M. J., and Colledge, W. H. (1993) Correction of the ion transport defect in cystic fibrosis transgenic mice by gene therapy. *Nature* **362(6417),** 250–255.
45. Jones, S. E., McHugh, J. D., Jomary, C., Shallal, A., and Neal, M. J. (1994) Assessment of liposomal transfection of ocular tissues in vivo. *Gene Ther.* **1(Suppl. 1),** S61.
46. Parker, S. E., Khatibi, S., Margalith, M., Anderson, D., Yankauckas, M., Gromkowski, S. H., Latimer, T., Lew, D., Marquet M., Manthorpe M., Hobart, P., Hersh, E., Stopeck, A. T., and Norman, J. (1996) Plasmid DNA gene therapy: studies with the human interleukin-2 gene in tumor cells in vitro and in the murine B16 melanoma model in vivo. *Cancer Gene Ther.* **3(3),** 175–185.
47. Egilmez, N. K., Cuenca, R., Yokota, S. J., Sorgi, F., and Bankert, R. B. (1996) In vivo cytokine gene therapy of human tumor xenografts in SCII) mice by liposome-mediated gene therapy. *Gene Ther.* **3(7),** 607–614.
48. Nabel, G. J., Gordon, D., Bishop, D. K., Nickoloff, B. J., Yang, Z. Y., Aruga, A., Cameron, M. J., Nabel, E. G., and Chang, A. E. (1996) Immune response in human melanoma after transfer of an allogeneic class I major histocompatibility complex gene with DNA-liposome complexes. *Proc. Natl. Acad. Sci. USA* **93(26),** 15,388–15,393.
49. Hickman, M. A., Malone, R. W., Lehmann-Bruinsma, K., Sih, T. R., Knoell, D., Szoka, F. C., Walzem, R., Carlson, D. M., and Powell, J. S. (1994) Gene expression following direct injection of DNA into the liver. *Hum. Gene Ther.* **5(12),** 1477–1483.
50. Caplen, N. J., Alton, E. W., Middleton, P. G., Dorin, J. R., Stevenson, B. J., Gao, X., Durham, S. R., Jeffery, P. K., Hodson, M. E., Coutelle, C., Huang, L., Porteous, D. J., Williamson, R., and Geddes, D. M. (1995) Liposome-mediated

CFTR gene transfer to the nasal epithelium of patients with cystic fibrosis. *Nat. Med.* **1(1),** 39–46.
51. Felgner, P. L., Tsai, Y. J., Sukhu, L., Wheeler, C. J., Manthorpe, M., Marshall, J., and Cheng, S. H. (1995) Improved cationic lipid formulations for in vivo gene therapy. *Ann. NY Acad. Sci.* **772,** 126–139.
52. Felgner, J. H., Kumar, R., Sridhar, C. N., Wheeler, C. J., Tsai, Y. J., Border, R., Ramsey, P., Martin, M., and Felgner, P. L. (1994) Enhanced gene delivery and mechanism studies with a novel series of cationic lipid formulations. *J. Biol. Chem.* **269(4),** 2550–2561.
53. Balasubramaniam, R. P., Bennett, M. J., Aberle, A. M., Malone, J. G., Nantz, M. H., and Malone, R. W. (1996) Structural and functional analysis of cationic transfection lipids: the hydrophobic domain. *Gene Ther.* **3(2),** 163–172.
54. Wheeler, C. J., Sukbu L., Yang G., Tsai Y., Bustamente C., Felgner P. L., Norman, J., and Manthorpe, M. (1996) Converting an alcohol to an amine in a cationic lipid dramatically alters the co-lipid requirement, cellular transfection activity and the ultrastructure of DNA-cytofectm complexes. *Biochim. Biophys. Acta* **1280,** 1–11.
55. Farhood, H., Serbina, N., and Huang, L. (1995) The role of dioleoyl phosphatidylethanolamine in cationic liposome mediated gene transfer. *Biochim. Biophys. Acta* **1235,** 289–295.
56. Wasan, E. K., Reimer, D. L., and Bally, M. B. (1996) Plasmid DNA is protected against ultrasonic cavitation-induced damage when complexed to cationic liposomes. *J. Pharm. Sci.* **85(4),** 427–433.
57. Wu, G. Y. and Wu, C. H. (1988) Evidence for targeted gene delivery to Hep G2 hepatoma cells in vivo. *Biochemistry* **27(3),** 887–892.
58. Wu, G. Y. and Wu, C. H. (1988) Receptor-mediated gene delivery and expression in vivo. *J. Biol. Chem.* **263(29)**, 14,621–14,624.
59. Wagner, E., Cotten, M., Foisner, R., and Birnstiel, M. L. (1991) Transferrin-polycation-DNA complexes: the effect of polylysine on the structure of the complex and DNA delivery to cells. *Proc. Natl. Acad. Sci. USA* **88(10),** 4255–4259.
60. Okada, N., Miyamoto, H., Yoshioka, T., Sakamoto, K., Katsume, A., Saito, H., Nakagawa, S., Ohsugi, Y., and Mayumi, T. (1997) Immunological studies of SK2 hybridoma cells microencapsulated with alginate-poly(L-lysine)-alginate (APA) membrane following allogenic transplantation. *Biochem. Biophys. Res. Comm.* **230(3),** 524–527.
61. Liu, H. W., Ofosu, F. A., and Chang, P. L. (1993) Expression of human factor IX by microencapsulated recombinant fibroblasts. *Hum. Gene Ther.* **4(3),** 291–301.
62. Halle, J. P., Bourassa, S., Leblond, F. A., Chevalier, S., Beudry, M., Chapdelaine, A., Cousineau, S., Saintonge, J., and Yale, J. F. (1993) Protection of islets of Langerhans from antibodies by microencapsulation with alginate-poly-L-lysine membranes. *Transplantation* **55(2),** 350–354.
63. Tomalia, D. A., Naylor, A. M., and Goddard, W. A. (1990) Starburst dendrimers: molecular-level control of size, shape surface chemistry, topology, and flexibility from atoms to macroscopic matter. *Angew. Chem. Int. Ed. Engl.* **29,** 138–175.

64. Tomalia, D. A. and Durst, H. D. (1993) Genealogically directed synthesis: starburst/cascade dendrimers and hyperbranched structures. *Top. Curr. Chem.* **165,** 193–313.
65. Legendre, J.-Y. and Szoka, F. C. (1993) Cyclic arnphipathic peptide-DNA complexes mediate high efficiency transfection of adherent mammalian cells. *Proc. Natl. Acad Sci. USA* **90,** 893–897.
66. Ohmori, N., Niidome, T., Wada, A., Hirayama, T., Hatakeyama, T., and Aoyagi, H. (1997) The enhancing effect of anionic alpha-helical peptide on cationic peptide-mediating transfection systems. *Biochem. Biophys. Res. Comm.* **235(3),** 726–729.
67. Buschle, M., Cotten, M., Kirlappos, H., Mechtler, K., Shaffner, G., Zauner, W., Birnstiel, M. C., and Wagner, E. (1995) Receptor-mediated gene transfer into human T lymphocytes via binding of DNA/CD3 antibody particles to the CD3 T cell receptor. *Hum. Gene Ther.* **6(6),** 753–761.
68. Merwin, J. R., Noell G. S., Thomas, W. L., Chiou, H. C., DeRome, M. E., McKee, T. D., Spitalny, G. L., and Findeis, M. A. (1994) Targeted delivery of DNA using; YEE(GalNAcAH)3, a synthetic glycopeptide ligand for the asialoglycoprotein receptor. *Bioconj. Chem.* **5(6),** 612–620.
69. McKee, T. D., DeRome, M. E., Wu, G. Y., and Findeis, M. A. (1994) Preparation of asialoorosomucoid-polylysine conjugates. *Bioconj. Chem.* **5(4),** 306–311.
70. Stankovics, J., Crane, A. M., Andrews, E., Wu, C. H., Wu, G. Y., and Ledley, F. D. (1994) Overexpression of human methylmalonyl CoA mutase in mice after in vivo gene transfer with asialoglycoprotein/polylysine/DNA complexes. *Hum. Gene Ther.* **5(9),** 1095–1104.
71. Ferkol, T., Pellicena-Palle, A., Eckrnan, E., Perales, J. C., Trzaska, T., Tosi, M., Redline, R., and Davis, P. B. (1996) Immunologic responses to gene transfer into mice via the polymeric immunoglobulin receptor. *Gene Ther.* **3(8),** 669–678.
72. Phillips, S. C. (1995) Receptor-mediated DNA delivery approaches to human gene therapy. *Biologicals* **23(1),** 13–16.
73. Lozier, J. N., Thompson, A. R., Hu, P. C., Read, M., Brinkhous, K. M., High, K. A., and Curiel, D. T. (1994) Efficient transfection of primary cells in a canine hemophilia B model using adenoviruspolylysine-DNA complexes. *Hum. Gene Ther.* **5(3),** 313–322.
74. Cristiano, R. J., Smith, L. C., Kay, M. A., Brinkely, B. R., and Woo, S. L. (1993) Hepatic gene therapy: efficient gene delivery and expression in primary hepatocytes utilizing a conjugated adenovirus-DNA complex. *Proc. Natl. Acad. Sci. USA* **90(24),** 11,548–11,552.
75. Cristiano, R. J., Smith, L. C., and Woo, S. L. (1993) Hepatic gene therapy: adenovirus enhancement of receptor-mediated gene delivery and expression in primary hepatocytes. *Proc. Natl. Acad. Sci USA* **90(6),** 2122–2126.
76. Plank, C., Katloukal, K., Cotten, M., Mechtler, K., and Wagner, E. (1992) Gene transfer into hepatocytes using asialoglycoprotein receptor mediated endocylosis of DNA complexed with an artificial tetra-antennary galactose ligand. *Bioconj. Chem.* **3,** 533–539.

77. Wagner, E., Plank, C., Katloukal, K., Cotten, M., and Birnstie, M. L. (1992) Influenza virus hemagglutinin HA-2 terminal fusogenic peptides augment gene transfer by transferrinpolylysine-DNA complexes: toward a synthetic virus-like gen~e transfer vehicle. *Proc. Natl. Acad. Sci. USA* **89(17),** 7934–793.
78. Fritz, J. D., Herweijer, H., Zhang, G., and Wolff, J. A. (1996) Gene transfer into mammalian cells using his/one-condensed plasmid DNA. *Hum. Gene Ther.* **7(12),** 1395–1404.
79. Papahadjopoulos, D., Hong, K., Kirpotin, D., Zheng, W., Shao, V., Park, J., and Benz, C. (1997) Ligand-directed targeting of liposomes in vivo: formulations for delivery of drugs and genes to tumors. *Control. Rel. Bioact. Mater.* **24,** 159,160.
80. Sambrook, J., Fritsch, E. F., and Maniatis, T., eds. (1989) *Molecular Cloning: A Laboratory Manual.* Cold Spring Harbor Laboratory, Cold Spring Harbor, New York.
81. Ausubel, F. M., Kingston, R. E., Moore, D. D., Seidman, J. G., Smith, J. A., and Struhl, K., eds. (1997) *Protocols in Molecular Biology.* Wiley, Boston, MA.
82. Haugland, R. P. (1996) *Handbook of Fluorescent Probes and Research Chemicals* (Spence, T. Z., ed.), Molecular Probes, Eugene, OR.
83. Hofland, H. E., Shephard, L., and Sullivan, S. M. (1996) Formation of stable cationic lipid/DNA complexes for gene transfer. *Proc. Natl. Acad. Sci. USA* **93(14),** 7305–7309.
84. Thurnher, M., Wagner, E., Clause,n H., Mechtler, K., Rusconi, S., Dinter, A., Birstiel, M. L., Berger, E. G., and Cotten, M. (1994) Carbohydrate receptor-mediated gene transfer to human T leukaemic cells. *Glycobiol.* **4(4)**, 429–435.
85. Erbacher, P., Bousser, M. T., Raimond, J., Monsigny, M., Midoux, P., and Roche, A. C. (1996) Gene transfer by DNA/glycosylated polylysine complexes into human blood monocyte-derived macrophages. *Hum. Gene Ther.* **7(6),** 721–729.
86. Holt, C., Parker, T. G., and Dalgleish, D. G. (1975) Measurement of particle sizes by elastic and quasi-elastic light scattering. *Biochim. Biaphys. Acta* **400(2),** 283–292.
87. Pecora, R. (1972) Quasi-elastic light scattering from macromolecules. *Ann. Rev. Biophys. Bioeng.* **1,** 257–276.
88. Sternberg, B., Sorgi, F. L., and Huang, L. (1994) New structwres in complex formation between DNA and cationic liposomes visualized by fireeze-fracture electron microscopy. *FEBS Lett.* **356,** 361–366.
89. Radler, J. O., Koltover, I., Salditt, T., and Safinya, C. R. (1997) Structure of DNA-cationic liposome complexes: DNA intercalation in multilarnellar membranes in distinct interhelical packing regimes. *Science* **275,** 810–814.
90. Hui, S. W., Langner, M., Zhao, Y. L., Ross, P., Hurley, E., and Chan, K. (1996) The role of helper lipids in cationic liposome-mediated gene transfer. *Biophys. J.* **71,** 590–599.
91. Gustafsson, J., Arvidson, G., Karlsson, G., and Almgren, M. (1995) Complexes between cationic liposomes and DNA visualized by cryo-TEM. *Biochim. Biophys. Acta* **1235(2),** 305–312.

92. Dubochet, J., Adrian, M., Chang, J. J., Homo, J. C., Lepault, J., McDowall, A. W., and Schultz, P. (1988) Cryo-electron microscopy of vitrified specimens. *Q. Rev. Biophys.* **21,** 129–288.
93. Bellare, J. R., Davis, H. T., Scrivep, L. E., and Talmon, Y. (1988) Controlled environment vitrification system (CEVS): an improved sample preparation technique. *J. Electron Miscrosc. Tech.* **10,** 87–111.
94. Bally, M. B., Zhang, Y.-P., Wong, F. M. P., Kong, S., Wasan, E., and Reimer, D. L. (1997) Lipid/DNA complexes as an intermediate in the preparation of particles for gene transfer: an alternative to cationic liposome/DNA aggregates. *Adv. Drug Deliv. Rev.* **24,** 275–290.
95. Struck, D. K., Hoekstra, D., and Pagano, R. E. (1981) Use of resonance energy transfer to monitor membrane fusion. *Biochemistry* **20,** 4093–4099.
96. Fung, B. K. K. and Stryer, L. (1978) Surface density determination by fluorescence energy transfer. *Biochemistry* **17(24),** 5241–5248.
97. Stryer, L. (1978) Fluorescence energy transfer as a spectroscopic ruler. *Ann. Rev. Biochem.* **47,** 819–832.
98. Holland, J. W., Hui, C., Cullis, P. R., and Madden, T. D. (1996) Poly(ethylene glycol)-lipid conjugates regulate the calcium-induced fusion of liposomes composed of phosphatidylethanolamine and phosphatidylserine. *Biochemistry* **35(8),** 2618–2624.
99. Duzgunes, N., Nir, S., Wilshut, J., Bentz, J., Newton, C., Portis, A., and Papahadjopoulos, D. (1981) Calcium- and magnesium-induced fusion of mixed phosphatidylserine/phosphatidylcholine vesicles: effect of ion binding. *J. Membr. Biol.* **59,** 115–125.
100. Stamatatos, L., Leventis, R., Zuckermann, M. J., and Silvius, J. R. (1988) Interactions of cationic lipid vesicles with negatively charged phospholipid vesicles and biological membranes. *Biochemistry* **27(11),** 3917–3925.
101. Wasan, E. K., Fairchild, A., and Bally, M. B. (1997) Cationic liposome-plasmid DNA complexes used for gene transfer retain a significant trapped volume. *J. Pharm. Sci.* **87(1),** 9–14.
102. Xu, Y. and Szoka, F. C. (1996) Mechanism of DNA release from cationic liposome/DNA complexes used in cell transfection. *Biochemistry* **35,** 5616–5623.
103. Harvie, P., Wong, F. M. P., Reimer, D. L., and Bally, M. B. (1998) Self-assembling lipid-DNA particles: anionic membrane-mediated dissociation. *Biophys. J.* **47(10),** 1611–1617.
104. Schott, H. (1969) Hydrophile-lipophile balance and cloud points of nonionic surfactants. *J. Pharm. Sci.* **58(12),** 1443–1449.
105. Smolarsky, M., Teitelbaum, D., Sela, M., and Gitler, C. (1977) A simple fluorescent method to determine complement mediated liposome immune lysis. *Immunol. Meth.* **15,** 255–265.
106. Ellens, H., Bentz, J., and Szoka, F. C. (1984) pH-induced destabilization of phosphatidylethanolamine-containing liposomes: role of bilayer contact. *Biochemistry* **23,** 1532–1538.
107. Wilschut, J. and Papahadjopoulos, D. (1979) Ca^{2+}-induced fusion of phospholipid vesicles monitored by mixing of aqueous contents. *Nature* **281,** 691,692.

108. Bailey, A. L. and Cullis, P. R. (1997) Membrane fusion with cationic liposomes: effects of target membrane lipid composition. *Biochemistry* **36(7),** 1628–1634.
109. Arscott, P. G., Li, A. Z., and Bloomfield, V. A. (1990) Condensation of DNA by trivalent cations. 1. Effects of DNA length and topology on the size and shape of condensed particles. *Biopolymers* **30,** 619–630.
110. Plum, G. E., Arscott, P. G., and Bloomfield, V. A. (1990) Condensation of DNA by trivalent cations. 2. Effects of cation structure. *Biopolymers* **30,** 631–643.
111. Blumfield, V. A. (1991) Condensation of DNA by multivalent cations: considerations on mechanism. *Biopolymers* **31,** 1471–1481.
112. Thierry, A. R., Rabinovich, P., Peng, B., Mahan, L. C., Bryant, J. L., and Gallo, R. C. (1997) Characterization of liposome-mediated gene delivery: expression, stability and pharmacokinetics of plasmid DNA. *Gene Ther.* **4(3),** 226–237.
113. Bligh, E. G. and Dyer, W. J. (1959) A rapid method of total lipid extraction and purification. *Can. J. Biochem. Physiol.* **37(8),** 911–917.
114. Lewis, J. G., Lin, K. Y., Kothvale, A., Flanagan, W. M., Matteucci, M. D., DePrince, R. B., Mook, R. A., Jr., Hendren, R. W., and Wagner, R. W. (1996) A serum-resistant cytofectin for cellular delivery of antisense oligodeoxynucleotides and plasmid DNA. *Proc. Natl. Acad. Sci. USA* **93(8),** 3176–3181.
115. Zabner, J., Fasbender, A. J., Moninger, T., Poellinger, K. A., and Welsh, M. J. (1995) Cellular and molecular barriers to gene transfer by a cationic lipid. *J. Biol. Chem.* **270(32),** 18,997–19,007.
116. Lasic, D. D. and Templeton, N. S. (1996) Liposomes in gene therapy. *Adv. Drug Del. Rev.* **20(2–3),** 221–266.
117. Hart, S. L., Harbottle, R. P., Cooner, R., Miller, A., Williamson, R., and Coutelle, C. (1995) Gene delivery and expression mediated by an integrin-binding peptide. *Gene Ther.* **2(8),** 552–554.
118. Hara, T., Liu, F., Liu, D., and Huang, L. (1997) Emulsion formulations as a vector for gene delivery in vitro and in vivo. *Adv. Drug Del. Rev.* **24,** 265–271.
119. Reimer, D. L., Kong, S., and Bally, M. E. (1997) Analysis of cationic liposome-mediated interactions of plasmid DNA with murine and human melanoma cells in vitro. *J. Biol. Chem.* **272(31),** 19,480–19,487.
120. Hirt, B. (1967) Selective extraction of polyoma DNA from infected mouse cell cultures. *J. Mol. Biol.* **26(2),** 365–369.
121. Kawabata, K., Takakura, Y., and Hashida, M. (1995) The fate of plasmid DNA after intravenous injection in mice-involvement of scavenger receptors in its hepatic uptake. *Pharm. Res.* **12(6),** 825–830.
122. Osaka, G., Carey, K., Cuthbertson, A., Godowski, P., Patapoff, T., Ryan, A., Gadek, T., and Mordenti, J. (1996) Pharmacokinetics, tissue distribution, and expression efficiency of plasmid [^{33}P]DNA following intravenous administration of DNA/cationic lipid complexes in mice—use of a novel radionuclide approach. *J. Pharm. Sci.* **85(6),** 612–618.
123. Nomura, T., Nakahima, S., Kawabata, K., Yamashita, F., Takakura, Y., and Hashida, M. (1997) Intratumoral pharmacokinetics and in vivo gene expression

of naked plasmid DNA and its cationic liposome complexes after direct gene transfer. *Cancer Res.* **57(13),** 2681–2686.

124. Reimer, D. L., Kong, S., Monk, M., Tan, P., Wasan, E., and Bally, M. B. (1997) Factors influencing in vivo liposome-mediated transfection of B 16/BL6 melanoma tumor models: a pharmacodynamic study. *J. Pharmacol. Exp. Ther. JPET* **289(2),** 807–815.
125. Levy, M. Y., Barron, L. G., Meyer, K. B., and Szoka, F. C. (1996) Characterization of plasmid DNA transfer into mouse skeletal muscle: evaluation of uptake mechanism, expression and secretion of gene products into blood. *Gene Ther.* **3,** 201–211.
126. Winegar, R. A., Monforte, J. A., Suing, K. D., Oloughlin, K. G., Rudd, C. J., and Macgregor, J. T. (1996) Determination of tissue distribution of an intramuscular plasmid vaccine using PCR and in situ DNA hybridization. *Hum. Gene Ther.* **7(17),** 2185–2194.
127. Porcher, C., Malinge, M. C., Picat, C., and Grandchamp, B. (1992) A simplified method for determination of specif~c DNA or RNA copy number using quantitative PCR and an automatic DNA sequencer. *Biotechnology* **13(1),** 106–114.
128. Sperisen, P., Wang, S. M., Reichenbach, P., and Nabholz, M. (1992) A PCR-based assay for reporter gene expression. *PCR Meth. Appl.* **1(3),** 164–170.
129. Friend, D. S., Papahadjopoulos, D., and Debs, R. J. (1996) Endocytosis and intracellular processing accompanying transfection mediated by cationic liposomes. *Biochim. Biophys. Acta* **1278(1),** 41–50.
130. Schwedener, R. A., Trub, T., Schott, H., Langhals, H., Barth, R. F., Groscurth, P., and Hengartner, H. (1990) Comparative studies of the preparation of immunoliposomes with the use of two bifunctional coupling agents and investigation of in vitro immunoliposome-target cell binding by cytofluorometry and electron microscopy. *Biochim. Biophys. Acta* **1026(1),** 69–79.
131. Flasher, D., Konopka, K., Chamow, S. M., Dazin, P., Ashkenazi, A., Pretzer, F. (1994) Liposome targeting to immune deficiency virus type 1-infected cells via recombinant soluble CD4 and CD4 immunoadhesin (CD4-IgG). *Biochim. Biophys. Acta* **1194(1),** 185–196.
132. Bally, M. B., May, L. D., Hope, M. J., and Nayar, R. (1993) Pharrnacodynamics of liposomal drug carriers: methodological considerations, in *Liposome Technology* (Gregoriadis, G., ed.), CRC, Boca Raton, FL, pp. 27–41.
133. Parker, S. E., Ducharme, D., Norman, J., and Wheeler, C. J. (1997) Tissue distribution of the cytofectin component of a plasmid DNA/cationic lipid complex following intravenous administration in mice. *Hum. Gene Ther.* **8(4),** 393–401.
134. Cowan, P. J., Shinkel, T. A., Witort, E. J., Barlow, H., Pearse, M. J., and d'Apice, A. J. (1996) Targeting gene expression to endothelial cells in transgenic mice using the human intercellular adhesion molecule 2 promoter. Transplantation **62(2),** 155–160.
135. Vile, R. G. and Hart, I. R. (1994) Targeting of cytokine gene expression to malignant melanoma cells using tissue-specific promoter sequences. *Ann. Oncol.* **5(Suppl. 4),** 59–65.

136. Gerloni, M., Billetta, R., Xiong, S. D., and Zanetti, M. (1997) Somatic transgene immunization with DNA encoding an irnmunoglobulin heavy chain. *DNA Cell Biol.* **16(5),** 611–625.
137. Liang, X., Hartikka, J., Sukhu, L., Manthorpe, M., and Hobart, P. (1996) Novel, high expressing and antibiotic-controlled plasmid vectors designed for use in gene therapy. *Gene Ther.* **3(4),** 350–356.
138. Fishman, G. I., Kaplan, M. L., and Buttrick, P. M. (1994) Tetracycline-regulated cardiac gene expression in vivo. *J. Clin. Invest.* **93(4),** 1864–1868.
139. Delort, J. P. and Capecchi, M. R. (1996) TAXI/WAS—a molecular switch to control expression of genes in vivo. *Hum. Gene Ther.* **7(7),** 809–820.
140. Hallahan, D. E., Mauceri, H. J., Seung, L. P., Dunphy, E. J., Wayne, J. D., Hanna, N. N., Toledano, A., Hellman, S., Kufe, D. W., and Weichselbaum, R. R. (1995) Spatial and temporal control of gene therapy using ionizing radiation. *Nature Med.* **1(8),** 786–791.
141. Mount, R. C., Jordan, B. E., and Hadfield, C. (1996) Reporter gene systems for assaying gene expression in yeast. *Meth. Mol. Biol.* **53,** 239–248.
142. Cui, C., Wani, M. A., Wight, D., Kopchick, J., and Stambrook, P. J. (1994) Reporter genes in transgenic mice. *Transgen. Res.* **3(3)**, 182–194.
143. Mittal, S. K., Bett, A. J., Prevec, L., and Graham, F. L. (1995) Foreign gene expression by human adenovirus type 5-based vectors studies using firefly luciferase and bacterial beta-galactosidase gene as reporters. *Virology* **210(1),** 226–230.
144. Hanna, Z., Fregeau, C., Prefontaine, G., and Brousseau, R. (1984) Construction of a family of universal expression plasmid vectors. *Gene* **30,** 247–250.
145. Shen Q., van Beusechem, V. W., Einerhand, M. P., Hendrikx, P. J., and Valerio, D. (1991) Construction and expression of an adenosine deaminase:lacZ fusion gene. *Gene* **98(2),** 283–287.
146. Srienc, F., Campbell, J. L., and Bailey, J. E. (1986) Flow cytometry analysis of recombinant Saccharomyces cerevisiae populations. *Cytometry* **7(2),** 132–141.
147. Lal, B., Cahan, M. A., Couraud, P. O., Goldstein, G. W., and Laterra, J. (1994) Development of endogenous beta-galactosidase and autofluorescence in rat brain microvessels: implications for cell tracking and gene transfer studies. *J. Histochem. Cytochem.* **42(7),** 953–956.
148. Jiao, S., Acsadi, G., Jani, A., Felgner, P. L., and Wolff, J. A. (1992) Persistence of plasmid DNA and expression in rat brain cells in vivo. *Exper. Neurol.* **15(3),** 400–413.
149. Yoshimura, K., Rosenfeld, M. A., Nakamura, H., Scherer, E. M., Pavirani, A., Lecocq, J. P., and Crystal, R. G. (1992) Expression of the human cystic fibrosis transmembrane conductance regulator gene in the mouse lung after in vivo intratracheal plasmid-mediated gene transfer. *Nucl. Acids Res.* **20(12),** 3233–3240.
150. Jiao, S., Williams, P., Berg, R. K., Hodgeman, B. A., Liu, L., Repetto, G., and Wolff, J. A. (1992) Direct gene transfer into nonhuman primate myofibers in vivo. *Hum. Gene Ther.* **3(1),** 21–33.

151. Gorman, C. M., Moffat, L. F., and Howard, B. H. (1982) Recombinant genomes which express chloramphenicol acetyltransferase in mammarlian cells. *Mol. Cell Biol.* **2(9),** 1044–1051.
152. Sleigh, M. J. (1986) A nonchromatographic assay for expression of the chloramphenicol acetyltransferase gene in eukaryotic cells. *Anal. Biochem.* **156(1),** 251–256.
153. de Wet, J. R., Wood, K. V., Helinski, D. R., and DeLuca, M. (1985) Cloning of firefly luciferase cDNA and the expression of active luciferase in Escherichia. coli. *Proc. Natl. Acad. Sci. USA* **82(23),** 7870–7873.
154. Chapman, G. D., Lim, C. S., Gammon, R. S., Culp, S. C., Desper, J. S., Bauman, R. P., Swain, J. L., and Stack, R. S. (1992) Gene transfer into coronary arteries of intact animals with a percutaneous balloon-catheter. *Circ. Res.* **71(1),** 27–33.
155. de Wet, J. R., Wood, K. V., DeLuca, M., Helinski, D. R., and Subramani, S. (1987) Firefly luciferase gene: structure and expression in mammalian cells. *Mol. Cell Biol.* **7(2),** 725–737.
156. Brasier, A. R., Tate, J. E., and Habener, J. F. (1989) Optimized use of firefly luciferase assay as a reporter gene in mammalian tell lines. *Biotechnology* **7(10),** 1116–1122.
157. Kricka, L. J. (1991) Chemiluminescence and bioluminescence. *Clin. Chem.* **37(9),** 1472–1481.
158. Fasbender, A., Marshall, J., Moninger, T. O., Grunst, T., Cheng, S., and Welsh, M. J. (1997) Effect of co-lipids in enhancing cationic lipid-medialed gene transfer in vitro and in vivo. *Gene Ther.* **4,** 716–725.
159. Marquet, M., Horn, N. A., and Meek, J. A. (1995) Process development for the manufacture of plasmid DNA vectors for use in gene therapy. *BioPharm.* **8(7),** 26–37.
160. Weber, M., Moller, K., Welzeck, M., and Schorr, J. (1995) The effects of lipopolysaccharide on transfection in eukaryotic cells. *Biotechnology* **19,** 930–940.
161. Chang, N.-S. and Mattison, J. (1996) Rapicl separation of DNA from ethidium bromide and cesium chloride in ultracentrifugation gradients by a desalting column. *Biotechnology* **14(3),** 342,343.
162. Davis, H. L., Schleef, M., Moritz, P., Mancini, M., Schorr, J., and Whalen, R. G. (1996) Comparison of plasmid DNA preparation methods for direct gene transfer and genetic immunization. *Biotechnology* **21(1),** 92–99.
163. Wicks, I. P., Howell, M. L., Hancock, T., Kohsaka, H., Olee, T., and Carson, D. A. (1995) Bacterial lipopolysaccharide copurifies with plasmid DNA: implications for gene therapy. *Hum. Gene Ther.* **6,** 317–323.
164. Cotten, M., Baker, A., Saltik, M., Wagner, E., and Buschle, M. (1994) Lipopolysaccharide is a frequent contaminant of plasmid DNA preparations and can be toxic to primary human cells in the presence of adenovirus. *Gene Ther.* **1,** 239–246.
165. Bywater, M., Bywater, R., and Hellman, C. (1983) A novel chromatographic procedure for purification of bacterial plasmids. *Anal. Biochem.* **132,** 219–224.

166. Vo-Quang, T., Malpiece, Y., Buffard, D., Kaminski, P. A., Vidal, D., and Strosberg, A. D. (1985) Rapid, large-scale purlfication of plasmid DNA by medium or low pressure gel filtration. Application: construction of thermo-amplifiable expression vectors. *Biosci. Rep.* **5,** 101–111.
167. Raymond, G. J., Bryant, P. K., Nelson, A., and Johnson, J. D. (1988) Large-scale isolation of covalently closed circular DNA (cccDNA) using gel filtration chromatography. *Anal. Biochem.* **173,** 125–133.
168. Weintraub, H., Cheng, P. F., and Conrad, K. (1996) Expression of transfected DNA depends on DNA topology. *Cell* **46,** 115–122.
169. Lis, J. T. (1980) Fractionation of DNA frapments by polyethylene glycol precipitation. *Meth. Enzymol.* **65,** 347–353.
170. Laws, G. M. and Adams, S. P. (1996) Measurement of 8-OHdG in DNA by HPLC-ECD: the importance of DNA purity. *Biotechnology* **20(1),** 36–38.
171. Okamoto, T., Mitsuhashi, M., and Kikkawa, Y. (1994) Fluorometric nuclear run-on assay with oligonucleotide probe immobilized on plastic plates. *Anal. Biochem.* **221,** 202–204.
172. Kichler, A., Mechtler, K., Behr, J.-P. and Wagner, E. (1997) Influence of membrane-active peptides on lipospermine/DNA complex mediated gene transfer. *Bioconj. Chem.* **8,** 213–221.
173. Arndt-Jovin, D. J. and Jovin, T. M. (1989) Florescence labeling and microscopy of DNA. *Meth. Cell Biol.* **30,** 417–448.
174. Szoka, F. and Papahadjopoulos, D. (1978) Procedure for preparation of liposomes with large internal aqueous space and high capture by reverse-phase evaporation. *Proc. Natl. Acad. Sci. USA* **75,** 4194–4198.
175. Mayhew, E., Lazo, R., and Vail, W. J. (1984) Preparation of liposomes entrapping cancer chemotherapeutic agents for experimental in vivo and in vitro uses, in *Liposome Technology* (Gregoriadis, G., ed.), CRC, Boca Raton, FL, pp. 19–31.
176. Barenholtz, Y., Amselem, S., and Lichtenberg, D. (1979) A new method for preparation of phospholipid vesicles (liposomes)—French press. *FEBS Lett.* **99(1),** 210–214.
177. Hope, M. J., Bally, M. B., Webb, G., and Cullis, P. R. (1985) Production of large unilamellar vesicles by a rapid extrusion procedure: characterization of size distribution, trapped volume, and ability to maintain a membrane potential. *Biochim. Biophys. Acta* **812,** 55–65.
178. Ellens, H., Bentz, J., and Szoka, F. C. (1986) Fusion of phosphatidylethanolamine-containing liposomes and mechanism of the La-H_{II} phase transition. *Biochemistry* **25,** 4141–4147.
179. Siegel, D. P., Green, W. J., and Talmon, Y. (1994) The mechanism of lamellar-to-inverted hexagonal phase transitions: a study using temperature-jump cryo-electron microscopy. *Biophys. J.* **66(2 Pt. 1)**, 402–414.
180. Harasym, T. O., Tardi, P., Longman, S. A., Ansell, S., Bally, M. B., Cullis, P. R., and Choi, L. S. (1995) Poly(ethylene glycol)-modified phospholipids prevent aggregation during covalent conjugation of proteins to liposomes. *Bioconj. Chem.* **6(2),** 187–194.

181. Lee, R. J. and Low, P. S. (1995) Folate-mediated tumor cell targeting of liposome-entrapped doxorubicin in vitro. *Biochim. Biophys. Acta* **1233(2),** 134–144.
182. Lee, R. J. and Huang, L. (1996) Folate-targeted anionic liposome-entrapped polylysinecondensed DNA for tumor-cell specific gene transfer. *J. Biol. Chem.* **271(4),** 8481–8487.
183. Thomas, W. H. and Lee, Y. K. (1994) Particles in intravenous solutions: a review. *NZ Med. J.* **80(522),** 170–178.
184. Cullis, P. R., Hope, M. J., Bally, M. B., Madden, T. D., Mayer, L. O., and Janoff, A. (1987) Liposomes as pharmaceuticals, in *Liposomes: From Biophysics to Therapeutics* (Ostro, M. J., ed.), Marcel Dekker, New York, pp. 39–72.
185. Abra, R. M. and Hunt, C. A. (1981) Liposome disposition in vivo. III. Dose and vesicle-size effects. *Biochim. Biophys. Acta* **666(3),** 493–503.
186. Allen, T. M., Austin, G. A., Chonn, A., Lin, L., and Lee, K. C. (1991) Uptake of liposomes by cultured mouse bone marrow macrophages: influence of liposome composition and size. *Biochim. Biophys. Acta* **1061(1),** 56–64.
187. Moghimi, S. M., Porter, C. J., Muir, I. S., Illum, L., and Davis, S. S. (1991) Non-phagocytic uptake of intravenously injected microspheres in rat spleen: influence of particle size and hydrophilic coating. *Biochem. Biophys. Res. Comm.* **177(2),** 861–866.
188. Kalin, B., Sellin, P., von Krusenstierna, S., Schnell, P. O., and Jacobsson, H. (1991) Effect of size fractionation on the distribution of an albumin colloid in the reticuloendothelial system of the mouse. *Intl. J. Rad Applic. Instrumen.—Part B, Nucl. Med Biol.* **18(7),** 817–820.
189. Siegel, D. P. (1986) Inverted micellar intermediates and the transitions between lamellar, cubic and inverted hexagonal lipid phases. I. Mechanism of the La to H_{II} phase transitions. *Biophys. J.* **49,** 1155–1170.
190. Siegel, D. P. (1986) Inverted micellar intermediates and the transitions between lamellar, cubic and inverted hexagonal lipid phases. II. Implications for membrane-membrane interactions and membrane fusion. *Biophys. J.* **49,** 1171–1183.
191. Boggs, J. M. (1987) Lipid intermolecular hydrogen bonding: influence on structural organization and membrane function. *Biochim. Biophys. Acta* **906,** 353–404.
192. Hui, S. W., Stewart, T. P., Yeagle, P. L., and Albert, A. D. (1981) Bilayer to non-bilayer transition in mixtures of phosphatidylethanolarnine and phosphatidylcholine: implications for membrane properties. *Arch. Biochem. Biophys.* **207(2),** 227–240.
193. Stegmann, T. and Legendre, J.-Y. (1997) Gene transfer mediated by cationic lipids: lack of correlation between lipid-mixing and transfection. *Biochim. Biophys. Acta* **1325,** 71–79.
194. Wolff, J. A., Ludtke, J. J., Acsadi, G., Williams, P., and Jani, A. (1992) Long-term persistence of plasmid DNA and foreign gene expression in mouse muscle. *Hum. Mol. Genet.* **1(6),** 363–369.
195. Acsadi, G., Dickson, G., Love, D. R., Jani, A., Walsh, F. S., Gurusinghe, A., Wolff, J. A., and Davies, K. E. (1991) Human dystrophin expression in mdx

mice after intramuscular injection of DNA constructs. *Nature* **352(6338),** 815–818.
196. Wolff, J. A., Williams, P., Acsadi, G., Jiao, S., Jani, A., and Chong, W. (1991) Conditions affecting direct gene transfer into rodent muscle in vivo. *Biotechnology* **11(4),** 474–485.
197. Bainton, D. (1991) The discovery of lysosomes. *J. Cell Biol.* **91,** 66S–76S.
198. Labat-Moleur, F., Steffan, A. M., Brisson, C., Perron, H., Feugeas, O., Furstenberger, P., Oberling, F., Brambilla, E., and Behr, J. P. (1996) An electron microscopy study into the mechanism of gene transfer with lipopolyamines. *Gene Ther.* **3(11),** 1010–1017.
199. Nakanishi, M., Uchida, T., and Sugawa, H. (1985) Efficient introduction of content of liposomes into cells using HVJ (Sendai virus). *Exp. Cell Res.* **159,** 399–409.
200. Chen, X., Li, Y., Xie, Y., Aizicovici, S., Snodgrass, R., Wagner, T. E., and Platika, D. (1995) A novel nonviral cytoplasmic gene expression system and its implications in cancer gene therapy. *Ca. Gene Ther.* **2(4)**, 281–289.
201. Kaneda, Y., Iwai, K., and Uchida, T. (1989) Increased expression of DNA cointroduced with nuclear protein in adult rat liver. *Science* **243,** 374–378.
202. Tomita, N., Higaki, J., Ogihara, T., Kondo, T., and Kaneda, Y. (1994) A novel gene-transfer technique mediated by HVJ (Sendai virus), nuclear protein, and liposomes. *Ca. Detec. Preven.* **18(6),** 485–491.
203. Tartakoff, A. M. (1987) *The Secretory and Endocytic Paths: Mechanism and Specificity of Vesicular Traffic in the Cell Cytoplasm.* Wiley, New York.